

**Characterisation of human and mouse SOD1-ALS
proteins *in vivo* and *in vitro***

Rachele Saccon

**A thesis presented in partial fulfilment of the requirements for the
degree of Doctor of Philosophy to the University of London**

**Department of Neurodegenerative Disease
Institute of Neurology
University College London**

Declaration

I, Rachele Saccon, confirm that the work presented in this thesis is my own. Where information has been derived from other sources, I confirm that this has been indicated in the thesis.

Abstract

Amyotrophic lateral sclerosis (ALS) is a fatal progressive neurodegenerative disease affecting motor neurons (MNs). It is primarily sporadic, however a proportion of cases are inherited and of these ~20 % are caused by mutations in the superoxide dismutase 1 (*SOD1*) gene. The work described in this thesis has focused on the characterisation of the role that the SOD1 protein plays in ALS, investigating the human and the mouse variants *in vivo* and *in vitro*.

SOD1 mutations result in ALS by an unknown gain of function mechanism, although mouse models suggest that complete loss of SOD1 is also detrimental to MN function. To investigate a possible role of SOD1 loss of function in SOD1-ALS, a meta-analysis was carried out on the literature reviewing measures of SOD1 activity from patients carrying SOD1 familial ALS mutations and the phenotype of *Sod1* knockout mice.

The first set of experiments aimed to phenotypically characterise a novel mouse model, *Sod1*^{D83G}, carrying a pathological mutation in the mouse *Sod1* gene. *Sod1*^{D83G/D83G} mice have no SOD1 activity, low levels of SOD1 protein, develop central MN degeneration and a distal peripheral neuropathy. Further the *Sod1*^{D83G} mice were crossed with *Sod1* knockout mice and mice overexpressing the human wild-type SOD1 to determine if it was possible to dissect elements of a loss of function (the peripheral axonopathy) and aspects of a gain of function (the central body degeneration).

ALS mutations generally cause SOD1 to become more aggregate-prone, but it is unclear whether the human and the mouse SOD1 proteins co-aggregate in mouse models of SOD1 familial ALS. To investigate possible interactions between human and mouse SOD1 variants, recombinant proteins were produced, characterised and their spontaneous aggregation propensity was assessed *in vitro*.

Finally a sensitised screen focused on the effect of unknown mutations on the life-span of a low copy *SOD1*^{G93A} transgenic model of ALS, identified one mouse line with reduced survival, named *Galabad*. The phenotype of the *Galabad* mouse progeny was examined and a quantitative trait loci analysis was carried out to try to identify possible modifying locus/loci interacting with the SOD1 G93A mutation.

The present work aims to shed light on the interaction between human and mouse SOD1 proteins and increase our understanding on the mechanism affecting central and peripheral degeneration of MNs in the context of SOD1 familial ALS mutations.

Acknowledgements

I would like to express my deep gratitude to Professor Elizabeth Fisher for giving me the opportunity of a lifetime, for always believing and encouraging me providing guidance and support throughout my PhD. Thank you for being such an amazing mentor.

Many thanks also to Dr Abraham Acevedo and Professor Linda Greensmith for giving me valuable and constructive advice every step of the way.

Thank you to all past and present members of the Fisher, Isaacs and Greensmith labs all of who have played their part in making my PhD a wonderful and fun learning experience. I would also like to thank the members of staff from the UCL Department of Neurodegenerative Disease and the MRC Prion Unit who were essential for the work I have presented in this thesis. So many people have supported me that there are too many to mention individually by name, but in particular I would like to thank Dr Sarah Mizielinska, Dr Emma Clayton, Dr Rosie Bunton-Stasyshyn, Dr Phil McGoldrick, Dr Pietro Fratta, Mark Batchelor, Robin Labesse-Garbal and Cristina Venturini.

Another particular whole hearted thanks go to my amazing friends Daniel, Elisa, Caterina, Alessia, Luca, Karinne and Christiane who have always encourage me and lift my spirit during this journey.

Finally, my heartfelt thanks to my parents, to my grandparents and Martino, I would not be who I am and where I am without you.

Table of contents

Declaration	2
Abstract	3
Acknowledgements	4
Table of contents	5
List of figures	15
List of tables	18
List of abbreviations	20
Chapter 1 Introduction	25
1.1 Amyotrophic lateral sclerosis (ALS)	25
1.1.1 Epidemiology.....	25
1.1.2 ALS clinical course	25
1.1.2.1 Motor neuron degeneration.....	25
1.1.2.2 Cognitive dysfunctions	26
1.1.3 Diagnosis.....	27
1.1.4 Treatments	27
1.1.5 Environmental risk factors.....	28
1.1.6 ALS pathological features.....	28
1.1.6.1 Degeneration of motor neurons	28
1.1.6.2 Gliosis	30
1.1.6.3 Inclusion bodies.....	30
1.1.6.4 Muscle atrophy.....	31
1.1.7 Genetics of ALS.....	31
1.2 SOD1-fALS	37
1.2.1 Clinical course and pathogenicity of SOD1-fALS.....	37
1.2.2 <i>SOD1</i> gene and inheritance pattern	37
1.3 SOD1 protein	39

1.3.1	Biological function.....	40
1.3.2	Structural features and protein stability	41
1.3.3	Properties of mutant SOD1 proteins.....	43
1.3.3.1	Effect of mutations on protein function	43
1.3.3.2	Effect of mutations on SOD1 biochemical properties.....	43
1.4	SOD1 mouse models	47
1.4.1	Why we use mouse models in ALS research	47
1.4.1.1	Mouse models of SOD1-ALS	47
1.4.2	SOD1 transgenic mice	48
1.4.2.1	Transgenic <i>SOD1^{G93A}</i> high copy mice	48
1.4.2.2	Transgenic <i>SOD1^{WT}</i> mice	50
1.4.3	<i>Sod1</i> knock out mice	51
1.4.4	Effect of background on mouse phenotypes	51
1.4.5	Limitations of current SOD1-ALS mouse models	54
1.5	How mutant SOD1 causes disease	55
1.5.1	SOD1-fALS proposed mechanisms of pathogenicity.....	55
1.5.1.1	Glutamate toxicity and calcium homeostasis	55
1.5.1.2	Endoplasmic reticulum (ER) stress and unfolded protein response (UPR)	56
1.5.1.3	Mitochondrial dysfunction.....	56
1.5.1.4	Oxidative stress.....	57
1.5.1.5	Axonal transport impairment	58
1.5.1.6	Non-cell autonomous mechanism	59
1.5.1.7	SOD1 involvement in RNA metabolism.....	60
1.5.2	Protein misfolding and aggregation	61
1.5.2.1	SOD1 protein aggregates	61
1.5.2.2	SOD1 pre-aggregate species	63
1.5.2.3	Prion-like protein misfolding mechanism.....	64

1.5.3	Role of wild-type SOD1 in the pathogenesis of ALS	65
1.6	Research aim and current questions in SOD1-fALS	66
1.6.1	Does SOD1 loss of function play a role in the disease?	66
1.6.2	Can we dissect the central and the peripheral effects of mutant SOD1 toxicity using a new mouse model of motor neuron disease?	67
1.6.3	Is there an interaction between human and mouse SOD1 proteins, and how does this change our interpretation of SOD1 mouse models?	67
1.6.4	Can we identify new genes involved in SOD1-ALS by creating new modifier mouse models?	68
Chapter 2	Materials and methods	70
2.1	Materials	70
2.1.1	Equipment	70
2.1.2	Chemicals and reagents	72
2.1.3	Commercial kits	74
2.1.4	Antibodies	74
2.1.4.1	Primary antibodies	74
2.1.4.2	Secondary antibodies	74
2.1.5	Software	75
2.2	Mice	75
2.2.1	Housing and husbandry of mice	76
2.2.2	C57BL/6J mice	77
2.2.3	<i>Sod1</i> knockout mice	77
2.2.4	Human wild-type <i>SOD1</i> transgenic mice	77
2.2.5	Human <i>SOD1</i> ^{G93A} transgenic high copy mice	77
2.2.6	<i>Sod1</i> ^{D83G} mice	78
2.2.7	<i>Galabad</i> mice	78
2.2.8	<i>Sod1</i> ^{D83G} X <i>Sod1</i> knockout cross	78
2.2.9	<i>Sod1</i> ^{D83G} X Human wild-type <i>SOD1</i> transgenic cross	79

2.2.10	<i>Galabad</i> X Human <i>SOD1</i> ^{G93A} transgenic high copy cross	80
2.3	Mouse experimental procedures	80
2.3.1	General mouse experimental procedures	80
2.3.1.1	Perfusion with paraformaldehyde.....	80
2.3.2	Mouse experimental procedures specific for <i>Galabad</i> mice	81
2.3.2.1	Neurological checks	81
2.3.2.2	Weekly weight.....	81
2.3.2.3	Grip-strength.....	81
2.3.2.4	Survival.....	82
2.4	Histology	82
2.4.1	Harvesting of fresh tissues	82
2.4.2	Harvesting and embedding of fixed tissues	82
2.4.3	Neuromuscular junction (NMJ).....	83
2.4.3.1	Sectioning of the extensor digitorum longus (EDL) muscle	83
2.4.3.2	Immunostaining.....	83
2.4.3.3	Analysis	84
2.5	General DNA protocols	84
2.5.1	Nucleic acids extraction and purification from mouse tissue	84
2.5.1.1	Fast DNA extraction	84
2.5.1.2	Proteinase K DNA extraction.....	85
2.5.2	Polymerase chain reaction (PCR)	85
2.5.2.1	<i>SOD1</i> transgene genotyping PCR	85
2.5.2.2	<i>Sod1</i> knockout genotyping PCR.....	87
2.5.2.3	Agarose gel electrophoresis (AGE)	88
2.5.3	<i>Galabad</i> chromosome single-nucleotide polymorphism PCR.....	88
2.5.4	Quantitative real time PCR (qPCR) for <i>SOD1</i> transgene copy number.....	90
2.6	<i>SOD1</i> protein protocols	91

2.6.1	Production and purification of wild-type and mutant SOD1 recombinant proteins	91
2.6.1.1	Protein expression, cell harvesting and cell lysis.....	92
2.6.1.2	Affinity chromatography Ni-NTA	94
2.6.2	Preparation of animal tissues for protein investigation.....	96
2.6.2.1	Brains preparation specific for <i>Sod1</i> ^{D83G} experiments	96
2.6.2.2	Spinal cord preparation specific for transmission experiments.....	97
2.6.3	Spectrophotometric protein concentration measurements	97
2.6.3.1	Absorbance.....	97
2.6.3.2	Colorimetric assays.....	97
2.6.4	Polyacrylamide gel electrophoresis.....	98
2.6.4.1	Coomassie blue staining	98
2.6.4.2	Western blot.....	98
2.6.4.3	Native western blot.....	99
2.6.4.4	SOD1 activity in-gel assay.....	101
2.6.5	Protein characterisation using circular dichroism (CD)	101
2.6.6	Conversion of SOD1 proteins into fibrils <i>in vitro</i>	101
2.7	Meta-analysis on SOD1 activity in SOD1-ALS affected patients	102
2.8	Statistical analysis	102
Chapter 3	SOD1 loss of function in SOD1-amyotrophic lateral sclerosis	103
3.1	Introduction.....	103
3.2	Aim	104
3.3	Results	104
3.3.1	SOD1 loss of function in SOD1-fALS patients	104
3.3.1.1	Methods of measuring SOD1 dismutase activity	104
3.3.1.2	Intrinsic and overall SOD1 activity	105
3.3.1.3	SOD1 dismutase activity is reduced in SOD1-fALS patients.....	106

3.3.1.4	Dismutase activity reduction might be enhanced in motor neurons	111
3.3.2	SOD1 loss of function in <i>Sod1</i> knockout mice	112
3.3.2.1	Absence of <i>Sod1</i> causes a progressive adult-onset motor axonopathy in <i>Sod1</i> ^{-/-} mice	113
3.3.2.2	Motor neurons of <i>Sod1</i> ^{-/-} mice have an increased vulnerability to stress	116
3.3.2.3	<i>Sod1</i> ^{-/-} develop other non-motor neuronal and extra neuronal phenotypes	117
3.3.2.4	<i>Sod1</i> ^{+/-} mice have a 50% reduction of SOD1 activity and develop abnormal neuronal function	118
3.3.3	SOD1 loss of function influence on SOD1-fALS mouse models	121
3.3.3.1	Loss of function of mouse endogenous SOD1 does not affect lifespan of transgenic SOD1-fALS mouse models	121
3.3.3.2	Influence of SOD1 overexpression on disease.....	121
3.3.3.3	Tissue specific expression and inactivation of mutant SOD1 suggest a modifying role for dismutase activity	122
3.4	Conclusions	123
3.4.1	<i>Sod1</i> knockout models share commonalities with ALS and indicate specific cell-type sensitivities	123
3.4.2	SOD1 activity is reduced in human SOD1-fALS patients	123
3.4.3	Absence of loss of function phenotypes in humans.....	124
3.4.4	SOD1 gain and loss of function could both play a role in ALS pathogenesis.....	124
3.4.5	SOD1 loss of function implications in ALS therapeutic approaches	126
3.5	Summary	126
Chapter 4	<i>Sod1</i>^{D83G} a mouse model for motor neuron disease	128
4.1	Introduction	128
4.2	Aim	131

4.3	Results	133
4.3.1	<i>Sod1</i> ^{D83G} mice characterisation	133
4.3.1.1	Neuromuscular junctions of the EDL	133
4.3.1.2	SOD1 protein levels of <i>Sod1</i> ^{D83G} mice	137
4.3.1.3	SOD1 enzymatic activity of <i>Sod1</i> ^{D83G} mice	138
4.3.2	<i>Sod1</i> ^{D83G} X <i>Sod1</i> knockout cross characterisation	142
4.3.2.1	SOD1 protein levels of <i>Sod1</i> ^{D83G} X <i>Sod1</i> knockout progeny at 15 weeks	142
4.3.2.2	SOD1 enzymatic activity of <i>Sod1</i> ^{D83G} X <i>Sod1</i> knockout progeny at 15 weeks	143
4.3.3	<i>Sod1</i> ^{D83G} X Tg <i>SOD1</i> ^{WT} cross characterisation	144
4.3.3.1	Ratio of <i>Sod1</i> ^{D83G} X Tg <i>SOD1</i> ^{WT}	144
4.3.3.2	SOD1 protein levels of <i>Sod1</i> ^{D83G} X Tg <i>SOD1</i> ^{WT} progeny at 15 weeks	145
4.3.3.3	SOD1 enzymatic activity of <i>Sod1</i> ^{D83G} X Tg <i>SOD1</i> ^{WT} progeny at 15 weeks	146
4.4	Conclusions	149
4.5	Summary	152
Chapter 5	Characterisation of SOD1 proteins	154
5.1	Introduction	154
5.1.1	Possible prion-like mechanism for SOD1 protein	154
5.1.1.1	SOD1 aggregation <i>in vitro</i>	155
5.1.1.2	SOD1 transmission <i>in vitro</i>	155
5.1.1.3	SOD1 transmission <i>in vivo</i>	156
5.1.2	Human and mouse SOD1 proteins	157
5.2	Aim	157
5.3	Results	158
5.3.1	SOD1 recombinant proteins	158

5.3.1.1	Production and purification of recombinant proteins	158
5.3.1.2	Sodium dodecyl sulphate - polyacrylamide gel electrophoresis of mouse and human purified SOD1 recombinant proteins.....	163
5.3.2	SOD1 recombinant proteins structural profile with circular dichroism...	164
5.3.3	Kinetics of spontaneous fibrillization of mouse and human SOD1 recombinant proteins	167
5.3.4	SOD1 transmission project	170
5.3.4.1	Western blot analysis.....	170
5.3.4.2	Native blot analysis	170
5.4	Conclusions	172
5.4.1	Comparison between SOD1 human and mouse proteins	172
5.4.2	Future work	173
5.4.2.1	Further mouse SOD1 proteins characterisation.....	173
5.4.2.2	Kinetics of mouse and human SOD1 proteins.....	173
5.5	Summary	174
Chapter 6 Galahad mouse		175
6.1	Introduction	175
6.1.1	ENU mutagenesis and the phenotype driven approach	175
6.1.1.1	ENU properties	176
6.1.1.2	ENU administration and breeding strategies	176
6.1.1.3	Mapping and cloning	178
6.1.2	A sensitised screen for modifiers in <i>SOD1^{G93A}</i> low copy mice	178
6.1.3	The <i>SOD1^{G93A}</i> low copy phenotype	180
6.1.3.1	Effects of genetic background on time to end stage in Tg <i>SOD1^{G93A(L)}</i> mice.....	180
6.1.3.2	Grip-strength analysis of C57BL/6J Tg <i>SOD1^{G93A(L)}</i> mice.....	181
6.2	Aim	182
6.3	Results	182

6.3.1	Phenotypic characterisation of the G2 <i>Galabad</i> progeny	183
6.3.1.1	<i>Galabad</i> breeding strategy	183
6.3.1.2	<i>Galabad</i> G2 genotype and ratios	184
6.3.1.3	Survival of Tg ^{G93A(L)} <i>Galabad</i> mice	185
6.3.1.4	Definition of two transgenic populations for phenotypic analysis	189
6.3.1.5	Correlation between transgene copy number and survival	191
6.3.1.6	<i>Galabad</i> G2 body weight analysis	192
6.3.1.7	<i>Galabad</i> G2 grip-strength analysis	194
6.3.2	Phenotypic characterisation of the G3 <i>Galabad</i> progeny	197
6.3.2.1	<i>Galabad</i> G2 breeding strategy	197
6.3.2.2	<i>Galabad</i> G3 genotype and ratios	197
6.3.2.3	Survival of G3 Tg ^{G93A(L)} <i>Galabad</i> mice.....	197
6.3.2.4	<i>Galabad</i> G3 body weight analysis	199
6.3.3	NTg <i>Galabad</i> X TgSOD1 ^{G93A(H)} cross	200
6.3.4	Genetic mapping.....	201
6.3.4.1	Genome wide scan.....	201
6.3.4.2	QTL analysis	202
6.4	Conclusions.....	210
6.4.1	Concluding remarks on <i>Galabad</i> mice.....	210
6.4.2	Future work	212
6.4.2.1	Further phenotypic characterisation.....	212
6.4.2.2	Further QTL analysis and next-generation sequencing.....	212
6.4.2.3	Pathology investigation.....	212
6.5	Summary	213
Chapter 7 Discussion.....		214
7.1	Gain and loss of function could coexist in SOD1-ALS.....	214
7.1.1	Reduction of SOD1 activity in SOD1-fALS patients	215

7.1.2	SOD1 loss of function worsens the phenotype of transgenic mouse models pointing to a neuroprotective role for SOD1 activity	215
7.1.3	<i>Sod1</i> knockout mice have specific cell-type sensitivities and share characteristics with ALS.....	215
7.1.4	<i>Sod1^{D83G}</i> a novel mouse model to investigate axonal and neuronal body degeneration.....	216
7.1.5	Separation of gain of function and loss of function phenotypes in the <i>SOD1^{D83G}</i> mouse model.....	218
7.1.6	Co-existence of a SOD1 gain and loss of function in ALS.....	220
7.2	Human and mouse SOD1 proteins in ALS.....	221
7.2.1	<i>In vivo</i> interaction of human and mouse SOD1 proteins	221
7.2.2	<i>In vitro</i> interactions of human and mouse SOD1 recombinant proteins ..	223
7.3	The importance of investigating SOD1 modifiers.....	224
7.4	Conclusions.....	225
Chapter 8	Appendices.....	228
8.1	Appendix 1 Table of SOD1 transgenic mice.....	228
8.2	Appendix 2 Vector and constructs	239
8.3	Appendix 3 Ni-NTA column recharged protocol.....	240
8.4	Appendix 4 <i>Sod1^{-/-}</i> other neuronal and extra-neuronal phenotypes	241
8.4.1	<i>Sod1^{-/-}</i> non-motor neuronal phenotypes	241
8.4.2	<i>Sod1^{-/-}</i> extra-neuronal phenotypes.....	242
8.5	Appendix 5 Identification of the <i>Sod1^{D83G}</i> mouse model by ENU mutagenesis.....	243
8.6	Appendix 6 Transmission project.....	244
8.7	Appendix 7 <i>Galahad</i> project.....	245
	References	256
	Publications.....	306

List of figures

Figure 1.1 Impairment of the neuromuscular system in ALS.....	29
Figure 1.2 Percentage of sALS and fALS explained by each gene.....	33
Figure 1.3 Human <i>SOD1</i> gene chromosomal location, DNA and mRNA structure.....	39
Figure 1.4 Human SOD1 protein structure.....	42
Figure 1.5 Human SOD1 secondary structure and mutations responsible for fALS.....	46
Figure 1.6 Genetic background effect on Tg <i>SOD1</i> ^{G93A(H)} mouse survival.....	53
Figure 2.1 Breeding scheme for <i>Sod1</i> ^{D83G} X <i>Sod1</i> KO.....	79
Figure 2.2 Breeding scheme for <i>Sod1</i> ^{D83G} X Tg <i>SOD1</i> ^{WT}	80
Figure 2.3 Example of transgene genotyping PCR.....	87
Figure 2.4 SOD1 protein production.....	93
Figure 2.5 SOD1 protein purification.....	96
Figure 3.1 Diagram of human SOD1 mutations dismutase activity in the current literature.....	107
Figure 3.2 The cycle of SOD1 loss of function, schematic representation of a potential co-operation between SOD1 loss and gain of function in SOD1 pathogenesis.....	125
Figure 4.1 Representative image of innervated NMJs from EDL muscle of a 52 weeks old wild-type mouse.....	134
Figure 4.2 Representative images of innervated, intermediate and denervated NMJs of the three <i>Sod1</i> ^{D83G} genotypes at 52 weeks of age.....	135
Figure 4.3 NMJs analysis from EDL muscle of <i>Sod1</i> ^{D83G} mice at 15 and 52 weeks.....	136
Figure 4.4 SOD1 western blots and activity gel assays of <i>Sod1</i> ^{D83G} mice and controls at 15 and 60 weeks of age.....	140
Figure 4.5 Quantification of SOD1 protein levels and activity of <i>Sod1</i> ^{D83G} mice and controls at 15 and 60 weeks of age.....	141
Figure 4.6 SOD1 western blots and activity gel assays of <i>Sod1</i> ^{D83G} X <i>Sod1</i> KO offspring and controls at 15 weeks.....	143
Figure 4.7 Quantification of SOD1 protein levels and activity of <i>Sod1</i> ^{D83G} X <i>Sod1</i> KO offspring at 15 weeks.....	143
Figure 4.8 SOD1 western blots and activity gel assays of <i>Sod1</i> ^{D83G} X Tg <i>SOD1</i> ^{WT} offspring at 15 weeks of age.....	147

Figure 4.9 Quantification of SOD1 protein levels and activity of <i>Sod1</i> ^{D83G} X Tg <i>SOD1</i> ^{WT} offspring at 15 weeks of age.....	148
Figure 4.10 Types of mouse model used in ALS research.....	149
Figure 5.1 Possible prion-like mechanism for SOD1 protein.....	154
Figure 5.2 Bacterial growth for human wild-type SOD1 protein pre and post IPTG induction.....	160
Figure 5.3 Human wild-type SOD1 protein first Ni-NTA affinity chromatography...	161
Figure 5.4 Human wild-type SOD1 protein before and after His-tag cleavage.....	162
Figure 5.5 Human wild-type SOD1 protein second Ni-NTA affinity chromatography.....	162
Figure 5.6 Western blot of purified human and mouse SOD1 recombinant proteins.....	163
Figure 5.7 Coomassie blue of purified human and mouse SOD1 recombinant proteins.....	164
Figure 5.8 CD spectra of human and mouse SOD1 recombinant proteins.....	165
Figure 5.9 CD spectra comparison between human and mouse SOD1 recombinant proteins.....	166
Figure 5.10 Spontaneous fibrillization of SOD1 human wild-type recombinant protein.....	168
Figure 5.11 Spontaneous fibrillization of SOD1 human and mouse D83G recombinant proteins.....	168
Figure 5.12 Spontaneous fibrillization of SOD1 mouse wild-type recombinant protein.....	169
Figure 5.13 Spontaneous fibrillization of SOD1 human D83G recombinant protein over 450 hours.....	169
Figure 5.14 Western blot of spinal cord homogenates.....	170
Figure 5.15 Native blot of spinal cord homogenates.....	171
Figure 6.1 Modifier screen in <i>SOD1</i> ^{G93A} low copy mice.....	179
Figure 6.2 Representative distribution of Tg <i>SOD1</i> ^{G93A(L)} mice survival on different genetic backgrounds.....	181
Figure 6.3 Grip-strength analysis of C57BL/6J Tg <i>SOD1</i> ^{G93A(L)} mice.....	182
Figure 6.4 <i>Galabad</i> breeding scheme.....	184
Figure 6.5 Quantile-quantile plot of Tg ^{G93A(L)} <i>Galabad</i> mice survival.....	186

Figure 6.6 Tg ^{G93A(L)} <i>Galahad</i> mice survival bimodal distribution.....	187
Figure 6.7 Tg ^{G93A(L)} <i>Galahad</i> males and females survival bimodal distribution.....	188
Figure 6.8 Definition of Tg <i>SOD1</i> ^{G93A(L)} and mTg ^{G93A(L)} <i>Galahad</i> populations for phenotypic analysis.....	190
Figure 6.9 Correlation between copy number and survival in G2 Tg ^{G93A(L)} <i>Galahad</i> mice.....	191
Figure 6.10 Normalised body weight of G2 <i>Galahad</i> mice.....	193
Figure 6.11 Normalised grip-strength of G2 <i>Galahad</i> mice.....	196
Figure 6.12 Normalised body weight of G3 <i>Galahad</i> females.....	200
Figure 6.13 SNPs genome coverage.....	202
Figure 6.14 Genotype data for the G2 <i>Galahad</i> mice.....	203
Figure 6.15 LOD scores for <i>Galahad</i> G2 progeny.....	204
Figure 6.16 Chromosome 6.....	207
Figure 6.17 Chromosome 12.....	208
Figure 6.18 Chromosome 18.....	209
Figure 8.1 <i>Sod1</i> ^{D83G} identification: ENU mutagenized mice breeding scheme.....	244
Figure 8.2 Genotype and recombination events per mouse along the 19 autosomal chromosomes.....	246

List of tables

Table 1.1 El Escorial diagnostic criteria for ALS.....	27
Table 1.2 ALS associated genes.....	34
Table 1.3 Classification of mutant SOD1 proteins to WTL and MBR categories.....	44
Table 2.1 Mouse genotypes nomenclature.....	76
Table 2.2 Classification of NMJs innervation status.....	84
Table 2.3 SOD1 transgene genotyping primers.....	86
Table 2.4 PCR cycling conditions for SOD1 transgene genotyping.....	86
Table 2.5 <i>Sod1</i> knockout genotyping primers.....	87
Table 2.6 PCR cycling conditions for <i>Sod1</i> knockout genotyping.....	88
Table 2.7 <i>Galabud</i> genotyping primers.....	89
Table 2.8 <i>Galabud</i> PCR cycling conditions.....	89
Table 2.9 SOD1 transgene copy number qPCR primers and probes.....	91
Table 2.10 <i>SOD1</i> transgene copy number qPCR cycling conditions.....	91
Table 2.11 Primary and secondary antibodies for native blots.....	100
Table 3.1 Methods of measuring SOD1 activity.....	105
Table 3.2 SOD1 overall and intrinsic activity of SOD1-fALS patients in the current literature.....	107
Table 3.3 Characteristic of D90A and L117V mutations.....	111
Table 3.4 Published <i>Sod1</i> knockout mouse lines.....	113
Table 3.5 <i>Sod1</i> ^{-/-} mice behavioural phenotypes.....	114
Table 3.6 <i>Sod1</i> ^{-/-} non-motor neuronal phenotypes.....	117
Table 3.7 <i>Sod1</i> ^{-/-} extra-neuronal phenotypes.....	118
Table 3.8 Consequences of mutant SOD1 excision in Tg <i>SOD1</i> ^{G37R} and Tg <i>SOD1</i> ^{G85R} mice.....	122
Table 4.1 <i>Sod1</i> ^{D83G} mice upper and lower motor neurons characterisation.....	129
Table 4.2 <i>Sod1</i> ^{D83G} mice behavioural tests.....	130
Table 4.3 <i>Sod1</i> ^{D83G} mice EDL and TA muscle force.....	131
Table 4.4 Percentage of innervated intermediate and denervated NMJs at 15 and 52 week.	137

Table 4.5 Total number of NMJs at 15 and 52 weeks.....	137
Table 4.6 Experimental genotypes for <i>Sod1</i> ^{D83G} X Tg <i>SOD1</i> ^{WT} characterisation.....	144
Table 4.7 Observed ratios of offspring from <i>Sod1</i> ^{D83G} X Tg <i>SOD1</i> ^{WT} cross.....	145
Table 5.1 Human and mouse SOD1 recombinant proteins produced.....	159
Table 6.1 ENU base pair substitution frequency.....	176
Table 6.2 Average survival of Tg <i>SOD1</i> ^{G93A(L)} mice on different genetic background..	181
Table 6.3 Tg <i>SOD1</i> ^{G93A} genotype ratios of <i>Galahad</i> G2 mice.....	185
Table 6.4 <i>Galahad</i> G2 mice normalised body weight pair-wise comparisons.....	192
Table 6.5 <i>Galahad</i> G2 mice normalised grip-strength pair-wise comparisons.....	195
Table 6.6 Haplotype of the G3 mTg ^{G93A(L)} <i>Galahad</i> females and G2 parents.....	198
Table 6.7 <i>Galahad</i> G3 normalised weight pair-wise comparisons.....	199
Table 6.8 Top LOD score marker per chromosome.....	205
Table 7.1 Comparison between <i>Sod1</i> ^{-/-} and <i>Sod1</i> ^{D83G/D83G} animals.....	218
Table 8.1 Transgenic mice expressing mutant or wild-type SOD1.....	232
Table 8.2 Ni-NTA resin recharge protocol.....	240

List of abbreviations

AD	Alzheimer disease
AGE	Agarose gel electrophoresis
ALS	Amyotrophic lateral sclerosis
<i>ALS2</i>	Alsin
AMD	Age related macular degeneration
AMPA	Alpha-amino-3-hydroxy-5-methyl-4-isoxazolepropionic acid
<i>ANG</i>	Angiogenin
<i>APP</i>	Amiooyd precursor protein
ARE	Adenine/uridine-rich elements
<i>ATXN2</i>	Ataxin 2
BBB	Blood brain barrier
BMAA	Neurotoxic non protein amino acid β - <i>N</i> -methylamino-L-alanine
bp	Base pair
BSA	Bovine serum albumin
<i>C9orf72</i>	Chromosome 9 reading frame 72
CaBP	Calcium-binding proteins
CaCl ₂	Calcium chloride
<i>CCS</i>	Copper chaperone for SOD1
CD	Circular dichroism
cDNA	Coding DNA
CH ₃ CH ₂ OH	Ethanol
CH ₃ OH	Methanol
<i>CHMP2B</i>	Chromatin modifying protein 2B
Chr	Chromosome
CK1 γ	Casein kinase 1-gamma
CNS	Central nervous system
COPII	Coatomer coat protein II
Cre-loxP	Causes recombination-locus for crossing over (x), P1
Ct	Threshold cycle

Cu ⁺ ZnSOD	Reduced cupric ion
Cu ²⁺	Copper
Cu ²⁺ ZnSOD	Cupric ion
CuSO ₄	Copper sulphate
Cys	Cysteine
DAO	d-amino acid oxidase
DAPI	4',6-diamidino-2-phenylindole
DRG	Dorsal root ganglia
<i>Dync1h1</i>	Cytoplasmic dynein heavy chain 1
EAAT2	Excitatory amino-acid transporter 2
EC	Endogenous control
ECL	Enhanced chemiluminescent substrate
EDL	Extensor digitorum longus
EDTA	Ethylenediaminetetraacetic acid
ELAV	Embryonic lethal abnormal visual
ENU	<i>N</i> -ethyl- <i>N</i> -nitrosourea
ER	Endoplasmic reticulum
ERAD	ER-associated degradation
ESC	Embryonic stem cells
fALS	Familiar amyotrophic lateral sclerosis
<i>FIG4</i>	Polyphosphoinositide phosphate
<i>FMRP</i>	Fragile X Mental Retardation Protein
FTD	Frontotemporal dementia
<i>FUS</i>	Fused in sarcoma
GluR2	Glutamate receptor 2
GOF	Gain of function
GuHCl	Guanidine hydrochloride
GWAS	Genome wide association studies
GWS	Genome-wide scan
H ₂ O ₂	Hydrogen peroxide

HCC	Hepatocellular carcinoma
HD	Huntington's disease
His	Histidine
hnRNPA1	Heterogenous nuclear ribonucleoprotein A1
Hr	Hours
HRP	Horseradish peroxidase
<i>Il2</i>	Interleukin 2
IMS	Inter-membrane space
iPSC	Induced pluripotent stem cell
IPTG	Isopropyl- β -D-thiogalactopyranoside
IVC	Individually ventilated cages
IVF	<i>In vitro</i> fertilisation
kb	Kilobase
l	Litre
LB	Luria Broth
LMN	Lower motor neuron
<i>Loa</i>	Legs-at-odd-angles
LOD	Logarithm of the odds
LOF	Loss of function
MBR	Metal-binding-regions
MN	Motor neuron
MRI	Magnetic resonance imaging
mutSOD1	Mutant SOD1
n	number
Na ₃ PO ₄	Sodium phosphate
NaCl	Sodium chloride
NFL	Molecular weight neurofilament
Ni-NTA	Nitrilotriacetic acid sepharose matrix
NMJ	Neuromuscular junction
nq	Not quantified

nr	Not reported
ntc	No template PCR control
O ₂	Molecular oxygen
O ₂ ⁻	Superoxide anions
OCT	Optimum cutting temperature freezing medium
OD	Optical density
<i>OPTN</i>	Optineurin
ORF	Open reading frame
PBS	Phosphate buffered saline
PBS	Phosphate Buffered Saline
PBS-T	50 % PBS with 0.05 % Tween
PCR	Polymerase chain reaction
PFA	Paraformaldehyde
<i>PFN1</i>	Profilin 1
<i>PRNP</i>	Prion protein gene
PrP	Prion protein
PrP ^c	Correctly folded cellular PrP
PrP ^{sc}	Misfolded PrP
PVDF	Polyvinylidene difluoride
qPCR	Quantity real time polymerase chain reaction
QQ	Quantile-quantile
QTL	Quantitative trait loci
RFU	Relative fluorescence units
ROS	Reactive oxygen species
sALS	Sporadic amyotrophic lateral sclerosis
SDS	Sodium dodecyl sulphate
SDS-PAGE	SDS-polyacrylamide gel electrophoresis
SEDI	SOD1 exposed dimer interface
SEM	Standard error of the mean
<i>SETX</i>	Senataxin

<i>SIGMAR1</i>	σ Non opioid receptor 1
SNP	Single nucleotide polymorphisms
<i>SOD1</i>	Superoxide dismutase 1
<i>SPG11</i>	Spatascin
<i>SQSTM1</i>	Sequestosome 1
S-S	Intrasubunit disulphide bond
T7 RNAP	T7 RNA polymerase
TA	Tibialis anterior
<i>TDP-43</i>	TAR DNA binding protein 43
TEMED	N,N,N',N'-tetramethylethylenediamine
ThT	Thioflavin-T
Tris	Trizma base
Tris-HCl	Tris hydrochloride
<i>UBQLN2</i>	Ubiquilin 2
UMN	Upper motor neuron
UPR	Unfolded protein response
UPS	Ubiquitin proteasome system
USOD	Unfolded SOD1
UTR	Untranslated region
<i>VAPB</i>	Vesicle-associated membrane protein-associated protein B
<i>VCP</i>	Valosin-containing protein
<i>VEGF</i>	Vascular endothelial growth factor
WT	Wild-type
WTL	Wild-type like
Zn ²⁺	Zinc
ZnSO ₄	Zinc sulphate
ϵ SOD1	SOD1 extinction coefficient

Mice genotype abbreviations are listed in Chapter 2 section 2.2

Chapter 1 Introduction

1.1 Amyotrophic lateral sclerosis (ALS)

Amyotrophic lateral sclerosis (ALS) is the most common adult onset motor neuron disease, characterised by the degeneration and death of upper and lower motor neurons (MNs). This relentless and fatal neurodegenerative disorder has a progressive clinical course typically starting with a focal onset of motor weakness which spreads through the body leading to paralysis and death within 3 to 5 years after diagnosis (Hirtz et al., 2007; Valdmanis and Rouleau, 2008).

1.1.1 Epidemiology

A meta-analysis study of global data provided a median incidence rate of ALS of 1.90 per 100,000 and a prevalence of 4.48 per 100,000 of total population. In considering this figure it is important to note that the great majority of research on ALS epidemiology has been conducted in Europe and that there is wide variability in the incidence and prevalence reported in literature (Chiò et al., 2013). Investigation of ALS sex ratios showed that men are 1.2-1.5 times more likely to develop ALS compared to women, and this difference decreases with age (Manjaly et al., 2010). The average age of onset is 65.2 for men and 67.0 for women, while the peak incidence is between the ages of 70-74 for men and 65-69 for women (Logroscino et al., 2010; Strong and Rosenfeld, 2003).

1.1.2 ALS clinical course

ALS affects both the upper and lower motor neurons. Upper motor neuron (UMN) degeneration presents itself clinically as weakness of the voluntary muscles, spasticity, and brisk reflexes. While symptoms of lower motor neuron (LMN) impairment are muscular atrophy, weakness of the skeletal muscles, cramping, fasciculation, twitching and flaccidity (Traynor et al., 2000).

1.1.2.1 Motor neuron degeneration

About 70 % of ALS patients develop a primary lumbar onset, which usually starts with asymmetric focal weakness of the extremities. In 25 % of the cases the onset is bulbar causing pronunciation problems (dysarthria) and swallowing difficulties (dysphagia) (Piao et al., 2003). While in the remaining 5 % of affected individuals the onset occurs in the trunk muscles, affecting the respiratory system (Kiernan et al., 2011). In most of

the cases, during the course of the disease symptoms become progressively more severe, developing from muscle weakness to paralysis and they also spread from a focal site of onset through the rest of body (Fujimura-Kiyono et al., 2011). Patients usually have preserved oculomotor muscles and voluntary sphincters of bowel and bladder functions (Eisen et al., 1992; Kiernan et al., 2011). Of note the majority of patients die from respiratory failure arising from paralysis of intercostal muscles, or related complications (Haverkamp et al., 1995; Mitchell and Borasio, 2007; Valdmanis and Rouleau, 2008).

Although ALS causes both upper and lower motor neuron degeneration, symptoms often have a wide clinical spectrum with cases showing predominantly UMN or LMN signs (Burrell et al., 2011). The age of onset ranges extensively from about 14 to 90 years of age (Andersen et al., 1996; Gouveia and de Carvalho, 2007). Also disease duration is heterogeneous, indeed even though the majority of patients die within 2.5 years of onset there are about 15-20 % who survive past 5 years (Talbot, 2009) and rare cases exhibiting survival of over 40 years (Grohme et al., 2001). Interestingly a shorter disease progression has been found to correlate with advanced age and body mass at onset, bulbar onset, respiratory dysfunctions, and fast spread from the initial site of onset (Fujimura-Kiyono et al., 2011; Magnus et al., 2002; Traxinger et al., 2013).

1.1.2.2 Cognitive dysfunctions

ALS was initially considered a pure motor system disorder (Strong et al., 1996), but a component of cognitive impairment gradually became apparent. Recent studies confirmed that 51 % of ALS patients develop significant cognitive dysfunction presenting symptoms such as impaired memory and alteration in behaviour, abstract reasoning, problem solving and language comprehension (Zimmerman et al., 2007). Histological evidence and neuroimaging studies support clinical findings showing degeneration of neurons in extra-motor neuron areas (Neumann et al., 2006) and regional atrophy of the frontal and temporal lobes of the brain (Chang et al., 2005). Indeed about 15 % of ALS patients also present frontotemporal dementia (FTD), (Ringholz et al., 2005). These two disorders share pathological and genetic features, see section 1.1.7 (Giordana et al., 2011; Orr, 2011).

1.1.3 Diagnosis

To date there is no specific diagnostic laboratory test or clinical procedure to recognise ALS. Physicians establish the presence of the disease through a standard diagnostic protocol involving positive inclusion and negative exclusion criteria: The Revised El Escorial Criteria (Brooks et al., 2000). Inclusion criteria are evidence of signs of impairment of LMNs or UMNs confirmed by clinical examination, electrophysiological or neuropathological changes. Exclusion criteria are employed to reject the presence of pathological characteristics of other diseases that explain the degeneration of motor neurons (Table 1.1). Despite the establishment of these diagnostic criteria, incorrect diagnoses are still frequent. In addition, the combination of UMN and LMN symptoms may not be evident until a late point in the disease meaning that there is often a latency period between onset of symptoms and diagnosis.

Diagnostic level	Description
Clinically definite	Either UMN signs with LMN signs in the bulbar region plus two other signs, or UMN and LMN signs in 3 or more spinal regions
Clinically probable	UMN and LMN signs in 2 spinal cord regions with some UMN signs rostral to LMN signs
Clinically probable Laboratory supported	Either UMN and LMN signs in 1 region, or UMN signs with EMG defined LMN signs in 2 regions
Clinically possible	Either UMN and LMN signs in 1 or UMN signs in 2 or more regions, or LMN signs rostral to UMN signs
UMN signs for diagnosis	Spasticity, increased muscle tone and clonus, bilateral facial weakness affecting lower face and dysarthria
LMN signs for diagnosis	Muscle weakness, atrophy, fasciculation and flaccid dysarthria

Table 1.1 El Escorial diagnostic criteria for ALS. (EMG) electromyography. (Brooks et al., 2000; Economides et al., 2013; Kiernan et al., 2011; Ravits et al., 2007a; Wijesekera and Leigh, 2009).

1.1.4 Treatments

ALS is an incurable disease, despite the large number of clinical trials testing the effect of over 50 different compounds only one drug is available for the treatment of this neurodegenerative disorder, Riluzole, which can increase survival by 2-3 months

(Miller et al., 2012a; Turner, 2001). Thus to date the main method in the care of ALS patients consists of symptomatic treatment via a multidisciplinary approach covering physiotherapy, nutrition, respiration and pain management to help improve life quality (Kiernan et al., 2011; Miller et al., 2009a, 2009b, 2012b).

1.1.5 Environmental risk factors

Environmental factors such as exposure to toxins, solvents, pesticides, formaldehyde, smoking, exercise, infectious agents, and physical trauma have been associated with increased risk of developing ALS.

For example, the elevated rate of ALS reported for the indigenous population of Guam was postulated to be the consequence of exposure to the neurotoxic non-protein amino acid β -N-methylamino-L-alanine (BMAA). This neurotoxin present in the cycad seeds was assumed by people in Guam through the consumption of home-grown plants and animals (Khabazian et al., 2002; Lee, 2011; Shaw and Wilson, 2003). Although it was clear that the etiologic agent could be an environmental neurotoxin an eventual genetic contribution to disease could not be excluded. Also intense physical activity has been suspected of being an environmental factor in ALS. For instance, increased risk of ALS has been reported in Italian professional soccer players actively engaged between 1970 and 2001. However, the absence of ALS cases in professional road cyclists and basketball players suggests that ALS is not related to physical activity in general (Chio et al., 2009).

Despite many studies none has produced consistent and convincing evidence that environmental factors can cause ALS; therefore to date other than age, gender and family history no other non-genetic risk factor is associated with the disease (Al-Chalabi and Hardiman, 2013; Ingre et al., 2015).

1.1.6 ALS pathological features

1.1.6.1 Degeneration of motor neurons

The main neuropathological feature of ALS is the degeneration of both upper and lower motor neurons causing the denervation of skeletal muscles, see Figure 1.1 (Mendonça et al., 2005; Miki et al., 2010; Ota et al., 2005; Ravits et al., 2007b).

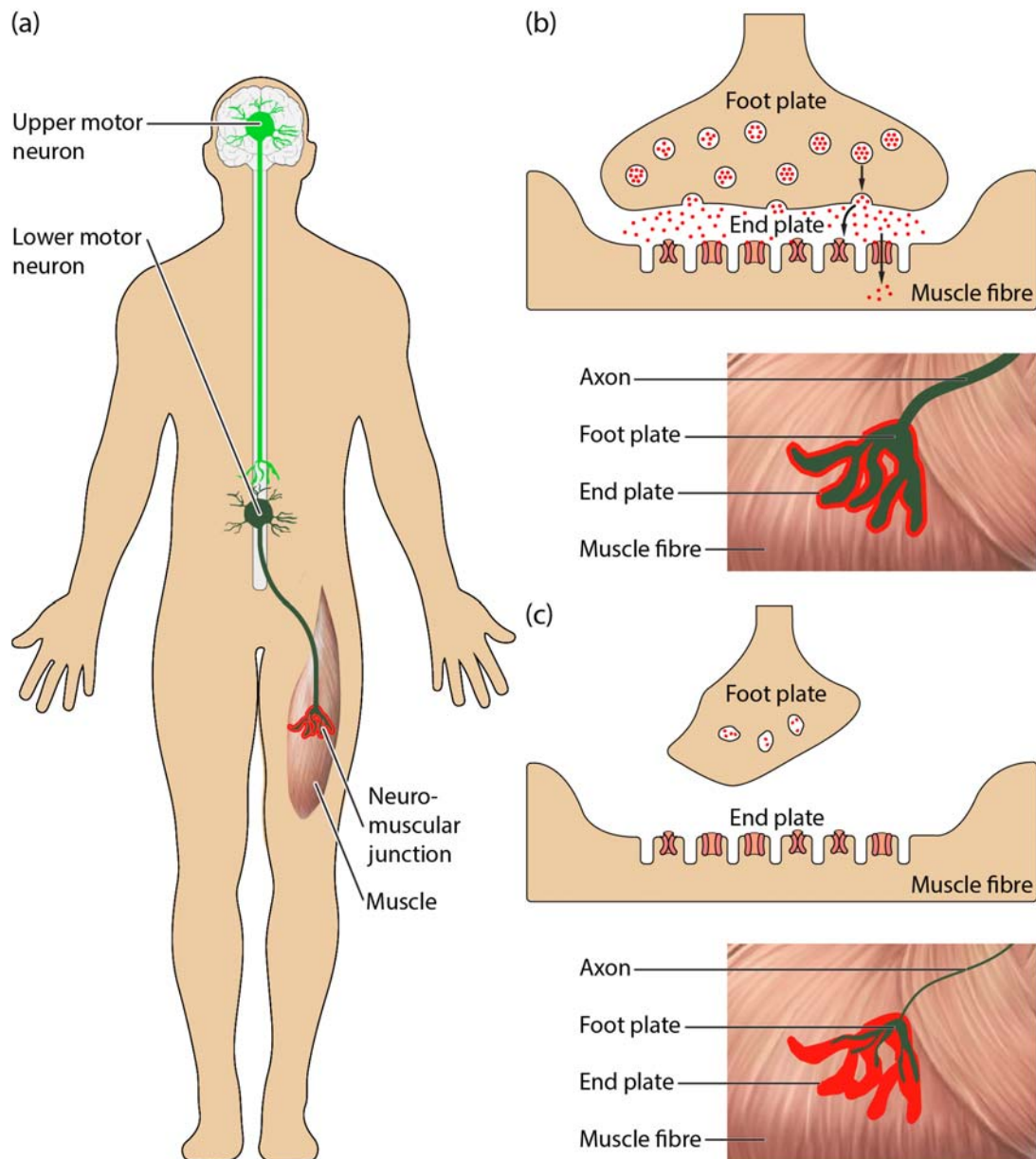


Figure 1.1 Impairment of the neuromuscular system in ALS. (a) Upper motor neurons (UMNs) are located in the motor cortex and their axons project down to the spinal cord where they form synapses with lower motor neurons (LMNs). The axons of LMNs project to the muscles forming synapses at the level of the neuromuscular junctions (NMJs). (b) In healthy individuals the motor cortex connects with the muscles through the MNs. At the muscle level each LMN axon branch innervates a single muscle fibre. The neurotransmitter acetylcholine (red dots) is released from the foot plate of the axon and received by nicotinic acetylcholine receptors located on end plate of the muscle fibre. In this case the NMJ, the foot plate and the end plate are closely aligned to ensure efficient signal transduction. (c) In a degenerating NMJ the foot plate and the axon degenerate progressively retracting and reducing the efficiency of signal between the axon terminal and the muscle, eventually losing contact.

The selective vulnerability of MNs to neurodegeneration might be explained by their structural and metabolic specialization. In humans MNs are typically large cells, with a

central body of approximately 50-60 μm and an axon of 1 m. To maintain such a large structure mitochondria have to meet high energy demands, consequentially increasing the production of reactive oxygen species (ROS) and therefore leaving the cell more prone to oxidative stress damages (Barber and Shaw, 2010). Moreover MNs have low levels of cytosolic calcium-binding proteins (CaBP) compared to other neuronal populations. The lack of CaBP, forces mitochondria to sequester calcium ions, triggering further an increase in ROS. In addition, MNs have low expression of the glutamate receptor 2 (GluR2) subunit of the Alpha-amino-3-hydroxy-5-methyl-4-isoxazolepropionic acid (AMPA) glutamate receptors, which imparts a high calcium permeability contributing once again to generate more ROS and ultimately to selectively damage MNs (Barber and Shaw, 2010; Jaiswal, 2014). Degeneration mostly takes place in the anterior and lateral columns of the spinal cord, but is evident also in the motor cortex and brain stem. Investigation of brain and spinal cord of ALS patients using magnetic resonance imaging (MRI) and diffusion tensor tomography techniques have shown an *in vivo* correlation between the severity of the atrophy and the clinical symptoms of the disease (Branco et al., 2014; Cohen-Adad et al., 2013; Schuster et al., 2013; Thorns et al., 2013). Furthermore post mortem LMN investigation has suggested that MNs loss is a contiguous process that progresses in parallel with the disease symptoms, with an average loss at end stage of 55 %, ranging from 8 % to 90 % (Ravits et al., 2007b).

1.1.6.2 Gliosis

Astrogliosis and microgliosis are hallmarks of ALS and they occur in the dorsal and ventral horns of the spinal cord (McGeer and McGeer, 2002; O'Reilly et al., 1995; Ota et al., 2005; Schiffer et al., 1996) and in motor and non-motor regions of the cortical grey matter (Kushner et al., 1991; Nagy et al., 1994; Sugiyama et al., 2013). The impairment within astrocytes and microglia has been suggested to accelerate disease progression, while intensity of microglial activation has been shown to correlate with the severity of MN damage (Lasiene and Yamanaka, 2011).

1.1.6.3 Inclusion bodies

A major pathological feature of ALS is the presence of cytoplasmic inclusions or aggregates in degenerating MNs and adjacent oligodendrocytes. Inclusions are present in the spinal cord, in the frontotemporal cortices, hippocampus and cerebellum of ALS patients (Al-Chalabi et al., 2012). The predominant inclusions found are ubiquitinated

aggregates that are classified either as Lewy body-like hyaline inclusions or skein-like inclusions, the first characterised by a round shape and the second characterised by bundles of filaments with granules. TDP-43 protein has been shown to be the major component of these ubiquitinated inclusions (Mackenzie et al., 2007; Nishihira et al., 2008), but also p62 immunoreactivity is present in these aggregates (Blokhuis et al., 2013; Leigh et al., 1991; Mizuno et al., 2006; Ota et al., 2005). Other neuropathological inclusions are: neurofilament heavy chain accumulations in spinal cord MN cell bodies and axons (Mendonça et al., 2005), phosphorylated neurofilament inclusions, often co-localising with ubiquitin (Takahashi et al., 1997; Troost et al., 1992), astrocytic hyaline-inclusions, similar to lewy-body-like hyaline but present in astrocytes (Kato et al., 1997) and Bunina bodies, small eosinophilic granules occasionally co-localising with TDP-43 (Miki et al., 2010; Ota et al., 2005). Of note hyaline inclusions containing SOD1 protein are found in ALS patients with SOD1 mutations (Shibata et al., 1996a), and present a fibrillar morphology reminiscent of the amyloid formation observed in many neurodegenerative diseases (Ross and Poirier, 2004).

1.1.6.4 Muscle atrophy

Atrophy of the muscles, due to loss of innervation of motor neurons is another important feature of ALS. In healthy individuals when motor neurons innervating a muscle bundle die the adjacent axons tend to re-innervate those muscle fibers exhibiting a non-random regrouping of muscle fiber type. However, it has been suggested that sprouting axons in ALS are unable to change fiber types of re-innervated muscle. In fact, ALS patients characteristically have an atrophic group containing mixed fiber types rather than a non-random regrouping muscle fiber type pattern (Baloh et al., 2007a; Daube et al., 2000).

1.1.7 Genetics of ALS

The majority of ALS cases are sporadic (sALS) since they lack a clear genetic component, however, a significant percentage are caused by inherited genetic mutations, termed familial ALS (fALS). The percentage of ALS patients with a family history has been appraised from a low 0.8 % up to 23 % of the ALS population; this might still be an underestimation since many cases labelled as sporadic might indeed be familial with a reduced disease penetrance (Andersen and Al-Chalabi, 2011). All genes found to be causative of fALS have also been found mutated in sALS patients. Moreover sALS and fALS are clinically indistinguishable in terms of disease

progression and neuropathology; but the average age of onset of fALS is approximately 10 years earlier than sALS (Andersen and Al-Chalabi, 2011; Siddique and Ajroud-Driss, 2011).

The first major breakthrough in understanding the genetic basis of ALS occurred in 1993, when Rosen and colleagues found that mutations in the superoxide dismutase 1 (*SOD1*) gene were causative of fALS (Rosen et al., 1993). To date over 160 *SOD1* mutations have been associated with ALS, variations in this gene account for about 12-24 % of fALS and for 2-7 % of sALS cases (Pasinelli and Brown, 2006; Renton et al., 2014; Valdmanis and Rouleau, 2008). Since the identification of *SOD1* other genes have been discovered to be causative of ALS; with varying levels of prevalence. The percentage of ALS explained by each gene in populations of European ancestry are reported in Table 1.2 and Figure 1.2 (Renton et al., 2014). Additionally several risk loci have been identified mainly on the basis of genome wide association studies (GWAS), and they have been predicted to be responsible for 60 % of the risk of developing ALS with the remaining 40 % being environmental (Al-Chalabi et al., 2010).

Of note the identification of an expanded hexanucleotide repeat in an intronic region of the uncharacterized gene *C9ORF72* strengthened the link between ALS and FTD. Normal individuals have at most 23 repeats while ALS or FTD patients can have up to several thousand of repeats (Rohrer et al., 2015). This pathogenic expansion repeats account for about 40 % of fALS cases, 7 % sALS cases, 25 % of familial FTD cases and 4 % of sporadic FTD cases (Andersen and Al-Chalabi, 2011; DeJesus-Hernandez et al., 2011; Gijssels et al., 2012; Renton et al., 2011). Indeed many of the ALS causative genes are mutated also in FTD, see Table 1.2. Moreover in some families individuals carrying these mutations may develop ALS or FTD or a combination of both diseases, reinforcing the hypothesis of a common genetic behind ALS and FTD (Orr, 2011).

In many cases mutations in a specific ALS causative gene can cause specific pathologies in patients. For example, *SOD1* protein aggregates are present in mutant *SOD1* cases (Kato et al., 2000). In a similar way mutation in *TDP-43* and *FUS* genes cause *TDP-43* and *FUS* protein to mislocalise into the cytoplasm (Blokhuis et al., 2013). While *C9orf72* repeat expansions are characterised by RNA aggregates and protein aggregates containing atypical products (Mackenzie et al., 2014).

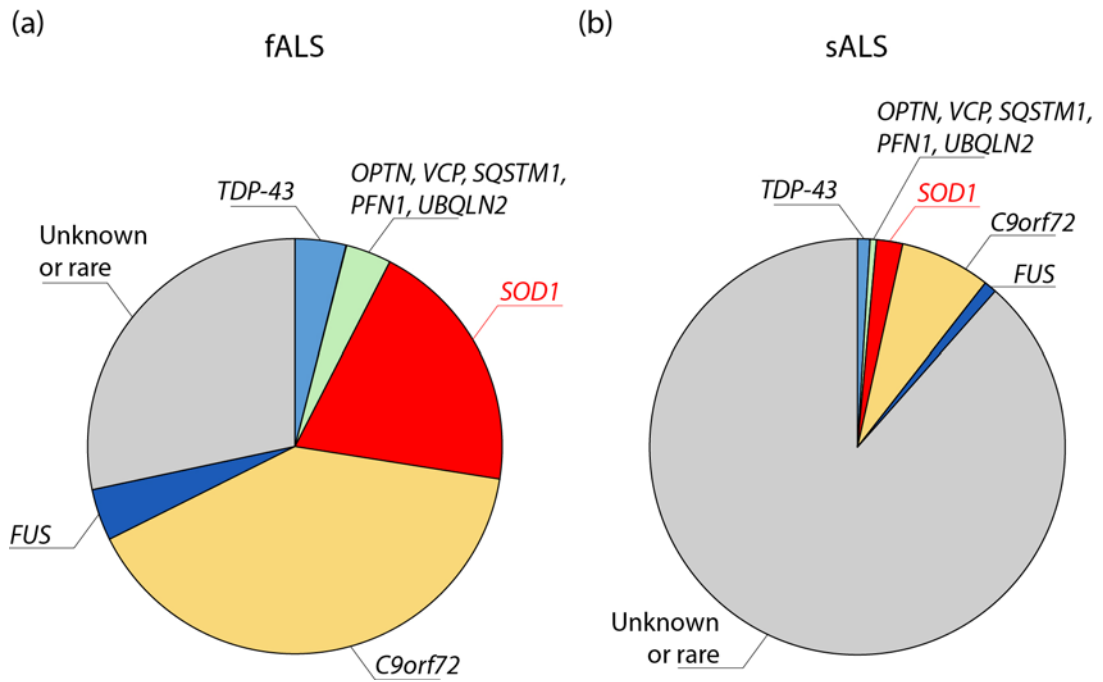


Figure 1.2 Percentage of sALS and fALS explained by each gene. (a) Percentage of fALS cases explained by the different genes: *C9orf72* = 40 %; *FUS* = 4 %; *SOD1* = 12 %; *TDP-43* = 4 %; *VCP* = 1 %; *SQSTM1* = 1 %; *OPTN*, *PFN1* and *UBQLN2* < 1 %. (b) Percentage of sALS cases explained by the different genes: *C9orf72* = 7 %; *FUS* = 1 %; *SOD1* = 1-2 %; *TDP-43* = 1%; *VCP* = 1 %; *SQSTM1*, *OPTN*, *PFN1* and *UBQLN2* < 1 %. Data according to Renton 2014, values are referred to populations of European ancestry (Renton et al., 2014).

Gene symbol	Gene name	Location	Inheritance	Frequency	Link to FTD	Putative function	References
	<i>Not identified (ALS3)</i>	18q21	AD	Rare	no	Unknown	(Hand et al., 2002)
	<i>Not identified (ALS7)</i>	20p13	AD	Rare	no	Unknown	(Sapp et al., 2003)
ALS2	<i>Alsin</i>	2q33.2	AR	Rare, juvenile	no	Endosomal trafficking and cell signalling	(Hadano et al., 2001)
ANG	<i>Angiogenin</i>	14q11.2	AD	Rare	yes	RNA processing	(Greenway et al., 2006)
ATXN2	<i>Ataxin 2</i>	12q24.12	AD	Rare	no	Endocytosis, RNA translation	(Elden et al., 2010)
C9orf72	<i>Chromosome 9 reading frame 72</i>	9p21-q22	AD	22.5-46 % fALS, 21 % sALS	yes	Homologue to guanine nucleotide exchange factor	(DeJesus-Hernandez et al., 2011; Levine et al., 2013)
CHMP2B	<i>Chromatin modifying protein 2B</i>	3p11	AD	Rare	yes	Vesicle trafficking	(Parkinson et al., 2006)
DAO	<i>d-amino acid oxidase</i>	12q24.11	AD	Rare	no	Glutamate excitotoxicity	(Mitchell et al., 2010)

Gene symbol	Gene name	Location	Inheritance	Frequency	Link to FTD	Putative function	References
FIG4	<i>Polyphosphoinositide phosphatase</i>	6q21	AD	Rare 1-2 % fALS	no	Endosomal trafficking and cell signalling	(Chow et al., 2009)
FUS	<i>Fused in sarcoma</i>	16q11.2	AD, AR, <i>de novo</i> mutation	4-5 % fALS juvenile	yes	RNA processing	(Kwiatkowski et al., 2009; Vance et al., 2009)
hnRNPA1	<i>Heterogenous nuclear ribonucleoprotein A1</i>	12q13.3	AD	Rare	no	RNA processing	(Kim et al., 2013)
OPTN	<i>Optineurin</i>	10p15-p14	AD and AR	Rare	no	Endosomal trafficking and cell signalling	(Maruyama et al., 2010)
PFN1	<i>Profilin 1</i>	17p13.2	AD	Rare	no	Cytoskeleton / transport	(Wu et al., 2012)
SETX	<i>Senataxin</i>	9q34	AD	Rare, juvenile	no	RNA processing	(Chen et al., 2004)
SIGMAR1	<i>σ Non opioid receptor 1</i>	9p13.3	AD and AR	Rare adult and juvenile	yes	Unknown	(Al-Saif et al., 2011; Luty et al., 2010)
SOD1	<i>Superoxide dismutase 1</i>	21q22.1	AD, AR, <i>de novo</i> mutation	20 % fALS 7 % sALS	no	Superoxide metabolism	(Rosen et al., 1993)

Gene symbol	Gene name	Location	Inheritance	Frequency	Link to FTD	Putative function	References
<i>SPG11</i>	<i>Spatacsin</i>	15q15-q21	AR	Rare, juvenile	no		(Orlacchio et al., 2010)
<i>SQSTM1</i>	<i>Sequestosome 1</i>	5q35	AD	1 % fALS	yes	Ubiquitination / autophagy	(Shimizu et al., 2013)
<i>TDP-43</i>	<i>TAR DNA-binding protein 43 (TDP-43)</i>	1p36.2	AD AR(rare)	5 % fALS	yes	RNA processing	(Sreedharan et al., 2008)
<i>UBQLN2</i>	<i>Ubiquilin 2</i>	Xp11	X-linked		yes		(Deng et al., 2011)
<i>VAPB</i>	<i>Vesicle-associated membrane protein-associated protein B</i>	20q13.3	AD	Rare	no	Endosomal trafficking and cell signalling	(Nishimura et al., 2004)
<i>VCP</i>	<i>Valosin-containing protein</i>	9p13-p12	AD	1 % fALS	yes	Ubiquitin / protein degradation	(Johnson et al., 2010)

Table 1.2 ALS associated genes. Autosomal dominant (AD); Autosomal recessive (AR).

1.2 SOD1-fALS

In 1993 Rosen and colleagues identified for the first time 11 missense mutations in the *SOD1* gene in 13 different fALS families (Rosen et al., 1993; Saccon et al., 2013). Since then over 160 SOD1 variants have been associated with ALS although pathogenicity has been confirmed only for 75 of them (Bunton-Stasyshyn et al., 2014)(ALS online Database (ALSoD) <http://alsod.iop.kcl.ac.uk/>).

1.2.1 Clinical course and pathogenicity of SOD1-fALS

The clinical course of SOD1-fALS is very similar to the one of SOD1-sALS regarding site of onset, progression and duration of the disease (Synofzik et al., 2010). Interestingly SOD1-fALS patients have been suggested to be less likely to develop cognitive deficits, nevertheless a low proportion SOD1-fALS families have been reported with cases of ALS-FTD (Battistini et al., 2005; Katz et al., 2012; Masè et al., 2001; Wicks et al., 2009). Of note the clinical phenotype deriving from the SOD1-fALS mutations can be very heterogeneous among patients, sometimes even between siblings of a single family (Ito et al., 2002).

Although mostly similar, the neuropathology of SOD1-fALS presents some differences compared to the one of non-SOD1-fALS and sALS. TDP-43 inclusions for example were thought to be absent in SOD1-fALS and have been used for a long time to discriminate between sporadic and familial SOD1-ALS cases (Mackenzie et al., 2007; Tan et al., 2007). However, recent studies reported TDP-43 pathology also in SOD1-fALS cases (Maekawa et al., 2009; Okamoto et al., 2011; Sumi et al., 2009). Bunina bodies are also thought to be absent in fALS (Nakamura et al., 2014; Shibata et al., 1996a; Tan et al., 2007) while neuronal and astrocytic SOD1 inclusions are ubiquitously expressed in SOD1-fALS but often absent in sALS and non-SOD1-fALS (Bruijn et al., 1998; Hinenno et al., 2012; Kato et al., 1996, 2000, 2001; Shibata et al., 1996a, 1996b).

1.2.2 *SOD1* gene and inheritance pattern

The *SOD1* gene, which encodes Cu/Zn superoxide dismutase 1, is located on human chromosome 21q22.11 and is 9,310 base pairs (bp) long (Wang et al., 2006; Wulfsberg et al., 1983). The gene is composed of 5 exons and is transcribed into 966 bp mRNA transcript (Figure 1.3) which encodes a 154 amino acid metalloenzyme, (described in section 1.3, Figure 1.4) (Wang et al., 2006).

Mutations in *SOD1* are scattered throughout the coding sequence of the gene and they are mainly missense substitutions. However there are also deletions, insertions, mutations in the non-coding areas of the gene and silent point mutations (Birve et al., 2010; Hu et al., 2012; Turner and Talbot, 2008; Valdmanis et al., 2009; Zinman et al., 2009; Zu et al., 1997). All *SOD1* mutations are associated with a dominant inheritance pattern with few exceptions such as N86S and D90A, which also behave as recessive traits (Andersen and Al-Chalabi, 2011; Turner and Talbot, 2008). The D90A mutation has also been found in association with D96N in recessive fALS (Hand et al., 2001), and as a neutral polymorphism in unaffected Scandinavian people (Turner and Talbot, 2008). Some mutations are found more frequently in populations than others for example, the D90A mutation is the most common worldwide, the A4V is the most common in the USA (Turner and Talbot, 2008), while I113T is the most common in the UK (Orrell et al., 1999). Mutations in the *SOD1* gene are thought to cause ALS through a still unknown toxic gain of function, even though the majority of the *SOD1*-fALS mutations reduce the activity of the *SOD1* protein in patients, see section 3.3.1 (Saccon et al., 2013). The effect of these mutations on the biological function of the *SOD1* protein will be discussed later in section 1.5.

A range of transcription factor binding sites have been identified for the *SOD1* gene, located between -1,200 and +1 bp from the transcriptional start site (Miao and St Clair, 2009; Park and Rho, 2002; Romanuik et al., 2009; Yoo et al., 1999a, 1999b). Further 2 functional transcripts with a different 3' untranslated region (UTR) have also been describe (Kilk et al., 1995; Sherman et al., 1983).

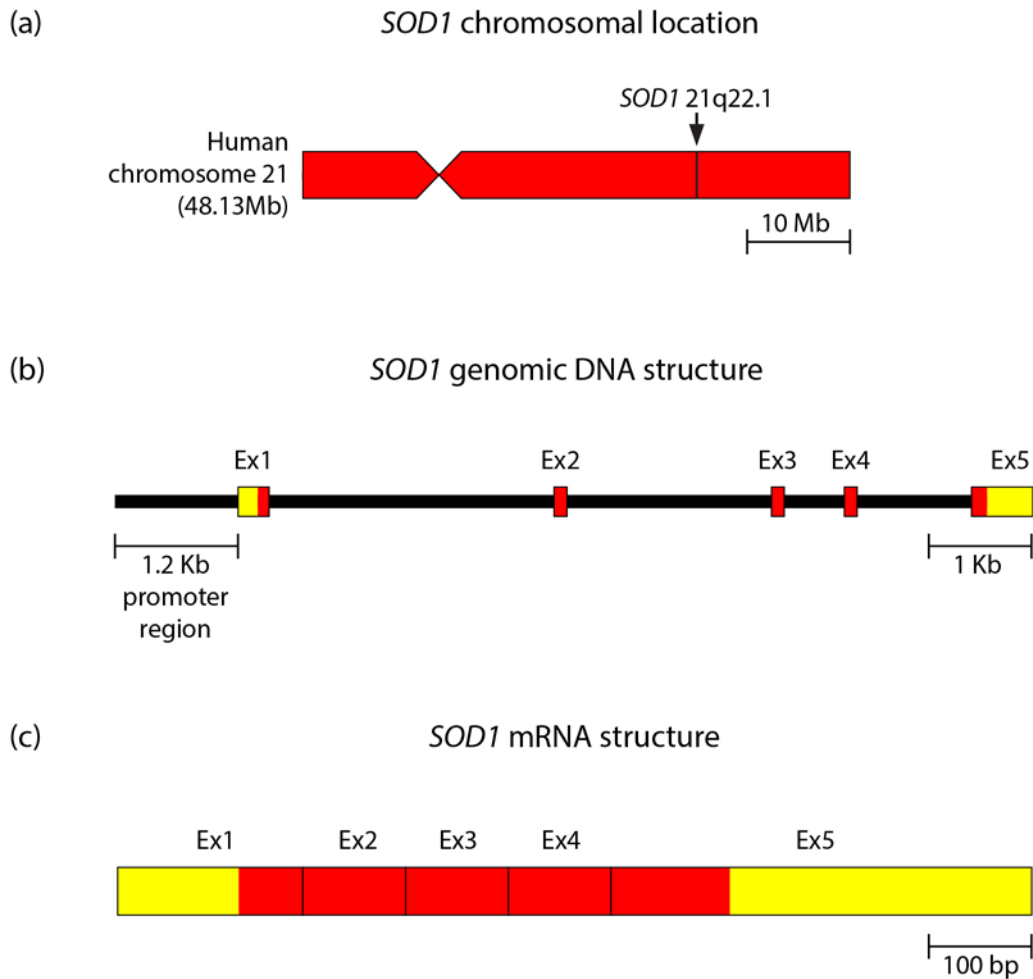


Figure 1.3 Human *SOD1* gene chromosomal location, DNA and mRNA structure. (a) Location of the human *SOD1* gene on chromosome 21. (b) *SOD1* gene structure. The gene is 9,310 bp long, including a 1.2 kb upstream encompassing the promoter region. Exons are labelled in red, introns in black and UTRs in yellow. (c) *SOD1* mRNA is 966 bp. Coding regions are labelled in red and UTRs in yellow.

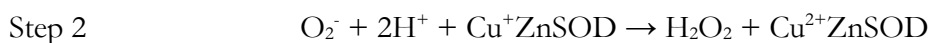
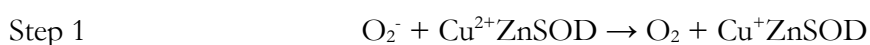
1.3 *SOD1* protein

SOD1 is an abundant copper and zinc containing protein ubiquitously expressed in all cell types, particularly abundant in the motor neurons of the spinal cord (Bordo et al., 1994; Lindenau et al., 2000). Protein expression levels *in vivo* are stable within tissues and across time independently from environmental factors (Miao and St Clair, 2009; Radyuk et al., 2004). This metalloenzyme is highly conserved across species (Fridovich, 1995), indeed 73 % of the amino acid sequence is shared across mammals (Wang et al., 2006). Within the cell, *SOD1* localises in the cytoplasm, nucleus, lysosomes and inter-membrane space of mitochondria (Chang et al., 1988; Crapo et al., 1992; Kawamata and Manfredi, 2010; Keller et al., 1991; Sturtz et al., 2001).

1.3.1 Biological function

SOD1 is an antioxidant enzyme and its main canonical function consists in the catalysis and conversion of toxic superoxide anions (O_2^-) to molecular oxygen (O_2) and hydrogen peroxide (H_2O_2), thus providing a defence against oxygen toxicity (Zelko et al., 2002).

The dismutase of O_2^- is a two-step process. First one molecule of O_2^- reduces the cupric ion ($Cu^{2+}ZnSOD$) to form O_2 , then a second molecule of O_2^- reoxidise the reduced cupric ion (Cu^+ZnSOD) to form H_2O_2 . This two-step reaction has been shown to work in a pH range of 5.0 to 9.5 (Valentine et al., 2005).



Another role for SOD1 in cellular metabolism has been recently identified by Reddi and Culotta, using yeast and human cell lines. In the mechanism proposed SOD1 is thought to act as an O_2 and glucose dependent regulator of respiration through stabilisation of casein kinase 1-gamma ($CK1\gamma$), via hydrogen peroxide (Bunton-Stasyshyn et al., 2014; Reddi and Culotta, 2013). SOD1 has also been suggested to work as a molecular switch that initiate endoplasmic reticulum (ER) stress in conditions of zinc deficiency. In particular the dissociation of zinc from wild-type SOD1 during zinc depletion induces a mutant-like conformation change that exposes the binding site for Derlin-1, a component of the ER-associated degradation machinery. The SOD1-Derlin-1 interaction has been proposed to activate homeostatic ER stress by triggering the unfolded protein response (UPR) and consequently preventing the accumulation of misfolded proteins (Homma et al., 2013). Furthermore mutant SOD1 has been proposed to activate ER stress by disrupting ER-Golgi trafficking through binding to the coatamer coat protein II (COPII) (Atkin et al., 2008; Bunton-Stasyshyn et al., 2014). Recent studies have suggested a potential role for SOD1 in nucleic acid metabolism; SOD1 might be able to control transcription by binding to nuclear promoters to regulate oxidative resistance genes (Hu et al., 2012; Tsang et al., 2014).

The SOD1 protein is produced at high levels and represents about 1 % of all cytoplasmic proteins in the cell. The functions described above do not account for

such a big quantity of SOD1, therefore it is likely that this protein plays other roles in the cellular metabolism that have not yet been identified (Bunton-Stasyshyn et al., 2014; Milani et al., 2013).

1.3.2 Structural features and protein stability

The human SOD1 protein functions as a 32 kDa homodimer, and as mentioned before has a highly conserved structure. Each monomer contains an intrasubunit disulphide bond (S-S), one copper (Cu^{2+}) and one zinc (Zn^{2+}). When the protein is metal loaded the copper and the zinc ions are located in close proximity and share an imidazole ligand, histidine 63 (His63) (Figure 1.4); their bond is further stabilised by a network of hydrogen bonds. Each subunit is made of an 8-stranded β -barrel connected by loops, and 1 helical structure in residues 134-137 (Figure 1.4 (b)). The two largest loops are particularly important for the correct function of the enzyme: the metal binding loop (residues 49-84) and the electrostatic loop (residues 122-143) (Rakhit et al., 2007). The disulphide bond is linked between two cysteine residues: cysteine 57 (Cys57) and cysteine 146 (Cys146) (Figure 1.4). The two monomers are connected by hydrophobic interactions, water mediated hydrogen bonding and main chain to main chain hydrogen bonding between the monomers (Elam et al., 2003).

Metallated SOD1 has been reported to be one of the most stable proteins in nature (Rakhit et al., 2007), in particular the intrasubunit S-S bond and the zinc ion act as a monodentate ligand contributing to protein stability. SOD1 when fully metallated has a melting temperature of 85-95 °C, and does not lose its enzymatically active in 8 M urea or in 1 % SDS or 4 M guanidine HCl (Rakhit and Chakrabartty, 2006; Rodriguez et al., 2002). However, SOD1 loses its stability and becomes intrinsically disordered when in the apo- and disulfide reduced forms (Rodriguez et al., 2005). Evidence from *in vitro* and *in vivo* experiments using non-metallated forms of SOD1 have suggested that a mixture of SOD1 species with varying degrees of metallation exists in cells and that instability caused by metal-deficiency can be a mechanism through which SOD1 mutations cause the disease (Hilton et al., 2015).

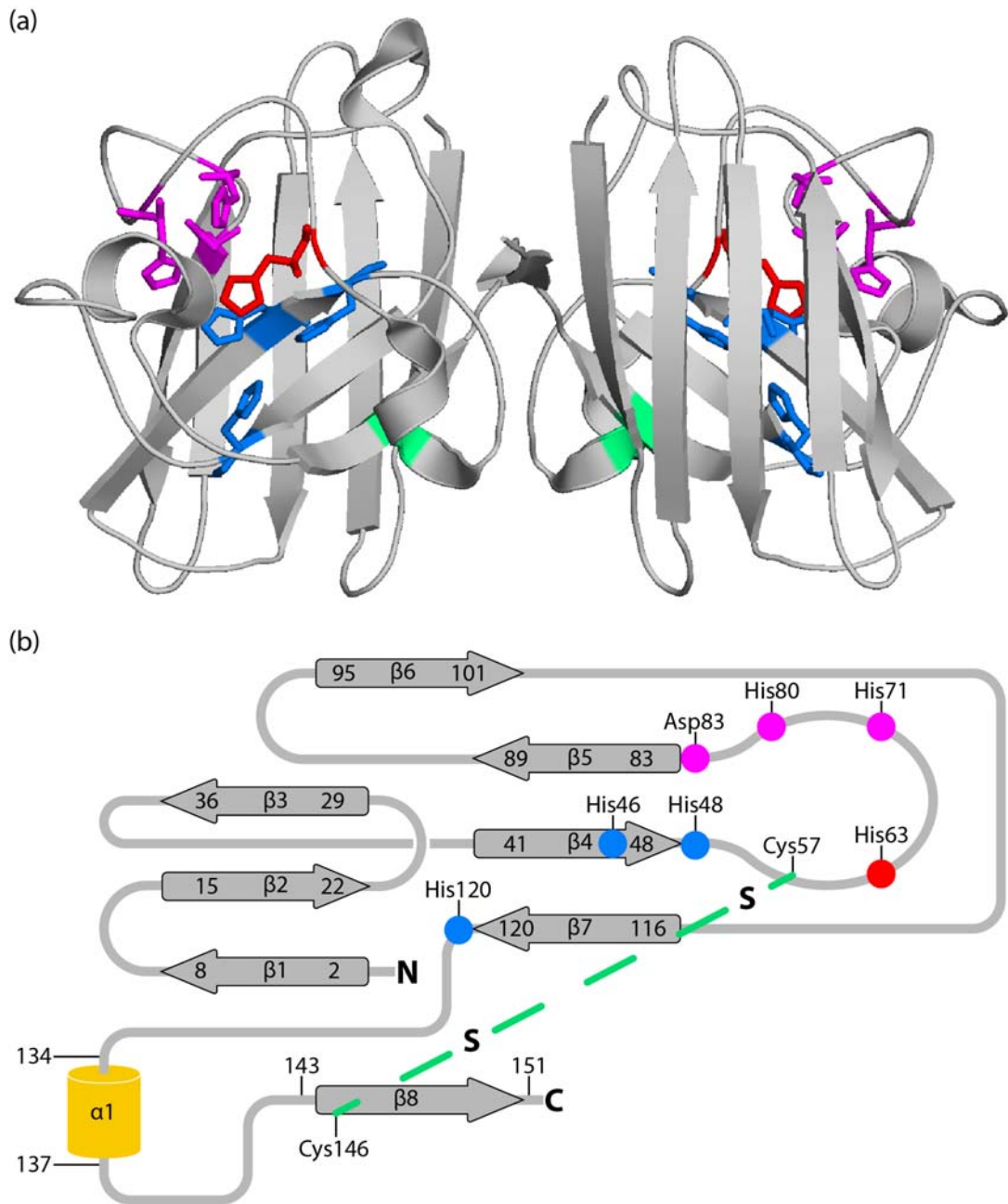


Figure 1.4 Human SOD1 protein structure. (a) 3-dimensional structure of dimeric SOD1. Residue His63 is involved both in copper and zinc binding (red); His71, His80 and Asp83 are involved in zinc binding (purple); His46, His48 and His120 are involved in copper binding (blue). Cysteine 57 and 146 form the disulfide bond (green). (b) Secondary structure elements of SOD1. The 8 β -strands are represented as arrows and numbered, the α -helix (α 1) that forms copper and zinc binding is shown in yellow. His63 is labelled in red, residues involved in zinc binding in purple and residues involved in copper binding in blue. The disulphide bond is highlighted as a green dotted line.

1.3.3 Properties of mutant SOD1 proteins

1.3.3.1 Effect of mutations on protein function

Since their first discovery in 1993 mutations in the *SOD1* gene are known to reduce the dismutase activity of the SOD1 protein. Initially it was hypothesised that this reduction in enzymatic activity was the mechanism through which SOD1 mutations were causing the disease. Subsequent findings carried out on mouse models soon dismissed that theory, and suggested that the disease is caused by a toxic gain of function (reviewed in chapter 3).

A study carried out in HEK cells transfected with 132 flag-SOD1 variants showed that 124 SOD1-ALS mutations have an exposed Derlin-1 binding site that is blocked in the wild-type protein (Fujisawa et al., 2012), suggesting that pathogenic SOD1 mutations may induce a common conformational change in SOD1 that leads to motor neuron toxicity through ER-stress activation (Fujisawa et al., 2012; Homma et al., 2013). Primary spinal MN culture experiments reinforced this hypothesis (Nishitoh et al., 2008). However, even though a Derlin-1 and mutant SOD1 CNS specific interaction have been shown in a transgenic SOD1-fALS mouse models, to date the functional consequence of this interaction has not yet been demonstrated outside of cell culture (Nishitoh et al., 2008). Further Derlin-1 has never been identified in screens for SOD1 interactors in SOD1-fALS mice (Watanabe et al., 2008; Zetterström et al., 2011).

Mutations of specific residues in the copper binding region have been shown to block SOD1 activity, and they might influence the role of SOD1 in respiration repression described by Reddi and Culotta (Reddi and Culotta, 2013).

1.3.3.2 Effect of mutations on SOD1 biochemical properties

Biophysical studies of mutant SOD1 investigating protein activity, metal content and spectroscopy, allowed the classification of these mutants into 2 main groups depending on their similarity with the wild-type SOD1 protein (Rodriguez et al., 2002). Mutants SOD1 with reduced activity and reduced protein stability are classified as metal-binding-region (MBR) since typically their mutations are located in the region close to zinc and copper ions. Variants that are shown to behave similarly to wild-type SOD1 are defined as wild-type-like (WTL) and typically their mutations are located away from the metal binding site (Rodriguez et al., 2002; Valentine et al., 2005). Table 1.3 shows

the classification of fALS mutant SOD1 proteins investigated in the present work, according to Valentine (2005).

WTL	MBR
G93A	D83G
D101G	
I113T	

Table 1.3 Classification of mutant SOD1 proteins to WTL and MBR categories. Mutant proteins employed in this thesis, are listed under one of the two groups WTL (wild-type-like) or MBR (metal-binding-region), (Valentine et al., 2005).

In vivo and *in vitro* studies trying to correlate disease severity with activity of enzyme, half-life, proteolysis resistance, mutation position, protein charge and aggregation propensity have not produce convincing results (Lindberg et al., 2002; Prudencio et al., 2009a; Ratovitski et al., 1999; Vassall et al., 2011). However some biophysical and biochemical properties of SOD1 mutations that have been shown to differ significantly from wild-type SOD1 are listed below:

- Resistance to proteinase K digestion: MBR mutants are more easily digested than WTL mutants (Ratovitski et al., 1999).
- Thermal stability: generally all SOD1 mutants show a reduction in thermal stability, but there is only a slight reduction in WTL mutants compared to a significant reduction in MBR mutants (Rodriguez et al., 2002). Furthermore a correlation between decreased disease duration and decreased thermal stability has been shown for a small number of MBR mutants (Kitamura et al., 2011; Lindberg et al., 2002).
- Sensitivity to disulfide reduction: MBR mutants are more susceptible to S-S reduction compared to WTL mutants and wild-type SOD1 (Rodriguez et al., 2005).
- Protein half-life: protein half-life did not correlate to whether mutations were MBR or WTL type, although generally SOD1 mutants had shorter half-lives than wild-type SOD1, correlating with protein stability (Sato et al., 2005). Further cell studies have shown that some MBR mutants with markedly

reduced stability have a comparable half-life to wild-type SOD1 (Borchelt et al., 1994; Ratovitski et al., 1999; Reaume et al., 1996).

- Degree of hydrophobic exposure: SOD1 mutants have a greater exposure of hydrophobic areas than wild-type SOD1 (Rakhit et al., 2002; Rodriguez et al., 2005).
- Net charge of protein: net charge of protein at physiological pH varies in different SOD1 mutants, independently of whether mutations are MBR or WTL type. A reduction in net charge of SOD1 mutants is likely to increase their propensity to aggregate especially in cellular environment of low and fluctuating pH, as would be found in the lysosomes and in the intermembrane space of the mitochondria (Lindberg et al., 2005).
- Dimer dissociation: SOD1 monomers have been identified as a common misfolding intermediate both in sporadic and familial SOD1-ALS (Rakhit et al., 2004). SOD1 dimer dissociation is a key step in aggregation and occurs due to mutations, glutathionylation and cellular stress. In particular SOD1 mutations located in the inter-subunit cleft are able to disrupt the dimer interface leading to more facile dissociation. Recently a link between the propensity of mutant SOD1 to monomerise and disease severity has been suggested specifically, when glutathionylation of SOD1 is taken into consideration (McAlary et al., 2013).

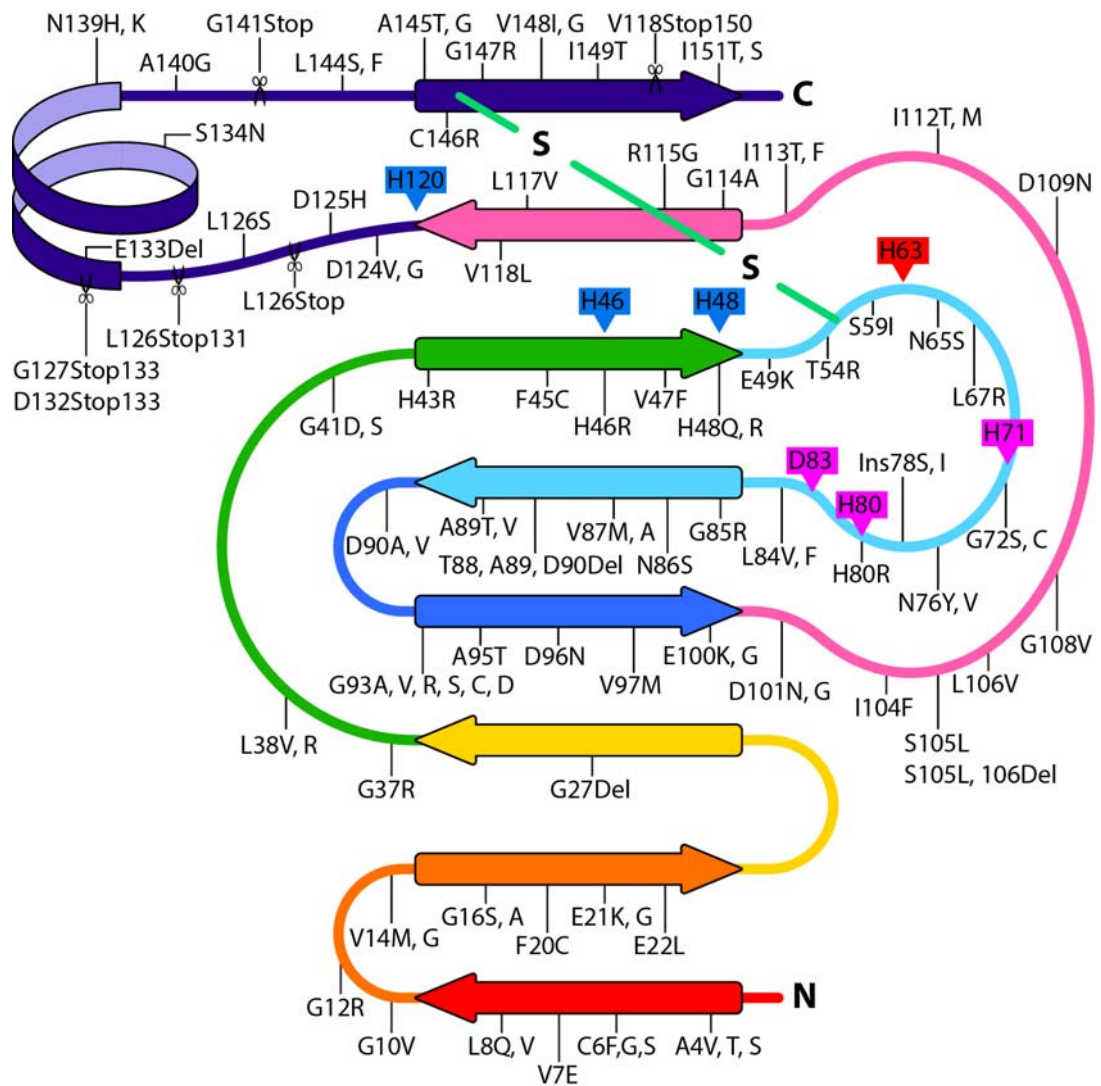


Figure 1.5 Human SOD1 secondary structure and mutations responsible for fALS. The 8 β -strands are represented as arrows, the α -helix that forms copper and zinc binding is in blue. His63 is labelled in red, residues involved in zinc binding in purple and residues involved in copper binding in blue. The disulphide bond is highlighted as a green dotted line. Mutations known to be causative of fALS are reported along the secondary structure of the protein. In the nomenclature, for amino acid substitutions the first letter indicates the residue in the wild-type form of the protein, the number indicates the amino acid position and the second letter the new residue. For example, D83G is a substitution of an asparagine for a glycine in position 83. Point mutations, deletions and insertions are indicated with a line, while mutations that cause a C-terminal truncation are illustrated with a scissor. Modified from (Valentine et al., 2005).

1.4 SOD1 mouse models

1.4.1 Why we use mouse models in ALS research

Mice are one of the most widely used model organisms in research. Indeed it is currently the most genetically tractable and cheap mammalian model (Huang et al., 2011; Niu et al., 2014). The mouse genome has been sequenced and it is 14 % smaller compared to humans; at the nucleotide level approximately 40 % of the human genome can be aligned to the mouse genome (Waterston et al., 2002). Mice were the first species in which an exogenous genetic sequence was introduced (Jaenisch and Mintz, 1974) and also the first species with embryonic stem cells (ESC) cultured *in vitro* (Evans and Kaufman, 1981; Martin, 1981). Both these techniques and many others lead to the creation of important mouse models and currently over 2,252 human diseases have at least one mouse model available (www.informatics.jax.org September 2015).

In the study of the nervous system mice are preferentially employed compared to other models such as the fruit fly or zebrafish, because they are genetically and physiologically more similar to humans. ALS research makes no exception and mice are the most widely employed model organism (Gurney et al., 1994). However, also rats (Howland et al., 2002), zebrafish (Lemmens et al., 2007), fruit flies (Mizielinska et al., 2014; Phillips et al., 1995), and nematodes (Oeda et al., 2001) are used to investigate this disease. A small amount of research has also been carried out in horses and dogs specifically regarding the SOD1 mutation (Coates and Wininger, 2010; de la Rúa-Domènech et al., 1996; Zeng et al., 2014).

1.4.1.1 Mouse models of SOD1-ALS

Since the identification of *SOD1* as a causative gene of fALS (Rosen et al., 1993), several different types of mouse model have been generated to investigate SOD1 mutations. From transgenic mouse models overexpressing either the human mutant or the wild-type SOD1 protein, to *Sod1* knockout models and also mice overexpressing the mouse SOD1 protein. Several experimental crosses have also been carried out using these animals to further elucidate the role of SOD1 in ALS. Some of these mouse models relevant to the present work are described below, details of other important lines are reported in the relevant chapters.

1.4.2 SOD1 transgenic mice

The first mouse expressing the human mutant *SOD1* transgene was presented in 1994 by Gurney and colleagues. Since then a great number of transgenic SOD1 mice have been produced, including mice expressing tagged proteins, experimental mutations, conditional/inducible lines, and one model overexpressing the mouse SOD1 (Deng et al., 2008; Pramatarova et al., 2001; Ripps et al., 1995; Wang, 2003; Watanabe et al., 2005). A comprehensive list of all these transgenic animals is reported in Table 8.1 of Appendix 8.1.

Almost all these transgenic SOD1 mouse lines, share similar behavioural phenotypes, disease progression patterns and neuropathological characteristics resembling of the pathology seen in ALS patients. However, they have different ages of onset and survival times which often correlate with the level of transgene expression or with the number of copies in the transgene array (Gurney et al., 1994; Tu et al., 1996; Watanabe et al., 2005; Wong et al., 1995).

Three SOD1 transgenic mouse lines have been employed in the present work: two overexpressing the mutant SOD1 G93A mutation at different levels, referred to as transgenic SOD1 G93A high copy (Tg*SOD1*^{G93A(H)}) (Chiu et al., 1995) and low copy (Tg*SOD1*^{G93A(L)}) (Zhang et al., 1997) and one overexpressing the human wild-type SOD1 protein (Tg*SOD1*^{WT}) (Gurney et al., 1994). Tg*SOD1*^{G93A(H)} and Tg*SOD1*^{WT} lines have been used through the whole thesis and are described here, while the Tg*SOD1*^{G93A(L)} line has been specifically employed for one project and is described in section 6.1.3.

1.4.2.1 Transgenic *SOD1*^{G93A} high copy mice

In 1994 Gurney and colleagues established for the first time four transgenic SOD1 mouse lines carrying the G93A mutation (Gurney et al., 1994). The mouse line employed in the present work, Tg(SOD1*G93A)1Gur, referred in the text as Tg*SOD1*^{G93A(H)}, derives from one of these original lines but has 40 % expansion resulting in 25 copies in the transgene array (Chiu et al., 1995). The transgene integration site has been mapped to band E of mouse chromosome 12 (Achilli et al., 2005).

The TgSOD1^{G93A(H)} line was originally maintained and described in a C57BL6-SJL background (Chiu et al., 1995). TgSOD1^{G93A(H)} mice are characterised by a gradual loss of body weight starting at approximately 10 week of age. Signs of motor disturbance typically starts at 13 weeks usually in the form of tremors in one or more limbs. Similarly to ALS patients these animals develop muscle weakness and atrophy along with symptoms such as spasticity, limb-grasping and clonus. With the progressive loss of strength in the hind limbs mice display a dropped pelvis and typically drag the body using the forelimbs. According to Chiu and colleagues (1995) mice reached the humane end point at 136 days of age, which was defined as 10 % loss of body weight or inability to right themselves within 30 seconds when placed on their side.

Electrophysiological studies confirmed the behavioural data describe above showing a loss of muscle strength from 40 days of age, compatible with a pattern of preferential loss of larger MNs innervating faster muscle fibres (Hegedus et al., 2007, 2008).

Further pathological studies revealed that, as occurs in ALS patients, these mice have a progressive loss of MNs starting at 100 days of age. In particular by end stage a 50 % loss of MNs is detected in the spinal cord (Chiu et al., 1995; Fischer et al., 2004; Gould et al., 2006). Vacuolation has been observed in the MNs of the spinal cord from 80 days of age and also in the mitochondria, which appear abnormal (Dal Canto and Gurney, 1994; Fischer et al., 2004). Events of denervation and reinnervation of skeletal muscles are detected from 47 days of age, moreover evidence of axonal degeneration is present in ventral roots from 80 days of age (Chiu et al., 1995; Fischer et al., 2004). Astrocytosis is also apparent in the spinal cord from 82 days of age (Tu et al., 1996). Several types of inclusion are detectable from an early stage for example spheroid neurofilament inclusions are visible in swollen axons of the ventral spinal cord from 82 days of age, (Gurney et al., 1994; Tu et al., 1996). There are also SOD1 inclusions, particularly in the MNs' ventral horn (Gurney et al., 1994) and p62 and ubiquitin aggregates, which have all been shown to co-localise by 120 days (Gal et al., 2007). Typically TDP-43 pathology is absent in this mouse line (Robertson et al., 2007), however TDP-43 mislocalisation has been reported once at end stage (Shan et al., 2009).

1.4.2.2 Transgenic *SOD1^{WT}* mice

Three wild-type SOD1 transgenic lines were generated together with the first G93A mutant SOD1 transgenic line by Gurney and colleagues in 1994 and one of them is employed in the present work: Tg(SOD1)2Gur, referred in text as Tg*SOD1^{WT}*. This line is thought to carry 7 copies of the SOD1 human wild-type transgene, and is typically used as control of the Tg*SOD1^{G93A(H)}* line since it has comparable levels of SOD1 protein expression and activity (Tu et al., 1996), even though not all studies agree (Jaarsma et al., 2000).

Initially the Tg*SOD1^{WT}* line was thought to be free from motor deficits (Chiu et al., 1995; Tu et al., 1996), but further phenotypic investigation revealed mild deficits from 58 week of age (Jaarsma et al., 2000).

Histological studies showed abundant SOD1 staining in the lateral ventral horn and throughout the spinal cord of the Tg*SOD1^{WT}* mice (Gurney et al., 1994). In particular at an early stage SOD1 staining is homogeneously distributed but from 30 weeks of age it appears enriched within the MNs' axons (Jaarsma et al., 2000). Further SOD1 inclusions are detected in MNs from 86 week of age (Jonsson et al., 2006a), and axonal degeneration and vacuolation are seen from 30-35 weeks of age, however, denervation or reinnervation events are never detected at this stage (Chiu et al., 1995; Dal Canto and Gurney, 1995; Jaarsma et al., 2000). Several other pathologies similar to those seen in Tg*SOD1^{G93A(H)}* mice, have been reported, but with milder characteristics and at a later point in life. Neurofilament and mitochondrial pathology are present and occur at a later age, for example neurofilament pathology is seen at 18.6 weeks rather than 11.7 (Dal Canto and Gurney, 1995; Jaarsma et al., 2000; Tu et al., 1996). The same happens for gliosis, MN vacuolation and MN degeneration (Jaarsma et al., 2000; Tu et al., 1996).

Of note, Graffmo and colleagues have recently investigated homozygous Tg*SOD1^{WT}* mice on a different background, due to failure to produce homozygotes in the original C57BL/6J background. Interestingly the same phenotype described for the Tg*SOD1^{G93A(H)}* mice has been reported but with a longer time scale. These mice show hind limb paralysis from 36 weeks, end stage at 52 weeks, presence of misfolded SOD1 and astrocytosis in the spinal cord and 40 % MNs loss at end stage (Graffmo et al., 2013).

1.4.3 *Sod1* knock out mice

Sod1 knockout mice are not considered a model of ALS since they do not develop typical disease phenotypes such as paralysis, loss of motor neuron or premature death (Saccon et al., 2013). Nonetheless these mice develop a series of ALS-like phenotypes and they have been extensively employed in the study of ALS. Furthermore they have been extremely helpful in the investigation of the role that a SOD1 loss of function might play in the disease. The *Sod1* knockout mice are described in Chapter 3 section 3.3.2.

Of note the mouse *Sod1* gene is located in mouse chromosome 16, is composed of 5 exons and is 5581 bp long. The mouse *Sod1* mRNA is 116 bp. Despite some difference in the gene compared to the human *SOD1* gene, the mouse *Sod1* encodes for a protein of 154 amino acid, very similar to the human homologues.

1.4.4 Effect of background on mouse phenotypes

Inbred mouse strain are often employed in research to isolate the effects of a particular mutation since they allow the minimisation of background genetic heterogeneity.

Several inbred strains have been employed in ALS research and since the phenotypes of a specific mutation can change depending on the background in which mice are bred, it is important to consider it when comparing results. Further, since genetic variability can result in phenotypic variations it is important to conduct characterisation studies using pure inbred or congenic lines. Congenic lines are obtained by backcrossing a donor line to a recipient inbred line for 10 generations. The result of such backcross is a ~99.8 % homozygous loci for the recipient allele (Acevedo-Arozena et al., 2008).

An example of a phenotypic change modulated by the background strain comes from Tg*SOD1*^{G93A(H)} mice. Indeed the time of end stage of these animals was found to be significantly different between mice kept on a C57BL/6J or on a C57B6-SJL background (Mead et al., 2011). Variance among background strains of Tg*SOD1*^{G93A(H)} mice was observed also for other factors, such as onset, disease progression and response to drugs (Mancuso et al., 2012; Nardo et al., 2013; Pan et al., 2012; Pizzasegola et al., 2009; Wooley et al., 2005). It is also important to note that variability among publications might be also due to different humane end points or inconsistency

of transgene copy number. Survival variability of Tg*SOD1*^{G93A(H)} mice in different backgrounds is reported in Figure 1.6.

Specific background strains have also been documented to increase gender differences in survival, onset and also behavioural tests such as grip-strength, both in Tg*SOD1*^{G93A(H)} and Tg*SOD1*^{G93A(L)} mice (Acevedo-Aroza et al., 2011; Heiman-Patterson et al., 2005; Mancuso et al., 2012; Pan et al., 2012). The same pattern has also been reported for other SOD1 transgenes (Kunst et al., 2000; Pan et al., 2012).

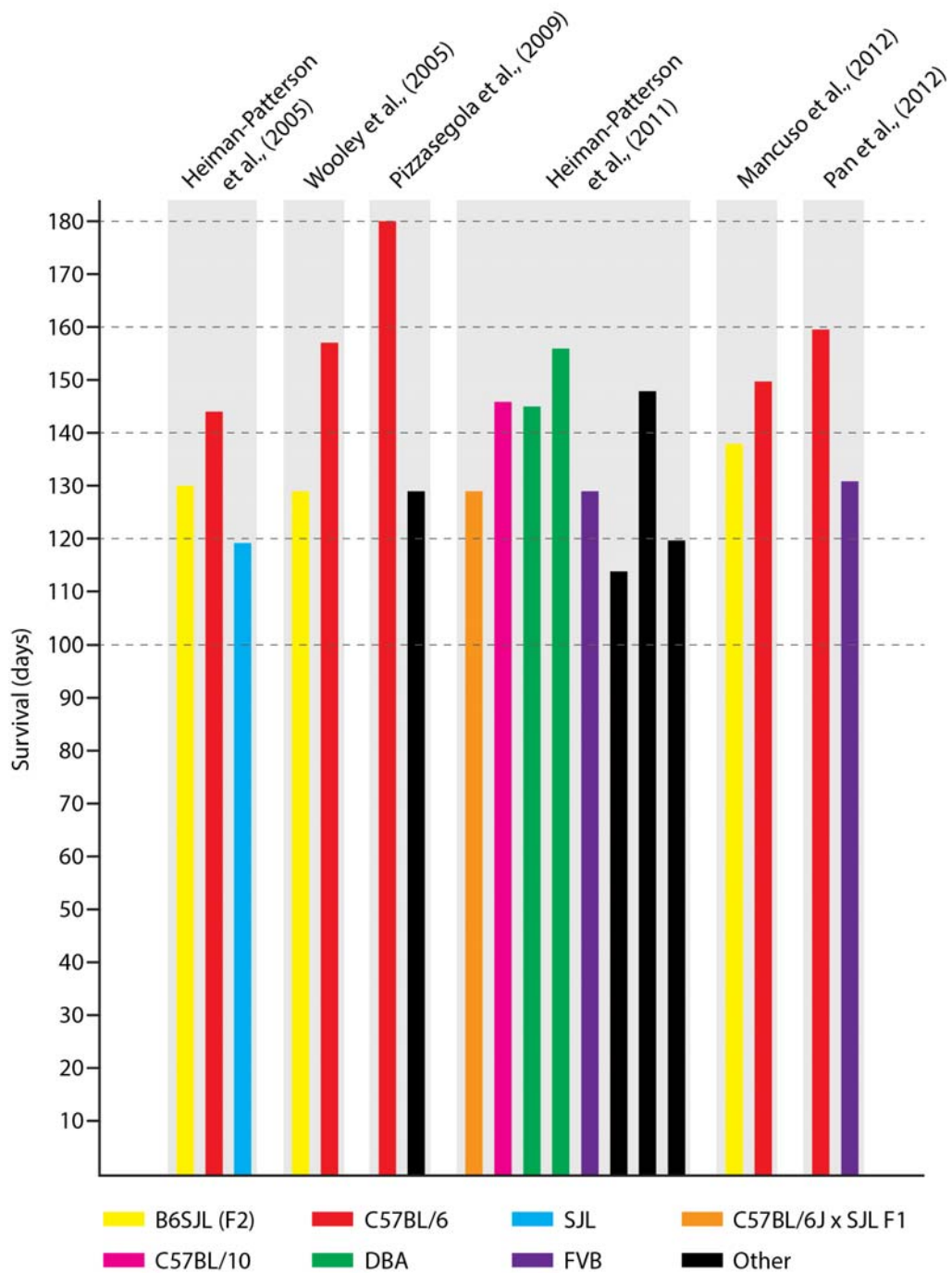


Figure 1.6 Genetic background effect on *TgSOD1^{G93A(H)}* mouse survival. Survival time expressed in days for *TgSOD1^{G93A(H)}* mice maintained in different background strains. Data come from different publications reporting results from two or more background strains (Heiman-Patterson et al., 2005, 2011; Mancuso et al., 2012; Pan et al., 2012; Pizzasegola et al., 2009; Wooley et al., 2005). Where survival was measured separately for each gender the average is plotted.

1.4.5 Limitations of current SOD1-ALS mouse models

Transgenic mouse models of SOD1-fALS and *Sod1* knock out models have been very useful in furthering our understanding of motor neuron disease, but as all model organisms they have some limitations.

The majority of the SOD1 transgenic mice, develop ALS symptoms and pathology but they are not a perfect genetic representation of the human disease since they overexpress the mutant *SOD1* gene in addition to the mouse endogenous *Sod1*. Tg*SOD1*^{G93A(H)} mice for example overexpress the human SOD1 protein up to 17 times the level of the endogenous mouse SOD1 in some studies and up to 25 times in some others, and such high levels of mutant protein have been proven to affect various aspect of the disease phenotype and pathology from onset to survival (Jaarsma et al., 2000; Jonsson et al., 2006b). *Sod1* knockout animals have also been crucial for investigating the effects of a 50 % reduction of SOD1 dismutase activity as seen in patients (Saccon et al., 2013). However, the absence of the *Sod1* gene does not mimic the human situation, since these animals do not develop motor neuron loss and premature death (Saccon et al., 2013). Further, as explained above different factors can influence animal pathology and phenotype such as background strain, transgene copy number and gender; therefore it is important to take them into consideration in interpreting existing results and designing new experiments (Perrin, 2014).

Despite these limitations to date SOD1 transgenic mice are the most commonly used and the most accurate models of ALS. Indeed, the majority of SOD1 transgenic mice available recapitulate the keys histopathological and biochemical features of the human disease and their onset and survival correlates with the level of the mutant protein expressed (Jucker, 2010). Moreover, SOD1 transgenic mice have been extensively employed as preclinical models and a substantial number of compounds that modulate their pathology have been identified, but only few have been successfully translated in clinical trial. Nevertheless there are examples of treatments developed in SOD1 mouse models, such as riluzole, the only approved drug for ALS, where the effects seen in transgenic SOD1 mice match the clinical experience, demonstrating that these animals are an invaluable tool in the study of ALS (Gurney et al., 1996; Ittner et al., 2015; Turner and Talbot, 2008).

1.5 How mutant SOD1 causes disease

1.5.1 SOD1-fALS proposed mechanisms of pathogenicity

Studies carried out in SOD-fALS and sALS patients and SOD1-fALS mouse models lead to the conclusion that SOD1-ALS is caused by one or more toxic functions of the mutant SOD1 protein, rather than a reduction of superoxide dismutase activity. A plethora of molecular mechanisms of pathogenesis have been proposed (Ilieva et al., 2009). However, to date it is still unknown which of these mechanisms are the cause of motor neuron degeneration and which are consequences of the disease. The most important of these proposed mechanisms relevant to SOD1-fALS are summarised below.

1.5.1.1 Glutamate toxicity and calcium homeostasis

High levels of glutamate have been observed in the central nervous system (CNS) of sporadic and familial ALS patients (Arundine and Tymianski, 2003; Foran and Trotti, 2009), and SOD1 mutant mouse models (Ilieva et al., 2009). Elevated concentrations of this excitatory neurotransmitter, that triggers motor neurons to fire, can initiate a cascade of toxic events in the motor neurons. Taking together these two observations it has been proposed that glutamate excitotoxicity can cause motor neuron death in ALS. In particular excess of glutamate provokes activation of the glutamate receptors which causes a prolonged opening of associated ion channels in mitochondria, resulting in increased levels of intracellular calcium and production of ROS (Mattson, 2003; Rothstein, 1995; Shaw and Ince, 1997). These findings are confirmed by data coming from mouse models of SOD1-fALS, where glutamate release and glutamate sensitivity are increased (Milanese et al., 2010; Tortarolo et al., 2006).

Moreover deficiency of the glutamate transporter excitatory amino-acid transporter 2 (EAAT2) has been reported in astrocytes of sALS and fALS patients and SOD1 mouse models, causing glutamate accumulation in the synapses (Howland et al., 2002; Rothstein, 1995; Yang et al., 2009, 2010).

Of note Riluzole which is the only drug used in the treatment of ALS is an anti-glutamnergic agent which regulates glutamate release (Foran and Trotti, 2009).

1.5.1.2 Endoplasmic reticulum (ER) stress and unfolded protein response (UPR)

Pathogenic mutants of SOD1 are involved in the activation of the ER stress (Fujisawa et al., 2012; Homma et al., 2013; Nishitoh et al., 2008). When perturbed the ER typically activates two stress responses: the UPR and the ER-associated degradation (ERAD) (Bunton-Stasyshyn et al., 2014). Indeed markers of UPR response and ERAD have been found in ALS patient tissues (Atkin et al., 2008; Ito et al., 2009; Walker and Atkin, 2011) and SOD1-fALS mice (Ito et al., 2009; Kikuchi et al., 2006; Saxena et al., 2009). In particular, as described above, the mechanisms through which SOD1 mutations have been proposed to cause ER stress are the interaction between SOD1 and COPII that disrupt the ER-Golgi trafficking (Atkin et al., 2014), and binding of SOD1 with Derlin-1 in situations of zinc deficiency (Homma et al., 2013).

Genetic and pharmacological manipulation of the UPR have been proven to affect degeneration in SOD1-fALS mice, presumably because the mice had a reduced capacity to turn down synthesis of misfolded SOD1 (Kalmar et al., 2008; Wang et al., 2011a). In interpreting these findings it is important to consider that in transgenic mouse models of SOD1-fALS the SOD1 protein is greatly overexpressed and the ER stress response seen might, at least in part, be caused by the presence of an abnormal amount of protein. Of note Kiskinis and colleagues showed that motor neurons are more susceptible to ER stress than other cell types, and this might be the reason why motor neurons are more vulnerable in ALS (Kiskinis et al., 2014).

1.5.1.3 Mitochondrial dysfunction

Ultrastructural studies revealed mitochondrial abnormalities in motor neurons of sALS patients. The same pathology is present also in transgenic SOD1 G93A mice (Gurney et al., 1994) and other SOD1-fALS mouse models (Dal Canto and Gurney, 1994, 1995; Kong and Xu, 1998; Martin et al., 2007; Wong et al., 1995).

Furthermore energy metabolism dysfunctions have been observed in mitochondria from CNS (central nervous system), blood and muscle of patients and also in motor neurons from SOD1-fALS mouse models (Crugnola et al., 2010; Martin et al., 2007; Mattiazzi et al., 2002; Swerdlow et al., 1998; Wiedemann et al., 1998). In particular it has been observed: an alteration of the mitochondrial electron transfer chain activity (Borthwick et al., 1999; Bowling et al., 1993), aberrant calcium homeostasis (Curti et al.,

1996; Siklós et al., 1996) and abnormal localization of SOD1 to the inner membrane space (IMS) (Mattiuzzi et al., 2002). In mice mutant SOD1 specifically targeted to the mitochondria IMS has been shown to impair the mitochondria respiratory chain and cause ALS like phenotypes such as loss of motor neurons and muscle weakness but not muscle denervation (Igoudjil et al., 2011). Therefore, there is evidence that in mice mutant SOD1 can cause mitochondrial dysfunction that results in some ALS features, but other mechanisms may be necessary to recapitulate all aspects of the ALS phenotype (Igoudjil et al., 2011).

1.5.1.4 Oxidative stress

Even though it is known that SOD1-ALS is caused by a toxic gain of function, the idea that the lack of SOD1 activity provoking oxidative stress might play a role in the disease has not yet been dismissed. Indeed SOD1-fALS patients show on average approximately 50 % reduced dismutase activity, see section 3.3.1 (Saccon et al., 2013). Moreover there are also other indications, independent from the loss of SOD1 enzymatic function suggesting a role for oxidative stress in ALS.

For example signs of increased oxidative damage of protein, lipids, DNA and mRNA together with other indicators of oxidative stress have been observed in spinal cord but also in urine, blood and cerebrospinal fluid of SOD1-fALS and sALS patients (Barber and Shaw, 2010; D'Amico et al., 2013). Moreover increased 3-nitrotyrosine levels, an oxidative stress marker have been detected in motor neurons of SOD1-fALS patients (Beal et al., 1997). Of note in a small number of cases oxidative stress damage has been also shown to correlate with disease measures (Abe et al., 1995; Babu et al., 2008; Beal et al., 1997; Bogdanov et al., 2000; Bowling et al., 1993; Chang et al., 2008; Cova et al., 2010; Ferrante et al., 1997a; Murata et al., 2008; Sasaki et al., 2000; Shaw et al., 1995; Shibata et al., 2001, 2004; Simpson et al., 2004; Smith et al., 1998; Tohgi et al., 1999).

Interestingly similar oxidative stress markers have been detected in SOD1-fALS mouse models providing further evidence that oxidative damage is implicated in motor neuron degeneration (Andrus et al., 1998; Casoni et al., 2005; Cha et al., 2000; Ferrante et al., 1997b; Lee et al., 2009; Liu et al., 2007, 1998; Poon et al., 2005). In mice SOD1 has been found to be oxidised, oxidation has indeed been implicated in the monomerisation and aggregation of wild-type and mutant SOD1 (Ezzi et al., 2007; Rakhit et al., 2002; Wilcox et al., 2009). Evidence that mRNA oxidation contributes to

motor neuron degeneration also comes from SOD1-fALS mouse models, and the majority of oxidised mRNA species identified in the spinal cord of the mice are implicated with ALS (Chang et al., 2008).

Recent findings underlined the central role of oxidative stress in SOD1-fALS showing that overexpression of oxidation resistance 1 (*OXR1*), a gene protective against oxidative stress, induced damage in neurons of transgenic SOD1 G93A mice, delays spinal cord and muscle pathology, extends survival and delays the non-cell-autonomous inflammatory response (Liu et al., 2015). Moreover, alterations in peroxiredoxin (PRDX) 1, 3 and 6, the enzymes responsible for reducing hydrogen peroxide levels, and reduction in several isoforms of glutathione S-transferase (GST) mu1, 2 and 5 have been demonstrated in SOD1 G93A ALS mouse and cell models, suggesting a crucial role of oxidative stress in disease (Allen et al., 2003; Jain et al., 2008; Strey et al., 2004).

From all these studies is possible to conclude that even if the role of oxidative stress is still unclear, the fact that it is involved in several pathogenic mechanisms of the disease suggests that it is an important factor in ALS (Barber and Shaw, 2010).

1.5.1.5 Axonal transport impairment

Disruption of axonal transport has been demonstrated in several SOD1-fALS mouse models and in primary MNs expressing mutant SOD1. In particular in several SOD1-fALS mice both slow anterograde and fast retrograde axonal transport system defects are present (Bilsland et al., 2010; Warita et al., 1999; Williamson and Cleveland, 1999; Zhang et al., 1997). While in primary MNs fast anterograde and retrograde transport are disrupted triggering mitochondrial reduction in the axon (De Vos et al., 2007). Also in human spinal cords the axonal anterograde transport has been suggested to be impaired causing mislocalisation of mitochondria (Sasaki and Iwata, 1996).

SOD1 has been shown to interact with a driver of retrograde transport, the dynein complex, in cell, mouse and rat models (Zhang et al., 2007). Interestingly in cell models it has been shown that perturbation of SOD1-dynein complex interaction correlates with reduction of SOD1 toxicity and aggregation (Ström et al., 2008).

In mice SOD1 aggregation together with a progressive motor phenotype are triggered by deficits in the axonal retrograde transport caused by a mutation in the cytoplasmic

dynein heavy chain 1 (*Dync1b1*) gene (Hafezparast et al., 2003). Further mutant and oxidised wild-type SOD1 can inhibit dynein based fast anterograde transport (Rotunno and Bosco, 2013).

A damaged axonal transport might cause problems with cytoskeletal structure, energy metabolism and seriously impair the transport of crucial proteins and organelles (De Vos *et al.*, 2007) creating a process in which all these components are mislocalised and the cell is unable to recycle them. MNs have been suggested to be more sensitive to this type of axonal impairment than other neuronal cells, due to their morphology (Chevalier-Larsen and Holzbaur, 2006).

1.5.1.6 Non-cell autonomous mechanism

Motor neuron degeneration is a hallmark of ALS but several other cell types are known to be involved in disease pathogenesis. Indeed studies carried out in SOD1-fALS mouse models have shown that the selective expression of mutant SOD1 in motor neurons or in astrocytes, fails to cause an ALS phenotype, suggesting a non-cell autonomous nature of the disease (Gong et al., 2000; Pramatarova et al., 2001). However, other experiments have found that the selective expression of mutant SOD1 in MNs, can give MN loss but no behavioural motor phenotype (Wang et al., 2008) or MN loss and behavioural phenotype (Jaarsma et al., 2008).

Subsequent studies carried out on chimeric mice and on mice in which the transgenes were excised from particular cell types, have provided more consistent results. Expression of mutant SOD1 in motor neurons determines disease onset and influences progression (Boillée et al., 2006; Wang et al., 2009b; Yamanaka et al., 2008a, 2008b). While mutant SOD1 expressed in astrocytes and microglia has been proposed to be the main key for determining the progression of degeneration (Beers et al., 2006; Boillée et al., 2006; Gong et al., 2000; Wang et al., 2009b, 2011b; Yamanaka et al., 2008b). Transgenic mice with mutant SOD1 expressed in skeletal muscle have shown muscle atrophy and reduced strength, but it is still unclear whether this can cause degeneration of MNs (Dobrowolny et al., 2008; Wong and Martin, 2010).

Co-culture experiments have revealed that astrocytes expressing mutant SOD1 are toxic to neurons (Fritz et al., 2013; Di Giorgio et al., 2008; Kunze et al., 2013; Marchetto et al., 2008; Nagai et al., 2007). Also mutant SOD1 microglial toxicity seems likely although the effect may be indirect (Thonhoff et al., 2012; Zhao et al., 2010).

All these results taken together suggest that the expression of mutant SOD1 in astrocytes and microglia is crucial for disease progression, but the expression of the mutant protein in motor neurons is necessary for the disease onset (Boillée et al., 2006).

Barber and Shaw proposed a mechanism in which damaged motor neurons activate glial cells through the release of ROS, which in turn activate other glial cells leading to further motor neuron damage (Barber and Shaw, 2010). The mechanism of this communication is still unknown however, a recent publication hypostasised that *OXR1* could act as mediator of the cross-talk between motor neurons and toxic mutant SOD1 microglia and astrocytes, extending MN survival (Liu et al., 2015).

1.5.1.7 SOD1 involvement in RNA metabolism

TDP-43 and FUS are RNA binding proteins, and are both causative of fALS when mutated; their discovery highlighted the possibility that RNA metabolism might play a crucial role in the pathogenesis of ALS (Ling et al., 2013). SOD1 has been also shown to be involved in RNA metabolism by binding and stabilising mRNAs.

For example mutant SOD1 may down regulate vascular endothelial growth factor (*VEGF*) expression by directly binding its mRNA transcript. Indeed *VEGF* mRNA expression is downregulated in the spinal cords of transgenic SOD1 G93A mice, and a luciferase reporter assay carried out in an *in vitro* culture model of glia cells expressing mutant SOD1, showed that mutant SOD1 protein has a high binding affinity for *VEGF* adenine/uridine-rich elements (ARE) (Lu et al., 2007; Miao and St Clair, 2009). Furthermore, *in vitro* mutant SOD1 has been shown to directly compete with HuR and neuronal HuC embryonic lethal abnormal visual (ELAV) RNA stabilizer proteins, specifically for *VEGF* mRNA binding. This gain of function of mutant SOD1 may disrupt ELAV protein function leading to loss of expression of *VEGF* that is essential for motor neuron survival (Li et al., 2009). Indeed *VEGF* increased expression has been shown to attenuate the phenotype of SOD1-fALS mice (Bunton-Stasyshyn et al., 2014; Keifer et al., 2014). Furthermore a polymorphism in the *VEGF* promoter has been related to increased risk of ALS and lower age of onset (Su et al., 2014) and a deletion in the promoter of the mouse gene has resulted in a MN degenerative phenotype characterised by late onset (Oosthuysen et al., 2001).

In a similar way mutant SOD1 also binds the 3' UTR of low molecular weight neurofilament (*NFL*) mRNA negatively affecting its stability (Bunton-Stasyshyn et al., 2014; Chen et al., 2014; Ge et al., 2005; Volkening et al., 2009). Experiments carried out in NSC34 cells showed that mutant SOD1 but not wild-type SOD1 interacts directly with hNFL mRNA and functions as a trans-acting hNFL mRNA stability determinant acting within the 3'-UTR (Ge et al., 2005). Further studies showed that a reduction in *NFL* mRNA mediated by mutant SOD1 induces axonal degeneration in sALS, SOD1-fALS mouse models and also in MNs differentiated from induced pluripotent stem cells (iPSC) derived from SOD1-fALS patients (Chen et al., 2014; Julien, 1999; Menzies et al., 2002). However in a SOD1-fALS mouse model the knockout of *NFL* resulted in a significant delay of disease onset (Williamson et al., 1998), therefore the reduction of the *NFL* mRNA is probably not the main pathogenic mechanism of SOD1-fALS.

1.5.2 Protein misfolding and aggregation

1.5.2.1 SOD1 protein aggregates

The presence of specific protein aggregates is a hallmark of several neurodegenerative diseases. In SOD1-fALS the presence of non-amyloid SOD1 aggregates in the MNs has been extensively reported (Kato et al., 1996, 1997; Kerman et al., 2010; Okamoto et al., 1991; Wang et al., 2002a). Nevertheless the role of such aggregates is still unknown. In particular it is unclear whether they are toxic pathogenic species or if they are the result of a coping mechanism used to protect the organism against other misfolded protein species like monomers and oligomers. (Mulligan and Chakrabarty, 2013; Ross and Poirier, 2005).

Investigation of SOD1-fALS mice suggested a link between SOD1 aggregation and the disease phenotype. Indeed SOD1 aggregates are preferentially located in the ALS affected tissues, and their level has a positive correlation with disease progression (Cheroni et al., 2005; Turner et al., 2003; Wang et al., 2002a, 2002b). Moreover Wang and colleagues suggested that SOD1 expression levels should reach a certain threshold to cause aggregation in order for ALS like symptoms to arise (Wang et al., 2002a).

Experiments carried out using double transgenic mice expressing both mutant and wild-type SOD1 showed increased aggregation and co-localization of the mutant SOD1 protein with the wild-type form. In general these animals have a reduced

survival compared to single transgenic mice and develop an early onset of ALS symptoms (Deng et al., 2006; Fukada et al., 2001; Jaarsma et al., 2000, 2008; Prudencio et al., 2010; Wang et al., 2009c). However how the presence of wild-type SOD1 modulate the aggressiveness of the phenotype and the quantity and nature of the aggregates might depend on the expression level of the wild-type SOD1 protein. A cross between the L126Z mutant SOD-fALS mouse and 2 lines of transgenic wild-type mice showed that higher levels of wild-type SOD1 increase toxicity leaving aggregation of mutant SOD1 unchanged; while lower levels of wild-type SOD1 do not affect the phenotype but higher levels of aggregation are observed (Prudencio et al., 2010).

Of note SOD1 aggregate inclusions are detected in mice always after the denervation of the muscles (Bruijn et al., 1997; Gould et al., 2006; Johnston et al., 2000; Koyama et al., 2006).

Cell culture model experiments confirmed findings from double transgenic mice showing that increased levels of soluble SOD1 correlates with increased toxicity, while increased levels of insoluble SOD1 correlates with reduced toxicity. Moreover when mutant and wild-type SOD1 are co-expressed aggregation is lessened while toxicity is increased (Brotherton et al., 2013; Prudencio et al., 2010; Weisberg et al., 2012; Witan et al., 2008, 2009).

Of note in SOD1-fALS mice high levels of misfolded SOD1 can overload the ubiquitin proteasome system (UPS) causing it to become dysfunctional and therefore increase aggregation of SOD1 (Bendotti et al., 2012; Urushitani et al., 2002). However, this mechanism is always detected after disease onset (Lee et al., 2002). UPS dysfunction is observed in SOD1-fALS mice, but not until after onset (Cheroni et al., 2009) and SOD1 aggregation caused by UPS inhibition is not necessarily toxic (Lee et al., 2002), suggesting that this is not a primary cause of mutant SOD1 toxicity.

The fact that aggregated SOD1 is mainly detected in symptomatic animals suggests that aggregates are not the primary cause of ALS, however pre-aggregated SOD1 forms present before disease onset might be toxic species (Karch et al., 2009). This does not exclude that SOD1 aggregates can cause secondary toxicity by sequestration of other important proteins (Bergemalm et al., 2010; Pasinelli et al., 2004; Weisberg et al., 2012), or by disrupting axonal transport (Sau et al., 2011).

1.5.2.2 SOD1 pre-aggregate species

Several SOD1 species are detected in the spinal cord of affected SOD1-fALS animals, such as: soluble, insoluble and detergent resistant monomers, soluble and insoluble dimers, oligomers and other high molecular weight SOD1 species (Koyama et al., 2006).

SOD1 mutants typically show an increased propensity of the SOD1 dimers to monomerise, together with defects in folding and dimerization of the protein (Bruns and Kopito, 2007; Khare et al., 2006; Rakhit et al., 2004). Since monomerisation is a crucial step for the formation of oligomers and aggregates (Rakhit et al., 2004; Ray et al., 2004) this propensity could accelerate the aggregation process of the SOD1 mutants. For instance, spinal cords from four different SOD1-fALS mouse mutant lines have been shown to be enriched in soluble hydrophobic disordered monomers compared to mice overexpressing the human wild-type SOD1 transgenic protein. The level of these monomers correlates with survival in the 4 mutant lines, associating monomeric SOD1 with disease (Zetterström et al., 2007, 2013).

Not only monomers but also other oligomeric soluble and insoluble SOD1 species have been identified in pre-symptomatic SOD1-fALS mice and they have been suggested to correlate with progression of the phenotype (Johnston et al., 2000; Wang et al., 2009a). Indeed staining of the MNs of SOD1-fALS mice using antibodies that specifically label misfolded forms of SOD1, revealed the presence of non-native dimeric species in pre-symptomatic mice and inclusions after disease onset (Liu et al., 2012; Rakhit et al., 2007).

The mechanisms through which these monomeric or oligomeric species of SOD1 might cause toxicity are still unknown, however, some assumptions have been made. Monomerisation could for example expose the SOD1 binding site for derlin-1 triggering ER stress (Fujisawa et al., 2012; Nishitoh et al., 2008), or could impair the copper binding causing oxidative stress (Kishigami et al., 2010). Oligomerisation has instead been proposed to disrupt retrograde axonal transport by competing with other transport targets overwhelming the system (Johnston et al., 2000).

1.5.2.3 Prion-like protein misfolding mechanism

Prion diseases are fatal neurodegenerative diseases characterised by misfolding of the prion protein (PrP). They can be sporadic, caused by mutation in the prion protein (*PRNP*) gene or caused by infection with misfolded PrP (PrP^{sc}). In particular the PrP^{sc} protein can induce the correctly folded cellular PrP (PrP^c) to misfold and take the characteristics of the infectious PrP^{sc}. The disease can be transmitted cell to cell, but also among animals via oral uptake, blood, or other sources of direct contact (Acquatella-Tran Van Ba et al., 2013; Grad et al., 2015; Lee and Kim, 2015).

There are several lines of evidence suggesting that ALS is a propagating process similar to prion diseases. First of all both SOD1 and TDP-43 are known to self-propagate within and between neuronal cells (Münch et al., 2011; Nonaka et al., 2013). Moreover ALS patients have aggregates of misfolded protein in their motor neurons and post mortem studies showed that the loss of motor neurons is more prominent in the region of onset and gradually decreases in the other affected areas, with distance from the focal onset (Ravits et al., 2007b; Verma, 2013). ALS might be therefore considered a prion-like disease. The term prion-like is used to describe two main features: one is the ability of a misfolded protein of seeding aggregation and misfold a correctly folded protein, and the other is the capacity of spreading this process between cells, see section 5.1.1 (Lee and Kim, 2015).

Even though amyloid features have never been detected in SOD1-fALS and sALS patients, the SOD1 protein has been shown to display prion-like mechanism *in vitro* showing both seeding and cell to cell transmission (Chia et al., 2010; Grad et al., 2014; Münch et al., 2011). Moreover recent findings suggest a cell to cell transmissibility of the SOD1 protein also in mice (Ayers et al., 2014). The SOD1 prion-like mechanism is discussed in detail in 5.1.1. It is important to note that the majority of SOD1-fALS studies are conducted in mouse models where beside the overexpression of the mutant forms of the human SOD1 protein also the endogenous mouse SOD1 protein is present. Investigating the possible interactions between the human and the mouse SOD1 variants will be extremely helpful to better understand and interpret the results from the many studies carried out in ALS research.

1.5.3 Role of wild-type SOD1 in the pathogenesis of ALS

As mentioned above SOD1 aggregates are present both in sporadic and familial ALS and typically wild-type SOD1 protein is detected in aggregates of SOD1-fALS patients in addition to mutant SOD1 (Bruijn et al., 1998; Matsumoto et al.; Shibata et al., 1994, 1996b; Watanabe et al., 2001). The advent of antibodies able to distinguish between misfolded and correctly folded SOD1 revealed the presence of misfolded SOD1 also in some sALS and non-SOD1-fALS cases (Bosco et al., 2010; Forsberg et al., 2010, 2011; Gruzman et al., 2007; Pokrishevsky et al., 2012).

Interestingly wild-type SOD1 can misfold and acquire characteristics of the SOD1 mutant proteins, becoming toxic to the motor neurons. This transformation of the wild-type SOD1 protein has been proposed to happen as consequence of a prion-like mechanism, initiated by mutant SOD1 proteins, by oxidative damage or demetalation (Ezzi et al., 2007; Lindberg et al., 2004; Rakhit et al., 2004; Redler et al., 2011; Urushitani et al., 2006). Further in cell models oxidation and misfolding of wild-type SOD1 has been reported after expression of wild-type TDP-43 and wild-type FUS (Pokrishevsky et al., 2012).

Transgenic mice expressing human wild-type SOD1, have been extensively investigated. Interestingly these animals show ALS-like phenotypes late in life (Dal Canto and Gurney, 1995). In particular when the wild-type SOD1 protein is greatly overexpressed mice develop motor neuron loss and misfolded SOD1 is detected (Graffmo et al., 2013; Jaarsma et al., 2000). Misfolded-oxidised wild-type SOD1 behaves as mutant SOD1 also in cellular and *in vitro* models, impairing anterograde axonal transport, activating ER-stress and causing mitochondrial damage (Bosco et al., 2010; Guareschi et al., 2012; Pasinelli et al., 2004; Sundaramoorthy et al., 2013).

Wild-type SOD1 has been proposed to increase mutant SOD1 toxicity in several ways. SOD1-fALS mouse model data showed, for example, that the presence of wild-type SOD1 can increase solubility of the mutant protein (Fukada et al., 2001). Also misfolded wild-type SOD1 lacking zinc has been observed to become more toxic in the presence of correctly folded wild-type SOD1 (Sahawneh et al., 2010). Further wild-type SOD1 has been suggested to increase the toxicity of mutant or misfolded SOD1 by forming homodimers with pre-aggregated toxic species, stabilizing them and

consequently slowing aggregation as reported in cellular models (Brotherton et al., 2013; Prudencio et al., 2010; Weisberg et al., 2012; Witan et al., 2008, 2009) .

Although all mechanisms have not yet been elucidated it is clear that overexpression of the wild-type SOD1 protein can cause toxicity.

1.6 Research aim and current questions in SOD1-fALS

1.6.1 Does SOD1 loss of function play a role in the disease?

Mutations in the *SOD1* gene were the first to be identified as causative of fALS (Rosen et al., 1993). Initially, two mechanisms have been suggested to cause motor neuron death in mutant SOD1-induced fALS: a toxic gain of function and a loss of function. Data from *Sod1* knock out and transgenic mice overexpressing mutant SOD1 provided evidence of a neuromuscular phenotype. However, it was soon clear that transgenic SOD1 mutant mice better mimicked the MN loss phenotype seen in patients. In 1998, a seminal paper showed that the SOD1 loss of function did not influence the survival of the gain of function disease models excluding a role of loss of function in SOD1 fALS (Bruijn et al., 1998).

Since then several groups further investigated the phenotype of *Sod1* knockout mice characterising and examining the specific neuromuscular involvement. These studies taken together with recent findings on mice overexpressing SOD1 (Ezzi et al., 2007; Khare et al., 2004; Rakhit et al., 2004; Wilcox et al., 2009) suggested a possible modifying role played by loss of SOD1 activity on the fALS disease course. Furthermore loss of function and gain of function mechanisms have been proposed to contribute to pathogenesis of TDP-43-ALS and FUS-ALS (Guo et al., 2011; Lagier-Tourenne and Cleveland, 2009). The contribution of both these mechanism to neurodegeneration has been reported also in other disease such as Huntington's disease (HD) (Zuccato et al., 2010), Parkinson's disease (Winklhofer et al., 2008) and spinocerebellar ataxia 1 (Crespo-Barreto et al., 2010; Lim et al., 2008).

In Chapter 3 papers reporting SOD1 activity data from SOD1-fALS patients and publications on *Sod1* knockout mice are reviewed to investigate if a possible role for SOD1 loss of function in SOD1-fALS pathogenesis exists and what can be done to definitively address this issue.

1.6.2 Can we dissect the central and the peripheral effects of mutant SOD1 toxicity using a new mouse model of motor neuron disease?

Many SOD1 transgenic mice have been generated in the last twenty years, and as explained above they have been implicated in many potential ALS pathological mechanisms (McGoldrick et al., 2013). However, these animals overexpress the mutant or the wild-type SOD1 protein and it is difficult to determine whether the phenotype and pathology that they exhibit are the cause of the disease or an effect of the large amount of SOD1 protein (Acevedo-Arozena et al., 2011; Chang et al., 2008; Deng et al., 2006; Graffmo et al., 2013; Prudencio et al., 2010). *Sod1* knock out mice have also been crucial in ALS research and develop a distal axonopathy, but the absence of the SOD1 protein is not capable of causing MN degeneration (Fischer et al., 2011, 2012).

Recently we described a new mouse model carrying a point mutation (D83G) in the mouse *Sod1* gene, identical to an ALS-causing SOD1 mutation in humans (Joyce et al., 2014; Millecamps et al., 2010). Animals homozygous for this mutation (*Sod1*^{D83G/D83G}) develop MN loss and also a distal neuropathy, due respectively to gain of function and loss of function effects (Joyce et al., 2014). In the work presented in Chapter 4 the morphological innervation patterns of endplate NMJs, SOD1 protein level and SOD1 activity of *Sod1*^{D83G} animals are investigated. Moreover to characterise further the gain of function and loss of function phenotypes, by dissecting the MN loss and the peripheral neuropathy of the *Sod1*^{D83G} mouse, *Sod1*^{D83G} mice were crossed with TgSOD1^{WT} animals to see if the overexpression of the human wild-type SOD1 could rescue the disease phenotype of *Sod1*^{D83G/D83G} mice. Further, *Sod1*^{D83G} were crossed with *Sod1* knockout mice to see if only once copy of the D83G allele was sufficient to cause both motor neuron loss and distal neuropathy.

1.6.3 Is there an interaction between human and mouse SOD1 proteins, and how does this change our interpretation of SOD1 mouse models?

In several transgenic mouse models of neurodegenerative disease overexpressing a mutant human protein, it has been shown that the presence of the homologous mouse protein affects the phenotype. For example, in mouse models of human prion disease the presence of both mouse and human PrP delays the disease onset and the phenotypes detected are more variable than when the mouse gene is knocked-out (Collinge et al., 1995; Telling et al., 1995). In mice expressing wild-type human tau no disease pathology is detected when the endogenous mouse *Mapt* gene is functional

(Duff et al., 2000). However, when the mouse *Maqt* is knocked-out, animals develop a pattern of pathology similar to that seen in Alzheimer disease (AD), including neuronal death (Andorfer et al., 2003, 2005).

A transgenic SOD1-fALS mutant line carrying the G85R mutation investigated both in presence and absence of the endogenous *Sod1* gene showed no difference in survival and phenotype (Bruijn et al., 1998). However, in a more recent study carried out on a similar cross with a G93A mutant SOD1 transgenic, a delay in disease onset and longer survival has been observed in absence of the mouse *Sod1* gene. Data from double transgenic animals have shown that the interaction between wild-type and mutant human SOD1 exacerbates the disease. Nevertheless, when wild-type human SOD1 has been expressed in a mouse carrying the mouse SOD1 G86R mutation no difference in the phenotype has been detected (Audet et al., 2010).

Cell studies have shown that both human and mouse wild-type SOD1 can slow the aggregation of mutant human SOD1, but the mouse and the human SOD1 protein have never been shown to co-aggregate (Grad et al., 2011; Prudencio et al., 2009b; Qualls et al., 2013).

In order to interpret results from SOD1 transgenic models it is important to understand if there is an interaction between the human and the mouse SOD1 protein, and if there is, how it influences the disease phenotype. The mouse SOD1 dimer is more stable compared to the human one and therefore predicted to form less aggregates (Jonsson et al., 2006b).

As described in Chapter 5, to investigate human and mouse aggregation propensity several human and mouse SOD1 recombinant proteins have been produced, purified and biochemically characterised and preliminary experiments have been carried out to assess their propensity to spontaneously aggregate.

1.6.4 Can we identify new genes involved in SOD1-ALS by creating new modifier mouse models?

Mouse models of SOD1-fALS have been used in the investigation of modifier genes that might positively or negatively influence the ALS phenotype. To do so the main approach that has been employed consists in crossing SOD1-fALS mouse models with

other mice that transgenically express or lack genes that are considered of interest (Liu et al., 2015; Riboldi et al., 2011; Turner and Talbot, 2008).

In order to investigate new modifiers of the *SOD1* gene a sensitized screen was carried out at MRC Harwell, in which *N*-ethyl-*N*-nitrosourea (ENU) mutagenized mice were crossed with animals carrying the transgenic *SOD1* G93A low copy mutation. As result of this screen one mouse with a reduced survival was identified as a phenodeviant of the Tg*SOD1*^{G93A(L)} line, named *Galabad*.

A phenotypic investigation of the *Galabad* mouse progeny and a quantitative trait loci (QTL) analysis to try to identify possible modifying locus/loci interacting with the *SOD1* G93A mutation are reported in Chapter 6.

Chapter 2 Materials and methods

2.1 Materials

2.1.1 Equipment

1 l polypropylene centrifuge bottle	Nalgene
2 l erlenmeyer flask	Nalgene
5 l beaker	Nalgene
96-well black microtiter plate	Griener
96-well PCR microplate	VWR
Balance	Mettler-Toledo
Beads	Hybaid Ribolyser
Bench top refrigerated microfuge Heraeus Fresco 17	Thermo Fisher
Bio-Rad Bio-Logic chromatography system	Bio-Rad
Centrifuge 5402 or 5424	Eppendorf
Centrifuge 6K15 rotor number: 12500; 12166	Sigma Laboratory
Centrifuge tube 50 ml	Oakridge
Chromatographic glass column	Bio-Rad
Confocal microscope LSM 710	Zeiss
Coverslips	VWR
Cryostat	Bright™
Dialysis cassette	Pierce
Dialysis membrane tubing (8 ml/cm, 8 kDa)	Spectra pro
Dissection tools	Dumont
Electrophoresis power pack	Bio-Rad
Epifluorescence microscope	Leica DMR
Filter unit	Sartolab
Fluorimeter plate reader Infinite M1000 PRO	Tecan
Gel cast for agarose gel	Scie-plas
Gel scanner	Hewlett-Packard (hp)
Gel tank submarine	Mupi
Gilson pipettes	Anachem Ltd

Grip-strength meter bio-GS3	BioSeb
Heat block	Grant Instruments
Homogeniser TissueRuptor	Qiagen
Incubator shaker	Orbital
Jasco J-715 Circular Dichroism Spectropolarimeter	Jasco
Magnetic flea stirrer	BIBBY
Microscope slides	VWR
Microwave	Sharp
Odyssey Classic imaging system	Licor
PAP pen	VWR
Pasteur pipette	VWR
Peltier Thermal Cyclers PTC-225	Bio-Rad
pH meter	Mettler-Toledo
Photo-film	Kodak
Plastic cuvettes	Starstedt
Plate incubator shaker	GrantBio
Poly-lysine coated slides	VWR
Polyvinylidene difluoride (PVDF) membrane	Millipore
Protein machine ÄKTA pure	GE Healthcare Life Sciences
qPCR machine	Applied Biosystems
Sonicator	Philip Harris Scientific
Sonicator Probe MS73	Sigma-Aldrich
Spectrophotometer NanoDrop® ND-1000	NanoDrop Technologies
Spectrophotometer Sunrise	Tecan
UV illuminator ChemiDoc XRS+	BioRad
UV/VIS disposable cuvettes	Kartell
Vacusafe pump	Integra Biosciences
XCell <i>SureLock</i> Mini-Cell Electrophoresis System	Life Technologies

2.1.2 Chemicals and reagents

16 % Tris-Glycine precast gel	Life Technologies
2-mercaptoethanol	Sigma-Aldrich
3-12 % NativePAGE Bis-Tris precast gels	Life Technologies
4-12 % NuPAGE Bis-Tris precast gels	Life Technologies
Acetic acid	VWR
Benzonase	VWR
Bovine Serum Albumins (BSA)	Sigma-Aldrich
Calcium chloride (CaCl ₂)	Sigma-Aldrich
Coomassie Brilliant Blue R	Sigma-Aldrich
Copper sulphate (CuSO ₄)	Sigma-Aldrich
EDTA free protease inhibitor cocktail	Roche
Ethanol (CH ₃ CH ₂ OH)	VWR
Ethidium bromide	Sigma-Aldrich
Ethylenediaminetetraacetic acid (EDTA)	Sigma-Aldrich
Extraction Solution	Sigma-Aldrich
Florescent mounting media	DAKO
Glutathione	Sigma-Aldrich
Glycerol	Sigma-Aldrich
Guanidine hydrochloride (GuHCl)	Sigma-Aldrich
HyperLadder IV	Bioline
Imidazole	Sigma-Aldrich
Isopropanol	VWR
Isopropyl-β-D-thiogalactopyranoside (IPTG)	Melford
Kanamycin	Sigma-Aldrich
Luria Broth (LB)	Sigma-Aldrich
Lysozyme	Sigma-Aldrich
MES SDS Running buffer 20X	Life Technologies
Methanol (CH ₃ OH)	VWR
N,N,N',N'-tetramethylethylenediamine (TEMED)	Sigma-Aldrich

NativeMark unstained protein standard	Life Technologies
NativePAGE Cathode buffer additive 20X	Life Technologies
NativePAGE Running buffer 20X	Life Technologies
NativePAGE Sample buffer 4X	Life Technologies
Neutralisation Solution B	Sigma-Aldrich
Nitro blue tetrazolium	Sigma-Aldrich
NuPAGE LDS Sample buffer 4X	Life Technologies
NuPAGE Transfer buffer 20X	Life Technologies
OCT	Sakura Finetek
Odyssey blocking buffer (PBS)	Licor
Paraformaldehyde	Sigma-Aldrich
Phosphate Buffered Saline (PBS)	Sigma-Aldrich
Potassium phosphate	Sigma-Aldrich
Proteinase K	Invitrogen
Riboflavin	Sigma-Aldrich
Seeblue plus2 protein standard	Life Technologies
Sodium acetate	Sigma-Aldrich
Sodium azide	Sigma-Aldrich
Sodium chloride (NaCl)	Sigma-Aldrich
Sodium dodecyl sulphate (SDS)	Sigma-Aldrich
Sodium pentobarbital	Euthatal
Sodium phosphate (Na ₃ PO ₄)	Sigma-Aldrich
Sucrose	Sigma-Aldrich
<i>Taq</i> polymerase REDTaq ReadyMix	Sigma-Aldrich
TaqMan Universal PCR Master Mix	Applied Biosystems
TBS	Sigma-Aldrich
Thioflavin-T (ThT)	Sigma-Aldrich
Thrombin	Sigma-Aldrich
Tissue Prep Solution	Sigma-Aldrich
Tris acetate	Sigma-Aldrich

Tris borate	Sigma-Aldrich
Tris hydrochloride (Tris-HCl)	Sigma-Aldrich
Tris-Glycine Electroblothing Buffer 10X	National Diagnostic
Tris-Glycine SDS Buffer 10X	National Diagnostic
Tris-Glycine SDS sample buffer 2X	Life Technologies
Triton X-100	Sigma-Aldrich
Trizma base (Tris)	Sigma-Aldrich
Tween-20	Sigma-Aldrich
UltraPure agarose	Invitrogen
Zinc sulphate (ZnSO ₄)	Sigma-Aldrich

2.1.3 Commercial kits

DC™ Protein Assay	Bio-Rad
ECL Enhanced chemiluminescent substrate	Pierce
M.O.M. Immunodetection basic kit	Vector Labs
Quick Start™ Bradford Protein Assay	Bio-Rad

2.1.4 Antibodies

2.1.4.1 Primary antibodies

4',6-diamidino-2-phenylindole (DAPI)	Sigma-Aldrich
Anti-β-actin	Sigma-Aldrich
Mouse monoclonal anti-neurofilament (165 k Da) (2H3)	Developmental Studies Hybridoma Bank
Mouse monoclonal anti-synaptic vesicle (SV2)	Developmental Studies Hybridoma Bank
SEDI (SOD1 exposed dimer interface)	(Rakhit et al., 2007)
SOD-100 rabbit pan-anti SOD1	Enzo
USOD (Unfolded SOD1)	(Kerman et al., 2010)

2.1.4.2 Secondary antibodies

IRDye Licor anti-mouse	Licor
IRDye Licor anti-rabbit	Licor
Polyclonal goat anti-mouse IgG-HRP	DAKO

Polyclonal goat anti-rabbit IgG-HRP	DAKO
Streptavidin Alexa Fluor 488	Invitrogen
α -bungarotoxin-rhodamine	Sigma-Aldrich

2.1.5 Software

Applied Biosystems 7500 software v2.0.1

Carl Zeiss software ZEN

GraphPad Prism 6

IBM SPSS Statistics 19

i-controlTM

ImageJ v1.47 for Windows

Jasco Standard Analysis software

Odyssey v2.1 from Licor

R (programming language)

2.2 Mice

All animals were maintained and animal experiments were executed in accordance with the Animals (Scientific Procedures) Act 1986 and Home Office Project licence No. 30/2290.

Humane end points were defined as loss of 20 % maximum body weight, presence of hind limb paralysis or loss of righting reflex. Animals were assessed daily and weighed at least twice a month.

In the present work an abbreviated nomenclature will be used to describe mouse genotypes, defined in Table 2.1.

Genotypes	Short nomenclature
<i>Sod1</i> wild-type	<i>Sod1</i> ^{+/+}
<i>Sod1</i> knockout heterozygous	<i>Sod1</i> ^{+/-}
<i>Sod1</i> knockout homozygous	<i>Sod1</i> ^{-/-}
Human wild-type <i>SOD1</i> hemizygous transgenic	Tg <i>SOD1</i> ^{WT}
Human <i>SOD1</i> ^{G93A} hemizygous high copy transgenic	Tg <i>SOD1</i> ^{G93A(H)}
Human <i>SOD1</i> ^{G93A} hemizygous low copy transgenic	Tg <i>SOD1</i> ^{G93A(L)}
<i>Sod1</i> ^{D83G} heterozygous	<i>Sod1</i> ^{+/D83G}
<i>Sod1</i> ^{D83G} homozygous	<i>Sod1</i> ^{D83G/D83G}
<i>Sod1</i> ^{D83G} compound heterozygous knockout	<i>Sod1</i> ^{-/D83G}
Human wild-type <i>SOD1</i> hemizygous transgenic; <i>Sod1</i> ^{D83G} heterozygous	Tg ^{WT} <i>Sod1</i> ^{+/D83G}
Human wild-type <i>SOD1</i> hemizygous transgenic; <i>Sod1</i> ^{D83G} homozygous	Tg ^{WT} <i>Sod1</i> ^{D83G/D83G}
<i>Galabad</i> without human <i>SOD1</i> ^{G93A} hemizygous low copy transgenic	NTg <i>Galabad</i>
<i>Galabad</i> with human <i>SOD1</i> ^{G93A} hemizygous low copy transgenic	Tg ^{G93A(L)} <i>Galabad</i>
<i>Galabad</i> with human <i>SOD1</i> ^{G93A} hemizygous high copy transgenic	Tg ^{G93A(H)} <i>Galabad</i>
<i>Galabad</i> with human <i>SOD1</i> ^{G93A} hemizygous low copy transgenic; possibly carrying ENU mutation/s	mTg ^{G93A(L)} <i>Galabad</i>

Table 2.1 Mouse genotypes nomenclature.

2.2.1 Housing and husbandry of mice

Mice were housed in two different facilities under constant conditions: 19-23 °C temperature, 55±10 % humidity, 12 hours light:dark cycle. All animals were kept in individually ventilated cages (IVCs) with constant access to food and water, and grade five dust-free autoclaved wood bedding. If mice became unable to move freely or experienced a weight loss between 10 and 15 %, paper was removed and hydrogel was placed in the cage at ground level.

2.2.2 C57BL/6J mice

C57BL/6J mice (Jax stock number: 000664) were purchased from the Jackson Laboratory, and maintained by animal technicians. These animals have been used as the background strain for all the mice employed in the present work.

2.2.3 *Sod1* knockout mice

B6;129S-*Sod1*^{tm1Lxb}/J mice (Matzuk et al., 1998) (Jax stock number: 002972) were purchased from the Jackson Laboratory on a C57BL/6J X 129S hybrid background. These animals were backcrossed to C57BL/6J for at least 5 generations before use, and maintained by animal technicians.

Within the present work this strain will be referred to as *Sod1* knockout (*Sod1* KO), while the three genotypes produced from it will be named: *Sod1*^{+/+} (homozygous for the *Sod1* wild-type allele); *Sod1*^{+/-} (heterozygous for the *Sod1* KO allele) and *Sod1*^{-/-} (homozygous for the *Sod1* KO allele).

Genotyping was carried out as described in section 2.5.2.2.

2.2.4 Human wild-type *SOD1* transgenic mice

B6JL-Tg(SOD1)2Gur/J mice (Gurney et al., 1994) (Jax stock code number: 002297) were purchased from the Jackson Laboratory on a C57BL/6J X SJL/J hybrid background. These animals were backcrossed to C57BL/6J for at least 5 generations before use, and maintained by animal technicians.

In the present work only hemizygous transgenic littermates coming from this strain have been employed in experiments and they will be referred to as Tg*SOD1*^{WT}.

Genotyping was carried out as described in section 2.5.2.1.

2.2.5 Human *SOD1*^{G93A} transgenic high copy mice

B6.Cg-Tg(SOD1*G93A)1Gur/J (Chiu et al., 1995; Gurney et al., 1994) (Jax stock code number: 004435) were purchased from the Jackson Laboratory, already congenic to C57BL/6J and maintained by animal technicians. Animals employed for breeding purposes were culled at 120 days of age, before development of symptoms.

In the present work only transgenic littermates coming from this strain have been employed in experiments and they will be referred as Tg*SOD1*^{G93A(H)}.

Genotyping was carried out as described in section 2.5.2.1.

2.2.6 *Sod1*^{D83G} mice

Sod1^{D83G} mice have been identified by screening genomic DNA from the MRC Harwell ENU mutagenesis archive for mutations in *Sod1* (Joyce et al., 2014). *Sod1*^{D83G} mice were originally on a C57BL/6J-C3H background and they have been backcrossed to C57BL/6J for at least 5 generations before use.

I maintained my own *Sod1*^{D83G} colony in collaboration with Dr Philip Mcgoldrick. All three genotypes generated from this mouse line have been employed in experiments: *Sod1*^{+/+} (homozygous for the *Sod1* wild-type allele); *Sod1*^{+/^{D83G} (heterozygous for the *Sod1*^{D83G} allele) and *Sod1*^{D83G/D83G} (homozygous for the *Sod1*^{D83G} allele).}

Genotyping was carried out by Dr Abraham Acevedo using pyrosequencing at MRC Harwell.

2.2.7 *Galahad* mice

Galahad mice were identified by an ENU mutagenesis modifier screen carried out by Dr Abraham Acevedo in collaboration with Prof Elizabeth Fisher see section 6.1.1. The colony founder mouse was on a C57BL/6J-BALB/c hybrid background, the line produced from it was then maintained on congenic C57BL/6J.

Two genotypes were generated from this line: Tg^{G93A(L)}*Galahad* (carrying the human transgene *SOD1*^{G93A} low copy) and NTg*Galahad* (mice non transgenic for the human *SOD1*^{G93A} low copy).

Genotyping was carried out as described in section 2.5.2.1.

2.2.8 *Sod1*^{D83G} X *Sod1* knockout cross

To produce this line *Sod1*^{D83G} mice were crossed to *Sod1* knockout mice in a two-step cross. In the first step *Sod1*^{+/^{D83G} males were mated with *Sod1*^{+/-} females, producing four possible genotypes: *Sod1*^{+/^{D83G}, *Sod1*^{+/-}, *Sod1*^{-/^{D83G} and *Sod1*^{+/+} as illustrated in Figure 2.1 (a). In the second step *Sod1*^{-/^{D83G} males were mated with *Sod1*^{+/-} and *Sod1*^{+/^{D83G} females, producing six possible genotypes: *Sod1*^{+/^{D83G}, *Sod1*^{+/-}, *Sod1*^{-/^{D83G}, *Sod1*^{-/-} and *Sod1*^{D83G/D83G} see Figure 2.1 (b).}}}}}}}

Genotyping for the presence of the *Sod1* knockout allele was carried out as described in section 2.5.2.2, while genotyping for the presence of the *Sod1*^{D83G} allele was carried out by Dr Abraham Acevedo using pyrosequencing at MRC Harwell.

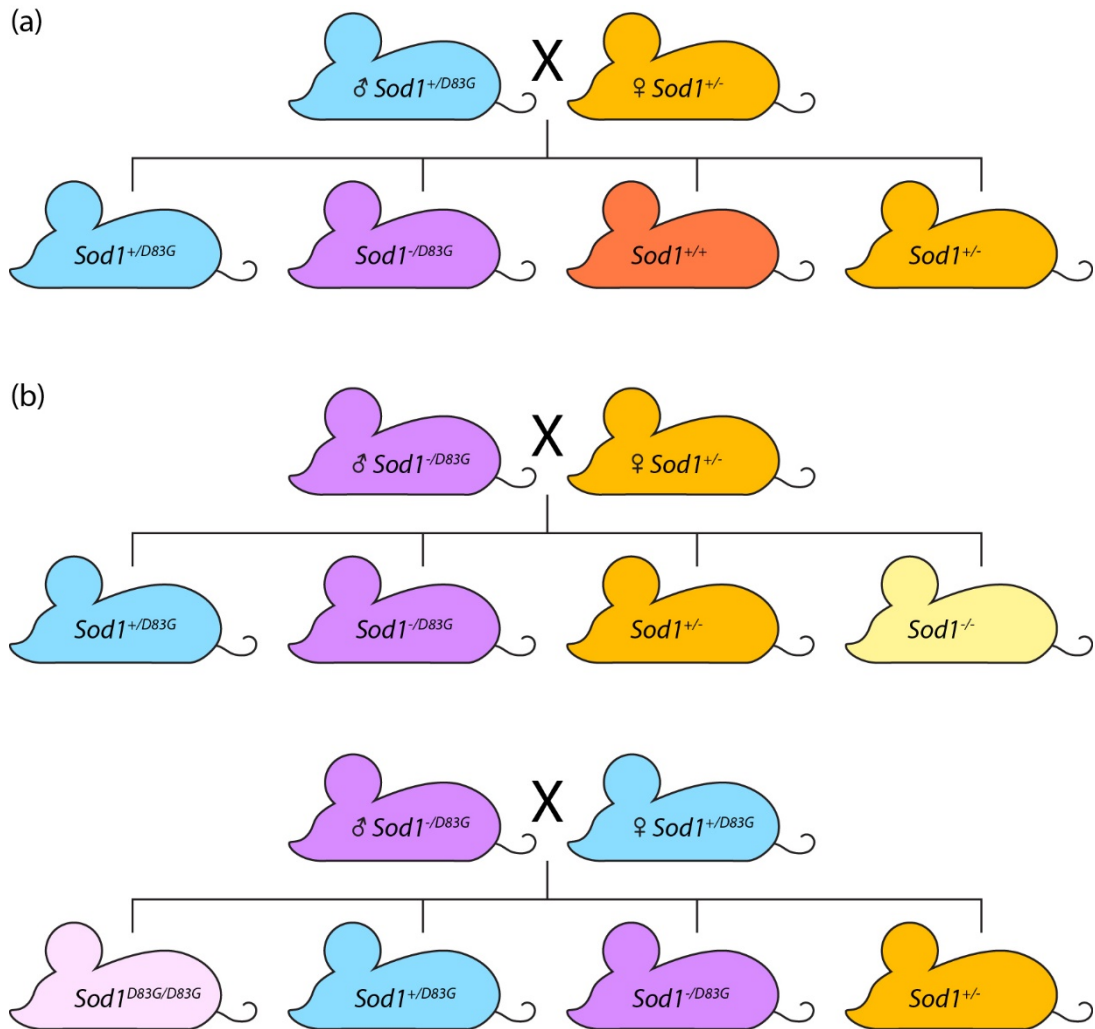


Figure 2.1 Breeding scheme for *Sod1*^{D83G} X *Sod1* KO.

2.2.9 *Sod1*^{D83G} X Human wild-type *SOD1* transgenic cross

To produce this line *Sod1*^{D83G} mice were crossed to Tg*SOD1*^{WT} mice in a two-step cross. In the first step hemizygous Tg*SOD1*^{WT} males were mated with *Sod1*^{+/D83G} females, producing four possible genotypes: Tg*SOD1*^{WT}, *Sod1*^{+/D83G}, *Sod1*^{+/+}, and Tg^{WT}*Sod1*^{+/D83G} see Figure 2.2 (a). In the second step Tg^{WT}*Sod1*^{+/D83G} males were mated with *Sod1*^{+/D83G} females, producing six possible genotypes: Tg*SOD1*^{WT}, Tg^{WT}*Sod1*^{+/D83G}, Tg^{WT}*Sod1*^{D83G/D83G}, *Sod1*^{+/+}, *Sod1*^{+/D83G} and *Sod1*^{D83G/D83G} as illustrated in Figure 2.2 (b).

Genotyping for the presence of the transgene allele was carried out as described in section 2.5.2.1 while genotyping for the presence of the *Sod1^{D83G}* allele was carried out by Dr Abraham Acevedo using pyrosequencing at MRC Harwell.

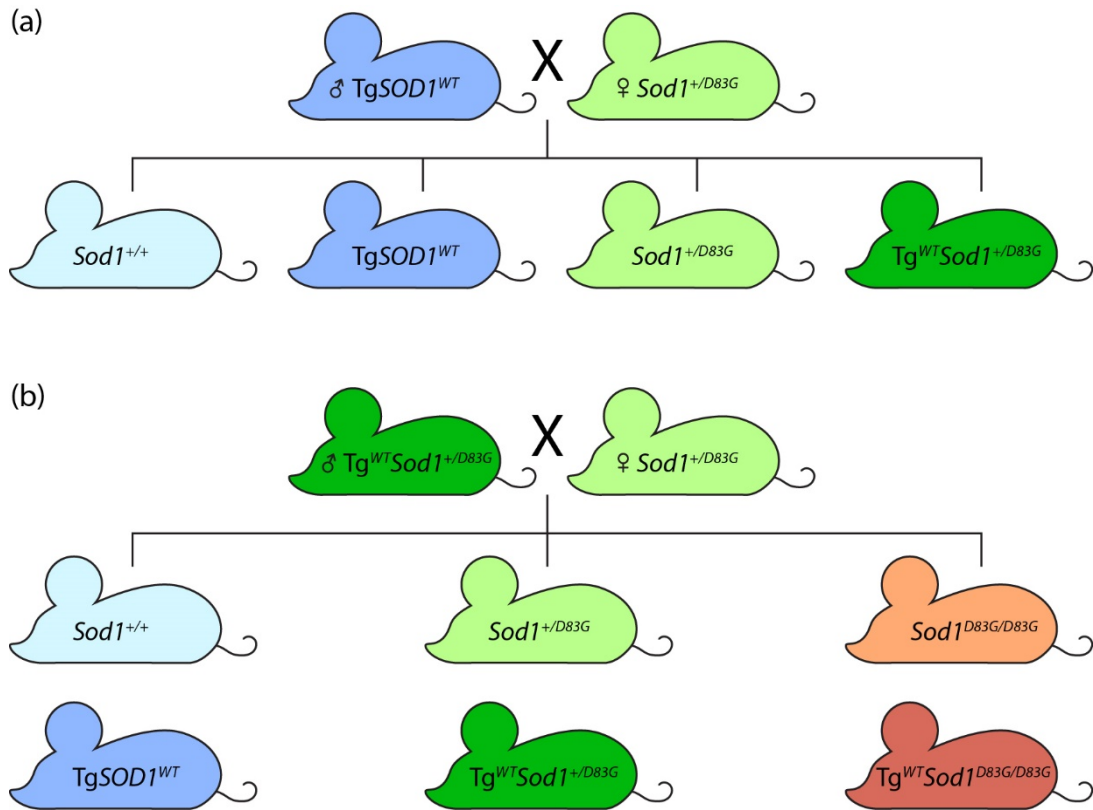


Figure 2.2 Breeding scheme for *Sod1^{D83G}* X *TgSOD1^{WT}*.

2.2.10 Galahad X Human *SOD1^{G93A}* transgenic high copy cross

To produce this line NTg*Galahad* females were crossed with hemizygous *TgSOD1^{G93A(H)}* males, producing two genotypes: NTg*Galahad* and *Tg^{G93A(H)}Galahad*. The line was maintained by crossing the *Tg^{G93A(H)}Galahad* males with wild-type C57BL/6J females, and NTg*Galahad* female with *TgSOD1^{G93A(H)}* males.

Genotyping was carried out as described in section 2.5.2.1.

2.3 Mouse experimental procedures

2.3.1 General mouse experimental procedures

2.3.1.1 Perfusion with paraformaldehyde

Mice were terminally anaesthetised by intraperitoneal injections with 200 μ l of 200 mg/ml sodium pentobarbital (Euthatal). Surgical plane of anaesthesia was

evaluated by blink reflex and paw pinch. Once unresponsive, the animal was pinned on its back, and the sternum was exposed by opening the abdominal cavity. An incision was made on the diaphragm along the entire length of the rib cage, which was subsequently cut on each side up to the collarbone. The sternum was lifted back to expose the heart and the pericardium was removed. A 27 gauge needle connected to a perfusion pump was carefully inserted into the left ventricle. The right atrium was cut and ice cold sterile 0.9 % NaCl (Sigma-Aldrich) was pumped into the heart for 4 minutes at 3 ml/min flow rate. The buffer was then changed and the animal was perfused with ice cold 4 % paraformaldehyde (PFA) (Sigma-Aldrich) in phosphate buffer saline (PBS) (Sigma-Aldrich) for 8 minutes at a flow rate of 3 ml/min flow rate.

2.3.2 Mouse experimental procedures specific for *Galabad* mice

2.3.2.1 Neurological checks

Galabad mice carrying a transgene were checked weekly by animal technicians for indications of neurological onset starting at 90 days of age for Tg^{G93A(H)}*Galabad* and at 150 days of age for Tg^{G93A(L)}*Galabad*. Animals were lifted by the tail and observed for the presence of the following symptoms: tremors, rear limbs moving towards the middle and paralysis.

2.3.2.2 Weekly weight

All *Galabad* mice were weighed weekly on a set day by technical staff starting at 90 days of age for Tg^{G93A(H)}*Galabad* and at 150 days of age for Tg^{G93A(L)}*Galabad* and NTg*Galabad*. When animals reached 10 % weight loss compared to their maximum body weight they were weighed daily. Weights have been analysed by ANOVA.

2.3.2.3 Grip-strength

Grip-strength of Tg^{G93A(L)}*Galabad* and NTg*Galabad* animals was evaluated once a week starting at 150 days of age. Measures were taken by technicians using Grip-strength meter bio-GS3 (BioSeb).

Each animal was lifted by the base of the tail and placed with all four feet on the mesh of the grip-strength meter. Once the mouse settled on a grip it was drawn back along the mesh in one single movement. Three individual measurements were taken for each time point, values were averaged and divided for the weight of the mouse of the correspondent week. Data were analysed by ANOVA.

2.3.2.4 Survival

Humane end points defined in section 2.2 have been used for *Galabud* mice. On reaching the human end points animals were perfused as described in section 2.3.1.1, and tissues were harvested as described below in section 2.4.2. Control mice that did not display ALS symptoms were kept until 315 days of age and then culled by exposure to rising concentration of CO₂.

Kaplan-Meier estimator was used for survival data analysis.

2.4 Histology

2.4.1 Harvesting of fresh tissues

For molecular biology experiments the following tissues were harvested fresh from each animal: brain, spinal cord, liver, sciatic nerves, tibialis anterior (TA) muscle, extensor digitorum longus (EDL) muscle and tail.

When collecting fresh samples animals were culled by cervical dislocation one at a time. The mouse was placed supine to dissect TA, EDL muscles and sciatic nerves. The skin on the leg was peeled off and the distal TA tendon was exposed. The ligament of the TA was cut and muscle was gently removed, the same was done for the EDL muscle. A deep cut was performed from the lumbar region of the vertebral column to the gluteal muscles to expose both sciatic nerves, which were then harvested. The mouse was turned on its back, a sample of the tail was taken and an incision on the abdomen was made to collect the liver. The head was then detached from the body and the brain was separated from the skull. Finally the whole column was removed from the body and the spinal cord was carefully pinned and dissected.

Immediately after dissection tissues were placed in cryotubes, snap frozen in liquid nitrogen and stored at -80 °C.

2.4.2 Harvesting and embedding of fixed tissues

Following perfusion fixed tissues were harvested from mice: brain, spinal cord, TA and EDL muscles.

TA and EDL muscles were dissected with the same technique used for fresh tissues described in section 2.4.1. They were then arranged on supports, post fixed for 3 hours in 4 % PFA at 4 °C and placed overnight in 40 % sucrose (Sigma-Aldrich), 0.001 %

sodium azide (Sigma-Aldrich) in PBS at 4 °C. The following day muscles were embedded in OCT freezing medium (Sakura) using aluminium foil moulds. Muscles were stored at -20 °C. Brain was dissected as described in section 2.4.1 and post fixed overnight in 4 % PFA at 4 °C. The following day it was placed in 40 % sucrose, 0.001 % sodium azide in PBS and stored at 4 °C. The column was removed from the body and post fixed overnight in 4 % PFA at 4 °C. The following day the spinal cord was dissected and stored in 40 % sucrose, 0.001 % sodium azide in PBS at 4 °C.

2.4.3 Neuromuscular junction (NMJ)

2.4.3.1 Sectioning of the extensor digitorum longus (EDL) muscle

A Bright™ cryostat was used to cut two series of 20 µm longitudinal sections of frozen EDL muscles. Muscles were cut through their entire length and since NMJs are approximately 40 µm in size all NMJs present in a muscle should be captured in each series. One of the two series cut per muscle was stained and analysed. Sections were collected onto poly-lysine coated slides (VWR), air dried at room temperature for 1 hour and stored at -20 °C.

2.4.3.2 Immunostaining

Muscle sections were defrosted, circled with a PAP pen (VWR) and air dried for 30 minutes. Slices were then placed in a humidified chamber at room temperature and kept there for the duration of the staining process.

Sections were washed 3 times for 5 minutes with TBS (Sigma-Aldrich) to remove OCT and then blocked for 1 hour with 3.5 % M.O.M. blocking reagent (Vector Labs) in TBS with 0.2 % Triton X-100 (Sigma-Aldrich) (referred to as TBS+). Slices were washed twice in TBS+ for 2 minutes and incubated for 30 minutes with 1:10 dilution of primary antibodies prepared in 7.5 % M.O.M. diluent (Vector Labs) in TBS+. The two primary antibodies used were mouse monoclonal anti-synaptic vesicle (SV2) (Developmental Studies Hybridoma Bank) and mouse monoclonal anti-neurofilament (2H3) (165 kDa) (Developmental Studies Hybridoma Bank). Sections were washed again in TBS+ and incubated for 10 minutes with M.O.M. biotinylated anti-mouse secondary antibody (Vector Labs) diluted 1:250 in M.O.M. diluent. Another TBS+ washing was applied to the section before incubation with fluorescent labelling performed as followed: 1:200 of streptavidin Alexa Fluor 488 (Invitrogen), 1:500 of α -bungarotoxin-rhodamine (Sigma-Aldrich) 1:500 of DAPI (Sigma-Aldrich) in TBS+ for

30 minutes in the dark. Sections were rinsed with TBS and cover slipped using florescent mounting media (DAKO), dried overnight at room temperature and stored at -20 °C.

2.4.3.3 Analysis

NMJs were manually counted using a Leica DMR epifluorescent microscope. The total number of NMJs in each muscle was assessed by identification of the end plates on the red florescence channel (stained by α -bungarotoxin-rhodamine). The innervation status of each NMJ, defined in Table 2.2, was evaluated by determining the co-localisation level between the muscle fibre end plate (red) and the foot plate of the motor neuron (green, stained by SV2 antibody). All analysis was carried out blind to genotype. Images were acquired on a laser scanner confocal microscope Zeiss LSM 710 using proprietary software (Carl Zeiss Ltd, Hertfordshire, UK).

Innervation status	Morphology
Innervated	Complete overlap between nerve terminal and endplate
Intermediate	Partial overlap between nerve terminal and endplate
Denervated	Absent overlap between nerve terminal and endplate
En-passant	Synapses that occur at a non-terminal region of an axon

Table 2.2 Classification of NMJs innervation status.

2.5 General DNA protocols

2.5.1 Nucleic acids extraction and purification from mouse tissue

DNA was extracted from 2 mm ear notches or from 0.5 mm tail biopsies. Two different extraction techniques have been employed: a fast DNA extraction for genotyping polymerase chain reaction (PCR), and a proteinase K DNA extraction for quantity real time polymerase chain reaction (qPCR) and pyrosequencing genotyping.

2.5.1.1 Fast DNA extraction

Tissues were incubated in 50 μ l Extraction Solution (Sigma-Aldrich) and 12.5 μ l Tissue Prep Solution (Sigma-Aldrich) for 20 minutes at room temperature then transferred at 95 °C for 4 minutes. Samples were centrifuged for 30 seconds at maximum speed in a bench top microfuge (Heraeus Fresco 17, Thermo Fisher). 50 μ l of Neutralisation Solution B (Sigma-Aldrich) were added and mixed by vortexing. Samples were then

centrifuged for 7 minutes at maximum speed. For genotyping PCR, 1 μ l of a 1:10 dilution in ddH₂O was used as template.

2.5.1.2 Proteinase K DNA extraction

Tissues were digested at 55 °C overnight in 210 μ l filtered lysis buffer: 20 mg/ml proteinase K (Invitrogen), 100 mM Tris (pH 8.0) (Sigma-Aldrich), 5 mM ethylenediaminetetraacetic acid (EDTA) (Sigma-Aldrich), 200 mM NaCl, 0.2 % sodium dodecyl sulphate (SDS) (Sigma-Aldrich). Once digested, the mixtures were centrifuged for 5 minutes, at 20817 $\times g$ at 4 °C to pellet non-digested tissues. Supernatants were transferred to clean 1.5 ml Eppendorf tubes. DNAs were precipitated by adding 200 μ l isopropanol (VWR) and pelleted by 10 minutes centrifugation at 20817 $\times g$ at 4 °C. The supernatants were then removed by pipetting, and the pellets were air-dried overnight at room temperature. DNA pellets were resuspended in 50 μ l TE buffer: 10 mM Tris-HCl (Sigma-Aldrich), 1 mM EDTA. One μ l of DNA diluted 1:10 in TE buffer was used as template for genotyping pyrosequencing and qPCR.

2.5.2 Polymerase chain reaction (PCR)

Primers were either supplied by collaborators ready to be used or purchased as desalted lyophilised pellets (Sigma-Aldrich). Purchased primers stocks were reconstituted to 100 μ M in ddH₂O and stored at -20 °C. Working dilutions were made to 5 μ M with ddH₂O and stored at -20 °C.

For genotyping PCR a 2X REDTaq ReadyMix (REDTaq) *Taq* polymerase from Sigma-Aldrich was used. Mega mix contained gel loading dye and buffer thus PCR products were loaded directly onto agarose gels.

2.5.2.1 SOD1 transgene genotyping PCR

This PCR protocol has been employed for genotyping all mouse lines with human *SOD1* wild-type or human *SOD1* G93A transgene: Tg*SOD1*^{WT}, Tg*SOD1*^{G93A(H)}, *Sod1*^{D83G} X Tg*SOD1*^{WT}, *Galabad* and *Galabad* X Tg*SOD1*^{G93A(H)} mice.

A 10 μ l master mix was used per sample, containing: 2X REDTaq, four primers defined in Table 2.3 at a concentration of 0.5 μ M, a template of 1 μ l of genomic DNA diluted 1:10 in ddH₂O or TE and appropriate quantity of ddH₂O to reach final volume. PCR was carried out using Peltier Thermal Cycler PTC-225 (Bio-Rad), cycling conditions are reported in Table 2.4. Products from PCR were resolved on a 2 %

agarose (Invitrogen), 45 mM Tris-borate (Sigma-Aldrich), 0.1 mM EDTA gel, (see below 2.5.2.3) running at 100 V for 30 minutes.

The success of the PCR was confirmed by the presence in all samples of a 324 bp fragment. This band amplifies across an intron 3/exon 3 boundary from the gene *Interleukin 2 (Il2)* on chromosome 3. While the presence of the transgene was established by a band of 236 bp which amplifies across exon 4 of the *SOD1* transgene, from intron 3 to intron 4 see Figure 2.3.

	Forward	Reverse
Control	CTAGGCCACAGAATTGAAAGATCT	GTAGGTGGAAATTCCTAGCATCATC
Transgene	CATCAGCCCTAATCCATCTGA	CGCGACTAACAATCAAAGTGA

Table 2.3 *SOD1* transgene genotyping primers.

Step	Condition	Temperature (°C)	Time (min)
1	denaturation	95	03:00
2	denaturation	95	00:30
3	annealing	60	00:30
4	extension	72	00:45
Cycle 35 times from step 2			
5	final extension	72	02:00
6	storing	4	forever

Table 2.4 PCR cycling conditions for *SOD1* transgene genotyping.

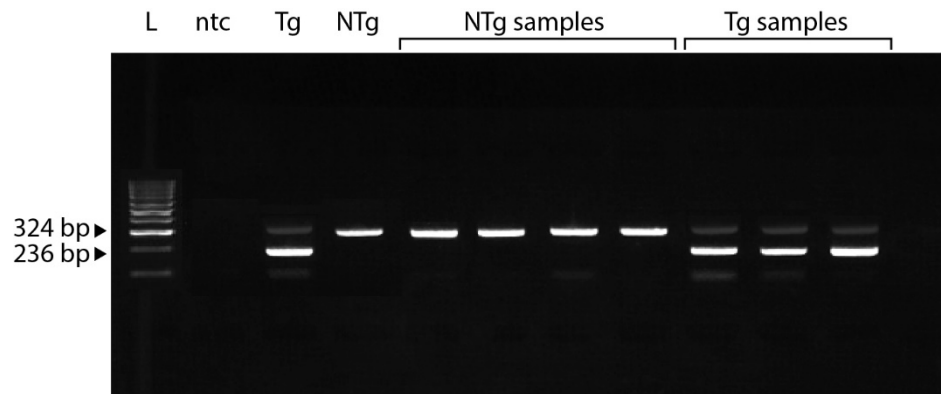


Figure 2.3 Example of transgene genotyping PCR. (L) Ladder, (ntc) no template control, (Tg) transgenic control, (NTg) non-transgenic control; non-transgenic and transgenic samples.

2.5.2.2 *Sod1* knockout genotyping PCR

This PCR protocol has been employed for genotyping all mouse lines with *Sod1* knockout allele: *Sod1* KO and *Sod1*^{D83G} X *Sod1* KO mice.

A 10 μ l master mix was used per sample, containing: 2X REDTaq, four primers defined in Table 2.5 at a concentration of 0.5 μ M, a template of 1 μ l of genomic DNA diluted 1:10 in ddH₂O or TE and appropriate quantity of ddH₂O to reach final volume. PCR was carried out using the cycling conditions defined in Table 2.6.

Products from PCR were resolved on a 2 % agarose, 45 mM Tris-borate, 0.1 mM EDTA gel, (see below 2.5.2.3) running at 100 V for 30 minutes.

The presence of a wild-type allele was revealed by a 123 bp band amplified from exon 2 to intron 2 of *Sod1* on chromosome 16. While the presence of the knockout allele was established by a band of 240 bp which presumably amplifies from the selection cassette used to replace exon 1 and exon 2, however the sequence was not published by (Matzuk et al., 1998) and details are not given on the Jax website.

	Forward	Reverse
Control	TGAACCAGTTGTGTGTCAGG	TCCATCACTGGTCACTAGCC
KO	TGTTCTCCTCTTCCTCATCTCC	ACCCTTCCAAATCCTCAGC

Table 2.5 *Sod1* knockout genotyping primers.

Step	Condition	Temperature (°C)	Time (min)
1	denaturation	95	03:00
2	denaturation	95	00:20
3	annealing	61	01:00
4	extension	72	01:00
Cycle 35 times from step 2			
5	final extension	72	05:00
6	storing	4	forever

Table 2.6 PCR cycling conditions for *Sod1* knockout genotyping.

2.5.2.3 Agarose gel electrophoresis (AGE)

For electrophoresis of PCR products 6 mm gels were prepared by dissolving 2 % Invitrogen UltraPure agarose in 100 ml 4.5 mM Tris-borate, 0.1 mM EDTA (TBE buffer). The solution was heated in a microwave for 1-2 minutes, allowed to cool slightly before adding 0.05 µg/ml of ethidium bromide (Sigma-Aldrich) and poured into gel casts (Scie-plas). Gels were left at room temperature to solidify for about 30-40 minutes.

Electrophoresis was carried out at 100 V at room temperature for 30 minutes in TBE buffer using horizontal submarine gel tanks (Mupi). Gels were visualized and imaged using a UV illuminator and digital imaging system (ChemiDoc XRS+ Bio-Rad). A quantitative DNA ladder was used to assess the size of the DNA bands: HyperLadder IV (Bioline).

2.5.3 *Galabad* chromosome single-nucleotide polymorphism PCR

This PCR protocol has been used to amplify DNA for pyrosequencing assays (carried out by collaborators at MRC Harwell) for *Galabad* and *Galabad* X Tg*SOD1*^{G93A(H)} mice.

Six PCRs were run per samples with different primers pairs defined in Table 2.7. A 10 µl master mix was used for each sample, containing: 2X REDTaq, a forward and a reverse primer both at a concentration of 0.2 µM, a template of 2 µl of genomic DNA diluted 1:10 in TE and appropriate quantity of ddH₂O to reach final volume. PCR was carried out using Peltier Thermal Cycler PTC-225, for cycling conditions see Table 2.8.

Chr1 166 Mb	Forward	GTTTACGATGTTGCATT
	Reverse	AAAATTCTGGTTTACGATGTTGCAT
	Biotinylated	TCCTTAGACATAGGCAATTACAGC
Chr1 181 Mb	Forward	GCGTGTAAAGCCCAA
	Reverse	TGCTGGGTGTGTTGAGGTTTG
	Biotinylated	CCTCTGCCAGTTCACAATGG
Chr1 191 Mb	Forward	CTGGCAGCTGGATG
	Reverse	TGAAATACTGGCAGCTGGATG
	Biotinylated	GGGAAGATTTTGCATCCTGTGAG
Chr7 40 Mb	Forward	ACGTACCAGGTCCAGT
	Reverse	AGGGTCTGCGGCTAATAG
	Biotinylated	ATATACACACCTCGACCTACCAC
Chr7 60 Mb	Forward	GAGCACATATTCAGGGT
	Reverse	AATGGGAAAAATCTGTGTTGT
	Biotinylated	TTGGCAGAAGCTTGACTTA
Chr7 90 Mb	Forward	ACAACCAACCCTCTTC
	Reverse	AAACAACCAACCCTCTTCA
	Biotinylated	CAGTGCCAAGATGACCAG

Table 2.7 *Galahad* genotyping primers.

Step	Condition	Temperature (°C)	Time (min)
1	denaturation	95	05:00
2	denaturation	95	00:15
3	annealing	60	00:30
4	extension	72	00:15
Cycle 44 times from step 2			
5	final extension	72	05:00
6	storing	4	forever

Table 2.8 *Galahad* PCR cycling conditions.

2.5.4 Quantitative real time PCR (qPCR) for *SOD1* transgene copy number

The qPCR protocol to determine transgene copy number was developed by Dr Rosie Bunton-Stasyshyn from the procedure published on Jackson Laboratory website: <http://jaxmice.jax.org>. Assays and the analysis were carried out by technical staff and used to assess copy number for the following mouse lines: Tg*SOD1*^{G93A(HI)}, *Galahad* and *Galahad* X Tg*SOD1*^{G93A(HI)}.

The assay used TaqMan (Applied Biosystems) reagents and relative standard curve quantitation of multiplex reactions, containing one measure of the transgene (Tg) and one internal endogenous control (EC).

Primers and probes defined in Table 2.9 have been purchased from Sigma-Aldrich as lyophilised pellets and resuspended to 100 µM. The endogenous control primers amplified 74 bp from exon 24 of the *Apob* gene on mouse chromosome 12. The transgene primers amplified 88 bp from intron 4 of the human *SOD1* transgene.

A 10 µl master mix was used for each sample, containing: 2X TaqMan Universal PCR Master Mix, 0.8 µM of EC forward and EC reverse primers, 0.1 µM of Tg forward and Tg reverse primers, 0.1 µM of EC and Tg probes, a template of 1 µl of genomic DNA diluted 1:20 and appropriate quantity of ddH₂O to reach final volume. For each assay plate a five point standard curve was created using a known copy number DNA by Jackson Laboratory at the following concentrations: 100, 20, 4, 0.8 and 0.16 ng/µl. Each point on the standard curve was replicate six times. Three replicates were measured for the *SOD1* Tg standard curve and three were measured for the EC standard curve. On each plate experimental DNA samples and two control DNAs (a Jackson Laboratory control and a known reduced copy number sample) were assayed over four replicate reactions. Applied Biosystems 7500 Software v2.0.1 was used to set up a standard run, using default baseline and threshold settings and the cycling conditions describe in Table 2.10. The delta threshold cycle (Ct) was calculated by subtracting the mean *SOD1* Tg Ct from the mean EC Ct for each replicate group. The delta-delta Ct was then calculated by subtracting the replicate group delta Ct from the Jackson Laboratory control delta Ct. Relative quantity was then calculated as 2 to the power of the negative delta-delta Ct.

Primers and probes	Sequence	5' label	3' label
Endogenous control (EC) forward primer	CACGTGGGCTCCAGCATT		
Endogenous control (EC) reverse primer	TCACCAGTCATTTCTGCC TTTG		
Transgene (Tg) forward primer	GGGAAGCTGTTGTCCCA AG		
Transgene (Tg) reverse primer	CAAGGGGAGGTAAAAGA GAGC		
EC probe	CCAATGGTCGGGCACTG CTCAA	Cy5	Black Hole Quencher 2
Tg probe	CTGCATCTGGTTCTTGCA AAACACCA	6-FAM	Black Hole Quencher 1

Table 2.9 *SOD1* transgene copy number qPCR primers and probes.

Step	Temperature (°C)	Time (min)
1	50	02:00
2	95	10:00
3	95	00:15
4	60	01:00

Cycle 39 times from step 3

Table 2.10 *SOD1* transgene copy number qPCR cycling conditions.

2.6 SOD1 protein protocols

2.6.1 Production and purification of wild-type and mutant SOD1 recombinant proteins

Human and mouse SOD1 proteins were produced and purified from an *E. coli* expression system. All expression constructs have been generated and cloned into vectors by Dr Ruth Chia, Dr David Emery and Julian Pietrzyk see Appendix 8.1 for more details. Constructs were transformed into *E. coli* strain BL21 (DE3) (Novagen) by Dr Chia Ruth and Mark Bachelor. To confirm that constructs were successfully

transformed, Dr Chia Ruth and Mark Bachelor also performed a small scale protein expression screen on each colony. Plasmids were isolated for sequence verification to ensure the construct did not change during transformation. Cells were stored at -80 °C in 15 % glycerol (Sigma-Aldrich).

2.6.1.1 Protein expression, cell harvesting and cell lysis

Protein expression

To produce a sufficient amount of proteins each construct was expressed in 9 l culture Figure 2.4 (a). A transformant colony was inoculated in 100 ml autoclaved 4 % Luria Broth in ddH₂O (LB) (Sigma-Aldrich) with 50 µg/ml kanamycin (Sigma-Aldrich) and grown overnight at 37 °C in a shaking incubator (200 rpm) (Orbital). The following day nine erlenmeyer flasks (Nalgene) containing 1 l of autoclaved LB and 50 µg/ml kanamycin each, were inoculated with 11 ml of overnight growth. Cells were grown at 37 °C in a shaking incubator (200 rpm) until the optical density at 600 nm (OD₆₀₀) was between 0.6-1.0 (about 2.5 hours). Cells were then induced overnight at 37 °C in a shaking incubator (250 rpm) by addition of 1 ml of 1 M isopropyl-β-D-thiogalactopyranoside (IPTG) (Melford).

Cell harvesting

Harvesting of cells was performed by successive centrifugation and decantation of supernatant in 1 l polypropylene bottles (Nalgene) at 17000 *x g* for 5 minutes at 10 °C using a Sigma Laboratory Centrifuge 6K15 (rotor Nr. 12500) see Figure 2.4 (b). If not used immediately cell pellets were stored at -80 °C, otherwise they were carefully resuspended in 100 ml of extraction buffer: 50 mM Tris-HCl, 200 mM NaCl, 0.1 % Tween-20 (Sigma-Aldrich), 50 U/ml benzonase (VWR), 10 µg/ml lysozyme (Sigma-Aldrich) at pH 8.0.

Cell lysis

Cells resuspended in extraction buffer were lysed by sonication (sonicator probe MS73, Sigma-Aldrich) with 2 minutes bursts at 45 % power repeated 3 times. The solution was clarified by centrifugation at 17000 *x g* for 30 minutes at 10 °C (rotor number: 12166) the supernatant was discarded and the pellet retained. The extraction step was repeated a second time using the same conditions to obtain a new pellet, Figure 2.4 (c).

Solubilisation

Pellet was resuspended in 40 ml solubilisation buffer: 6 M GuHCl (Sigma-Aldrich), 50 mM Tris-HCl, and 0.8 % 2-mercaptoethanol (Sigma-Aldrich) at pH 8.0. The solution was sonicated with 2 minutes bursts at 45 % power repeated 3 times and clarified by centrifugation at $21000 \times g$ for 45 minutes at 10°C . Supernatant was retained, pellet was resuspended again in 40 ml solubilisation buffer, and the process was repeated at the same conditions. The pellet was now discard and the supernatant was combined with the one obtained before and stored at -20°C , see Figure 2.4 (d).

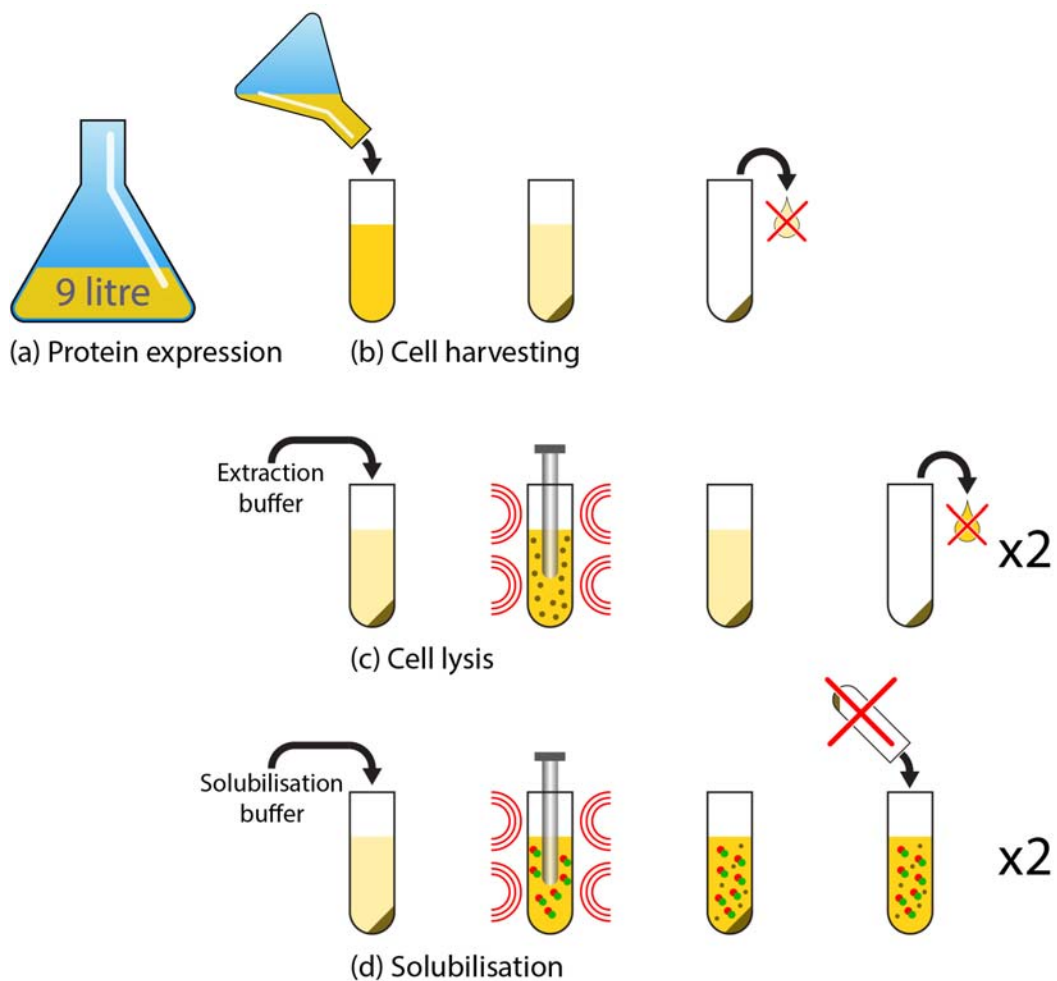


Figure 2.4 SOD1 protein production. (a) Each construct was expressed in 9 l culture. (b) Bacterial growth was centrifuged and cell pellet retained. (c) Cell pellet was resuspended in extraction buffer. Suspension was sonicated centrifuged, and pellet retained. The process was repeated twice. (d) Pellet was resuspended in solubilisation buffer, sonicated and supernatant containing His-tagged SOD1 protein was retained. The process was repeated twice.

2.6.1.2 Affinity chromatography Ni-NTA

Metal chelate affinity chromatography with nickel ions immobilised on a nitrilotriacetic acid sepharose matrix (Ni-NTA) was used to purify SOD1 proteins. A technique based on the high specificity bond between immobilised nickel ions and histidine residues in the His-tag fused to SOD1 proteins.

Ni-NTA runs were performed at room temperature using an ÄKTA pure (GE Healthcare Life Sciences) chromatography system. Each purification process required two Ni-NTA column runs. The first run removed contaminated proteins from the cell lysate, the second removed the free His-tag after cleavage from SOD1.

Column details

A 65 ml glass column (BioRad) packed with 150 ml Ni-NTA resin (Qiagen) was used for protein purification. The column resin was recharged with metal ions every 6 runs, see protocol in section 8.3. The column was stored at room temperature in 20 % ethanol (VWR).

First column

A column was flushed with 120 ml ddH₂O and equilibrated with 120 ml of filter sterilised buffer A: 6 M GuHCl, 10 mM Tris-HCl, 100 mM Na₃PO₄ (Sigma-Aldrich), 10 mM glutathione (GSH) (Sigma-Aldrich) at pH 8.0. The column was then loaded with solubilised protein preparation previously defrosted and filtered, and flushed with 120 ml of buffer A. Protein was refolded on-column overnight with a gradient of 0-100 % filter sterilised buffer B (10 mM Tris-HCl, 100 mM Na₃PO₄ at pH 8.0) over 30 column volumes. The following day protein was eluted with a gradient of 0-100 % filter sterilised buffer C (10 mM Tris-HCl, 100 mM Na₃PO₄, 2 M imidazole (Sigma-Aldrich) at pH 7.0) over 2 column volumes. See Figure 2.5 (a).

Dialysis and cleavage

Protein was transferred within a dialysis membrane (Spectra pro) and dialysed at room temperature for 3 hours in 5 l of 25 mM Tris-HCl, 150 mM NaCl at pH 8.4 in ddH₂O over 3 buffer changes. Concentration of the protein sample was measured using absorbance at OD₂₈₀. His-tags were then cleaved from the protein by addition 0.1 U thrombin (VWR) per 1 mg of protein and CaCl₂ (Sigma-Aldrich) at a final concentration of 2.5 mM see Figure 2.5 (b). The solution was left shaking overnight at room temperature to assure complete cleavage.

Second column

A column was flushed with 120 ml ddH₂O and equilibrated with 120 ml of filter sterilised buffer D: 20 mM Tris-HCl, 300 mM NaCl at pH 8.0. The protein solution was loaded into the column and eluted over 5 column volume of 0-100 % gradient of filter sterilised buffer E: 20 mM Tris-HCl, 300 mM NaCl, 2 M imidazole at pH 8.0 as illustrated in Figure 2.5 (c).

After use column was cleaned with 150 ml of 6 M GuHCl, 2 M imidazole to remove flushed with 120 ml of ddH₂O and stored in 20 % ethanol.

Dialysis and Cu/Zn metal loading

Protein obtained from the second column run was dialysed at room temperature for 3 hours in 20 mM Tris-HCl, pH 8.0 over 3 buffer changes.

Protein was then either stored at -80 °C in 15 % glycerol or metal loaded with copper and zinc by subsequent dialysis at room temperature. The first dialysis was carried out for 3 hours in 5 l of 100 mM Tris-HCl, 300 mM NaCl, 150 µM of CuSO₄ (Sigma-Aldrich) in ddH₂O at pH 8.0; the second for 3 hours in 5 l of 100 mM Tris-HCl, 300 mM NaCl, 150 µM of ZnSO₄ (Sigma-Aldrich) in ddH₂O at pH 8.0. Finally the protein was dialysed in storage buffer containing 20 mM Tris-HCl in ddH₂O at pH 7.5, snap freeze and stored at -80 °C.

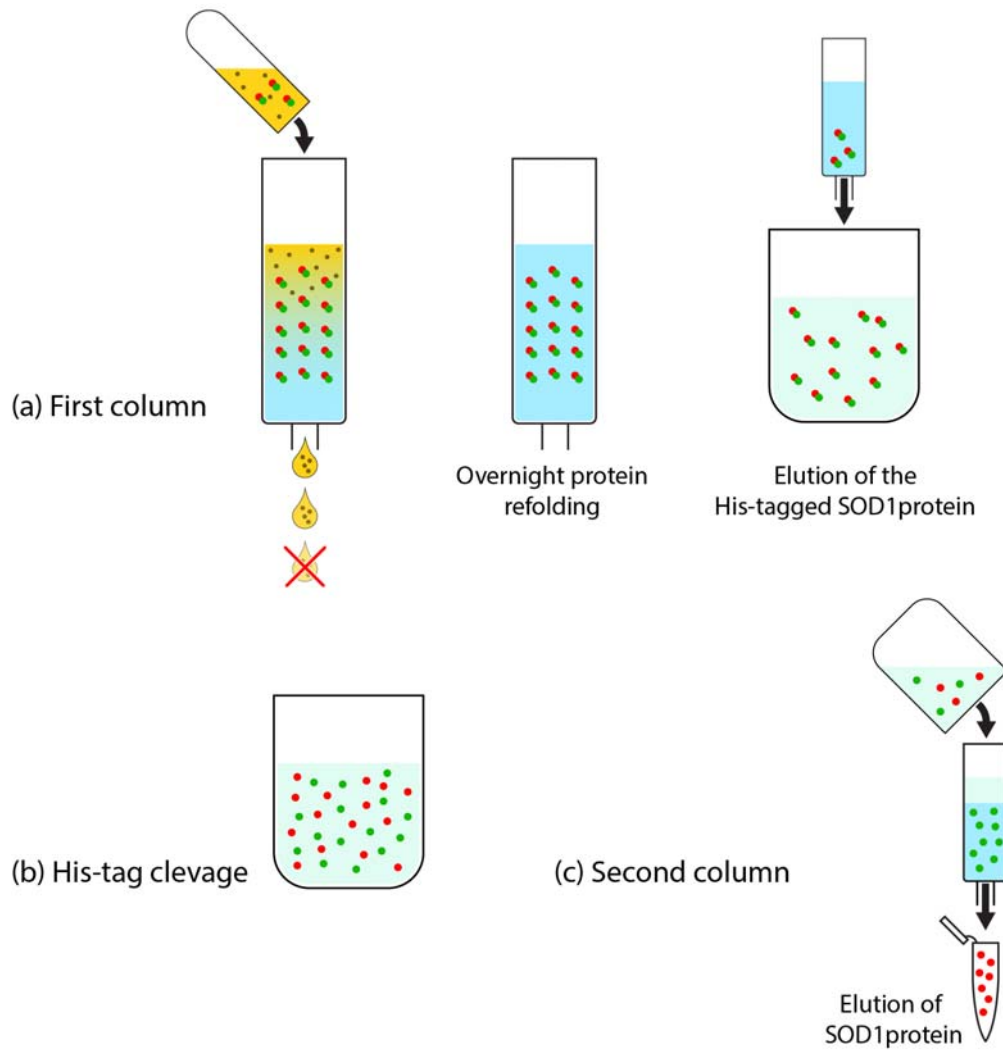


Figure 2.5 SOD1 protein purification. (a) Solubilised protein preparation was loaded to the column. Contaminates were removed and protein refolded overnight. His-tagged SOD1 protein was collected. (b) Overnight cleavage of the His-tags from SOD1 protein. (c) Cleaved solution was loaded to the column, only free His-tags attached to the resin and SOD1 protein was collected.

2.6.2 Preparation of animal tissues for protein investigation

2.6.2.1 Brains preparation specific for *Sod1*^{D83G} experiments

Frozen mouse brains collected as described in section 2.4.1 were rinsed in PBS and weighed. Brains were homogenised using a TissueRuptor (Qiagen) in ice cold lysis buffer 0.1 M Tris-HCl at pH 7.4, 0.5 % Triton X-100, 1 mM EDTA and complete EDTA-free protease inhibitors (Roche) to make a 10 % weight/volume solution. Crude homogenates were kept on ice for 20 minutes and centrifuged at 14000 $\times g$ for 10 minutes at 4 °C. Supernatants were collected and stored at -80 °C.

2.6.2.2 Spinal cord preparation specific for transmission experiments

Frozen mouse spinal cords collected as described in section 2.4.1 were homogenised using TissueRuptor in ice cold PBS to make a 10 % weight/volume solution. Crude homogenates were kept on ice for 20 minutes, filtered using a syringe with a 20 gauge needle and stored at -80 °C.

2.6.3 Spectrophotometric protein concentration measurements

2.6.3.1 Absorbance

While performing affinity chromatography (2.6.1.2) protein concentration of samples was estimated using absorbance. One ml of protein sample diluted 5 times was measured for absorbance at 280 nm using NanoDrop® ND-1000 Spectrophotometer. The concentration for SOD1 was calculated using an experimentally determined extinction coefficient (ϵ_{SOD1}) at 280 nm of $10800 \text{ M}^{-1}\text{cm}^{-1}$ (Choi et al., 2005) calculated using the following formula:

$$\text{SOD1 concentration (M)} = \text{OD}_{280} / \epsilon_{\text{SOD1}}$$

2.6.3.2 Colorimetric assays

Two different type of colorimetric protein assay kits with different reactivity to detergents have been employed to measure protein concentration: Bradford assay (Bio-Rad) and DC protein assay (Bio-Rad).

Bradford assay

This assay was used, according to manufacturer's instructions, to determine the concentration of solubilised proteins towards the addition of an acidic dye. A differential colour change of the day occurred in response to different protein concentration. Absorbance measured at 595 nm with a 96 well microplate reader (Sunrise, Tecan) and comparison to a standard curve provided a relative quantification of protein concentration.

DC protein assay

The DC protein assay was used, according to manufacturer's instructions, to measure the relative concentration of solubilized protein. The assay was based a reaction of the protein with alkaline copper tartrate solution followed by the reduction of the folin reagents with the copper treated-protein which produce several reduced species with a

characteristic blue colour. Measurement of the absorbance at 750 nm using a 96 well microplate reader and comparison with a standard curve provided quantification of the relative protein concentration.

2.6.4 Polyacrylamide gel electrophoresis

Gel electrophoresis and blotting were carried out using XCell *SureLock* Mini-Cell Electrophoresis System from Life Technologies. All types of precast polyacrylamide gels, buffers and protein standards have been also purchased from Life Technologies unless specified differently. Gels and blots were quantified using ImageJ software.

2.6.4.1 Coomassie blue staining

SDS-polyacrylamide gel electrophoresis (SDS-PAGE)

For coomassie blue staining proteins were separated by polyacrylamide gels electrophoresis on 16 % Tris-glycine precast gels with 1X Tris-glycine SDS running buffer (National Diagnostic). Prior to running, samples were mixed with 1X Tris-glycine SDS sample buffer, 2 % 2-mercaptoethanol, heated at 100 °C for 2 minutes and loaded onto the gel. Electrophoresis was performed at room temperature at 125 V for 90 minutes. A BSA (Sigma-Aldrich) control of a known concentration and SeeBlue plus2 protein standard were include in all experiments.

Proteins visualisation

Proteins were visualised by soaking the gel for 1 hour in coomassie brilliant blue solution containing: 10 % acetic acid (VWR), 60 mg / l of Coomassie Blue R (Sigma-Aldrich) in ddH₂O. Gels were destained in ddH₂O until they become colourless and only protein bands were visible. All gels were imaged using an hp scanner. For protein concentration analysis the proteins of interest were compared to the BSA control.

2.6.4.2 Western blot

SDS-polyacrylamide gel electrophoresis

For reducing and denaturing western blots, proteins were separated by polyacrylamide gels electrophoresis on 4-12 % NuPAGE Bis-Tris precast gels with 1X MES running buffer. Prior to running, samples to a final concentration of 30 µg were mixed with 2X LDS sample buffer, 2 % 2-mercaptoethanol and heated at 70 °C for 10 minutes. Electrophoresis was performed at room temperature at 200 V for 35 minutes, SeeBlue

ladder was used in all experiments in order to identify the molecular weight of the proteins of interest.

Transfer

Proteins were transferred by electro-blotting from the gel to a polyvinylidene difluoride (PVDF) membranes (Millipore). Each PVDF membrane was pre-wet in methanol (VWR) at least for 2 minutes before use. Electro-blot was performed at room temperature at 35 V for 2 hours using a transfer buffer made up with 1X Tris-Glycine Electroblotting buffer (National Diagnostic), 10 % methanol.

Blocking

The membrane was blocked in blocking solution (Odyssey blocking buffer (PBS) Licor) for 1 hour at room temperature.

Immunodetection of SOD1

The membrane was incubated overnight at 4 °C with SOD-100 primary antibody (Enzo) (1:2000) and anti- β -actin (Sigma-Aldrich) (1:10000) in 50 % blocking solution, 50 % PBS with 0.05 % Tween (PBS-T). The unbound antibodies were removed by 3 washes of 5 minutes in PBS-T. Membrane was then exposed for 2 hours in the dark to infrared secondary antibodies: IRDye Licor anti-mouse (1:10000) and IRDye Licor anti-rabbit (1:10000) in 50 % blocking solution, 50 % PBS-T. The membrane was washed 2 times for 5 minutes with PBS-T and 1 time for 5 minutes with PBS prior imaging using Odyssey Classic from Licor. For quantification proteins were normalized for β -actin internal control.

2.6.4.3 Native western blot

Native-polyacrylamide gel electrophoresis

For native western blots proteins were separated by polyacrylamide gels electrophoresis on 3-12 % NativePAGE Bis-Tris precast gels in non-denaturing and non-reducing conditions. Samples to a final concentration of 30 μ g were mixed with 1X NativePAGE sample buffer and loaded onto the gel. Electrophoresis was performed at room temperature in two stages. In the first stage the outer chamber of the electrophoresis tank was filled with 600 ml of 1X NativePAGE running buffer and the inner chamber was filled with 200 ml of dark blue cathode buffer (1X NativePAGE running buffer, 1X NativePAGE cathode buffer additive). The gel was electrophoresed for 40 minutes at 120 V until the dye front migration was 1/3rd of the gel. For the

second stage the inner chamber buffer was substituted with 200 ml of light blue cathode buffer (1X NativePAGE running buffer, 0.1X NativePAGE cathode buffer additive). Proteins were resolved on the gel for another hour at 120 V. NativeMark unstained protein standard was used in all experiments.

Transfer

Proteins were transferred to a PVDF membrane by electro-blotting. The membrane was pre-wet in methanol at least for 2 minutes and the gel was soaked for 15 minutes in 50 ml of 0.1 % SDS in ddH₂O. Electro-blotting was performed at room temperature at 35 V for 2 hours using 1X NuPAGE transfer buffer.

Blocking

To prevent diffusion of proteins, the membrane was soaked in 20 ml of 8 % acetic acid for 15 minutes, washed with ddH₂O and air dried for at least 30 minutes. The membrane was then reactivated in methanol for 2 minutes rinsed in ddH₂O and blocked in Odyssey blocking solution for 1 hour at room temperature.

Immunodetection of SOD1

Three different antibodies against SOD1 have been employed in native western blot experiments, concentrations and secondary antibodies details are given in Table 2.11. Membrane was incubated overnight at 4 °C with primary antibody diluted in 50 % blocking solution, 50 % PBS-T. The following day unbound antibodies were removed by 3 washes of 5 minutes in PBS-T. Membrane was incubate for 2 hours with horseradish peroxidase (HRP) conjugated secondary antibody diluted in 50 % blocking solution, 50 % PBS-T and was washed 2 time for 5 minutes with PBS-T and 1 time for 5 minutes with PBS. Enhanced chemiluminescent substrate (ECL) (Pierce) was applied to each membrane for 5 minutes to detect HRP. In the dark room photo-films were exposed to a membrane and developed. Exposure time varied as needed for optimal detection.

Primary antibody	Secondary antibody
SOD-100 (Enzo) 1:1000	Goat anti-rabbit IgG-HRP (DAKO) 1:5000
SEDI (Rakhit et al., 2007) 1:1000	Goat anti-rabbit IgG-HRP (DAKO) 1:5000
USOD (Kerman et al., 2010) 1:100	Goat anti-rabbit IgG-HRP (DAKO) 1:5000

Table 2.11 Primary and secondary antibodies for native blots.

2.6.4.4 SOD1 activity in-gel assay

To perform an in-gel assay for SOD1 activity quantification, 30 µg of brain homogenates were resolved using 3-12 % NativePAGE Bis-Tris precast gels in 1X NativePAGE running buffer. Samples were mixed with 2X NativePAGE sample buffer and electrophoresed at 120 V for 50 minutes. The gel was then soaked for 45 minutes in the dark with 50 mM potassium phosphate (Sigma-Aldrich) at pH 7.8, 275 µg/ml nitro blue tetrazolium (Sigma-Aldrich), 65 µg/ml riboflavin (Sigma-Aldrich), and 3.2 µl/ml TEMED (Sigma-Aldrich). The gel was rinsed with ddH₂O and developed by exposure to light.

2.6.5 Protein characterisation using circular dichroism (CD)

Secondary structure of purified SOD1 proteins was determined by circular dichroism (CD) spectroscopy. Prior to analysis, SOD1 proteins were dialysed over 3 buffer change in 20 mM sodium phosphate (Sigma-Aldrich) at pH 7.5. CD spectra at far-UV 250-190 nm was performed with a J-715 Circular Dichroism Spectropolarimeter (Jasco) using 0.1 mm path length circular cuvette. Data were collected at a stop resolution of 1 nm, a scan speed of 50 nm/minute, and 1 second response time. Each protein sample was measured over 10 accumulations and corrected against storage buffer. Protein concentrations were approximately 1.0 mg/ml, and CD measurements were converted to units of molar ellipticity ([θ]). Corrections and processing were performed using the Jasco Standard Analysis Software (Jasco).

2.6.6 Conversion of SOD1 proteins into fibrils *in vitro*

To form amyloid fibrils each recombinant protein was diluted to a final protein concentration of 10 µM in filtered 20 mM Tris acetate buffer (Sigma-Aldrich) with 0.5 M GuHCl at pH 3.0, containing a final concentration of 10 µM Thioflavin-T (ThT) (Sigma-Aldrich). The assay was carried out on a 96 well plate with transparent flat bottom, prearranged with 4 Hybaid Ribolyser beads per well. For each sample 200 µl of reaction mixture was pipetted into 6 wells and the plate was covered with optically corrected adhesive film. The plates was incubated with continuous shaking at 830 rpm at 37 °C using GrantBio plate incubator shaker. The kinetics of fibril formation were monitored daily by measuring fluorescence emission at 485 nm when excited at 450 nm using a fluorimeter plate reader (Infinite M1000 PRO, Tecan) with i-control™ software.

The lag phase of amyloid formation was determined by fitting the time-dependent changes in the fluorescence of ThT (F) overtime of the reaction (t) to using the equation:

$$F = A + B / (1 + \exp [k * (t_m - t)])$$

In the equation above (A) is the base lave of florescence during the lag phase, (B) difference between final fluorescence level at plateau and the initial level during the lag phase, (k) is the rate constant of fibril growth (h^{-1}), and (t_m) is the observed time at transition midpoint. The lag time (t_l) of fibril formation was calculated as: $t_l = t_m - 2 / k$ (Chia et al., 2010) .

2.7 Meta-analysis on SOD1 activity in SOD1-ALS affected patients

Data for meta-analysis were collected by searching Pubmed, ALSoD and Medline electronic databases between 1993 and April 2015. Reference lists from relevant articles and from all papers obtained were also checked. The search terms used are listed below and they have been employed both alone and in combination with each other.

Search terms: amyotrophic lateral sclerosis, SOD1 enzymatic activity, fALS, loss of function, red blood cells, fibroblasts, lymphoblast cells lines, in-gel activity assay. All names of *SOD1* mutations have also been used as search terms in combination with the words “enzymatic activity” for example: “SOD1 G93A enzymatic activity”.

Original papers but no abstracts or reports from meetings were considered. Studies were grouped according to the type of data presented and examined for sources and type of SOD1 enzymatic activity measurements taken. Only articles where SOD1 activity was assessed from red blood cells, fibroblasts and lymphoblast cells lines of fALS patients were taken into consideration for analysis.

2.8 Statistical analysis

Statistical analysis was carried out using IBM SPSS, GraphPad Prism 6 and R with the exception of Chi Square test for calculation of inheritance ratios that was carried out using Graph Pad online <http://graphpad.com/quickcalcs/chisquared1.cfm>.

Chapter 3 SOD1 loss of function in SOD1-amyotrophic lateral sclerosis

3.1 Introduction

In 1993 Rosen and colleagues identified the first ALS causative mutations, 11 missense substitutions spread throughout the *SOD1* gene. This result together with the finding of loss of dismutase activity in ALS patients, initially suggested a loss of function as a disease causative mechanism (Deng et al., 1993; Rosen et al., 1993).

However, in 1994 analysis of a mutant SOD1 transgenic mouse model (Tg*SOD1*^{G93A}) gave the first indication for a gain of function mechanism as the cause of ALS (Gurney et al., 1994). Tg*SOD1*^{G93A} mice indeed exhibited an increased SOD1 activity together with a progressive adult onset motor phenotype with loss of lower MNs.

Subsequent data from human and mouse studies supported the hypothesis that ALS arises from a gain of function mechanism. For example, in humans SOD1 dismutase activity did not correlate with aggressiveness of clinical features (Ratovitski et al., 1999). Mice lacking the *Sod1* gene (*Sod1*^{-/-}) had no SOD1 activity and did not display ALS-like phenotypes (Reaume et al., 1996). Moreover most of the transgenic mouse models overexpressing mutant human SOD1 (Joyce et al., 2011) showed an increased SOD1 activity and loss of MNs.

The idea that a loss of function played a role in the disease was abandoned without question in 1998, when Bruijn and colleagues compared the survival of a transgenic SOD1 mouse model (Tg*SOD1*^{G85R}) on a normal wild-type background and on a *Sod1*^{-/-} background. The two mouse lines showed no change in survival, demonstrating that survival was influenced by a gain of function mechanism while was independent from mouse SOD1 loss of function (Bruijn et al., 1998).

Further studies on SOD1-ALS together with the identification of other ALS causative genes confirmed the undeniable presence of a still unknown toxic gain of function as cause of this disease. Several mechanisms by which this gain of function might occur have been proposed and reviewed (Ilieva et al., 2009; Rothstein, 2009; Turner and Talbot, 2008). However, recently additional investigations on transgenic SOD1 mice and *Sod1*^{-/-} mice pointed to the possibility that a loss of dismutase activity may contribute to SOD1-fALS.

3.2 Aim

The aim of the work described in this chapter was to re-examine over twenty years of human and mouse research on SOD1 dismutase activity to see if SOD1 loss of function may play a modifying role in SOD1-ALS.

In particular published data regarding SOD1 enzymatic activity of SOD1-ALS patients, and phenotypic data of *Sod1* knockout mice were analysed and reviewed.

3.3 Results

3.3.1 SOD1 loss of function in SOD1-fALS patients

Published papers about SOD1 enzymatic activity measured in SOD1-fALS patients were collected and reviewed as described in section 2.7.

3.3.1.1 Methods of measuring SOD1 dismutase activity

In mammals there are three unique and highly compartmentalized superoxide dismutases: SOD1 localised in the cytoplasm, SOD2 (Mn-SOD) localised in the mitochondrial matrix (Fridovich, 1986; Zelko et al., 2002) and SOD3 (Fe-SOD) which is mainly extracellular (Marklund et al., 1982). The presence of other two antioxidant enzymes similar to SOD1 complicates the measures of its activity.

Two methods have been employed to assess SOD1 activity in patients: the “activity assay” and the “gel assay”. The activity assay (explained in Table 3.1) measures the total activity of the three dismutase enzymes and then subtracts SOD2 and SOD3 activity to obtain a measure of SOD1 activity alone. In the gel assay the three proteins are separated by electrophoresis and only the band corresponding to SOD1 is used to determine its activity.

Activity assay	Xanthine-xanthine oxidase is added to samples to generate superoxide anions ($O_2^{\cdot-}$), and then a chromogen is used as an indicator of $O_2^{\cdot-}$ production. In the presence of SOD, $O_2^{\cdot-}$ concentration is reduced, resulting in a decreased colorimetric signal. However, all three SOD isoforms contribute to the measure of activity, therefore SOD1 activity is obtained indirectly by subtraction of SOD2 and SOD3 from total SOD activity. This is achieved by running a parallel assay with the addition of potassium cyanide which preferentially inhibits SOD1 (Roe et al., 1988).
Gel assay	Proteins are separated by electrophoresis using a native gel. The gel is stained using a solution of NBT and riboflavin (a source of superoxide anions after exposure to light). When the gel is exposed to light the superoxide anions interact with NBT, reducing the yellow tetrazolium within the gel to a blue precipitate and staining the gel blue. However, SOD inhibits this reaction, resulting in colourless bands where SOD is present. Quantification of activity is inferred by measuring the intensity of the bands at the correct molecular weight using a digital software (Weydert and Cullen, 2010).

Table 3.1 Methods of measuring SOD1 activity.

3.3.1.2 Intrinsic and overall SOD1 activity

In the literature SOD1 dismutase activity was measured either outside (intrinsic activity) or within a biological system (overall activity).

The intrinsic activity of SOD1 was assessed using SOD1 recombinant proteins normalised for their quantity. This particular measure reflects only the enzymatic efficiency of the SOD1 protein.

Conversely the overall activity was calculated within biological samples and normalised to the tissue quantity. This measure therefore reflects the amount of activity present in a biological contexts and takes into account known and unknown factors that affect the quantity, biological availability and functionality of SOD1. The intrinsic activity itself is one of these factors, others are: SOD1 mRNA half-life, SOD1 protein half-life, correct folding of SOD1, Cu^{++} loading of SOD1 and other post-translational modifications (Wilcox et al., 2009).

3.3.1.3 SOD1 dismutase activity is reduced in SOD1-fALS patients

Data of SOD1 intrinsic activity were found only for eight mutant recombinant proteins, see Figure 3.1. Intrinsic activity values ranged between 0 % and 150 % of human wild-type SOD1 activity, and did not show any correlation with clinical aspects of the disease (Borchelt et al., 1994; Ratovitski et al., 1999).

SOD1 overall activity instead was more frequently measured from patients' red blood cells, fibroblasts and lymphoblast cell lines. Data from 48 different SOD1-fALS mutations were found in literature (Figure 3.1 and Table 3.2). The majority of them had a reduced overall SOD1 activity (Table 3.2), with a remarkable average loss of 58 % (± 17 , S.D.) of normal values (Figure 3.1).

These results were consistent and more homogenous than measures of intrinsic activity considering that they were produced by different laboratories and that there is a naturally occurring variation in activity assessed in blood samples (Borchelt et al., 1994; de Lustig et al., 1993; Robberecht et al., 1994). Only in two of the 48 mutations SOD1 overall activity was found to be normal or slightly reduced: D90A expressed both in heterozygosity and homozygosity and L117V when expressed in heterozygosity. Further literature investigation on these two mutations revealed some atypical characteristics (Table 3.3) and suggested that they might have a propensity to aggregate which is sufficient to start the disease process but not sufficient to determine misfolding and loss of SOD1 activity in the peripheral tissues.

No correlation was found between intrinsic and overall SOD1 activity in the eight mutations where activity was assessed both from recombinant proteins and in patients. The G37R mutation was the most striking example having an overall activity of 40 % and an intrinsic activity of 150 % compared to wild-type. As mentioned the intrinsic activity is considered to be only one of the many factors that contribute to the overall activity, other determinants such as stability of mutant SOD1 proteins need to be investigated to account for this difference. Protein half-life for instance is variable among SOD1 mutants, but consistently reduced compared to the wild-type protein (Sato et al., 2005). A study that combined protein half-life and intrinsic SOD1 activity of six SOD1-fALS mutations predicted overall activity of 50 % of normal levels (Borchelt et al., 1994). This result is in accordance with Figure 3.1 and with other findings (Birve et al., 2010; Deng et al., 1993). Of note most of the data collected in

this meta-analysis are measures of SOD1 activity from patients' red blood cells, which are a particularly reliable system for the detection of protein half-life changes due to their lack of active protein synthesis (Broom et al., 2008).

SOD1 activity was found to be reduced to similar levels both in red blood cells and post mortem CNS tissues, the similarity was even more striking when compared within the same subset of patients (Bowling et al., 1993; Browne et al., 1998; Jonsson et al., 2004; Rosen et al., 1994; Watanabe et al., 1997b).

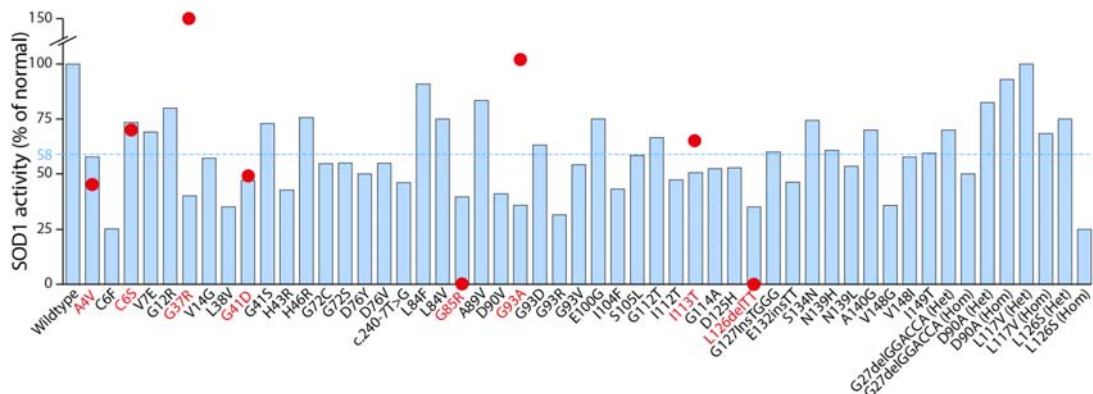


Figure 3.1 Diagram of human SOD1 mutations dismutase activity in the current literature. Measurements from patients carrying 48 SOD1 fALS mutations between 1993 and April 2015; original references are cited in Table 3.2. All intrinsic activity measures fall below 100% of controls activity. Three mutations found in homozygous individuals are shown on the right hand side of the figure. Red circles show measures of intrinsic activity where these are known. We note that all mutations shown here are familial, not sporadic, and have supporting data indicating they are causative of ALS (Table 3.2). Where more than one publication reports overall activity for an individual mutation the value from the report with the highest sample size has been plotted. Heterozygous (Het); homozygous (Hom) (Saccon et al., 2013).

SOD1 mutation	% of SOD1 activity	Reference
A4V	57.8 %	(Bowling et al., 1993)
A4V	45 % intrinsic activity	(Borchelt et al., 1994)
C6F	25.3 %	(Morita et al., 1996)
C6S	73.5 %	(Brotherton et al., 2011)
C6S	70 % intrinsic activity	(Marin et al., 2012)

SOD1 mutation	% of SOD1 activity	Reference
V7E	69.1 %	(Hirano et al., 1994)
G12R	80 %	(Penco et al., 1999)
V14G	57.2 %	(Andersen et al., 1997)
G37R	40 %	(Borchelt et al., 1994)
G37R	150 % intrinsic activity	(Borchelt et al., 1994)
L38V	35 %	(Robberecht et al., 1994)
G41D	47 %	(Fujii et al., 1995)
G41D	49 % intrinsic activity	(Borchelt et al., 1994)
G41S	73 %	(Tsuda et al., 1994)
H43R	42.7 %	(Rosen et al., 1993)
H46R	75.7 %	(Abe et al., 1996)
c.240-7T>G	46. %	(Birve et al., 2010)
G72C	54.7 %	(Stewart et al., 2006)
G72S	55 %	(Orrell et al., 1997a)
D76Y	50 %	(Andersen et al., 1997)
D76V	54.9 %	(Segovia-Silvestre et al., 2002)
L84F *	80.5 %; 69.8 %	(Curti et al., 2002)
L84V	74.8 %	(Abe et al., 1996)
G85R	39.5 %	(Deng et al., 1993)
G85R	0 % intrinsic activity	(Borchelt et al., 1994)

SOD1 mutation	% of SOD1 activity	Reference
A89V	83.5 %	(Jacobsson et al., 2001)
D90V	41 %	(Morita et al., 1996)
G93A	35.8 %	(Deng et al., 1993)
G93A	102 % intrinsic activity	(Chia et al., 2010)
G93D	63.2 %	(Bowling et al., 1993)
G93R	31.7 %	(Orrell et al., 1997b)
G93V	54.2 %	(Orrell et al., 1997b)
E100G	75 %	(Calder et al., 1995)
I104F	43.1 %	(Abe et al., 1996)
S105L	58.4 %	(Jacobsson et al., 2001)
G112T	66.6 %	(Esteban et al., 1994)
I112T	47.3 %	(Bowling et al., 1993)
I113T	50.6 %	(Orrell et al., 1997b)
I113T	65 % intrinsic activity	(Borchelt et al., 1994)
G114A	52.4 %	(Jacobsson et al., 2001)
D125H	52.8 %	(Orrell et al., 1997b)
L126delTT	35 %	(Nakashima et al., 1995)
L126delTT	0 % intrinsic activity	(Zu et al., 1997)
G127insTGG	60 %	(Andersen et al., 1997)
E132insTT	46.3 %	(Orrell et al., 1997b)

SOD1 mutation	% of SOD1 activity	Reference
S134N	74.4 %	(Watanabe et al., 1997a)
N139H	60.8 %	(Nogales-Gadea et al., 2004)
N139K	53.5 %	(Pramatarova et al., 1995)
A140G	70 %	(Naini et al., 2002)
V148G	35.7 %	(Deng et al., 1993)
V148I	57.7 %	(Abe et al., 1996)
I149T	59.5 %	(Pramatarova et al., 1995)
G27delGGACCA heterozygous	70 %	(Zinman et al., 2009)
G27delGGACCA homozygous	50 %	(Zinman et al., 2009)
D90A heterozygous	82.5 %	(Andersen et al., 1995)
D90A homozygous	93 %	(Andersen et al., 1995)
L117V heterozygous	100 %	(Synofzik et al., 2012)
L117V homozygous	66.8 %	(Synofzik et al., 2012)
L126S heterozygous	75 %	(Takehisa et al., 2001)
L126S homozygous	25 %	(Takehisa et al., 2001)

Table 3.2 SOD1 overall and intrinsic activity of SOD1-fALS patients in the current literature. (Figure 3.1). SOD1 overall activities, unless intrinsic where shown. The overall and intrinsic activity of each SOD1 mutations is represented with its corresponding reference. In case where the activity of a given SOD1 mutant was determined by more than one study, the one with the greatest number of clinical samples was reported (Saccon et al., 2013). * 80.5 % is the mean of percentage activity compared to wild-type SOD1, as determined in 5 patients carrying the L84F mutation (one was asymptomatic). For 3 of these patients the SOD1 activity has been measured 3 times at one year intervals and the average activity for these 3 measurements is 69.8 %.

	D90A	L117V
Presence of misfolded SOD1 in cells derived from patients	Not present	Not present
Frequency of homozygosis	Majority of patients	1 in 4 patients
Penetrance in heterozygosity	Low	Low
Disease progression	Slow	Slow

Table 3.3 Characteristic of D90A and L117V mutations.

3.3.1.4 Dismutase activity reduction might be enhanced in motor neurons

The level of SOD1 activity in patients' motor neurons and other specific cell types, known to be affected in ALS, is unknown. This is mainly due to technical difficulties in the measurement and availability of post-mortem tissues. However, studies on SOD1 mRNA, aggregation and oxidative stress suggests that dismutase activity may be reduced in motor neurons.

In normal conditions the half-life of SOD1 mRNA in brain and spinal cord tissues was found to be prolonged after formation of complexes with ribonucleoproteins. Though, in the presence of SOD1 mutations this complex formation was impaired, reducing the half-life of mutant SOD1 mRNA preferentially in the central nervous system of SOD1-fALS patients (Ge et al., 2006).

Other indirect evidence that SOD1 activity might be reduced in specific cells types comes from aggregation studies. For example a reduction of SOD1 activity was detected in cells where SOD1 G93A and amyloid- β were co-expressed, suggesting that aggregation triggers reduction of dismutase activity (Yoon et al., 2009). Moreover in mice overexpressing the human wild-type SOD1 protein, SOD1 aggregates were found in brain and spinal cord but not in liver and muscle samples. Interestingly the levels of the SOD1 protein were similarly increased among the four different tissues; but the dismutase activity was increased accordingly only in liver and muscle and not in brain and spinal cord, suggesting a link between aggregation and loss of SOD1 enzymatic activity (Graffmo et al., 2013). Even if the dismutase activity is retained in SOD1

aggregates, it is unknown whether they are able to accomplish the normal SOD1 function when SOD1 dimer is correctly targeted to the appropriate cell compartments. Furthermore, misfolding and aggregation are a hallmark of SOD1-fALS (Jonsson et al., 2008), and have been recently found also in SOD1-sALS patients (Bosco et al., 2010). All these findings from aggregation studies taken together make a dominant negative loss of function in SOD1-ALS feasible.

Lastly oxidative stress it is known to induce monomerisation of SOD1 making it dismutase inactive (Ezzi et al., 2007; Khare et al., 2004; Rakhit et al., 2004; Wilcox et al., 2009). This mechanism might be particularly prominent in motor neurons since susceptibility to oxidative stress was proven to be more prominent in MNs than in other cells (Barber and Shaw, 2010).

In conclusion these findings on tissue specific changes in SOD1 protein and SOD1 mRNA suggest that dismutase activity might be lower in motor neurons and other affected cells compared to that assessed in patients' red blood cells. Further, SOD1 overall activity is consistently reduced in SOD1-fALS patients compared to wild-type controls. This is caused by changes in protein activity and protein half-life, and possibly there is also a tissue-specific dismutase reduction in affected neurons.

3.3.2 SOD1 loss of function in *Sod1* knockout mice

Sod1 knockout mice have been extensively employed in SOD1-ALS research even if they do not model ALS disease. To get more insight on the role of SOD1 loss of function in SOD1-ALS, historical and more recent papers about these mice have been collected and reviewed using the criteria described in section 2.7.

Up to now five *Sod1* knockout mouse lines have been published (Table 3.4), all were generated by homologous recombination in mouse embryonic stem cells. In the five models, different regions of the *Sod1* gene are deleted, ranging from a single exon to the entire genomic sequence. Despite the presence of different *Sod1* gene regions, the five mouse lines present a strikingly similar phenotype and they have been compared in several papers (Huang et al., 1997; Kondo et al., 1997; Kostrominova, 2010). Importantly SOD1 protein is undetectable in all homozygous mice and SOD1 dismutase activity is either absent or very low; detection of low activity levels may be caused by the presence of alternative scavenging enzyme or assay background (Reaume et al., 1996). Another example that confirms similarity among these mouse lines is the

development in three of them of an accelerated age-related muscle denervation (Kostrominova, 2010).

Of note the majority of the studies collected for this meta-analysis have been conducted using *Sod1* knockout mice on a congenic C57BL/6J background, making results from different laboratories comparable.

Since the first studies on *Sod1*^{-/-} mice it was clear that these animals do not develop MN degeneration. In 1996 Reaume and colleagues did not find a reduction in the number *Sod1*^{-/-} MNs up until 4 months of age. However, they detected a higher number of small neurons and astrocytes from spinal cord tissues (Reaume et al., 1996). Later papers confirmed the absence of MN loss also at 6, 9 and 17 months of age and ruled out the presence of other hallmarks of ALS such as vacuolation and chromatolysis in mice of 4 and 18 months of age (Fischer et al., 2012; Flood et al., 1999). Also microgliosis and ubiquitinated protein accumulation in MNs were excluded, but mild astrocytosis was found at 4 and 18-months (Fischer et al., 2012).

Even though *Sod1*^{-/-} mice do not have motor neuron loss they develop a series of phenotypes, some of which relevant to ALS. Also *Sod1*^{+/-} have been shown to have several neuronal dysfunction. Therefore investigating the phenotype of both *Sod1* knockout homozygous and heterozygous mice might be crucial to elucidate the role of SOD1 loss of function.

Mouse line	Reference
<i>Sod1</i> ^{tm1Cpe}	(Reaume et al., 1996)
<i>Sod1</i> ^{tm1Cje}	(Huang et al., 1997)
<i>Sod1</i> ^{tm1Lem}	(Matzuk et al., 1998)
<i>Sod1</i> ^{tm1Ysb}	(Ho et al., 1998)
<i>Sod1</i> ^{tm1Dkd}	(Yoshida et al., 2000)

Table 3.4 Published *Sod1* knockout mouse lines.

3.3.2.1 Absence of *Sod1* causes a progressive adult-onset motor axonopathy in *Sod1*^{-/-} mice

Several studies show that homozygous *Sod1* knockout mice develop an adult onset motor axonopathy, and other phenotypes relevant to ALS disease.

Behavioural data

Behavioural analysis from different laboratories showed that even if at birth *Sod1*^{-/-} mice were indistinguishable from wild-type littermates, with age they developed several neuromuscular deficits. All behavioural data collected are gathered together in Table 3.5.

Age (months)	Phenotype	Reference
3	Decrease in voluntary wheel running	(Muller et al., 2006)
5	Body weight reduced by 20 % compared to wild-type littermates *	(Reaume et al., 1996)
9	Progressive deficit in rotarod	(Flood et al., 1999)
9	Progressive deficit in stride-length analysis	(Muller et al., 2006)
12	Deficit in grip-strength	(Fischer and Glass, 2010)
12	Presence of tremors	(Fischer and Glass, 2010)

Table 3.5 *Sod1*^{-/-} mice behavioural phenotypes. * The light body weight detected in these mice might be explained by an impairment in intestine lipid metabolism (Kurahashi et al., 2012) and by a reduction lipoprotein secretion in the liver (Uchiyama et al., 2006).

Neurophysiological data

Neurophysiological investigations also showed the presence of ALS related phenotypes, revealing a clear muscle denervation as well as deficits in motor axons and functional motor units. Firstly direct stimulation of muscles showed a reduction in muscle strength from 8 months of age. While, muscle strength generated by nerve stimulation became increasingly worse compared to measures from direct muscle stimulation suggesting a progressive deficit in innervation (Larkin et al., 2011). Secondly a progressive reduction in motor unit number was detected starting at 3-months of age (Shefner et al., 1999). Finally at 6 months of age analysis of nerve conduction velocity and latency performed on sensory and mixed nerves, revealed a

reduction only where a motor component was present suggesting a deficit in the largest motor axons (Flood et al., 1999).

Axonal damage and neuromuscular junctions denervation

Investigating neuromuscular junctions (and early pathological disease target in SOD1-fALS mouse models) revealed a progressive denervation of both fast and slow twitch muscles (Fischer et al., 2012; Flood et al., 1999; Larkin et al., 2011). The pattern was found to be more aggressive in fast twitch muscles with a reduction of TA muscle innervation to 70 % of endplates by 4 months of age, and to 34 % by 18 months of age (Fischer et al., 2012; Jang et al., 2010). These results highlighted that as occurs in ALS patients and mouse models of fALS, functional SOD1 is also crucial for maintenance of motor axons and their terminals in *Sod1*^{-/-} mice.

Muscle pathology is secondary to denervation

Analysis of *Sod1*^{-/-} muscles showed a progressive loss of muscle mass, and the presence of angular muscle fibres (an indicator of denervation). Specifically gastrocnemius mass was reduced by 20 % at 3 months of age and hind limb muscles were reduced by 40 % at 20 months of age (Jang et al., 2010; Larkin et al., 2011; Muller et al., 2006). No reduction was detected in other organs such as liver, heart and kidney (Muller et al., 2006). Angular muscle fibres were found to be present starting at 2 months of age and increased overtime (Flood et al., 1999). Furthermore at 8 months massive reduction in fibre number was detected preferentially in fibres innervated by large motor neurons (Larkin et al., 2011; Reaume et al., 1996). The muscle profile of *Sod1*^{-/-} mice was found to be similar to the one described for transgenic mouse models of SOD1-fALS (Frey et al., 2000; Kennel et al., 1996) and suggested that muscle pathology is secondary to axonal impairment. Confirmation of this hypothesis came from a study where *Sod1*^{-/-} mice were crossed with transgenic mice expressing the *Sod1* gene in the CNS but not in muscles. Although *Sod1* was not present in muscles of double mutant mice, the muscle pathology was fully rescued in these animals (Flood et al., 1999). Other evidence proving that muscle denervation is secondary to axonal damage came from examination of the redox state of the tibial nerve and gastrocnemius muscle in 4 months old *Sod1*^{-/-} mice, showing a selective involvement of the nerve (Fischer et al., 2012). These results taken together indicate that in *Sod1*^{-/-} mice muscle changes are secondary to denervation.

3.3.2.2 Motor neurons of *Sod1*^{-/-} mice have an increased vulnerability to stress

The selective involvement of MNs and their susceptibility to stress are a hallmark of ALS. Even if *Sod1*^{-/-} do not develop MN loss, lack of SOD1 activity was shown to induce phenotypes that preferentially affected these neuronal cells, such as susceptibility to damage, vulnerability after injuries and mitochondrial function impairments.

Selective susceptibility to damage of the motor system

Histopathological examination of L3 dorsal and ventral roots in 19 month old *Sod1*^{-/-} mice revealed signs of degeneration and regeneration only in the ventral roots suggesting a preferential motor involvement (Flood et al., 1999). Also epidermal nerves, which are the most distal tracts of the sensory axons were unaffected while NMJs were impaired as described in section 3.3.2.1 (Fischer et al., 2012).

Other insights on MNs susceptibility came from *Sod1*^{-/-} primary embryonic MNs culture experiments. Firstly MNs from *Sod1*^{-/-} animals did not survive more than 72 hours in culture while wild-type mouse embryonic MNs lived for about 10 days (L. Greensmith, UCL, personal communication). Secondly analysis of initial stages of *Sod1*^{-/-} MNs culture showed reduced mitochondrial density, a significant oxidation of thioredoxin 2 and reduced axonal length and outgrowth, that depend on the intrinsic levels of oxidative stress (Acevedo-Arozena et al., 2011; Fischer et al., 2012) Finally dorsal root ganglia (DRG) cultures from the same mice were normal for two days and then showed a significant reduction in axonal growth (Fischer and Glass, 2010; Fischer et al., 2011).

Motor neuron vulnerability after injury

SOD1 activity was shown to be important for motor neuron survival after injury. Facial axotomy conducted on 5 month old *Sod1*^{-/-} mice and wild-type littermates showed that after 5 weeks there was a significant increase in MN loss in *Sod1*^{-/-} animals compared to controls (Reaume et al., 1996).

Mitochondrial function is affected by loss of SOD1

ALS and mitochondrial dysfunction studies underlined the crucial role of mitochondria for preservation of functional distal axons (Baloh et al., 2007b; Cassereau et al., 2011; Faes and Callewaert, 2011). For example mitochondrial abnormalities were shown in

transgenic mouse models of ALS (De Vos et al., 2007), and abnormal mitochondrial accumulations were described in lower MNs and proximal axons from, ALS patients post-mortem (Sasaki et al., 2009). Interestingly investigation of *Sod1*^{-/-} mice revealed a reduction in mitochondrial density in axons, which could be rescued together with the neuromuscular phenotype by replacing SOD1 selectively in the mitochondrial intermembrane space of these mice (Fischer et al., 2011). This may be explained by the fact that mitochondria of *Sod1*^{-/-} animals release high levels of free radicals due to the absence of dismutase, consequently increasing oxidative stress (Jang et al., 2010).

Thus, even if mice do not develop MNs degeneration, MNs are more vulnerable to damage.

3.3.2.3 *Sod1*^{-/-} develop other non-motor neuronal and extra neuronal phenotypes

In addition to the neuronal phenotypes described above, *Sod1*^{-/-} mice were found to develop other neuronal characteristics not directly related to ALS, listed in Table 3.6 (more details are provided in Appendix 8.4). These animals also presented a series of extra-neuronal phenotypes described in Table 3.7 the most relevant of all was the susceptibility to hepatocellular carcinoma a feature known to be present in humans and in Sod1D83G mice (Elchuri et al., 2005; Joyce et al., 2014), more details are provided in Appendix 8.4.

Phenotype	Reference
Hearing deficit and ganglion neurons loss	(Keithley et al., 2005)
Progressive retinal degeneration	(Hashizume et al., 2008; Imamura et al., 2006)
Blood brain barrier disruption and increased lethality after cerebral ischemia	(Kim et al., 2003; Kondo et al., 1997)
Increased damage after brain trauma	(Lewén et al., 2000; Mikawa et al., 1996)
Increased susceptibility to neurodegeneration	(Bechara et al., 2009; Murakami et al., 2011)

Table 3.6 *Sod1*^{-/-} non-motor neuronal phenotypes.

Phenotype	Reference
Decrease survival and hepatocellular carcinoma	(Elchuri et al., 2005; Takahashi et al. 2002)
Impaired endothelial-dependent relaxation	(Didion et al., 2002)
Skin thinning and osteoporosis	(Murakami et al., 2009)
Infertility	(Ho et al., 1998; Matzuk et al., 1998; Tsunoda et al., 2012)

Table 3.7 *Sod1*^{-/-} extra-neuronal phenotypes.

3.3.2.4 *Sod1*^{+/-} mice have a 50% reduction of SOD1 activity and develop abnormal neuronal function

Heterozygous *Sod1* knockout mice retain 50 % of SOD1 dismutase activity (Reaume et al., 1996) mimicking the physiological levels described in SOD1-fALS patients (Figure 3.1). Several papers have highlighted the presence of an abnormal range of phenotypes in *Sod1*^{+/-} animals such as: progressive cellular damage and deficits in reaction to injury and toxic stimuli. Here the relevance of these phenotypes to ALS is investigated.

***Sod1*^{+/-} MNs are more susceptible to cell death after axon injury**

Following facial nerve axotomy *Sod1*^{+/-} mice lost a significantly higher number of MNs compared to wild-type controls, but a significantly lower number compared to *Sod1*^{-/-} mice. This intermediate situation suggests a dose-dependent effect, and shows that in mouse retaining 50 % SOD1 activity is not sufficient for normal MN function in response to injury (Reaume et al., 1996).

Of note, facial nerve axotomy was also performed on copper chaperone for SOD1 knockout mice (*Ccs*^{-/-}). These animals retain only 20 % of SOD1 activity, due to the lack of this crucial protein for delivery of copper to SOD1. As happened for *Sod1* knockout mice, MN survival was significantly reduced in *Ccs*^{-/-} mice (Subramaniam et al., 2002). Results from all these mice, are important in light of the potential role for injury and trauma as a trigger in ALS pathogenesis (Yip and Malaspina, 2012).

Spontaneous denervation, MN sensitivity and reduction in mitochondrial numbers, show trends but are not significant in *Sod1*^{+/-}

Neuromuscular junction analysis and other studies carried out in *Sod1*^{+/-} mice failed to show a significant pattern of denervation. However, these results even if not statistically significant, highlighted a denervation trend. For example in 18 months of age *Sod1*^{+/-} animals 20 % of TA muscle endplates (NMJs) were denervated compared to 8 % in controls (Fischer et al., 2011, 2012).

Of note cultured *Sod1*^{+/-} MNs (unlikely *Sod1*^{-/-} MNs) showed a non-significant trend in reduction of axon length and mitochondrial density, whereas axon length and surface area of DRGs was normal (Fischer and Glass, 2010).

Enhanced Glutamate toxicity in *Sod1*^{+/-} mice

As mentioned glutamate toxicity is implicated in disease in ALS patients and in animal models (Ilieva et al., 2009). Importantly overexpression of SOD1 is known to be protective against glutamate toxicity (Cadet et al., 1994; Chan et al., 1990). When SOD1 neuronal sensitivity to glutamate toxicity was assessed *in vivo* by intrastriatal injection of and *N*-methyl-*D*-aspartic acid and kainite glutamate receptor agonist; *Sod1*^{+/-} mice were susceptible to the neurotoxic effects while mice overexpressing SOD1 were not (Schwartz et al., 1998). Thus, SOD1 partial loss of function could play a role in facilitating damage from glutamate toxicity, which may have relevance to ALS.

Increased susceptibility to cerebral ischemia in *Sod1*^{+/-} mice

After induced focal cerebral ischemia, *Sod1*^{+/-} mice had decreased survival along with increased early blood brain barrier (BBB) disruption and increased infarct volume causing brain swelling (Kondo et al., 1997). Furthermore, augmented apoptotic neuronal death demonstrated enhanced ischemia-reperfusion injury (Kondo et al., 1997). Interestingly, an important mechanism involved in ischemia-reperfusion injury is glutamate excitotoxicity (section 1.5.1.1) (Beal, 1992). Of note BBB disruption was seen also in transgenic SOD1-ALS mouse models and indirect indication of disruption, such as increased cerebrospinal fluid albumin/plasma albumin ratios, was documented in ALS patients (Apostolski et al., 1991; Leonardi et al., 1984).

Increased memory deficits and plaque formation in an AD model on a *Sod1*^{+/-} background

Overexpression of the amyloid precursor protein (*APP*) gene carrying the Swedish mutation on a *Sod1*^{+/-} background, resulted in increased deficits in memory behavioural tests and in increased senile plaque formation. Thus, in contrast with what happened with a 100 % loss of SOD1 activity, a 50 % loss failed to increase the development of a neurodegenerative phenotype *in vivo*.

Increased ganglion neuron loss with ageing in *Sod1*^{+/-} mice

Sod1^{+/-} mice did not display hearing deficits or altered auditory brainstem response thresholds as observed in *Sod1* homozygous knockout animals. However, ganglion cell density was significantly reduced at 15 months of age demonstrating that a 50 % reduction in SOD1 activity results in reduced neuronal survival *in vivo* (Keithley et al., 2005).

Reduction of DNA methylation in *Sod1*^{+/-} mice

DNA methylation in prostate tissue of 2 months old *Sod1*^{+/-} mice was significantly reduced, suggesting once again that a reduction of SOD1 activity increases oxidative stress (Bhusari et al., 2010). Even though this study was not carried out on ALS-affected tissues, it could be relevant to the disease since DNA methyltransferases, the enzymes involved in DNA methylation, and 5-methylcytosine, the end-product of DNA methylation, were found to be upregulated in human ALS (Chestnut et al., 2011).

Development of a contractile vascular phenotype with ageing in *Sod1*^{+/-} mice

Loss of 50 % of dismutase activity was sufficient to increase vascular superoxide levels and produced vascular contractile dysfunction with ageing in mice (Didion et al., 2006).

In summary loss of SOD1 activity to 50 % of normal levels does not cause death of MNs. However, *Sod1*^{+/-} animals are a valuable tool to investigate SOD1-ALS. Indeed, the increased loss of specific cell types and susceptibility to injury present in these mice are mechanisms postulated in human ALS pathogenesis.

3.3.3 SOD1 loss of function influence on SOD1-fALS mouse models

3.3.3.1 Loss of function of mouse endogenous SOD1 does not affect lifespan of transgenic SOD1-fALS mouse models

The role of SOD1 loss of function in ALS pathogenesis has been investigated by analysing the double mutant progeny of *Sod1*^{-/-} or of *Ccs*^{-/-} mice crossed to three transgenic SOD1-ALS lines overexpressing the human mutations: G93A, G37R and G85R.

Experiments carried out by crossing G93A and G37R mutants were not informative regarding the role of SOD1 loss of function in ALS, for several reasons. Firstly both these mutants retained dismutase activity see Figure 3.1. Secondly they had an increase of over 6 fold of SOD1 activity, compared to non-transgenic control mice (Bruijn et al., 1997; Deng et al., 2006; Subramaniam et al., 2002) As a result of this, even on a *Ccs*^{-/-} background, these two transgenic lines still had SOD1 activity levels comparable to those of non-transgenic wild-type mice (Subramaniam et al., 2002).

On the other hand data from G85R mutants were very informative since this mutation was known to have no detectable intrinsic activity (Borchelt et al., 1994; Bruijn et al., 1997). SOD1 activity was predicted to be 0 % when *TgSOD1*^{G85R} were crossed with *Sod1*^{-/-} and 20% when crossed with *Ccs*^{-/-} (Bruijn et al., 1998; Subramaniam et al., 2002). Furthermore *TgSOD1*^{G85R} mice had a late disease onset (8-10 months of age) compared to other transgenic SOD1 mouse models of ALS making them ideal for evaluating potential modifying effects of lack of SOD1 (Bruijn et al., 1998). Double mutant mice coming from both crosses (*Sod1*^{-/-} n=5 and *Ccs*^{-/-} n=10) did not showed significant effects on lifespan, but unfortunately no analysis was done on age of disease onset and pathology (Bruijn et al., 1997; Subramaniam et al., 2002). Thus it is possible to conclude only that lack of SOD1 activity does not affect survival, but it is still unclear if it affects other features such as age of onset or disease progression.

3.3.3.2 Influence of SOD1 overexpression on disease

To investigate if overexpression of wild-type SOD1 had an effect on disease, transgenic SOD1-ALS animals were crossed with *TgSOD1*^{WT} mice. The double mutant progeny showed an earlier age of onset and a reduced survival compared to single mutant transgenic SOD1-ALS animals (Bruijn et al., 1998; Deng et al., 2006; Fukada et al., 2001; Jaarsma et al., 2000; Prudencio et al., 2010; Wang et al., 2009b, 2009c).

However, it is important to consider that *TgSOD1^{WT}* mice develop spontaneous MN and axon loss and have misfolded SOD1 accumulations (Jaarsma et al., 2000).

3.3.3.3 Tissue specific expression and inactivation of mutant SOD1 suggest a modifying role for dismutase activity

Experiments using *Cre-loxP* (causes recombination - locus for crossing over \times P1) technology were conducted to conditionally eliminate mutant SOD1 expression in different cell lineages or used specific promoters to overexpress mutant SOD1 in selected cell types. *Cre-loxP* is a type of site specific recombinase (SSR) widely employed to carry out deletions, insertions, translocations and inversions at specific sites in the DNA. Briefly Cre recombinase is an enzyme that when expressed can recognize and splice specific *loxP* sites; therefore, depending on the position of the *loxP* sequences specific genes can be activated or repressed in particular tissues and at particular developmental time points. The analysis of site specific mutagenized SOD1 transgenic mice demonstrated a central role for neurons in the determination of age of onset and disease progression in SOD1-fALS, and pointed to a role for other cell types, such as astrocytes and microglia in influencing the course of the disease (Ilieva et al., 2009). *Cre-loxP* experiments were conducted using two mutant transgenic SOD1 mouse lines: conditional *TgSOD1^{G37R}*, which retained intrinsic dismutase activity, and conditional *TgSOD1^{G85R}*, which lacked activity (data are gathered in Table 3.8). This data suggested a protective role of SOD1 dismutase activity, at least in some cell types, on non-cell-autonomous degeneration and disease in SOD1-ALS.

Excision	<i>TgSOD1^{G37R}</i>	<i>TgSOD1^{G85R}</i>
Neurons	<ul style="list-style-type: none"> • Increased survival • Delay of disease onset 	<ul style="list-style-type: none"> • Increased survival • Delay of disease onset
Microglia	<ul style="list-style-type: none"> • No change in disease onset 	<ul style="list-style-type: none"> • Delay of disease onset
Astrocytes	<ul style="list-style-type: none"> • No change in disease onset 	<ul style="list-style-type: none"> • Delay of disease onset
Shwann cells	<ul style="list-style-type: none"> • Increased disease progression 	<ul style="list-style-type: none"> • Delay of disease onset • Increased survival • Pathology amelioration

Table 3.8 Consequences of mutant SOD1 excision in *TgSOD1^{G37R}* and *TgSOD1^{G85R}* mice.

3.4 Conclusions

3.4.1 *Sod1* knockout models share commonalities with ALS and indicate specific cell-type sensitivities

Sod1 homozygous knockout mice have been the most useful tool to investigate *in vivo* a possible modifying role for SOD1 loss of function in ALS. These animals do not develop motor neuron degeneration and therefore are not considered a model of the human disease. However, several studies pointed out striking features related to ALS. To begin with *Sod1*^{-/-} mice develop a progressive distal motor axonopathy, as happens in early stages of ALS (Murray et al., 2010). The most affected motor units in these mice are fast-twitch, as observed in other ALS models (Frey et al., 2000). Even if MNs are not lost they have a great susceptibility to injury and they are preferentially affected compared to other neuronal cells, as seen in patients (Pupillo et al., 2012). Lack of SOD1 activity in the mitochondrial intermembrane and decrease in mitochondrial density in axons have been demonstrated to be causative of the neuronal phenotype of these mice (Fischer et al., 2011). This is not surprising since mitochondrial contribution has been proven not only in ALS but also in other motor neuronal diseases (Acsadi et al., 2009; Baloh et al., 2007a; Faes and Callewaert, 2011; Sasaki et al., 2009; De Vos et al., 2007; Wen et al., 2010). Finally as described above, homozygous *Sod1* knockout mice present many other phenotypes related to the disease.

3.4.2 SOD1 activity is reduced in human SOD1-fALS patients

The meta-analysis conducted on SOD1-fALS patients clearly shows a reduction in SOD1 activity of approximately 50 % compared to normal levels Figure 3.1 (Saccon et al., 2013). Many papers suggest that this reduction could be even bigger in specific tissues and cell types mainly due to mutant SOD1 mRNA half-life decrease in the CNS or due to possible effects of SOD1 protein misfolding and aggregation on activity. Data from *Sod1*^{+/-} mice support these hypothesis and match what is known from patients. In these animals decrease in SOD1 dismutase activity causes neuronal loss, susceptibility to injury, to MN axonal damage and to glutamate toxicity. Moreover *Sod1*^{+/-} mice show spontaneous loss of spiral ganglion cells and increased vulnerability of the BBB after injury, as described both in patients and in mouse models of ALS. Finally exacerbation of neurodegeneration in an AD mouse model when on a *Sod1*^{+/-} background indicates that 50 % loss of SOD1 activity affects neuronal survival.

3.4.3 Absence of loss of function phenotypes in humans

In this meta-analysis both homozygous and heterozygous *Sod1* knockout mice were found to have many phenotypes relevant to ALS, but as expected, no studies suggested that a loss of SOD1 activity in humans could cause the disease. Indeed, though over 160 mutation have been reported to be causative of ALS none of them generates a null allele. Furthermore no patients with full loss of SOD1 activity were identified in the literature search. Even if to date there is no evidence of loss of function phenotypes in SOD1-fALS patients, the studies analysed here underlined the importance of investigating this aspect in humans. A modifying role for SOD1 loss of function could point to new directions in researching therapies for ALS.

3.4.4 SOD1 gain and loss of function could both play a role in ALS pathogenesis

The mouse data reviewed here show that a reduction in SOD1 dismutase activity is not causative for ALS, however, this leaves open the possibility that it may modify disease. This disease modification might happen through a direct or indirect increase in susceptibility to neurodegeneration, such as for example, effects on respiration in MNs. Indeed SOD1 was recently reported to be implicated in energy metabolism by repressing respiration, integrating O₂, glucose and superoxide levels, through casein kinase signalling (Reddi and Culotta, 2013). Loss of SOD1 could therefore affect cellular metabolism, and many other patterns still unknown.

In other neurodegenerative diseases like Huntington's disease, Parkinson's disease, spinocerebellar ataxia and myotonic dystrophy (DM) mechanisms of gain and loss of function coexist (Crespo-Barreto et al., 2010; Lim et al., 2008; Winklhofer et al., 2008; Zuccato et al., 2010). For example in DM type 1 the expansion of unstable CTG trinucleotide repeats in the 3' UTR of the dystrophia myotonica protein kinase (*DMPK*) gene, leads to disease through the misregulation of two RNA binding proteins; specifically causing a gain of function of CUG-binding protein 1 (CUGBP1) and loss of function of muscleblind-like 1 (MBNL-1). Furthermore, the hypothesis that a loss of function mechanism might contribute to ALS has been formulated not only for SOD1-ALS but also for TDP43-ALS and FUS-ALS (Guo et al., 2011; Lagier-Tourenne and Cleveland, 2009). SOD1 protein has a crucial role in superoxide clearance and its absence increases oxidative stress. SOD1 is also a major target of oxidation in transgenic SOD1-ALS mouse models, (Andrus et al., 1998) and in the

presence of oxidative stress, its two monomers have been shown to dissociate after oxidation and glutathionylation (Ezzi et al., 2007; Khare et al., 2004; Rakhit et al., 2004; Wilcox et al., 2009). These findings reported by several groups point once more to the possibility of a co-occurrence of SOD1 loss and gain of function in ALS. Indeed, a vicious circle was hypothesized in which oxidized SOD1 has increased propensity to misfold, causing seeding and aggregation of SOD1 and a reduction of dismutase activity, which therefore feeds more potential oxidative stress to the beginning of the loop (Saccon et al., 2013) see Figure 3.2.

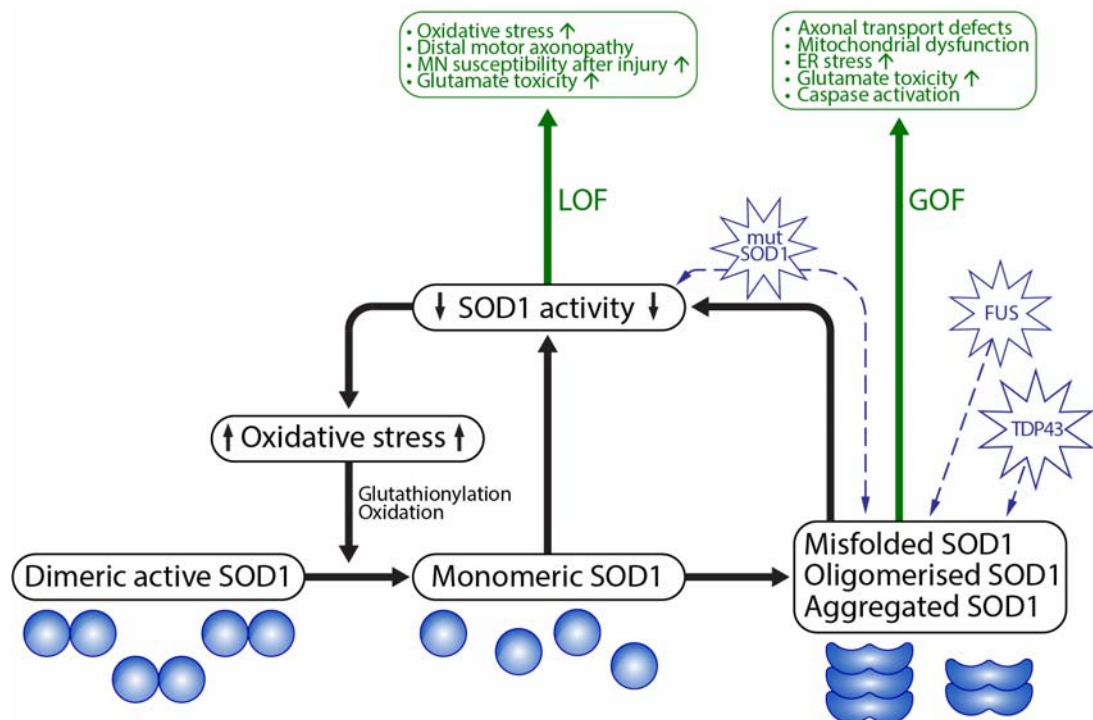


Figure 3.2 The cycle of SOD1 loss of function, schematic representation of a potential co-operation between SOD1 loss and gain of function in SOD1 pathogenesis. SOD1 loss of function (LOF) increases levels of oxidative stress, which through glutathionylation and oxidation, can facilitate the monomerisation of dimeric SOD1. Once monomerized, SOD1 is more prone to become misfolded, oligomerized and aggregated. The monomerization of previously active dimeric SOD1 and the recruitment of SOD1 into aggregates further enhance the loss of function, feeding back to the beginning of the loop. In this way the gain of function (GOF) effects of misfolded, oligomerized and aggregated SOD1, which are known to cause motor neuron degeneration, are amplified by the loss of function circle. Mutant SOD1 (mutSOD1) has both a direct effect on reduction of SOD1 activity and induces SOD1 misfolding and aggregation. Mislocalisation of both TDP-43 and FUS result in misfolding of SOD1. ER = endoplasmic reticulum; MN = motor neuron (Saccon et al., 2013).

3.4.5 SOD1 loss of function implications in ALS therapeutic approaches

Therapies for dominant mutations diseases are being developed using knockdown of the mutant allele RNA (Kordasiewicz et al., 2012; Lu and Yang, 2012; Smith et al., 2006), many of them, for example, against Huntington's disease, seem very promising. Interestingly these approaches have been tested also for SOD1-ALS (Ralph et al., 2005; Raoul et al., 2005; Saito et al., 2005; Smith et al., 2006; Towne et al., 2011; Wang et al., 2010; Wright et al., 2012). In particular a phase 1 clinical trial has been conducted (Fratta, 2013; Miller et al., 2013) employing antisense oligonucleotides that silence both mutant and wild-type SOD1, known to be effective in rats (Smith et al., 2006). The results of this preliminary study only assessed that the treatment was well-tolerated by patients for a short period of time. However, it is still unknown if downregulation of SOD1 triggers negative effects. Data on *Sod1* knockout mouse models give insights for the development of these type of strategies (Elchuri et al., 2005). First of all the incidence of liver cancer in these animals suggests that it is necessary to monitor non-neuronal effects also in patients and carefully optimise delivery routes and protein levels. Even if it is important to consider that *Sod1*^{-/-} mice lack *Sod1* from birth, and it will be more relevant to patients to investigate the case in which *Sod1* is knocked down in adulthood. Secondly *Sod1*^{+/-} mice findings raise the necessity to investigate other aspects of SOD1-ALS in patients such as: incidence of cardiovascular disease, stroke and liver cancer. Lastly, *Sod1* knockout animals loss of dismutase activity associate with abnormal phenotypes suggest that SOD1-ALS patients should also be screened for other non-fatal characteristics for example, age-related macular degeneration, progressive hearing loss.

3.5 Summary

- SOD1 activity is reduced to approximately half of normal in SOD1-fALS patients
- *Sod1*^{-/-} mice develop and adult-onset progressive motor axonopathy
- *Sod1*^{-/-} mice do not develop MN loss but they have an increased susceptibility to MNs degeneration
- *Sod1*^{-/-} mice develop a wide range of other neuronal and extra-neuronal phenotypes

- *Sod1*^{+/-} mice have 50 % reduction of SOD1 activity and develop abnormal phenotypes also within the motor system
- Mutant SOD1 tissue specific expression and inactivation suggest a modifying role for dismutase activity
- SOD1 loss of function by increasing oxidative stress could facilitate gain of function effects such as monomerisation, misfolding and aggregation of SOD1 which in turn could feed more potential oxidative stress to the loss of function mechanism

Chapter 4 *Sod1*^{D83G} a mouse model for motor neuron disease

4.1 Introduction

Transgenic mouse models overexpressing the *SOD1* gene have been extremely useful tools in the study of ALS. To date there are number of different transgenic mouse lines overexpressing either the wild-type or mutant forms of the human *SOD1* gene, and one overexpressing a mutant form of the mouse *Sod1* gene, see Table 8.1 (Graffmo et al., 2013; Gurney et al., 1994; Joyce et al., 2011; McGoldrick et al., 2013; Ripps et al., 1995; Turner and Talbot, 2008). The majority of these animals are considered models of SOD1-ALS since they develop the same features seen in patients: progressive motor deficits, hind limb paralysis, degeneration of motor neurons, and premature death (Joyce et al., 2011; McGoldrick et al., 2013; Turner and Talbot, 2008). However, these mice largely overexpress the mutant SOD1 protein and although they model the toxic gain of function that leads to motor neuron degeneration they are not a direct genetic representation of human ALS. Such raised expression levels might indeed affect aspects of the phenotype like disease onset or survival (Acevedo-Arozena et al., 2011; Joyce et al., 2014). For example, mice overexpressing the human SOD1 G93A mutant at different levels also present a different disease progression: the higher the number of copies of the mutant human *SOD1* transgene, the more accelerated the disease (Acevedo-Arozena et al., 2011; Jonsson et al., 2006b), indicating that SOD1 dose is important in determining the phenotype. Moreover mice overexpressing the *SOD1* gene generally present an increased SOD1 activity thus they do not model the effects that a reduction in dismutase activity may have in the pathogenesis of the disease, as observed in SOD1-fALS patients (Saccon et al., 2013).

To investigate the effects of SOD1 mutations at endogenous level and to create a model that is genetically more representative of human SOD1-ALS our group in collaboration with Linda Greensmith and Abraham Acevedo identified and characterised a new mutant line that carries an *N*-ethyl-*N*-nitrosourea (ENU)-induced point mutation in the mouse *Sod1* gene (Joyce et al., 2014) (see Appendix 8.5). This mutation is an adenosine to guanidine change that results in a D83G substitution and is identical to a pathological change found in several ALS families, mainly characterised by early onset and slow disease progression (Millecamps et al., 2010). Of note this

mutation is predicted to disrupt SOD1 activity and protein stability since it lies in the zinc-binding residue (Krishnan et al., 2006).

Characterisation of the *Sod1*^{D83G} mice has revealed several interesting phenotypes especially in the homozygous animals. *Sod1*^{D83G/D83G} mice indeed develop degeneration of both upper and lower motor neurons between 6 and 29 weeks of age, but differently from fALS patients and transgenic mouse models of SOD1-ALS, motor neuron cell death does not progress to paralysis and premature death (Joyce et al., 2014). A complete characterisation of *Sod1*^{D83G} homozygous and heterozygous mice was published in 2014 (Joyce et al., 2014), the data I collected are presented in the results section of this chapter while other findings most relevant to this work are summarised below.

Loss of upper and lower motor neurons

To investigate loss of upper and lower motor neurons in the *Sod1*^{D83G} model, the number of LMN in the sciatic motor pool of lumbar spinal cord and the survival of corticospinal motor neurons were assessed in *Sod1*^{D83G} homozygous, heterozygous and wild-type littermates see Table 4.1. As mentioned *Sod1*^{D83G/D83G} mice were found to develop loss of both upper and lower MNs that does not progress to paralysis, while *Sod1*^{+/D83G} appeared to be normal. Furthermore astrogliosis and microgliosis were detected in lumbar spinal cords of 15 weeks old homozygous animals and were shown to aggravate with age (Joyce et al., 2014).

Phenotype	Age (weeks)	<i>Sod1</i> ^{+/D83G}	<i>Sod1</i> ^{D83G/D83G}
% of LMNs compared to wild-type	6	100 %	100 %
	15	100 %	77 %
	52	100 %	77 %
% of UMNs compared to wild-type	15	100 %	100 %
	29	100 %	78 %

Table 4.1 *Sod1*^{D83G} mice upper and lower motor neurons characterisation. *Sod1*^{D83G/D83G} animals develop lower MNs loss by 15 week of age and upper MNs loss by 29 week of age. Data from (Joyce et al., 2014).

Analysis of functional motor units

The number of functional motor neurons that innervate the EDL muscle was determined by physiological analysis of motor unit survival in *Sod1^{D83G}* homozygous, heterozygous and wild-type littermates at 15 and 52 weeks of age. *Sod1^{+ /D83G}* animals did not reveal any significant difference in the number of EDL motor units compared to wild-type littermates at both time points. However, *Sod1^{D83G/D83G}* showed a significant reduction in the number of motor units in the EDL at 52 week of age, in accordance with the loss of MNs detected in these animals (Joyce et al., 2014).

Behavioural deficits

A series of behavioural tests were carried out to investigate *Sod1^{D83G}* motor functions. *Sod1^{D83G/D83G}* animals presented several behavioural deficits that progressively worsen with age, the most important results for homozygous and heterozygous mice are gathered in Table 4.2 (Joyce et al., 2014).

Test	<i>Sod1^{+ /D83G}</i>	<i>Sod1^{D83G/D83G}</i>
Weight	Normal	Weight loss, starting at 4 weeks
Grip-strength	Normal	Reduced from 6 weeks
Accelerating rotarod	No deficit	Deficit at 23 weeks for females and at 67 weeks for males
Wheel running	Not tested	Impaired from 44 weeks
Tremors	About 20 % mice develop tremors by 96 weeks of age	100 % of mice develop tremors by 22 weeks of age

Table 4.2 *Sod1^{D83G}* mice behavioural tests. All data are compared to wild-type littermates (Joyce et al., 2014).

Analysis of muscle force

Physiological analysis of TA and EDL muscles of females *Sod1^{D83G/D83G}*, *Sod1^{+ /D83G}* and wild-type mice revealed a progressive loss of muscle strength in homozygous animals between 15 and 52 weeks of age see Table 4.3.

Genotype	Age (weeks)	% of TA tetanic force compared to wild-type	% of EDL tetanic force compared to wild-type
<i>Sod1^{+/D83G}</i>	15	100 %	100 %
	52	100 %	100 %
	96	100 %	100 %
<i>Sod1^{D83G/D83G}</i>	15	65 %	100 %
	52	55 %	65 %

Table 4.3 *Sod1^{D83G}* mice EDL and TA muscle force. TA force of *Sod1^{D83D83G}* animals is affected starting at 15 weeks of age, while EDL force is affected starting at 52 weeks of age. Data from (Joyce et al., 2014).

Survival and incidence of hepatocellular carcinoma

Survival of *Sod1^{D83G}* homozygous mice was significantly reduced compared to heterozygous and wild-type littermates, with a higher incidence in males. Interestingly 85 % of *Sod1^{D83G/D83G}* animals develop hepatocellular carcinoma, a feature typical of *Sod1* knockout models (section 3.3.2) (Elchuri et al., 2005). Of note *Sod1^{D83G/D83G}* mice were not produced with a Mendelian ratio (Joyce et al., 2014).

In conclusion, *Sod1^{D83G}* is the first mouse model carrying a pathological point mutation in the *Sod1* gene which is expressed at endogenous levels, and the presence of a non-progressive motor neuron degeneration in homozygous *Sod1^{D83G}* animals make them a good system for studying early stages of ALS. Of note another mouse model with a spontaneous point mutation in the mouse *Sod1* gene has been previously described but the equivalent mutation in humans has not been identified as pathogenic (Joyce et al., 2014; Luche et al., 1997).

4.2 Aim

This chapter aims to characterise further the *Sod1^{D83G}* model and use it to investigate the gain of function mechanisms and a possible role of the loss of dismutase function in SOD1-ALS.

To better understand this new model an immunohistochemical, biochemical and molecular analysis was carried out for *Sod1^{D83G}* animals in comparison to wild-type

littermates. In particular the morphological innervation pattern of endplate NMJs of the EDL muscle was investigated at two different time points using an immunohistochemical approach. First to confirm the development of an axonopathy in *Sod1^{D83G/D83G}* animals and second to examine whether in this model axonal impairment precedes neuronal body degeneration or if these are two separate events. Further, since the D83 residue is predicted to interfere with the correct folding of SOD1 and potentially affect its function (Krishnan et al., 2006), SOD1 protein levels were measured by western blot and SOD1 dismutase activity was assessed by in gel assay, in homozygous and heterozygous *Sod1^{D83G}* animals compared to wild-type littermates at two different time points.

Sod1^{D83G} homozygous characterisation revealed that these mice present elements of both a gain of function and of a loss of function mechanism (Joyce et al., 2014). In order to try to dissect these two aspects *Sod1^{D83G}* mice were crossed with *Sod1* knockout animals and with mice overexpressing the human wild-type *SOD1* gene. In particular:

- To investigate whether the *Sod1^{D83G}* phenotype is dose-dependent, the protein levels and the SOD1 activity of the progeny generated by the cross between *Sod1^{D83G}* mice and *Sod1* knockout mice were analysed by western blot and in gel assay respectively. Specifically SOD1 activity and protein levels of the compound heterozygous animals *Sod1^{-/D83G}* were compared with that of *Sod1^{D83G/D83G}* mice. If the *Sod1^{D83G}* phenotype is dose-dependent SOD1 protein activity levels of *Sod1^{-/D83G}* mice are expected to be lower compared to those of *Sod1^{D83G/D83G}*.
- To investigate if the presence of human SOD1 protein rescues the MNs loss or if it exacerbates the ALS-like phenotypes described for *Sod1^{D83G}* animals, SOD1 protein levels and activity of the progeny generated by the cross between *Sod1^{D83G}* mice and mice overexpressing the human wild-type *SOD1* gene, were examined by western blot and in gel assay. Specifically the *TgSod1^{D83G/D83G}* were compared to *Sod1^{D83G/D83G}* mice, to confirm the overexpression of the human SOD1 protein.

4.3 Results

4.3.1 *Sod1*^{D83G} mice characterisation

In the experiments described in this section female mice were employed to investigate NMJ morphology, and male mice were used to assess SOD1 protein level and activity in order to minimise gender variability.

4.3.1.1 Neuromuscular junctions of the EDL

Neuromuscular junction denervation is considered to be a hallmark of ALS; and several studies suggested that the distal degeneration of the skeletal muscle plays a role in disease progression (Fischer et al., 2004; Murray et al., 2010). Furthermore investigations carried out using SOD1 transgenic mouse models and *Sod1* knockout mice demonstrated that NMJ degeneration occurs in the early disease stages, long before loss of MNs (Kanning et al., 2010).

To examine the innervation pattern of the EDL muscle in the *Sod1*^{D83G} line a morphological analysis of the endplate neuromuscular junctions was performed for *Sod1*^{D83G/D83G}, *Sod1*^{+ /D83G}, and wild-type littermates at 15 and 52 weeks of age. For each muscle the total number of NMJs was counted and NMJs were classified in three groups depending on the level of innervation of the postsynaptic apparatus: innervated, intermediate and denervated (Table 2.2, Figure 4.1 and Figure 4.2). In particular the innervation status of each NMJ was evaluated by determining the co-localisation between synaptic vesicles of the axon terminal, and acetylcholine receptors present in the foot plate of the skeletal muscle see Figure 4.1 and Figure 4.2. The three genotypes were compared at both time points for the total number of NMJs and for each classification group using a one-way ANOVA.

At 15 weeks no significant difference was detected in the number of denervated endplates NMJs, or in any of the other categories among the three genotypes (Figure 4.3 (a) (d); Table 4.4). However, at 52 weeks of age significant denervation had taken place in the *Sod1*^{D83G/D83G} mice compared to wild-type and *Sod1*^{+ /D83G} littermates (Figure 4.3 (b) (d); Table 4.4). Furthermore the number of partially innervated endplates (intermediate) was higher in *Sod1*^{D83G/D83G} animals compared to other genotypes but it was significantly different only to *Sod1*^{+ /D83G} littermates (Figure 4.3 (b); Table 4.4).

There was no difference in the total number of endplate NMJs counted among genotypes at 15 week, but at 52 weeks the number of NMJs counted was significantly reduce in *Sod1*^{D83G} homozygous animals compared to heterozygous and wild-type littermates (Figure 4.3 (c); Table 4.5).

This analysis confirmed the presence of a distal progressive denervation between 15 and 52 weeks of age in *Sod1*^{D83G/D83G} mice (Joyce et al., 2014).

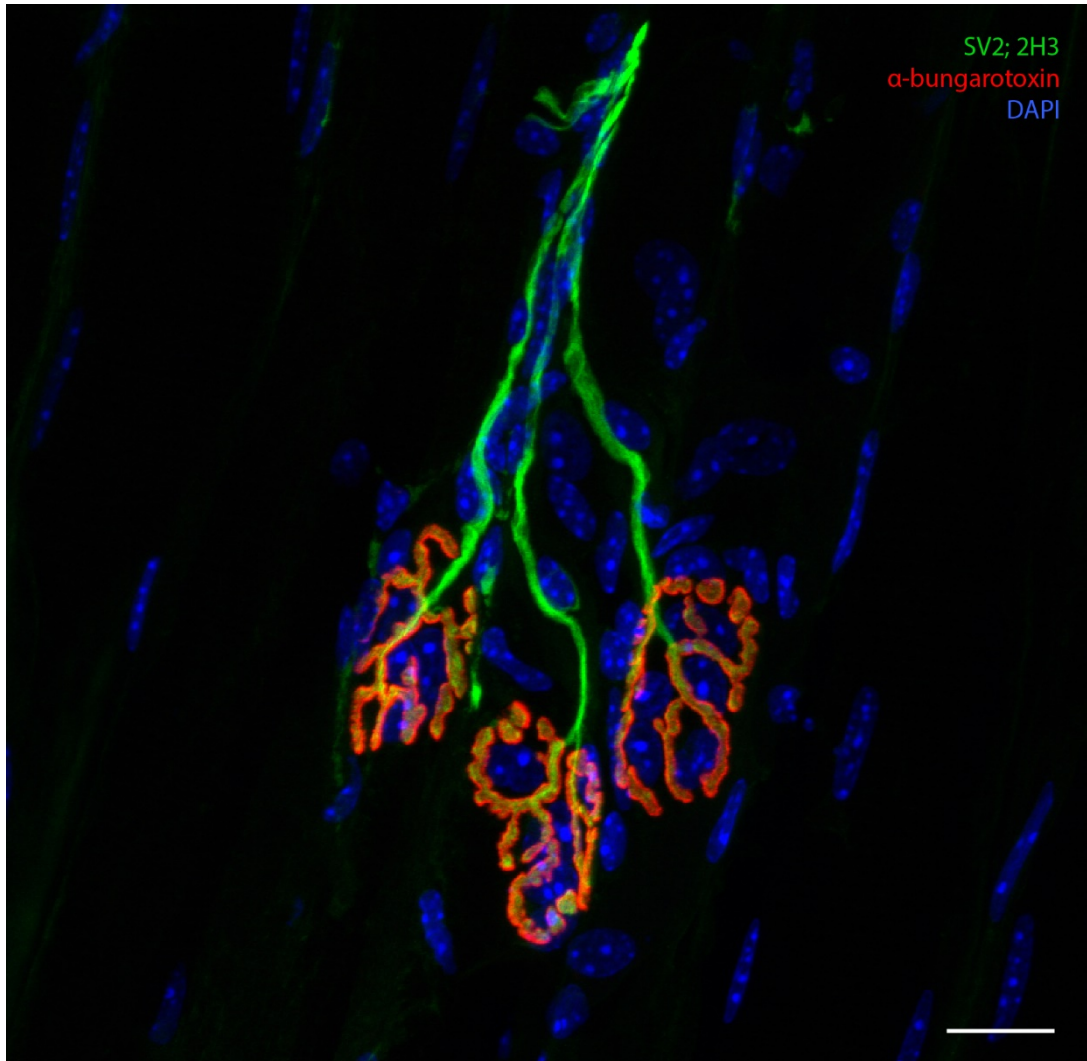


Figure 4.1 Representative image of innervated NMJs from EDL muscle of a 52 weeks old wild-type mouse. Axon projections and axonal terminals are identified respectively by 2H3 antibody staining neurofilaments (green) and SV2 antibody staining synaptic vesicles (green). Motor endplates are identified by α -bungarotoxin staining of acetylcholine receptors (red). Nuclei are stained by DAPI (blue). Scale bar = 20 μ m.

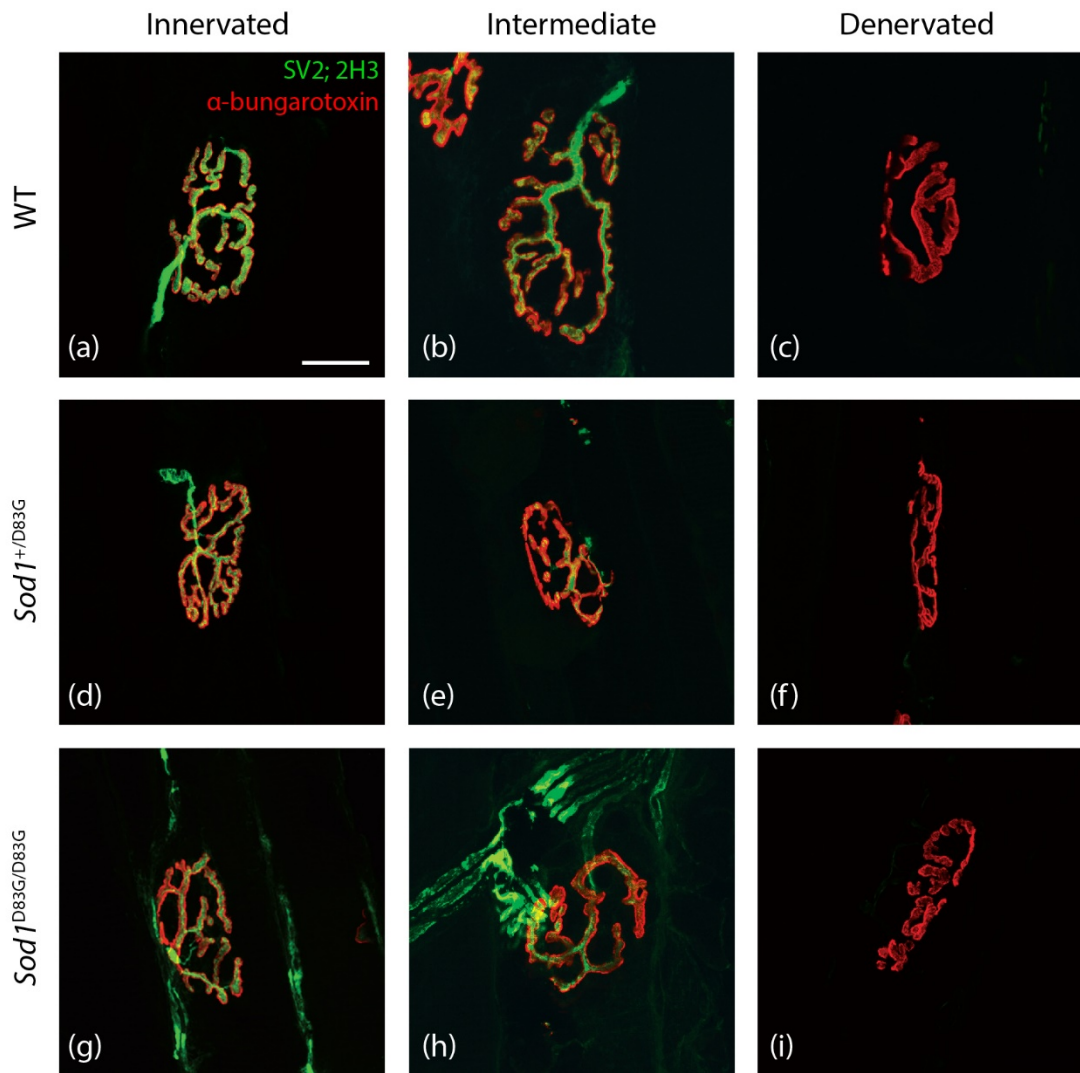


Figure 4.2 Representative images of innervated, intermediate and denervated NMJs of the three *Sod1*^{*D83G*} genotypes at 52 weeks of age. (a; b; c) Wild-type (WT); (d; e; f) *Sod1*^{+/*D83G*}; (g; h; i) *Sod1*^{*D83G*/*D83G*}. The synaptic vesicles and the axon terminals were visualized with SV2 and 2H3 antibodies respectively (both in green), while the acetylcholine receptors in skeletal muscle were labelled with α -bungarotoxin (red). Scale bar = 20 μ m.

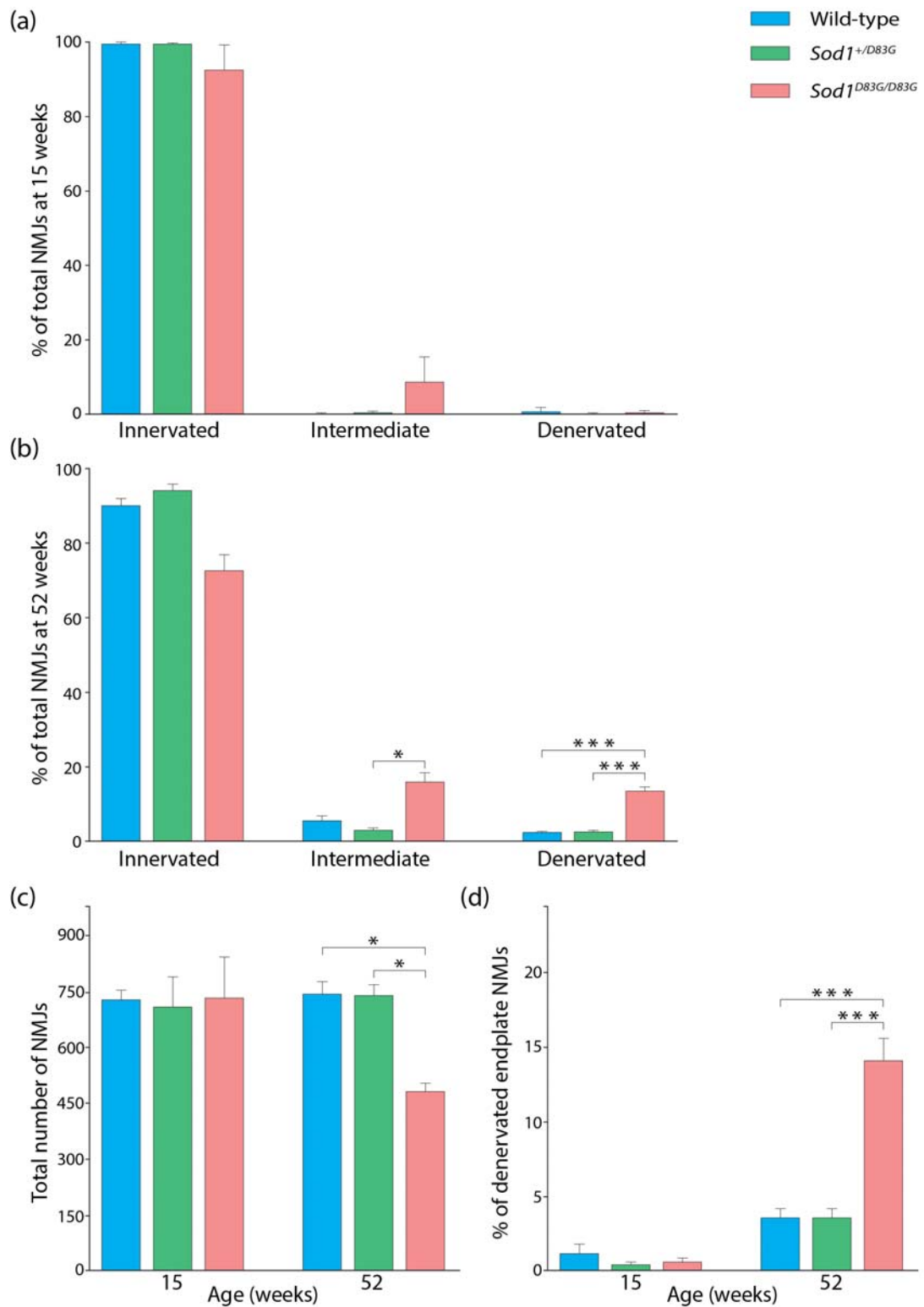


Figure 4.3 NMJs analysis from EDL muscle of *Sod1^{D83G}* mice at 15 and 52 weeks. (a) Percentage of innervated, intermediate and denervated NMJs for the 3 *Sod1^{D83G}* genotypes at 15 weeks, and (b) at 52 weeks. (c) Total number of NMJs at 15 and 52 weeks for the 3 genotypes. (d) Percentage of denervated NMJs at 15 and 52 weeks for the 3 genotypes. For all measurements $p < 0.001 = ***$; $p < 0.01 = **$; $p < 0.05 = *$ $n=5$ for all genotypes.

15 weeks			
Genotype	Innervated (% of total)	Intermediate (% of total)	Denervated (% of total)
Wild-type	99.0 % ± 0.6 %	0.2 % ± 0.1 %	0.7 % ± 0.6 %
<i>Sod1^{+/D83G}</i>	99.2 % ± 0.5 %	0.5 % ± 0.3 %	0.3 % ± 0.2 %
<i>Sod1^{D83G/D83G}</i>	91.0 % ± 7.5 %	8.5 % ± 7.6 %	0.5 % ± 0.3 %

52 weeks			
Genotype	Innervated (% of total)	Intermediate (% of total)	Denervated (% of total)
Wild-type	90.5 % ± 3.3 %	6.0 % ± 2.7 %	2.5 % ± 1.0 %
<i>Sod1^{+/D83G}</i>	94.2 % ± 3.0 %	3.1 % ± 1.5 %	2.7 % ± 1.5 %
<i>Sod1^{D83G/D83G}</i>	74.0 % ± 6.1 %	16.8 % ± 4.0 %	14.1 % ± 1.0 %

Table 4.4 Percentage of innervated intermediate and denervated NMJs at 15 and 52 weeks. Values represent the mean percentage ± SEM of the total number of NMJs calculate on an n = 5 per genotype.

Genotype	Total NMJs at	Total NMJs at
	15 weeks	52 weeks
Wild-type	714 ± 33	742 ± 39
<i>Sod1^{+/D83G}</i>	705 ± 82.5	740 ± 36
<i>Sod1^{D83G/D83G}</i>	719 ± 100	463 ± 30

Table 4.5 Total number of NMJs at 15 and 52 week. Values represent the mean of the total NMJs counted ± SEM, n = 5 per genotype.

4.3.1.2 SOD1 protein levels of *Sod1^{D83G}* mice

In order to investigate protein stability SOD1 levels were assessed by western blot (section 2.6.4.2) from brain homogenates of *Sod1^{D83G/D83G}*, *Sod1^{+/D83G}* and wild-type mice at 15 and 60 weeks of age. To confirm experimental conditions accuracy SOD1 levels were also measured for 15 weeks old control mice: *Sod1^{-/-}*, *Sod1^{+/-}*, wild-type and

TgSOD1^{G93A(H)}. Values from control genotypes at 15 weeks and from *Sod1*^{D83G} animals at 15 and 60 weeks were compared using one-way ANOVA.

As expected, *Sod1*^{-/-} controls were significantly lacking the SOD1 protein (0.4 % ± 0.4 %) compared to wild-type animals (100 % ± 2.7 %) and *Sod1*^{+/-} mice had a significant protein reduction of 53.6 % ± 8.1 % compared to normal. Further TgSOD1^{G93A(H)} mice SOD1 protein levels were over six fold (627.1 % ± 2.6 %) of wild-type, see Figure 4.4 (a) and Figure 4.5 (a).

SOD1 protein levels of homozygous and heterozygous *Sod1*^{D83G} mice were significantly reduced compared to wild-type littermates both at 15 and 60 week of age. In particular at 15 weeks SOD1 protein of *Sod1*^{D83G/D83G} mice was reduced down to 11.8 % ± 0.4 % of wild-type littermates (100 % ± 9.4 %), while *Sod1*^{+ /D83G} mice retained 70.4 % ± 5.3 % of SOD1 protein compared to wild-type (Figure 4.4 (c) and Figure 4.5 (c)). Similarly at 60 weeks SOD1 protein levels were reduced to 14.6 % ± 0.4 % in homozygous *Sod1*^{D83G} animals and to 57.0 % ± 0.7 % in heterozygous mice compared to wild-type littermates (100 % ± 4.3 %) see Figure 4.4 (e) and Figure 4.5 (e).

4.3.1.3 SOD1 enzymatic activity of *Sod1*^{D83G} mice

To investigate SOD1 enzymatic activity gel assays were carried out using brain homogenate from *Sod1*^{D83G/D83G}, *Sod1*^{+ /D83G} and wild-type mice at 15 and 60 week of age; and also from *Sod1*^{-/-}, *Sod1*^{+/-}, wild-type and TgSOD1^{G93A(H)} animals at 15 weeks (section 2.6.4.4). Values from control genotypes at 15 weeks and from *Sod1*^{D83G} animals at 15 and 60 weeks were compared using one-way ANOVA.

Confirming published data *Sod1*^{-/-} mice were completely lacking SOD1 activity (0.40 % ± 1.6 %) (Reaume et al., 1996), *Sod1*^{+/-} animals retained 33.8 % ± 9.1 % of activity and TgSOD1^{G93A(H)} mice presented a 291.3 % ± 5.3 % increase of dismutase activity compared to wild-type-littermates (100 % ± 6.4 %) see Figure 4.4 (b) and Figure 4.5 (b).

As for SOD1 protein levels also SOD1 dismutase activity of homozygous and heterozygous *Sod1*^{D83G} mice was significantly reduced compared to wild-type littermates at both time points. Specifically, at 15 weeks SOD1 activity of *Sod1*^{D83G/D83G} mice was 1.3 % ± 2.1 %, and SOD1 activity of *Sod1*^{+ /D83G} mice was 55.9 % ± 7.0 % of wild-type littermates (100 % ± 14.4 %), see Figure 4.4 (d) and Figure 4.5 (d). While at 60 weeks

SOD1 activity was reduced to $1.5 \% \pm 5.3 \%$ in homozygous *Sod1^{D8G3}* animals and to $34.2 \% \pm 5.3\%$ in heterozygous *Sod1^{D8G3}* mice compared to wild-type littermates ($100 \% \pm 2.9 \%$), see Figure 4.4 (f) and Figure 4.5 (f).

The SOD1 activity bands detected from brain homogenates of Tg*SOD1^{G93A(H)}* mice migrated faster in the gel compared to the SOD1 activity bands from brain homogenates of wild-type, *Sod1^{+/-}* and *Sod1^{D83G}* mice. Gel electrophoresis was carried out in non-denaturing and non-reducing conditions, therefore the electrophoretic mobility of the proteins depended only on their charge-to-mass ratio and physical shape. Of note in these assays it was not possible to use native ladder markers to detect the size of the SOD1 activity bands.

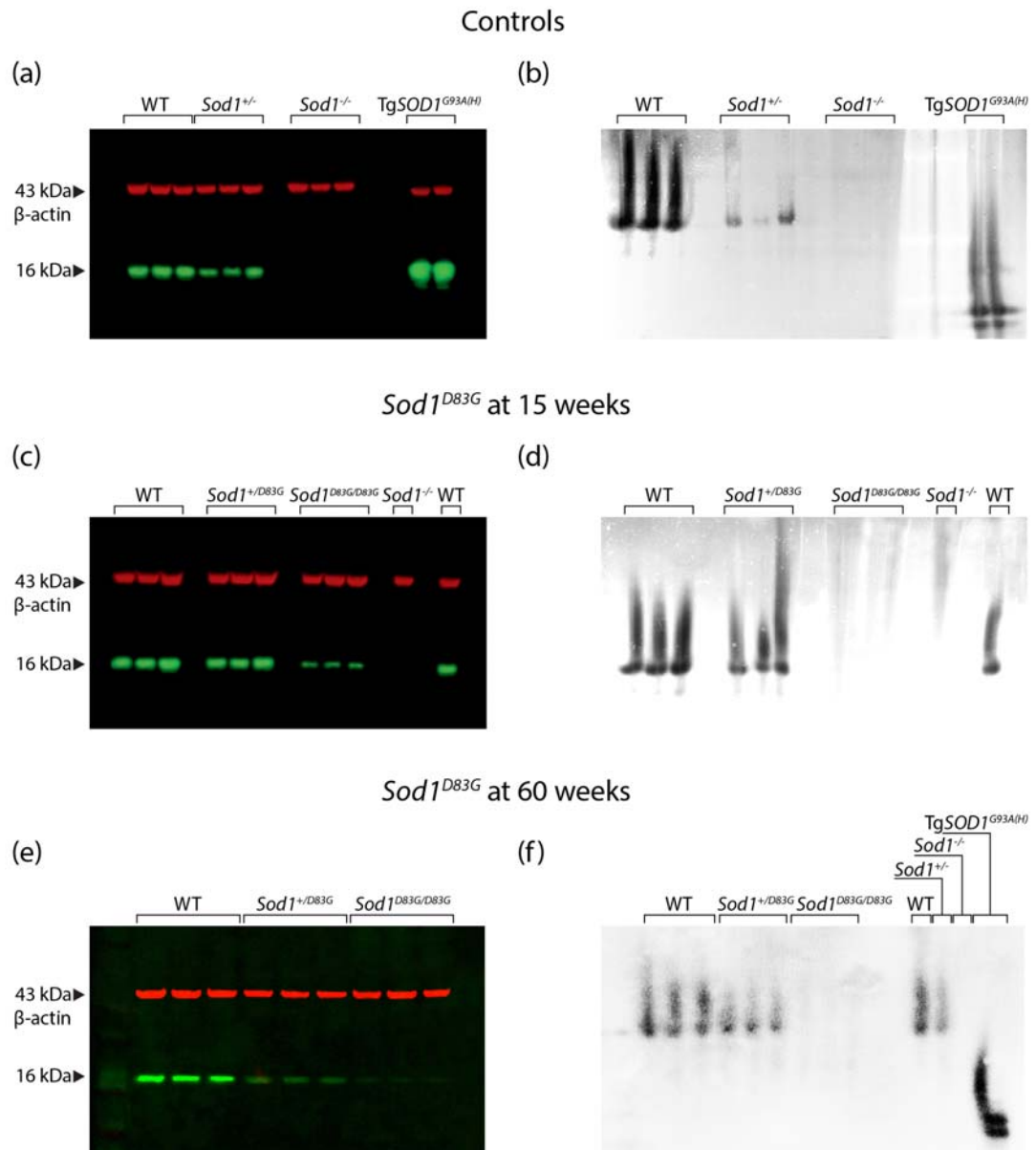


Figure 4.4 SOD1 western blots and activity gel assays of *Sod1*^{D83G} mice and controls at 15 and 60 weeks of age. (a) Western blot and (b) activity gel assay of *Sod1*^{-/-}, *Sod1*^{+/-}, wild-type (WT) and Tg*SOD1*^{G93A(H)} animals. (c) Western blot and (d) activity gel assay of *Sod1*^{D83G} homozygous, heterozygous and wild-type (WT) littermates at 15 weeks. (e) Western blot and (f) activity gel assay of *Sod1*^{D83G} homozygous, heterozygous and wild-type (WT) littermates at 60 weeks; n = 3 per genotype. 20 µg of protein for western blot and 30 µg of protein for activity assay were added per well. In activity gel assays SOD1 bands from Tg*SOD1*^{G93A(H)} mice migrate faster compared to SOD1 bands from wild-type, *Sod1*^{+/-} and *Sod1*^{D83G} mice.

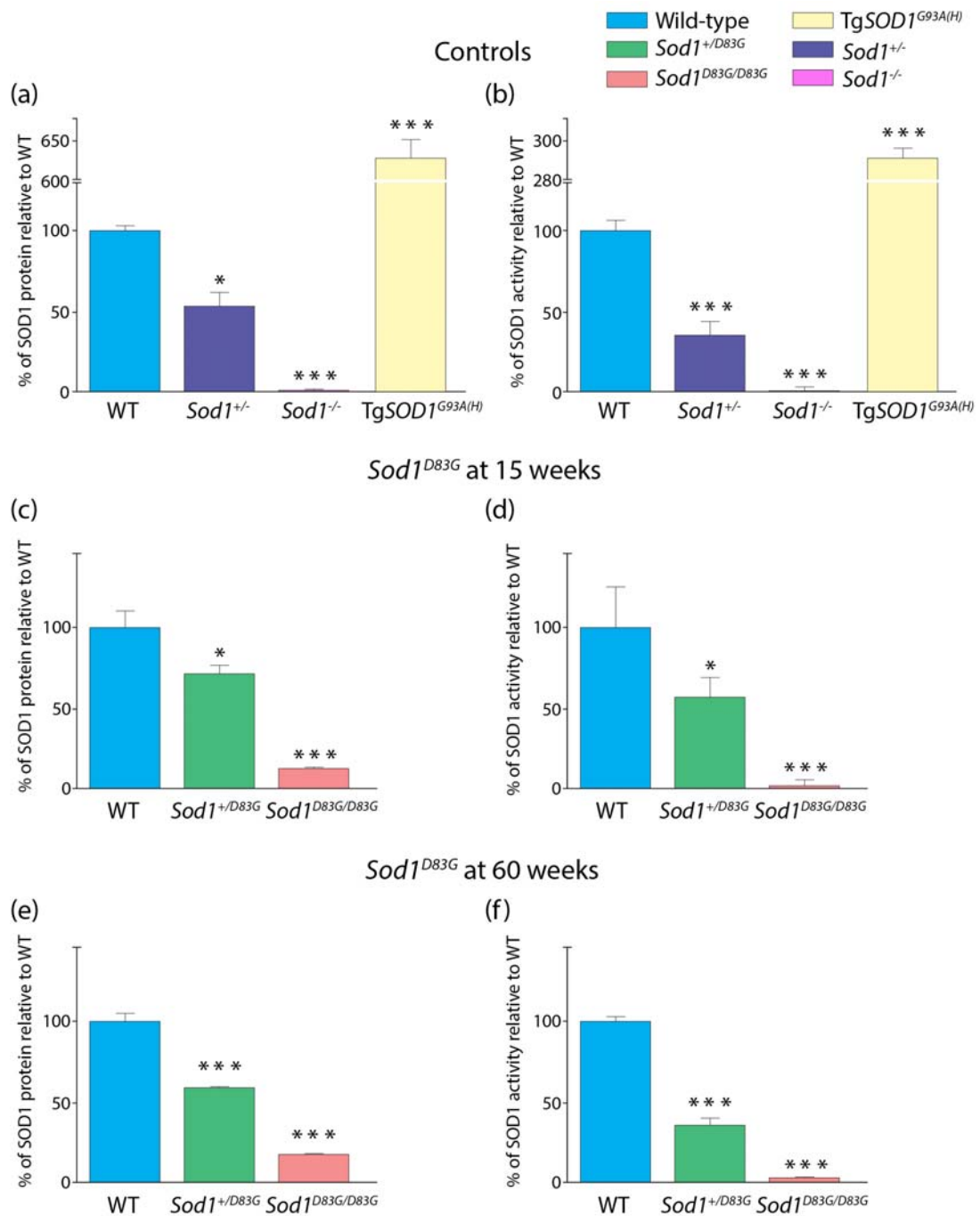


Figure 4.5 Quantification of SOD1 protein levels and activity of *Sod1*^{D83G} mice and controls at 15 and 60 weeks of age. (a) SOD1 protein levels and (b) activity of *Sod1*^{-/-}, *Sod1*^{+/-}, wild-type (WT) and Tg*SOD1*^{G93A(H)} animals. (c) SOD1 protein levels and (d) activity of *Sod1*^{D83G} homozygous, heterozygous and wild-type (WT) littermates at 15 weeks. (e) SOD1 protein levels and (f) activity of *Sod1*^{D83G} homozygous, heterozygous and wild-type (WT) littermates at 60 weeks. Values represent the mean \pm SEM from 3 independent experiments, expressed as % of wild-type, SOD1 protein levels are normalised for β -actin. For all measurements $p < 0.001 = ***$; $p < 0.01 = **$; $p < 0.05 = *$, $n = 3$ per genotype per experiment.

4.3.2 *Sod1*^{D83G} X *Sod1* knockout cross characterisation

Characterisation of the *Sod1*^{D83G} line showed that *Sod1*^{D83G/D83G} phenocopy several aspects of *Sod1*^{-/-} mice, such as reduced survival, development of hepatocellular carcinoma, NMJ denervation, development of axonopathy and lack of dismutase activity (Joyce et al., 2011; McGoldrick et al., 2013; Turner and Talbot, 2008). However, unlike *Sod1*^{-/-} mice, *Sod1*^{D83G/D83G} animals retain about 12 % of SOD1 protein and have an additional toxic gain of function that causes degeneration of motor neurons (Joyce et al., 2014). To investigate if the gain of function element seen in *Sod1*^{D83G} mice is dose dependent and how it affects axonopathy and motor neuron loss, *Sod1*^{D83G} animals were crossed with the *Sod1* knockout line (see breeding scheme in section 2.2.8). In particular the phenotype of the compound heterozygous *Sod1*^{-/D83G} was analysed in comparison with *Sod1*^{D83G/D83G} and *Sod1*^{-/-} animals. If the *Sod1*^{D83G} line have a dose dependent gain of function mechanism, as expected, the compound animals should have a phenotype less severe than the *Sod1*^{D83G/D83G} mice.

Mice from this cross were maintained and sampled in collaboration with Dr. Philip McGoldrick. Here are present data of SOD1 protein levels and dismutase activity. Motor neuron counts, muscle force and EDL motor unit number from the same colony were measured by Dr. Philip McGoldrick (data not yet published).

4.3.2.1 SOD1 protein levels of *Sod1*^{D83G} X *Sod1* knockout progeny at 15 weeks

SOD1 protein levels were assessed by western blot (section 2.6.4.2) from brain homogenate of 15 weeks *Sod1*^{+/D83G}, *Sod1*^{-/D83G} and *Sod1*^{D83G/D83G} mice. Values were compared using one-way ANOVA. Control mice and *Sod1*^{+/D83G} protein levels relative to wild-type are reported in Figure 4.5 (a) and (c).

SOD1 protein levels of heterozygous *Sod1*^{D83G} mice (100 % ± 4.7 %) were significantly higher compared to homozygous (20.5 % ± 1.6 %) and compound heterozygous knockout mice (7 % ± 0.5 %). Furthermore *Sod1*^{-/D83G} protein levels were significantly reduced also compared to *Sod1*^{D83G/D83G} animals, confirming that the absence of one D83G allele results in a reduction of SOD1 protein see Figure 4.6 (a) and Figure 4.7 (a).

4.3.2.2 SOD1 enzymatic activity of *Sod1^{D83G}* X *Sod1* knockout progeny at 15 weeks

SOD1 enzymatic activity was measured by activity gel assays (section 2.6.4.4) using brain homogenate of 15 weeks *Sod1^{+ /D83G}*, *Sod1^{- /D83G}* and *Sod1^{D83G /D83G}* mice. Values were compared using one-way ANOVA. Controls and *Sod1^{+ /D83G}* measures relative to wild-type can be found in Figure 4.5 (b) and (d).

SOD1 activity of heterozygous *Sod1^{D83G}* mice (100 % ± 13.9 %) was significantly higher compared to both homozygous (1.2 % ± 0.6 %) and compound heterozygous knockout mice (0.4 % ± 0.2 %), where activity was absent as expected, see Figure 4.6 (b) Figure 4.7 (b).

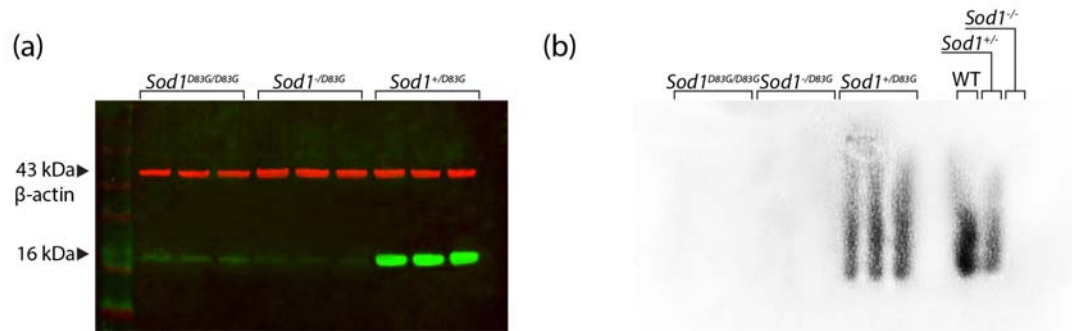


Figure 4.6 SOD1 western blots and activity gel assays of *Sod1^{D83G}* X *Sod1* KO offspring and controls at 15 weeks. (a) Western blot and (b) activity gel assay of *Sod1^{+ /D83G}*, *Sod1^{- /D83G}* and *Sod1^{D83G /D83G}* mice; n = 3 per genotype. 20 µg of protein for western blot and 30 µg of protein for activity assay were added per well.

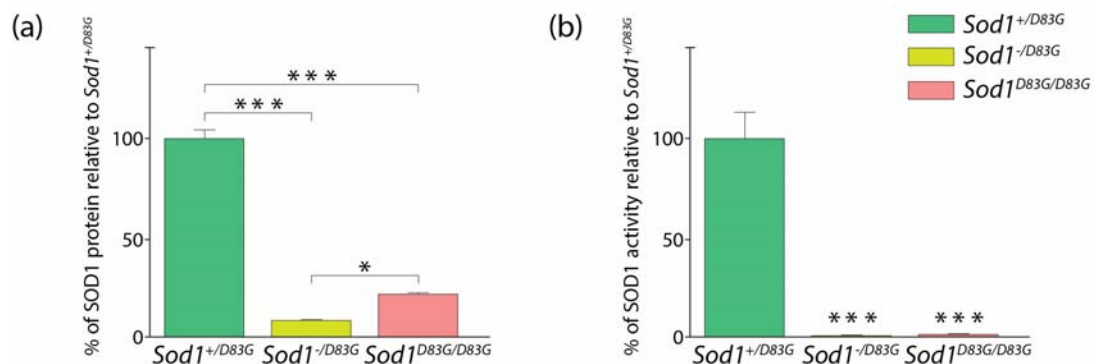


Figure 4.7 Quantification of SOD1 protein levels and activity of *Sod1^{D83G}* X *Sod1* KO offspring at 15 weeks. (a) SOD1 protein levels and (b) activity of *Sod1^{+ /D83G}*, *Sod1^{- /D83G}* and *Sod1^{D83G /D83G}* animals at 15 weeks. Values represent the mean ± SEM from 3 independent experiments, expressed as % of *Sod1^{+ /D83G}*, SOD1 protein levels are normalised for β-actin. For all measurements $p < 0.001 = ***$; $p < 0.01 = **$; $p < 0.05 = *$ n = 3 per genotype per experiment.

4.3.3 *Sod1^{D83G}* X Tg*SOD1^{WT}* cross characterisation

To see if it was possible to dissect elements of a loss of function and gain of function mechanism in the *Sod1^{D83G}* mice, this line was crossed with mice overexpressing the human wild-type SOD1 protein, see breeding scheme in section 2.2.9. In particular the aim was to investigate the phenotype of Tg*Sod1^{D83G/D83G}* mice to see if the presence of the human SOD1 protein can rescue elements of a loss of function, while maintaining the gain of function mechanism, or if its presence exacerbates ALS-like features.

Mice from this cross were maintained and sampled by me in collaboration with Dr. Philip McGoldrick. Data of SOD1 protein levels and dismutase activity are presented in this section. Motor neuron counts, muscle force and EDL motor unit number from the same colony were measured by Dr. Philip McGoldrick (data not published).

The six genotypes generated from this cross plus a Tg*SOD1^{G93A(H)}* control were used in the experiments described in this section. All genotypes are listed in Table 4.6.

Transgenic allele	<i>Sod1^{D83G}</i> allele	Nomenclature
Non-transgenic	Wild-type (<i>Sod1^{+/+}</i>)	Wild-type
Non-transgenic	<i>Sod1^{+/D83G}</i>	<i>Sod1^{+/D83G}</i>
Non-transgenic	<i>Sod1^{D83G/D83G}</i>	<i>Sod1^{D83G/D83G}</i>
<i>SOD1^{WT}</i> transgenic	Wild-type (<i>Sod1^{+/+}</i>)	Tg <i>SOD1^{WT}</i>
<i>SOD1^{WT}</i> transgenic	<i>Sod1^{+/D83G}</i>	Tg ^{WT} <i>Sod1^{+/D83G}</i>
<i>SOD1^{WT}</i> transgenic	<i>Sod1^{D83G/D83G}</i>	Tg ^{WT} <i>Sod1^{D83G/D83G}</i>
<i>SOD1^{G93A(H)}</i> transgenic	Wild-type (<i>Sod1^{+/+}</i>)	Tg <i>SOD1^{G93A(H)}</i>

Table 4.6 Experimental genotypes for *Sod1^{D83G}* X Tg*SOD1^{WT}* characterisation.

4.3.3.1 Ratio of *Sod1^{D83G}* X Tg*SOD1^{WT}*

Pervious data showed that *Sod1^{D83G}* mice ratios, significantly differ from expected Mendelian ratios (Joyce et al., 2014). The number of offspring of the 6 potential genotypic ratios from the *Sod1^{D83G}* X Tg*SOD1^{WT}* cross (Figure 2.2) was monitored from 6 trios (two females and one male). The observed ratios were significantly different from the expected ratios $\chi^2(5) = 14.97$ $p = 0.0105$. Results are summarised in Table 4.7.

Genotype	Number of animals	Observed ratios	Expected ratios
Wild-type	25	0.173	0.125
<i>Sod1</i> ^{+/D83G}	37	0.256	0.25
<i>Sod1</i> ^{D83G/D83G}	6	0.041	0.125
Tg <i>SOD1</i> ^{WT}	25	0.173	0.125
Tg ^{WT} <i>Sod1</i> ^{+/D83G}	38	0.263	0.25
Tg ^{WT} <i>Sod1</i> ^{D83G/D83G}	6	0.090	0.125
Total	144	1	1

Table 4.7 Observed ratios of offspring from *Sod1*^{D83G} X Tg*SOD1*^{WT} cross. The omnibus χ^2 showed that observed ratios differ significantly from expected ratios.

4.3.3.2 SOD1 protein levels of *Sod1*^{D83G} X Tg*SOD1*^{WT} progeny at 15 weeks

SOD1 protein levels of transgenic and non-transgenic animals, generated from the *Sod1*^{D83G} X Tg*SOD1*^{WT} cross, were evaluated by western blot (section 2.6.4.2) using brain homogenate of 15-week old mice. Since these transgenic animals generally have a level of SOD1 protein that is about five-fold of wild-type mice, transgenic and non-transgenic genotypes were assessed in separate blots and compared among each other. A control experiment was performed to show the difference in SOD1 protein between transgenic and wild-type non-transgenic animals. Values were compared using one-way ANOVA.

The control experiment confirmed that SOD1 protein levels of Tg*SOD1*^{WT} (464 % \pm 29.5 %) and Tg*SOD1*^{G93A(H)} (498 % \pm 19.9 %) animals were significantly higher compare to SOD1 levels of wild-type mice (100 % \pm 5.3 %), see Figure 4.8 (a) and Figure 4.9 (a).

As expected SOD1 protein levels of non-transgenic homozygous and heterozygous mice were significantly reduced compared to wild-type littermates. In particular SOD1 protein in *Sod1*^{D83G/D83G} mice was reduced down to 21.8 % \pm 1.4 % of wild-type littermates (100 % \pm 1.6 %), while *Sod1*^{+/D83G} mice retained 70.7 % \pm 5.1 % of SOD1 protein compared to wild-type (Figure 4.8 (c) and Figure 4.9 (c)).

Instead SOD1 protein levels of the 3 transgenic genotypes were all similar among each other. In particular SOD1 protein levels of Tg^{WT}*Sod1*^{+/*D83G*} mice were 101.3 % ± 0.9 % compare to SOD1 protein levels of Tg*SOD1*^{WT} (100 % ± 2.4 %) animals, while Tg^{WT}*Sod1*^{*D83G*/*D83G*} SOD1 protein levels (90.9 % ± 4 %) were slightly reduced but not significantly different from Tg*SOD1*^{WT} animals, see Figure 4.8 (e) and Figure 4.9 (e).

4.3.3.3 SOD1 enzymatic activity of *Sod1*^{*D83G*} X Tg*SOD1*^{WT} progeny at 15 weeks

SOD1 enzymatic activity of transgenic and non-transgenic animals, generated from the *Sod1*^{*D83G*} X Tg*SOD1*^{WT} cross, was measured by activity gel assays (section 2.6.4.4) using brain homogenate of 15-week old mice. As for SOD1 protein levels, SOD1 activity is much higher in transgenic animals compared to wild-type; therefore dismutase activity of transgenic and non-transgenic genotypes was assessed in separate gel assays. A control experiment showed the difference in SOD1 dismutase activity between transgenic and wild-type non-transgenic animals, see Figure 4.8 (b) and Figure 4.9 (b). Values were compared using one-way ANOVA.

SOD1 activity of Tg*SOD1*^{WT} (479.6 % ± 64.8 %) and Tg*SOD1*^{*G93A(H)*} (532.4 % ± 96.2 %) animals was significantly higher compare to dismutase activity of wild-type mice (100 % ± 6.2 %), see Figure 4.8 (b) and Figure 4.9 (b). As found in previous experiments, SOD1 activity of non-transgenic *Sod1*^{*D83G*} homozygous and heterozygous mice was significantly reduced compared to wild-type littermates. Specifically *Sod1*^{*D83G*/*D83G*} mice did not have any SOD1 activity (0.0% ± 0.0 %) compared to wild-type littermates (100 % ± 8 %), while *Sod1*^{+/*D83G*} mice retained 49.9 % ± 4 % of SOD1 activity compared to normal (Figure 4.8 (d) and Figure 4.9 (d)). Conversely, there was no significant difference among SOD1 activity of transgenic animals. SOD1 activity of Tg^{WT}*Sod1*^{+/*D83G*} mice was 124 % ± 11.6 % compared to Tg*SOD1*^{WT} (100 % ± 10.9 %) littermates and Tg^{WT}*Sod1*^{*D83G*/*D83G*} SOD1 activity was 134.5 % ± 4.1 % of Tg*SOD1*^{WT}, see Figure 4.8 (f) and Figure 4.9 (f).

The SOD1 activity bands detected from brain homogenates of Tg*SOD1*^{*G93A(H)*}, Tg*SOD1*^{WT}, Tg^{WT}*Sod1*^{+/*D83G*} and Tg^{WT}*Sod1*^{*D83G*/*D83G*} mice migrated faster compared to bands of wild-type and *Sod1*^{*D83G*} mice. Gel electrophoresis was carried out in native conditions, therefore the electrophoretic mobility of the proteins depended only on their charge-to-mass ratio and physical shape. Of note in these assays it was not possible to use native ladder markers to detect the size of the SOD1 activity bands.

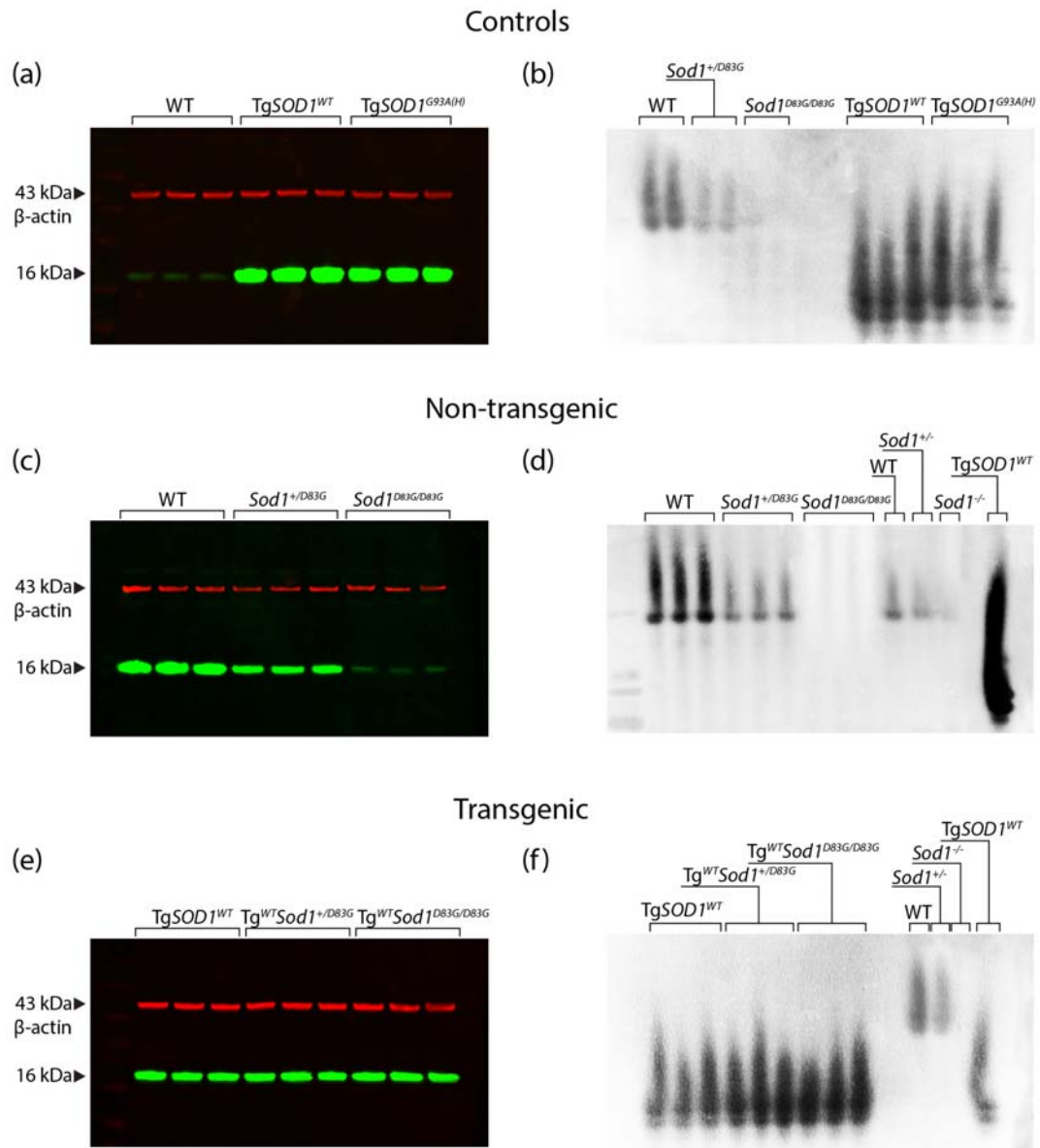


Figure 4.8 SOD1 western blots and activity gel assays of *Sod1*^{D83G} X *TgSOD1*^{WT} offspring at 15 weeks of age. (a) Western blot and (b) activity gel assay of wild-type (WT), *TgSOD1*^{WT} and *TgSOD1*^{G93A(H)} animals. (c) Western blot and (d) activity gel assay of non-transgenic offspring: *Sod1*^{D83G} homozygous, heterozygous and wild-type littermates. (e) Western blot and (f) activity gel assay of transgenic offspring: *Tg*^{WT}*Sod1*^{+/D83G}, *Tg*^{WT}*Sod1*^{D83G/D83G} and *TgSOD1*^{WT}; n = 3 per genotype. 20 μg of protein for western blot and 30 μg of protein for activity assay were added per well. In activity gel assays SOD1 bands from *TgSOD1*^{G93A(H)}, *TgSOD1*^{WT}, *Tg*^{WT}*Sod1*^{+/D83G} and *Tg*^{WT}*Sod1*^{D83G/D83G} mice migrate faster compared to SOD1 bands from wild-type and *Sod1*^{D83G} mice.

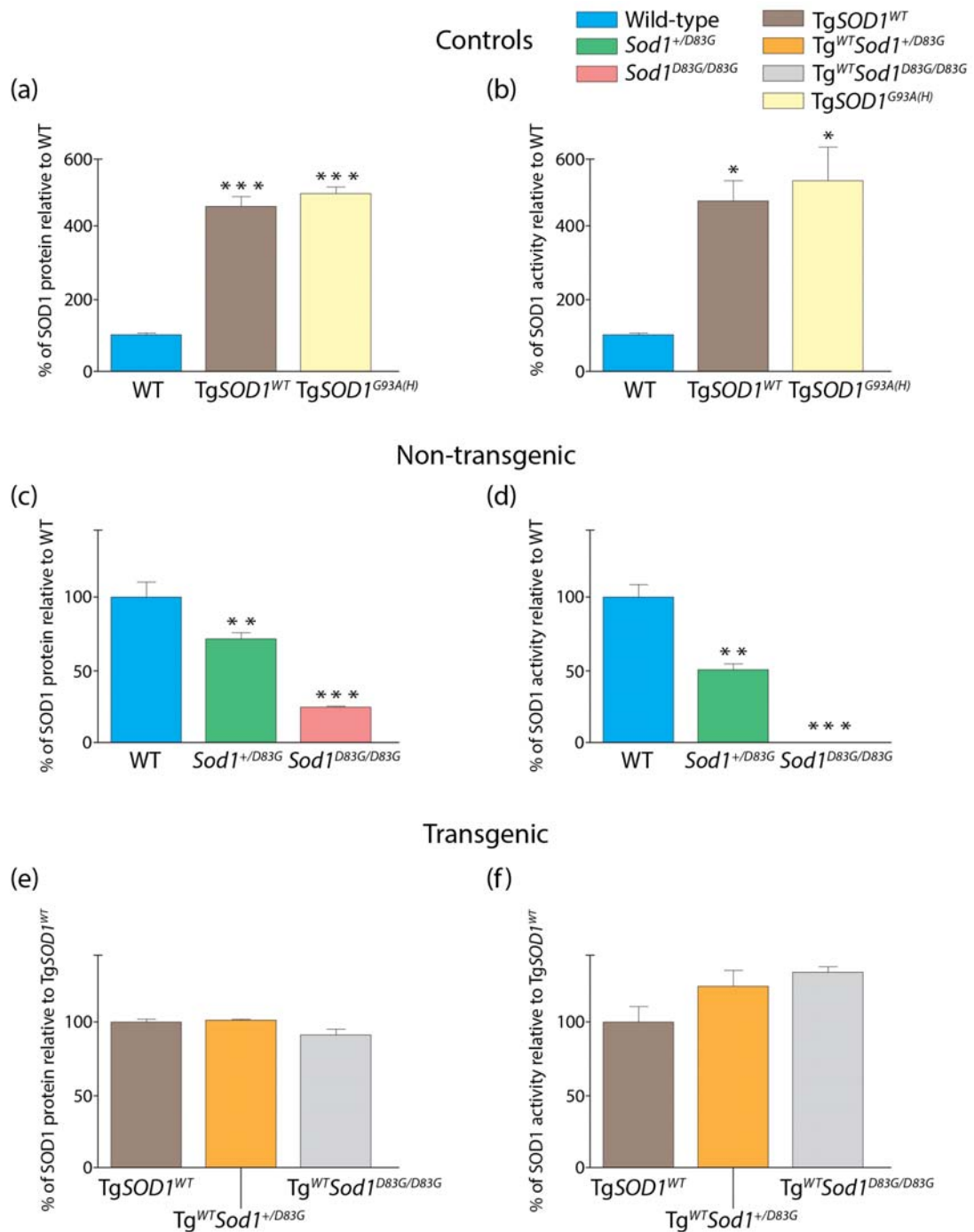


Figure 4.9 Quantification of SOD1 protein levels and activity of *Sod1*^{D83G} X *TgSOD1*^{WT} offspring at 15 weeks of age. (a) SOD1 protein levels and (b) activity of wild-type (WT), *TgSOD1*^{WT} and *TgSOD1*^{G93A(H)} animals. (c) SOD1 protein levels and (d) activity of non-transgenic offspring: *Sod1*^{D83G} homozygous, heterozygous and wild-type littermates. (e) SOD1 protein levels and (f) activity of transgenic offspring: *Tg*^{WT}*Sod1*^{+/D83G}, *Tg*^{WT}*Sod1*^{D83G/D83G} and *TgSOD1*^{WT}. Values represent the mean \pm SEM from 3 independent experiments, expressed as % of wild-type (a, b, c and d) or % of *TgSOD1*^{WT} (e and f). SOD1 protein levels are normalised for β -actin. For all measurements $p < 0.001 = ***$; $p < 0.01 = **$; $p < 0.05 = *$, $n = 3$ per genotype per experiment.

4.4 Conclusions

Transgenic mouse models overexpressing either wild-type or mutant human *SOD1* have been largely employed in the study of ALS (Joyce et al., 2011). In particular mice overexpressing the mutant human *SOD1* gene recapitulate many characteristics of human ALS and have been crucial in our understanding of this disease. However, they are not a close genetic representation of human ALS, as they overexpress the human SOD1 protein at high levels, alongside the endogenous mouse SOD1 protein (Figure 4.10). Also *Sod1* knockout models have been key in SOD1-ALS research. These mice have a slow progressive axonopathy and a range of ALS-like phenotypes but do not develop motor neuron degeneration therefore they are not a model of human ALS (Figure 4.10). *Sod1*^{D83G} is the first mouse model described to date that carries the equivalent of a human pathogenic mutation in the mouse *Sod1* gene expressed at endogenous levels (Joyce et al., 2014; Millecamps et al., 2010), and in this mouse line the mutant SOD1 protein is endogenous and not overexpressed (Figure 4.10). Investigation of the *Sod1*^{D83G} line demonstrated that mutations in the mouse endogenous *Sod1* gene model some human ALS features, which are different from the characteristics modelled by mice overexpressing human mutant SOD1 transgenes, making *Sod1*^{D83G} a useful tool to study new aspects of ALS.

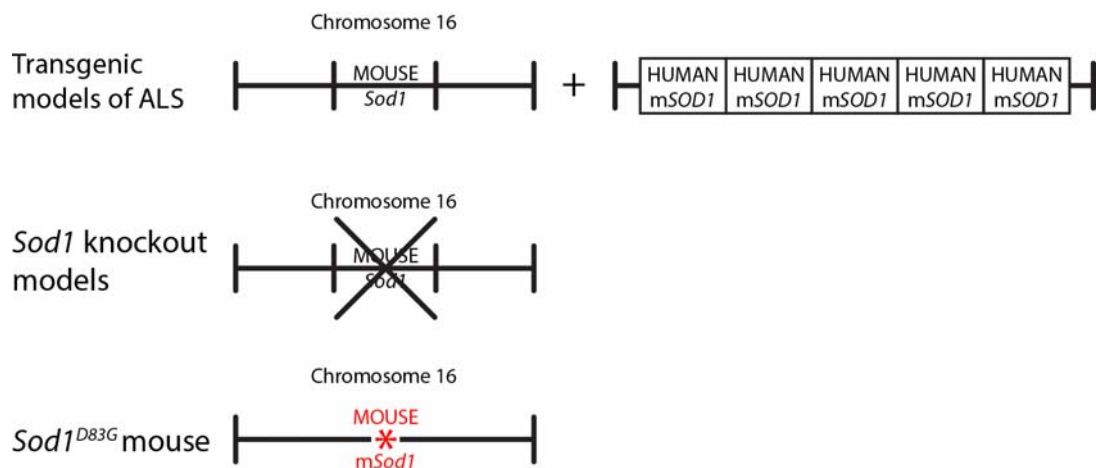


Figure 4.10 Types of mouse model used in ALS research. Transgenic mouse models of ALS express endogenous mouse *Sod1* gene (mouse chromosome 16) and overexpress the human mutant *SOD1* gene; *Sod1* knockout models lack the endogenous *Sod1* gene; *Sod1*^{D83G} mouse carries a mutation in the endogenous *Sod1* gene. Mutant human *SOD1* gene (m*SOD1*); mutant mouse *Sod1* gene (m*Sod1*).

Characterisation of the *Sod1*^{D83G} line showed that homozygous *Sod1*^{D83G} animals develop a distal axonopathy and have progressive loss of upper and lower motor neurons. This motor neuron degeneration appears to stop in early adulthood, does not lead to paralysis and is likely caused by a toxic gain of function mechanism as occurs in fALS patients. Heterozygous mice do not have motor neuron loss, at least up until one year of age, probably because the dose of mutant SOD1 protein is not sufficient to cause degeneration or because wild-type SOD1 has a protective effect. Both homozygous and heterozygous mice develop a series of other ALS related phenotypes (Joyce et al., 2014).

Data presented in this chapter highlighted some interesting features of this mouse model. Morphological examination of the EDL muscle showed that at 52 weeks of age *Sod1*^{D83G/D83G} animals have a significantly higher percentage of denervated NMJs compared to littermates. Also, the total number of NMJs counted is significantly smaller compared to the other genotypes, probably because some neuromuscular endplates are no longer detectable from muscle sections. Suggesting that the degeneration process occurs between 15 and 52 weeks of age. Since in *Sod1*^{D83G/D83G} motor neuron degeneration occurs between 6 and 15 weeks and does not progress further with age (Joyce et al., 2014); taken together these findings point to the hypothesis that the loss of EDL neuromuscular junction detected in these mice is a peripheral neuropathy that is not caused by motor neuron death.

Investigation of SOD1 protein by western blot showed a dose-dependent decrease of SOD1 in homozygous and heterozygous animals, which does not change with age. *Sod1*^{D83G/D83G} mice have a reduction in SOD1 protein to approximately 10 % of wild-type, while *Sod1*^{+ /D83G} retain about 70 % of SOD1 protein. Analysis of the mRNA levels revealed that these SOD1 protein reductions are not caused by allele-specific differences in transcription (Joyce et al., 2014), but more likely are the result of mutant SOD1 instability and degeneration. Indeed, the D83 residue was predicted to coordinate zinc and therefore be crucial for SOD1 stability, see Figure 1.4 (Choi et al., 2011; Krishnan et al., 2006; Nordlund et al., 2009); moreover mutant SOD1 was shown to have a decreased half-life compare to wild-type protein and consequently degenerate faster (Kabuta et al., 2006). The low SOD1 protein detected in *Sod1*^{D83G/D83G} mice might explain why the motor neuron loss does not progress with age in these animals. It is known from SOD1 transgenic mouse models that there is a positive

correlation between toxicity and SOD1 dose. Therefore it is possible to speculate that the low SOD1 protein level detected in homozygous animals is sufficient to trigger motor neuron denervation but not at the same levels seen in SOD1-ALS patients.

Activity gel analysis showed that SOD1 dismutase activity in 15 and 60-week old *Sod1*^{D83G/D83G} is approximately 1 % of wild-type animals, while *Sod1*^{+ /D83G} retain about 50 % of SOD1 activity, similarly to SOD1-fALS patients (section 3.3.1) and to *Sod1* knockout mice (section 3.3.2 and Figure 4.5 (b)). Interestingly homozygous *Sod1*^{D83G} animals share commonalities with *Sod1*^{-/-} mice (discussed in section 7.1.4), the most striking example is the development of a progressive peripheral motor neuropathy. This shared phenotype, may be caused by a loss of dismutase function mechanism, which might increase the vulnerability of motor axons to oxidative stress (Fischer et al., 2004) or simply be the result of a lack of a yet unknown SOD1 function. Of note the SOD1 protein activity bands detected from brain homogenates of mice carrying either the human wild-type or mutant SOD1 G93A transgene, migrated faster in the gel compared to the bands from mouse wild-type and mutant D83G samples. This difference in migration pattern in native conditions may be explained by diverse biochemical and biophysical characteristics of the human and mouse SOD1 proteins.

Studies carried out in SOD1 transgenic mouse models and ALS patients led to the concept that ALS is a “dying back” disorder, meaning that in the disease muscle denervation occurs prior to motor neuron cell body death (Fischer et al., 2004; Murray et al., 2010). Thus suggesting that a gain of toxic function can contribute to the peripheral neuropathy seen in *Sod1*^{D83G/D83G} animals. However, data presented here and findings from other SOD1 mouse models point to the hypothesis that axonal and neuron body degeneration are separate events, which may be regulated by different genes. The *Sod1*^{D83G/D83G} mouse may be a good system in which it is possible to dissect the early stages of the human ALS and separate the effects of a mutant SOD1 toxic gain of function from a loss of function.

To try and investigate the gain and loss of function mechanisms, *Sod1*^{D83G} animals were crossed with *Sod1* knockout and TgSOD1^{WT} mice. To date only SOD1 protein levels and activity have been measured from the offspring of these crosses. Data on motor neuron counts, muscle force and EDL motor unit survival have not yet been analysed.

SOD1 protein levels of the compound heterozygous animals $Sod1^{-/D83G}$, produced from the cross with the $Sod1$ knockout line, are significantly reduced compared to $Sod1^{+/D83G}$ and also compared to $Sod1^{D83G/D83G}$ littermates, while SOD1 activity is absent. Investigation of spinal cord and muscles of these animals will tell if the $Sod1^{D83G}$ phenotype is dose-dependent and whether one mutant D83G allele is sufficient to cause motor neuron degeneration. Moreover it will shed some light on the causes of the peripheral axonopathy and the motor neuron loss seen in $Sod1^{D83G/D83G}$ animals. Indeed, if a gain of function mechanism is present, the $Sod1^{-/D83G}$ phenotype should be less severe than the one of $Sod1^{D83G/D83G}$ mice.

SOD1 protein levels and activity measured from offspring of the $Sod1^{D83G}$ X TgSOD1^{WT} confirmed previous results from $Sod1^{D83G}$ animals and showed five-fold increase in protein level and SOD1 activity in transgenic animals compared to wild-type. Investigation of motor neurons of transgenic offspring will tell if the presence of a human wild-type SOD1 protein has a protective effect and rescues the loss of motor neurons seen in homozygous $Sod1^{D83G}$ animals or if its exacerbates ALS phenotypes.

The present work on the $Sod1^{D83G}$ model together with further analysis will hopefully give new insights on the contribution of both central neuronal loss and peripheral neuronal dysfunction in SOD1-ALS.

4.5 Summary

- $Sod1^{D83G/D83G}$ mice develop a distal progressive motor axonopathy between 15 and 52 weeks of age
- SOD1 protein levels are reduced to ~65 % in $Sod1^{+/D83G}$ and to ~10 % in $Sod1^{D83G/D83G}$ compared to wild-type littermates both at 15 and 60 weeks of age
- SOD1 dismutase activity is reduced to 50 % in $Sod1^{+/D83G}$ and it is almost absent in $Sod1^{D83G/D83G}$ compared to wild-type littermates both at 15 and 60 weeks of age
- SOD1 protein levels of $Sod1^{-/D83G}$ mice are significantly reduced compared to $Sod1^{+/D83G}$ and $Sod1^{D83G/D83G}$ littermates

- SOD1 activity of *Sod1*^{-/D83G} mice is almost absent and significantly reduced compared to *Sod1*^{+ /D83G} littermates
- Tg*SOD1*^{WT}, Tg^{WT}*Sod1*^{+ /D83G} and Tg^{WT}*Sod1*^{D83G /D83G} have similar SOD1 protein levels and activity which are significantly increased compared to wild-type littermates

Chapter 5 Characterisation of SOD1 proteins

5.1 Introduction

5.1.1 Possible prion-like mechanism for SOD1 protein

SOD1 displays prion-like properties both *in vitro* and *in vivo*, as happens for proteins causative of other neurodegenerative diseases such as Parkinson's and Alzheimer's disease (Marciniuk et al., 2013). Proteins that have prion-like properties are able to sequester the wild-type form of the protein, seed its aggregation or misfolding, and act as transmissible agents between cells (Bunton-Stasyshyn et al., 2014; Polymenidou and Cleveland, 2012), Figure 5.1.

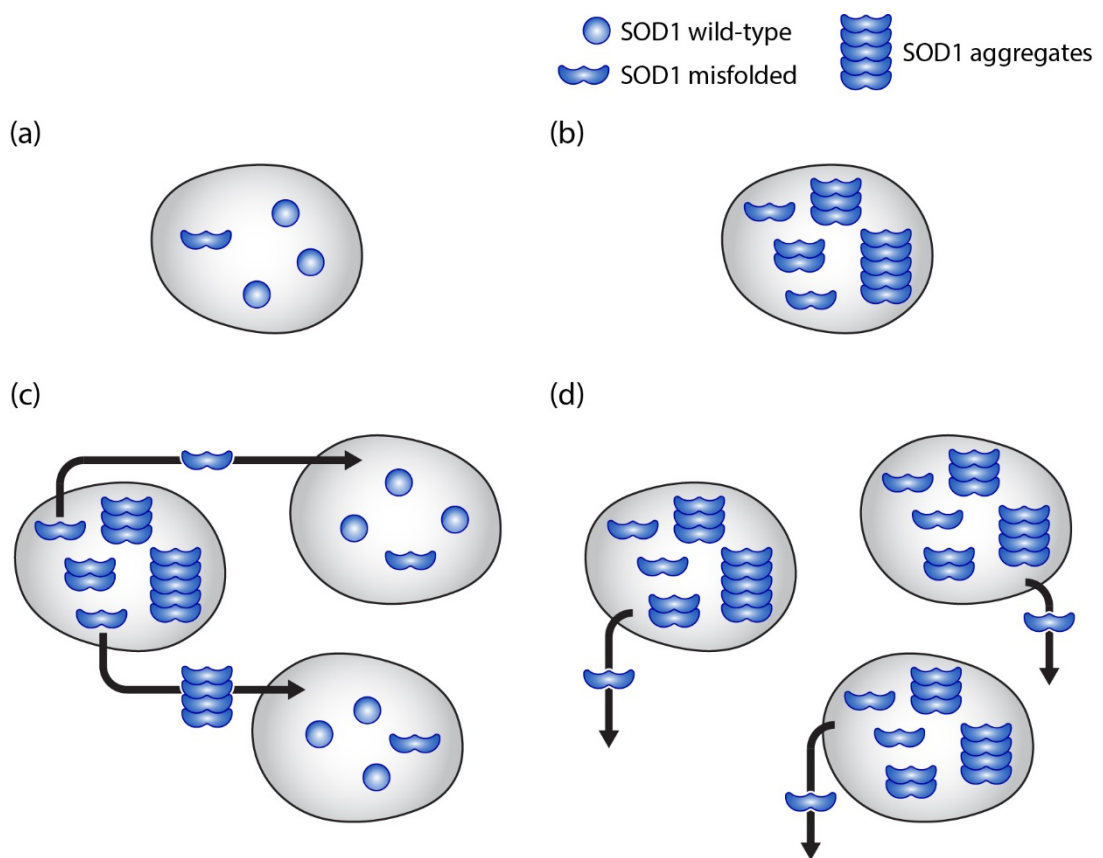


Figure 5.1 Possible prion-like mechanism for SOD1 protein. (a) Misfolded SOD1 within a cell could (b) sequester and misfold wild-type SOD1 and eventually producing aggregates. (c) If secreted and taken up by neighbouring cells misfolded SOD1/aggregated SOD1 could (d) cause a chain reaction of misfolding, aggregate formation and transmission in a prion-like manner.

Indeed, SOD1 protein can form aggregates, which are a well-known hallmarks of SOD1-fALS, and have been found also in sALS cases (Bosco et al., 2010; Forsberg et al., 2010; Grad and Cashman, 2014). Moreover SOD1 has been shown to seed its own

aggregation *in vitro* and to transmit in human and mouse cell lines and recently also in SOD1-fALS mouse models (Ayers et al., 2014; Chia et al., 2010; Furukawa et al., 2013; Münch et al., 2011; Weisberg et al., 2012). These findings are in accordance with the fact that ALS has a focal start and is a non-cell autonomous disease (Ilieva et al., 2009), and point to the hypothesis that mutant forms of the SOD1 proteins are the toxic species causative of SOD1-ALS. Indeed non-amyloid SOD1 inclusions are found in SOD1-fALS MNs (Kato et al., 1996, 1997, 2000; Kerman et al., 2010), and there is a correlation between disease phenotype and aggregation pathology in SOD1-fALS mice (Turner et al., 2003; Wang et al., 2002a, 2002b, 2005a). Furthermore investigation of aggregate toxicity in cell culture models has yielded evidence suggesting that increasing the level of soluble SOD1 increases toxicity, while increasing recruitment of mutant SOD1 into insoluble inclusions decreased toxicity (Brotherton et al., 2013; Weisberg et al., 2012).

5.1.1.1 SOD1 aggregation *in vitro*

In vitro Thioflavin-T (ThT) assays, measuring protein aggregation propensity, demonstrated that both wild-type and mutant human SOD1 recombinant proteins can spontaneously aggregate, seed aggregation of themselves (self-seeding) and of each other (cross-seeding), in an autocatalytic manner (Chia et al., 2010). The lag time of fibrillization both for self-seeded and cross-seeded reactions was shorter compared to spontaneous seeding (Chia et al., 2010). Further, spinal cord homogenates from TgSOD1^{G93A(H)} mice were shown to successfully self-seed and cross-seed aggregation *in vitro* with recombinant wild-type and mutant SOD1 proteins (Chia et al., 2010). Of note the seeding of SOD1 amyloid fibrils occurred at acidic pH and in the presence of a chaotropic and a misfolding agent (Bunton-Stasyshyn et al., 2014; Chia et al., 2010). Finally self-seeding and cross-seeding with recombinant proteins were shown to produce aggregate species with structural properties similar to aggregates found in SOD1-fALS (Hwang et al., 2010).

5.1.1.2 SOD1 transmission *in vitro*

Cells experiments showed that mutant SOD1 was secreted extracellularly in exosomes from primary astrocytes and neuronal-like stable cell lines (Basso et al., 2013; Grad and Cashman, 2014). Moreover, mutant SOD1 protein was detected in medium from primary cultures of spinal cord and of astrocytes from SOD1-ALS transgenic mice (Basso et al., 2013; Urushitani et al., 2006). Interestingly astrocytes derived from

SOD1-fALS mice showed increased secretion of SOD1 in exosomes compared to mice overexpressing the wild-type human SOD1 protein and these exosomes resulted toxic to primary cultures (Basso et al., 2013).

Internalisation of recombinant mutant and wild-type SOD1 proteins also occurred in cell models, either via macropinocytosis in neuronal-like stable cell lines (Grad and Cashman, 2014; Münch et al., 2011; Sundaramoorthy et al., 2013), or via exosome internalisation in primary mouse spinal cord cultures and neuronal-like cell lines (Basso et al., 2013; Grad and Cashman, 2014).

Investigations carried out using a mouse neuroblastoma-derived cell line confirmed *in vitro* results showing that once internalised, aggregates of recombinant mutant SOD1 could self-seed aggregations of stable mutant SOD1 protein, even after the exogenous seeds were no longer present in the cells (Münch et al., 2011). Further aggregated and non-aggregated recombinant mutant SOD1 could cross-seed the wild-type form of the protein, which could also be self-seeded by aggregated recombinant wild-type SOD1 (Bunton-Stasyshyn et al., 2014; Sundaramoorthy et al., 2013).

In a human cell line, exogenously applied recombinant mutant SOD1 (both aggregated and non-aggregated) and aggregated wild-type SOD1 caused aggregation of endogenous SOD1, but also activated ER stress and apoptotic cell death (Sundaramoorthy et al., 2013), demonstrating ALS relevant toxicity related to self-seeded and cross-seeded reactions. Of note self-seeding aggregation of endogenous SOD1 was reported in stable cell lines and could be blocked by immune-depletion of misfolded SOD1 or by knocking down the *SOD1* gene (Grad and Cashman, 2014; Grad et al., 2011).

5.1.1.3 SOD1 transmission *in vivo*

In a recent study Ayers and colleagues investigated the prion-like transmissibility of mutant SOD1 and motor neuron disease pathology *in vivo*. Spinal cord homogenates from TgSOD1^{G93A(H)} mice were injected in spinal cords of different SOD1 transgenic mice. After injection motor neuron disease was induced in and otherwise unaffected transgenic animals expressing low level of mutant SOD1 G85R (TgSOD1^{G85R}). Interestingly when spinal cord homogenate from induced mice was used to inoculate new animals, as happened in prion models, the disease onset of recipient mice was early compared to the first passage animals. Also one-third of the TgSOD1^{G85R} animals

inoculated with homogenates from TgSOD1^{WT} animals developed degeneration of motor neurons. Of note self-seeding experiments carried out by the same group in other transgenic mice did not change the phenotype of these animals. There are therefore evidence suggesting that mutant SOD1 and motor neuron degeneration may be transmitted with a prion-like mechanism but is still unclear if misfolded SOD1 is required and sufficient for this to happen (Ayers et al., 2014).

5.1.2 Human and mouse SOD1 proteins

Human and mouse SOD1 proteins share a similar structure and are 84 % identical in amino acid sequence (Seetharaman et al., 2010). Both mouse and human SOD1 function as a dimer and accomplish the same function of scavenging superoxide radicals from the body. In SOD1 transgenic mouse models the wild-type or mutant human SOD1 protein is overexpressed together with the endogenous mouse SOD1 protein. The presence of SOD1 aggregates in these animals and the possible pathogenic role for misfolded SOD1 highlighted the importance of investigating the interaction between human and mouse SOD1. Cell culture and mouse model experiments showed that when co-expressed with human SOD1 mutants the endogenous mouse SOD1 does not co-aggregate (Wang, 2003). However, when mutant human SOD1 and wild-type human SOD1 are co-expressed the wild-type form of the protein co-aggregates with the pathogenic variant (Prudencio et al., 2009c; Seetharaman et al., 2010). Further a recent study on a mouse line carrying the G86R mutation (equivalent of human G85R) in the endogenous mouse *Sod1* gene demonstrated that raising levels of wild-type human SOD1 does not affect disease in these animals (Audet et al., 2010). A subsequent study by Qualls and colleagues using cell culture models, showed that misfolded mouse SOD1 G86R interacts readily with mouse wild-type SOD1 protein and poorly with human wild-type SOD1 (Qualls et al., 2013).

5.2 Aim

Mutant and wild-type human SOD1 recombinant proteins are known to spontaneously aggregate, self-seed and cross seed *in vitro* (Chia et al., 2010). Furthermore, both human and mouse SOD1 proteins are found in aggregates in SOD1 transgenic mouse models, however, it is still unclear whether the mouse and the human variants can co-aggregate *in vitro* and *in vivo*.

In order to investigate possible interactions between the human and the mouse SOD1, the aggregation propensity of human and mouse SOD1 recombinant proteins was examined *in vitro*. In particular human and mouse SOD1 recombinant proteins were produced using an *E. coli* system and purified by affinity chromatography. The purity of the preparations was then assessed by measuring protein quantity via western blot and coomassie blue. All SOD1 recombinant proteins were characterised by investigating their secondary structure with CD, focusing on the possible differences between human and mouse structure. Further, two preliminary experiments were carried out to investigate whether the mouse SOD1 recombinant proteins can spontaneously seed aggregation *in vitro* as happen for human SOD1.

As part of a bigger project to study whether SOD1 can act in a prion-like way seeding aggregations (Appendix 8.6), mouse spinal cord homogenates were analysed by polyacrylamide gel electrophoresis to confirm the presence of SOD1 and possibly detect misfolded forms of the protein.

5.3 Results

5.3.1 SOD1 recombinant proteins

To investigate the aggregation propensity of mouse and human SOD1 protein and its capacity to co-aggregate, eight SOD1 protein variants were produced, purified and characterised. Preliminary experiments were then carried out to study SOD1 protein aggregation.

5.3.1.1 Production and purification of recombinant proteins

Five human SOD1 and three mouse SOD1 recombinant proteins (Table 5.1) were produced using a prokaryotic expression system: *E. coli* BL21 (DE3), as in (Chia et al., 2010). The cDNA of the eight SOD1 variants employed in this study had been previously cloned by Dr Chia Ruth into pET28a expression vectors downstream of a sequence encoding a string of six histidines, so that the SOD1 protein produced would be His-tagged. Expression of the SOD1 protein was based on an IPTG induction system see sections 2.6.1 and Appendix 8.1.

Species	Variants
Human	Wild-type
	G93A
	D83G
	I113T
	D101G
Mouse	Wild-type
	G93A
	D83G

Table 5.1 Human and mouse SOD1 recombinant proteins produced.

A protein scale preparation from 9 litre culture was carried out for each SOD1 variant. *E. coli* strains transformed with plasmids carrying the SOD1 cDNAs of interest were grown as described in section 2.6.1. Once the desired cell density was reached, SOD1 protein expression was induced using IPTG. Samples of SOD1 protein preparations pre-IPTG and post-IPTG treatment were collected and tested by coomassie blue to confirm induction (see example for human SOD1 wild-type in Figure 5.2). Prior to purification SOD1 proteins were extracted and solubilised as described in 2.6.1.1.

Affinity chromatography purification was carried out using a Ni-NTA column on an ÄKTA pure machine. The soluble fraction from the crude cell extract of each preparation was loaded on the Ni-NTA column to remove the contaminating proteins from the His-SOD1 protein. After overnight on-column refolding (Figure 5.3 (a)) the His-SOD1 protein was eluted (Figure 5.3 (b)), dialysed and incubated with thrombin to cleave the His-tag. All SOD1 variants were separated by polyacrylamide gel electrophoresis and stained using coomassie blue to confirm cleavage (see example for human SOD1 wild-type Figure 5.4). The free His-tag was removed by a second Ni-NTA affinity chromatography (Figure 5.5) and the SOD1 protein preparation was collected and dialysed against storage buffer, see 2.6.1.2. Prior to experiments, all SOD1 proteins were loaded with copper and zinc by subsequent dialysis to ensure acquisition of their full enzymatic activity see 2.6.1.2.

The amount of SOD1 protein produced varied between 20 and 130 mg depending on the protein preparation. While the final concentrations of the recombinant proteins ranged between 0.5 and 2 mg / ml per SOD1 variant. Protein concentration was a crucial parameter for characterisation and aggregation experiments, it was therefore carefully calculated using three different methods: absorbance, DC protein assay and coomassie blue staining compared to a sample of known concentration, (section 2.6.3 and 2.6.4.1). Results obtained were consistent among the three methods.

The images presented in this section are representative of the human wild-type SOD1 protein, the same procedure was carried out for all other variants.

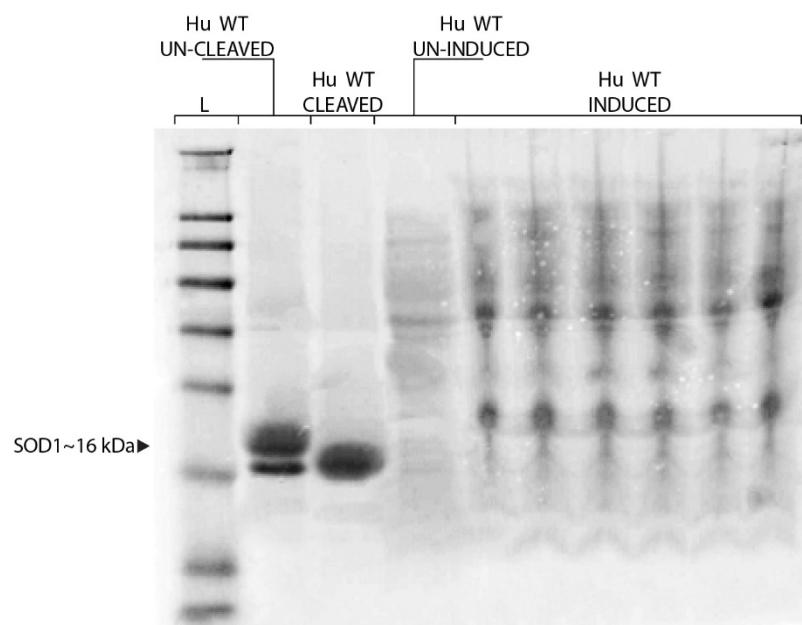


Figure 5.2 Bacterial growth for human wild-type SOD1 protein pre and post IPTG induction. From the left ladder (L); His-tagged human SOD1 wild-type protein (Hu WT un-cleaved); non-His-tagged variant (Hu WT cleaved); human SOD1 wild-type bacterial growth before IPTG induction (Hu WT un-induced); human SOD1 wild-type bacterial growth after IPTG induction (Hu WT induced). Approximately 15 μ g of protein were loaded on each well.

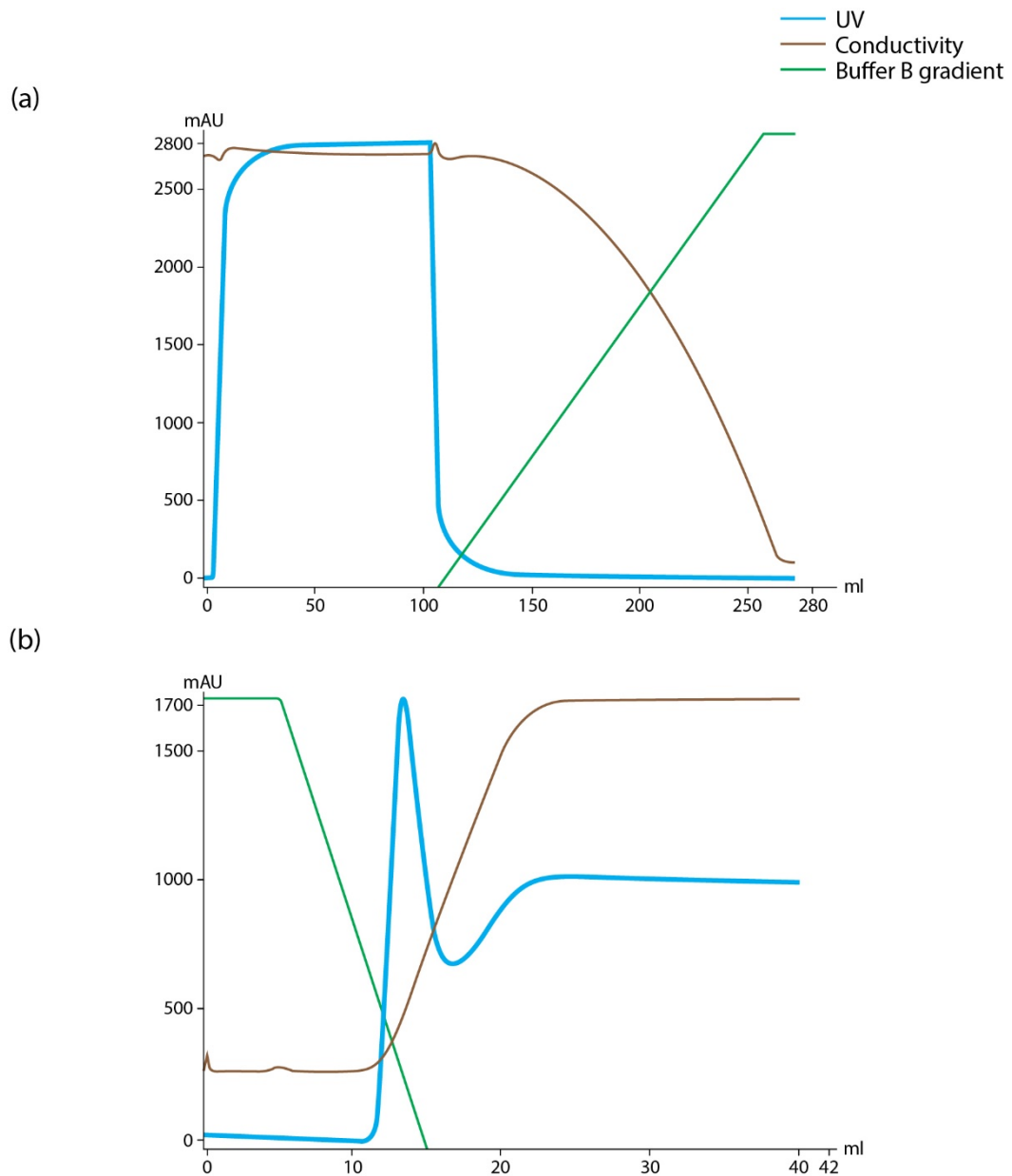


Figure 5.3 Human wild-type SOD1 protein first Ni-NTA affinity chromatography. (a) Human wild-type SOD1 protein preparation solubilised in a chaotrope buffer was loaded on the column causing an increase in the UV (blue line). During this process the His-tagged SOD1 bound to the column while the contaminating proteins flushed through. The His-SOD1 protein was then allowed to refold overnight on column over a gradient of 0 to 100% of a non chaotropic buffer (buffer B; green line), causing the UV to drop to zero. (b) The His-SOD1 protein was eluted from the column over a reducing gradient of buffer B and an increased concentration of an imidazole buffer, to displace the His-tag from nickel co-ordination. The UV peak on the graph corresponds to the His-SOD1 protein elution. Due to the presence of imidazole UV does not plateau at zero but approximately at 600 mAU. The brown line indicates the conductivity of the buffer.

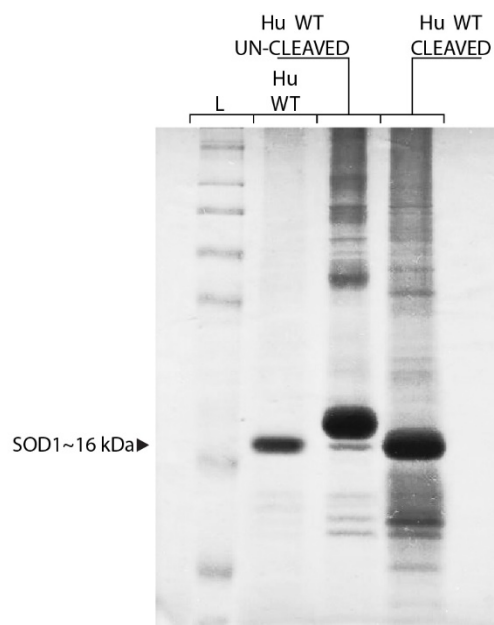


Figure 5.4 Human wild-type SOD1 protein before and after His-tag cleavage. The His-tagged human SOD1 wild-type protein (Hu WT un-cleaved) has a higher molecular weight compared to the non-His-tagged variant (Hu WT cleaved) therefore migrates slower on the gel. (Hu WT) purified and metal loaded recombinant human wild-type SOD1 protein; (L) ladder. Approximately 15 μ g of protein were loaded on each well.

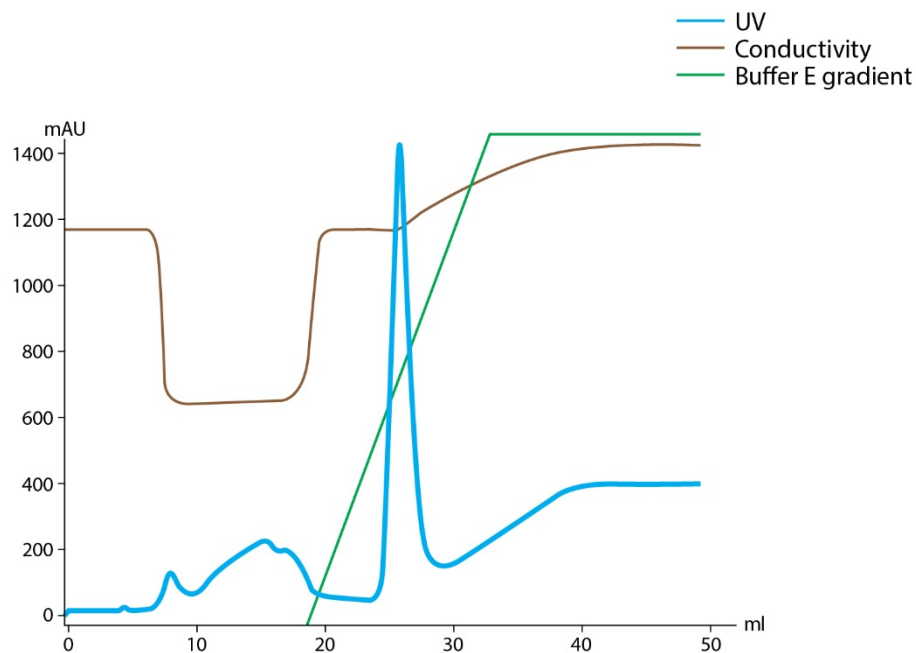


Figure 5.5 Human wild-type SOD1 protein second Ni-NTA affinity chromatography. The human wild-type SOD1 protein was loaded on the column and eluted over an increasing gradient of imidazole buffer (buffer E), the peak in the UV correspond to the non-His-tagged SOD1 protein. Of note due to the presence of imidazole mAU do not plateau at zero. The brown line indicates the conductivity of the buffer.

5.3.1.2 Sodium dodecyl sulphate - polyacrylamide gel electrophoresis of mouse and human purified SOD1 recombinant proteins

To confirm that the recombinant proteins produced were mouse or human SOD1 variants and that the preparations were not contaminated by other proteins, all samples were separated by SDS-PAGE and tested by western blot and coomassie blue staining.

Western blot analysis using a commercial polyclonal antibody (SOD-100) that detects both mouse and human SOD1, confirmed that the metal loaded recombinant proteins produced were SOD1 variants. Both human and mouse SOD1 proteins migrated as a monomer with a molecular weight of approximately 16 kDa, see Figure 5.6.

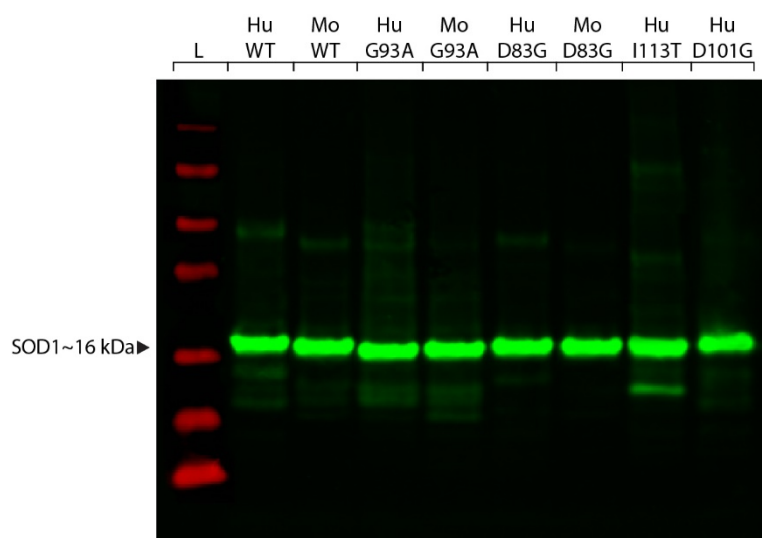


Figure 5.6 Western blot of purified human and mouse SOD1 recombinant proteins. From the left ladder (L); human wild-type SOD1 (Hu WT); mouse-wild-type SOD1 (Mo WT); human G93A SOD1 (Hu G93A); mouse G93A SOD1 (Mo G93A); human D83G SOD1 (Hu D83G); mouse D83G SOD1 (Mo D83G); human I113T SOD1 (Hu I113T) and human D101G SOD1 (Hu D101G). SOD1 migrated as a monomer with a molecular weight of about 16 kDa; 20 μ g of protein were loaded per well.

To test the purity of the SOD1 protein preparations, metal loaded samples were separated by SDS-PAGE gel and stained by coomassie blue. As in the western blot, a single band of approximately 16 kDa was visible in all samples indicating that the only protein present in the preparations was SOD1, Figure 5.7. Both wild-type and mutant mouse SOD1 proteins migrated slightly faster than human wild-type SOD1. While most of human SOD1 mutants migrated as human wild-type SOD1 with the exception of human SOD1 G93A, see Figure 5.7. This difference in migration pattern might be due to the difference in metal binding capacity among these SOD1 variants.

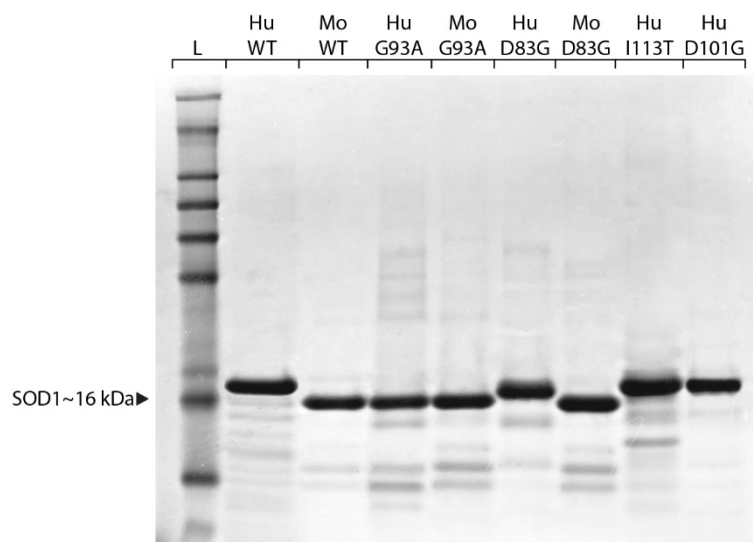


Figure 5.7 Coomassie blue of purified human and mouse SOD1 recombinant proteins. From the left ladder (L); human wild-type SOD1 (Hu WT); mouse-wild-type SOD1 (Mo WT); human G93A SOD1 (Hu G93A); mouse G93A SOD1 (Mo G93A); human D83G SOD1 (Hu D83G); mouse D83G SOD1 (Mo D83G); human I113T SOD1 (Hu I113T) and human D101G SOD1 (Hu D101G). SOD1 migrated as a monomer with a molecular weight of about 16 kDa. 20 μ g of protein were loaded per well.

5.3.2 SOD1 recombinant proteins structural profile with circular dichroism

In order to confirm that the SOD1 recombinant proteins produced were correctly folded their secondary structure was investigated by circular dichroism (CD), a form of spectroscopy that measures the differential interaction of circularly polarised light with proteins in solution (Beychok, 1966). To examine proteins' secondary structure CD is typically measured at a UV interval of 190-250 nm (far-UV). Three possible protein conformations are identifiable by the CD spectrum at a far-UV: α -helix, β -sheet and random coil.

Purified SOD1 proteins stored in 20 mM Tris-HCl at pH 7.5, were dialysed in a 20 mM phosphate buffer at pH 7.5. Tris-HCl indeed absorbs highly in the UV wavelength of interest and might interfere with a protein CD spectrum. Each recombinant protein was measured for its CD at a far-UV over a series of 10 accumulations (Figure 5.8 and Figure 5.9). The CD spectra obtained for all the SOD1 variants, showed a negative peak at approximately 208 nm, with the exception of mouse wild-type and mouse G93A SOD1. In particular the CD spectra of human SOD1 variants were all very similar among each other and resembled of proteins containing β -sheet conformation, as published by Chia and colleagues in 2010 (Figure 5.8 (a)). Further the CD spectra of mouse SOD1 variants were similar, however, the

mouse G93A SOD1 showed a deviation of the negative peak to 200 nm compared to the other 2 mouse SOD1 variants, which indicates of an increase in random coil conformation (Figure 5.8 (b)). Interestingly when comparing the CD spectra of homologous human and mouse SOD1 recombinant proteins (SOD1 wild-type, D83G and G93A), the negative peak of the mouse SOD1 variants were always slightly shifted towards 200 nm compared to the human forms (Figure 5.9). These results taken together indicate that the SOD1 proteins examined have a β -sheet conformation, which is consistent with previous SOD1 structural and conformational studies (Chia et al., 2010; Getzoff et al., 1989; Khare et al., 2004; Rakhit and Chakrabartty, 2006; Tainer et al., 1982).

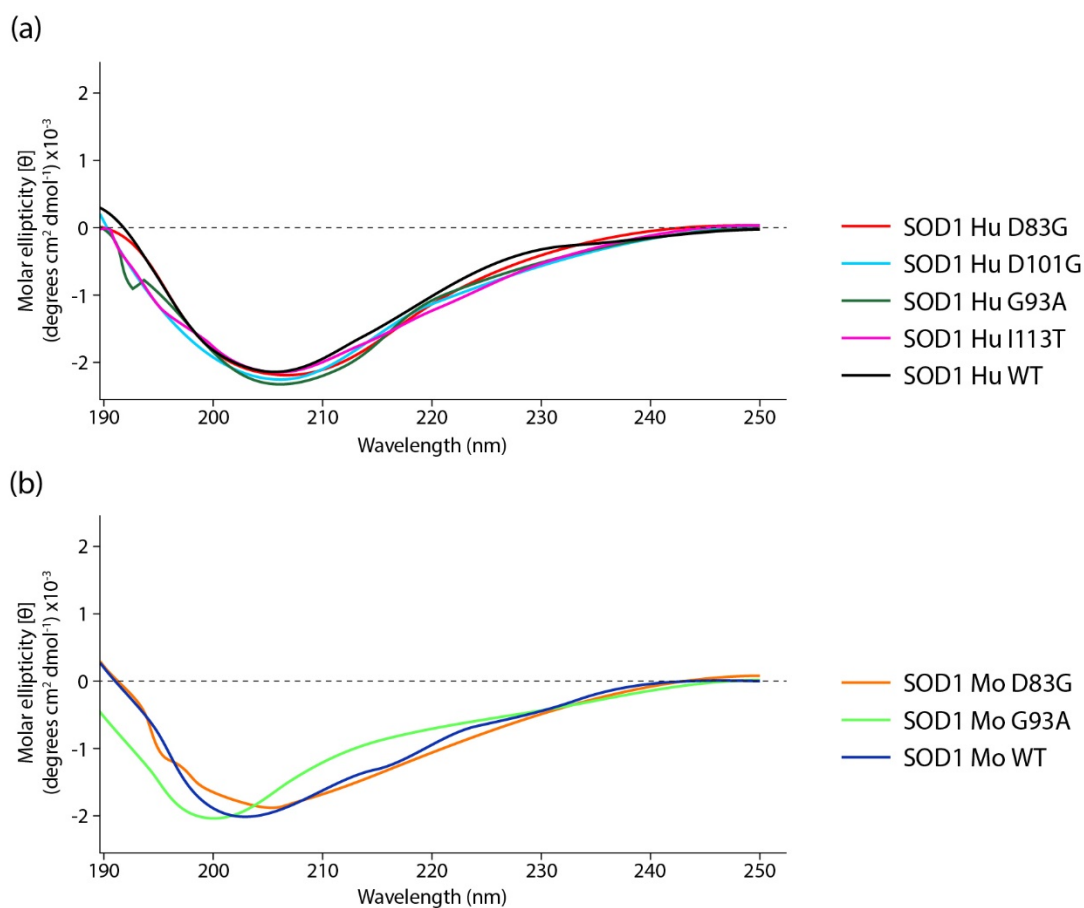


Figure 5.8 CD spectra of human and mouse SOD1 recombinant proteins. CD spectra were measured at a wavelength interval of 190 to 250 nm. (a) Wild-type and mutants human SOD1 recombinant proteins; (b) wild-type and mutants mouse SOD1 recombinant proteins. All SOD1 recombinant proteins, except mouse G93A SOD1 have a comparable CD spectra resembling of proteins containing β -sheet conformation. Mouse G93A SOD1 CD spectrum is the only one resembling a random coil confirmation.

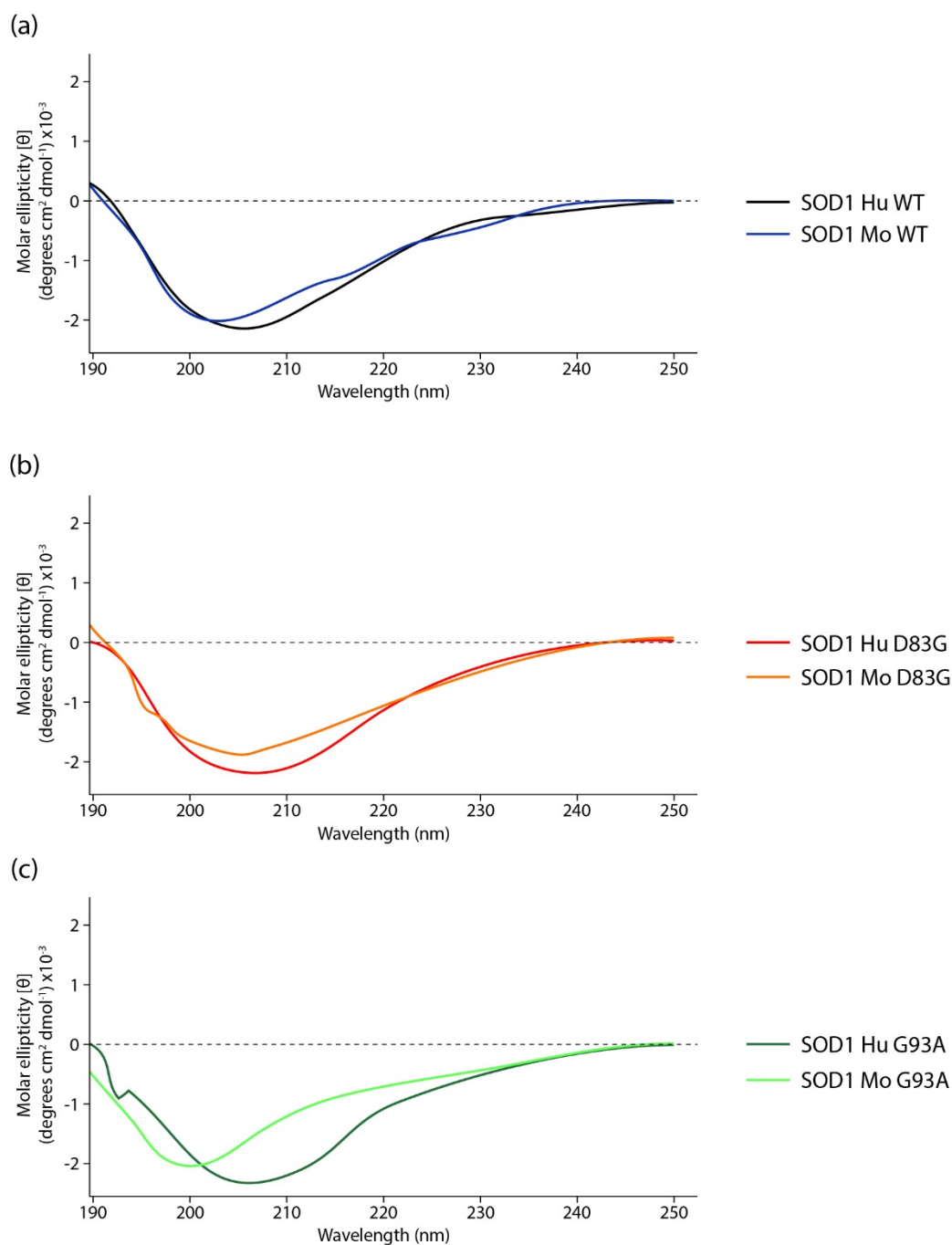


Figure 5.9 CD spectra comparison between human and mouse SOD1 recombinant proteins. CD spectra were measured at a wavelength interval of 190 to 250 nm. (a) SOD1 wild-type human and mouse proteins; (b) SOD1 human and mouse D83G proteins; (c) SOD1 human and mouse G93A proteins. All mouse SOD1 recombinant proteins, have a CD spectra slightly shifted towards the far-UV compared to the human variants, resembling a random coil confirmation.

5.3.3 Kinetics of spontaneous fibrillization of mouse and human SOD1 recombinant proteins

In order to study the kinetics of human and mouse SOD1 fibrillization, some preliminary fibrillization assays for spontaneous reactions were carried out using the SOD1 recombinant proteins produced.

For all SOD1 variants, fibrillization was carried using a protein concentration of 20 μM in a solution at pH 3.0 in mild denaturing conditions (0.5 GuHCl) similar to what described in Chia et al., 2010. Spontaneous fibril formation of SOD1 proteins was monitored by following the change in fluorescence of Thioflavin-T (section 2.6.6). The fibrillization lag time of the proteins was calculated using the equation described in 2.6.6. In all the figures fibril formation is reported as % of maximum ThT relative fluorescence units (RFU) shown as a function of time (in hours).

To optimise experimental conditions, two preliminary assays were conducted, testing the spontaneous fibrillization for all 8 SOD1 variant over 6 repetitions. In the first experiment ThT fluorescence was measured over a period of 250 hours. Formation of fibrils occurred evenly among the 6 sample repeats only for human wild-type SOD1 (Figure 5.10) and mouse and human D83G SOD1 proteins (Figure 5.11). The lag time of human wild-type SOD1 was of 125 hours, which is very short compared to previously published data where the same recombinant protein was tested under similar conditions (Chia et al., 2010). While fibril formation for both human and mouse D83G SOD1 occurred at approximately 200 hours, only 50 hours before the conclusion of the experiment.

Since human and mouse D83G SOD1 fibrillization seemed to start only at 200 hours, in the second experiment ThT fluorescence was measured over a period of 450 hours. In this case fibril formation occurred evenly among the 6 sample repeats for mouse wild-type SOD1 (Figure 5.12) and human D83G SOD1 (Figure 5.13). The lag time of mouse wild-type SOD1 was of approximately 225 hours. While similarly to the previous experiment fibril formation for human D83G SOD1 occurred at 200 hours. These results are preliminary, and more experiments are necessary to optimise the fibrillization assay. However, these first analysis confirmed that human SOD1 recombinant proteins can spontaneously form fibrils *in vitro* and suggest that also mouse SOD1 recombinant proteins can spontaneously fibrillize under similar conditions.

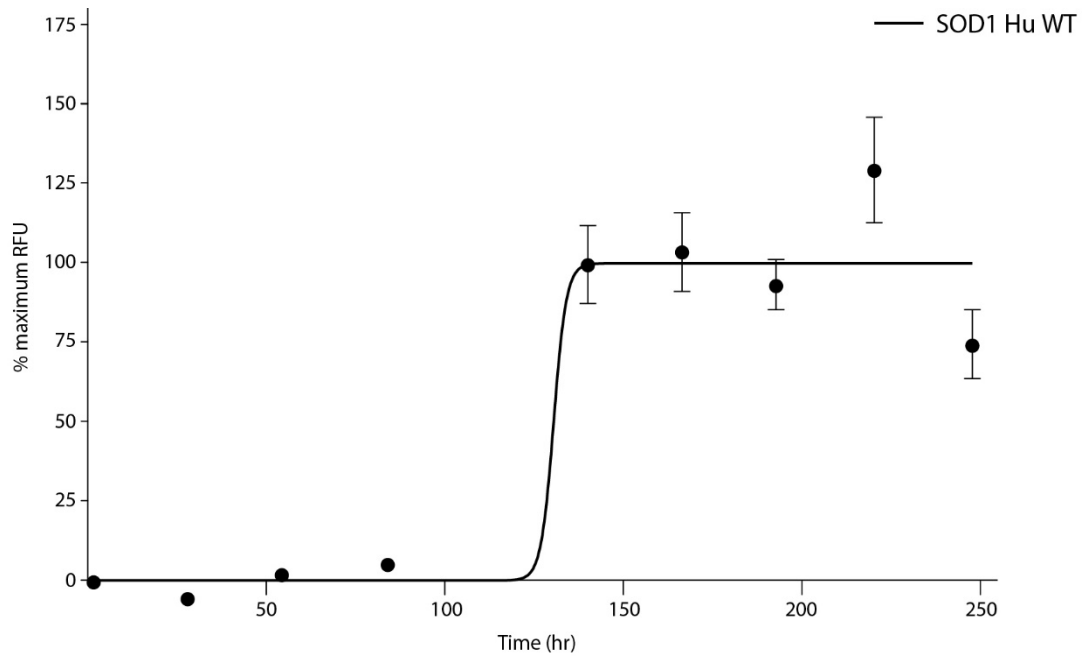


Figure 5.10 Spontaneous fibrillization of SOD1 human wild-type recombinant protein. Data shown are average values from 6 replicates (\pm SEM) from an independent assay. SOD1 human wild-type recombinant protein (SOD1 Hu WT).

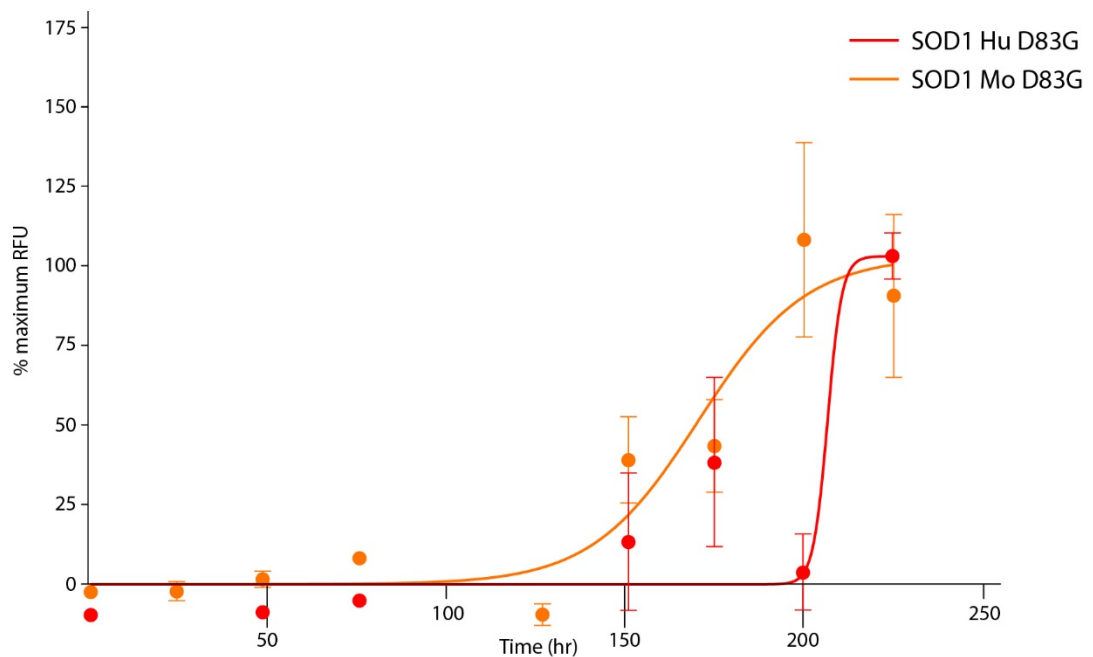


Figure 5.11 Spontaneous fibrillization of SOD1 human and mouse D83G recombinant proteins. Data shown are average values from 6 replicates (\pm SEM) from an independent assay. SOD1 human D83G recombinant protein (SOD1 Hu D83G); SOD1 mouse D83G recombinant protein (SOD1 Mo D83G).

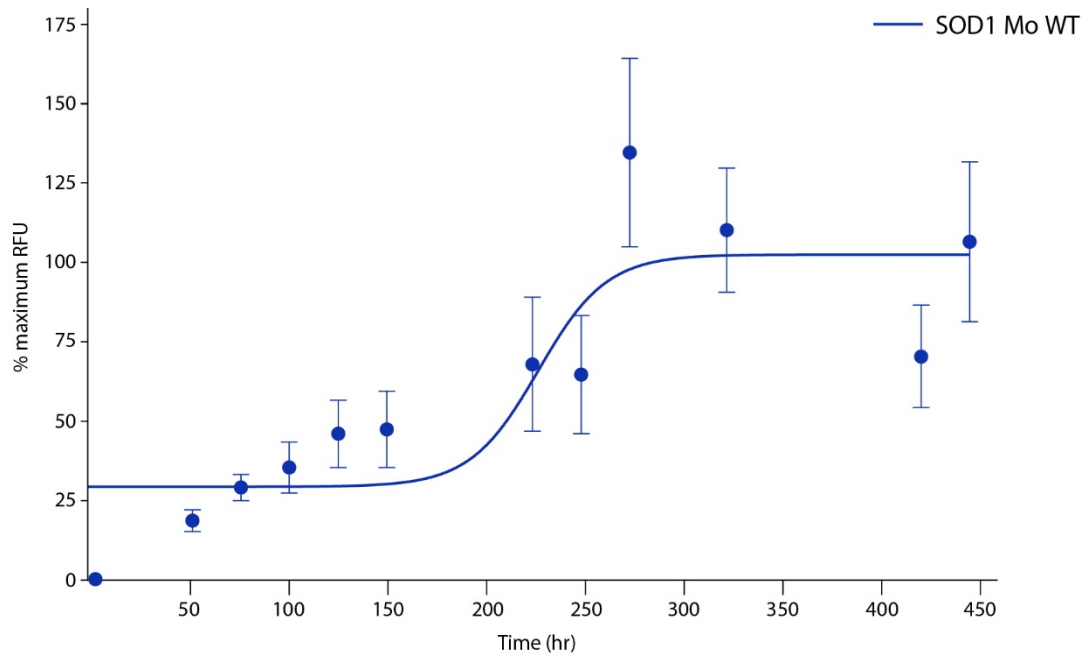


Figure 5.12 Spontaneous fibrillization of SOD1 mouse wild-type recombinant protein. Data shown are average values from 6 replicates (\pm SEM) from an independent assay. SOD1 mouse wild-type recombinant protein (SOD1 Mo WT).

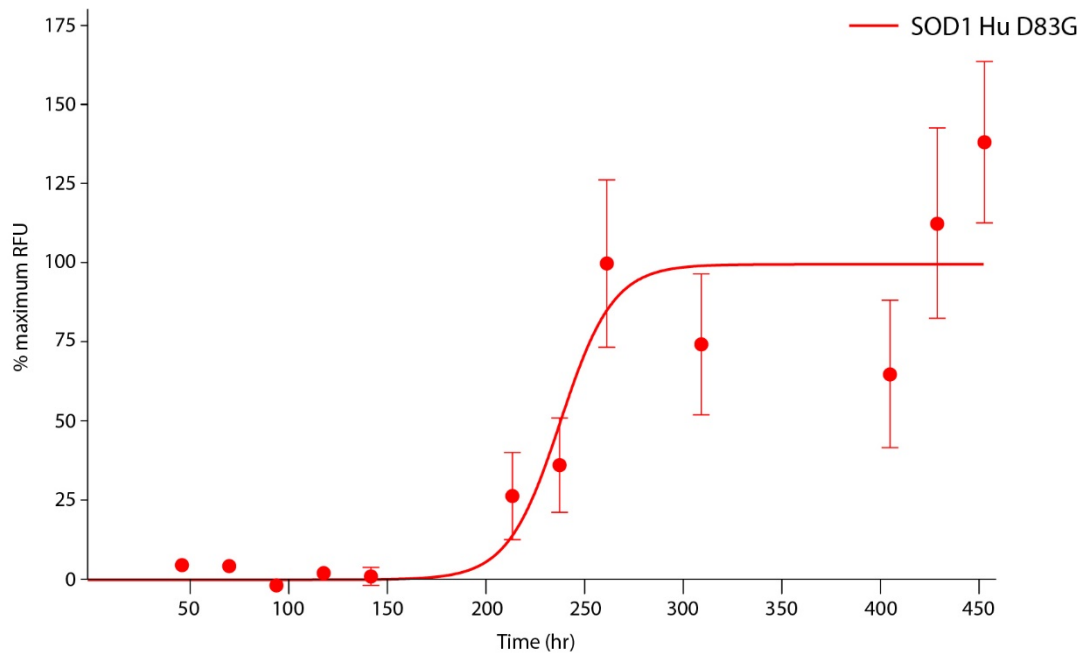


Figure 5.13 Spontaneous fibrillization of SOD1 human D83G recombinant protein over 450 hours. Data shown are average values from 6 replicates (\pm SEM) from an independent assay. SOD1 human D83G recombinant protein (SOD1 Hu D83G).

5.3.4 SOD1 transmission project

As part of the transmission project (Appendix 8.6) mouse spinal cord homogenates used to inoculate TgSOD1^{G93A(H)} animals were separated by SDS-PAGE and the SOD1 protein was detected by western and native blot.

The inoculum tested by SDS-PAGE were 1 % spinal cord homogenates of *Sod1*^{-/-}, TgSOD1^{G93A(H)} and TgSOD1^{WT} mice in PBS, plus a wild-type controls prepared in the same manner.

5.3.4.1 Western blot analysis

Western blot analysis (section 2.6.4.2) carried out using a commercial polyclonal antibody against SOD1 protein (SOD-100) confirms that SOD1 was absent in *Sod1*^{-/-} homogenates and that it was overexpressed in TgSOD1^{G93A(H)} and TgSOD1^{WT} samples compared to wild-type control (Figure 5.14).

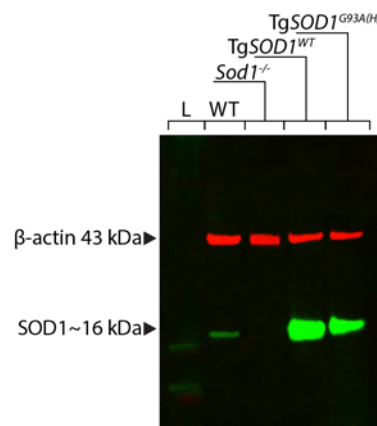


Figure 5.14 Western blot of spinal cord homogenates. SOD1 protein is overexpressed in transgenic samples and absent in the *Sod1* knockout sample. Ladder (L); wild-type (WT) control. 20 µg of protein per well.

5.3.4.2 Native blot analysis

Native blot analysis was carried as described in section 2.6.4.3 using three different antibodies. A commercial polyclonal antibody against SOD1 protein (SOD-100), and two conformation specific SOD1 antibodies: SEDI (SOD1 exposed dimer interface) (Rakhit et al., 2007) and USOD (unfolded SOD1) (Kerman et al., 2010). In particular these two antibodies were shown to detect misfolded SOD1 by immunohistochemistry and immunoprecipitation, but accordingly to published date they were never employed in native blot analysis.

Native blot probed using USOD and SEDI failed to reveal misfolded SOD1 bands in any of the samples, probably because these two antibodies are not suitable for the detection of SOD1 protein in blots (Figure 5.15 (a) and (b)). Though, the native blot probed using SOD1-100 antibody confirmed the result seen in the western blot analysis, that SOD1 protein was absent in the *Sod1*^{-/-} homogenate and it was overexpressed in TgSOD1^{G93A(H)} and TgSOD1^{WT} samples compared to wild-type control. Interestingly in non-denaturing and non-reducing conditions mouse wild-type SOD1 protein appears to migrate slower compared to the human SOD1 variants (Figure 5.15 (c)). All bands identified by the SOD1-100 antibody had a molecular weight bigger than 20 kDa, suggesting that the SOD1 proteins detected are not in the monomeric form. Of note these native blots have been purposely overexposed to reveal possible bands corresponding to misfolded SOD1.

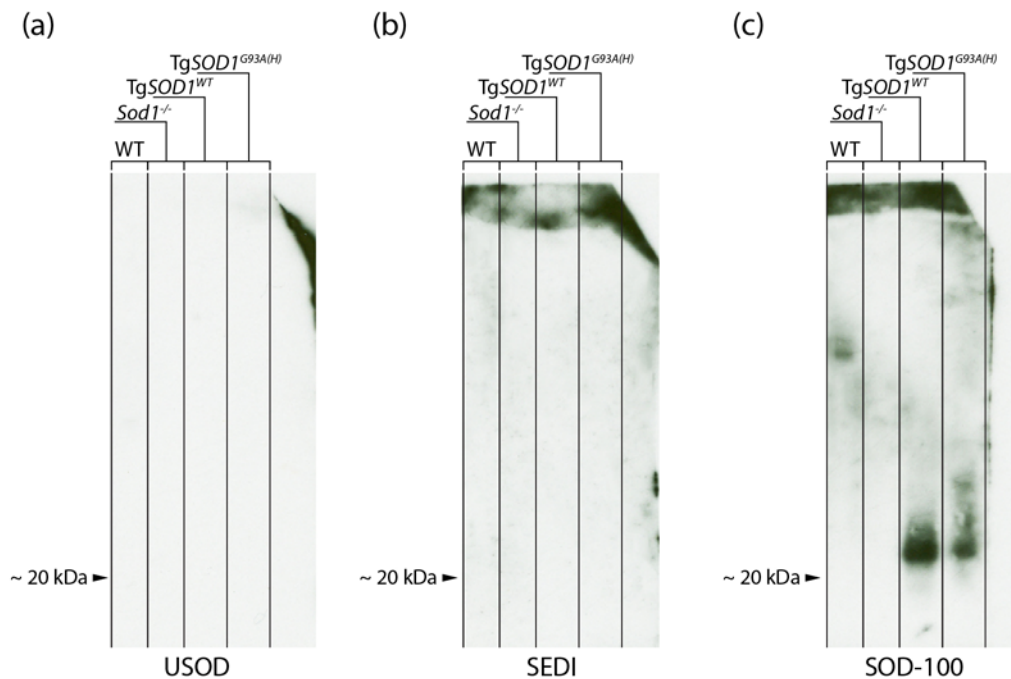


Figure 5.15 Native blot of spinal cord homogenates. (a), (b) SOD1 protein is not detected by USOD and SEDI antibodies. (c) SOD1 is overexpressed in transgenic samples and absent in the *Sod1* knockout sample, mouse wild-type SOD1 (WT) migrates slower compared to human SOD1 variants (TgSOD1^{G93A(H)} and TgSOD1^{WT}); all SOD1 products detected have a higher molecular weight than monomeric SOD1 (16 kDa). 30 µg of protein per well.

5.4 Conclusions

5.4.1 Comparison between SOD1 human and mouse proteins

Data presented in this chapter showed that it is possible to produce and purify both human and mouse SOD1 recombinant proteins from an *E. coli* system. Western blot analysis established that the proteins produced were SOD1. While coomassie blue staining confirmed the purity of all the preparations and also showed the presence of a different migrations pattern among SOD1 variants, suggesting a diverse metal binding capacity between human and mouse SOD1 and also among human SOD1 variants.

Characterisation of the SOD1 protein folding state by CD showed the presence of β -sheet conformations in most of the SOD1 variants. The CD spectra of human SOD1 proteins appeared very similar among each other as describe in Chia et al., 2010. Also mouse SOD1 CD spectra seemed comparable among each other with the exception of SOD1 mouse G93A, which resembled of a random coil conformation. Comparison between SOD1 wild-type human and mouse proteins and SOD1 human and mouse carrying the same mutations, revealed that the mouse CD spectra is always deviated slightly toward 200 nm, possibly indicating an increase in random coil conformation.

Preliminary fibrillization experiments showed that both SOD1 human wild-type and mutant D83G recombinant proteins can spontaneously form fibrils *in vitro* under non physiological conditions, as indicated in literature (Chia et al., 2010). However, in this first analysis, differently from what was published by Chia and colleagues, the lag time of human wild-type SOD1 (Figure 5.10) was shorter compare to the lag time of the human SOD1 D83G mutant (Figure 5.11 and Figure 5.13), (Chia et al., 2010). Furthermore the experiments presented in this section showed that SOD1 mouse wild-type and mutant D83G proteins could form fibrils *in vitro* under the same conditions used for the human variants. Specifically the lag time of the SOD1 mouse wild-type protein was shorter compare to the lag time of the mouse D83G mutant. Of note the lag time of human wild-type SOD1 protein was shorter compare to the lag time of the homologous mouse SOD1. While in the case of the D83G mutation the human variant had a slightly longer lag time compare to the mouse variant.

Further investigation are necessary to optimise the experimental procedure to conduct fibrillization assays, but it is possible to conclude that both human and mouse SOD1 recombinant proteins can spontaneously seed *in vitro* under non physiological

conditions. Supporting the idea that the ability to fibrilize is a generic and intrinsic property of the SOD1 proteins conserved among species.

Results from native blots of mouse spinal cord indicated that the wild-type mouse SOD1 protein migrates slower compared to the wild-type and mutant G93A human SOD1 in non-reducing and non-denaturing conditions, possibly suggesting conformational and charge differences between the human and the mouse SOD1 proteins.

5.4.2 Future work

5.4.2.1 Further mouse SOD1 proteins characterisation

Other experiments can be done in order to further characterise the mouse SOD1 proteins produced, as was extensively done for the human SOD1 variants (Rakhit and Chakrabartty, 2006; Valentine et al., 2005). For example the conformational and the aggregation state of the proteins could be investigated by analytical ultracentrifugation; their stability could be examined by differential scanning fluorimetry and their activity could be assessed by gel assays.

5.4.2.2 Kinetics of mouse and human SOD1 proteins

In order to optimise the fibrillization assay for SOD1 recombinant proteins it will be necessary to investigate a matrix of different experimental conditions. Important parameters that could be changed in order to potentiate fibril formations are: pH, temperature, experimental time and denaturant concentration. For example it was shown that apo-wild-type SOD1 proteins could form ThT-binding structures under a more physiological condition (pH 7.0), with very long periods of time (approximately 5100 hours) (Banci et al., 2008).

Once optimised fibrillization assays can be used to investigate self-seeding and cross seeding aggregation of mouse and human SOD1 proteins. Cross-seeding experiments will be crucial to determine whether mouse and human SOD1 variant have the ability to co-aggregate *in vitro*. Moreover, answering this question will be relevant to understand the results from the transmission project and the D83G project where human and mouse SOD1 proteins coexist and might interact within a living biological system.

5.5 Summary

- Eight SOD1 human and mouse recombinant proteins were produced and purified
- Purity and correct folding state were confirmed for all SOD1 recombinant proteins
- All mouse SOD1 and human SOD1 G93A recombinant proteins migrate slightly faster compare to other human SOD1 recombinant variants including wild-type
- The CD spectra of mouse SOD1 recombinant proteins always deviated to 200 nm compared to the homologous human SOD1 recombinant proteins
- Mouse SOD1 wild-type and D83G recombinant proteins can spontaneously form fibrils *in vitro*
- In non-reducing and non-denaturant conditions mouse SOD1 wild-type migrates slower compared to human SOD1 wild-type and G93A mutant

Chapter 6 *Galahad* mouse

6.1 Introduction

Mouse models carrying genetic mutations have been extensively employed in neuroscience research since they often present pathologies that mimic the human disease state, and they are able to perform behavioural tasks and respond to drugs in a comparable way to humans (Acevedo-Arozena et al., 2008; Oliver and Davies, 2012).

Two complementary strategies are typically applied to generate mouse models: the gene driven approach and the phenotype driven approach. In the gene driven approach the genome is manipulated to create genetically modified animals starting from a known gene, while in the phenotype driven approach mice carrying random mutations are screened for abnormal phenotypes (Acevedo-Arozena et al., 2008). Of note mice may also have mutations that occur naturally, examples of spontaneous mouse models of motor neuron degeneration are: the *SOD/Ei* mouse carrying a spontaneous mutation in the endogenous mouse *Sod1* gene (Luche et al., 1997) and the motor neuron degeneration mouse (*mnd*) (Bertamini et al., 2002).

The gene driven approach employing homologous recombination in embryonic stem cells has been extensively used to create knockout mice modelling human diseases and for the study of the disruption of specific genes in the whole organism. However, in nature many disorders are not caused by complete loss of gene function, but more likely they are the consequence of more subtle changes such as: protein structure modifications, binding affinity disruption, changes in expression or activity levels and more. In the phenotype driven approach *N*-ethyl-*N*-nitrosurea (ENU) chemical mutagenesis is used to generate point mutations in mice giving rise to a range of subtle mutant effects that model the diversity and complexity of human diseases, providing the tools to analyse compound genotypes and identify new pathways, genes or function involved in pathological mechanisms (Acevedo-Arozena et al., 2008; Justice et al., 1999; Oliver and Davies, 2012).

6.1.1 ENU mutagenesis and the phenotype driven approach

In the last 20 years ENU mutagenesis screenings in conjunction with large-scale phenotype-driven approaches have been used to identify mouse models of human disorders and also to investigate new genes and pathways involved in complex disease pathologies (Acevedo-Arozena et al., 2008).

6.1.1.1 ENU properties

ENU is a mutagen that since its discovery in 1979 has been largely employed to induce random point mutations in mouse (Russell et al., 1979). In particular when injected in mice ENU can transfer its ethyl group to oxygen or nitrogen radicals of deoxyribonucleotides causing random single base pair substitutions in the DNA during replication, in a dose-dependent manner, if not removed by DNA repair mechanisms (Justice et al., 1999; O'Neill, 2000). ENU preferentially modifies A/T base pairs, causing some amino acid changes to be more frequent than others (Table 6.1), nevertheless this limitation has not yet prevented the identification of new mutant models (Acevedo-Arozena et al., 2008; Justice et al., 1999).

Base pair change		%
A/T → T/A	transversions	44
A/T → G/C	transitions	38
G/C → A/T	transitions	8
G/C → C/G	transversions	3
A/T → C/G	transitions	5
G/C → T/A	transitions	2

Table 6.1 ENU base pair substitution frequency. ENU induced point mutations exhibit a preference towards specific nucleotide substitutions (Justice et al., 1999).

6.1.1.2 ENU administration and breeding strategies

Typically ENU is administrated to male mice as a sequence of two or three intraperitoneal injections at a dose of approximately 80-100 mg/kg. The dosage and the number of injections vary according to the mouse strain employed. It has been estimated that an optimal dose protocol should produce a mutation every 1-1.5 Mb, consequently the mutation rate of each gene varies depending on its size (Acevedo-Arozena et al., 2008).

ENU mutagenesis is used to carry out various types of screenings; different strategies and breeding schemes are applied depending on the chosen approach (genotype or phenotype driven), the allelic characteristics (recessive or dominant) and the strains required for subsequent genetic mapping (Acevedo-Arozena et al., 2008; Brown and Nolan, 1998). For example in a screen for dominant genome-wide mutations, ENU is

injected in male mice, causing random base-pair substitution preferentially in the spermatogonial stem cells. Mutagenized males are then mated with wild-type females and their progeny is screened for aberrant phenotypes through behavioural and physiological tests, followed by analysis of specific features of interest (Acevedo-Arozena et al., 2008; Justice et al., 1999) (Appendix 8.5 and Figure 8.1). Furthermore ENU can be used to undertake sensitised screens to identify modifying loci that interact with specific mutations, and investigate new genetic pathways. In these screens ENU mutagenized male mice are crossed with females that are on a different genetic background and are mutant for a disease of interest. Different breeding strategies are employed depending on the nature of the mutant model, and the progeny are screened for aberrant phenotypes (Acevedo-Arozena et al., 2008). Of note in modifier screens analysis of the phenotype is crucial but also very challenging. Indeed animals that are not ENU mutant also present disease characteristics of the original model, thus it is essential to determine a baseline disease associate-phenotype and variation for the non-mutagenized population in order to determine a suitable phenotyping strategy for the modifier screen (Acevedo-Arozena et al., 2008).

Sensitised screens have been successfully employed in invertebrate models such as the fly *Drosophila melanogaster*, the nematode *Caenorhabditis elegans* and the zebrafish *Danio rerio* (St Johnston, 2002). Indeed the first pioneer screen using mutagenesis in a multicellular organism was carried out in *Drosophila melanogaster* and lead to the identification of 15 loci that when mutated alter the segmental pattern of the larva (Nüsslein-Volhard and Wieschaus, 1980). Since then many other sensitised chemical mutagenesis screens in lower organisms have provided models of neurological mutations related to human disease (Bach et al., 2003; Bonini and Fortini, 2003; Driscoll and Gerstbrein, 2003) and more recently this sensitised genetic systems have been developed also in mouse (Rubio-Aliaga et al., 2007). Using mouse models for sensitised screens is expensive, but to date mice are still the best model organism for the study of mammalian gene function and complex neurodegenerative disorders in the context of the whole organism. Indeed mice can be easily genetic manipulated and bred. Furthermore the complete genome is known for many inbred lines; therefore mutagenesis screens are a great tool for systematically generate new mutants. Also, mice complex behaviour makes them an effective model for human neurological disorders, hence sensitised screen, by producing a wide range of mutations, can not

only identify new mutants but also help elucidate intricate neurological pathways (Oliver and Davies, 2005).

6.1.1.3 Mapping and cloning

Once an ENU mutant is selected inheritance tests and positional cloning techniques are applied to isolate and identify the causative mutation of the new phenotype (Acevedo-Arozena et al., 2008; Oliver and Davies, 2012). The mutation is only inherited from the ENU mutagenized parent. Initial mapping commonly uses heterozygosity to detect areas of linkage, which is assisted by having two different inbred backgrounds for the parents. For inheritance testing in dominant screens if on the G0 (mutagenized generation and wild-type cross) animals have different backgrounds the ENU mutants of the G1 (first generation after mutagenesis) are backcrossed to the non-mutagenized strain of the G0, and the G2 (second generation after mutagenesis) is used for mapping. Conversely, if the G0 animals have the same background, it is not possible to test inheritance in the G2 but two other mating with a different inbred strain are required before positional cloning (Acevedo-Arozena et al., 2008). While for recessive screens, regardless of the background of the G0, G2 mice are either intercrossed or mated to the original G1 ENU mutagenized parent, recessive mutations can be detected in the resultant G3 progeny.

Causative mutations can be identified by genome mapping of a number of affected mice using single nucleotide polymorphisms (SNPs) as markers, in order to identify areas of linkage, followed by a candidate gene approach. Detecting newly induced causal variants in a forward genetic screen using these techniques is expensive and time consuming however, this process can now be accelerated using next-generation sequencing technologies which allow affordable whole-genome sequencing (Boles et al., 2009; Sun et al., 2012).

6.1.2 A sensitised screen for modifiers in *SOD1*^{G93A} low copy mice

A sensitised screen focused on the identification of new genetic loci interacting with the mutant *SOD1* gene was carried out as part of the Harwell ENU mutagenesis programme. BALB/c male mice were treated with a sequence of two 100 mg / kg ENU intraperitoneal injections. Mutagenized BALB/c males were then mated with hemizygous human *SOD1*^{G93A} transgenic low copy females (Tg*SOD1*^{G93A(L)/+}) on a C57BL/6J background (see breeding scheme in Figure 6.1). *SOD1* transgenic animals

from the G1 underwent a phenotyping analysis starting at 12 weeks of age and were compared to a non-mutagenized population of TgSOD1^{G93A(L)/+} on a hybrid C57BL/6J-BALB/c background (Acevedo-Arozena et al., 2011). Specifically every 2 weeks transgenic G1 mice were tested using the SHIRPA protocol, and measures of weight, and grip-strength were taken. During this screen several mice were identified as phenodeviant of the SOD1^{G93A} transgenic low copy line, but inheritance tests confirmed transmission of the ENU induced phenotype only from one male mouse, named *Galahad*. This animal developed paralysis at 27 weeks of age, showing an early disease onset compared to the non-mutagenized population, where the average age of paralysis is 35.6 weeks (Figure 6.2) (Acevedo-Arozena et al., 2011). Sperm samples from the affected G1 male mouse were collected to allow further breeding and *in vitro* fertilisation (IVF) (Thornton et al., 1999).

A first IVF was carried out in Harwell soon after the identification of the *Galahad* mouse. Phenotyping of 32 G2 mice carrying the SOD1^{G93A} low copy transgene confirmed the presence of an early paralysis onset in some of them, but it was not possible to identify any other phenotype. An initial genetic mapping on 9 animals that reached paralysis before 33 weeks of age suggested 3 possible regions of interest, however in order to confirm these areas of linkage a bigger number of G2 animals and a more in depth phenotyping approach will be necessary.

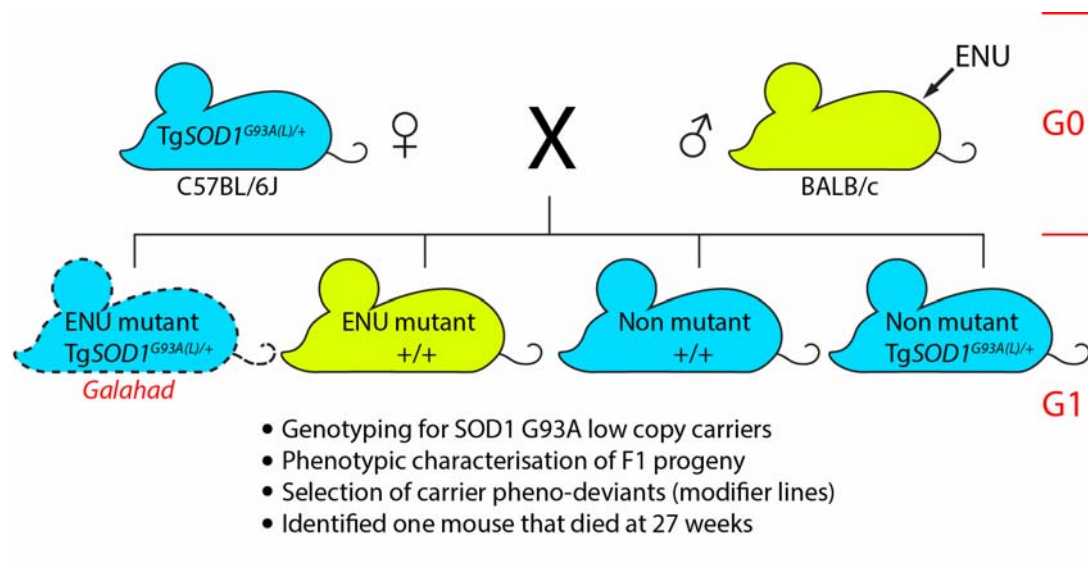


Figure 6.1 Modifier screen in SOD1^{G93A} low copy mice. In the G0 (mutagenized generation) ENU mutagenized BALB/c male mice were crossed with C57BL/6J hemizygous SOD1^{G93A} low copy females. Transgenic animals of the G1 (first generation after mutagenesis) progeny were phenotypically screened

for modifications of the transgenic phenotypes. One phenodeviant mouse with an early paralysis onset was identified, named *Galabad*.

6.1.3 The *SOD1*^{G93A} low copy phenotype

Transgenic human *SOD1*^{G93A} low copy mice (Tg(*SOD1**G93A)^{d1}1Gur) carry approximately eight to ten copies of the human *SOD1*^{G93A} transgene. This mouse line, here referred as Tg*SOD1*^{G93A(L)}, derives from a deletion in the transgene array of the Jackson Laboratory *SOD1*^{G93A} high copy (<http://jaxmice.jax.org/strain/002299.html>). Tg*SOD1*^{G93A(L)} are considered a model for human ALS, indeed these mice present progressive motor neuron loss, accumulations of mutant SOD1 in both spinal cord and brain and develop paralysis between 24 and 34 weeks of age that results in premature death (Acevedo-Arozena et al., 2011; Alexander et al., 2004; Teuling et al., 2008). Compared to *SOD1*^{G93A} high copy Tg*SOD1*^{G93A(L)} animals have a slow progressive pathology that make them invaluable for understanding early-stage disease mechanisms and testing therapies. Acevedo-Arozena and colleagues carried out a comprehensive phenotypic analysis of the Tg*SOD1*^{G93A(L)} mice investigating the effects of five different genetic backgrounds on lifespan, motor neuron, muscle function and pathology (Acevedo-Arozena et al., 2011). Findings relevant to the present study are reported below.

6.1.3.1 Effects of genetic background on time to end stage in Tg*SOD1*^{G93A(L)} mice

The average time to end stage was assessed for Tg*SOD1*^{G93A(L)} animals on a C57BL/6J and on a hybrid C57BL/6J-BALB/c background. The humane endpoint was defined as loss of 20 % bodyweight, first sign of hind limb paralysis or loss of righting reflex. On both backgrounds approximately 92 % of mice were culled for leg paralysis, while the remaining 8 % was culled due to substantial weight loss. When on C57BL/6J background Tg*SOD1*^{G93A(L)} mice had an average time to endpoint of 37.8 weeks, while on a hybrid C57BL/6J-BALB/c background the average survival was of 35.6 weeks (Figure 6.2 and Table 6.2). The difference between the average survival of the two backgrounds was statistically non-significant. Interestingly gender was shown to affect survival on the C57BL/6J-BALB/c background with females reaching end point significantly later compared to males, while it had no effect on the C57BL/6J background (Table 6.2) (Acevedo-Arozena et al., 2011).

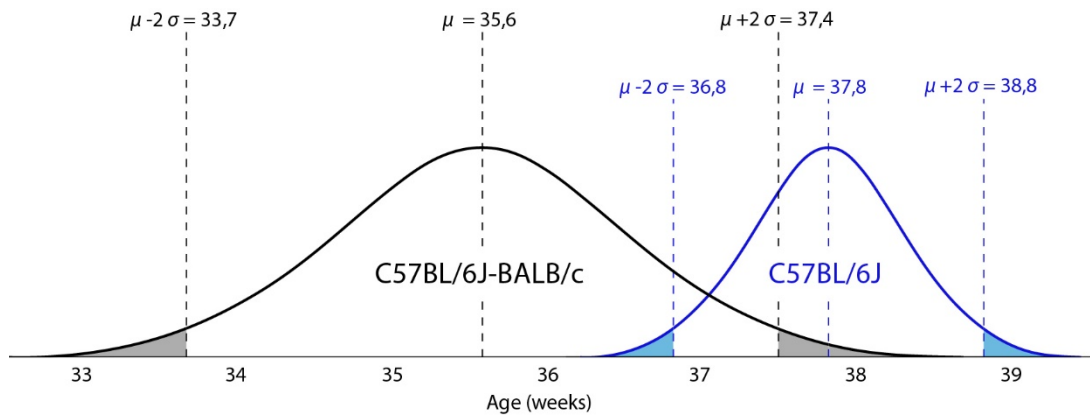


Figure 6.2 Representative distribution of TgSOD1^{G93A(L)} mice survival on different genetic backgrounds. Mean average survival (μ) of TgSOD1^{G93A(L)} mice on a C57BL/6J background (blue) and on a hybrid C57BL/6J-BALB/c background (black). The area of the two curves that fall between 2 standard deviations (σ) of the mean, $\mu - 2\sigma$ and $\mu + 2\sigma$, represent 95 % of the values.

Genetic background	Survival (weeks)		
	Females	Males	Total
C57BL/6J	37.5	38.1	37.8
C57BL/6J-BALB/c	37.6	32.6	35.6

Table 6.2 Average survival of TgSOD1^{G93A(L)} mice on different genetic backgrounds. Survival was calculated on at least 6 animals per category. For the C57BL/6J-BALB/c survival was significantly different between genders ($p = 0.001$) (Acevedo-Arozena et al., 2011).

6.1.3.2 Grip-strength analysis of C57BL/6J TgSOD1^{G93A(L)} mice

Grip-strength analysis of TgSOD1^{G93A(L)} mice on a C57BL/6J background revealed that females were significantly different compared to gender matched wild-type littermates starting at 24 weeks of age (Figure 6.3 (a)) while males showed a difference from 28 weeks of age (Figure 6.3 (b)). Interestingly at 30 and 32 weeks of age there was a significant difference in grip-strength between TgSOD1^{G93A(L)} males and females, and the males appeared to be more severely affected (30 weeks: $p = 0.020$; 32 weeks $p < 0.001$) (Acevedo-Arozena et al., 2011).

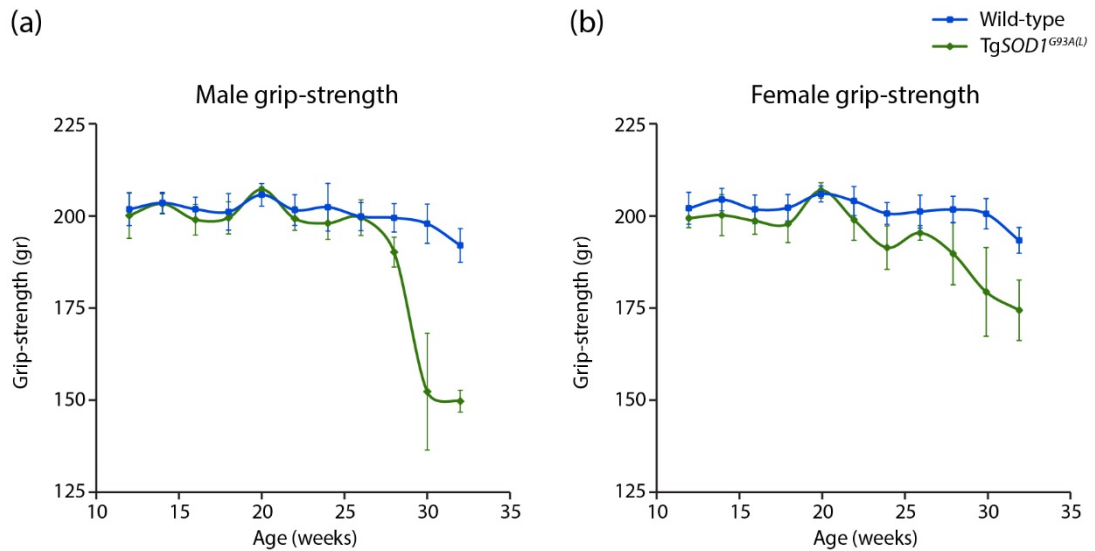


Figure 6.3 Grip-strength analysis of C57BL/6J TgSOD1^{G93A(L)} mice. (a) Male grip-strength. N = 5 per genotype, except for week 20 where only four wild-type males were assessed. A significant difference was detected from 24 weeks of age (ANOVA; 28 weeks: $p = 0.005$; 30 and 32 weeks: $p < 0.001$). (b) Female grip-strength. N = 5 per genotype, except for week 20 where only two TgSOD1^{G93A(L)} females were assessed. A significant difference was detected from 24 weeks of age (ANOVA; 24 weeks: $p = 0.006$; 26 weeks: $p = 0.073$; 28 weeks: $p = 0.007$; 30 weeks: $p = 0.001$; 32 weeks: $p = 0.003$). The graphs shows the average grip-strength \pm SEM per genotype and time point (Acevedo-Arozena et al., 2011).

6.2 Aim

The present work aimed to investigate the progeny of the ENU mutagenized *Galabad* mouse in order to try and identify possible modifying locus/loci interacting with the *SOD1* G93A mutation.

In particular the G2 and the G3 generation were phenotypically characterised to confirm the abnormal phenotype of the founder and a cross with TgSOD1^{G93A(H)} animals was set up to try exacerbate the *Galabad* phenotype. Moreover a quantitative trait locus (QTL) approach was applied to identify regions where the mutation might lay.

6.3 Results

In this chapter all mice generated from the *Galabad* founder are named *Galabad* whether they carry or not the ENU mutation.

6.3.1 Phenotypic characterisation of the G2 *Galahad* progeny

In order to phenotypically characterize the G2 *Galahad* progeny, and possibly identify other distinctive features of the ENU mutagenized animals, the following measure of disease progression were investigated: survival, weight and grip-strength.

6.3.1.1 *Galahad* breeding strategy

The *Galahad* mouse was identified during an ENU sensitised screen at the MRC Mammalian Genetics Unit of Harwell, and it was generated by a cross between a BALB/c mutagenized male and a C57BL/6J hemizygous Tg*SOD1*^{G93A(L)} female (see G0 and G1 in Figure 6.4). The *Galahad* mouse was found to have an early paralysis onset at 27 weeks of age compare to the average described for a Tg*SOD1*^{G93A(L)} line on the same hybrid C57BL/6J-BALB/c background, which was of 35.6 weeks (Figure 6.2) (Acevedo-Arozena et al., 2011). To recover the *Galahad* phenotype and characterise the second generation of animals after mutagenesis, three IVFs were carried out at MRC Harwell, using the sperm of the G1 *Galahad* founder and oocytes from wild-type C57BL/6J females. Mice of the G2 progeny were then, genotyped, phenotyped and their DNA was used for positional cloning studies (see G2 in Figure 6.4).

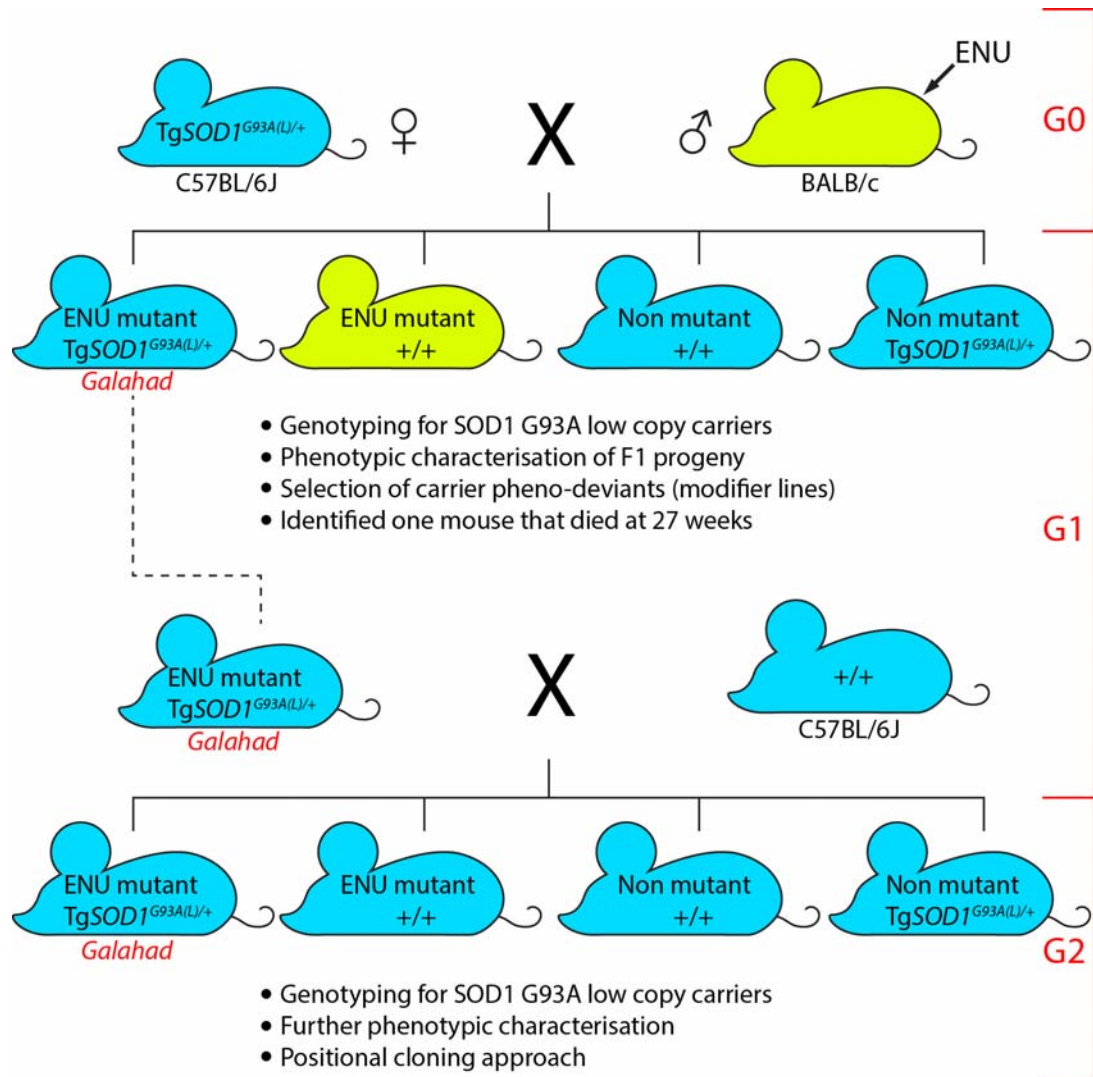


Figure 6.4 Galahad breeding scheme. In the G0 ENU mutagenized BALB/c males were crossed with C57BL/6J hemizygous *SOD1*^{G93A} low copy females. Transgenic animals of the G1 were phenotypically screened for modifications of the transgenic phenotypes. One phenodeviant mouse with an early paralysis onset was identified, named *Galahad*. IVFs were carried out using the sperm of the *Galahad* mouse and wild-type C57BL/6J females. Mice from the G2 were then genotyped for the *SOD1*^{G93A} transgene, phenotypically characterised and their DNA was used for mapping.

6.3.1.2 Galahad G2 genotype and ratios

A total of 142 animals were generated from the three *Galahad* IVFs. G2 mice were genotyped for the presence of the human *SOD1*^{G93A} transgene as described in section 2.5.2.1. Ratios and numbers of *SOD1*^{G93A} transgenic (Tg^{G93A(L)}*Galahad*), and non-transgenic (NTg*Galahad*) animals are reported in Table 6.3. The observed ratios were not significantly different from the expected ratios $\chi^2(1) = 2.208$ $p = 0.131$ for

inheritance of the low copy SOD1 transgene. Of note 50 % of the Tg^{G93A(L)}*Galahad* and 50 % of the NTg*Galahad* should also carry the ENU mutation of the founder.

Genotype	Number of animals			Observed ratios	Expected ratios
	Females	Males	Total		
NTg <i>Galahad</i>	34	28	62	0.44	0.5
Tg ^{G93A(L)} <i>Galahad</i>	40	40	80	0.56	0.5
Total	74	68	142	1	1

Table 6.3 TgSOD1^{G93A} genotype ratios of *Galahad* G2 mice. The omnibus χ^2 showed that observed ratios do not differ from expected ratios.

6.3.1.3 Survival of Tg^{G93A(L)}*Galahad* mice

In this study the humane endpoint for the *Galahad* line was defined as first paralysis onset, loss of 20 % bodyweight and loss of righting reflex.

Fifty Tg^{G93A(L)}*Galahad* mice were employed in survival analysis, among them 64 % were culled due to development of hind limb paralysis while the remaining 36 % reached the humane end point because of loss of 20 % bodyweight. Of note no NTg*Galahad* animals reached the humane endpoint within the timescale of the Tg^{G93A(L)}*Galahad* littermates, suggesting that the ENU mutation alone does not have an effect on survival. The survival distribution of Tg^{G93A(L)}*Galahad* mice was investigated to try and understand if it was possible to distinguish between two populations: one carrying only the SOD1^{G93A} low copy mutation and a phenodeviant population with an early paralysis onset, carrying both the SOD1^{G93A} low copy and the ENU mutation of the founder. The Shapiro-Wilk normality test gave a p value of $p = 0.848$, accepting the null hypothesis that the data are normally distributed. However, when a graphical assessment of normality was carried out using a quantile-quantile (QQ) plot, it was observed that the sample quantiles matched the theoretical quantiles only at the median and the extremes, suggesting a bimodal distribution of the data (Figure 6.5). A further investigation using the EM algorithm of the R mixtools package (Benaglia et al., 2009), confirmed that the survival frequency distribution of Tg^{G93A(L)}*Galahad* mice was a continuous curve with two different peaks (black dotted line Figure 6.6) compatible with a mixture of two normal distributions. One curve with a mean (μ) and a standard

deviation (σ) of $\mu = 32.05$; $\sigma = 2.4$ weeks, and the other with $\mu = 37.3$; $\sigma = 2.97$ weeks that most likely represent respectively the population of $SOD1^{G93A}$ low copy mice carrying the *Galabad* founder ENU mutation (mTg^{G93A(L)}*Galabad*) and the $SOD1^{G93A}$ low copy population (Tg $SOD1^{G93A(L)}$) (Figure 6.6). Since it is known that gender affects survival in Tg $SOD1^{G93A(L)}$ mice on a hybrid C57BL/6J-BALB/c background (Acevedo-Arozena et al., 2011), the survival frequency of Tg^{G93A(L)}*Galabad* males and females was plotted separately, to see if it was still possible to distinguish between two normal distributions. In the case of the males two normal distributions were identified one with $\mu = 32.1$; $\sigma = 2.5$ weeks and the other with $\mu = 35.8$; $\sigma = 3.3$ weeks (Figure 6.7 (a)). While in the case of the females only one normal curve was identified with $\mu = 37.5$; $\sigma = 3.1$ weeks, while the other curve appeared as a distribution with a positive kurtosis (Figure 6.7 (b)); a bigger sample number will be needed to separate the two populations.

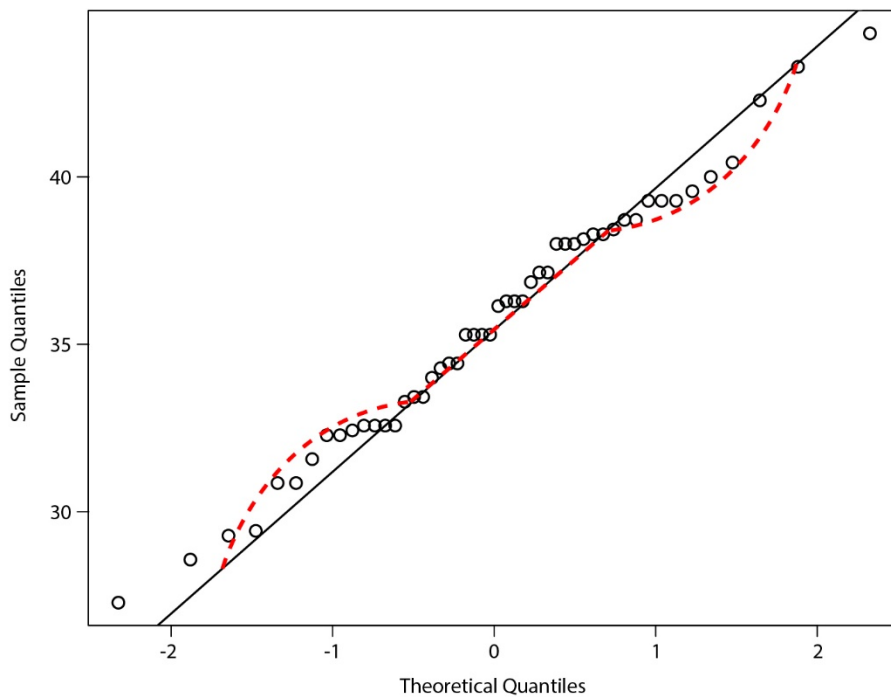


Figure 6.5 Quantile-quantile plot of Tg^{G93A(L)}*Galabad* mice survival. Survival data of males and females are analysed together. The y axis represents the observed values (Sample quantiles), $n = 50$. The x axis represents the predicted values (Theoretical quantiles) which are equally spaced quantiles of a normal distribution that has the same mean and standard deviation of the sample dataset. The dots indicate each predicted value matched by rank with the corresponding observed value. If the data are sampled from a normal distribution the dots are expected to line up to the line of identity (black line). In this case the dots line up only at the median and the extremes of the line of identity, showing two kinks (red dotted line), characteristic of a bimodal distribution.

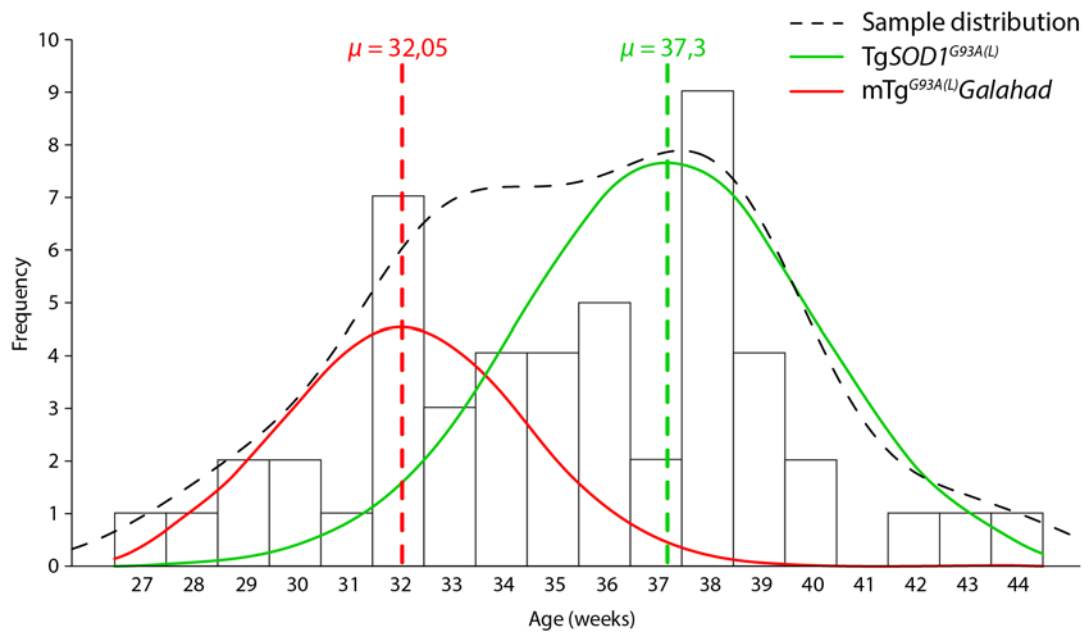


Figure 6.6 $Tg^{G93A(L)}Galahad$ mice survival bimodal distribution. The survival frequency of the $Tg^{G93A(L)}Galahad$ mice, $n = 50$, is represented by the histograms. The sample distribution, (black dotted line) shows two peaks compatible with two normal distributions. One with a mean of $\mu = 32.05$ (red line) corresponding to the $mTg^{G93A(L)}Galahad$ population, and one with a mean of $\mu = 37.3$ (green line) corresponding the $TgSOD1^{G93A(L)}$ population.

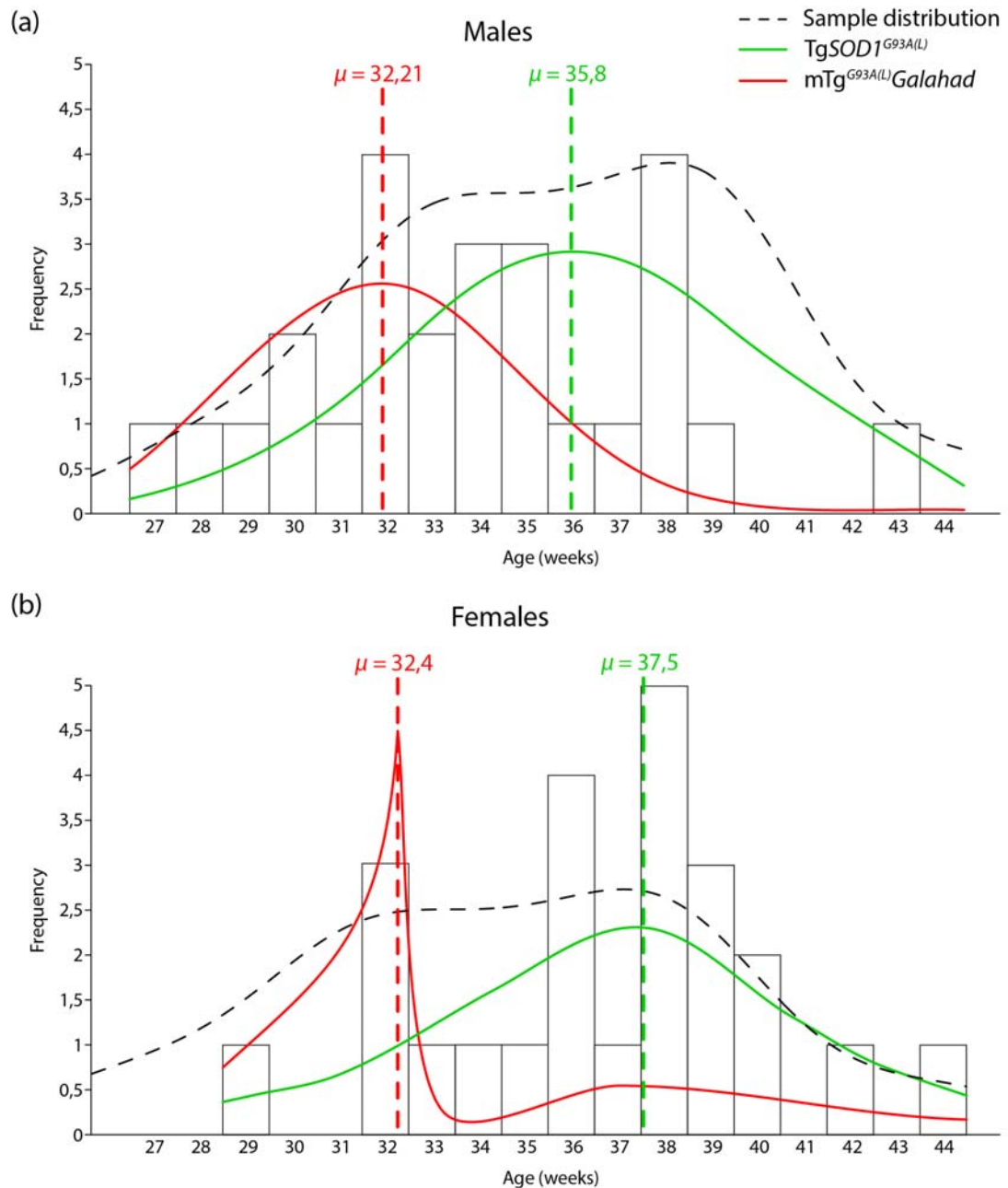


Figure 6.7 Tg^{G93A(L)}Galahad males and females survival bimodal distribution. (a) The survival frequency of the Tg^{G93A(L)}Galahad male mice, $n = 26$, is represented by the histograms. The sample distribution, (black dotted line) shows two peaks compatible with two normal distributions. One with a mean of $\mu = 32.1$; $\sigma = 2.5$; (red line) corresponding to the mTg^{G93A(L)}Galahad population, and one with a mean of $\mu = 35.8$; $\sigma = 3.3$; (green line) corresponding the TgSOD1^{G93A(L)} population. (b) The survival frequency of the Tg^{G93A(L)}Galahad female mice, $n = 24$, is represented by the histograms. The sample distribution, (black dotted line), seems to be compatible with two normal distributions. However, the first curve, corresponding to the mTg^{G93A(L)}Galahad population, is not normally distributed (red line) and has $\mu = 32.4$; $\sigma = 0.1$, the second curve is a normal distribution with $\mu = 37.5$; $\sigma = 3.1$; (green line) corresponding the TgSOD1^{G93A(L)} population. A bigger n number is needed to distinguish between the two populations.

6.3.1.4 Definition of two transgenic populations for phenotypic analysis

In order to analyse weight and grip-strength data of the G2 *Galabad* progeny, and try to identify other phenotypes characteristic of $SOD1^{G93A}$ transgenic ENU mutagenized animals, it was crucial to determine which of the transgenic G2 mice to score $mTg^{G93A(L)}Galabad$, and which mice to score $TgSOD1^{G93A(L)}$. Since the survival distribution of the transgenic *Galabad* population is continuous and the two normal curves describing it greatly overlap (Figure 6.6), for the phenotypic analysis it was defined that: all the mice with survival greater than the mean of the $mTg^{G93A(L)}Galabad$ curve plus two standard deviations ($\mu + 2\sigma = 36.8$) were classified as $TgSOD1^{G93A(L)}$ (Figure 6.8 (a)); whereas animals with survival smaller than the mean of the $TgSOD1^{G93A(L)}$ curve minus two standard deviations ($\mu - 2\sigma = 31.36$) were classified as $mTg^{G93A(L)}Galabad$ (Figure 6.8 (b)). Hence theoretically only 2.1 % of the $TgSOD1^{G93A(L)}$ animals were included in the $mTg^{G93A(L)}Galabad$ population and vice versa only 2.1 % of the $mTg^{G93A(L)}Galabad$ mice were included in the $TgSOD1^{G93A(L)}$ population. A total of 7 animals were defined as $mTg^{G93A(L)}Galabad$ and 25 mice were defined as $TgSOD1^{G93A(L)}$. All animals with a time to end point between 31.36 and 36.85 weeks of age were excluded from the phenotypical analysis, since it was impossible to statistically categorise them into one of the two populations.

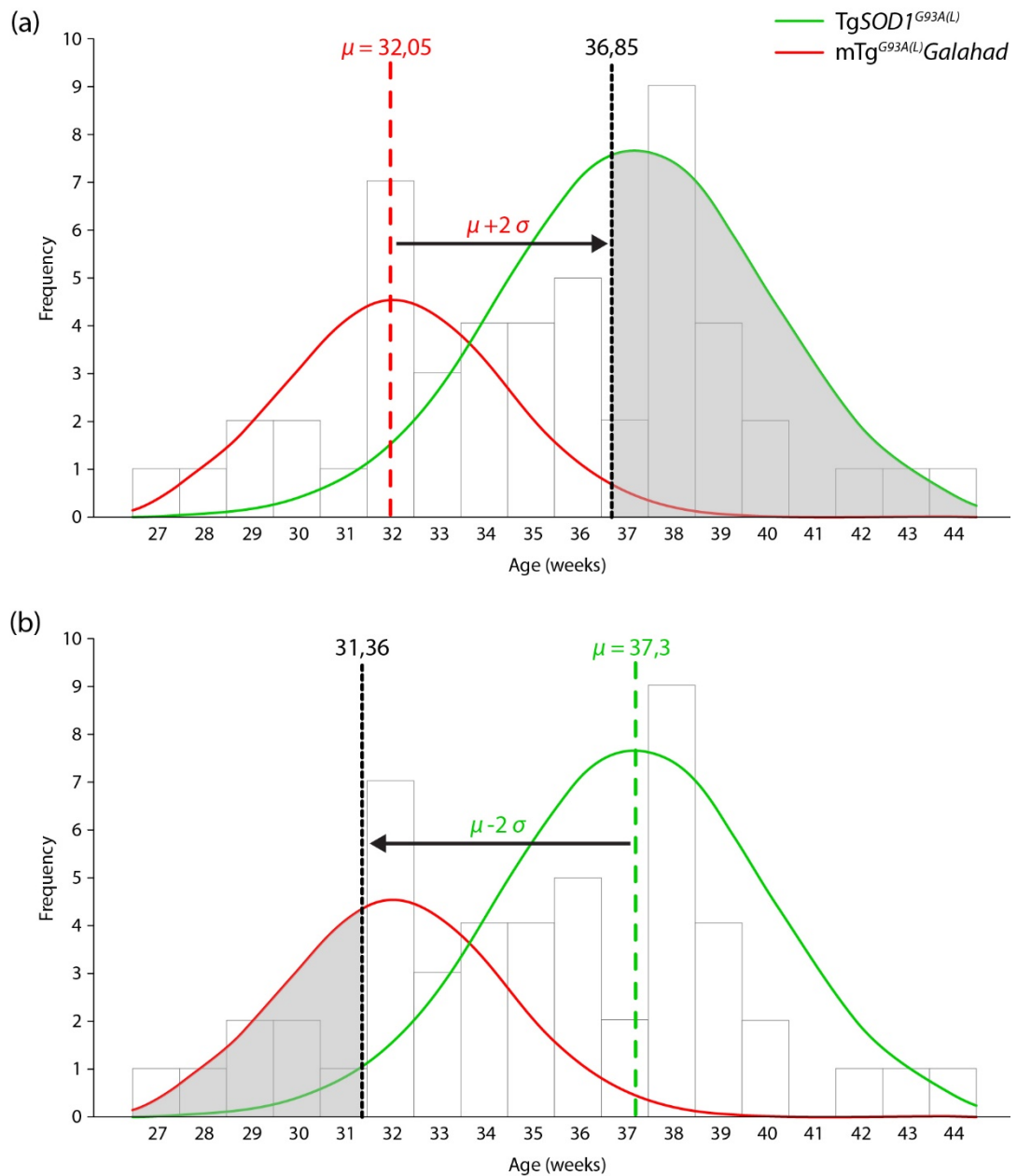


Figure 6.8 Definition of $TgSOD1^{G93A(L)}$ and $mTg^{G93A(L)}Galahad$ populations for phenotypic analysis. (a) All $TgSOD1^{G93A(L)}$ mice that had a survival equal or greater than the mean of the $mTg^{G93A(L)}Galahad$ curve plus 2 standard deviations ($\mu + 2\sigma = 36.85$ weeks) were considered for the phenotypic analysis (grey area). Only 2.1 % of the $mTg^{G93A(L)}Galahad$ data might be included in the non-mutagenized population during analysis (right tail of the red curve). (b) All $mTg^{G93A(L)}Galahad$ mice that had a survival equal or smaller than the mean of the $TgSOD1^{G93A(L)}$ curve minus 2 standard deviations ($\mu - 2\sigma = 31.36$ weeks) were considered for the phenotypic analysis (grey area). Only 2.1 % of the $TgSOD1^{G93A(L)}$ data might be included in the mutagenized population during analysis (left tail of the green curve).

6.3.1.5 Correlation between transgene copy number and survival

There is a positive correlation between the copy number of the *SOD1* G93A transgene array and the phenotype of the mice (Alexander et al., 2004). To verify whether the copy number of G2 Tg^{G93A(L)}*Galahad* mice might influence their survival, a correlation was calculated between the copy number and the survival of 21 animals.

A quantitative real time PCR (qPCR) was carried out as described in section 2.5.4. The data presented in Figure 6.9 proves the existence of a significant correlation between these two parameters: $p = 0.01$. The negative r of the correlation test ($r = -0.5731$) confirmed that with a decrease in copy number, there was an increase in survival. Finally the r^2 ($r^2 = 0.328$) showed that 32.8 % of variance was shared between the two variables. However, the copy number of animals that died before 31.36 weeks seemed to be quite variable (Figure 6.9, below dotted line), a bigger number of mTg^{G93A(L)}*Galahad* animals will be needed to verify if there is correlation with copy number within this population.

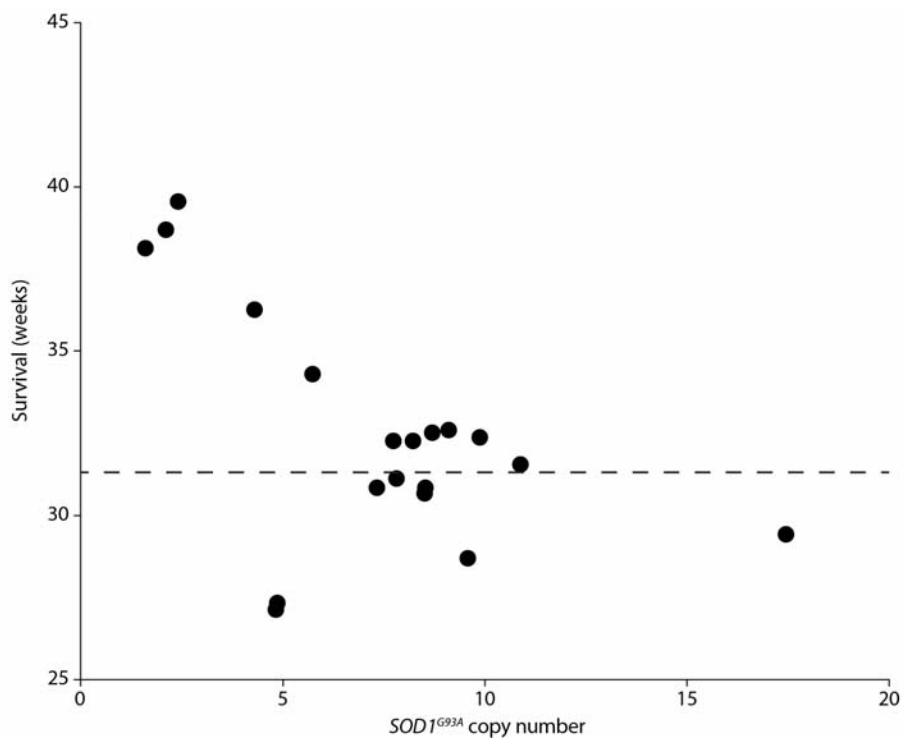


Figure 6.9 Correlation between copy number and survival in G2 Tg^{G93A(L)}*Galahad* mice. The r^2 ($r^2 = 0.328$) confirmed that 32.8 % of variance is shared between the copy number and survival. Indeed a reduced copy number corresponds to an increase in survival. $N = 21$; $r = -0.5731$, $p = 0.01$.

6.3.1.6 *Galabad* G2 body weight analysis

To investigate if the presence of the *Galabad* mutation together with the *SOD1^{G93A}* low copy transgene could cause body weight deficits, weight measures of mTg^{G93A(L)}*Galabad* mice were examined in comparison to Tg*SOD1^{G93A(L)}* and NTg*Galabad* littermates. Weight was assessed weekly as described in section 2.3.2.2. A one-way analysis of variance (ANOVA) with Bonferroni post-hoc test was used to evaluate the difference in body weight between the 3 genotypes from 24 to 27 weeks of age. The analysis was carried out combining the results from the two sexes and for male mice. Of note the number of mTg^{G93A(L)}*Galabad* females was too small to be able to conduct a female only analysis. To minimise gender variation and also size variation that might occur due to the hybrid background all weight measures of each individual were normalised to its maximum bodyweight.

For the whole cohort the overall ANOVA was significant at 26 weeks ($p = 0.007$) and 27 weeks of age ($p < 0.001$). Similarly for the males the overall ANOVA was significant at 26 weeks ($p = 0.005$) and 27 weeks of age ($p = 0.009$). In both analysis the pair-wise comparison found that mTg^{G93A(L)}*Galabad* animals were significantly different from Tg*SOD1^{G93A(L)}* and NTg*Galabad* littermates at 26 and 27 weeks of age. No difference was found between Tg*SOD1^{G93A(L)}* and NTg*Galabad* mice (Table 6.4 and Figure 6.10).

	Weeks	mTg ^{G93A(L)} <i>Galabad</i>		Tg <i>SOD1^{G93A(L)}</i>	
		vs	Tg <i>SOD1^{G93A(L)}</i>	vs	NTg <i>Galabad</i>
Males and females	24	$p = 1$	$p = 1$	$p = 1$	$p = 1$
	25	$p = 0.180$	$p = 0.313$	$p = 1$	$p = 1$
	26	$p = 0.005$ **	$p = 0.037$ *	$p = 1$	$p = 1$
	27	$p < 0.001$ ***	$p = 0.001$ ***	$p = 1$	$p = 1$
Males	24	$p = 1$	$p = 1$	$p = 1$	$p = 1$
	25	$p = 0.213$	$p = 0.361$	$p = 1$	$p = 1$
	26	$p = 0.008$ **	$p = 0.013$ *	$p = 1$	$p = 1$
	27	$p = 0.027$ *	$p = 0.014$ *	$p = 1$	$p = 1$

Table 6.4 *Galabad* G2 mice normalised body weight pair-wise comparisons. Results of Bonferroni post-hoc analysis between the three genotypes, for the whole cohort and males only. Significant p -values are indicated with (*) $p \leq 0.05$; (**) $p \leq 0.01$; (***) $p \leq 0.001$.

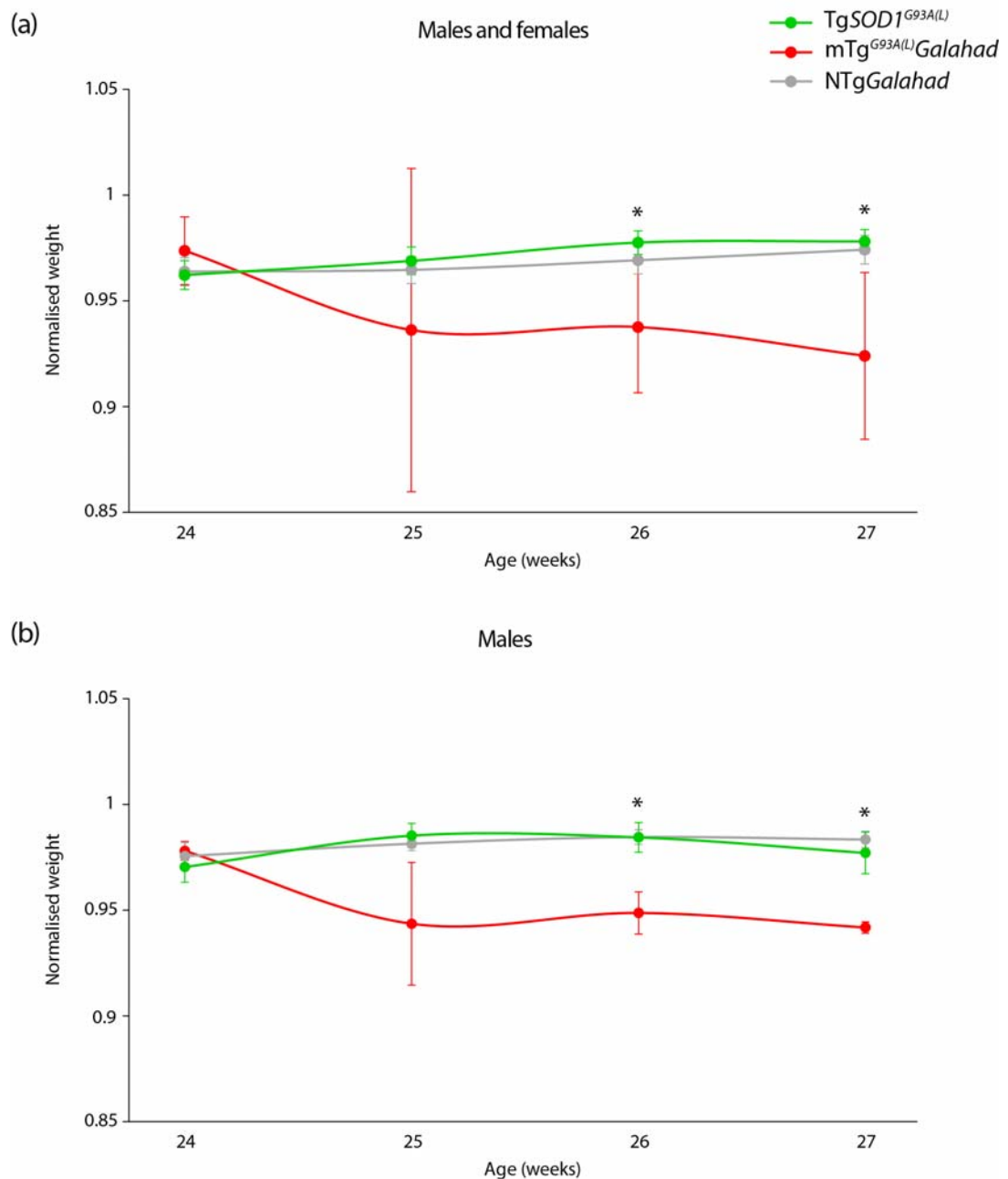


Figure 6.10 Normalised body weight of G2 Galahad mice. (a) Male and female normalised body weight. At least 7 animals per genotype were assessed. mTg^{G93A(L)}Galahad mice are significantly different from TgSOD1^{G93A(L)} and NTgGalahad littermates at 26 and 27 weeks of age. (b) Male normalised body weight. At least 6 animals per genotype were assessed. Also for males only by 26 weeks of age mTg^{G93A(L)}Galahad mice are significantly different from TgSOD1^{G93A(L)} and NTgGalahad littermates. The graphs represent the average normalised weight \pm SEM per genotype and time point. (*) indicates the significant differences between the two transgenic genotypes: mTg^{G93A(L)}Galahad and TgSOD1^{G93A(L)}, other significant results are reported in Table 6.4.

6.3.1.7 *Galabad* G2 grip-strength analysis

To gain more details on the disease progression of the *Galabad* line, grip-strength was assessed weekly for mTg^{G93A(L)}*Galabad*, TgSOD1^{G93A(L)} and NTg*Galabad* littermates, as described in section 2.3.2.3. A one-way ANOVA with Bonferroni post-hoc test was used to evaluate the difference in grip-strength between the 3 genotypes from 23 to 28 weeks of age. Since it is known that gender has an effect on the grip-strength of TgSOD1^{G93A(L)} animals (see above), the analysis was carried out both combining the results from the two sexes and for male mice. As for the weight, also for grip-strength the n number of the mTg^{G93A(L)}*Galabad* females was too small to allow a female only investigation. To minimise variations each grip-strength measure was corrected for the corresponding body weight.

For the whole cohort the overall ANOVA was significant at all weeks tested: 23 weeks ($p = 0.006$); 24 weeks ($p = 0.04$), 25 weeks ($p = 0.014$); 26 weeks ($p = 0.021$), 27 weeks ($p = 0.012$) and 28 weeks ($p = 0.001$). While for the males the overall ANOVA was significant at 23 week ($p = 0.017$), 27 weeks ($p = 0.037$) and 28 weeks of age ($p = 0.003$). In the whole cohort analysis, the pair-wise comparison found that mTg^{G93A(L)}*Galabad* animals were significantly different from TgSOD1^{G93A(L)} at 23, 25, 26, 27 and 28 weeks of age, while they differ significantly from NTg*Galabad* littermates only at 27 and 28 weeks of age. No difference was found between TgSOD1^{G93A(L)} and NTg*Galabad* mice (Figure 6.11 (a) and Table 6.5). When only male mice were investigated a significant difference was found between mTg^{G93A(L)}*Galabad* and TgSOD1^{G93A(L)} littermates at 27 and 28 weeks of age. mTg^{G93A(L)}*Galabad* were also significantly different from NTg*Galabad* mice at 28 weeks of age. Of note at 23 weeks of age the grip-strength of NTg*Galabad* animals appeared significantly reduced compared to TgSOD1^{G93A(L)} littermates, however a difference was detected only for the first time point examined, suggesting that there is not a real variance between the two groups (Figure 6.11 (b) and Table 6.5).

Weeks	<i>mTg^{G93A(L)} Galahad</i>	<i>mTg^{G93A(L)} Galahad</i>	<i>TgSOD1^{G93A(L)}</i>	
	vs <i>TgSOD1^{G93A(L)}</i>	vs <i>NTg Galahad</i>	vs <i>NTg Galahad</i>	
Males and females	23	$p = 0.011$ *	$p = 0.433$	$p = 0.7$
	24	$p = 0.064$	$p = 0.747$	$p = 0.207$
	25	$p = 0.012$ *	$p = 0.057$	$p = 1$
	26	$p = 0.024$ *	$p = 0.541$	$p = 0.207$
	27	$p = 0.012$ *	$p = 0.024$ *	$p = 1$
	28	$p = 0.001$ ***	$p = 0.001$ ***	$p = 1$
Males	23	$p = 0.058$	$p = 1$	$p = 0.036$ *
	24	$p = 0.819$	$p = 1$	$p = 1$
	25	$p = 0.163$	$p = 1$	$p = 0.869$
	26	$p = 0.581$	$p = 1$	$p = 0.483$
	27	$p = 0.041$ *	$p = 0.151$	$p = 1$
	28	$p = 0.003$ **	$p = 0.012$ *	$p = 1$

Table 6.5 Galahad G2 mice normalised grip-strength pair-wise comparison. Results of Bonferroni post-hoc analysis between the three genotypes, for the whole cohort and males only. Significant p -values are indicated with (*) $p \leq 0.05$; (**) $p \leq 0.01$; (***) $p \leq 0.001$.

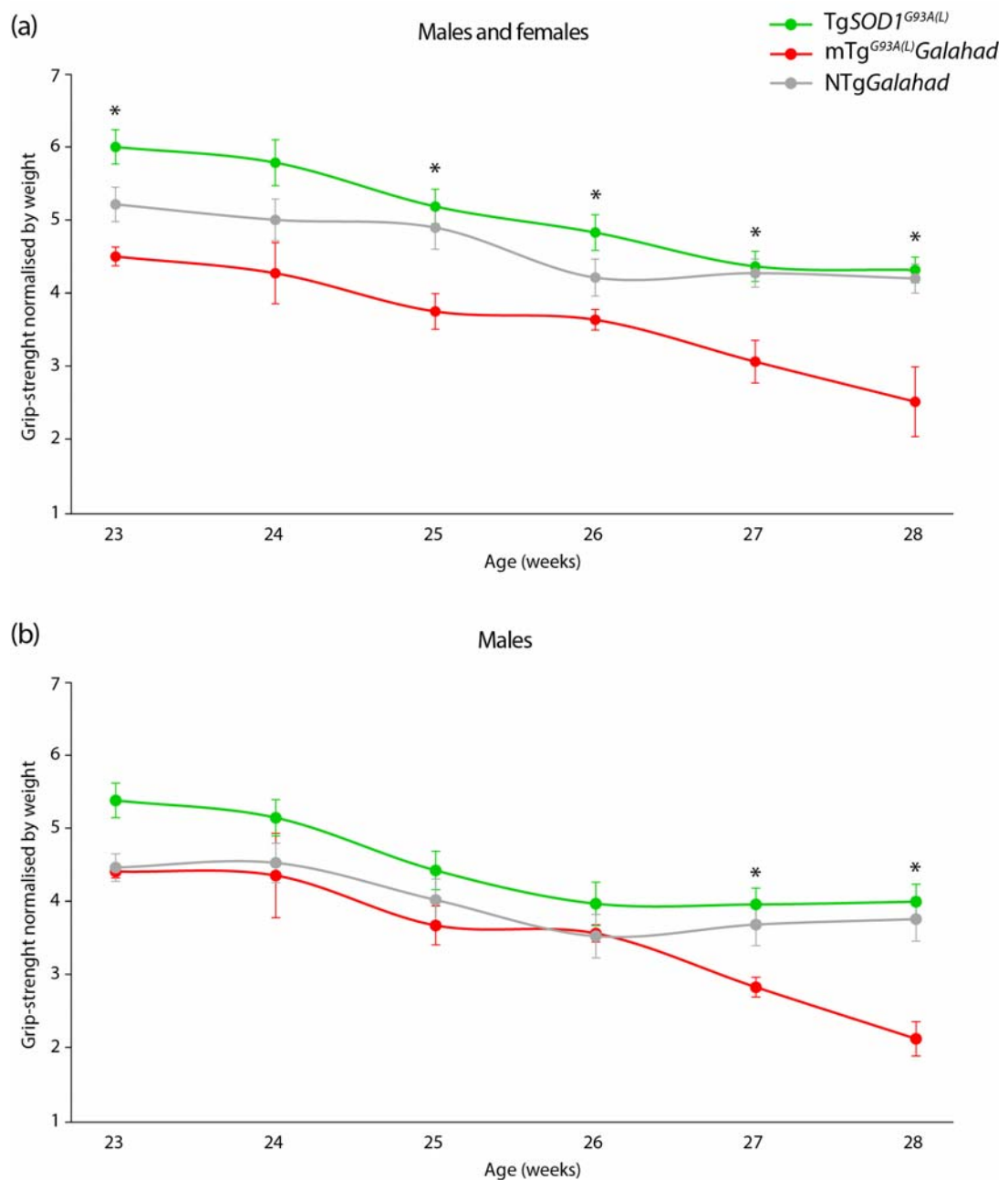


Figure 6.11 Normalised grip-strength of G2 Galahad mice (a) Males and females' normalised grip-strength. At least 6 animals per genotype were assessed for every time point. mTg^{G93A(L)}Galahad mice are significantly different from TgSOD1^{G93A(L)} littermates at all-time points except 24 weeks, and they are significantly different from NTgGalahad mice at 27 and 28 weeks of age. (b) Males normalised body weight. At least 5 animals per genotype were assessed for every time point. mTg^{G93A(L)}Galahad mice are significantly different from TgSOD1^{G93A(L)} littermates at 27 and 28 weeks, and they are significantly different from NTgGalahad mice at 28 weeks of age. There is also a significant difference between NTgGalahad and TgSOD1^{G93A(L)} at 23 weeks. The graphs represent the average grip-strength normalised by weight \pm SEM per genotype and time point. (*) indicates the significant differences between the two transgenic genotype: mTg^{G93A(L)}Galahad and TgSOD1^{G93A(L)}, the other significant difference are noted in Table 6.5.

6.3.2 Phenotypic characterisation of the G3 *Galahad* progeny

A first genome-wide scan (GWS) carried out at MRC Harwell on G2 *SOD1^{G93A(L)}* transgenic *Galahad* mice that reached paralysis before 33 weeks of age, suggested 3 potential areas of linkage for the ENU mutation, located in chromosomes 1, 3 and 10. In order to see if the selected regions were of interest and if it was possible to refine their map position, it was necessary to carry out additional backcrossing followed by a phenotypical investigation and genetic mapping of the new progenies.

6.3.2.1 *Galahad* G2 breeding strategy

G2 *SOD1^{G93A(L)}* transgenic *Galahad* animals were genotyped for markers specific for the 3 regions of interest, which were polymorphic between BALB/c and C57BL/6J background strains (see section 2.5.3). Since the *Galahad* founder (hybrid C57BL/6J-BALB/c) was backcrossed to C57BL/6J mice and the ENU mutation must within DNA from the inbred strain used for chemical mutagenesis (BALB/c), G2 mice that were heterozygous in one or more of the 3 regions of interest were selected for further backcrosses. Twelve G2 Tg^{G93A(L)}*Galahad* mice, 7 females and 5 males were backcrossed with C57BL/6J mice in 9 crosses. Females that were heterozygous for the same regions were crossed in trio matings.

6.3.2.2 *Galahad* G3 genotype and ratios

A total of 132 animals were generated from the 9 crosses. Interestingly the number of males produced was considerably higher than the number of females, respectively 80 and 48. The observed sex ratios were indeed significantly different from the expected $\chi^2(1) = 8.00$ $p = 0.0047$.

Only G3 females were kept and genotyped for the presence of the human *SOD1^{G93A}* transgene as described in section 2.5.2.1. Among them 22 were Tg^{G93A(L)}*Galahad* and 26 were NTg*Galahad*, in this case the observed ratios between transgenic and non-transgenic females was not significantly different from the expected: $\chi^2(1) = 0.333$ $p = 0.564$.

6.3.2.3 Survival of G3 Tg^{G93A(L)}*Galahad* mice

Because of the low number of Tg^{G93A(L)}*Galahad* females it was not possible to statistically investigate if the survival data could fit a bimodal curve, as it was done for the G2 progeny. Hence, the same parameters applied for the G2 mice were used to

define which of the $SOD1^{G93A(L)}$ transgenic G3 females were $mTg^{G93A(L)}Galahad$ and which were $TgSOD1^{G93A(L)}$ (Figure 6.8). Five female mice reached the humane end point before 31.36 weeks and were defined as $mTg^{G93A(L)}Galahad$, and 9 mice reached the humane endpoint after 36.85 weeks and were defined as $TgSOD1^{G93A(L)}$. Interestingly all $mTg^{G93A(L)}Galahad$ were culled due to substantial weight loss. Of note among all the transgenic $SOD1^{G93A(L)}$ females only 13.6 % reached the humane end point because of paralysis while the remaining 86.4 % were culled due to weight loss.

The five $mTg^{G93A(L)}Galahad$ females from the G3 progeny were genotyped for the 3 regions of interest selected by the MRC Harwell GWS, their genotype together with the genotype of the corresponding G2 parents are reported in Table 6.6.

Cross	G	Sex	Survival (weeks)	Chr 1 20 Mb	Chr 1 59 Mb	Chr 3 58 Mb	Chr 3 108 Mb	Chr 10 105 Mb
1	G2	f	36.3	B/B	B/B	B/B	B/B	B/C
	G2	f	36.3	B/B	B/B	B/B	B/B	B/C
	G3	f	28.7	B/B	B/B	B/B	B/B	B/C
2	G2	f	38.7	B/C	B/C	B/B	B/B	B/B
	G2	f	38.1	B/C	B/C	B/B	B/B	B/B
	G3	f	27.14	B/C	B/C	B/B	B/B	B/B
3	G2	f	39.6	B/B	B/B	B/C	B/C	B/C
	G2	f	38	B/B	B/B	B/C	B/C	B/C
	G3	f	30.7	B/B	B/B	B/B	B/B	B/B
	G3	f	31.3	B/B	B/B	B/B	B/C	B/B
4	G2	m	34.2	B/C	B/C	B/C	B/C	B/B
	G3	f	31.1	B/B	B/B	B/B	B/C	B/B

Table 6.6 Haplotype of the G3 $mTg^{G93A(L)}Galahad$ females and G2 parents. Four crosses produced $mTg^{G93A(L)}Galahad$ females. Column (Cross) indicates the cross number, column (G) indicates the generation: parental generation (G2) and progeny generation (G3). Five SNPs were employed for the genotype of the 3 interesting regions, they are labelled by chromosome (chr) location. Regions of heterozygosity between C57BL/6J and BALB/c are indicated in yellow (B/C) while regions on homozygosity (both alleles C57BL/6J), are indicated in grey (B/B). Of note even though the G3 animals reached the humane end point before 31.36 weeks of age, none of the parents died within that period.

6.3.2.4 *Galahad* G3 body weight analysis

To investigate whether the significant difference in bodyweight detected in G2 mTg^{G93A(L)}*Galahad* mice compared to littermates was presented also in the G3 progeny; body weight of G3 mTg^{G93A(L)}*Galahad*, TgSOD1^{G93A(L)} and NTg*Galahad* was assessed weekly (see 2.3.2.2). Analysis was carried out using a one-way ANOVA with Bonferroni post-hoc correction, from 24 to 27 weeks of age. All weight measures of each individual were normalised for its maximum bodyweight.

The overall ANOVA was significant only at 27 weeks ($p < 0.0001$), and the pair-wise comparison found that mTg^{G93A(L)}*Galahad* animals were significantly different from TgSOD1^{G93A(L)} and NTg*Galahad* littermates at 27 weeks of age while no difference was found between TgSOD1^{G93A(L)} and NTg*Galahad* mice (Table 6.7 and Figure 6.12)

Weeks	mTg ^{G93A(L)} <i>Galahad</i>	mTg ^{G93A(L)} <i>Galahad</i>	TgSOD1 ^{G93A(L)}
	vs TgSOD1 ^{G93A(L)}	vs NTg <i>Galahad</i>	vs NTg <i>Galahad</i>
24	$p = 0.569$	$p = 0.241$	$p = 1$
25	$p = 1$	$p = 1$	$p = 1$
26	$p = 1$	$p = 0.594$	$p = 0.790$
27	$p = 0.001$ ***	$p < 0.001$ ***	$p = 1$

Table 6.7 *Galahad* G3 normalised weight pair-wise comparisons. Results of Bonferroni post-hoc analysis between the three genotypes, for females only. Significant p -values are indicated with (*) $p \leq 0.05$; (**) $p \leq 0.01$; (***) $p \leq 0.001$.

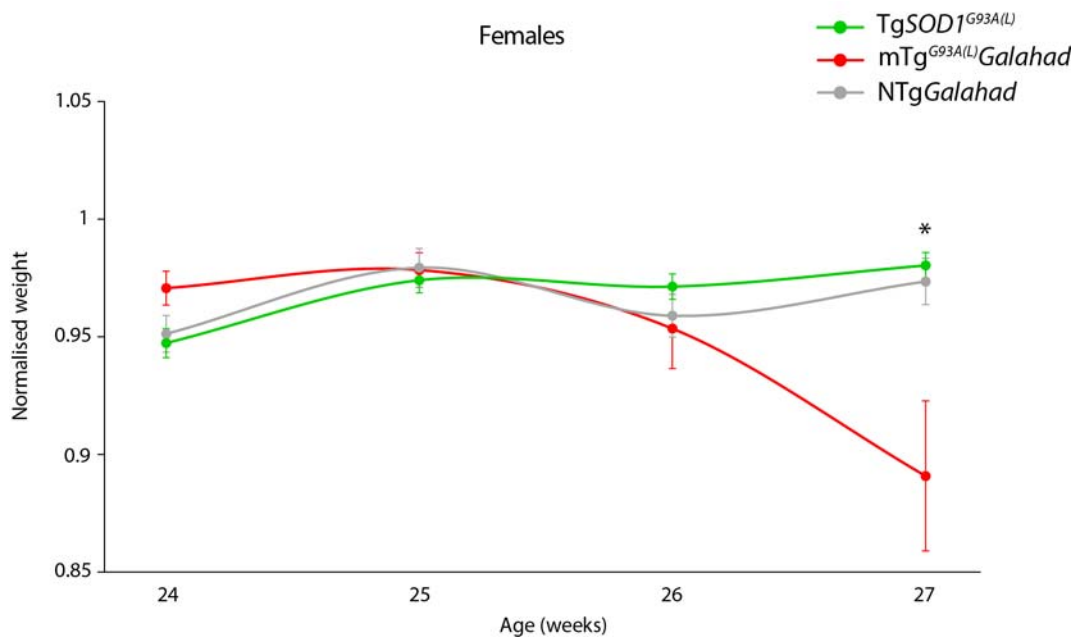


Figure 6.12 Normalised body weight of G3 Galahad females. At least 5 animals per genotype were assessed for every time point. mTg^{G93A(L)}Galahad mice are significantly different from TgSOD1^{G93A(L)} and NTgGalahad littermates at 27 weeks of age. The graphs represent the average normalised weight \pm SEM per genotype and time point. (*) indicates the significant differences between the two transgenic genotype: mTg^{G93A(L)}Galahad and TgSOD1^{G93A(L)}, other significant results are reported in Table 6.7.

6.3.3 NTgGalahad X TgSOD1^{G93A(H)} cross

Preliminary results of a second GWS carried out on the IVF1 G2 progeny, suggested two potential regions of linkage in chromosome 1 and 7 (data not shown). Considering the difficulties in the identification of this new ENU mutation, NTgGalahad animals carrying the potential areas of linkage were crossed with TgSOD1^{G93A(H)} mice, to investigate whether it was possible to exacerbate the Galahad phenotype by having more copies of the human SOD1^{G93A} transgene.

In particular G2 NTgGalahad animals were genotyped for markers specific for the 2 regions of interest, which were polymorphic between BALB/c and C57BL/6J background strains (as described section 2.5.3). Eight NTgGalahad females carrying one or more regions of interest were then crossed with TgSOD1^{G93A(H)} males. A total of 52 animals were generated: 28 females and 24 males, the observed sex ratios were not significantly different from the expected $\chi^2(1) = 0.308$ $p = 0.5791$. Among 52 mice, 24 were non-transgenic for SOD1^{G93A(H)} (NTgGalahad), 23 were transgenic (Tg^{G93A(H)}Galahad) and 5 died for other causes and were not genotyped. From these

mice the observed ratios between transgenic and non-transgenic animals was not significantly different from the expected: $\chi^2(1) = 0.021$ $p = 0.884$.

The average survival for Tg*SOD1*^{G93A(H)} animals on a C57BL/6J background is of 19.5 weeks of age (data from Dr. Rosie Bunton-Stasyshyn), so far 16 Tg^{G93A(H)}*Galabad* mice reached the humane end point with an average survival of 20 weeks. A bigger sample number will be necessary to statistically investigate if it possible to distinguish between a non-mutagenized and an ENU-mutagenized population, and determine whether the ENU mutation can worsen the phenotype of Tg*SOD1*^{G93A(H)} mice.

6.3.4 Genetic mapping

The breeding strategy applied to generate the *Galabad* line was based on the cross between two different inbred strains: BALB/c (ENU-mutagenized) and C57BL/6J. Animals from inbred strains are as genetically alike as possible, being homozygous at virtually all of their loci. Therefore when the *Galabad* founder was backcrossed to the non-mutagenized paternal strain (C57BL/6J), the G2 progeny produced were obligate heterozygous (BALB/c-C57BL/6J) at the mutation affected locus/loci. Furthermore recombination events and the presence of C57BL/6J homozygosity excluded unlinked areas.

6.3.4.1 Genome wide scan

To try to identify the *Galabad* mutation the DNAs of 28 G2 Tg^{G93A(L)}*Galabad* animals that died between 26 and 39.6 weeks of age were sent for GWS. The 19 mouse autosomal chromosomes were genotyped for 1358 polymorphic SNPs markers, that were uniformly distributed at a density of approximately three SNPs every 5 Mb intervals across the genome. The genome coverage by chromosome is reported in Figure 6.13. Of note the marker position is expressed in centimorgan (cM) a unit of linkage that represent the genetic distance between two loci determined by recombination frequency. The genetic distance does not always correspond to the physical distance expressed in base pair, since recombination rate is not constant along the length of the chromosomes.

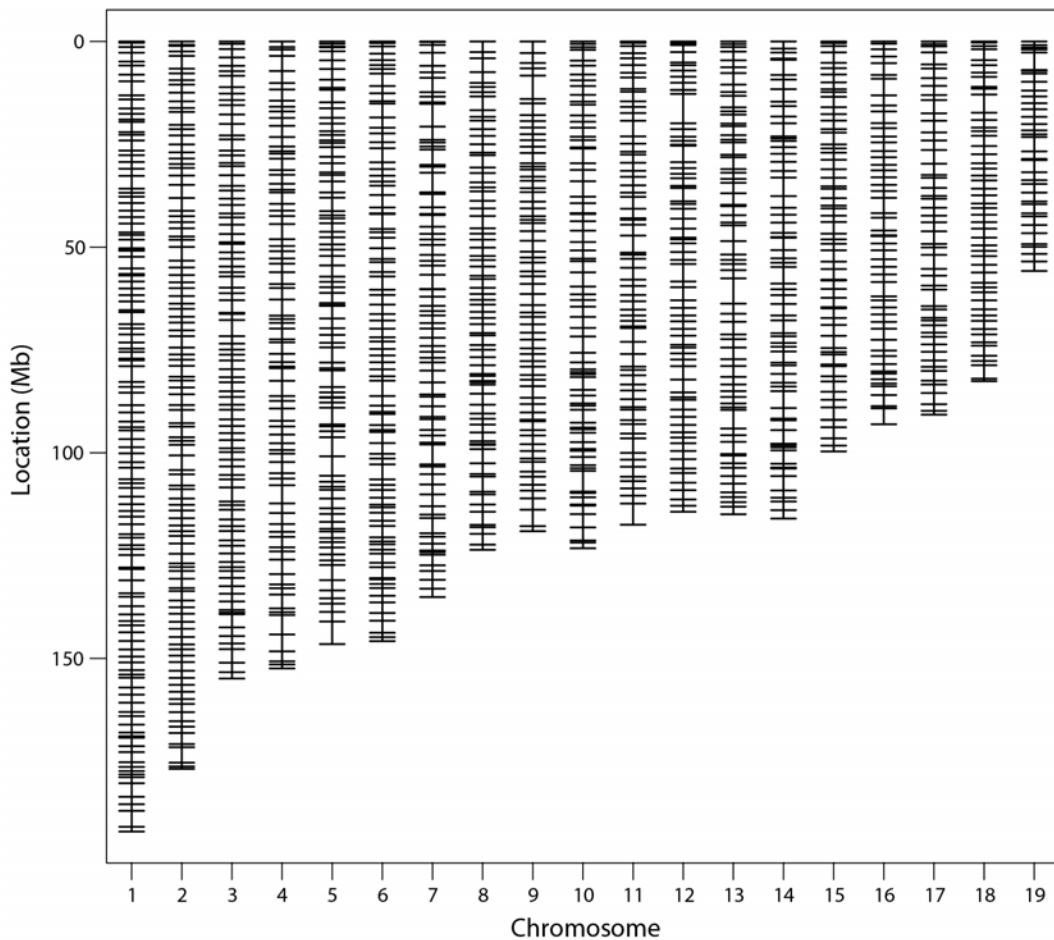


Figure 6.13 SNPs genome coverage. The image shows the coverage density in Mb for every autosomal chromosome. This SNP array provided a medium density genome coverage.

6.3.4.2 QTL analysis

A quantitative trait locus (QTL) analysis was carried out to try and link the phenotypic data (survival) and genotypic data (SNP markers) in an attempt to identify the new modifier mutation/s.

In particular a single QTL genome scan analysis was performed in R using the method of maximum likelihood via the EM algorithm (Lander and Botstein, 1989). Briefly the hidden Markov model was used to calculate QTL genotype probability and correct for missing values, using a step size of 1 cM. For each marker, a logarithm of the odds (LOD) score was calculated, which is an estimation of the probability that the difference seen between homozygous and heterozygous individuals in a specific locus is linked to the phenotype tested; details of the genotype data per chromosome per mouse are shown in Figure 6.14.

The results of the QTL analysis are presented in Figure 6.15 as a plot of the LOD score against the chromosomal map position. Results of the top LOD score obtained for each chromosome are listed in Table 6.8. Of note for the purpose of this analysis a threshold of significance for the LOD score was not calculated, the significance depends on a series of factors, such as species, genome length and recombination, and requires complex algorithms. Instead the 3 highest LOD scores obtained for chromosome 6, 12 and 18 were graphically investigated.

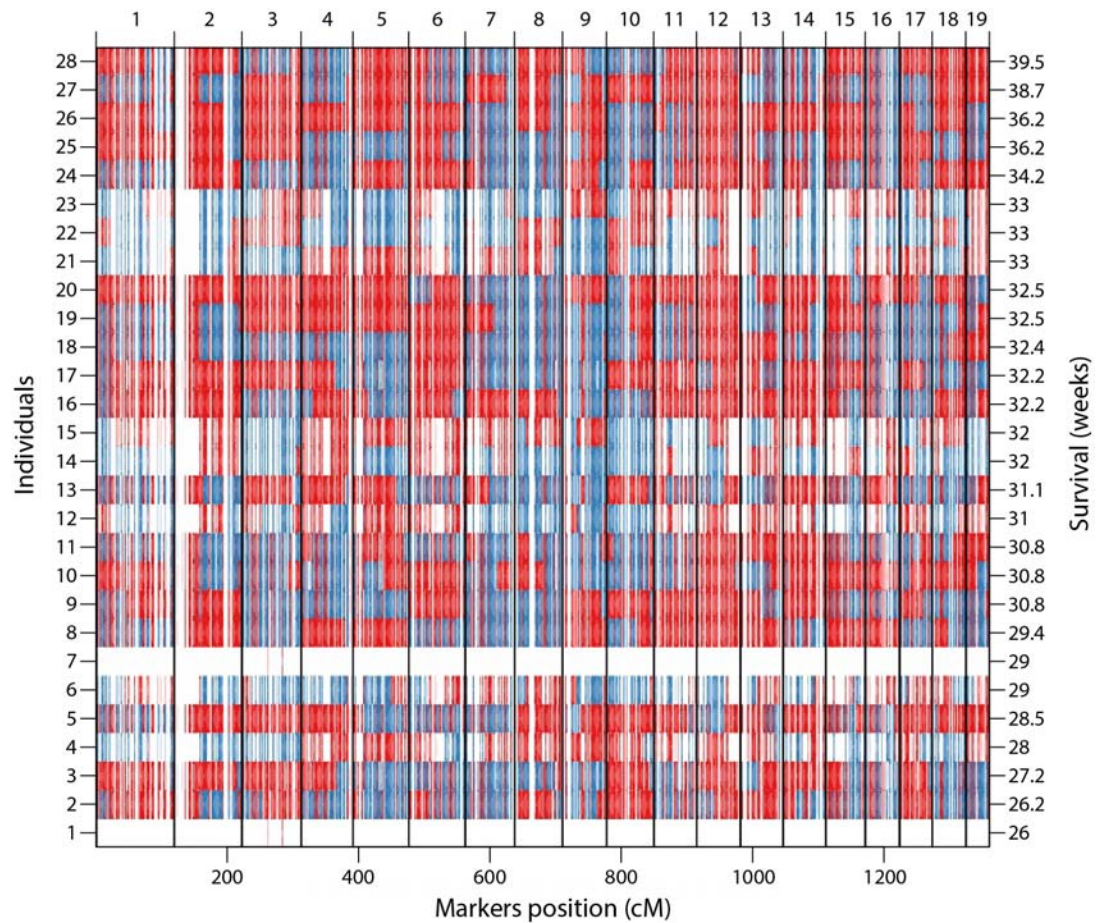


Figure 6.14 Genotype data for the G2 *Galahad* mice. Regions of homozygosity (red), regions of heterozygosity (blue), and missing data (white) plotted for each G2 mouse for every chromosome.

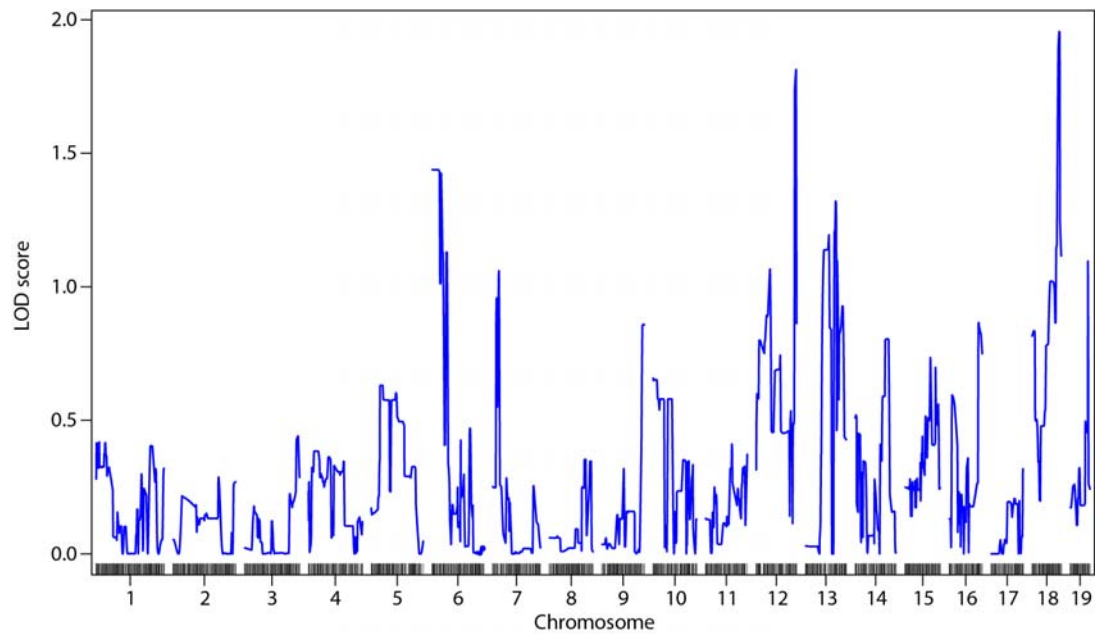


Figure 6.15 LOD scores for *Galahad G2* progeny. Logarithm of the likelihood odds ratio (LOD) score curves along the genome (minus the X chromosome). The positions of the markers are shown as black lines on each chromosome. A significance threshold has not been calculated for this data set, however it was possible to identify 3 peaks: on chromosome 6, 12 and 18.

Chr	Position (cM)	Marker	LOD
1	12.19	c1.loc9	0.419
2	131.99	rs4223511	0.288
3	154.84	rs13477506	0.441
4	26.96	rs13477617	0.384
5	34.91	rs13459085	0.6308
6	16.06	rs13478641	1.438
7	22.23	c7.loc18	1.060
8	106.80	gnf08.108.032	0.353
9	121.91	rs13459114	0.859
10	4.96	rs6185923	0.658
11	77.55	c11.loc74	0.411
12	117.72	rs3692361	1.814
13	99.09	c14.loc91	1.321
14	92.09	c14.loc84	0.804
15	74.85	rs8259436	0.735
16	87.49	rs4214396	0.866
17	94.13	rs3706382	0.318
18	79.94	rs3720876	1.955
19	53.44	rs13483682	1.095

Table 6.8 Top LOD score marker per chromosome. The markers with the highest LOD score values per chromosome (Chr) are shown with relative position in cM.

The three most significant markers identified by QTL analysis were located on chromosomes 6, 12 and 18. To further investigate these three SNPs the genotypes of each animal were plotted against the corresponding survival values and the heterozygosity and homozygosity regions of each mouse were plotted for the corresponding chromosome (Figure 6.16, Figure 6.17 and Figure 6.18). This graphic analysis suggested that regions located in chromosome 6 and 18 were possible areas of linkage since the majority of animals that reached an early time to end point presented areas of heterozygosity along the chromosomes in contrast to mice that displayed a

longer survival (Figure 6.16 (a), Figure 6.18 (a)). Furthermore on the top hit markers the mean of the heterozygous animals was significantly lower compared to the homozygous: $p = 0.005$ for chromosome 6 top hit marker and $p = 0.001$ for chromosome 18 top hit marker (Figure 6.16 (b), Figure 6.18 (b)). Instead chromosome 12 appeared to be a false positive, indeed the majority of animals were homozygous for C57BL/6J along the whole chromosome (Figure 6.17(a)), and on the top hit marker the mean of the heterozygous animals was higher compared to one of the homozygous (Figure 6.17 (b)). Plots showing the regions of homozygosity and heterozygosity with recombination events, for all mice per each chromosome are presented in Appendix 8.7.

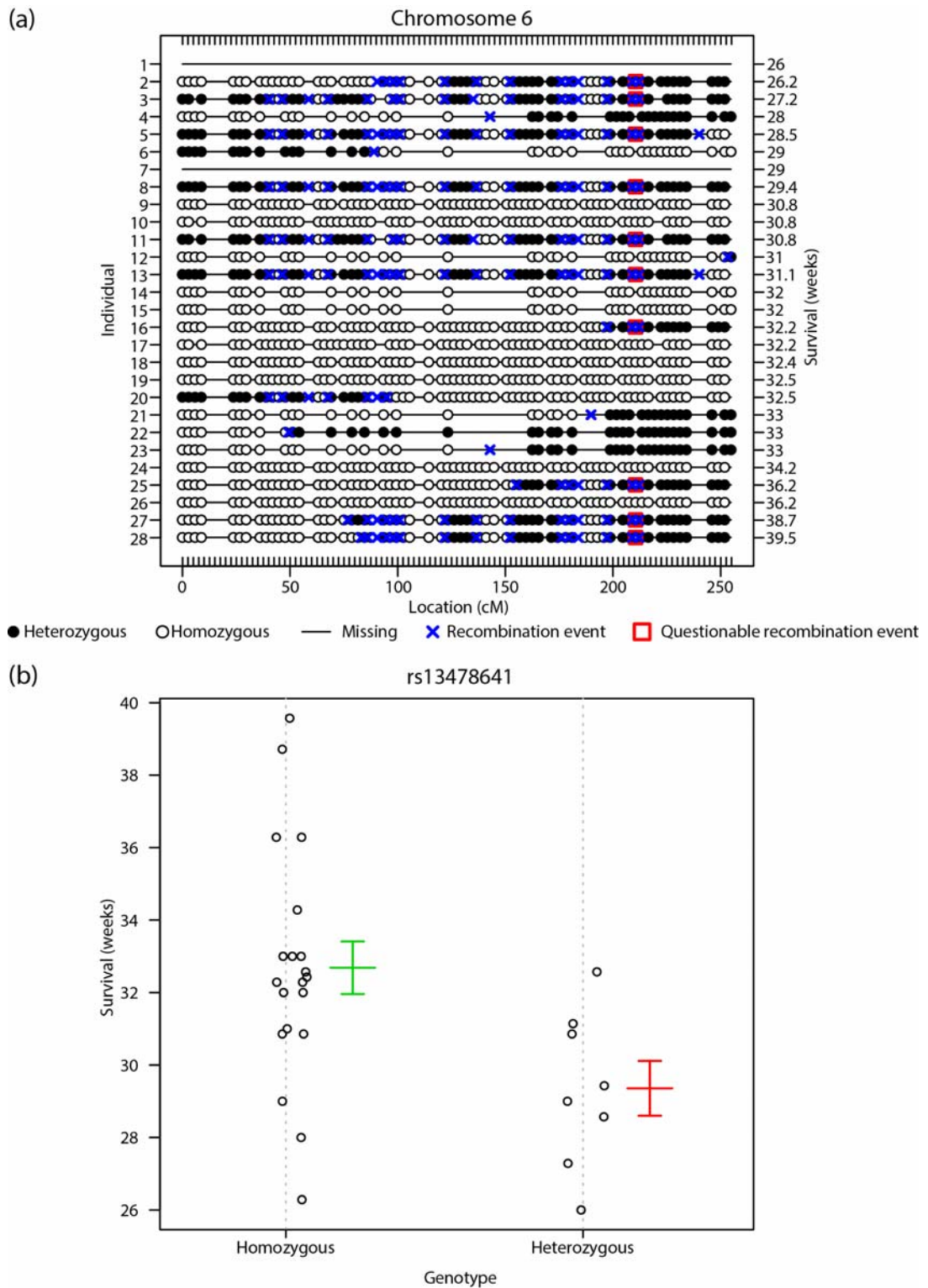


Figure 6.16 Chromosome 6. (a) Genotype and recombination events per mouse along chromosome 6. (b) Maximum LOD score marker for chromosome 6 (LOD = 1.438). Each animal is plotted for the genotype (homozygous or heterozygous, x axis) and survival (y axis). The bars indicate the average survival time for animals that are heterozygous (green) and homozygous (red) in that position.

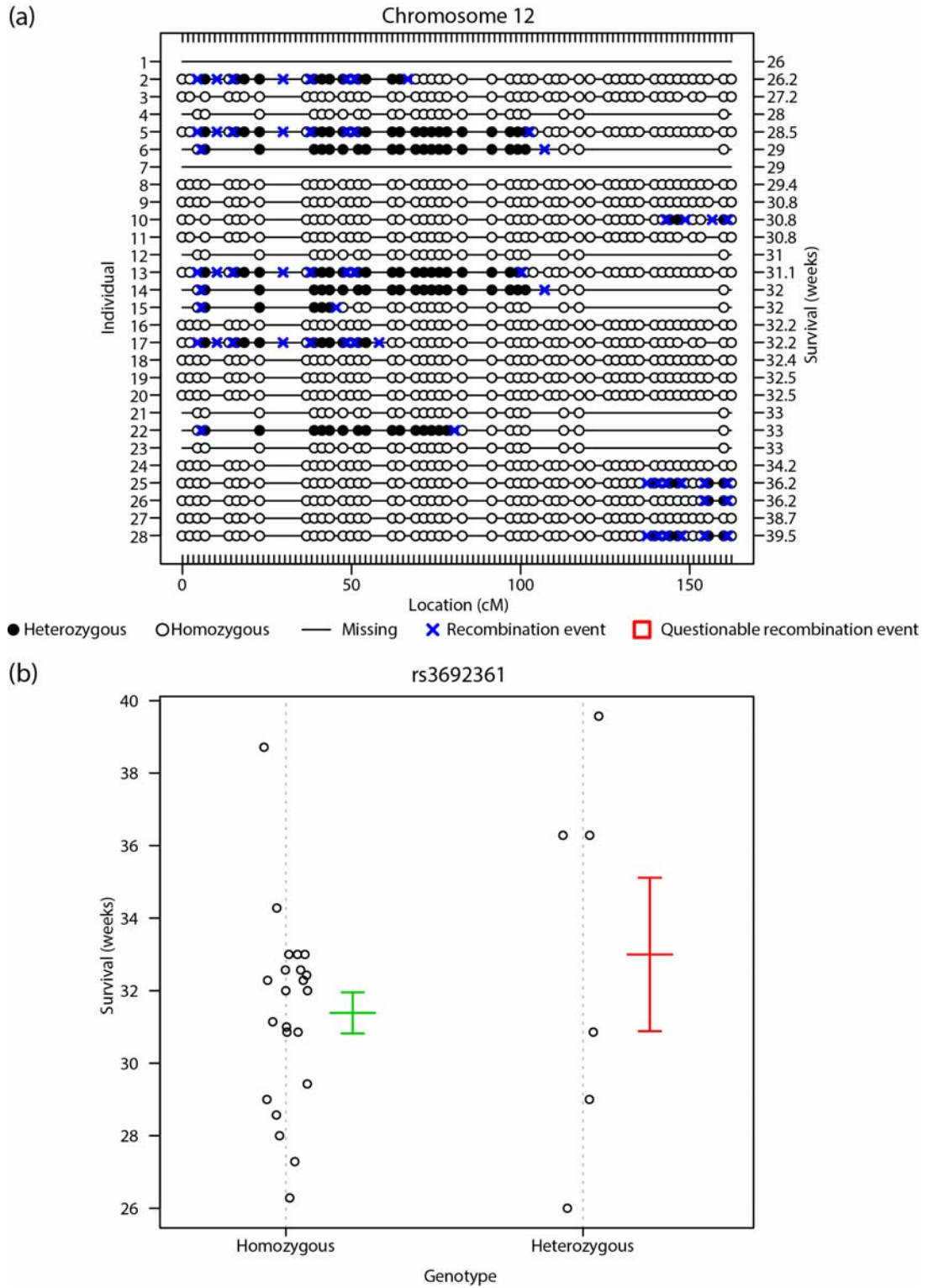


Figure 6.17 Chromosome 12. (a) Genotype and recombination events per mouse along chromosome 12. (b) Maximum LOD score marker for chromosome 12 (LOD = 1.814). Each animal is plotted for its genotype (homozygous or heterozygous, x axis) and survival (y axis). The bars indicate the average survival time for animals that are heterozygous (green) and homozygous (red) in that position. In this case the high LOD score is a false positive.

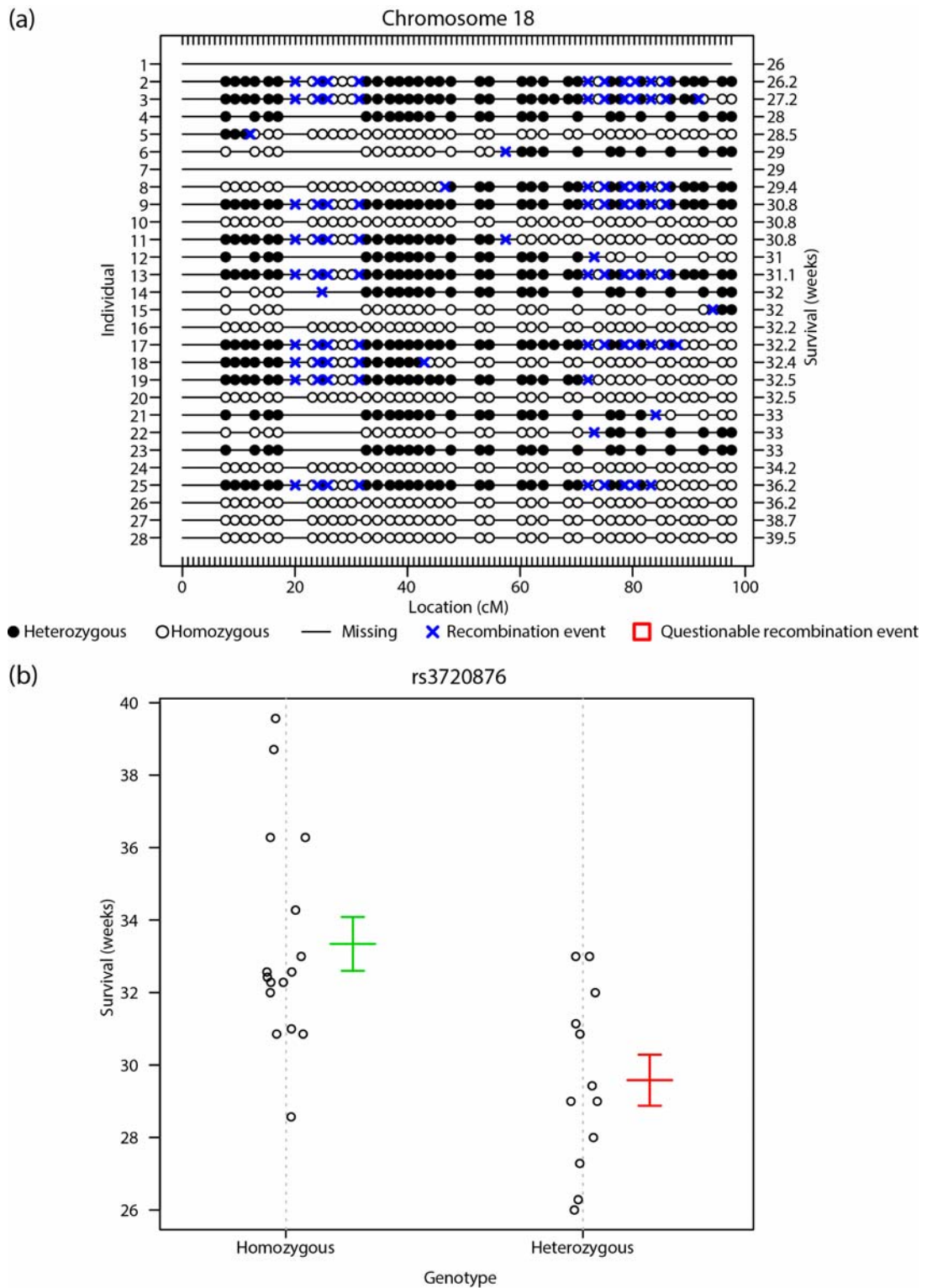


Figure 6.18 Chromosome 18. (a) Genotype and recombination events per mouse along chromosome 18. (b) Maximum LOD score marker for chromosome 18 (LOD = 1.955). Each animal is plotted for the genotype (homozygous or heterozygous, x axis) and survival (y axis). The bars indicate the average survival time for animals that are heterozygous (green) and homozygous (red) in that position.

6.4 Conclusions

6.4.1 Concluding remarks on *Galabad* mice

The aim of the work presented in this chapter was to phenotypically characterise the progeny of the ENU mutagenized *Galabad* mouse and identify possible modifying locus/loci interacting with the *SOD1* G93A mutation.

The results from the behavioural screen provided valuable data towards the characterisation of the *Galabad* mice.

Investigation of the survival phenotype of the second generation of *Galabad* after mutagenesis, confirmed the presence of an early onset phenotype in a subset of Tg^{G93A(L)}*Galabad* mice. Analysis of transgenic *SOD1*^{G93A(L)} survival distribution showed that it was possible to discern between two normal populations, allowing the identification of statistical criteria to classify the Tg^{G93A(L)}*Galabad* mice as ENU mutagenized (mTg^{G93A(L)}*Galabad*) or non-mutagenized (Tg*SOD1*^{G93A(L)}).

A correlation between survival and the number of *SOD1* G93A transgene copies was found in Tg^{G93A(L)}*Galabad* animals. However, a measure of copy number should not be applied as a strategy to identify mTg^{G93A(L)}*Galabad* within the transgenic *Galabad* population, since the copy number of the mice with the smallest survival appeared to be extremely variable.

A significant reduction in body weight was detected in mTg^{G93A(L)}*Galabad* mice compared to Tg*SOD1*^{G93A(L)} and NTg*Galabad* littermates from 26 weeks of age. Of note, even if not significant, a reduction in mTg^{G93A(L)}*Galabad* body weight was visible already at 25 weeks. This was true both when the males and females were analysed together and for males alone. However, a body weight reduction a few weeks before death is expected in mice carrying several copies of the human *SOD1* G93A transgene.

A significant and progressive reduction in grip-strength was found in mTg^{G93A(L)}*Galabad* compared to Tg*SOD1*^{G93A(L)} littermates, starting at 25 weeks of age when males and females were assessed together and from 27 weeks in males only. Interestingly in the whole cohort there was a significant difference between the two transgenic populations already at 23 weeks of age, suggesting that the impairment in grip-strength might start even earlier in mTg^{G93A(L)}*Galabad* animals. Further analysis at earlier time points will be needed to confirm this hypothesis, however if true, grip-strength analysis could be

employed as a strategy to identify mTg^{G93A(L)}*Galabad* mice within the transgenic population. mTg^{G93A(L)}*Galabad* showed a reduction in grip-strength also in comparison to NTg*Galabad* animals, from 27 weeks of age in the mixed gender group and from 28 weeks in males. Of note a significant difference in grip-strength was detected also in NTg*Galabad* animals compare to Tg*SOD1*^{G93A(L)} littermates at a single time point of 23 weeks of age. In the literature wild-type animals show difference in grip-strength compared to Tg*SOD1*^{G93A(L)} from 24 weeks of age (Acevedo-Arozena et al., 2011). Grip-strength investigation on a bigger number of animals will clarify whether this is a random difference or if this might be due to presence of ENU mutagenized animals within the NTg*Galabad* group that may display a subtle phenotype in reduction of grip-strength.

Analyses of body weight of Galahad G3 female mice confirmed the same pattern seen in the G2 generation. Indeed the body weight of mTg^{G93A(L)}*Galabad* mice was significantly reduced at 27 weeks of age compared to littermates. Interestingly all these animals were culled due to loss of body weight and none of them reached paralysis. This might be an effect of the backcross to the C57BL/6J background as it was shown that *SOD1* G93A transgenic mice display a milder phenotype when on a C57BL/6J background compare to others strains (Acevedo-Arozena et al., 2011; Heiman-Patterson et al., 2005). However, the G2 mice that generated the G3 progeny were chosen on the basis of a GWS carried out on a small number of animals and is important to note that the QTL analysis presented in this work excluded those areas as possible regions of linkage. Furthermore none of the G2 parental animals reached the humane end point early enough to be considered mTg^{G93A(L)}*Galabad*, therefore there is the possibility that none of the transgenic animals of the G3 generation that were analysed were carrying the ENU mutation/s of interest.

So far a cross between the G2 NTg*Galabad* and Tg*SOD1*^{G93A(H)} mice did not exacerbate the phenotype of the progeny compared to the parental Tg*SOD1*^{G93A(H)} animals. This might be simply because a bigger number of samples is needed, or because the animals selected on the base of a previous GWS were not carrying the ENU mutation of the founder. Alternatively no difference in survival can be detected because the presence of the high copy *SOD1*^{G93A} transgene causes such a severe phenotype that the ENU mutation if present gives rise only to subtle changes.

The QTL analysis carried out on the G2 progeny suggested two main regions of linkage, one located in chromosome 6 and one located in chromosome 18. The fact that the exact location of these regions is still unclear suggests that the effect of the *Galabad* ENU mutation on the $SOD1^{G93A(L)}$ phenotype might be caused either by a dominant mutation with low penetrance or by a more than one mutations.

6.4.2 Future work

6.4.2.1 Further phenotypic characterisation

To further phenotypically characterise the *Galabad* line it would be necessary to generate a bigger number of animals both for the G2 and the G3 generation. This should allow the investigation of survival, weight and grip-strength of males and females separately, to see if the gender has effect as happens in Tg $SOD1^{G93A(L)}$ mice when in a hybrid background (Acevedo-Arozena et al., 2011). Analysis of the grip-strength from an earlier time point should also reveal if this measure can be employed as a strategy to select ENU mutagenized animals.

The G3 mice that have been investigated should be genotyped for the new areas of linkage identified by the QTL analysis, in order to further investigate the reasons for the differences detected in the sex ratios and the high percentage of animals reaching the humane end point because of weight loss and not paralysis.

6.4.2.2 Further QTL analysis and next-generation sequencing

For the QTL analysis it will be crucial to increase the number of animals in the analysis to better identify the locus/loci that are related to the early onset of the founder. It will be also important to calculate the threshold for the LOD score based on the data to see if there are significant QTLs. Furthermore the whole genome of the *Galabad* founder has now been sequenced using next-generation sequencing technology. These new sequence data together with the result of the QTL analysis will possibly allow the identification of candidate modifier genes of the $SOD1^{G93A(L)}$ phenotype.

6.4.2.3 Pathology investigation

During this study, spinal cord, brain, TA and EDL samples have been collected from a large number of *Galabad* animals. It will be very interesting to carry out experiments such as motor neuron counts in the spinal cords, and neuromuscular junction counting to investigate the pathology of this line.

6.5 Summary

- Survival data from the transgenic $SOD1^{G93A(L)}$ G2 progeny can fit two normal distributions
- From the transgenic $SOD1^{G93A(L)}$ G2 progeny it was possible to define statistical criteria to classify *Galabad* transgenic $SOD1^{G93A(L)}$ mice as ENU mutagenized or non-mutagenized
- There is a correlation between $SOD1^{G93A(L)}$ copy number and survival in the G2 progeny
- G2 mTg^{G93A(L)}*Galabad* mice have a reduction in body weight compared to littermates starting at 26 weeks of age
- G2 mTg^{G93A(L)}*Galabad* mice appear to have early grip-strength impairment, that might be help to distinguish them from the Tg $SOD1^{G93A(L)}$ population
- In the G3 progeny *Galabad* transgenic $SOD1^{G93A(L)}$ animals that have a short survival all reach a humane end point because of substantial weight loss
- The QTL analysis suggests two areas of linkage, on chromosomes 6 and 18
- Chromosome 12 appears to have an area of linkage but is a false positive

Chapter 7 Discussion

The work described in this thesis has focused on the characterisation of the role that the SOD1 protein plays in ALS, investigating the human and the mouse variants *in vivo* and *in vitro*. In particular a meta-analysis was carried out on the literature to review measures of SOD1 activity from SOD1-fALS patients and the phenotype of *Sod1* knockout animals, aiming to understand if a loss of SOD1 function could play a role in disease. Further the phenotype of a novel mouse model, *Sod1^{D83G}*, carrying a point mutation in the endogenous mouse *Sod1* gene was investigated. Then the *Sod1^{D83G}* mouse was crossed with *Sod1* knockout mice and mice overexpressing the human wild-type SOD1 to see if it was possible to dissect elements of a loss of function (the peripheral axonopathy) and aspects of a gain of function (the central body degeneration). Recombinant SOD1 proteins were produced, purified and characterised and preliminary spontaneous aggregation experiments were conducted, to try to investigate human-mouse SOD1 protein interactions. Finally the phenotype of the progeny of the *Galahad* ENU mutagenized mouse was examined and a QTL analysis was carried out in order to try to identify possible modifying locus/loci interacting with the *SOD1* G93A mutation.

7.1 Gain and loss of function could coexist in SOD1-ALS

When in 1993 mutations in the *SOD1* gene were identified as causative of fALS, it was thought that the absence of functional SOD1 could increase oxidative stress, causing neurodegeneration (Smith et al., 1991; Stadtman, 1992; Stadtman and Berlett, 1997). Indeed patients showed oxidative stress markers in tissues and reduction of SOD1 activity in blood (Deng et al., 1993; Fitzmaurice et al., 1996; Rosen et al., 1993; Shaw et al., 1995). However, subsequent findings carried out in SOD1-fALS mouse models soon dismissed the idea that SOD1-ALS could arise from a loss of SOD1 function demonstrating that the disease is caused by a toxic gain of function (Bruijn et al., 1998). Only in recent years, a number of studies investigating *Sod1* knockout and SOD1 transgenic mice reopened the possibility that a loss of SOD1 function could play a role in SOD1-ALS (Saccon et al., 2013). Loss and gain of function mechanisms are already known to coexist in other neurodegenerative diseases such as Huntington's disease and Parkinson's disease (Winklhofer et al., 2008; Zuccato et al., 2010) and have been both hypothesised to contribute to TDP-43-ALS and FUS-ALS (Lagier-Tourenne and Cleveland, 2009; Petkova et al., 2005).

7.1.1 Reduction of SOD1 activity in SOD1-fALS patients

In the present work published data was analysed from patients carrying SOD1-fALS mutations and it was found that on average the overall SOD1 activity is reduced to approximately 50 % (Figure 3.1). However, we did not find any description of ALS patients with complete loss of SOD1 activity, not even when SOD1 mutations were present in homozygosity. Moreover from human genetic studies no evidence was found suggesting that SOD1 loss of function alone causes ALS. Of note none of the 160 mutations linked to SOD1-ALS generate an effectively null allele, reflecting the situation of *Sod1*^{-/-} mice. Indeed there are no truncation mutations in the N-terminal of the SOD1 protein (Figure 1.5). The only described SOD1 mutation that might be a null is a frameshift in exon 2 predicting a protein of 35 amino acid, but segregation data are unclear therefore no assumption can be made (Hu et al., 2012).

7.1.2 SOD1 loss of function worsens the phenotype of transgenic mouse models pointing to a neuroprotective role for SOD1 activity

Although data from transgenic mouse models of SOD1-fALS show that ALS arises from a toxic gain of function, some experiments also point to the possibility that a loss of SOD1 activity might worsen the disease phenotype of these animals.

As reviewed in 3.3.3.3 selective excision of mutant SOD1 from microglia and astrocytes improves the phenotype of transgenic SOD1 mouse models, producing a greater amelioration when the SOD1 mutation is dismutase inactive (Ilieva et al., 2009; Wang et al., 2011b). Further knockdown of mutant SOD1 from Schwann cells worsens the disease progression of enzymatically active SOD1 mutants and ameliorates disease from dismutase inactive SOD1 mutants (Kiernan et al., 2011; Lobsiger et al., 2009; Wang et al., 2012). These results suggest that, in addition to the gain of function, microglia cells and astrocytes of dismutase active mutant SOD1 mice have a neuroprotective effect on the disease, thanks to the presence of residual SOD1 activity.

7.1.3 *Sod1* knockout mice have specific cell-type sensitivities and share characteristics with ALS

Sod1 knockout mice do not develop motor neuron loss and therefore are not a model of ALS, but they are considered a model of chronic oxidative stress. These mice are indeed the most useful tool to investigate the effects of the absence of SOD1 protein *in vivo*.

The meta-analysis carried out in the present work shows that although *Sod1*^{-/-} mice do not develop MN degeneration, they present several ALS-related phenotypes. For example, these mice are characterised by a progressive distal axonopathy (Murray et al., 2010) and their motor neurons are preferentially affected and susceptible to injuries compared to sensory neurons (Pupillo et al., 2012). Furthermore they develop other phenotypes such as increased susceptibility to APP-induced neurodegeneration, or progressive loss of auditory ganglion neurons and retinal cells, that emphasise the importance of SOD1 in neurodegeneration.

Interestingly also heterozygous knockout animals present an increased neuronal loss and susceptibility to injury. Confirming that in mice a 50 % reduction in SOD1 activity, as in SOD1-fALS patients, has direct consequences on neuronal survival and increases predisposition to neurodegeneration. This is different from other human disease data involving loss of enzyme activity, where usually 50 % loss of activity is not sufficient to cause disease related phenotypes (Mitchell et al., 2011).

7.1.4 *Sod1*^{D83G} a novel mouse model to investigate axonal and neuronal body degeneration

We have recently published a paper describing the characterisation of a novel mouse model carrying an ENU-induced point mutation in the mouse *Sod1* gene, which is identical to a human fALS causative mutation (Joyce et al., 2014; Millicamps et al., 2010).

Since the *Sod1*^{D83G} mouse mutation is within the endogenous mouse *Sod1* gene, it overcomes one of the limitations of the transgenic mouse model of SOD-ALS: the overexpression of mutant human SOD1, which is known to affect various features of the disease phenotype and pathology (Jaarsma et al., 2000; Jonsson et al., 2006b). Analysis of the *Sod1*^{D83G} mouse has shown that homozygous *Sod1*^{D83G/D83G} mice develop both upper and lower motor neuron degeneration, modelling the situation in humans, but with a different profile than in mice carrying a human mutant SOD1 transgene array. Indeed, although the degeneration of motor neurons in *Sod1*^{D83G/D83G} animals is progressive, LMN death appears to stop in early adulthood and mice do not become paralysed. Since MN degeneration is never reported in *Sod1*^{-/-} animals (Table 7.1) we believe that the MN loss phenotype in these mice arises from the same toxic gain of function seen in patients (Fischer et al., 2011; Flood et al., 1999). The fact that MN loss in *Sod1*^{D83G/D83G} does not progress to paralysis could be explained by the fact that the

SOD1 protein in these mice is present at a reduced level, ~10 % compared to wild-type (Figure 4.4 and Figure 4.5). Since SOD1 expression levels show a dose-dependent toxicity in other fALS models (Acevedo-Arozena et al., 2011; Jonsson et al., 2006b), this dose of SOD1 protein in *Sod1*^{D83G/D83G} mice may be sufficient to cause some degree of MN degeneration but not at the same levels seen in SOD1-fALS mouse models or in patients. Such low levels of SOD1 protein could be explained by the location of the D83G mutation. The D83 is one of the four residues implicated in the zinc binding (Figure 1.4) (Valentine et al., 2005), and its mutation is predicted to disrupt the metal binding site of the SOD1 dimer causing it to become unstable and more likely to monomerise (Choi et al., 2011; Krishnan et al., 2006; Nordlund et al., 2009). Of note *Sod1*^{+ /D83G} heterozygous do not develop LMN loss up to one year of age, this might be because the presence of a wild-type SOD1 allele has a protective effect. Alternatively *Sod1*^{+ /D83G} heterozygotes mice might develop MN loss later in life, given that the dose of mutant SOD1 protein is known to correlate with the progression of ALS-like phenotypes (Acevedo-Arozena et al., 2011).

Investigation of the innervation pattern of endplate NMJs presented in Chapter 4 (Figure 4.2 and Figure 4.3) shows that *Sod1*^{D83G/D83G} animals develop a severe peripheral neuropathy between 15 and 52 weeks of age, similar to the one described for *Sod1*^{-/-} mice. This result is also confirmed by physiological analysis of motor unit survival (Joyce et al., 2014). Interestingly analysis of SOD1 protein levels and activity revealed that in *Sod1*^{D83G/D83G} the SOD1 dismutase activity is only 1 % of the wild-type animals (Figure 4.5). These findings together with details, gathered in Table 7.1 show that *Sod1*^{D83G/D83G} mice mimic several characteristics of the *Sod1*^{-/-} animals suggesting that the peripheral neuropathy present in this novel mouse may be due to a loss of SOD1 function, potentially leading to oxidative stress and consequently to an increased vulnerability of motor neuron axons. Another indication that SOD1 loss of function plays a role in the pathology of SOD-ALS comes from the analysis of the mitochondrial membrane potentials of embryonic MN cultures of *Sod1*^{+ /D83G} and *Sod1*^{+ /-} mice, which are both hyperpolarised, suggesting that mitochondria abnormalities can be caused by loss of dismutase activity (Joyce et al., 2014).

Although ALS has been proposed to be a ‘dying back’ disorder because NMJ denervation appeared to precede motor neuron cell body death (Bilsland et al., 2008; Duchen et al., 2003). Data on the *Sod1*^{D83G} mouse presented in this thesis and in Joyce

et al., 2014 suggest that axonal and neuronal cell body degeneration may be two separate events. Experiments carried out in SOD1 G93A transgenic mouse models where the BCL2-associated X protein (*Bax*) is ablated support this hypothesis. In these animals indeed *Bax* deficiency protects MN cell bodies from degeneration without altering muscle denervation and mice survival, compared to normal SOD1 G93A transgenic animals (Gould et al., 2006).

Overall, our data suggest that *Sod1*^{D83G/D83G} mice model early stages of human ALS, and are a good system in which is possible to separate the effects of central neuronal loss from the peripheral distal neuropathy.

Phenotype	<i>Sod1</i> ^{-/-}	<i>Sod1</i> ^{D83G/D83G}
Weight loss	Reduced from 20 weeks (Larkin et al., 2011)	Reduced from 4 weeks
Rotarod	Reduced from 36 weeks (Flood et al., 1999)	Reduced from 23 weeks
Grip-strength	Reduced from 52 weeks (Fischer and Glass, 2010)	Reduced from 6 weeks
Motor unit number	Reduced from 15 weeks (data from our group)	Reduced from 52 weeks
NMJ innervation	Denervation from 16 weeks (data from our group)	Denervation at 52 weeks
Development of HCC	56 % females, 79 % males (Elchuri et al., 2005)	78 % females, 91 % males
Survival	Reduced to ~86 weeks (Elchuri et al., 2005)	Reduced to ~86 weeks
MN loss	No MN loss (data from our group)	MN loss occurs from 15 weeks

Table 7.1 Comparison between *Sod1*^{-/-} and *Sod1*^{D83G/D83G} animals. Data refer to *Sod1*^{-/-} and *Sod1*^{D83G/D83G} mice on a C57BL/6J background.

7.1.5 Separation of gain of function and loss of function phenotypes in the *SOD1*^{D83G} mouse model

As explained above the work described in this thesis suggests that mice carrying a D83G mutation in the *Sod1* gene develop phenotypes typical of gain and loss of SOD1 function, in the absence of protein overexpression. To confirm that motor neuron loss and distal neuropathy arise respectively from a gain of function and loss of function of

SOD1, we have crossed *Sod1*^{D83G} mice with *Sod1*^{-/-} and Tg*SOD1*^{WT} mice to examine the effects of varying SOD1 activity on these phenotypes.

Our preliminary findings seem to confirm that the distal neuropathy in *Sod1*^{D83G/D83G} mice was due to a loss of SOD1 function. Indeed *Sod1*^{-/D83G} mice show a reduction in TA force similar to *Sod1*^{D83G/D83G} animals, but no lower motor neuron loss was detected in contrast to the 20 % loss of lower motor neurons seen in *Sod1*^{D83G/D83G} mice (courtesy of Dr Philip McGoldrick). Data presented in Chapter 4 show that SOD1 protein levels in the compound heterozygous animals *Sod1*^{-/D83G} are significantly reduced compared to *Sod1*^{+/D83G} and also compared to *Sod1*^{D83G/D83G} littermates, but are not absent as in *Sod1*^{-/-} mice (Figure 4.4 and Figure 4.5). Taken together these results suggest that the distal neuropathy seen in *Sod1*^{D83G/D83G} mice occurs independently of motor neuron loss, which is dependent on the dose of SOD1 protein and occurs due to a toxic gain of function of mutant SOD1. As mentioned before dose-dependent toxicity of mutant SOD1 has been reported for other transgenic mice overexpressing mutant SOD1 (Acevedo-Arozena et al., 2011; Deng et al., 2006; McGoldrick et al., 2013).

The cross between *Sod1*^{D83G} and Tg*SOD1*^{WT} mice further confirmed that the distal axonopathy of *Sod1*^{D83G/D83G} mice was due to a loss of SOD1 function. Indeed TA force data show that the distal neuropathy of *Sod1*^{D83G/D83G} mice and of *Sod1*^{-/-} mice can be completely rescued by the presence of human wild-type SOD1 (courtesy of Dr Philip McGoldrick). These results are consistent with previously published reports in which central nervous system specific expression of SOD1 could rescue distal neuropathy in *Sod1*^{-/-} mice (Flood et al., 1999).

Analysis of SOD1 protein levels and activity of the transgenic progeny generated from the cross between *Sod1*^{D83G} and Tg*SOD1*^{WT} mice, confirms as expected the presence of a high level of SOD1 and dismutase activity (Figure 4.8 and Figure 4.9). Data from double transgenic mutant mice overexpressing the wild-type human SOD1 together with the mutant protein, have been shown to accelerate ALS-like phenotypes (Deng et al., 2006). Crucially our Tg^{WT}*Sod1*^{D83G/D83G} mice have not shown any exacerbation of the mutant SOD1-mediated phenotypes. This might be because the human wild-type SOD1 and the mutant mouse SOD1 D83G fail to interact (Sakellariou et al., 2014). Alternatively it may be because wild-type SOD1 only exacerbates mutant SOD1 toxicity in a transgenic line showing high expression of mutant SOD1 (Deng et al.,

2006). If the latter is true it may suggest that a threshold limit of mutant SOD1 expression is needed for the manifestation of ALS-like phenotypes. Most probably this limit is not reached in *Sod1*^{D83G/D83G} mice, since SOD1 protein level is 10 % of wild-type and only a non-progressive motor neuron degeneration is present in these mice. *In vitro* experiments using mouse and human recombinant SOD1 proteins described in Chapter 5 could elucidate whether mouse and human SOD1 proteins can interact, and if there is a threshold under which cross-seeding of two SOD1 variants does not occur (Chia et al., 2010).

Preliminary data from these crosses seems to confirm that motor neuron degeneration in *Sod1*^{D83G/D83G} mice is due to a gain of function of mutant SOD1 while the peripheral axonopathy is the result of a loss of SOD1 function.

Although the role of SOD1 loss of function still needs to be investigated and it is insufficient to provoke motor neuron degeneration, the data presented in this thesis suggest that it is crucial for normal motor neuron function. Interestingly many new roles for the SOD1 protein are emerging and understanding them might help to elucidate the roles that an absence of SOD1 protein may play in the pathogenesis of SOD1-ALS.

7.1.6 Co-existence of a SOD1 gain and loss of function in ALS

Superoxide clearance is the best known function of SOD1 and its loss of function causes oxidative stress. SOD1 has also been demonstrated to be a target of oxidation in transgenic SOD1-fALS mice (Andrus et al., 1998). Additionally following oxidative stress, SOD1 oxidation and glutathionylation, increase the propensity of the dimer to dissociate and become misfolded (Ezzi et al., 2007; Khare et al., 2004; Rakhit et al., 2004; Wilcox et al., 2009). All these findings together with the work presented in this thesis support our hypothesis, previously published, of a potential co-operation of SOD1 loss of function and gain of function in ALS pathogenesis (Saccon et al., 2013). Confirming that a vicious circle can be postulated in which oxidized SOD1 has increased propensity to misfold, causing seeding and aggregation of SOD1 and determining a reduction of dismutase activity, which therefore feeds more potential oxidative stress to the beginning of the loop (Figure 3.2). Evidence from recent findings suggest that this mechanism can be relevant not only to SOD1-fALS but also to sporadic cases (Bosco et al., 2010; Forsberg et al., 2010) and to non SOD1-ALS;

indeed misfolding of SOD1 was shown to be induced by both TDP-43 and FUS mislocalisation (Pokrishevsky et al., 2012).

7.2 Human and mouse SOD1 proteins in ALS

Mutant SOD1 proteins have been intensively investigated in the study of ALS, but the mechanism through which they exert toxicity is still unknown (Bruijn et al., 2004; Seetharaman et al., 2009). Over the years a number of transgenic mouse models recapitulating the features of human SOD-ALS have been generated, introducing the human *SOD1* gene into mice. In all of these mouse models of SOD1-fALS it is possible to detect accumulation of mutant SOD1, as happen in patients, leading to the concept that SOD1-ALS is a protein misfolding disorder. This feature together with the focality of the clinical onset and the regional spreading of neurodegeneration pointed to the idea that ALS spreads through a prion-like mechanism (Grad et al., 2015; Lee and Kim, 2015). Such mechanism of seeded aggregation and spread of pathology have been demonstrated both *in vivo* and *in vitro* for many neurodegenerative diseases such as Alzheimer disease and Parkinson's disease (Marciniuk et al., 2013). Genetic mutation is not the only way through which SOD1 can misfold and aggregate. Indeed post-translational modification and aberrant oxidation of wild-type SOD1 have been shown to drive aggregation *in vivo* (Casoni et al., 2005; Rakhit et al., 2004), and human wild-type SOD1 has been found to co-aggregate with mutant SOD1 variants in cell cultures. This discovery underlined the importance that in SOD1-fALS transgenic mouse models the mutant human and the mouse wild-type SOD1 protein coexist, and to interpret mouse SOD1-ALS research it is crucial to understand whether the human and the mouse SOD1 variants interact.

7.2.1 *In vivo* interaction of human and mouse SOD1 proteins

Evidence from previous studies suggest that there is no interaction between mouse and human SOD1 in mouse models of SOD1-fALS. When human wild-type SOD1 protein was overexpressed in a mutant mouse carrying a several copies of the G86R mutation in the mouse *Sod1*, no effect was detected on the motor phenotype or survival of the G86R mouse line, and the mouse and the human variants were not co-aggregating (Audet et al., 2010; Ripps et al., 1995). Further in SOD1-fALS mouse models endogenous mouse SOD1 has previously been reported as having little or no effect on the phenotype (Bruijn et al., 1998; Deng et al., 2006) and wild-type mouse SOD1 is

usually absent from mutant human SOD1 aggregates (Bruijn et al., 1998; Deng et al., 2006; Jonsson et al., 2004).

Results presented in this thesis show that the presence of the D83G mutant mouse SOD1 protein at endogenous levels does not exacerbate the phenotype of TgSOD1^{WT} mice. Although, the presence of the overexpressed wild-type SOD1 protein rescues the phenotype of the *Sod1*^{D83G/D83G} mice. In accordance with previous findings these data suggests that there is no interaction between the human and the mouse SOD1 protein, and the rescue of the D83G phenotype appears to occur in a dose-dependent manner, where high levels of wild-type SOD1 are present. Indeed in double transgenic mice in which an exacerbation of the phenotype is seen, the amount of wild-type human SOD1 has a dose-dependent effect, with higher levels of expression resulting in more profound exacerbation of the phenotype (Prudencio et al., 2010)

The work presented in this thesis show that when SOD1 enzymatic activity is measured from mouse brain homogenates, using non-denaturing and non-reducing conditions the human wild-type and human G93A SOD1 transgenic proteins migrate faster in the gel, compared to the wild-type and D83G mutant mouse SOD1 variants (Figure 4.4, Figure 4.6, Figure 4.7, Figure 4.8). In general transgenic human SOD1 animals display high levels of activity and the signal detected in activity gel assays is considerably more intense compared to that of wild-type or *Sod1*^{D83G} mice. Thus in Tg^{WT}*Sod1*^{D83G/D83G} and Tg^{WT}*Sod1*^{+/D83G} mice it is not possible to distinguish between the human transgenic SOD1 protein and the mouse D83G SOD1, due to the intensity of the transgenic SOD1 signal. Further the native blot in Chapter 5 comparing SOD1 protein from brain homogenates of wild-type, *Sod1*^{-/-}, TgSOD1^{WT} and TgSOD1^{G93A(H)} mice using a commercial antibody against SOD1, confirms that the human SOD1 transgenic protein migrates faster than the mouse SOD1.

Unfortunately in native gels it is difficult to determine the size of the protein products since their electrophoretic mobility depends only on the charge-to-mass ratio and on the physical shape of the protein. Moreover in activity gel experiments it is not possible to stain the gel in order to identify the ladder. Besides these limitations it is possible to say that the protein products detected using activity gel assays corresponded to dimeric SOD1 proteins, or other functional SOD1 forms, but not to monomeric SOD1. Indeed monomeric SOD1 is not active and therefore undetectable by activity assays. Additionally in the native blot shown in Figure 5.15 (c) the minimum sized SOD1

bands electrophoresed higher on the gel than expected for SOD1 monomers. Further experiments measuring SOD1 activity and protein levels under native conditions from human and mouse brain samples could help clarify whether this difference in protein migration is due to species specific SOD1 protein charge or conformation, or if the fast migration pattern seen in transgenic SOD1-fALS is a consequence of protein overexpression.

The hypothesis that these differences in migration pattern are due to diverse biochemical and biophysical characteristics of the human and mouse SOD1 protein is supported by several publications. Indeed, wild-type human SOD1, but not wild-type mouse SOD1, was found to co-aggregate with mutant human SOD1 (Prudencio et al., 2010) while wild-type mouse SOD1, but not wild-type human SOD1, co-aggregates with mutant mouse SOD1 (Qualls et al., 2013). Further experiments carried out in cells by Grad and colleagues showed that residue tryptophan 32 is crucial for the conversion of human wild-type SOD1 to a misfolded form; but that mouse SOD1 possesses a serine residue at position 32, which is unable to participate in misfolding reactions with human wild-type SOD1 (Grad et al., 2011, 2015). These results taken together suggest that there are limited interactions between human and mouse SOD1 and that the tryptophan at residue 32 is implicated in species specific interaction limiting the co-aggregation of human and mouse SOD1.

7.2.2 *In vitro* interactions of human and mouse SOD1 recombinant proteins

To further investigate human and mouse SOD1 interactions, and their role in ALS we produced and characterised recombinant human and mouse SOD1 proteins, and carried out preliminary spontaneous aggregation experiments. It has already been demonstrated that human mutant and wild-type SOD1 proteins can form aggregates *in vitro*. Aggregation can occur either by self-seeding or by cross-seeding with other pre-formed aggregates, or with SOD1-fALS transgenic mice spinal cord homogenates (Chia et al., 2010). In Chapter 5 it is shown that human and mouse SOD1 protein share similar conformation characteristics of their secondary structure, this is expected since they are 84 % identical in amino acid sequence (Seetharaman et al., 2010). Interestingly when proteins were electrophoresed in denaturing and reducing conditions and stained by coomassie blue, the mouse SOD1 variants appeared to migrate slightly faster compared to the majority of the human variants (Figure 5.7). We hypothesise that this difference in migration might be due to a difference in metal

binding capacity among the SOD1 variants. Our preliminary experiments also show that the wild-type and mutant D83G human and mouse recombinant proteins that we produced can aggregate *in vitro*. Further cross-seeding experiments can be conducted to investigate whether the human and the mouse protein can co-aggregate *in vitro* and will help us to understand if the conversion of wild-type SOD1 by misfolded templates is a sequence or structure dependent process subject to species specific barriers.

7.3 The importance of investigating SOD1 modifiers

In ALS research transgenic SOD1-fALS mouse models have been extensively employed in the investigation of genetic modifiers of disease expression, that could potentially contribute to the susceptibility or neuroprotection of motor neuron degeneration (Heiman-Patterson et al., 2011). Both types of modifiers are quite valuable: suppressors can be used as targets for new drugs, and together with enhancers they might highlight new disease genes or pathways and lead to new therapeutic targets (Acevedo-Arozena et al., 2008). Modifiers can sometimes act both as enhancers and suppressors of different genes. For example, the ENU *Legs-at-odd-angles* (*Lod*) mutation in *Dync1h1* is known to act as an enhancer modifier in HD (Ravikumar et al., 2005) and as a suppressor in SOD1-ALS (Kieran et al., 2005). New interesting genes and pathways that may contribute to the disease have been mainly investigated by crossing transgenic SOD1-fALS mouse models with other mouse models expressing or lacking genes of interest (Oliver et al., 2011; Riboldi et al., 2011; Turner and Talbot, 2008). At MRC Harwell ENU mutagenesis, which can create a range of mutations from loss to gain of function, has been employed in combination with transgenic SOD1 G93A low copy mice to find possible new modifiers of SOD1-ALS. One mouse with reduced survival was identified: the *Galabad* mouse. In the present work the survival, weight and grip-strength of the G2 progeny generated from the *Galabad* founder were investigated. The results of this study confirmed that the only phenodeviant feature of these animals compared to SOD1 G93A low copy mice is a subtle reduction in survival. Indeed as shown in Figure 6.8 the average survival for the mTg^{G93A(L)}*Galabad* population is of 32.05 weeks while the average survival for the TgSOD1^{G93A(L)} population is of 36.85 weeks. Such subtle difference in survival makes the analysis of behavioural data very difficult for two reasons. First the normal distribution of the two populations greatly overlap therefore, the majority of the animals, 31 out of 50, could not be included in the statistical analysis of the weight and

the grip-strength. Second because we could identify whether a mouse was mTg^{G93A(L)}*Galabad* or not only at the time of end stage, it was not possible to carry out more accurate behavioural experiments since it would have been too costly to investigate all transgenic *Galabad* mice at the same time. Nevertheless, the results of the phenotypic analysis presented here suggests that it might be possible to select phenodeviant animals on the basis of their grip-strength, a few weeks before symptoms onset. Furthermore a genome scan investigation followed by a QTL analysis helped identifying a few regions of linkage where a possible mutation/s may be located. QTL analysis has already produced good results in the identification of important loci in SOD1-ALS. Indeed genome scan investigations have revealed the presence of modifier loci in chromosome 13 for SOD1-G86R mice and in chromosome 17 for SOD1-G93A mice (Kunst et al., 2000; Sher et al., 2014). However, to date next-generation sequencing technology is a fast and affordable approach in the identification of newly induced causal variants that might be favoured over QTL analysis in ENU sensitised screens.

As mentioned above genetic modifiers are important in the investigation of therapeutics for ALS. However, several reports showed that many therapeutic modifiers of mouse ALS did not translate successfully into patients (Perrin, 2014; Turner and Talbot, 2008). Indeed when working with SOD1-ALS mouse models it is crucial to take into consideration some experimental design guidelines to help ensure a standardisation of interpretation. It is therefore important to control for parameters such as background effect, a copy number and gender (Perrin, 2014; Turner and Talbot, 2008).

7.4 Conclusions

The work presented in this thesis proposes that loss of SOD1 function might play a modulating role in SOD-fALS, and shows that the *Sod1*^{D83G} mice represent a good mouse model in which is possible to dissect elements of a gain of function and of a loss of function mechanism. Further characterisation of SOD1 protein *in vivo* and *in vitro* suggests that although the mouse and the human SOD1 proteins are capable of forming spontaneous aggregates, their conformational differences may prevent them from interacting in mouse models. Finally using ENU mutagenesis and QTL analysis two regions of linkage have been identified where might lie a possible modifying locus/loci interacting with the *SOD1* G93A mutation.

SOD1 research has significantly contribute to broad our understanding of ALS however, in the last ten years several new causative genes have been identified, such as *TDP-43*, *FUS*, and *C9orf72*, providing new unforeseen insights into the pathogenesis of this disease. For example mutations in the RNA binding proteins TDP-43 and FUS exert toxicity through abnormal RNA metabolism or processing (Sreedharan et al., 2008; Vance et al., 2009), while C9orf72 repeat expansion is hypothesized to drive repeat-associated non-ATG (RAN) translation that results in toxic peptides (Mackenzie et al., 2014; Mizielinska and Isaacs, 2014). All these mechanisms seem not to be implicated in SOD1-ALS suggesting that this disease cannot be explained solely by studying mutations in the SOD1 gene. Nevertheless several evidence point to the hypothesis that *SOD1* might be implicated in the pathogenic mechanism of other causative ALS genes and vice versa. For example, as discussed in Chapter 3 mutant TDP-43 and FUS, and wild-type TDP-43, but not wild-type FUS can trigger misfolding of wild-type SOD1 in neural cells (Pokrishevsky et al., 2012). Moreover SOD1-immunoreactive inclusions were detectable in the spinal cords of fALS patients with and without SOD1 mutations (Forsberg et al., 2010). Recent reports also suggested that SOD1 mutations share similar toxic mechanisms with other ALS causative gene mutations. For instance motor protein kinesin 14 (KIF14) and an oxidative stress-related catalase CAT were commonly upregulated in transcripts from iPSCs derived from patients with C9orf72 expansion and SOD1 A4V mutation (Kiskinis et al., 2014). Of note SOD1 has also been suggested to work as a RNA binding protein similarly to TDP-43 and FUS (Chen et al., 2014; Lu et al., 2007; Volkening et al., 2009).

Since nearly all ALS associated mutants target motor neurons, it is possible that multiple causative gene products share the same targets. Therefore investigating SOD1-fALS models can help elucidate important mechanism relative not only to SOD1-fALS but also to ALS in general. SOD1 mouse models are the best established models of ALS and in the last 30 years they helped elucidate disease mechanism and treatments (Ittner et al., 2015). The research carried out in the present work shows how studying novel mouse models of SOD1-fALS gives us new insights on disease and also reassess concepts of ALS pathology mechanism. Indeed the investigation of the *Sod1*^{D83G} mouse described in Chapter 4, together with other findings, discredited the hypothesis that ALS is a dying back disorder, suggesting that the axonal and neuronal body degeneration, typical of ALS, may be two separate events possibly modulated by

different sets of genes. Further, the preliminary data on SOD1 recombinant proteins, reported in Chapter 5 confirmed that not only human SOD1 but also mouse SOD1 variants can spontaneously aggregate *in vitro*, contributing to the current notion that SOD1 can propagate in a prion-like manner. A similar mechanism has been proposed also for TDP-43 and other neurodegenerative diseases, suggesting once again that studying SOD1-ALS might give important contributions not only to ALS but also to the broader field of neurodegenerative diseases. Additionally exploring human-mouse SOD1 interaction in the context of SOD1-fALS mouse models will help interpret SOD1 transgenic mouse models pathology data and their translation into clinical trials.

Chapter 8 Appendices

8.1 Appendix 1 Table of SOD1 transgenic mice

Transgenic SOD1 mouse lines are reported in Table 8.1. Rows are arranged by the location of the mutation used. All figures are for hemizygous mice unless specified. The protein level and dismutase activity reported were assayed from spinal cord, unless specified.

Mutation	Promoter	Tg copy number	Protein level (fold increase to endogenous SOD1 level)	SOD1 activity (fold difference to non-transgenic)	Onset (weeks)	Survival (weeks)	Notes	References
Wild-type	hSOD1	7	50; 24 fold in (Jonsson et al., 2006b)	8.6	36 (hom)	52 (hom)		(Graffmo et al., 2013; Gurney et al., 1994; Jonsson et al., 2006b)
A4V	hSOD1	~5	nr	~1.4	None			(Gurney et al., 1994)
G37R (line 106)	hSOD1	nr	4.2 brain; 5.3 spinal cord	7.2	22-30	25-29		(Wong et al., 1995)
G37R (line 29)	hSOD1	nr	4 brain; 5 spinal cord	7	24-32			(Wong et al., 1995)
G37R (line 42)	hSOD1	nr	8 brain; 10.5 spinal cord	14.5	14-16			(Wong et al., 1995)
G37R (line 9)	hSOD1	nr	5.4 brain 6.2 spinal cord	9	20-24			(Wong et al., 1995)

Mutation	Promoter	Tg copy number	Protein level (fold increase to endogenous SOD1 level)	SOD1 activity (fold difference to non-transgenic)	Onset (weeks)	Survival (weeks)	Notes	References
G37R	Neurofilament light chain promoter	nr	4.3 (line 3156) and 2.8 (line 4012)	nr	None until 1.5 years	None until 1.5 years	Neuron specific expression, two lines reported	(Pramatarova et al., 2001)
G37R (see notes)	Mouse prion promoter	nr	nq	nq	28-36 (hom)	1 or 2 weeks after onset	Co-integration of SOD1 transgene with construct encoding wild-type human presenilin 1 (hPS1) with PrP promoter)	(Wang et al., 2005a)
G37R (floxed)	nr	nr	nq	nr	26-30	37-48		(Boillée et al., 2006)
G37R and G93A (see notes)	Chicken skilket muscle α_{sk} actin	1-8			32-40		Two mutants (G37R and G93A, plus the WT) created, results do not specify which mutant.	(Wong and Martin, 2010)
H46R	hSOD1	nr	nr	nr	22-26	4 weeks after onset		(Nagai, 2000)

Mutation	Promoter	Tg copy number	Protein level (fold increase to endogenous SOD1 level)	SOD1 activity (fold difference to non-transgenic)	Onset (weeks)	Survival (weeks)	Notes	References
H46R	hSOD1	nr	nr	nr	20	24		(Chang-Hong et al., 2005)
H46R/H48Q (line 139)	hSOD1	nr	nq	1	nr	17-26		(Wang et al., 2002b)
H46R/H48Q (line 58)	hSOD1	nr	nq	nr	nr	12-47		(Wang, 2003; Wang et al., 2002b)
H46R/H48Q/H63G/H120G (line 121)	hSOD1	nr	nq	nr	nr	Over 69 weeks	Experimental mutations to disrupt copper binding	(Wang, 2003)
H46R/H48Q/H63G/H120G (line 125)	hSOD1	nr	nq	1	nr	39-52	Experimental mutations to disrupt copper binding	(Wang, 2003)
H46R/H48Q/H63G/H120G (line 187)	hSOD1	nr	nq	nr	nr	35-48	Experimental mutations to disrupt copper binding	(Wang, 2003)

Mutation	Promoter	Tg copy number	Protein level (fold increase to endogenous SOD1 level)	SOD1 activity (fold difference to non-transgenic)	Onset (weeks)	Survival (weeks)	Notes	References
E77X	hSOD1	nq	nr	nr	None	Normal	Experiential to see if truncated proteins can cause disease (RNA barely detectable)	(Deng et al., 2008)
L84V	hSOD1	nr	nr	nr	22-26	26		(Kato, 2001; Tobisawa et al., 2003)
G85R (line 148)	hSOD1	nr	1	1	33	35		(Bruijn et al., 1997)
G85R (line 74)	hSOD1	nr	0.2	nr	51-61	2 weeks after onset		(Bruijn et al., 1997)
G85R	Thy1.2		nq	nq	None up to 87 weeks	nr	Bicistronic expression of SOD1 and EGFP in postnatal motor neurons	(Lino et al., 2002)
G85R (floxed)	nr	nr	1.5	1	44	50	LoxP flanked transgene	(Wang et al., 2009c)

Mutation	Promoter	Tg copy number	Protein level (fold increase to endogenous SOD1 level)	SOD1 activity (fold difference to non-transgenic)	Onset (weeks)	Survival (weeks)	Notes	References
G85R (YFP fusion line 641)	nr		nr	nr	36 (hom)			(Wang et al., 2009a)
G83R (mouse)	nr	nr	nr	1	13-17	13-17		(Pramatarova et al., 2001; Ripps et al., 1995)
G86R (mouse) (line 2)	Mouse GFAP	nq	nq		None up until 70 weeks		Astrocyte specific expression	(Gong et al., 2000)
G86R (mouse) (line 29)	Mouse GFAP	10	nq		None up until 70 weeks		Astrocyte specific expression	(Gong et al., 2000)
D90A (line 134)	nr	nr	nr	~6-9	50 (hom)	58 (hom)		(Jonsson et al., 2006a)

Mutation	Promoter	Tg copy number	Protein level (fold increase to endogenous SOD1 level)	SOD1 activity (fold difference to non-transgenic)	Onset (weeks)	Survival (weeks)	Notes	References
K91X (stop)	hSOD1	nq	nr	nr	None	Normal	Experiential to see if truncated proteins can cause disease (RNA barely detectable)	(Deng et al., 2008)
G93A (line G1)	hSOD1	18	nr	~4	12-16	20		(Gurney et al., 1994)
G93A (line G20)	hSOD1	1.7	nr	~1.6	nr	49		(Dal Canto and Gurney, 1995; Gurney et al., 1994)
G93A (line G1H)	hSOD1	25	17	<4; as 8.9 in (Wang et al., 2008)	13	19.4	High transgene copy number derived from G1	(Chiu et al., 1995; Tu et al., 1996)
G93A (line G1del)	hSOD1	8	nr	nr	28	36	Low transgene copy derived form G1line	(Gurney, 1997; Zhang et al., 1997)

Mutation	Promoter	Tg copy number	Protein level (fold increase to endogenous SOD1 level)	SOD1 activity (fold difference to non-transgenic)	Onset (weeks)	Survival (weeks)	Notes	References
G93A	Rat myosin light chain (MLC1)	nr	nq	nq	Muscle atrophy from 4 weeks	nr	Muscle specific	(Dobrowolny et al., 2008)
G93A (T1xT3) (see notes)	Thy1.2	nr			77-104	84-104	Compound hemizygous T1 and T3 transgene. Postnatal motor neurons specific	(Jaarsma et al., 2008)
G93A (line T1)	Thy1.2	nr			None	Normal	Postnatal motor neurons specific	(Jaarsma et al., 2008)
G93A (line T3)	Thy1.2	nr	nq		None (54-104 for hom)	62-104 (hom)	Postnatal motor neurons specific	(Jaarsma et al., 2008)

Mutation	Promoter	Tg copy number	Protein level (fold increase to endogenous SOD1 level)	SOD1 activity (fold difference to non-transgenic)	Onset (weeks)	Survival (weeks)	Notes	References
G93A (with luciferase reporter)	BiTetO				None	Over 64 weeks	BiTetO (bicistronic tetracycline-repressible transactivator) promoter expressing a SOD1-G93A and luciferase transgene. WT line also made	(Wang et al., 2008)
G93A	MLC1f/3f						Skeletal muscle specific.	(Dobrowolny et al., 2008)
G93A	TRE				None		Bidirectional tetracycline/doxycycline response (TRE) transgene	(Bao-Cutrona and Moral, 2009)
I113T	nr	nr	nr	nr	52	nr		(Kikugawa, 2000)
T116X (stop)	hSOD1	nr	nr	nr	2 weeks before survival	43 (hom)	Experiential to see if truncated proteins can cause disease	(Deng et al., 2008)

Mutation	Promoter	Tg copy number	Protein level (fold increase to endogenous SOD1 level)	SOD1 activity (fold difference to non-transgenic)	Onset (weeks)	Survival (weeks)	Notes	References
L126delTT (see notes)	nr	nr	nr	nr	None		Mouse created to model ALS but resultant phenotype was due to insertional disruption of the single stranded DNA binding protein 1	(Nishioka et al., 2005)
L126delTT (line D1)	hSOD1	1	nr	nr	None			(Watanabe et al., 2005)
L126delTT (line D2)	hSOD1	5		1	63 (34 for hom)	68 (36 for home)		(Watanabe et al., 2005)
L126delTT-FLAG (line DF2)	hSOD1	3	nr	nr	None		FLAG tagged SOD1	(Watanabe et al., 2005)
L126delTT-FLAG (line DF7)	hSOD1	4	nq	1	49 (17 for hom)	53 (18 for hom)	FLAG tagged SOD1	(Watanabe et al., 2005)

Mutation	Promoter	Tg copy number	Protein level (fold increase to endogenous SOD1 level)	SOD1 activity (fold difference to non-transgenic)	Onset (weeks)	Survival (weeks)	Notes	References
L126Z (stop)	hSOD1	nr	0-0.5	nr	30-39	nq	SOD1 locus with engineered fusion exon 3,4 and 5	(Wang et al., 2005b)
L126Z (stop)	nr	nr	0-1	nr	48	51		(Deng et al., 2006)
SOD1G127insTGGG (line 716)	nr	19	0.45-0.97	1	7-10 weeks before survival (hom)	64 (36 for hom)		(Jonsson et al., 2004)
SOD1G127insTGGG (line 832)	nr	28	nr	nr	nr	30 (18 for hom)		(Jonsson et al., 2004)

Table 8.1 Transgenic mice expressing mutant or wild-type SOD1. Transgene (Tg); homozygous (hom); not reported (nr); measured but not quantified (nq).

8.2 Appendix 2 Vector and constructs

The open reading frame (ORF) sequence of the human wild-type SOD1 cDNA was determined by sequencing an 'in house' plasmid stock, pSP64 Poly(A)Vector, containing SOD1 insert. This insert sequence was compared to available sequence (accession No.: NM_000454) from the Nucleotide Database on NCBI (<http://www.ncbi.nlm.nih.gov>). Using this as template, site directed mutagenesis was performed to generate constructs for other mutants, human G93A, human D101G. Constructs were cloned into the pET28 expression vector (Novagen), downstream of the T7 promoter between the *NdeI* and *XhoI* restriction sites. The SOD1 expression was based on IPTG induction of the T7 RNA polymerase (T7 RNAP). Once expressed T7 RNAP drove the expression of SOD1 at the IPTG inducible T7 promoter, located upstream of the cloned SOD1 cDNA. The constructs were cloned such that a thrombin cleavage site was created between the protein and the N-terminally added His-tag. Mutant constructs were generated by Dr. David Emery (University of Bristol), Dr Ruth Chia and Julian Pietrzyk (Institute of Neurology, University College London).

8.3 Appendix 3 Ni-NTA column recharged protocol

After 6 uses the resin of Ni-NTA columns needs to be recharged with nickel ions. The protocol consists in a series of washed with different buffers, see Table 8.2

Buffer	Volume (column/volume)
6 M GuHCl, 0.2 M acetic acid in ddH ₂ O	2
ddH ₂ O	5
2 % SDS in ddH ₂ O	3
25 % ethanol in ddH ₂ O	1
50 % ethanol in ddH ₂ O	1
75 % ethanol in ddH ₂ O	1
100 % ethanol	5
75 % ethanol in ddH ₂ O	1
50 % ethanol in ddH ₂ O	1
25 % ethanol in ddH ₂ O	1
ddH ₂ O	5
100 mM NiSO ₄ in ddH ₂ O	2
ddH ₂ O	2
6 M GuHCl, 0.2 M acetic acid in ddH ₂ O	2
ddH ₂ O	2
20 % ethanol in ddH ₂ O	2

Table 8.2 Ni-NTA resin recharge protocol.

8.4 Appendix 4 *Sod1*^{-/-} other neuronal and extra-neuronal phenotypes

8.4.1 *Sod1*^{-/-} non-motor neuronal phenotypes

Hearing deficit with loss of ganglion neurons

Keithley and colleagues found that at 12 months of age all *Sod1*^{-/-} mice developed a hearing loss with an increased auditory threshold. This phenotype was accompanied by a decrease in ganglion cell density at 7 months (Keithley et al., 2005).

Progressive retinal degeneration and age related macular degeneration (AMD)

Sod1^{-/-} mice developed a progressive retinal degeneration with manifestation of necrotic cells, and decreasing of wave amplitudes, similarly to AMD patients (Hashizume et al., 2008). Furthermore they displayed other human AMD features, such as overtime build-up of drusen (extracellular accumulations in Bruch's membrane of the eye) detectable in over 85% of eyes by 10 months of age. At 12 months Bruch's membrane was strikingly thickened and 15 months old mice showed a choroidal neovascularization. Drusen number could also be increase in young animals by exposure to light (Imamura et al., 2006).

Blood-brain-barrier disruption and increased lethality following focal cerebral ischemia

Sod1^{-/-} mice were shown to be susceptible to ischemic brain damage. Mortality 24 hours after ischemic insult occurred in 100 % of *Sod1*^{-/-} animals, compared to 11 % of wild-type littermates, with evidence of early and severe blood-brain-barrier (BBB) disruption (Kondo et al., 1997). Also, BBB disruption following noxious stimuli was increased in homozygous *Sod1* knockout mice (Kim et al., 2003).

Increased damage following brain trauma

Superoxide is known to be produced in vulnerable regions after traumatic brain injury, for example in the dentate gyrus or in cortex. Indeed *Sod1*^{-/-} mice experiencing traumatic brain developed increased lesion volume and levels of apoptotic cell death compared to wild-type controls (Lewén et al., 2000). In accordance, previous data showed a protective role of SOD1 overexpression after brain injury (Mikawa et al., 1996).

Increased susceptibility to neurodegeneration

Murakami et al. crossed *Sod1*^{-/-} mice with mice overexpressing the amyloid precursor protein (APP). The double mutant progeny obtained showed significantly increased memory loss, tau phosphorylation, A β oligomerisation and plaque formation, pointing to a modulation role of neurodegeneration progression for SOD1 (Murakami et al., 2011). Furthermore it was shown that *Sod1* mRNA binds the Fragile X Mental Retardation Protein (FMRP), increasing translation of SOD1 protein. Thus, SOD1 protein levels were reduced in *Fmrp1* knockout mice suggesting that this reduction played a role in the physiopathology of Fragile X syndrome (Bechara et al., 2009).

8.4.2 *Sod1*^{-/-} extra-neuronal phenotypes

Decreased survival, hepatocellular carcinoma

Survival of *Sod1*^{-/-} mice was significantly decreased compared to wild-type littermates (20.8 months versus 29.8 months for controls) due to increased incidence of hepatocellular carcinoma (HCC). Tumour nodules and hepatocyte injury were found on 70 % of end stage *Sod1*^{-/-} animals on a C57BL/6J background; which is proven to be protective against development of HCC (Elchuri et al., 2005; Takahashi et al 2002). Preferential development of HCC in these mice might occur because of the high amount of ROS that are constantly generated in the liver, due to lack of SOD1 activity. Indeed clinical studies carried out in patients with different stages of HCC showed a strong correlation between low levels of SOD and the severity of HCC (Casaril et al., 1994; Liaw et al., 1997). Furthermore HCC patient's data demonstrated a positive correlation between SOD1 activity in tumours and post-surgery survival time (Lin et al., 2001).

Impaired endothelial-dependent relaxation

Sod1^{-/-} mice developed increased myogenic tone, augmented vasoconstrictor response and impaired endothelium-dependent relaxation in large arteries and microvessels (Didion et al., 2002). These phenotypes might occur due to increased levels of superoxide that rapidly inactivates nitric oxide, which is released by endothelial cells and induces vasodilatation (Fukai and Ushio-Fukai, 2011). This is in accordance with previous observations that ROS play an important role in endothelial cell dysfunction, which can be rescued by SOD1 (Niwa et al., 2000) and prevented by SOD1 overexpression (Iadecola et al., 1999).

Skin thinning and osteoporosis

Sod1^{-/-} mice have atrophic skin morphology at 4 months of age, accompanied by degeneration of collagen and elastic fibres and reduction of skin hydroxyproline. Vitamin C derivate treatment were shown to ameliorate these conditions regenerating collagen and elastin (Murakami et al., 2009).

In vivo and *in vitro* studies demonstrate that *Sod1*^{-/-} mice have a number of key features of human bone aging such as: decreased bone density and cortical areas (typical signs of osteopenia), loss of bone volume and quality (involving a significant reduction in enzymatic collagen cross-linking) resulting in bone fragility. Vitamin C treatment reduced bone loss, leading to normalization of bone strength (Nojiri et al., 2011).

Infertility

Fertility of *Sod1*^{-/-} males was described as normal. However, *Sod1*^{-/-} sperm suffered from oxidative damage during *in-vitro* fertilization (Tsunoda et al., 2012). Only in some studies fertility of *Sod1*^{-/-} females was reported as decreased due to ovarian defects (Ho et al., 1998; Matzuk et al., 1998).

8.5 Appendix 5 Identification of the *Sod1*^{D83G} mouse model by ENU mutagenesis

ENU mutagenesis is a powerful technique largely used to generate mouse models of human disease. In particular ENU is a chemical that that when injected in mice induces random point mutations in the DNA in a dose dependent manner (approximately one mutation every 1-1.5 Mb). To produce animals carrying a point mutation in specific genes male mice are treated with ENU, which selectively kills spermatogonial cells. After a period of sterility spermatogonial cells of mutagenized animals repopulate and each of them express an assortment of point mutations along the genome. Treated males are then mated with wild-type females, the sperm from their offspring is stored while tissue is used to screen for mutations in the gene of interest (Acevedo-Arozena et al., 2008; Quwailid et al., 2004). To identify the *Sod1*^{D83G} model genomic DNA from Harwell ENU-induced mutagenesis archive of over 10000 mice was screened for mutations in the *Sod1* gene (Joyce et al., 2014).

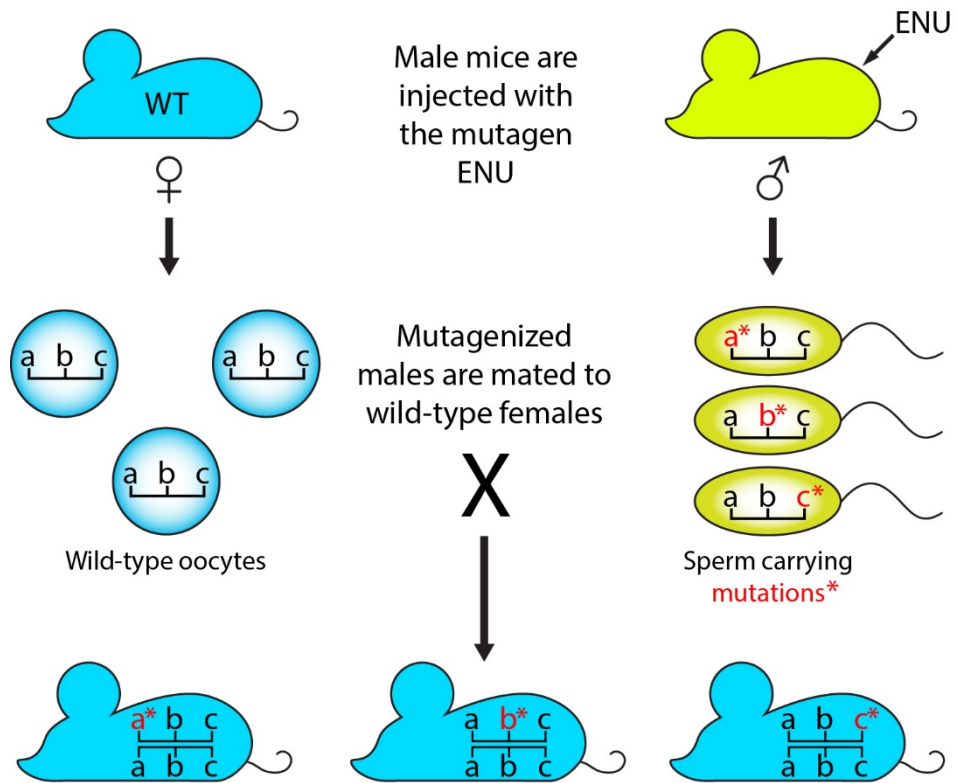


Figure 8.1 *Sod1^{D83G}* identification: ENU mutagenized mice breeding scheme.

8.6 Appendix 6 Transmission project

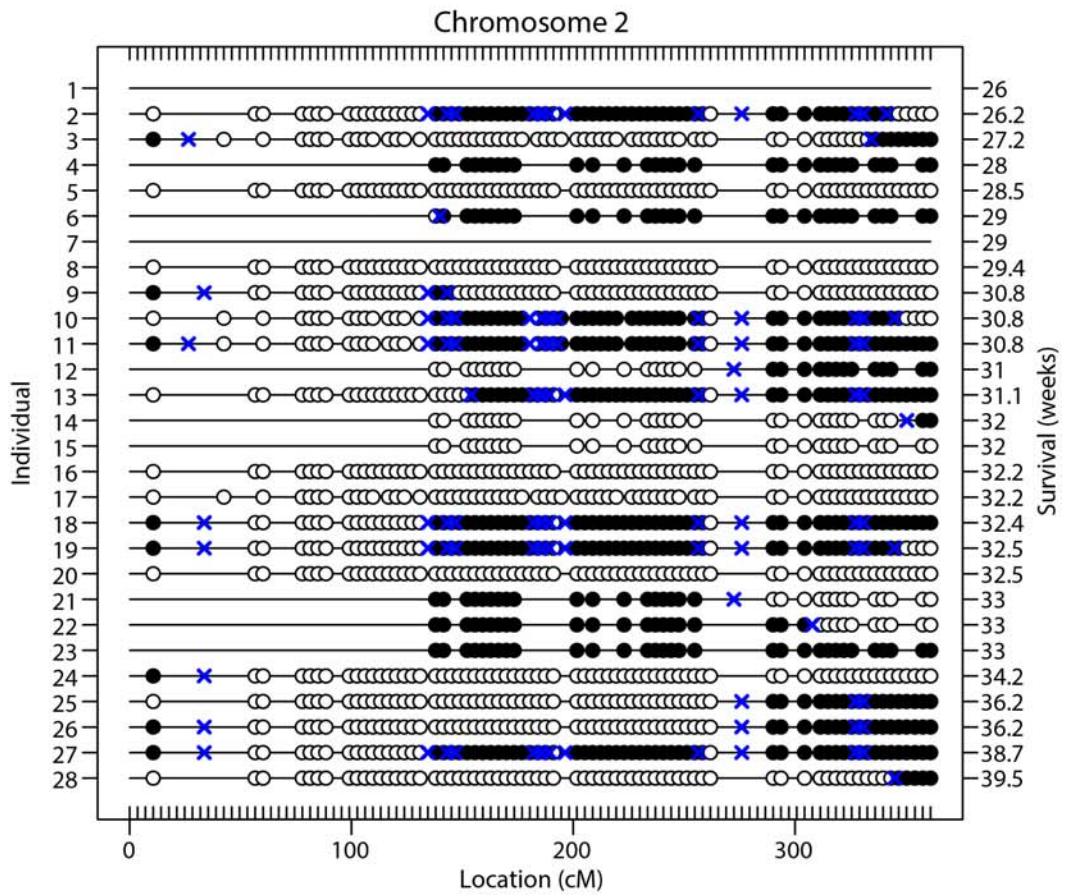
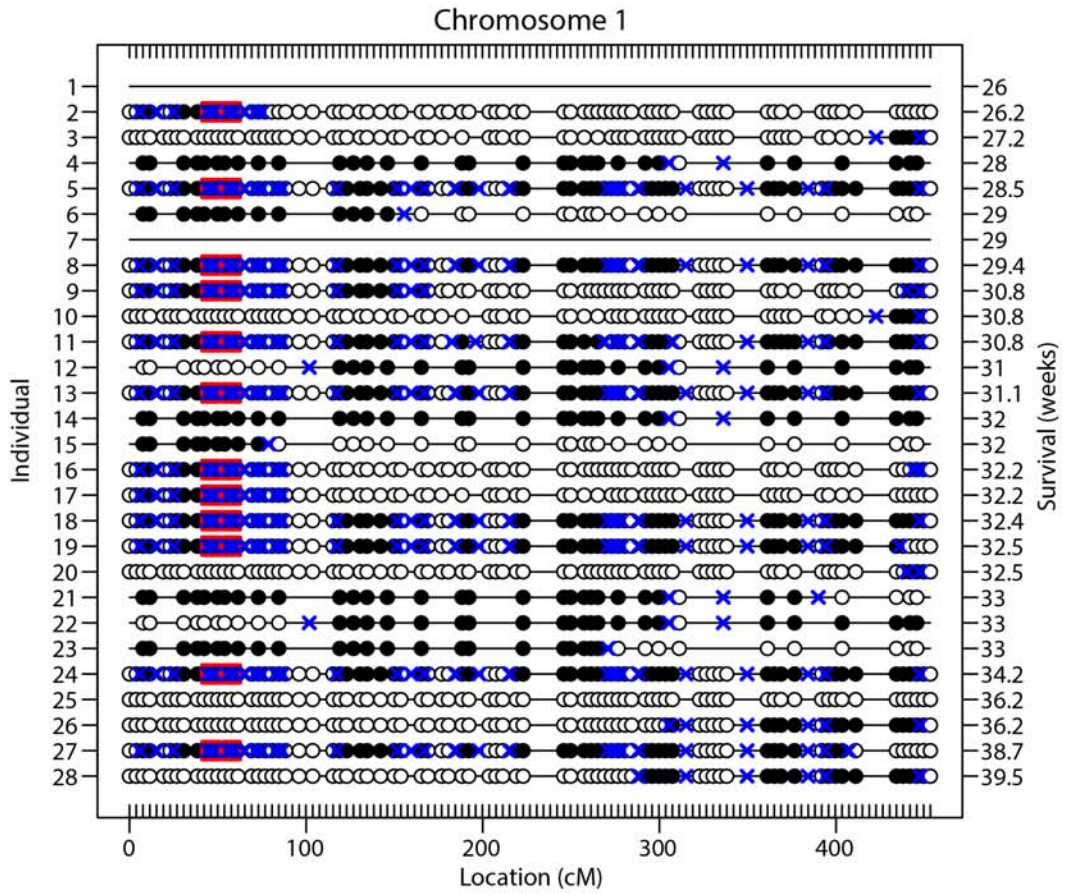
To investigate if SOD1 can seed aggregation in mouse model in a prion-like manner, transgenic mice overexpressing human SOD1 were intracerebrally inoculated with tissue homogenates of mutant human SOD1 species, or with control homogenates or a vehicle only control to assess misfolded SOD1 aggregate pathology.

To evaluate SOD1 self-seeded aggregation potential, spinal cord homogenates of Tg*SOD1^{G93A(I1)}* mice were inoculated in animals of the same line. While, to assess cross-seeded aggregation potential, spinal cord homogenates of Tg*SOD1^{G93A(I1)}* mice, and homogenates of motor cortex human SOD1-fALS carrying the I113T and the D101G mutations were inoculated in Tg*SOD1^{WT}* mice.

All animals employed for this project were bred on to a *Sod1^{-/-}* background, to avoid the possible interaction between the human SOD1 proteins and the endogenous mouse SOD1 protein.

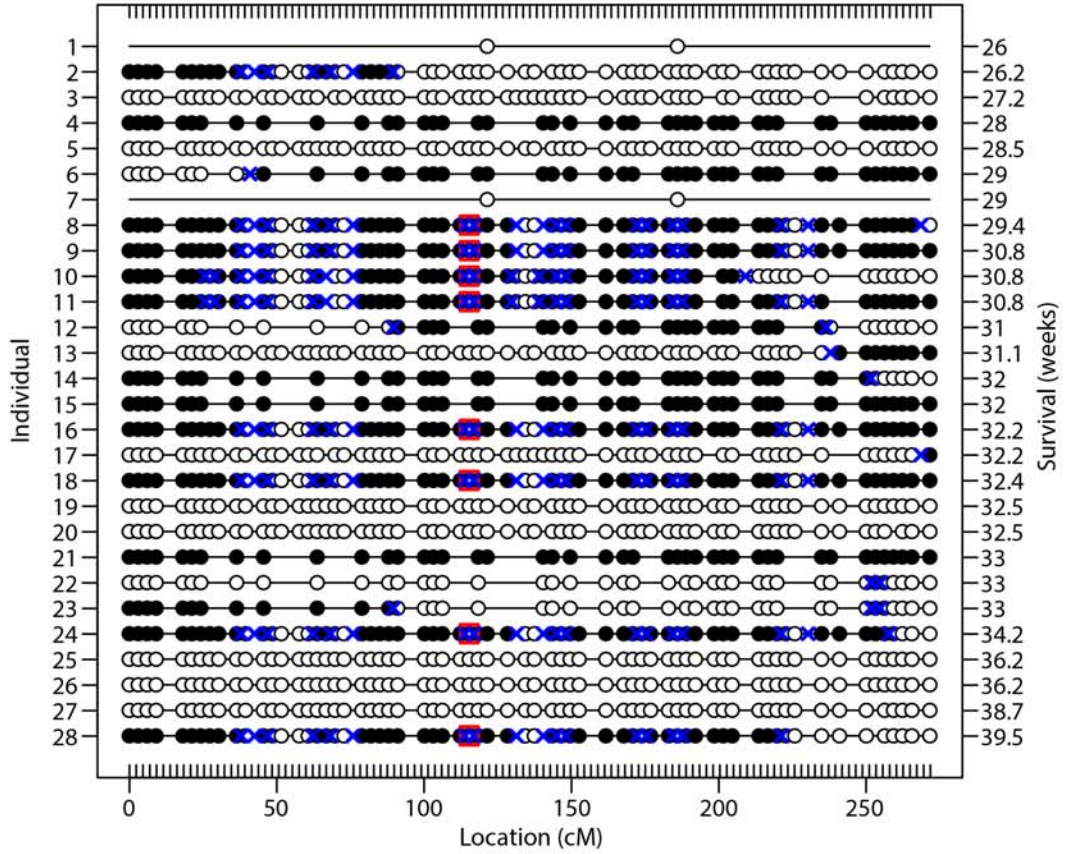
8.7 Appendix 7 *Galahad* project

Plots showing the genotype and recombination events along the different chromosome for all the G2 animals employed in the QTL analysis are reported below in Figure 8.2.

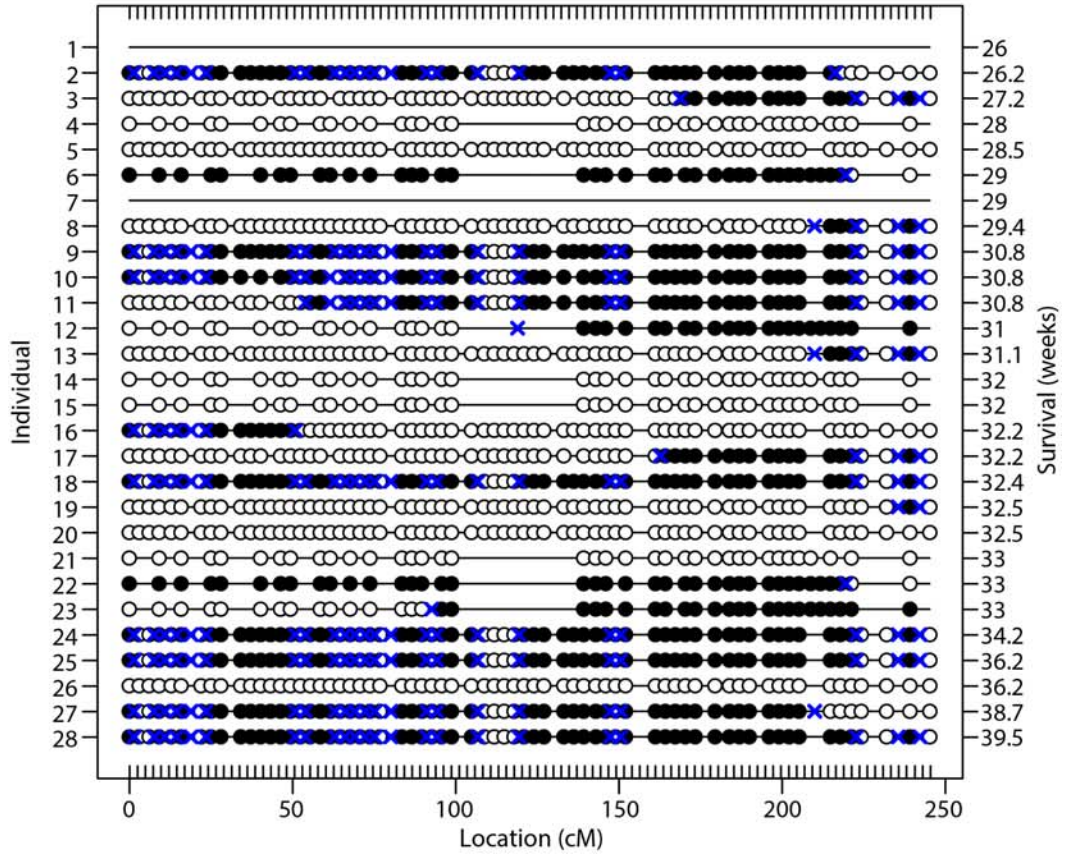


● Heterozygous ○ Homozygous — Missing × Recombination event ◻ Questionable recombination event

Chromosome 3

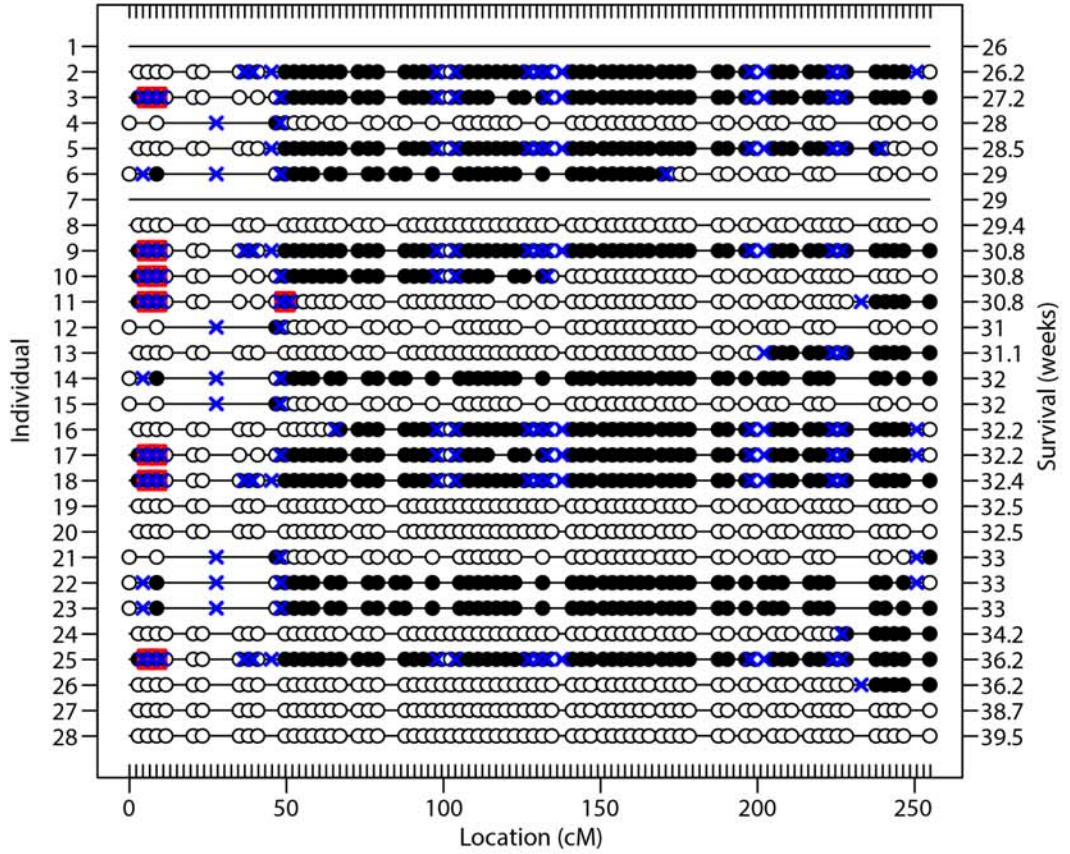


Chromosome 4

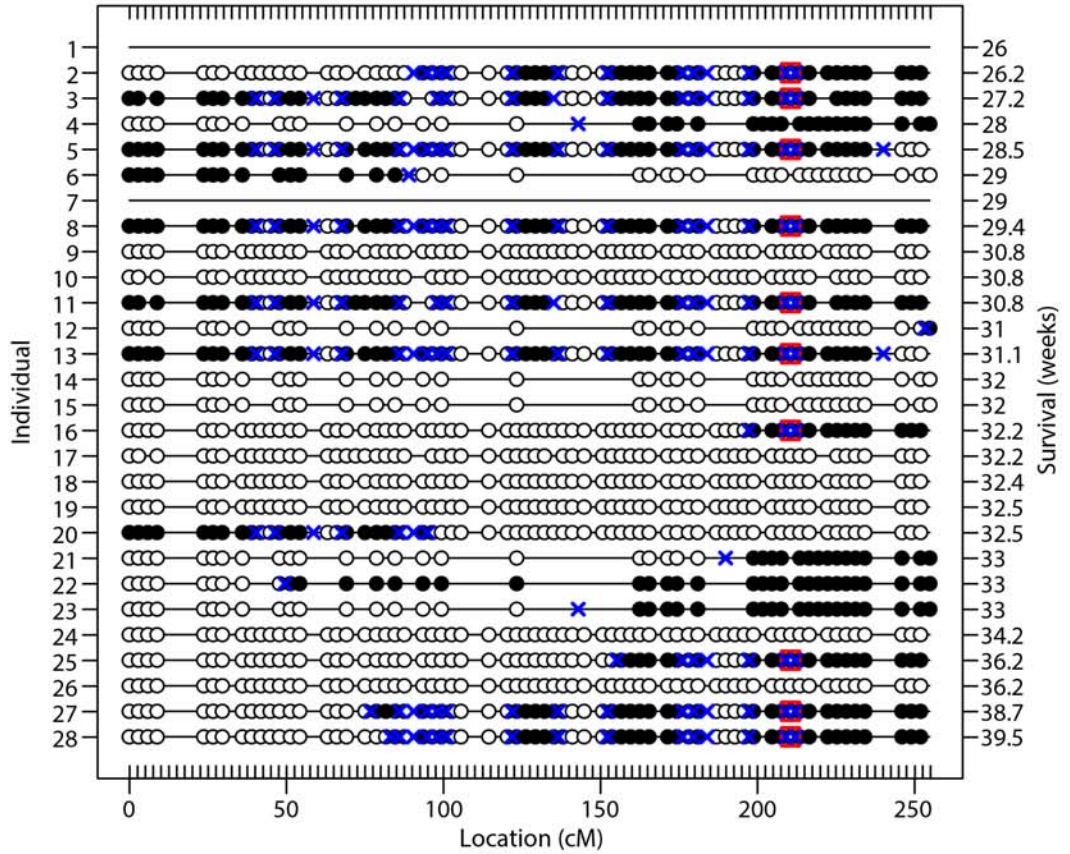


● Heterozygous ○ Homozygous — Missing × Recombination event ◻ Questionable recombination event

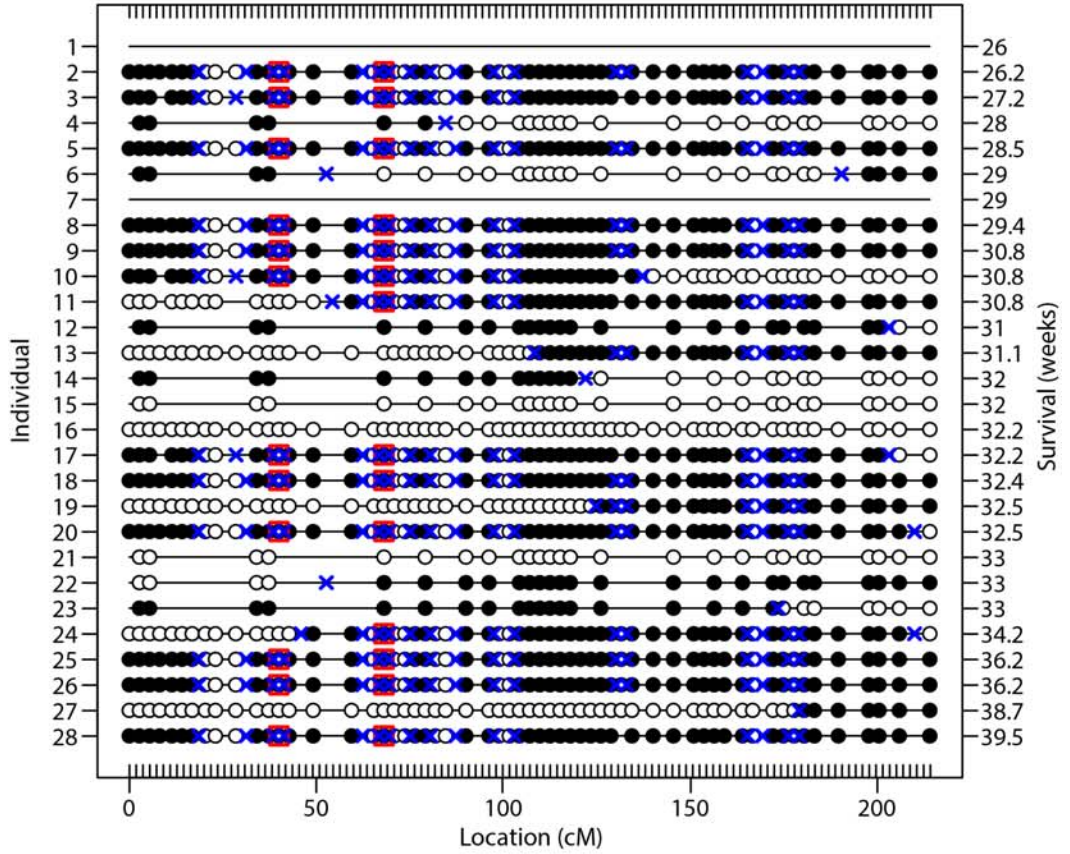
Chromosome 5



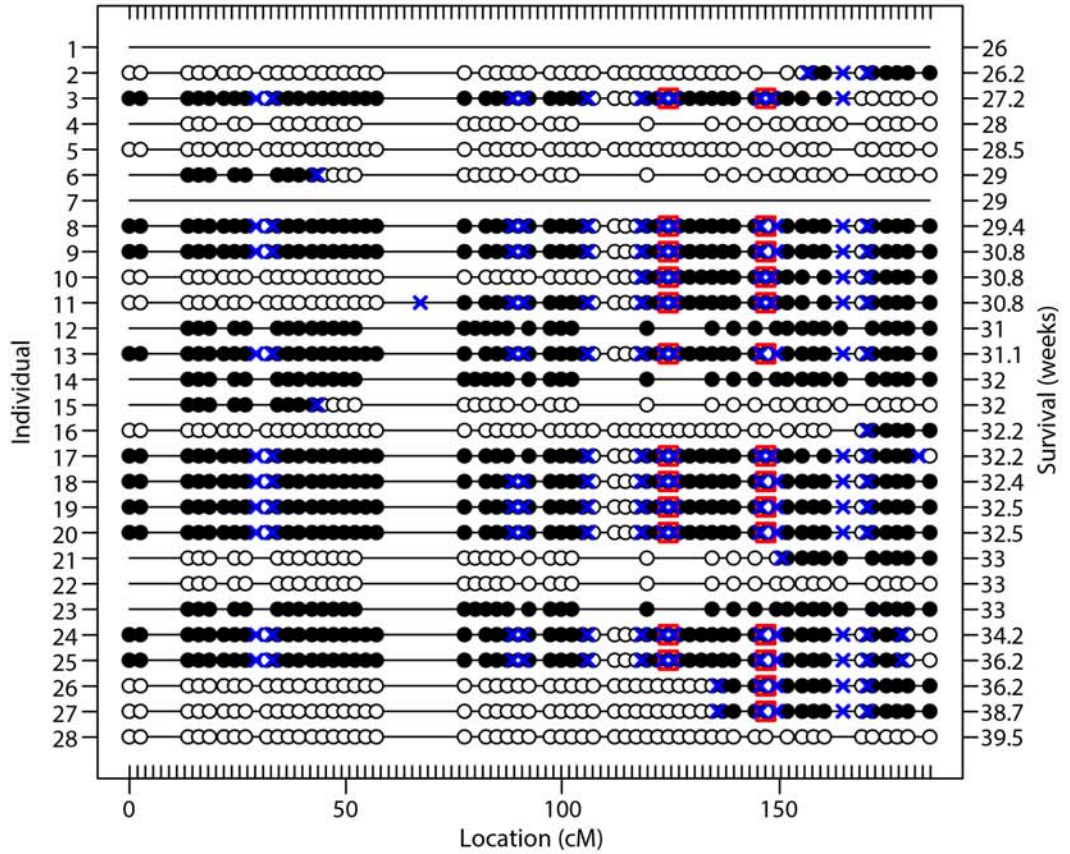
Chromosome 6



Chromosome 7

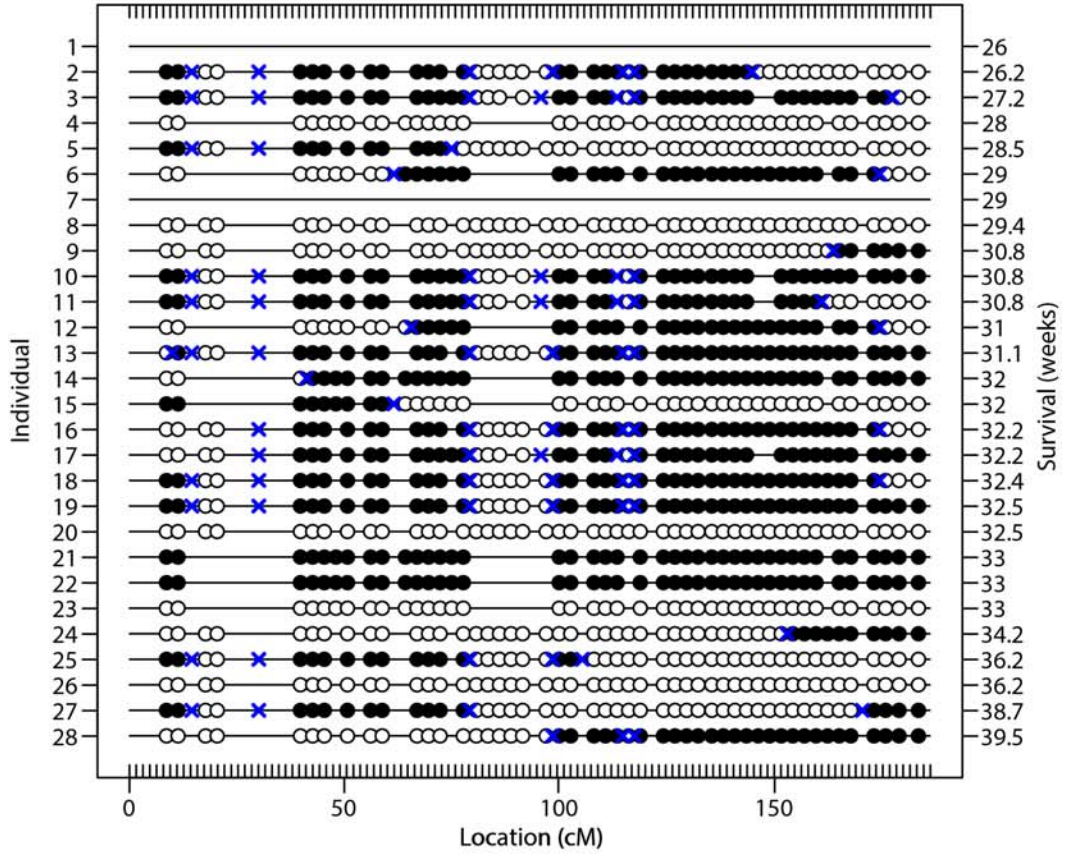


Chromosome 8

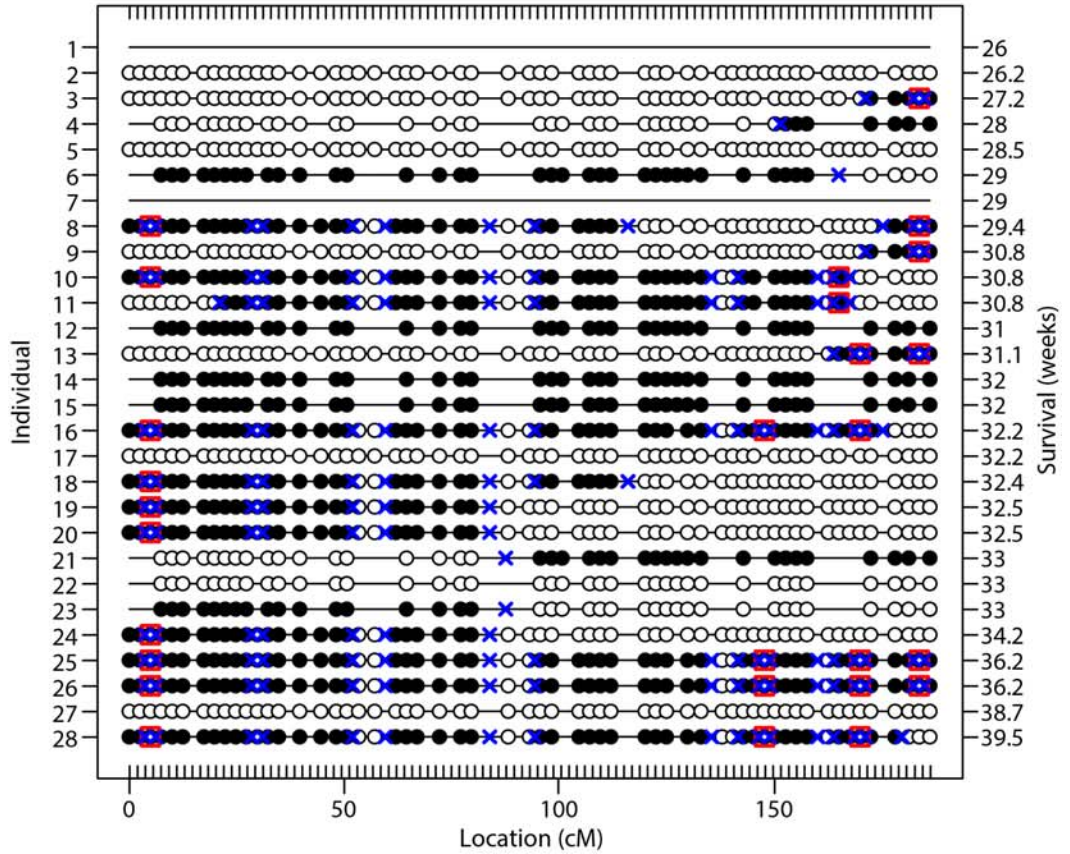


● Heterozygous ○ Homozygous — Missing × Recombination event ◻ Questionable recombination event

Chromosome 9

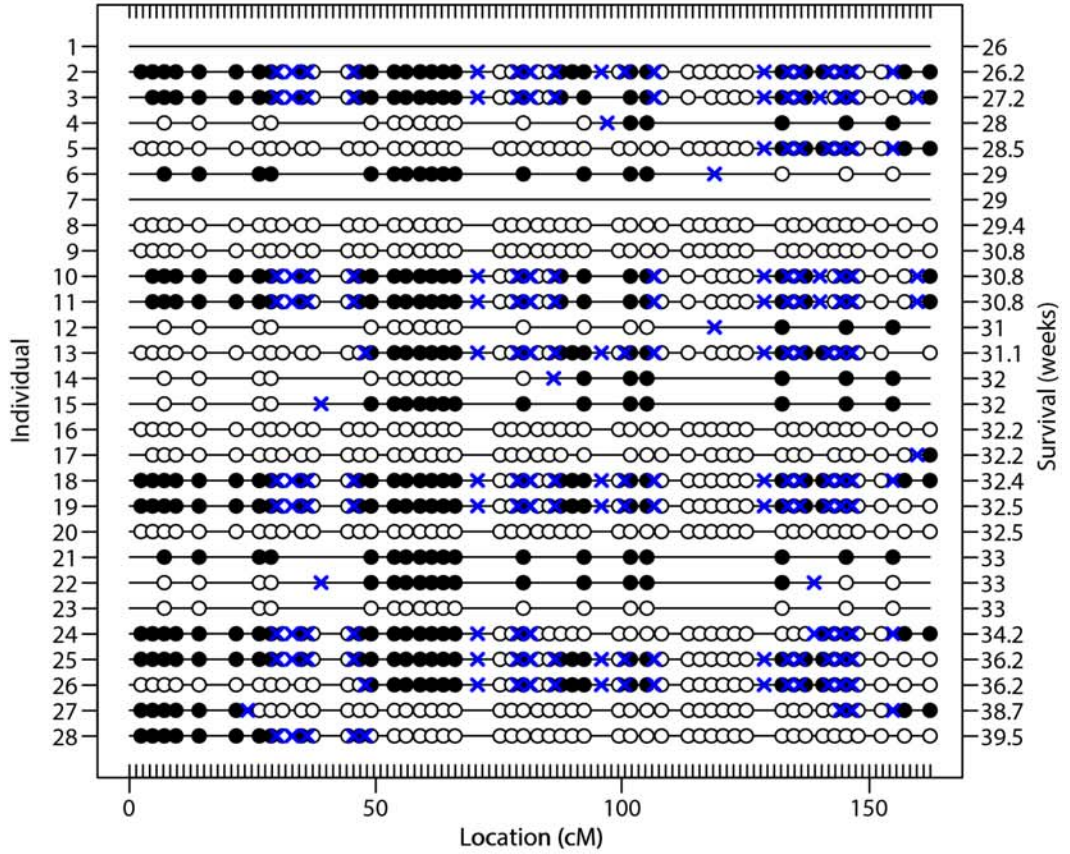


Chromosome 10

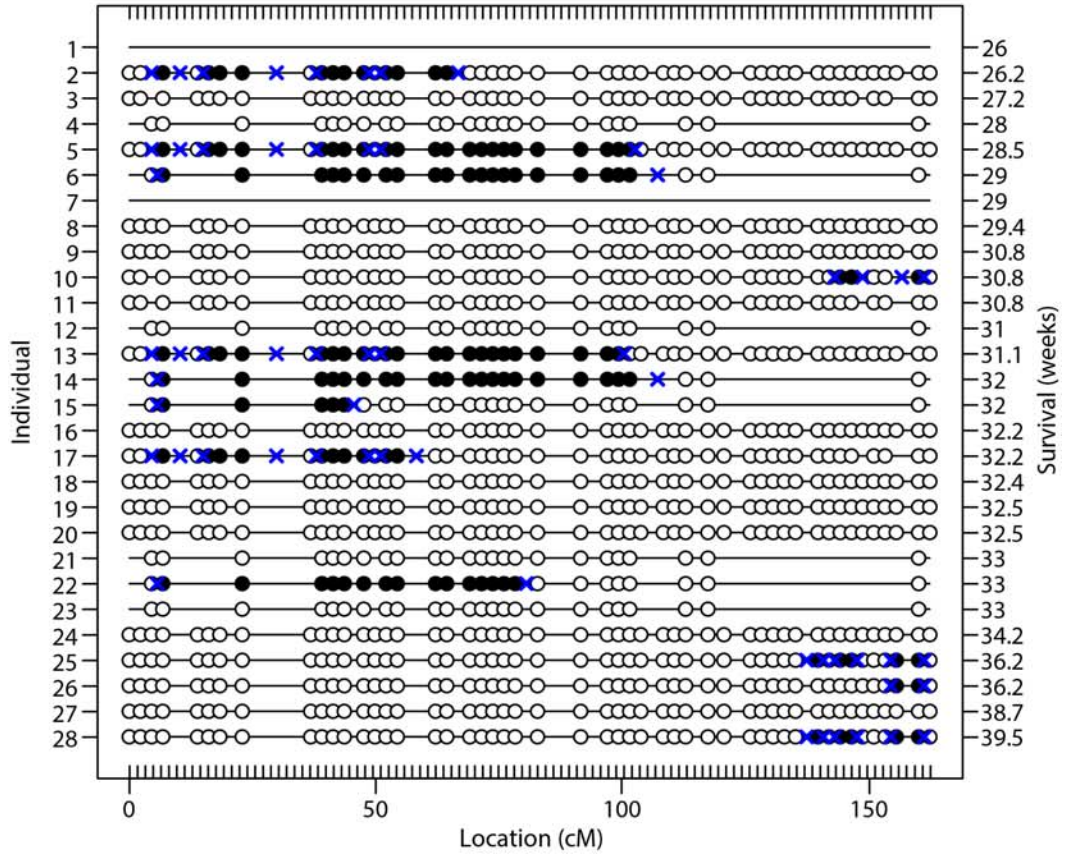


● Heterozygous ○ Homozygous — Missing × Recombination event □ Questionable recombination event

Chromosome 11

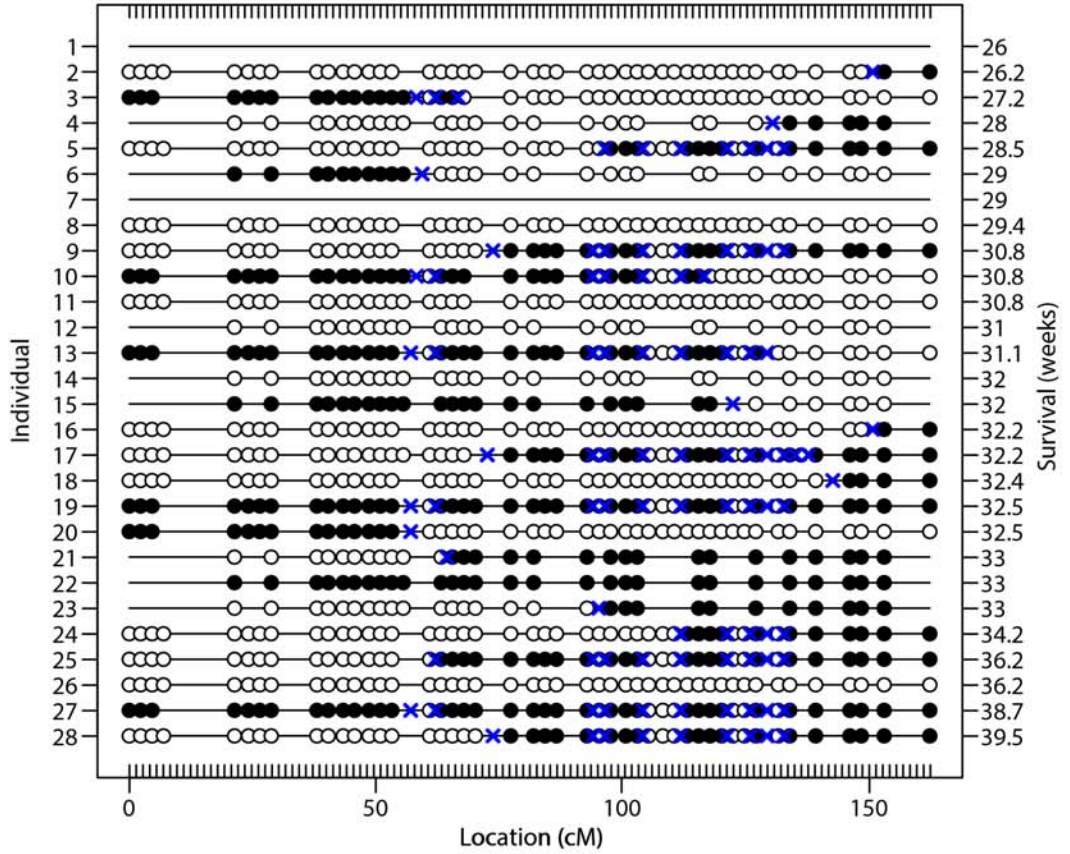


Chromosome 12

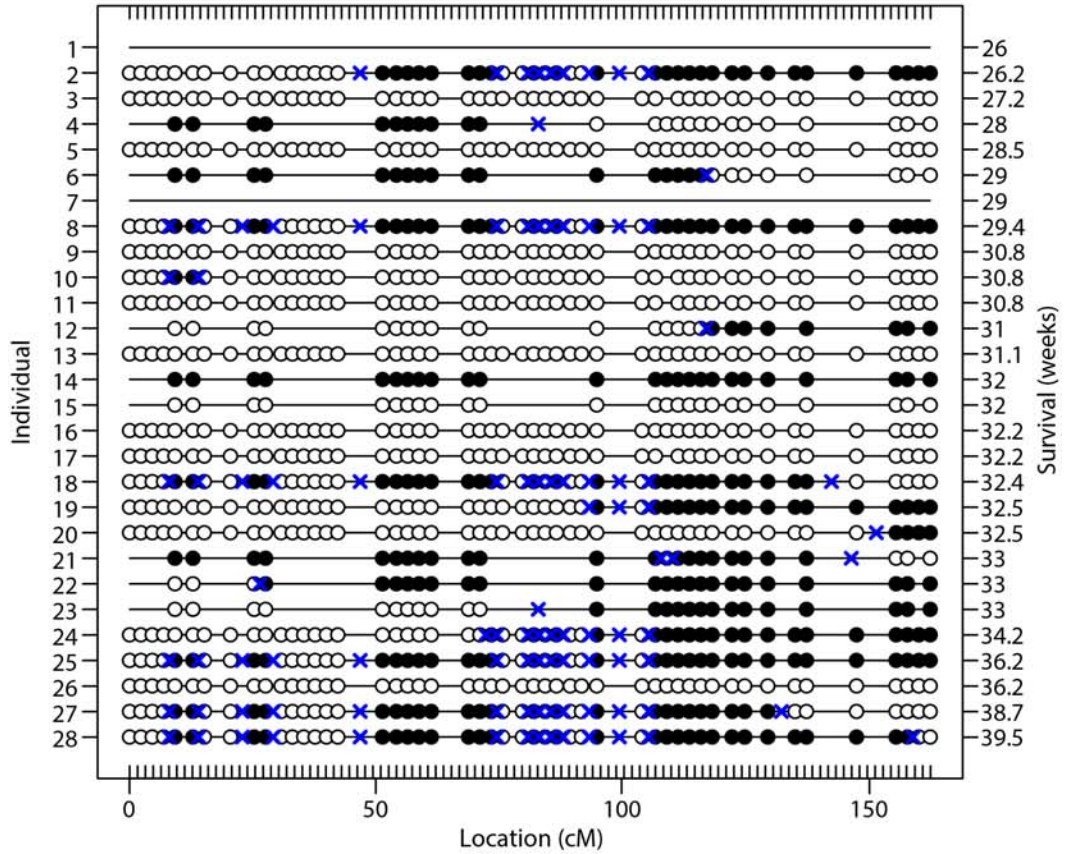


● Heterozygous ○ Homozygous — Missing × Recombination event ◻ Questionable recombination event

Chromosome 13

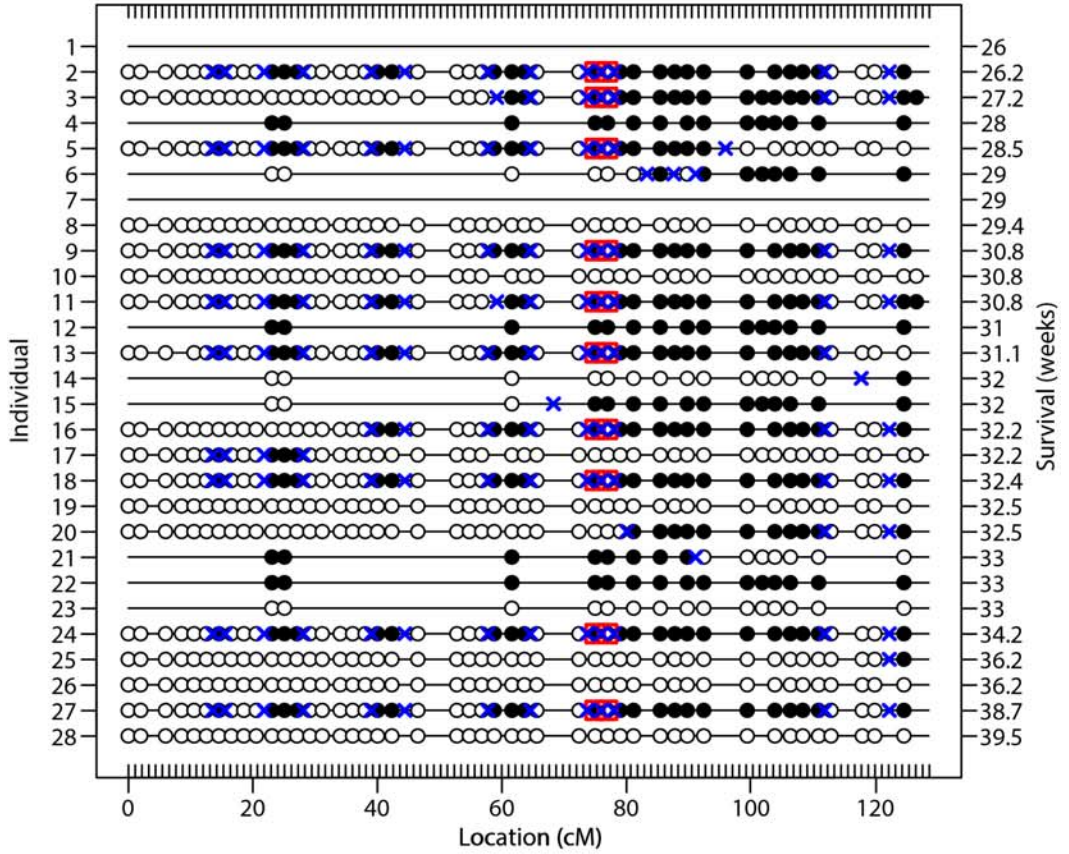


Chromosome 14

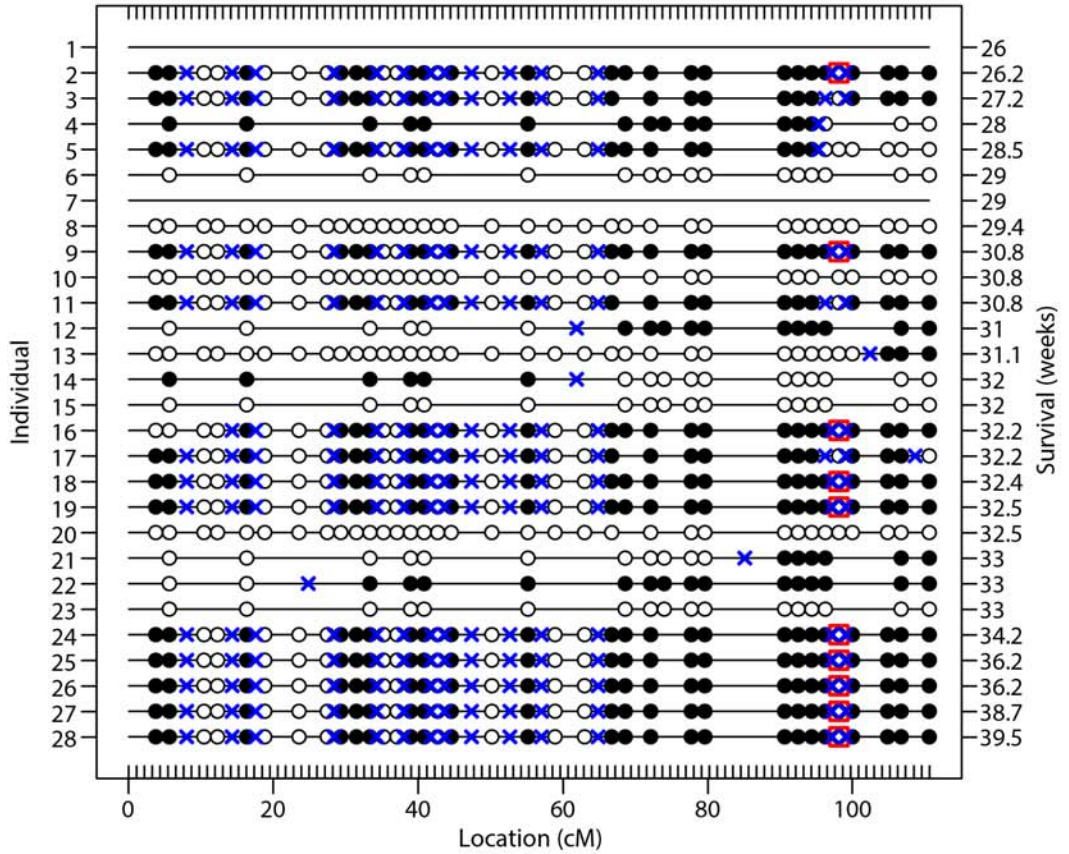


● Heterozygous ○ Homozygous — Missing × Recombination event □ Questionable recombination event

Chromosome 15

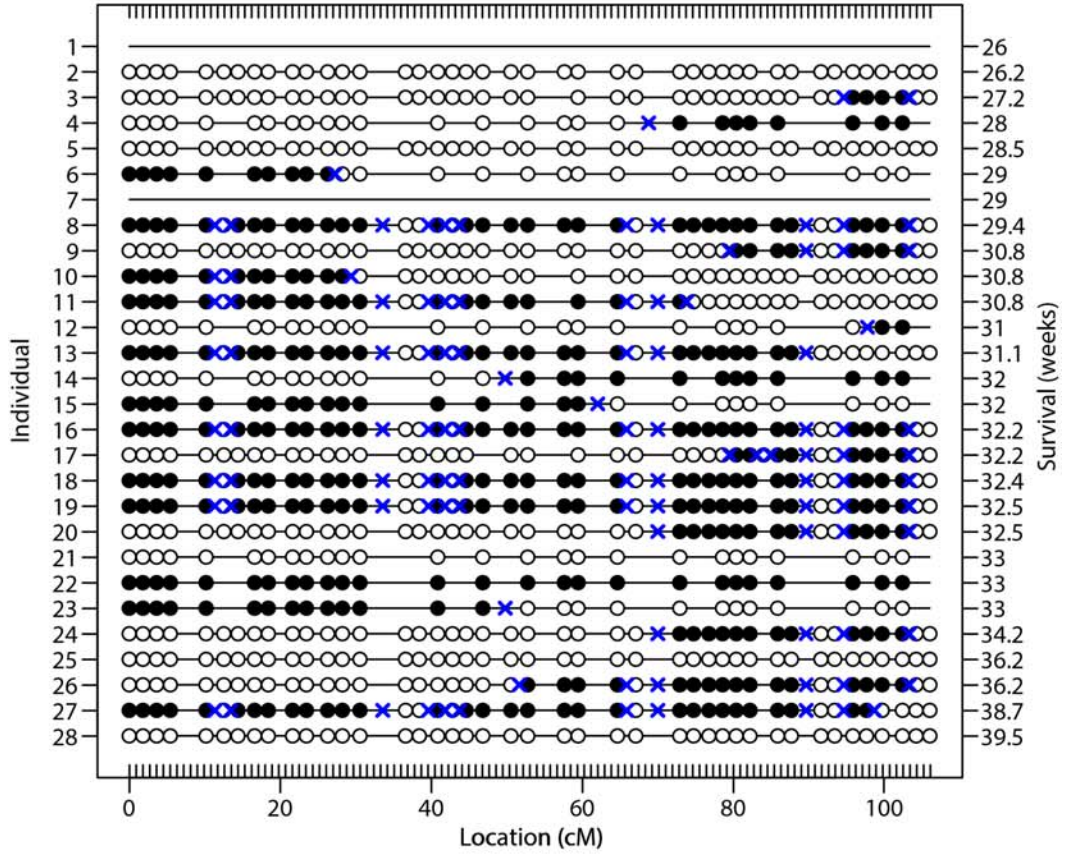


Chromosome 16

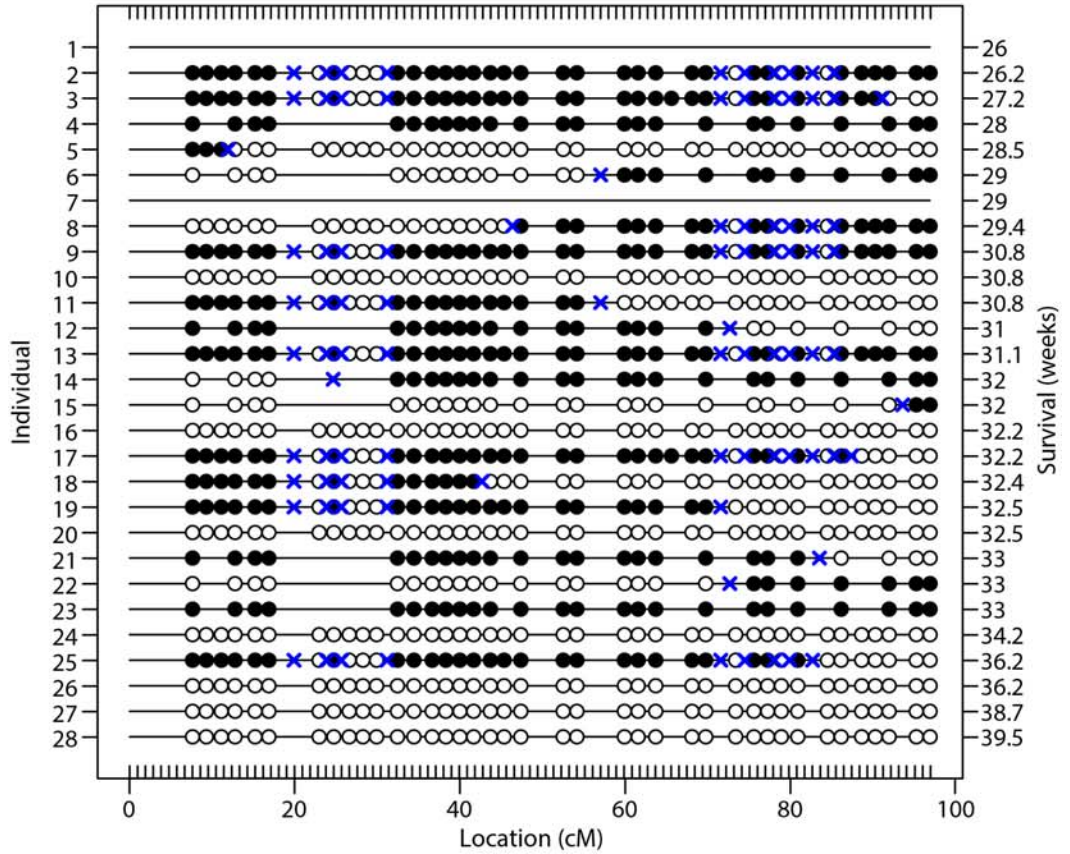


● Heterozygous ○ Homozygous — Missing × Recombination event ◻ Questionable recombination event

Chromosome 17



Chromosome 18



● Heterozygous ○ Homozygous — Missing × Recombination event ◻ Questionable recombination event

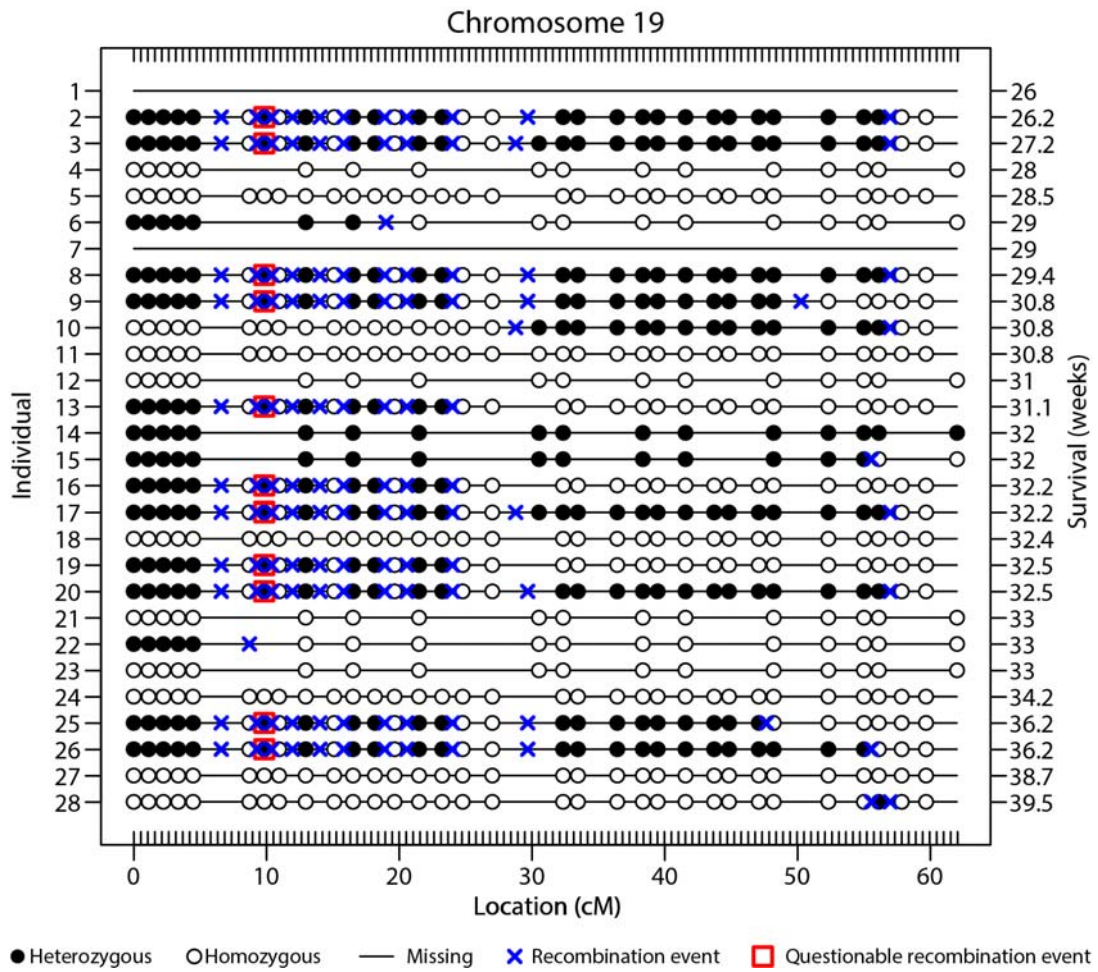


Figure 8.2 Genotype and recombination events per mouse along the 19 autosomal chromosomes. Animals are listed in crescent order of survival from top to bottom. Chromosomes 6 and 18 appears to be the most interesting.

References

- Abe, K., Pan, L.H., Watanabe, M., Kato, T., and Itoyama, Y. (1995). Induction of nitrotyrosine-like immunoreactivity in the lower motor neuron of amyotrophic lateral sclerosis. *Neurosci. Lett.* *199*, 152–154.
- Abe, K., Aoki, M., Ikeda, M., Watanabe, M., Hirai, S., and Itoyama, Y. (1996). Clinical characteristics of familial amyotrophic lateral sclerosis with Cu/Zn superoxide dismutase gene mutations. *J. Neurol. Sci.* *136*, 108–116.
- Acevedo-Arozena, A., Wells, S., Potter, P., Kelly, M., Cox, R.D., and Brown, S.D.M. (2008). ENU mutagenesis, a way forward to understand gene function. *Annu. Rev. Genomics Hum. Genet.* *9*, 49–69.
- Acevedo-Arozena, A., Kalmar, B., Essa, S., Ricketts, T., Joyce, P., Kent, R., Rowe, C., Parker, A., Gray, A., Hafezparast, M., et al. (2011). A comprehensive assessment of the SOD1G93A low-copy transgenic mouse, which models human amyotrophic lateral sclerosis. *Dis. Model. Mech.* *4*, 686–700.
- Achilli, F., Boyle, S., Kieran, D., Chia, R., Hafezparast, M., Martin, J.E., Schiavo, G., Greensmith, L., Bickmore, W., and Fisher, E.M.C. (2005). The SOD1 transgene in the G93A mouse model of amyotrophic lateral sclerosis lies on distal mouse chromosome 12. *Amyotroph. Lateral Scler. Other Motor Neuron Disord.* *6*, 111–114.
- Acquatella-Tran Van Ba, I., Imberdis, T., and Perrier, V. (2013). From prion diseases to prion-like propagation mechanisms of neurodegenerative diseases. *Int. J. Cell Biol.* *2013*, 975832.
- Acsadi, G., Lee, I., Li, X., Khaidakov, M., Pecinova, A., Parker, G.C., and Hüttemann, M. (2009). Mitochondrial dysfunction in a neural cell model of spinal muscular atrophy. *J. Neurosci. Res.* *87*, 2748–2756.
- Al-Chalabi, A., and Hardiman, O. (2013). The epidemiology of ALS: a conspiracy of genes, environment and time. *Nat. Rev. Neurol.* *9*, 617–628.
- Al-Chalabi, A., Fang, F., Hanby, M.F., Leigh, P.N., Shaw, C.E., Ye, W., and Rijdsdijk, F. (2010). An estimate of amyotrophic lateral sclerosis heritability using twin data. *J. Neurol. Neurosurg. Psychiatry* *81*, 1324–1326.
- Al-Chalabi, A., Jones, A., Troakes, C., King, A., Al-Sarraj, S., and van den Berg, L.H. (2012). The genetics and neuropathology of amyotrophic lateral sclerosis. *Acta Neuropathol.* *124*, 339–352.
- Alexander, G.M., Erwin, K.L., Byers, N., Deitch, J.S., Augelli, B.J., Blankenhorn, E.P., and Heiman-Patterson, T.D. (2004). Effect of transgene copy number on survival in the G93A SOD1 transgenic mouse model of ALS. *Brain Res. Mol. Brain Res.* *130*, 7–15.
- Allen, S., Heath, P.R., Kirby, J., Wharton, S.B., Cookson, M.R., Menzies, F.M., Banks, R.E., and Shaw, P.J. (2003). Analysis of the cytosolic proteome in a cell culture model of familial amyotrophic lateral sclerosis reveals alterations to the proteasome,

antioxidant defenses, and nitric oxide synthetic pathways. *J. Biol. Chem.* *278*, 6371–6383.

Al-Saif, A., Al-Mohanna, F., and Bohlega, S. (2011). A mutation in sigma-1 receptor causes juvenile amyotrophic lateral sclerosis. *Ann. Neurol.* *70*, 913–919.

Andersen, P.M., and Al-Chalabi, A. (2011). Clinical genetics of amyotrophic lateral sclerosis: what do we really know? *Nat. Rev. Neurol.* *7*, 603–615.

Andersen, P.M., Nilsson, P., Ala-Hurula, V., Keränen, M.L., Tarvainen, I., Haltia, T., Nilsson, L., Binzer, M., Forsgren, L., and Marklund, S.L. (1995). Amyotrophic lateral sclerosis associated with homozygosity for an Asp90Ala mutation in CuZn-superoxide dismutase. *Nat. Genet.* *10*, 61–66.

Andersen, P.M., Forsgren, L., Binzer, M., Nilsson, P., Ala-Hurula, V., Keränen, M.L., Bergmark, L., Saarinen, A., Haltia, T., Tarvainen, I., et al. (1996). Autosomal recessive adult-onset amyotrophic lateral sclerosis associated with homozygosity for Asp90Ala CuZn-superoxide dismutase mutation. A clinical and genealogical study of 36 patients. *Brain* *119*, 1153–1172.

Andersen, P.M., Nilsson, P., Keränen, M.L., Forsgren, L., Hägglund, J., Karlsborg, M., Ronnevi, L.O., Gredal, O., and Marklund, S.L. (1997). Phenotypic heterogeneity in motor neuron disease patients with CuZn-superoxide dismutase mutations in Scandinavia. *Brain* *120*, 1723–1737.

Andorfer, C., Kress, Y., Espinoza, M., de Silva, R., Tucker, K.L., Barde, Y.-A., Duff, K., and Davies, P. (2003). Hyperphosphorylation and aggregation of tau in mice expressing normal human tau isoforms. *J. Neurochem.* *86*, 582–590.

Andorfer, C., Acker, C.M., Kress, Y., Hof, P.R., Duff, K., and Davies, P. (2005). Cell-cycle reentry and cell death in transgenic mice expressing nonmutant human tau isoforms. *J. Neurosci.* *25*, 5446–5454.

Andrus, P.K., Fleck, T.J., Gurney, M.E., and Hall, E.D. (1998). Protein oxidative damage in a transgenic mouse model of familial amyotrophic lateral sclerosis. *J. Neurochem.* *71*, 2041–2048.

Apostolski, S., Nikolić, J., Bugarski-Prokopljević, C., Miletić, V., Pavlović, S., and Filipović, S. (1991). Serum and CSF immunological findings in ALS. *Acta Neurol. Scand.* *83*, 96–98.

Arundine, M., and Tymianski, M. (2003). Molecular mechanisms of calcium-dependent neurodegeneration in excitotoxicity. *Cell Calcium* *34*, 325–337.

Atkin, J.D., Farg, M.A., Walker, A.K., McLean, C., Tomas, D., and Horne, M.K. (2008). Endoplasmic reticulum stress and induction of the unfolded protein response in human sporadic amyotrophic lateral sclerosis. *Neurobiol. Dis.* *30*, 400–407.

Atkin, J.D., Farg, M.A., Soo, K.Y., Walker, A.K., Halloran, M., Turner, B.J., Nagley, P., and Horne, M.K. (2014). Mutant SOD1 inhibits ER-Golgi transport in amyotrophic lateral sclerosis. *J. Neurochem.* *129*, 190–204.

- Audet, J.-N., Gowing, G., and Julien, J.-P. (2010). Wild-type human SOD1 overexpression does not accelerate motor neuron disease in mice expressing murine Sod1G86R. *Neurobiol. Dis.* *40*, 245–250.
- Ayers, J.I., Fromholt, S., Koch, M., DeBosier, A., McMahon, B., Xu, G., and Borchelt, D.R. (2014). Experimental transmissibility of mutant SOD1 motor neuron disease. *Acta Neuropathol.* *128*, 791–803.
- Babu, G.N., Kumar, A., Chandra, R., Puri, S.K., Singh, R.L., Kalita, J., and Misra, U.K. (2008). Oxidant-antioxidant imbalance in the erythrocytes of sporadic amyotrophic lateral sclerosis patients correlates with the progression of disease. *Neurochem. Int.* *52*, 1284–1289.
- Bach, E.A., Vincent, S., Zeidler, M.P., and Perrimon, N. (2003). A sensitized genetic screen to identify novel regulators and components of the *Drosophila* janus kinase/signal transducer and activator of transcription pathway. *Genetics* *165*, 1149–1166.
- Baloh, R.H., Rakowicz, W., Gardner, R., and Pestronk, A. (2007a). Frequent atrophic groups with mixed-type myofibers is distinctive to motor neuron syndromes. *Muscle Nerve* *36*, 107–110.
- Baloh, R.H., Schmidt, R.E., Pestronk, A., and Milbrandt, J. (2007b). Altered axonal mitochondrial transport in the pathogenesis of Charcot-Marie-Tooth disease from mitofusin 2 mutations. *J. Neurosci.* *27*, 422–430.
- Banci, L., Bertini, I., Boca, M., Girotto, S., Martinelli, M., Valentine, J.S., and Vieru, M. (2008). SOD1 and amyotrophic lateral sclerosis: mutations and oligomerization. *PLoS One* *3*, e1677.
- Bao-Cutrona, M., and Moral, P. (2009). Unexpected expression pattern of tetracycline-regulated transgenes in mice. *Genetics* *181*, 1687–1691.
- Barber, S.C., and Shaw, P.J. (2010). Oxidative stress in ALS: key role in motor neuron injury and therapeutic target. *Free Radic. Biol. Med.* *48*, 629–641.
- Basso, M., Pozzi, S., Tortarolo, M., Fiordaliso, F., Bisighini, C., Pasetto, L., Spaltro, G., Lidonnici, D., Gensano, F., Battaglia, E., et al. (2013). Mutant copper-zinc superoxide dismutase (SOD1) induces protein secretion pathway alterations and exosome release in astrocytes: Implications for disease spreading and motor neuron pathology in amyotrophic lateral sclerosis. *J. Biol. Chem.* *288*, 15699–15711.
- Battistini, S., Giannini, F., Greco, G., Bibbò, G., Ferrera, L., Marini, V., Causarano, R., Casula, M., Lando, G., Patrosso, M.C., et al. (2005). SOD1 mutations in amyotrophic lateral sclerosis. Results from a multicenter Italian study. *J. Neurol.* *252*, 782–788.
- Beal, M.F. (1992). Role of excitotoxicity in human neurological disease. *Curr. Opin. Neurobiol.* *2*, 657–662.

- Beal, M.F., Ferrante, R.J., Browne, S.E., Matthews, R.T., Kowall, N.W., and Brown, R.H. (1997). Increased 3-nitrotyrosine in both sporadic and familial amyotrophic lateral sclerosis. *Ann. Neurol.* *42*, 644–654.
- Bechara, E.G., Didiot, M.C., Melko, M., Davidovic, L., Bensaid, M., Martin, P., Castets, M., Pognonec, P., Khandjian, E.W., Moine, H., et al. (2009). A novel function for fragile X mental retardation protein in translational activation. *PLoS Biol.* *7*, e16.
- Beers, D.R., Henkel, J.S., Xiao, Q., Zhao, W., Wang, J., Yen, A.A., Siklos, L., McKercher, S.R., and Appel, S.H. (2006). Wild-type microglia extend survival in PU.1 knockout mice with familial amyotrophic lateral sclerosis. *Proc. Natl. Acad. Sci. U. S. A.* *103*, 16021–16026.
- Benaglia, T., Chauveau, D., Hunter, D.R., and Young, D.S. (2009). mixtools: An R Package for Analyzing Finite. *J. Stat. Softw.* *32*, 1–29.
- Bendotti, C., Marino, M., Cheroni, C., Fontana, E., Crippa, V., Poletti, A., and De Biasi, S. (2012). Dysfunction of constitutive and inducible ubiquitin-proteasome system in amyotrophic lateral sclerosis: implication for protein aggregation and immune response. *Prog. Neurobiol.* *97*, 101–126.
- Bergemalm, D., Forsberg, K., Srivastava, V., Graffmo, K.S., Andersen, P.M., Brännström, T., Wingsle, G., and Marklund, S.L. (2010). Superoxide dismutase-1 and other proteins in inclusions from transgenic amyotrophic lateral sclerosis model mice. *J. Neurochem.* *114*, 408–418.
- Bertamini, M., Marzani, B., Guarneri, R., Guarneri, P., Bigini, P., Mennini, T., and Curti, D. (2002). Mitochondrial oxidative metabolism in motor neuron degeneration (mnd) mouse central nervous system. *Eur. J. Neurosci.* *16*, 2291–2296.
- Beychok, S. (1966). Circular dichroism of biological macromolecules. *Science* *154*, 1288–1299.
- Bhusari, S.S., Dobosy, J.R., Fu, V., Almassi, N., Oberley, T., and Jarrard, D.F. (2010). Superoxide dismutase 1 knockdown induces oxidative stress and DNA methylation loss in the prostate. *Epigenetics* *5*, 402–409.
- Bilsland, L.G., Nirmalanathan, N., Yip, J., Greensmith, L., and Duchen, M.R. (2008). Expression of mutant SOD1 in astrocytes induces functional deficits in motoneuron mitochondria. *J. Neurochem.* *107*, 1271–1283.
- Bilsland, L.G., Sahai, E., Kelly, G., Golding, M., Greensmith, L., and Schiavo, G. (2010). Deficits in axonal transport precede ALS symptoms in vivo. *Proc. Natl. Acad. Sci. U. S. A.* *107*, 20523–20528.
- Birve, A., Neuwirth, C., Weber, M., Marklund, S.L., Nilsson, A.-C., Jonsson, P.A., and Andersen, P.M. (2010). A novel SOD1 splice site mutation associated with familial ALS revealed by SOD activity analysis. *Hum. Mol. Genet.* *19*, 4201–4206.

- Blokhuis, A.M., Groen, E.J.N., Koppers, M., van den Berg, L.H., and Pasterkamp, R.J. (2013). Protein aggregation in amyotrophic lateral sclerosis. *Acta Neuropathol.* *125*, 777–794.
- Bogdanov, M., Brown, R.H., Matson, W., Smart, R., Hayden, D., O'Donnell, H., Flint Beal, M., and Cudkowicz, M. (2000). Increased oxidative damage to DNA in ALS patients. *Free Radic. Biol. Med.* *29*, 652–658.
- Boillée, S., Yamanaka, K., Lobsiger, C.S., Copeland, N.G., Jenkins, N. a, Kassiotis, G., Kollias, G., and Cleveland, D.W. (2006). Onset and progression in inherited ALS determined by motor neurons and microglia. *Science* *312*, 1389–1392.
- Boles, M.K., Wilkinson, B.M., Wilming, L.G., Liu, B., Probst, F.J., Harrow, J., Grafham, D., Hentges, K.E., Woodward, L.P., Maxwell, A., et al. (2009). Discovery of candidate disease genes in ENU-induced mouse mutants by large-scale sequencing, including a splice-site mutation in nucleoredoxin. *PLoS Genet.* *5*, e1000759.
- Bonini, N.M., and Fortini, M.E. (2003). Human neurodegenerative disease modeling using *Drosophila*. *Annu. Rev. Neurosci.* *26*, 627–656.
- Borchelt, D.R., Lee, M.K., Slunt, H.S., Guarnieri, M., Xu, Z.S., Wong, P.C., Brown, R.H., Price, D.L., Sisodia, S.S., and Cleveland, D.W. (1994). Superoxide dismutase 1 with mutations linked to familial amyotrophic lateral sclerosis possesses significant activity. *Proc. Natl. Acad. Sci. U. S. A.* *91*, 8292–8296.
- Bordo, D., Djinić, K., and Bolognesi, M. (1994). Conserved patterns in the Cu,Zn superoxide dismutase family. *J. Mol. Biol.* *238*, 366–386.
- Borthwick, G.M., Johnson, M.A., Ince, P.G., Shaw, P.J., and Turnbull, D.M. (1999). Mitochondrial enzyme activity in amyotrophic lateral sclerosis: implications for the role of mitochondria in neuronal cell death. *Ann. Neurol.* *46*, 787–790.
- Bosco, D.A., Morfini, G., Karabacak, N.M., Song, Y., Gros-Louis, F., Pasinelli, P., Goolsby, H., Fontaine, B.A., Lemay, N., McKenna-Yasek, D., et al. (2010). Wild-type and mutant SOD1 share an aberrant conformation and a common pathogenic pathway in ALS. *Nat. Neurosci.* *13*, 1396–1403.
- Bowling, A.C., Schulz, J.B., Brown, R.H., and Beal, M.F. (1993). Superoxide dismutase activity, oxidative damage, and mitochondrial energy metabolism in familial and sporadic amyotrophic lateral sclerosis. *J. Neurochem.* *61*, 2322–2325.
- Branco, L.M.T., De Albuquerque, M., De Andrade, H.M.T., Bergo, F.P.G., Nucci, A., and França, M.C. (2014). Spinal cord atrophy correlates with disease duration and severity in amyotrophic lateral sclerosis. *Amyotroph. Lateral Scler. Frontotemporal Degener.* *15*, 93–97.
- Brooks, B.R., Miller, R.G., Swash, M., and Munsat, T.L. (2000). El Escorial revisited: revised criteria for the diagnosis of amyotrophic lateral sclerosis. *Amyotroph. Lateral Scler. Other Motor Neuron Disord.* *1*, 293–299.

- Broom, W.J., Greenway, M., Sadri-Vakili, G., Russ, C., Auwarter, K.E., Glajch, K.E., Dupre, N., Swingler, R.J., Purcell, S., Hayward, C., et al. (2008). 50bp deletion in the promoter for superoxide dismutase 1 (SOD1) reduces SOD1 expression in vitro and may correlate with increased age of onset of sporadic amyotrophic lateral sclerosis. *Amyotroph. Lateral Scler.* *9*, 229–237.
- Brotherton, T., Polak, M., Kelly, C., Birve, A., Andersen, P., Marklund, S.L., and Glass, J.D. (2011). A novel ALS SOD1 C6S mutation with implications for aggregation related toxicity and genetic counseling. *Amyotroph. Lateral Scler.* *12*, 215–219.
- Brotherton, T.E., Li, Y., and Glass, J.D. (2013). Cellular toxicity of mutant SOD1 protein is linked to an easily soluble, non-aggregated form in vitro. *Neurobiol. Dis.* *49*, 49–56.
- Brown, S.D., and Nolan, P.M. (1998). Mouse mutagenesis-systematic studies of mammalian gene function. *Hum. Mol. Genet.* *7*, 1627–1633.
- Browne, S.E., Bowling, A.C., Baik, M.J., Gurney, M., Brown, R.H., and Beal, M.F. (1998). Metabolic dysfunction in familial, but not sporadic, amyotrophic lateral sclerosis. *J. Neurochem.* *71*, 281–287.
- Bruijn, L.I., Becher, M.W., Lee, M.K., Anderson, K.L., Jenkins, N.A., Copeland, N.G., Sisodia, S.S., Rothstein, J.D., Borchelt, D.R., Price, D.L., et al. (1997). ALS-linked SOD1 mutant G85R mediates damage to astrocytes and promotes rapidly progressive disease with SOD1-containing inclusions. *Neuron* *18*, 327–338.
- Bruijn, L.I., Houseweart, M.K., Kato, S., Anderson, K.L., Anderson, S.D., Ohama, E., Reaume, A.G., Scott, R.W., and Cleveland, D.W. (1998). Aggregation and motor neuron toxicity of an ALS-linked SOD1 mutant independent from wild-type SOD1. *Science* *281*, 1851–1854.
- Bruijn, L.I., Miller, T.M., and Cleveland, D.W. (2004). Unraveling the mechanisms involved in motor neuron degeneration in ALS. *Annu. Rev. Neurosci.* *27*, 723–749.
- Bruns, C.K., and Kopito, R.R. (2007). Impaired post-translational folding of familial ALS-linked Cu, Zn superoxide dismutase mutants. *EMBO J.* *26*, 855–866.
- Bunton-Stasyshyn, R.K.A., Saccon, R.A., Fratta, P., and Fisher, E.M.C. (2014). SOD1 Function and Its Implications for Amyotrophic Lateral Sclerosis Pathology: New and Renascent Themes. *Neurosci.*
- Burrell, J.R., Vucic, S., and Kiernan, M.C. (2011). Isolated bulbar phenotype of amyotrophic lateral sclerosis. *Amyotroph. Lateral Scler.* *12*, 283–289.
- Cadet, J.L., Sheng, P., Ali, S., Rothman, R., Carlson, E., and Epstein, C. (1994). Attenuation of methamphetamine-induced neurotoxicity in copper/zinc superoxide dismutase transgenic mice. *J. Neurochem.* *62*, 380–383.
- Calder, V.L., Domigan, N.M., George, P.M., Donaldson, I.M., and Winterbourn, C.C. (1995). Superoxide dismutase (glu100-->gly) in a family with inherited motor neuron

disease: detection of mutant superoxide dismutase activity and the presence of heterodimers. *Neurosci. Lett.* 189, 143–146.

Casaril, M., Corso, F., Bassi, A., Capra, F., Gabrielli, G.B., Stanzial, A.M., Nicoli, N., and Corrocher, R. (1994). Decreased activity of scavenger enzymes in human hepatocellular carcinoma, but not in liver metastases. *Int. J. Clin. Lab. Res.* 24, 94–97.

Casoni, F., Basso, M., Massignan, T., Gianazza, E., Cheroni, C., Salmona, M., Bendotti, C., and Bonetto, V. (2005). Protein nitration in a mouse model of familial amyotrophic lateral sclerosis: possible multifunctional role in the pathogenesis. *J. Biol. Chem.* 280, 16295–16304.

Cassereau, J., Chevrollier, A., Gueguen, N., Desquiret, V., Verny, C., Nicolas, G., Dubas, F., Amati-Bonneau, P., Reynier, P., Bonneau, D., et al. (2011). Mitochondrial dysfunction and pathophysiology of Charcot-Marie-Tooth disease involving GDAP1 mutations. *Exp. Neurol.* 227, 31–41.

Cha, C.I., Chung, Y.H., Shin, C.M., Shin, D.H., Kim, Y.S., Gurney, M.E., and Lee, K.W. (2000). Immunocytochemical study on the distribution of nitrotyrosine in the brain of the transgenic mice expressing a human Cu/Zn SOD mutation. *Brain Res.* 853, 156–161.

Chan, P.H., Chu, L., Chen, S.F., Carlson, E.J., and Epstein, C.J. (1990). Reduced neurotoxicity in transgenic mice overexpressing human copper-zinc-superoxide dismutase. *Stroke.* 21, III80–III82.

Chang, J.L., Lomen-Hoerth, C., Murphy, J., Henry, R.G., Kramer, J.H., Miller, B.L., and Gorno-Tempini, M.L. (2005). A voxel-based morphometry study of patterns of brain atrophy in ALS and ALS/FTLD. *Neurology* 65, 75–80.

Chang, L.Y., Slot, J.W., Geuze, H.J., and Crapo, J.D. (1988). Molecular immunocytochemistry of the CuZn superoxide dismutase in rat hepatocytes. *J. Cell Biol.* 107, 2169–2179.

Chang, Y., Kong, Q., Shan, X., Tian, G., Ilieva, H., Cleveland, D.W., Rothstein, J.D., Borchelt, D.R., Wong, P.C., and Lin, C.-L.G. (2008). Messenger RNA oxidation occurs early in disease pathogenesis and promotes motor neuron degeneration in ALS. *PLoS One* 3, e2849.

Chang-Hong, R., Wada, M., Koyama, S., Kimura, H., Arawaka, S., Kawanami, T., Kurita, K., Kadoya, T., Aoki, M., Itoyama, Y., et al. (2005). Neuroprotective effect of oxidized galectin-1 in a transgenic mouse model of amyotrophic lateral sclerosis. *Exp. Neurol.* 194, 203–211.

Chen, H., Qian, K., Du, Z., Cao, J., Petersen, A., Liu, H., Blackbourn, L.W., Huang, C.-L., Errigo, A., Yin, Y., et al. (2014). Modeling ALS with iPSCs reveals that mutant SOD1 misregulates neurofilament balance in motor neurons. *Cell Stem Cell* 14, 796–809.

Chen, Y.-Z., Bennett, C.L., Huynh, H.M., Blair, I.P., Puls, I., Irobi, J., Dierick, I., Abel, A., Kennerson, M.L., Rabin, B.A., et al. (2004). DNA/RNA helicase gene mutations in

a form of juvenile amyotrophic lateral sclerosis (ALS4). *Am. J. Hum. Genet.* *74*, 1128–1135.

Cheroni, C., Peviani, M., Cascio, P., Debiassi, S., Monti, C., and Bendotti, C. (2005). Accumulation of human SOD1 and ubiquitinated deposits in the spinal cord of SOD1G93A mice during motor neuron disease progression correlates with a decrease of proteasome. *Neurobiol. Dis.* *18*, 509–522.

Cheroni, C., Marino, M., Tortarolo, M., Veglianesi, P., De Biasi, S., Fontana, E., Zuccarello, L.V., Maynard, C.J., Dantuma, N.P., and Bendotti, C. (2009). Functional alterations of the ubiquitin-proteasome system in motor neurons of a mouse model of familial amyotrophic lateral sclerosis. *Hum. Mol. Genet.* *18*, 82–96.

Chestnut, B.A., Chang, Q., Price, A., Lesuisse, C., Wong, M., and Martin, L.J. (2011). Epigenetic regulation of motor neuron cell death through DNA methylation. *J. Neurosci.* *31*, 16619–16636.

Chevalier-Larsen, E., and Holzbaur, E.L.F. (2006). Axonal transport and neurodegenerative disease. *Biochim. Biophys. Acta* *1762*, 1094–1108.

Chia, R., Tattum, M.H., Jones, S., Collinge, J., Fisher, E.M.C., and Jackson, G.S. (2010). Superoxide dismutase 1 and tgSOD1 mouse spinal cord seed fibrils, suggesting a propagative cell death mechanism in amyotrophic lateral sclerosis. *PLoS One* *5*, e10627.

Chio, A., Calvo, A., Dossena, M., Ghiglione, P., Mutani, R., and Mora, G. (2009). ALS in Italian professional soccer players: the risk is still present and could be soccer-specific. *Amyotroph. Lateral Scler.* *10*, 205–209.

Chiò, A., Logroscino, G., Traynor, B.J., Collins, J., Simeone, J.C., Goldstein, L.A., and White, L.A. (2013). Global epidemiology of amyotrophic lateral sclerosis: a systematic review of the published literature. *Neuroepidemiology* *41*, 118–130.

Chiu, A.Y., Zhai, P., Dal Canto, M.C., Peters, T.M., Kwon, Y.W., Prattis, S.M., and Gurney, M.E. (1995). Age-dependent penetrance of disease in a transgenic mouse model of familial amyotrophic lateral sclerosis. *Mol. Cell. Neurosci.* *6*, 349–362.

Choi, I., Yang, Y.I., Song, H.D., Lee, J.S., Kang, T., Sung, J.-J., and Yi, J. (2011). Lipid molecules induce the cytotoxic aggregation of Cu/Zn superoxide dismutase with structurally disordered regions. *Biochim. Biophys. Acta* *1812*, 41–48.

Choi, J., Rees, H.D., Weintraub, S.T., Levey, A.I., Chin, L.-S., and Li, L. (2005). Oxidative modifications and aggregation of Cu,Zn-superoxide dismutase associated with Alzheimer and Parkinson diseases. *J. Biol. Chem.* *280*, 11648–11655.

Chow, C.Y., Landers, J.E., Bergren, S.K., Sapp, P.C., Grant, A.E., Jones, J.M., Everett, L., Lenk, G.M., McKenna-Yasek, D.M., Weisman, L.S., et al. (2009). Deleterious variants of FIG4, a phosphoinositide phosphatase, in patients with ALS. *Am. J. Hum. Genet.* *84*, 85–88.

- Coates, J.R., and Wininger, F.A. (2010). Canine degenerative myelopathy. *Vet. Clin. North Am. Small Anim. Pract.* *40*, 929–950.
- Cohen-Adad, J., El Mendili, M.-M., Morizot-Koutlidis, R., Lehericy, S., Meininger, V., Blanche, S., Rossignol, S., Benali, H., and Pradat, P.-F. (2013). Involvement of spinal sensory pathway in ALS and specificity of cord atrophy to lower motor neuron degeneration. *Amyotroph. Lateral Scler. Frontotemporal Degener.* *14*, 30–38.
- Collinge, J., Palmer, M.S., Sidle, K.C., Hill, a F., Gowland, I., Meads, J., Asante, E., Bradley, R., Doey, L.J., and Lantos, P.L. (1995). Unaltered susceptibility to BSE in transgenic mice expressing human prion protein. *Nature* *378*, 779–783.
- Cova, E., Bongioanni, P., Cereda, C., Metelli, M.R., Salvaneschi, L., Bernuzzi, S., Guareschi, S., Rossi, B., and Ceroni, M. (2010). Time course of oxidant markers and antioxidant defenses in subgroups of amyotrophic lateral sclerosis patients. *Neurochem. Int.* *56*, 687–693.
- Crapo, J.D., Oury, T., Rabouille, C., Slot, J.W., and Chang, L.Y. (1992). Copper,zinc superoxide dismutase is primarily a cytosolic protein in human cells. *Proc. Natl. Acad. Sci. U. S. A.* *89*, 10405–10409.
- Crespo-Barreto, J., Fryer, J.D., Shaw, C.A., Orr, H.T., and Zoghbi, H.Y. (2010). Partial loss of ataxin-1 function contributes to transcriptional dysregulation in spinocerebellar ataxia type 1 pathogenesis. *PLoS Genet.* *6*, e1001021.
- Crugnola, V., Lamperti, C., Lucchini, V., Ronchi, D., Peverelli, L., Prella, A., Sciacco, M., Bordoni, A., Fassone, E., Fortunato, F., et al. (2010). Mitochondrial respiratory chain dysfunction in muscle from patients with amyotrophic lateral sclerosis. *Arch. Neurol.* *67*, 849–854.
- Curti, D., Malaspina, A., Facchetti, G., Camana, C., Mazzini, L., Tosca, P., Zerbi, F., and Ceroni, M. (1996). Amyotrophic lateral sclerosis: oxidative energy metabolism and calcium homeostasis in peripheral blood lymphocytes. *Neurology* *47*, 1060–1064.
- Curti, D., Rognoni, F., Alimonti, D., Malaspina, A., Feletti, F., Tessera, S., Finotti, N., Rehak, L., Mazzini, L., Zerbi, F., et al. (2002). SOD1 activity and protective factors in familial ALS patients with L84F SOD1 mutation. *Amyotroph. Lateral Scler. Other Motor Neuron Disord.* *3*, 115–122.
- D’Amico, E., Factor-Litvak, P., Santella, R.M., and Mitsumoto, H. (2013). Clinical perspective on oxidative stress in sporadic amyotrophic lateral sclerosis. *Free Radic. Biol. Med.* *65*, 509–527.
- Dal Canto, M.C., and Gurney, M.E. (1994). Development of central nervous system pathology in a murine transgenic model of human amyotrophic lateral sclerosis. *Am. J. Pathol.* *145*, 1271–1279.
- Dal Canto, M.C., and Gurney, M.E. (1995). Neuropathological changes in two lines of mice carrying a transgene for mutant human Cu,Zn SOD, and in mice overexpressing wild type human SOD: a model of familial amyotrophic lateral sclerosis (FALS). *Brain Res.* *676*, 25–40.

- Daube, J.R., Gooch, C., Shefner, J., Olney, R., Felice, K., and Bromberg, M. (2000). Motor unit number estimation (MUNE) with nerve conduction studies. *Suppl. Clin. Neurophysiol.* *53*, 112–115.
- DeJesus-Hernandez, M., Mackenzie, I.R., Boeve, B.F., Boxer, A.L., Baker, M., Rutherford, N.J., Nicholson, A.M., Finch, N.A., Flynn, H., Adamson, J., et al. (2011). Expanded GGGGCC hexanucleotide repeat in noncoding region of C9ORF72 causes chromosome 9p-linked FTD and ALS. *Neuron* *72*, 245–256.
- Deng, H.X., Hentati, A., Tainer, J.A., Iqbal, Z., Cayabyab, A., Hung, W.Y., Getzoff, E.D., Hu, P., Herzfeldt, B., and Roos, R.P. (1993). Amyotrophic lateral sclerosis and structural defects in Cu,Zn superoxide dismutase. *Science* *261*, 1047–1051.
- Deng, H.-X., Shi, Y., Furukawa, Y., Zhai, H., Fu, R., Liu, E., Gorrie, G.H., Khan, M.S., Hung, W.-Y., Bigio, E.H., et al. (2006). Conversion to the amyotrophic lateral sclerosis phenotype is associated with intermolecular linked insoluble aggregates of SOD1 in mitochondria. *Proc. Natl. Acad. Sci. U. S. A.* *103*, 7142–7147.
- Deng, H.-X., Han-Xiang, D., Jiang, H., Hujun, J., Fu, R., Ronggen, F., Zhai, H., Hong, Z., Shi, Y., Yong, S., et al. (2008). Molecular dissection of ALS-associated toxicity of SOD1 in transgenic mice using an exon-fusion approach. *Hum. Mol. Genet.* *17*, 2310–2319.
- Deng, H.-X., Chen, W., Hong, S.-T., Boycott, K.M., Gorrie, G.H., Siddique, N., Yang, Y., Fecto, F., Shi, Y., Zhai, H., et al. (2011). Mutations in UBQLN2 cause dominant X-linked juvenile and adult-onset ALS and ALS/dementia. *Nature* *477*, 211–215.
- Didion, S.P., Ryan, M.J., Didion, L.A., Fegan, P.E., Sigmund, C.D., and Faraci, F.M. (2002). Increased superoxide and vascular dysfunction in CuZnSOD-deficient mice. *Circ. Res.* *91*, 938–944.
- Didion, S.P., Kinzenbaw, D.A., Schrader, L.I., and Faraci, F.M. (2006). Heterozygous CuZn superoxide dismutase deficiency produces a vascular phenotype with aging. *Hypertension* *48*, 1072–1079.
- Dobrowolny, G., Aucello, M., Rizzuto, E., Beccafico, S., Mammucari, C., Boncompagni, S., Boncompagni, S., Belia, S., Wannenes, F., Nicoletti, C., et al. (2008). Skeletal muscle is a primary target of SOD1G93A-mediated toxicity. *Cell Metab.* *8*, 425–436.
- Driscoll, M., and Gerstbrein, B. (2003). Dying for a cause: invertebrate genetics takes on human neurodegeneration. *Nat. Rev. Genet.* *4*, 181–194.
- Duchen, M.R., Surin, A., and Jacobson, J. (2003). Imaging mitochondrial function in intact cells. *Methods Enzymol.* *361*, 353–389.
- Duff, K., Knight, H., Refolo, L.M., Sanders, S., Yu, X., Picciano, M., Malester, B., Hutton, M., Adamson, J., Goedert, M., et al. (2000). Characterization of pathology in transgenic mice over-expressing human genomic and cDNA tau transgenes. *Neurobiol. Dis.* *7*, 87–98.

- Economides, A.N., Frendewey, D., Yang, P., Dominguez, M.G., Dore, A.T., Lobov, I.B., Persaud, T., Rojas, J., McClain, J., Lengyel, P., et al. (2013). Conditionals by inversion provide a universal method for the generation of conditional alleles. *Proc. Natl. Acad. Sci. U. S. A.* *110*, E3179–E3188.
- Eisen, A., Kim, S., and Pant, B. (1992). Amyotrophic lateral sclerosis (ALS): a phylogenetic disease of the corticomotoneuron? *Muscle Nerve* *15*, 219–224.
- Elam, J.S., Taylor, A.B., Strange, R., Antonyuk, S., Doucette, P.A., Rodriguez, J.A., Hasnain, S.S., Hayward, L.J., Valentine, J.S., Yeates, T.O., et al. (2003). Amyloid-like filaments and water-filled nanotubes formed by SOD1 mutant proteins linked to familial ALS. *Nat. Struct. Biol.* *10*, 461–467.
- Elchuri, S., Oberley, T.D., Qi, W., Eisenstein, R.S., Jackson Roberts, L., Van Remmen, H., Epstein, C.J., and Huang, T.-T. (2005). CuZnSOD deficiency leads to persistent and widespread oxidative damage and hepatocarcinogenesis later in life. *Oncogene* *24*, 367–380.
- Elden, A.C., Kim, H.-J., Hart, M.P., Chen-Plotkin, A.S., Johnson, B.S., Fang, X., Armarkola, M., Geser, F., Greene, R., Lu, M.M., et al. (2010). Ataxin-2 intermediate-length polyglutamine expansions are associated with increased risk for ALS. *Nature* *466*, 1069–1075.
- Esteban, J., Rosen, D.R., Bowling, A.C., Sapp, P., McKenna-Yasek, D., O'Regan, J.P., Beal, M.F., Horvitz, H.R., and Brown, R.H. (1994). Identification of two novel mutations and a new polymorphism in the gene for Cu/Zn superoxide dismutase in patients with amyotrophic lateral sclerosis. *Hum. Mol. Genet.* *3*, 997–998.
- Evans, M.J., and Kaufman, M.H. (1981). Establishment in culture of pluripotential cells from mouse embryos. *Nature* *292*, 154–156.
- Ezzi, S.A., Urushitani, M., and Julien, J.-P. (2007). Wild-type superoxide dismutase acquires binding and toxic properties of ALS-linked mutant forms through oxidation. *J. Neurochem.* *102*, 170–178.
- Faes, L., and Callewaert, G. (2011). Mitochondrial dysfunction in familial amyotrophic lateral sclerosis. *J. Bioenerg. Biomembr.* *43*, 587–592.
- Ferrante, R.J., Browne, S.E., Shinobu, L.A., Bowling, A.C., Baik, M.J., MacGarvey, U., Kowall, N.W., Brown, R.H., and Beal, M.F. (1997a). Evidence of increased oxidative damage in both sporadic and familial amyotrophic lateral sclerosis. *J. Neurochem.* *69*, 2064–2074.
- Ferrante, R.J., Shinobu, L.A., Schulz, J.B., Matthews, R.T., Thomas, C.E., Kowall, N.W., Gurney, M.E., and Beal, M.F. (1997b). Increased 3-nitrotyrosine and oxidative damage in mice with a human copper/zinc superoxide dismutase mutation. *Ann. Neurol.* *42*, 326–334.
- Fischer, L.R., and Glass, J.D. (2010). Oxidative stress induced by loss of Cu,Zn-superoxide dismutase (SOD1) or superoxide-generating herbicides causes axonal degeneration in mouse DRG cultures. *Acta Neuropathol.* *119*, 249–259.

- Fischer, L.R., Culver, D.G., Tennant, P., Davis, A.A., Wang, M., Castellano-Sanchez, A., Khan, J., Polak, M.A., and Glass, J.D. (2004). Amyotrophic lateral sclerosis is a distal axonopathy: evidence in mice and man. *Exp. Neurol.* *185*, 232–240.
- Fischer, L.R., Igoudjil, A., Magrané, J., Li, Y., Hansen, J.M., Manfredi, G., and Glass, J.D. (2011). SOD1 targeted to the mitochondrial intermembrane space prevents motor neuropathy in the Sod1 knockout mouse. *Brain* *134*, 196–209.
- Fischer, L.R., Li, Y., Asress, S.A., Jones, D.P., and Glass, J.D. (2012). Absence of SOD1 leads to oxidative stress in peripheral nerve and causes a progressive distal motor axonopathy. *Exp. Neurol.* *233*, 163–171.
- Fitzmaurice, P.S., Shaw, I.C., Kleiner, H.E., Miller, R.T., Monks, T.J., Lau, S.S., Mitchell, J.D., and Lynch, P.G. (1996). Evidence for DNA damage in amyotrophic lateral sclerosis. *Muscle Nerve* *19*, 797–798.
- Flood, D.G., Reaume, A.G., Gruner, J.A., Hoffman, E.K., Hirsch, J.D., Lin, Y.G., Dorfman, K.S., and Scott, R.W. (1999). Hindlimb motor neurons require Cu/Zn superoxide dismutase for maintenance of neuromuscular junctions. *Am. J. Pathol.* *155*, 663–672.
- Foran, E., and Trotti, D. (2009). Glutamate transporters and the excitotoxic path to motor neuron degeneration in amyotrophic lateral sclerosis. *Antioxid. Redox Signal.* *11*, 1587–1602.
- Forsberg, K., Jonsson, P.A., Andersen, P.M., Bergemalm, D., Graffmo, K.S., Hultdin, M., Jacobsson, J., Rosquist, R., Marklund, S.L., and Brännström, T. (2010). Novel antibodies reveal inclusions containing non-native SOD1 in sporadic ALS patients. *PLoS One* *5*, e11552.
- Forsberg, K., Andersen, P.M., Marklund, S.L., and Brännström, T. (2011). Glial nuclear aggregates of superoxide dismutase-1 are regularly present in patients with amyotrophic lateral sclerosis. *Acta Neuropathol.* *121*, 623–634.
- Fratta, P. (2013). Antisense makes sense for amyotrophic lateral sclerosis. *Lancet Neurol.* *12*, 416–417.
- Frey, D., Schneider, C., Xu, L., Borg, J., Spooren, W., and Caroni, P. (2000). Early and selective loss of neuromuscular synapse subtypes with low sprouting competence in motoneuron diseases. *J. Neurosci.* *20*, 2534–2542.
- Fridovich, I. (1986). Superoxide dismutases. *Adv. Enzymol. Relat. Areas Mol. Biol.* *58*, 61–97.
- Fridovich, I. (1995). Superoxide radical and superoxide dismutases. *Annu. Rev. Biochem.* *64*, 97–112.
- Fritz, E., Izaurieta, P., Weiss, A., Mir, F.R., Rojas, P., Gonzalez, D., Rojas, F., Brown, R.H., Madrid, R., and van Zundert, B. (2013). Mutant SOD1-expressing astrocytes release toxic factors that trigger motoneuron death by inducing hyperexcitability. *J. Neurophysiol.* *109*, 2803–2814.

- Fujii, J., Myint, T., Seo, H.G., Kayanoki, Y., Ikeda, Y., and Taniguchi, N. (1995). Characterization of wild-type and amyotrophic lateral sclerosis-related mutant Cu,Zn-superoxide dismutases overproduced in baculovirus-infected insect cells. *J. Neurochem.* *64*, 1456–1461.
- Fujimura-Kiyono, C., Kimura, F., Ishida, S., Nakajima, H., Hosokawa, T., Sugino, M., and Hanafusa, T. (2011). Onset and spreading patterns of lower motor neuron involvements predict survival in sporadic amyotrophic lateral sclerosis. *J. Neurol. Neurosurg. Psychiatry* *82*, 1244–1249.
- Fujisawa, T., Homma, K., Yamaguchi, N., Kadowaki, H., Tsuburaya, N., Naguro, I., Matsuzawa, A., Takeda, K., Takahashi, Y., Goto, J., et al. (2012). A novel monoclonal antibody reveals a conformational alteration shared by amyotrophic lateral sclerosis-linked SOD1 mutants. *Ann. Neurol.* *72*, 739–749.
- Fukada, K., Nagano, S., Satoh, M., Tohyama, C., Nakanishi, T., Shimizu, A., Yanagihara, T., and Sakoda, S. (2001). Stabilization of mutant Cu/Zn superoxide dismutase (SOD1) protein by coexpressed wild SOD1 protein accelerates the disease progression in familial amyotrophic lateral sclerosis mice. *Eur. J. Neurosci.* *14*, 2032–2036.
- Fukai, T., and Ushio-Fukai, M. (2011). Superoxide dismutases: role in redox signaling, vascular function, and diseases. *Antioxid. Redox Signal.* *15*, 1583–1606.
- Furukawa, Y., Kaneko, K., Watanabe, S., Yamanaka, K., and Nukina, N. (2013). Intracellular seeded aggregation of mutant Cu,Zn-superoxide dismutase associated with amyotrophic lateral sclerosis. *FEBS Lett.* *587*, 2500–2505.
- Gal, J., Ström, A.-L., Kilty, R., Zhang, F., and Zhu, H. (2007). p62 accumulates and enhances aggregate formation in model systems of familial amyotrophic lateral sclerosis. *J. Biol. Chem.* *282*, 11068–11077.
- Ge, W., Leystra-Lantz, C., Sanelli, T.R., McLean, J., Wen, W., Strong, W., and Strong, M.J. (2006). Neuronal tissue-specific ribonucleoprotein complex formation on SOD1 mRNA: alterations by ALS SOD1 mutations. *Neurobiol. Dis.* *23*, 342–350.
- Ge, W.-W., Wen, W., Strong, W., Leystra-Lantz, C., and Strong, M.J. (2005). Mutant copper-zinc superoxide dismutase binds to and destabilizes human low molecular weight neurofilament mRNA. *J. Biol. Chem.* *280*, 118–124.
- Getzoff, E.D., Tainer, J.A., Stempien, M.M., Bell, G.I., and Hallewell, R.A. (1989). Evolution of CuZn superoxide dismutase and the Greek key beta-barrel structural motif. *Proteins* *5*, 322–336.
- Gijssels, I., Van Langenhove, T., van der Zee, J., Slegers, K., Philtjens, S., Kleinberger, G., Janssens, J., Bettens, K., Van Cauwenberghe, C., Pereson, S., et al. (2012). A C9orf72 promoter repeat expansion in a Flanders-Belgian cohort with disorders of the frontotemporal lobar degeneration-amyotrophic lateral sclerosis spectrum: a gene identification study. *Lancet. Neurol.* *11*, 54–65.

- Giordana, M.T., Ferrero, P., Grifoni, S., Pellerino, A., Naldi, A., and Montuschi, A. (2011). Dementia and cognitive impairment in amyotrophic lateral sclerosis: a review. *Neurol. Sci.* *32*, 9–16.
- Di Giorgio, F.P., Boulting, G.L., Bobrowicz, S., and Eggan, K.C. (2008). Human embryonic stem cell-derived motor neurons are sensitive to the toxic effect of glial cells carrying an ALS-causing mutation. *Cell Stem Cell* *3*, 637–648.
- Gong, Y.H., Parsadanian, A.S., Andreeva, A., Snider, W.D., and Elliott, J.L. (2000). Restricted expression of G86R Cu/Zn superoxide dismutase in astrocytes results in astrocytosis but does not cause motoneuron degeneration. *J. Neurosci.* *20*, 660–665.
- Gould, T.W., Buss, R.R., Vinsant, S., Prevette, D., Sun, W., Knudson, C.M., Milligan, C.E., and Oppenheim, R.W. (2006). Complete dissociation of motor neuron death from motor dysfunction by Bax deletion in a mouse model of ALS. *J. Neurosci.* *26*, 8774–8786.
- Gouveia, L.O., and de Carvalho, M. (2007). Young-onset sporadic amyotrophic lateral sclerosis: a distinct nosological entity? *Amyotroph. Lateral Scler.* *8*, 323–327.
- Grad, L.I., and Cashman, N.R. (2014). Prion-like activity of Cu/Zn superoxide dismutase: implications for amyotrophic lateral sclerosis. *Prion* *8*, 33–41.
- Grad, L.I., Guest, W.C., Yanai, A., Pokrishevsky, E., O'Neill, M.A., Gibbs, E., Semenchenko, V., Yousefi, M., Wishart, D.S., Plotkin, S.S., et al. (2011). Intermolecular transmission of superoxide dismutase 1 misfolding in living cells. *Proc. Natl. Acad. Sci. U. S. A.* *108*, 16398–16403.
- Grad, L.I., Yerbury, J.J., Turner, B.J., Guest, W.C., Pokrishevsky, E., O'Neill, M.A., Yanai, A., Silverman, J.M., Zeineddine, R., Corcoran, L., et al. (2014). Intercellular propagated misfolding of wild-type Cu/Zn superoxide dismutase occurs via exosome-dependent and -independent mechanisms. *Proc. Natl. Acad. Sci. U. S. A.* *111*, 3620–3625.
- Grad, L.I., Fernando, S.M., and Cashman, N.R. (2015). From molecule to molecule and cell to cell: prion-like mechanisms in amyotrophic lateral sclerosis. *Neurobiol. Dis.* *77*, 257–265.
- Graffmo, K.S., Forsberg, K., Bergh, J., Birve, A., Zetterström, P., Andersen, P.M., Marklund, S.L., and Brännström, T. (2013). Expression of wild-type human superoxide dismutase-1 in mice causes amyotrophic lateral sclerosis. *Hum. Mol. Genet.* *22*, 51–60.
- Greenway, M.J., Andersen, P.M., Russ, C., Ennis, S., Cashman, S., Donaghy, C., Patterson, V., Swingler, R., Kieran, D., Prehn, J., et al. (2006). ANG mutations segregate with familial and “sporadic” amyotrophic lateral sclerosis. *Nat. Genet.* *38*, 411–413.
- Grohme, K., Maravic, M. V, Gasser, T., and Borasio, G.D. (2001). A case of amyotrophic lateral sclerosis with a very slow progression over 44 years. *Neuromuscul. Disord.* *11*, 414–416.

- Gruzman, A., Wood, W.L., Alpert, E., Prasad, M.D., Miller, R.G., Rothstein, J.D., Bowser, R., Hamilton, R., Wood, T.D., Cleveland, D.W., et al. (2007). Common molecular signature in SOD1 for both sporadic and familial amyotrophic lateral sclerosis. *Proc. Natl. Acad. Sci. U. S. A.* *104*, 12524–12529.
- Guareschi, S., Cova, E., Cereda, C., Ceroni, M., Donetti, E., Bosco, D.A., Trotti, D., and Pasinelli, P. (2012). An over-oxidized form of superoxide dismutase found in sporadic amyotrophic lateral sclerosis with bulbar onset shares a toxic mechanism with mutant SOD1. *Proc. Natl. Acad. Sci. U. S. A.* *109*, 5074–5079.
- Guo, W., Chen, Y., Zhou, X., Kar, A., Ray, P., Chen, X., Rao, E.J., Yang, M., Ye, H., Zhu, L., et al. (2011). An ALS-associated mutation affecting TDP-43 enhances protein aggregation, fibril formation and neurotoxicity. *Nat. Struct. Mol. Biol.* *18*, 822–830.
- Gurney, M.E. (1997). The use of transgenic mouse models of amyotrophic lateral sclerosis in preclinical drug studies. *J. Neurol. Sci.* *152 Suppl*, S67–S73.
- Gurney, M.E., Pu, H., Chiu, A.Y., Dal Canto, M.C., Polchow, C.Y., Alexander, D.D., Caliendo, J., Hentati, A., Kwon, Y.W., and Deng, H.X. (1994). Motor neuron degeneration in mice that express a human Cu,Zn superoxide dismutase mutation. *Science* *264*, 1772–1775.
- Gurney, M.E., Cutting, F.B., Zhai, P., Doble, A., Taylor, C.P., Andrus, P.K., and Hall, E.D. (1996). Benefit of vitamin E, riluzole, and gabapentin in a transgenic model of familial amyotrophic lateral sclerosis. *Ann. Neurol.* *39*, 147–157.
- Hadano, S., Hand, C.K., Osuga, H., Yanagisawa, Y., Otomo, A., Devon, R.S., Miyamoto, N., Showguchi-Miyata, J., Okada, Y., Singaraja, R., et al. (2001). A gene encoding a putative GTPase regulator is mutated in familial amyotrophic lateral sclerosis 2. *Nat. Genet.* *29*, 166–173.
- Hafezparast, M., Klocke, R., Ruhrberg, C., Marquardt, A., Ahmad-Annuar, A., Bowen, S., Lalli, G., Witherden, A.S., Hummerich, H., Nicholson, S., et al. (2003). Mutations in dynein link motor neuron degeneration to defects in retrograde transport. *Science* *300*, 808–812.
- Hand, C.K., Mayeux-Portas, V., Khoris, J., Briolotti, V., Clavelou, P., Camu, W., and Rouleau, G.A. (2001). Compound heterozygous D90A and D96N SOD1 mutations in a recessive amyotrophic lateral sclerosis family. *Ann. Neurol.* *49*, 267–271.
- Hand, C.K., Khoris, J., Salachas, F., Gros-Louis, F., Lopes, A.A.S., Mayeux-Portas, V., Brewer, C.G., Brown, R.H., Meininger, V., Camu, W., et al. (2002). A novel locus for familial amyotrophic lateral sclerosis, on chromosome 18q. *Am. J. Hum. Genet.* *70*, 251–256.
- Hashizume, K., Hirasawa, M., Imamura, Y., Noda, S., Shimizu, T., Shinoda, K., Kurihara, T., Noda, K., Ozawa, Y., Ishida, S., et al. (2008). Retinal dysfunction and progressive retinal cell death in SOD1-deficient mice. *Am. J. Pathol.* *172*, 1325–1331.

- Haverkamp, L.J., Appel, V., and Appel, S.H. (1995). Natural history of amyotrophic lateral sclerosis in a database population. Validation of a scoring system and a model for survival prediction. *Brain* 118, 707–719.
- Hegedus, J., Putman, C.T., and Gordon, T. (2007). Time course of preferential motor unit loss in the SOD1 G93A mouse model of amyotrophic lateral sclerosis. *Neurobiol. Dis.* 28, 154–164.
- Hegedus, J., Putman, C.T., Tyreman, N., and Gordon, T. (2008). Preferential motor unit loss in the SOD1 G93A transgenic mouse model of amyotrophic lateral sclerosis. *J. Physiol.* 586, 3337–3351.
- Heiman-Patterson, T.D., Deitch, J.S., Blankenhorn, E.P., Erwin, K.L., Perreault, M.J., Alexander, B.K., Byers, N., Toman, I., and Alexander, G.M. (2005). Background and gender effects on survival in the TgN(SOD1-G93A)1Gur mouse model of ALS. *J. Neurol. Sci.* 236, 1–7.
- Heiman-Patterson, T.D., Sher, R.B., Blankenhorn, E.A., Alexander, G., Deitch, J.S., Kunst, C.B., Maragakis, N., and Cox, G. (2011). Effect of genetic background on phenotype variability in transgenic mouse models of amyotrophic lateral sclerosis: a window of opportunity in the search for genetic modifiers. *Amyotroph. Lateral Scler.* 12, 79–86.
- Hilton, J.B., White, A.R., and Crouch, P.J. (2015). Metal-deficient SOD1 in amyotrophic lateral sclerosis. *J. Mol. Med. (Berl.)* 93, 481–487.
- Hineno, A., Nakamura, A., Shimojima, Y., Yoshida, K., Oyanagai, K., and Ikeda, S. (2012). Distinctive clinicopathological features of 2 large families with amyotrophic lateral sclerosis having L106V mutation in SOD1 gene. *J. Neurol. Sci.* 319, 63–74.
- Hirano, M., Fujii, J., Nagai, Y., Sonobe, M., Okamoto, K., Araki, H., Taniguchi, N., and Ueno, S. (1994). A new variant Cu/Zn superoxide dismutase (Val7-->Glu) deduced from lymphocyte mRNA sequences from Japanese patients with familial amyotrophic lateral sclerosis. *Biochem. Biophys. Res. Commun.* 204, 572–577.
- Hirtz, D., Thurman, D.J., Gwinn-Hardy, K., Mohamed, M., Chaudhuri, A.R., and Zalutsky, R. (2007). How common are the “common” neurologic disorders? *Neurology* 68, 326–337.
- Ho, Y.S., Gargano, M., Cao, J., Bronson, R.T., Heimler, I., and Hutz, R.J. (1998). Reduced fertility in female mice lacking copper-zinc superoxide dismutase. *J. Biol. Chem.* 273, 7765–7769.
- Homma, K., Fujisawa, T., Tsuburaya, N., Yamaguchi, N., Kadowaki, H., Takeda, K., Nishitoh, H., Matsuzawa, A., Naguro, I., and Ichijo, H. (2013). SOD1 as a molecular switch for initiating the homeostatic ER stress response under zinc deficiency. *Mol. Cell* 52, 75–86.
- Howland, D.S., Liu, J., She, Y., Goad, B., Maragakis, N.J., Kim, B., Erickson, J., Kulik, J., DeVito, L., Psaltis, G., et al. (2002). Focal loss of the glutamate transporter EAAT2

in a transgenic rat model of SOD1 mutant-mediated amyotrophic lateral sclerosis (ALS). *Proc. Natl. Acad. Sci. U. S. A.* *99*, 1604–1609.

Hu, J., Chen, K., Ni, B., Li, L., Chen, G., and Shi, S. (2012). A novel SOD1 mutation in amyotrophic lateral sclerosis with a distinct clinical phenotype. *Amyotroph. Lateral Scler.* *13*, 149–154.

Huang, G., Ashton, C., Kumbhani, D.S., and Ying, Q.-L. (2011). Genetic manipulations in the rat: progress and prospects. *Curr. Opin. Nephrol. Hypertens.* *20*, 391–399.

Huang, T.T., Yasunami, M., Carlson, E.J., Gillespie, A.M., Reaume, A.G., Hoffman, E.K., Chan, P.H., Scott, R.W., and Epstein, C.J. (1997). Superoxide-mediated cytotoxicity in superoxide dismutase-deficient fetal fibroblasts. *Arch. Biochem. Biophys.* *344*, 424–432.

Hwang, Y.-M., Stathopoulos, P.B., Dimmick, K., Yang, H., Badiei, H.R., Tong, M.S., Rumfeldt, J.A.O., Chen, P., Karanassios, V., and Meiering, E.M. (2010). Nonamyloid aggregates arising from mature copper/zinc superoxide dismutases resemble those observed in amyotrophic lateral sclerosis. *J. Biol. Chem.* *285*, 41701–41711.

Iadecola, C., Zhang, F., Niwa, K., Eckman, C., Turner, S.K., Fischer, E., Younkin, S., Borchelt, D.R., Hsiao, K.K., and Carlson, G.A. (1999). SOD1 rescues cerebral endothelial dysfunction in mice overexpressing amyloid precursor protein. *Nat. Neurosci.* *2*, 157–161.

Igoudjil, A., Magrané, J., Fischer, L.R., Kim, H.J., Hervias, I., Dumont, M., Cortez, C., Glass, J.D., Starkov, A.A., and Manfredi, G. (2011). In vivo pathogenic role of mutant SOD1 localized in the mitochondrial intermembrane space. *J. Neurosci.* *31*, 15826–15837.

Ilieva, H., Polymenidou, M., and Cleveland, D.W. (2009). Non-cell autonomous toxicity in neurodegenerative disorders: ALS and beyond. *J. Cell Biol.* *187*, 761–772.

Imamura, Y., Noda, S., Hashizume, K., Shinoda, K., Yamaguchi, M., Uchiyama, S., Shimizu, T., Mizushima, Y., Shirasawa, T., and Tsubota, K. (2006). Drusen, choroidal neovascularization, and retinal pigment epithelium dysfunction in SOD1-deficient mice: a model of age-related macular degeneration. *Proc. Natl. Acad. Sci. U. S. A.* *103*, 11282–11287.

Ingre, C., Roos, P.M., Piehl, F., Kamel, F., and Fang, F. (2015). Risk factors for amyotrophic lateral sclerosis. *Clin. Epidemiol.* *7*, 181–193.

Ito, K., Uchiyama, T., Fukutake, T., Arai, K., Kanesaka, T., and Hattori, T. (2002). [Different clinical phenotypes of siblings with familial amyotrophic lateral sclerosis showing Cys146Arg point mutation of superoxide dismutase 1 gene]. *Rinsho Shinkeigaku* *42*, 175–177.

Ito, Y., Yamada, M., Tanaka, H., Aida, K., Tsuruma, K., Shimazawa, M., Hozumi, I., Inuzuka, T., Takahashi, H., and Hara, H. (2009). Involvement of CHOP, an ER-stress

apoptotic mediator, in both human sporadic ALS and ALS model mice. *Neurobiol. Dis.* 36, 470–476.

Ittner, L.M., Halliday, G.M., Kril, J.J., Götz, J., Hodges, J.R., and Kiernan, M.C. (2015). FTD and ALS—translating mouse studies into clinical trials. *Nat. Rev. Neurol.* 11, 360–366.

Jaarsma, D., Haasdijk, E.D., Grashorn, J.A., Hawkins, R., van Duijn, W., Verspaget, H.W., London, J., and Holstege, J.C. (2000). Human Cu/Zn superoxide dismutase (SOD1) overexpression in mice causes mitochondrial vacuolization, axonal degeneration, and premature motoneuron death and accelerates motoneuron disease in mice expressing a familial amyotrophic lateral sclerosis mutant SO. *Neurobiol. Dis.* 7, 623–643.

Jaarsma, D., Teuling, E., Haasdijk, E.D., De Zeeuw, C.I., and Hoogenraad, C.C. (2008). Neuron-specific expression of mutant superoxide dismutase is sufficient to induce amyotrophic lateral sclerosis in transgenic mice. *J. Neurosci.* 28, 2075–2088.

Jacobsson, J., Jonsson, P.A., Andersen, P.M., Forsgren, L., and Marklund, S.L. (2001). Superoxide dismutase in CSF from amyotrophic lateral sclerosis patients with and without CuZn-superoxide dismutase mutations. *Brain* 124, 1461–1466.

Jaenisch, R., and Mintz, B. (1974). Simian virus 40 DNA sequences in DNA of healthy adult mice derived from preimplantation blastocysts injected with viral DNA. *Proc. Natl. Acad. Sci. U. S. A.* 71, 1250–1254.

Jain, M.R., Ge, W.-W., Elkabes, S., and Li, H. (2008). Amyotrophic lateral sclerosis: Protein chaperone dysfunction revealed by proteomic studies of animal models. *Proteomics. Clin. Appl.* 2, 670–684.

Jaiswal, M.K. (2014). Selective vulnerability of motoneuron and perturbed mitochondrial calcium homeostasis in amyotrophic lateral sclerosis: implications for motoneurons specific calcium dysregulation. *Mol. Cell. Ther.* 2, 26.

Jang, Y.C., Lustgarten, M.S., Liu, Y., Muller, F.L., Bhattacharya, A., Liang, H., Salmon, A.B., Brooks, S. V, Larkin, L., Hayworth, C.R., et al. (2010). Increased superoxide in vivo accelerates age-associated muscle atrophy through mitochondrial dysfunction and neuromuscular junction degeneration. *FASEB J.* 24, 1376–1390.

Johnson, J.O., Mandrioli, J., Benatar, M., Abramzon, Y., Van Deerlin, V.M., Trojanowski, J.Q., Gibbs, J.R., Brunetti, M., Gronka, S., Wu, J., et al. (2010). Exome sequencing reveals VCP mutations as a cause of familial ALS. *Neuron* 68, 857–864.

Johnston, J.A., Dalton, M.J., Gurney, M.E., and Kopito, R.R. (2000). Formation of high molecular weight complexes of mutant Cu, Zn-superoxide dismutase in a mouse model for familial amyotrophic lateral sclerosis. *Proc. Natl. Acad. Sci. U. S. A.* 97, 12571–12576.

Jonsson, P.A., Ernhill, K., Andersen, P.M., Bergemalm, D., Brännström, T., Gredal, O., Nilsson, P., and Marklund, S.L. (2004). Minute quantities of misfolded mutant superoxide dismutase-1 cause amyotrophic lateral sclerosis. *Brain* 127, 73–88.

- Jonsson, P.A., Graffmo, K.S., Brännström, T., Nilsson, P., Andersen, P.M., and Marklund, S.L. (2006a). Motor neuron disease in mice expressing the wild type-like D90A mutant superoxide dismutase-1. *J. Neuropathol. Exp. Neurol.* *65*, 1126–1136.
- Jonsson, P.A., Graffmo, K.S., Andersen, P.M., Brännström, T., Lindberg, M., Oliveberg, M., and Marklund, S.L. (2006b). Disulphide-reduced superoxide dismutase-1 in CNS of transgenic amyotrophic lateral sclerosis models. *Brain* *129*, 451–464.
- Jonsson, P.A., Bergemalm, D., Andersen, P.M., Gredal, O., Brännström, T., and Marklund, S.L. (2008). Inclusions of amyotrophic lateral sclerosis-linked superoxide dismutase in ventral horns, liver, and kidney. *Ann. Neurol.* *63*, 671–675.
- Joyce, P.I., Fratta, P., Fisher, E.M.C., and Acevedo-Arozena, A. (2011). SOD1 and TDP-43 animal models of amyotrophic lateral sclerosis: recent advances in understanding disease toward the development of clinical treatments. *Mamm. Genome* *22*, 420–448.
- Joyce, P.I., Mcgoldrick, P., Saccon, R. a., Weber, W., Fratta, P., West, S.J., Zhu, N., Carter, S., Phatak, V., Stewart, M., et al. (2014). A novel SOD1-ALS mutation separates central and peripheral effects of mutant SOD1 toxicity. *Hum. Mol. Genet.* *24*, 1883–1897.
- Jucker, M. (2010). The benefits and limitations of animal models for translational research in neurodegenerative diseases. *Nat. Med.* *16*, 1210–1214.
- Julien, J.P. (1999). Neurofilament functions in health and disease. *Curr. Opin. Neurobiol.* *9*, 554–560.
- Justice, M.J., Noveroske, J.K., Weber, J.S., Zheng, B., and Bradley, A. (1999). Mouse ENU mutagenesis. *Hum. Mol. Genet.* *8*, 1955–1963.
- Kabuta, T., Suzuki, Y., and Wada, K. (2006). Degradation of amyotrophic lateral sclerosis-linked mutant Cu,Zn-superoxide dismutase proteins by macroautophagy and the proteasome. *J. Biol. Chem.* *281*, 30524–30533.
- Kalmar, B., Novoselov, S., Gray, A., Cheetham, M.E., Margulis, B., and Greensmith, L. (2008). Late stage treatment with arimoclomol delays disease progression and prevents protein aggregation in the SOD1 mouse model of ALS. *J. Neurochem.* *107*, 339–350.
- Kanning, K.C., Kaplan, A., and Henderson, C.E. (2010). Motor neuron diversity in development and disease. *Annu. Rev. Neurosci.* *33*, 409–440.
- Karch, C.M., Prudencio, M., Winkler, D.D., Hart, P.J., and Borchelt, D.R. (2009). Role of mutant SOD1 disulfide oxidation and aggregation in the pathogenesis of familial ALS. *Proc. Natl. Acad. Sci. U. S. A.* *106*, 7774–7779.
- Kato, S. (2001). Transgenic mice with ALS-linked SOD1 mutant L84V. *Neurosci. Meet. Planner. San Diego, CA Soc. Neurosci.*
- Kato, S., Shimoda, M., Watanabe, Y., Nakashima, K., Takahashi, K., and Ohama, E. (1996). Familial amyotrophic lateral sclerosis with a two base pair deletion in

superoxide dismutase 1: gene multisystem degeneration with intracytoplasmic hyaline inclusions in astrocytes. *J. Neuropathol. Exp. Neurol.* *55*, 1089–1101.

Kato, S., Hayashi, H., Nakashima, K., Nanba, E., Kato, M., Hirano, A., Nakano, I., Asayama, K., and Ohama, E. (1997). Pathological characterization of astrocytic hyaline inclusions in familial amyotrophic lateral sclerosis. *Am. J. Pathol.* *151*, 611–620.

Kato, S., Takikawa, M., Nakashima, K., Hirano, A., Cleveland, D.W., Kusaka, H., Shibata, N., Kato, M., Nakano, I., and Ohama, E. (2000). New consensus research on neuropathological aspects of familial amyotrophic lateral sclerosis with superoxide dismutase 1 (SOD1) gene mutations: inclusions containing SOD1 in neurons and astrocytes. *Amyotroph. Lateral Scler. Other Motor Neuron Disord.* *1*, 163–184.

Kato, S., Nakashima, K., Horiuchi, S., Nagai, R., Cleveland, D.W., Liu, J., Hirano, A., Takikawa, M., Kato, M., Nakano, I., et al. (2001). Formation of advanced glycation end-product-modified superoxide dismutase-1 (SOD1) is one of the mechanisms responsible for inclusions common to familial amyotrophic lateral sclerosis patients with SOD1 gene mutation, and transgenic mice expressing human . *Neuropathology* *21*, 67–81.

Katz, J.S., Katzberg, H.D., Woolley, S.C., Marklund, S.L., and Andersen, P.M. (2012). Combined fulminant frontotemporal dementia and amyotrophic lateral sclerosis associated with an I113T SOD1 mutation. *Amyotroph. Lateral Scler.* *13*, 567–569.

Kawamata, H., and Manfredi, G. (2010). Import, maturation, and function of SOD1 and its copper chaperone CCS in the mitochondrial intermembrane space. *Antioxid. Redox Signal.* *13*, 1375–1384.

Keifer, O.P., O'Connor, D.M., and Boulis, N.M. (2014). Gene and protein therapies utilizing VEGF for ALS. *Pharmacol. Ther.* *141*, 261–271.

Keithley, E.M., Canto, C., Zheng, Q.Y., Wang, X., Fischel-Ghodsian, N., and Johnson, K.R. (2005). Cu/Zn superoxide dismutase and age-related hearing loss. *Hear. Res.* *209*, 76–85.

Keller, G.A., Warner, T.G., Steimer, K.S., and Hallewell, R.A. (1991). Cu,Zn superoxide dismutase is a peroxisomal enzyme in human fibroblasts and hepatoma cells. *Proc. Natl. Acad. Sci. U. S. A.* *88*, 7381–7385.

Kennel, P.F., Finiels, F., Revah, F., and Mallet, J. (1996). Neuromuscular function impairment is not caused by motor neurone loss in FALS mice: an electromyographic study. *Neuroreport* *7*, 1427–1431.

Kerman, A., Liu, H.-N., Croul, S., Bilbao, J., Rogaeva, E., Zinman, L., Robertson, J., and Chakrabartty, A. (2010). Amyotrophic lateral sclerosis is a non-amyloid disease in which extensive misfolding of SOD1 is unique to the familial form. *Acta Neuropathol.* *119*, 335–344.

Khabazian, I., Bains, J.S., Williams, D.E., Cheung, J., Wilson, J.M.B., Pasqualotto, B.A., Pelech, S.L., Andersen, R.J., Wang, Y.-T., Liu, L., et al. (2002). Isolation of various

forms of sterol beta-D-glucoside from the seed of *Cycas circinalis*: neurotoxicity and implications for ALS-parkinsonism dementia complex. *J. Neurochem.* *82*, 516–528.

Khare, S.D., Caplow, M., and Dokholyan, N. V (2004). The rate and equilibrium constants for a multistep reaction sequence for the aggregation of superoxide dismutase in amyotrophic lateral sclerosis. *Proc. Natl. Acad. Sci. U. S. A.* *101*, 15094–15099.

Khare, S.D., Caplow, M., and Dokholyan, N. V (2006). FALS mutations in Cu, Zn superoxide dismutase destabilize the dimer and increase dimer dissociation propensity: a large-scale thermodynamic analysis. *Amyloid* *13*, 226–235.

Kieran, D., Hafezparast, M., Bohnert, S., Dick, J.R.T., Martin, J., Schiavo, G., Fisher, E.M.C., and Greensmith, L. (2005). A mutation in dynein rescues axonal transport defects and extends the life span of ALS mice. *J. Cell Biol.* *169*, 561–567.

Kiernan, M.C., Vucic, S., Cheah, B.C., Turner, M.R., Eisen, A., Hardiman, O., Burrell, J.R., and Zoing, M.C. (2011). Amyotrophic lateral sclerosis. *Lancet* *377*, 942–955.

Kikuchi, H., Almer, G., Yamashita, S., Guégan, C., Nagai, M., Xu, Z., Sosunov, A.A., McKhann, G.M., and Przedborski, S. (2006). Spinal cord endoplasmic reticulum stress associated with a microsomal accumulation of mutant superoxide dismutase-1 in an ALS model. *Proc. Natl. Acad. Sci. U. S. A.* *103*, 6025–6030.

Kikugawa, K. (2000). Generation of mutant SOD1-expressing mice. *Progr. 41st Annu. Meet. Soc. Neurol. Jpn. Soc. Neurol. Jpn.*

Kilk, A., Laan, M., and Torp, A. (1995). Human CuZn superoxide dismutase enzymatic activity in cells is regulated by the length of the mRNA. *FEBS Lett.* *362*, 323–327.

Kim, G.W., Gasche, Y., Grzeschik, S., Copin, J.-C., Maier, C.M., and Chan, P.H. (2003). Neurodegeneration in striatum induced by the mitochondrial toxin 3-nitropropionic acid: role of matrix metalloproteinase-9 in early blood-brain barrier disruption? *J. Neurosci.* *23*, 8733–8742.

Kim, H.J., Kim, N.C., Wang, Y.-D., Scarborough, E.A., Moore, J., Diaz, Z., MacLea, K.S., Freibaum, B., Li, S., Molliex, A., et al. (2013). Mutations in prion-like domains in hnRNPA2B1 and hnRNPA1 cause multisystem proteinopathy and ALS. *Nature* *495*, 467–473.

Kishigami, H., Nagano, S., Bush, A.I., and Sakoda, S. (2010). Monomerized Cu, Zn-superoxide dismutase induces oxidative stress through aberrant Cu binding. *Free Radic. Biol. Med.* *48*, 945–952.

Kiskinis, E., Sandoe, J., Williams, L.A., Boulting, G.L., Moccia, R., Wainger, B.J., Han, S., Peng, T., Thams, S., Mikkilineni, S., et al. (2014). Pathways disrupted in human ALS motor neurons identified through genetic correction of mutant SOD1. *Cell Stem Cell* *14*, 781–795.

Kitamura, F., Fujimaki, N., Okita, W., Hiramatsu, H., and Takeuchi, H. (2011). Structural instability and Cu-dependent pro-oxidant activity acquired by the apo form

- of mutant SOD1 associated with amyotrophic lateral sclerosis. *Biochemistry* *50*, 4242–4250.
- Kondo, T., Reaume, A.G., Huang, T.T., Carlson, E., Murakami, K., Chen, S.F., Hoffman, E.K., Scott, R.W., Epstein, C.J., and Chan, P.H. (1997). Reduction of CuZn-superoxide dismutase activity exacerbates neuronal cell injury and edema formation after transient focal cerebral ischemia. *J. Neurosci.* *17*, 4180–4189.
- Kong, J., and Xu, Z. (1998). Massive mitochondrial degeneration in motor neurons triggers the onset of amyotrophic lateral sclerosis in mice expressing a mutant SOD1. *J. Neurosci.* *18*, 3241–3250.
- Kordasiewicz, H.B., Stanek, L.M., Wancewicz, E. V, Mazur, C., McAlonis, M.M., Pytel, K.A., Artates, J.W., Weiss, A., Cheng, S.H., Shihabuddin, L.S., et al. (2012). Sustained therapeutic reversal of Huntington's disease by transient repression of huntingtin synthesis. *Neuron* *74*, 1031–1044.
- Kostrominova, T.Y. (2010). Advanced age-related denervation and fiber-type grouping in skeletal muscle of SOD1 knockout mice. *Free Radic. Biol. Med.* *49*, 1582–1593.
- Koyama, S., Arawaka, S., Chang-Hong, R., Wada, M., Kawanami, T., Kurita, K., Kato, M., Nagai, M., Aoki, M., Itoyama, Y., et al. (2006). Alteration of familial ALS-linked mutant SOD1 solubility with disease progression: its modulation by the proteasome and Hsp70. *Biochem. Biophys. Res. Commun.* *343*, 719–730.
- Krishnan, U., Son, M., Rajendran, B., and Elliott, J.L. (2006). Novel mutations that enhance or repress the aggregation potential of SOD1. *Mol. Cell. Biochem.* *287*, 201–211.
- Kunst, C.B., Messer, L., Gordon, J., Haines, J., and Patterson, D. (2000). Genetic mapping of a mouse modifier gene that can prevent ALS onset. *Genomics* *70*, 181–189.
- Kunze, A., Lengacher, S., Dirren, E., Aebischer, P., Magistretti, P.J., and Renaud, P. (2013). Astrocyte-neuron co-culture on microchips based on the model of SOD mutation to mimic ALS. *Integr. Biol. (Camb)*. *5*, 964–975.
- Kurahashi, T., Konno, T., Otsuki, N., Kwon, M., Tsunoda, S., Ito, J., and Fujii, J. (2012). A malfunction in triglyceride transfer from the intracellular lipid pool to apoB in enterocytes of SOD1-deficient mice. *FEBS Lett.* *586*, 4289–4295.
- Kushner, P.D., Stephenson, D.T., and Wright, S. (1991). Reactive astrogliosis is widespread in the subcortical white matter of amyotrophic lateral sclerosis brain. *J. Neuropathol. Exp. Neurol.* *50*, 263–277.
- Kwiatkowski, T.J., Bosco, D.A., Leclerc, A.L., Tamrazian, E., Vanderburg, C.R., Russ, C., Davis, A., Gilchrist, J., Kasarskis, E.J., Munsat, T., et al. (2009). Mutations in the FUS/TLS gene on chromosome 16 cause familial amyotrophic lateral sclerosis. *Science* *323*, 1205–1208.

- De la Rúa-Domènech, R., Wiedmann, M., Mohammed, H.O., Cummings, J.F., Divers, T.J., and Batt, C.A. (1996). Equine motor neuron disease is not linked to Cu/Zn superoxide dismutase mutations: sequence analysis of the equine Cu/Zn superoxide dismutase cDNA. *Gene* *178*, 83–88.
- Lagier-Tourenne, C., and Cleveland, D.W. (2009). Rethinking ALS: the FUS about TDP-43. *Cell* *136*, 1001–1004.
- Lander, E.S., and Botstein, D. (1989). Mapping mendelian factors underlying quantitative traits using RFLP linkage maps. *Genetics* *121*, 185–199.
- Larkin, L.M., Davis, C.S., Sims-Robinson, C., Kostrominova, T.Y., Van Remmen, H., Richardson, A., Feldman, E.L., and Brooks, S. V (2011). Skeletal muscle weakness due to deficiency of CuZn-superoxide dismutase is associated with loss of functional innervation. *Am. J. Physiol. Regul. Integr. Comp. Physiol.* *301*, R1400–R1407.
- Lasiene, J., and Yamanaka, K. (2011). Glial cells in amyotrophic lateral sclerosis. *Neurol. Res. Int.* *2011*, 718987.
- Lee, S.E. (2011). Guam dementia syndrome revisited in 2011. *Curr. Opin. Neurol.* *24*, 517–524.
- Lee, S., and Kim, H.-J. (2015). Prion-like Mechanism in Amyotrophic Lateral Sclerosis: are Protein Aggregates the Key? *Exp. Neurobiol.* *24*, 1–7.
- Lee, J., Ryu, H., and Kowall, N.W. (2009). Differential regulation of neuronal and inducible nitric oxide synthase (NOS) in the spinal cord of mutant SOD1 (G93A) ALS mice. *Biochem. Biophys. Res. Commun.* *387*, 202–206.
- Lee, J.P., Gerin, C., Bindokas, V.P., Miller, R., Ghadge, G., and Roos, R.P. (2002). No correlation between aggregates of Cu/Zn superoxide dismutase and cell death in familial amyotrophic lateral sclerosis. *J. Neurochem.* *82*, 1229–1238.
- Leigh, P.N., Whitwell, H., Garofalo, O., Buller, J., Swash, M., Martin, J.E., Gallo, J.M., Weller, R.O., and Anderton, B.H. (1991). Ubiquitin-immunoreactive intraneuronal inclusions in amyotrophic lateral sclerosis. Morphology, distribution, and specificity. *Brain* *114*, 775–788.
- Lemmens, R., Van Hoecke, A., Hersmus, N., Geelen, V., D'Hollander, I., Thijs, V., Van Den Bosch, L., Carmeliet, P., and Robberecht, W. (2007). Overexpression of mutant superoxide dismutase 1 causes a motor axonopathy in the zebrafish. *Hum. Mol. Genet.* *16*, 2359–2365.
- Leonardi, A., Abbruzzese, G., Arata, L., Cocito, L., and Vische, M. (1984). Cerebrospinal fluid (CSF) findings in amyotrophic lateral sclerosis. *J. Neurol.* *231*, 75–78.
- Levine, T.P., Daniels, R.D., Gatta, A.T., Wong, L.H., and Hayes, M.J. (2013). The product of C9orf72, a gene strongly implicated in neurodegeneration, is structurally related to DENN Rab-GEFs. *Bioinformatics* *29*, 499–503.

- Lewén, A., Matz, P., and Chan, P.H. (2000). Free radical pathways in CNS injury. *J. Neurotrauma* *17*, 871–890.
- Li, X., Lu, L., Bush, D.J., Zhang, X., Zheng, L., Suswam, E.A., and King, P.H. (2009). Mutant copper-zinc superoxide dismutase associated with amyotrophic lateral sclerosis binds to adenine/uridine-rich stability elements in the vascular endothelial growth factor 3'-untranslated region. *J. Neurochem.* *108*, 1032–1044.
- Liaw, K.Y., Lee, P.H., Wu, F.C., Tsai, J.S., and Lin-Shiau, S.Y. (1997). Zinc, copper, and superoxide dismutase in hepatocellular carcinoma. *Am. J. Gastroenterol.* *92*, 2260–2263.
- Lim, J., Crespo-Barreto, J., Jafar-Nejad, P., Bowman, A.B., Richman, R., Hill, D.E., Orr, H.T., and Zoghbi, H.Y. (2008). Opposing effects of polyglutamine expansion on native protein complexes contribute to SCA1. *Nature* *452*, 713–718.
- Lin, M.T., Wang, M.Y., Liaw, K.Y., Lee, P.H., Chien, S.F., Tsai, J.S., and Lin-Shiau, S.Y. (2001). Superoxide dismutase in hepatocellular carcinoma affects patient prognosis. *Hepatogastroenterology.* *48*, 1102–1105.
- Lindberg, M.J., Tibell, L., and Oliveberg, M. (2002). Common denominator of Cu/Zn superoxide dismutase mutants associated with amyotrophic lateral sclerosis: decreased stability of the apo state. *Proc. Natl. Acad. Sci. U. S. A.* *99*, 16607–16612.
- Lindberg, M.J., Normark, J., Holmgren, A., and Oliveberg, M. (2004). Folding of human superoxide dismutase: disulfide reduction prevents dimerization and produces marginally stable monomers. *Proc. Natl. Acad. Sci. U. S. A.* *101*, 15893–15898.
- Lindberg, M.J., Byström, R., Boknäs, N., Andersen, P.M., and Oliveberg, M. (2005). Systematically perturbed folding patterns of amyotrophic lateral sclerosis (ALS)-associated SOD1 mutants. *Proc. Natl. Acad. Sci. U. S. A.* *102*, 9754–9759.
- Lindenau, J., Noack, H., Possel, H., Asayama, K., and Wolf, G. (2000). Cellular distribution of superoxide dismutases in the rat CNS. *Glia* *29*, 25–34.
- Ling, S.-C., Polymenidou, M., and Cleveland, D.W. (2013). Converging mechanisms in ALS and FTD: disrupted RNA and protein homeostasis. *Neuron* *79*, 416–438.
- Lino, M.M., Schneider, C., and Caroni, P. (2002). Accumulation of SOD1 mutants in postnatal motoneurons does not cause motoneuron pathology or motoneuron disease. *J. Neurosci.* *22*, 4825–4832.
- Liu, D., Bao, F., Wen, J., and Liu, J. (2007). Mutation of superoxide dismutase elevates reactive species: comparison of nitration and oxidation of proteins in different brain regions of transgenic mice with amyotrophic lateral sclerosis. *Neuroscience* *146*, 255–264.
- Liu, H.-N., Tjostheim, S., Dasilva, K., Taylor, D., Zhao, B., Rakhit, R., Brown, M., Chakrabartty, A., McLaurin, J., and Robertson, J. (2012). Targeting of monomer/misfolded SOD1 as a therapeutic strategy for amyotrophic lateral sclerosis. *J. Neurosci.* *32*, 8791–8799.

Liu, K.X., Edwards, B., Lee, S., Finelli, M.J., Davies, B., Davies, K.E., and Oliver, P.L. (2015). Neuron-specific antioxidant OXR1 extends survival of a mouse model of amyotrophic lateral sclerosis. *Brain* 138, 1167–1181.

Liu, R., Althaus, J.S., Ellerbrock, B.R., Becker, D.A., and Gurney, M.E. (1998). Enhanced oxygen radical production in a transgenic mouse model of familial amyotrophic lateral sclerosis. *Ann. Neurol.* 44, 763–770.

Lobsiger, C.S., Boillee, S., McAlonis-Downes, M., Khan, A.M., Feltri, M.L., Yamanaka, K., and Cleveland, D.W. (2009). Schwann cells expressing dismutase active mutant SOD1 unexpectedly slow disease progression in ALS mice. *Proc. Natl. Acad. Sci. U. S. A.* 106, 4465–4470.

Logroscino, G., Traynor, B.J., Hardiman, O., Chiò, A., Mitchell, D., Swingler, R.J., Millul, A., Benn, E., and Beghi, E. (2010). Incidence of amyotrophic lateral sclerosis in Europe. *J. Neurol. Neurosurg. Psychiatry* 81, 385–390.

Lu, X.-H., and Yang, X.W. (2012). “Huntingtin holiday”: progress toward an antisense therapy for Huntington’s disease. *Neuron* 74, 964–966.

Lu, L., Zheng, L., Viera, L., Suswam, E., Li, Y., Li, X., Estévez, A.G., and King, P.H. (2007). Mutant Cu/Zn-superoxide dismutase associated with amyotrophic lateral sclerosis destabilizes vascular endothelial growth factor mRNA and downregulates its expression. *J. Neurosci.* 27, 7929–7938.

Luche, R.M., Maiwald, R., Carlson, E.J., and Epstein, C.J. (1997). Novel mutations in an otherwise strictly conserved domain of CuZn superoxide dismutase. *Mol. Cell. Biochem.* 168, 191–194.

De Lustig, E.S., Serra, J.A., Kohan, S., Canziani, G.A., Famulari, A.L., and Dominguez, R.O. (1993). Copper-zinc superoxide dismutase activity in red blood cells and serum in demented patients and in aging. *J. Neurol. Sci.* 115, 18–25.

Luty, A.A., Kwok, J.B.J., Dobson-Stone, C., Loy, C.T., Coupland, K.G., Karlström, H., Sobow, T., Tchorzewska, J., Maruszak, A., Barcikowska, M., et al. (2010). Sigma nonopioid intracellular receptor 1 mutations cause frontotemporal lobar degeneration-motor neuron disease. *Ann. Neurol.* 68, 639–649.

Mackenzie, I.R.A., Bigio, E.H., Ince, P.G., Geser, F., Neumann, M., Cairns, N.J., Kwong, L.K., Forman, M.S., Ravits, J., Stewart, H., et al. (2007). Pathological TDP-43 distinguishes sporadic amyotrophic lateral sclerosis from amyotrophic lateral sclerosis with SOD1 mutations. *Ann. Neurol.* 61, 427–434.

Mackenzie, I.R.A., Frick, P., and Neumann, M. (2014). The neuropathology associated with repeat expansions in the C9ORF72 gene. *Acta Neuropathol.* 127, 347–357.

Maekawa, S., Leigh, P.N., King, A., Jones, E., Steele, J.C., Bodi, I., Shaw, C.E., Hortobagyi, T., and Al-Sarraj, S. (2009). TDP-43 is consistently co-localized with ubiquitinated inclusions in sporadic and Guam amyotrophic lateral sclerosis but not in familial amyotrophic lateral sclerosis with and without SOD1 mutations. *Neuropathology* 29, 672–683.

- Magnus, T., Beck, M., Giess, R., Puls, I., Naumann, M., and Toyka, K. V (2002). Disease progression in amyotrophic lateral sclerosis: predictors of survival. *Muscle Nerve* 25, 709–714.
- Mancuso, R., Oliván, S., Mancera, P., Pastén-Zamorano, A., Manzano, R., Casas, C., Osta, R., and Navarro, X. (2012). Effect of genetic background on onset and disease progression in the SOD1-G93A model of amyotrophic lateral sclerosis. *Amyotroph. Lateral Scler.* 13, 302–310.
- Manjaly, Z.R., Scott, K.M., Abhinav, K., Wijesekera, L., Ganesalingam, J., Goldstein, L.H., Janssen, A., Dougherty, A., Willey, E., Stanton, B.R., et al. (2010). The sex ratio in amyotrophic lateral sclerosis: A population based study. *Amyotroph. Lateral Scler.* 11, 439–442.
- Marchetto, M.C.N., Muotri, A.R., Mu, Y., Smith, A.M., Cezar, G.G., and Gage, F.H. (2008). Non-cell-autonomous effect of human SOD1 G37R astrocytes on motor neurons derived from human embryonic stem cells. *Cell Stem Cell* 3, 649–657.
- Marciniuk, K., Taschuk, R., and Napper, S. (2013). Evidence for prion-like mechanisms in several neurodegenerative diseases: potential implications for immunotherapy. *Clin. Dev. Immunol.* 2013, 473706.
- Marin, E.P., Derakhshan, B., Lam, T.T., Davalos, A., and Sessa, W.C. (2012). Endothelial cell palmitoylproteomic identifies novel lipid-modified targets and potential substrates for protein acyl transferases. *Circ. Res.* 110, 1336–1344.
- Marklund, S.L., Holme, E., and Hellner, L. (1982). Superoxide dismutase in extracellular fluids. *Clin. Chim. Acta.* 126, 41–51.
- Martin, G.R. (1981). Isolation of a pluripotent cell line from early mouse embryos cultured in medium conditioned by teratocarcinoma stem cells. *Proc. Natl. Acad. Sci. U. S. A.* 78, 7634–7638.
- Martin, L.J., Liu, Z., Chen, K., Price, A.C., Pan, Y., Swaby, J.A., and Golden, W.C. (2007). Motor neuron degeneration in amyotrophic lateral sclerosis mutant superoxide dismutase-1 transgenic mice: mechanisms of mitochondriopathy and cell death. *J. Comp. Neurol.* 500, 20–46.
- Maruyama, H., Morino, H., Ito, H., Izumi, Y., Kato, H., Watanabe, Y., Kinoshita, Y., Kamada, M., Nodera, H., Suzuki, H., et al. (2010). Mutations of optineurin in amyotrophic lateral sclerosis. *Nature* 465, 223–226.
- Masè, G., Ros, S., Gemma, A., Bonfigli, L., Carraro, N., Cazzato, G., Rolfo, M., Zanconati, F., Sepcic, J., Jurjevic, A., et al. (2001). ALS with variable phenotypes in a six-generation family caused by leu144phe mutation in the SOD1 gene. *J. Neurol. Sci.* 191, 11–18.
- Matsumoto, S., Kusaka, H., Ito, H., Shibata, N., Asayama, T., and Imai, T. Sporadic amyotrophic lateral sclerosis with dementia and Cu/Zn superoxide dismutase-positive Lewy body-like inclusions. *Clin. Neuropathol.* 15, 41–46.

- Mattiazzi, M., D'Aurelio, M., Gajewski, C.D., Martushova, K., Kiaei, M., Beal, M.F., and Manfredi, G. (2002). Mutated human SOD1 causes dysfunction of oxidative phosphorylation in mitochondria of transgenic mice. *J. Biol. Chem.* *277*, 29626–29633.
- Mattson, M.P. (2003). Excitotoxic and excitoprotective mechanisms: abundant targets for the prevention and treatment of neurodegenerative disorders. *Neuromolecular Med.* *3*, 65–94.
- Matzuk, M.M., Dionne, L., Guo, Q., Kumar, T.R., and Lebovitz, R.M. (1998). Ovarian function in superoxide dismutase 1 and 2 knockout mice. *Endocrinology* *139*, 4008–4011.
- McAlary, L., Yerbury, J.J., and Aquilina, J.A. (2013). Glutathionylation potentiates benign superoxide dismutase 1 variants to the toxic forms associated with amyotrophic lateral sclerosis. *Sci. Rep.* *3*, 3275.
- McGeer, P.L., and McGeer, E.G. (2002). Inflammatory processes in amyotrophic lateral sclerosis. *Muscle Nerve* *26*, 459–470.
- McGoldrick, P., Joyce, P.I., Fisher, E.M.C., and Greensmith, L. (2013). Rodent models of amyotrophic lateral sclerosis. *Biochim. Biophys. Acta* *1832*, 1421–1436.
- Mead, R.J., Bennett, E.J., Kennerley, A.J., Sharp, P., Sunyach, C., Kasher, P., Berwick, J., Pettmann, B., Battaglia, G., Azzouz, M., et al. (2011). Optimised and rapid pre-clinical screening in the SOD1(G93A) transgenic mouse model of amyotrophic lateral sclerosis (ALS). *PLoS One* *6*, e23244.
- Mendonça, D.M.F., Chimelli, L., and Martinez, A.M.B. (2005). Quantitative evidence for neurofilament heavy subunit aggregation in motor neurons of spinal cords of patients with amyotrophic lateral sclerosis. *Braz. J. Med. Biol. Res.* *38*, 925–933.
- Menzies, F.M., Grierson, A.J., Cookson, M.R., Heath, P.R., Tomkins, J., Figlewicz, D.A., Ince, P.G., and Shaw, P.J. (2002). Selective loss of neurofilament expression in Cu/Zn superoxide dismutase (SOD1) linked amyotrophic lateral sclerosis. *J. Neurochem.* *82*, 1118–1128.
- Miao, L., and St Clair, D.K. (2009). Regulation of superoxide dismutase genes: implications in disease. *Free Radic. Biol. Med.* *47*, 344–356.
- Mikawa, S., Kinouchi, H., Kamii, H., Gobbel, G.T., Chen, S.F., Carlson, E., Epstein, C.J., and Chan, P.H. (1996). Attenuation of acute and chronic damage following traumatic brain injury in copper, zinc-superoxide dismutase transgenic mice. *J. Neurosurg.* *85*, 885–891.
- Miki, Y., Mori, F., Nunomura, J., Ookawa, K., Yajima, N., Yagihashi, S., and Wakabayashi, K. (2010). Sporadic amyotrophic lateral sclerosis with pallido-nigro-luysian degeneration: a TDP-43 immunohistochemical study. *Neuropathology* *30*, 149–153.
- Milanese, M., Zappettini, S., Jacchetti, E., Bonifacino, T., Cervetto, C., Usai, C., and Bonanno, G. (2010). In vitro activation of GAT1 transporters expressed in spinal cord

gliosomes stimulates glutamate release that is abnormally elevated in the SOD1/G93A(+) mouse model of amyotrophic lateral sclerosis. *J. Neurochem.* *113*, 489–501.

Milani, P., Ambrosi, G., Gammoh, O., Blandini, F., and Cereda, C. (2013). SOD1 and DJ-1 converge at Nrf2 pathway: a clue for antioxidant therapeutic potential in neurodegeneration. *Oxid. Med. Cell. Longev.* *2013*, 836760.

Millecamps, S., Salachas, F., Cazeneuve, C., Gordon, P., Bricka, B., Camuzat, A., Guillot-Noël, L., Russaouen, O., Bruneteau, G., Pradat, P.-F., et al. (2010). SOD1, ANG, VAPB, TARDBP, and FUS mutations in familial amyotrophic lateral sclerosis: genotype-phenotype correlations. *J. Med. Genet.* *47*, 554–560.

Miller, R.G., Jackson, C.E., Kasarskis, E.J., England, J.D., Forshew, D., Johnston, W., Kalra, S., Katz, J.S., Mitsumoto, H., Rosenfeld, J., et al. (2009a). Practice parameter update: the care of the patient with amyotrophic lateral sclerosis: drug, nutritional, and respiratory therapies (an evidence-based review): report of the Quality Standards Subcommittee of the American Academy of Neurology. *Neurology* *73*, 1218–1226.

Miller, R.G., Jackson, C.E., Kasarskis, E.J., England, J.D., Forshew, D., Johnston, W., Kalra, S., Katz, J.S., Mitsumoto, H., Rosenfeld, J., et al. (2009b). Practice parameter update: the care of the patient with amyotrophic lateral sclerosis: multidisciplinary care, symptom management, and cognitive/behavioral impairment (an evidence-based review): report of the Quality Standards Subcommittee of the American. *Neurology* *73*, 1227–1233.

Miller, R.G., Mitchell, J.D., Lyon, M., and Moore, D.H. (2012a). Riluzole for amyotrophic lateral sclerosis (ALS)/motor neuron disease (MND). *Cochrane Database Syst. Rev.* CD001447.

Miller, R.G., Mitchell, J.D., and Moore, D.H. (2012b). Riluzole for amyotrophic lateral sclerosis (ALS)/motor neuron disease (MND)(Review). *Forbes* *3*, 1–34.

Miller, T.M., Pestronk, A., David, W., Rothstein, J., Simpson, E., Appel, S.H., Andres, P.L., Mahoney, K., Allred, P., Alexander, K., et al. (2013). An antisense oligonucleotide against SOD1 delivered intrathecally for patients with SOD1 familial amyotrophic lateral sclerosis: a phase 1, randomised, first-in-man study. *Lancet. Neurol.* *12*, 435–442.

Mitchell, J.D., and Borasio, G.D. (2007). Amyotrophic lateral sclerosis. *Lancet* *369*, 2031–2041.

Mitchell, J., Paul, P., Chen, H.-J., Morris, A., Payling, M., Falchi, M., Habgood, J., Panoutsou, S., Winkler, S., Tisato, V., et al. (2010). Familial amyotrophic lateral sclerosis is associated with a mutation in D-amino acid oxidase. *Proc. Natl. Acad. Sci. U. S. A.* *107*, 7556–7561.

Mitchell, J.J., Trakadis, Y.J., and Scriver, C.R. (2011). Phenylalanine hydroxylase deficiency. *Genet. Med.* *13*, 697–707.

- Mizielinska, S., and Isaacs, A.M. (2014). C9orf72 amyotrophic lateral sclerosis and frontotemporal dementia: gain or loss of function? *Curr. Opin. Neurol.* *27*, 515–523.
- Mizielinska, S., Grönke, S., Niccoli, T., Ridler, C.E., Clayton, E.L., Devoy, A., Moens, T., Norona, F.E., Woollacott, I.O.C., Pietrzyk, J., et al. (2014). C9orf72 repeat expansions cause neurodegeneration in *Drosophila* through arginine-rich proteins. *Science* *345*, 1192–1194.
- Mizuno, Y., Amari, M., Takatama, M., Aizawa, H., Mihara, B., and Okamoto, K. (2006). Immunoreactivities of p62, an ubiquitin-binding protein, in the spinal anterior horn cells of patients with amyotrophic lateral sclerosis. *J. Neurol. Sci.* *249*, 13–18.
- Morita, M., Aoki, M., Abe, K., Hasegawa, T., Sakuma, R., Onodera, Y., Ichikawa, N., Nishizawa, M., and Itoyama, Y. (1996). A novel two-base mutation in the Cu/Zn superoxide dismutase gene associated with familial amyotrophic lateral sclerosis in Japan. *Neurosci. Lett.* *205*, 79–82.
- Muller, F.L., Song, W., Liu, Y., Chaudhuri, A., Pieke-Dahl, S., Strong, R., Huang, T.-T., Epstein, C.J., Roberts, L.J., Csete, M., et al. (2006). Absence of CuZn superoxide dismutase leads to elevated oxidative stress and acceleration of age-dependent skeletal muscle atrophy. *Free Radic. Biol. Med.* *40*, 1993–2004.
- Mulligan, V.K., and Chakrabartty, A. (2013). Protein misfolding in the late-onset neurodegenerative diseases: common themes and the unique case of amyotrophic lateral sclerosis. *Proteins* *81*, 1285–1303.
- Münch, C., O'Brien, J., and Bertolotti, A. (2011). Prion-like propagation of mutant superoxide dismutase-1 misfolding in neuronal cells. *Proc. Natl. Acad. Sci. U. S. A.* *108*, 3548–3553.
- Murakami, K., Inagaki, J., Saito, M., Ikeda, Y., Tsuda, C., Noda, Y., Kawakami, S., Shirasawa, T., and Shimizu, T. (2009). Skin atrophy in cytoplasmic SOD-deficient mice and its complete recovery using a vitamin C derivative. *Biochem. Biophys. Res. Commun.* *382*, 457–461.
- Murakami, K., Murata, N., Noda, Y., Tahara, S., Kaneko, T., Kinoshita, N., Hatsuta, H., Murayama, S., Barnham, K.J., Irie, K., et al. (2011). SOD1 (copper/zinc superoxide dismutase) deficiency drives amyloid β protein oligomerization and memory loss in mouse model of Alzheimer disease. *J. Biol. Chem.* *286*, 44557–44568.
- Murata, T., Ohtsuka, C., and Terayama, Y. (2008). Increased mitochondrial oxidative damage in patients with sporadic amyotrophic lateral sclerosis. *J. Neurol. Sci.* *267*, 66–69.
- Murray, L.M., Talbot, K., and Gillingwater, T.H. (2010). Review: neuromuscular synaptic vulnerability in motor neurone disease: amyotrophic lateral sclerosis and spinal muscular atrophy. *Neuropathol. Appl. Neurobiol.* *36*, 133–156.
- Nagai, M. et al (2000). Transgenic mice with ALS-linked SOD1 mutant H46R. *Neurosci. Meet. Planner.* New Orleans, LA Soc. Neurosci.

- Nagai, M., Re, D.B., Nagata, T., Chalazonitis, A., Jessell, T.M., Wichterle, H., and Przedborski, S. (2007). Astrocytes expressing ALS-linked mutated SOD1 release factors selectively toxic to motor neurons. *Nat. Neurosci.* *10*, 615–622.
- Nagy, D., Kato, T., and Kushner, P.D. (1994). Reactive astrocytes are widespread in the cortical gray matter of amyotrophic lateral sclerosis. *J. Neurosci. Res.* *38*, 336–347.
- Naini, A., Musumeci, O., Hayes, L., Pallotti, F., Del Bene, M., and Mitsumoto, H. (2002). Identification of a novel mutation in Cu/Zn superoxide dismutase gene associated with familial amyotrophic lateral sclerosis. *J. Neurol. Sci.* *198*, 17–19.
- Nakamura, S., Wate, R., Kaneko, S., Ito, H., Oki, M., Tsuge, A., Nagashima, M., Asayama, S., Fujita, K., Nakamura, M., et al. (2014). An autopsy case of sporadic amyotrophic lateral sclerosis associated with the I113T SOD1 mutation. *Neuropathology* *34*, 58–63.
- Nakashima, K., Watanabe, Y., Kuno, N., Nanba, E., and Takahashi, K. (1995). Abnormality of Cu/Zn superoxide dismutase (SOD1) activity in Japanese familial amyotrophic lateral sclerosis with two base pair deletion in the SOD1 gene. *Neurology* *45*, 1019–1020.
- Nardo, G., Iennaco, R., Fusi, N., Heath, P.R., Marino, M., Trolese, M.C., Ferraiuolo, L., Lawrence, N., Shaw, P.J., and Bendotti, C. (2013). Transcriptomic indices of fast and slow disease progression in two mouse models of amyotrophic lateral sclerosis. *Brain* *136*, 3305–3332.
- Neumann, M., Sampathu, D.M., Kwong, L.K., Truax, A.C., Micsenyi, M.C., Chou, T.T., Bruce, J., Schuck, T., Grossman, M., Clark, C.M., et al. (2006). Ubiquitinated TDP-43 in frontotemporal lobar degeneration and amyotrophic lateral sclerosis. *Science* *314*, 130–133.
- Nishihira, Y., Tan, C.-F., Onodera, O., Toyoshima, Y., Yamada, M., Morita, T., Nishizawa, M., Kakita, A., and Takahashi, H. (2008). Sporadic amyotrophic lateral sclerosis: two pathological patterns shown by analysis of distribution of TDP-43-immunoreactive neuronal and glial cytoplasmic inclusions. *Acta Neuropathol.* *116*, 169–182.
- Nishimura, A.L., Mitne-Neto, M., Silva, H.C.A., Richieri-Costa, A., Middleton, S., Cascio, D., Kok, F., Oliveira, J.R.M., Gillingwater, T., Webb, J., et al. (2004). A mutation in the vesicle-trafficking protein VAPB causes late-onset spinal muscular atrophy and amyotrophic lateral sclerosis. *Am. J. Hum. Genet.* *75*, 822–831.
- Nishioka, N., Nagano, S., Nakayama, R., Kiyonari, H., Ijiri, T., Taniguchi, K., Shawlot, W., Hayashizaki, Y., Westphal, H., Behringer, R.R., et al. (2005). *Ssd1* regulates head morphogenesis of mouse embryos by activating the *Lim1-Ldb1* complex. *Development* *132*, 2535–2546.
- Nishitoh, H., Kadowaki, H., Nagai, A., Maruyama, T., Yokota, T., Fukutomi, H., Noguchi, T., Matsuzawa, A., Takeda, K., and Ichijo, H. (2008). ALS-linked mutant SOD1 induces ER stress- and ASK1-dependent motor neuron death by targeting Derlin-1. *Genes Dev.* *22*, 1451–1464.

- Niu, Y., Shen, B., Cui, Y., Chen, Y., Wang, J., Wang, L., Kang, Y., Zhao, X., Si, W., Li, W., et al. (2014). Generation of gene-modified cynomolgus monkey via Cas9/RNA-mediated gene targeting in one-cell embryos. *Cell* *156*, 836–843.
- Niwa, K., Carlson, G.A., and Iadecola, C. (2000). Exogenous A beta1-40 reproduces cerebrovascular alterations resulting from amyloid precursor protein overexpression in mice. *J. Cereb. Blood Flow Metab.* *20*, 1659–1668.
- Nogales-Gadea, G., Garcia-Arumi, E., Andreu, A.L., Cervera, C., and Gamez, J. (2004). A novel exon 5 mutation (N139H) in the SOD1 gene in a Spanish family associated with incomplete penetrance. *J. Neurol. Sci.* *219*, 1–6.
- Nojiri, H., Saita, Y., Morikawa, D., Kobayashi, K., Tsuda, C., Miyazaki, T., Saito, M., Marumo, K., Yonezawa, I., Kaneko, K., et al. (2011). Cytoplasmic superoxide causes bone fragility owing to low-turnover osteoporosis and impaired collagen cross-linking. *J. Bone Miner. Res.* *26*, 2682–2694.
- Nonaka, T., Masuda-Suzukake, M., Arai, T., Hasegawa, Y., Akatsu, H., Obi, T., Yoshida, M., Murayama, S., Mann, D.M.A., Akiyama, H., et al. (2013). Prion-like properties of pathological TDP-43 aggregates from diseased brains. *Cell Rep.* *4*, 124–134.
- Nordlund, A., Leinartaite, L., Saraboji, K., Aisenbrey, C., Gröbner, G., Zetterström, P., Danielsson, J., Logan, D.T., and Oliveberg, M. (2009). Functional features cause misfolding of the ALS-provoking enzyme SOD1. *Proc. Natl. Acad. Sci. U. S. A.* *106*, 9667–9672.
- Nüsslein-Volhard, C., and Wieschaus, E. (1980). Mutations affecting segment number and polarity in *Drosophila*. *Nature* *287*, 795–801.
- O’Neill, J.P. (2000). DNA damage, DNA repair, cell proliferation, and DNA replication: how do gene mutations result? *Proc. Natl. Acad. Sci. U. S. A.* *97*, 11137–11139.
- O’Reilly, S.A., Roedica, J., Nagy, D., Hallewell, R.A., Alderson, K., Marklund, S.L., Kuby, J., and Kushner, P.D. (1995). Motor neuron-astrocyte interactions and levels of Cu,Zn superoxide dismutase in sporadic amyotrophic lateral sclerosis. *Exp. Neurol.* *131*, 203–210.
- Oeda, T., Shimohama, S., Kitagawa, N., Kohno, R., Imura, T., Shibasaki, H., and Ishii, N. (2001). Oxidative stress causes abnormal accumulation of familial amyotrophic lateral sclerosis-related mutant SOD1 in transgenic *Caenorhabditis elegans*. *Hum. Mol. Genet.* *10*, 2013–2023.
- Okamoto, K., Hirai, S., Yamazaki, T., Sun, X.Y., and Nakazato, Y. (1991). New ubiquitin-positive intraneuronal inclusions in the extra-motor cortices in patients with amyotrophic lateral sclerosis. *Neurosci. Lett.* *129*, 233–236.
- Okamoto, Y., Ihara, M., Urushitani, M., Yamashita, H., Kondo, T., Tanigaki, A., Oono, M., Kawamata, J., Ikemoto, A., Kawamoto, Y., et al. (2011). An autopsy case of SOD1-related ALS with TDP-43 positive inclusions. *Neurology* *77*, 1993–1995.

- Oliver, P.L., and Davies, K.E. (2005). Analysis of human neurological disorders using mutagenesis in the mouse. *Clin. Sci. (Lond)*. *108*, 385–397.
- Oliver, P.L., and Davies, K.E. (2012). New insights into behaviour using mouse ENU mutagenesis. *Hum. Mol. Genet.* *21*, R72–R81.
- Oliver, P.L., Finelli, M.J., Edwards, B., Bitoun, E., Butts, D.L., Becker, E.B.E., Cheeseman, M.T., Davies, B., and Davies, K.E. (2011). *Oxr1* is essential for protection against oxidative stress-induced neurodegeneration. *PLoS Genet.* *7*, e1002338.
- Oosthuysen, B., Moons, L., Storkebaum, E., Beck, H., Nuyens, D., Brusselmans, K., Van Dorpe, J., Hellings, P., Gorselink, M., Heymans, S., et al. (2001). Deletion of the hypoxia-response element in the vascular endothelial growth factor promoter causes motor neuron degeneration. *Nat. Genet.* *28*, 131–138.
- Orlacchio, A., Babalini, C., Borreca, A., Patrono, C., Massa, R., Basaran, S., Munhoz, R.P., Rogaeva, E.A., St George-Hyslop, P.H., Bernardi, G., et al. (2010). SPATACSIN mutations cause autosomal recessive juvenile amyotrophic lateral sclerosis. *Brain* *133*, 591–598.
- Orr, H.T. (2011). FTD and ALS: genetic ties that bind. *Neuron* *72*, 189–190.
- Orrell, R.W., Marklund, S.L., and deBellerocche, J.S. (1997a). Familial ALS is associated with mutations in all exons of SOD1: a novel mutation in exon 3 (Gly72Ser). *J. Neurol. Sci.* *153*, 46–49.
- Orrell, R.W., Habgood, J.J., Gardiner, I., King, A.W., Bowe, F.A., Hallewell, R.A., Marklund, S.L., Greenwood, J., Lane, R.J., and deBellerocche, J. (1997b). Clinical and functional investigation of 10 missense mutations and a novel frameshift insertion mutation of the gene for copper-zinc superoxide dismutase in UK families with amyotrophic lateral sclerosis. *Neurology* *48*, 746–751.
- Orrell, R.W., Habgood, J.J., Malaspina, A., Mitchell, J., Greenwood, J., Lane, R.J., and deBellerocche, J.S. (1999). Clinical characteristics of SOD1 gene mutations in UK families with ALS. *J. Neurol. Sci.* *169*, 56–60.
- Ota, S., Tsuchiya, K., and Akiyama, H. (2005). “Forme fruste” of amyotrophic lateral sclerosis with dementia: a report of five autopsy cases without dementia and with ubiquitinated intraneuronal inclusions. *Neuropathology* *25*, 326–335.
- Pan, L., Yoshii, Y., Otomo, A., Ogawa, H., Iwasaki, Y., Shang, H.-F., and Hadano, S. (2012). Different human copper-zinc superoxide dismutase mutants, SOD1G93A and SOD1H46R, exert distinct harmful effects on gross phenotype in mice. *PLoS One* *7*, e33409.
- Park, E.Y., and Rho, H.M. (2002). The transcriptional activation of the human copper/zinc superoxide dismutase gene by 2,3,7,8-tetrachlorodibenzo-p-dioxin through two different regulator sites, the antioxidant responsive element and xenobiotic responsive element. *Mol. Cell. Biochem.* *240*, 47–55.

- Parkinson, N., Ince, P.G., Smith, M.O., Highley, R., Skibinski, G., Andersen, P.M., Morrison, K.E., Pall, H.S., Hardiman, O., Collinge, J., et al. (2006). ALS phenotypes with mutations in CHMP2B (charged multivesicular body protein 2B). *Neurology* 67, 1074–1077.
- Pasinelli, P., and Brown, R.H. (2006). Molecular biology of amyotrophic lateral sclerosis: insights from genetics. *Nat. Rev. Neurosci.* 7, 710–723.
- Pasinelli, P., Belford, M.E., Lennon, N., Bacskai, B.J., Hyman, B.T., Trotti, D., and Brown, R.H. (2004). Amyotrophic lateral sclerosis-associated SOD1 mutant proteins bind and aggregate with Bcl-2 in spinal cord mitochondria. *Neuron* 43, 19–30.
- Penco, S., Schenone, A., Bordo, D., Bolognesi, M., Abbruzzese, M., Bugiani, O., Ajmar, F., and Garrè, C. (1999). A SOD1 gene mutation in a patient with slowly progressing familial ALS. *Neurology* 53, 404–406.
- Perrin, S. (2014). Make mouse studies work. *Nature* 507, 423.
- Petkova, A.T., Leapman, R.D., Guo, Z., Yau, W.-M., Mattson, M.P., and Tycko, R. (2005). Self-propagating, molecular-level polymorphism in Alzheimer's beta-amyloid fibrils. *Science* 307, 262–265.
- Phillips, J.P., Tainer, J.A., Getzoff, E.D., Boulianne, G.L., Kirby, K., and Hilliker, A.J. (1995). Subunit-destabilizing mutations in *Drosophila* copper/zinc superoxide dismutase: neuropathology and a model of dimer dysequilibrium. *Proc. Natl. Acad. Sci. U. S. A.* 92, 8574–8578.
- Piao, Y.-S., Wakabayashi, K., Kakita, A., Yamada, M., Hayashi, S., Morita, T., Ikuta, F., Oyanagi, K., and Takahashi, H. (2003). Neuropathology with clinical correlations of sporadic amyotrophic lateral sclerosis: 102 autopsy cases examined between 1962 and 2000. *Brain Pathol.* 13, 10–22.
- Pizzasegola, C., Caron, I., Daleno, C., Ronchi, A., Minoia, C., Carri, M.T., and Bendotti, C. (2009). Treatment with lithium carbonate does not improve disease progression in two different strains of SOD1 mutant mice. *Amyotroph. Lateral Scler.* 10, 221–228.
- Pokrishevsky, E., Grad, L.I., Yousefi, M., Wang, J., Mackenzie, I.R., and Cashman, N.R. (2012). Aberrant localization of FUS and TDP43 is associated with misfolding of SOD1 in amyotrophic lateral sclerosis. *PLoS One* 7, e35050.
- Polymenidou, M., and Cleveland, D.W. (2012). Prion-like spread of protein aggregates in neurodegeneration. *J. Exp. Med.* 209, 889–893.
- Poon, H.F., Hensley, K., Thongboonkerd, V., Merchant, M.L., Lynn, B.C., Pierce, W.M., Klein, J.B., Calabrese, V., and Butterfield, D.A. (2005). Redox proteomics analysis of oxidatively modified proteins in G93A-SOD1 transgenic mice—a model of familial amyotrophic lateral sclerosis. *Free Radic. Biol. Med.* 39, 453–462.
- Pramatarova, A., Figlewicz, D.A., Krizus, A., Han, F.Y., Ceballos-Picot, I., Nicole, A., Dib, M., Meininger, V., Brown, R.H., and Rouleau, G.A. (1995). Identification of new

- mutations in the Cu/Zn superoxide dismutase gene of patients with familial amyotrophic lateral sclerosis. *Am. J. Hum. Genet.* *56*, 592–596.
- Pramatarova, A., Laganière, J., Roussel, J., Brisebois, K., and Rouleau, G.A. (2001). Neuron-specific expression of mutant superoxide dismutase 1 in transgenic mice does not lead to motor impairment. *J. Neurosci.* *21*, 3369–3374.
- Prudencio, M., Hart, P.J., Borchelt, D.R., and Andersen, P.M. (2009a). Variation in aggregation propensities among ALS-associated variants of SOD1: Correlation to human disease. *Hum. Mol. Genet.* *18*, 3217–3226.
- Prudencio, M., Hart, P.J., Borchelt, D.R., and Andersen, P.M. (2009b). Variation in aggregation propensities among ALS-associated variants of SOD1: Correlation to human disease. *Hum. Mol. Genet.* *18*, 3217–3226.
- Prudencio, M., Durazo, A., Whitelegge, J.P., and Borchelt, D.R. (2009c). Modulation of mutant superoxide dismutase 1 aggregation by co-expression of wild-type enzyme. *J. Neurochem.* *108*, 1009–1018.
- Prudencio, M., Durazo, A., Whitelegge, J.P., and Borchelt, D.R. (2010). An examination of wild-type SOD1 in modulating the toxicity and aggregation of ALS-associated mutant SOD1. *Hum. Mol. Genet.* *19*, 4774–4789.
- Pupillo, E., Messina, P., Logroscino, G., Zoccolella, S., Chiò, A., Calvo, A., Corbo, M., Lunetta, C., Micheli, A., Millul, A., et al. (2012). Trauma and amyotrophic lateral sclerosis: a case-control study from a population-based registry. *Eur. J. Neurol.* *19*, 1509–1517.
- Qualls, D.A., Prudencio, M., Roberts, B.L.T., Crosby, K., Brown, H., and Borchelt, D.R. (2013). Features of wild-type human SOD1 limit interactions with misfolded aggregates of mouse G86R Sod1. *Mol. Neurodegener.* *8*, 46.
- Quwailid, M.M., Hugill, A., Dear, N., Vizor, L., Wells, S., Horner, E., Fuller, S., Weedon, J., McMath, H., Woodman, P., et al. (2004). A gene-driven ENU-based approach to generating an allelic series in any gene. *Mamm. Genome* *15*, 585–591.
- Radyuk, S.N., Klichko, V.I., and Orr, W.C. (2004). Profiling Cu,Zn-superoxide dismutase expression in *Drosophila melanogaster*--a critical regulatory role for intron/exon sequence within the coding domain. *Gene* *328*, 37–48.
- Rakhit, R., and Chakrabartty, A. (2006). Structure, folding, and misfolding of Cu,Zn superoxide dismutase in amyotrophic lateral sclerosis. *Biochim. Biophys. Acta* *1762*, 1025–1037.
- Rakhit, R., Cunningham, P., Furtos-Matei, A., Dahan, S., Qi, X.-F., Crow, J.P., Cashman, N.R., Kondejewski, L.H., and Chakrabartty, A. (2002). Oxidation-induced misfolding and aggregation of superoxide dismutase and its implications for amyotrophic lateral sclerosis. *J. Biol. Chem.* *277*, 47551–47556.
- Rakhit, R., Crow, J.P., Lepock, J.R., Kondejewski, L.H., Cashman, N.R., and Chakrabartty, A. (2004). Monomeric Cu,Zn-superoxide dismutase is a common

misfolding intermediate in the oxidation models of sporadic and familial amyotrophic lateral sclerosis. *J. Biol. Chem.* *279*, 15499–15504.

Rakhit, R., Robertson, J., Vande Velde, C., Horne, P., Ruth, D.M., Griffin, J., Cleveland, D.W., Cashman, N.R., and Chakrabartty, A. (2007). An immunological epitope selective for pathological monomer-misfolded SOD1 in ALS. *Nat. Med.* *13*, 754–759.

Ralph, G.S., Radcliffe, P.A., Day, D.M., Carthy, J.M., Leroux, M.A., Lee, D.C.P., Wong, L.-F., Bilsland, L.G., Greensmith, L., Kingsman, S.M., et al. (2005). Silencing mutant SOD1 using RNAi protects against neurodegeneration and extends survival in an ALS model. *Nat. Med.* *11*, 429–433.

Raoul, C., Abbas-Terki, T., Bensadoun, J.-C., Guillot, S., Haase, G., Szulc, J., Henderson, C.E., and Aebischer, P. (2005). Lentiviral-mediated silencing of SOD1 through RNA interference retards disease onset and progression in a mouse model of ALS. *Nat. Med.* *11*, 423–428.

Ratovitski, T., Corson, L.B., Strain, J., Wong, P., Cleveland, D.W., Culotta, V.C., and Borchelt, D.R. (1999). Variation in the biochemical/biophysical properties of mutant superoxide dismutase 1 enzymes and the rate of disease progression in familial amyotrophic lateral sclerosis kindreds. *Hum. Mol. Genet.* *8*, 1451–1460.

Ravikumar, B., Acevedo-Arozena, A., Imarisio, S., Berger, Z., Vacher, C., O’Kane, C.J., Brown, S.D.M., and Rubinsztein, D.C. (2005). Dynein mutations impair autophagic clearance of aggregate-prone proteins. *Nat. Genet.* *37*, 771–776.

Ravits, J., Paul, P., and Jorg, C. (2007a). Focality of upper and lower motor neuron degeneration at the clinical onset of ALS. *Neurology* *68*, 1571–1575.

Ravits, J., Laurie, P., Fan, Y., and Moore, D.H. (2007b). Implications of ALS focality: rostral-caudal distribution of lower motor neuron loss postmortem. *Neurology* *68*, 1576–1582.

Ray, S.S., Nowak, R.J., Strokovich, K., Brown, R.H., Walz, T., and Lansbury, P.T. (2004). An intersubunit disulfide bond prevents in vitro aggregation of a superoxide dismutase-1 mutant linked to familial amyotrophic lateral sclerosis. *Biochemistry* *43*, 4899–4905.

Reaume, A.G., Elliott, J.L., Hoffman, E.K., Kowall, N.W., Ferrante, R.J., Siwek, D.F., Wilcox, H.M., Flood, D.G., Beal, M.F., Brown, R.H., et al. (1996). Motor neurons in Cu/Zn superoxide dismutase-deficient mice develop normally but exhibit enhanced cell death after axonal injury. *Nat. Genet.* *13*, 43–47.

Reddi, A.R., and Culotta, V.C. (2013). SOD1 integrates signals from oxygen and glucose to repress respiration. *Cell* *152*, 224–235.

Redler, R.L., Wilcox, K.C., Proctor, E.A., Fee, L., Caplow, M., and Dokholyan, N. V. (2011). Glutathionylation at Cys-111 induces dissociation of wild type and FALS mutant SOD1 dimers. *Biochemistry* *50*, 7057–7066.

- Renton, A.E., Majounie, E., Waite, A., Simón-Sánchez, J., Rollinson, S., Gibbs, J.R., Schymick, J.C., Laaksovirta, H., van Swieten, J.C., Myllykangas, L., et al. (2011). A hexanucleotide repeat expansion in C9ORF72 is the cause of chromosome 9p21-linked ALS-FTD. *Neuron* *72*, 257–268.
- Renton, A.E., Chiò, A., and Traynor, B.J. (2014). State of play in amyotrophic lateral sclerosis genetics. *Nat. Neurosci.* *17*, 17–23.
- Riboldi, G., Nizzardo, M., Simone, C., Falcone, M., Bresolin, N., Comi, G.P., and Corti, S. (2011). ALS genetic modifiers that increase survival of SOD1 mice and are suitable for therapeutic development. *Prog. Neurobiol.* *95*, 133–148.
- Ringholz, G.M., Appel, S.H., Bradshaw, M., Cooke, N.A., Mosnik, D.M., and Schulz, P.E. (2005). Prevalence and patterns of cognitive impairment in sporadic ALS. *Neurology* *65*, 586–590.
- Ripps, M.E., Huntley, G.W., Hof, P.R., Morrison, J.H., and Gordon, J.W. (1995). Transgenic mice expressing an altered murine superoxide dismutase gene provide an animal model of amyotrophic lateral sclerosis. *Proc. Natl. Acad. Sci. U. S. A.* *92*, 689–693.
- Robberecht, W., Sapp, P., Viaene, M.K., Rosen, D., McKenna-Yasek, D., Haines, J., Horvitz, R., Theys, P., and Brown, R. (1994). Cu/Zn superoxide dismutase activity in familial and sporadic amyotrophic lateral sclerosis. *J. Neurochem.* *62*, 384–387.
- Robertson, J., Sanelli, T., Xiao, S., Yang, W., Horne, P., Hammond, R., Piro, E.P., and Strong, M.J. (2007). Lack of TDP-43 abnormalities in mutant SOD1 transgenic mice shows disparity with ALS. *Neurosci. Lett.* *420*, 128–132.
- Rodriguez, J.A., Valentine, J.S., Eggers, D.K., Roe, J.A., Tiwari, A., Brown, R.H., and Hayward, L.J. (2002). Familial amyotrophic lateral sclerosis-associated mutations decrease the thermal stability of distinctly metallated species of human copper/zinc superoxide dismutase. *J. Biol. Chem.* *277*, 15932–15937.
- Rodriguez, J.A., Shaw, B.F., Durazo, A., Sohn, S.H., Doucette, P.A., Nersissian, A.M., Faull, K.F., Eggers, D.K., Tiwari, A., Hayward, L.J., et al. (2005). Destabilization of apoprotein is insufficient to explain Cu,Zn-superoxide dismutase-linked ALS pathogenesis. *Proc. Natl. Acad. Sci. U. S. A.* *102*, 10516–10521.
- Roe, J.A., Butler, A., Scholler, D.M., Valentine, J.S., Marky, L., and Breslauer, K.J. (1988). Differential scanning calorimetry of Cu,Zn-superoxide dismutase, the apoprotein, and its zinc-substituted derivatives. *Biochemistry* *27*, 950–958.
- Rohrer, J.D., Isaacs, A.M., Mizlienska, S., Mead, S., Lashley, T., Wray, S., Sidle, K., Fratta, P., Orrell, R.W., Hardy, J., et al. (2015). C9orf72 expansions in frontotemporal dementia and amyotrophic lateral sclerosis. *Lancet. Neurol.* *14*, 291–301.
- Romanuik, T.L., Wang, G., Holt, R.A., Jones, S.J.M., Marra, M.A., and Sadar, M.D. (2009). Identification of novel androgen-responsive genes by sequencing of LongSAGE libraries. *BMC Genomics* *10*, 476.

- Rosen, D.R., Siddique, T., Patterson, D., Figlewicz, D.A., Sapp, P., Hentati, A., Donaldson, D., Goto, J., O'Regan, J.P., and Deng, H.X. (1993). Mutations in Cu/Zn superoxide dismutase gene are associated with familial amyotrophic lateral sclerosis. *Nature* 362, 59–62.
- Rosen, D.R., Bowling, A.C., Patterson, D., Usdin, T.B., Sapp, P., Mezey, E., McKenna-Yasek, D., O'Regan, J., Rahmani, Z., and Ferrante, R.J. (1994). A frequent ala 4 to val superoxide dismutase-1 mutation is associated with a rapidly progressive familial amyotrophic lateral sclerosis. *Hum. Mol. Genet.* 3, 981–987.
- Ross, C.A., and Poirier, M.A. (2004). Protein aggregation and neurodegenerative disease. *Nat. Med.* 10 *Suppl*, S10–S17.
- Ross, C.A., and Poirier, M.A. (2005). Opinion: What is the role of protein aggregation in neurodegeneration? *Nat. Rev. Mol. Cell Biol.* 6, 891–898.
- Rothstein, J.D. (1995). Excitotoxic mechanisms in the pathogenesis of amyotrophic lateral sclerosis. *Adv. Neurol.* 68, 7–20; discussion 21–27.
- Rothstein, J.D. (2009). Current hypotheses for the underlying biology of amyotrophic lateral sclerosis. *Ann. Neurol.* 65 *Suppl* 1, S3–S9.
- Rotunno, M.S., and Bosco, D. a (2013). An emerging role for misfolded wild-type SOD1 in sporadic ALS pathogenesis. *Front. Cell. Neurosci.* 7, 253.
- Rubio-Aliaga, I., Soewarto, D., Wagner, S., Klaften, M., Fuchs, H., Kalaydjiev, S., Busch, D.H., Klempt, M., Rathkolb, B., Wolf, E., et al. (2007). A genetic screen for modifiers of the delta1-dependent notch signaling function in the mouse. *Genetics* 175, 1451–1463.
- Russell, W.L., Kelly, E.M., Hunsicker, P.R., Bangham, J.W., Maddux, S.C., and Phipps, E.L. (1979). Specific-locus test shows ethylnitrosourea to be the most potent mutagen in the mouse. *Proc. Natl. Acad. Sci. U. S. A.* 76, 5818–5819.
- Saccon, R.A., Bunton-Stasyshyn, R.K.A., Fisher, E.M.C., and Fratta, P. (2013). Is SOD1 loss of function involved in amyotrophic lateral sclerosis? *Brain* 136, 2342–2358.
- Sahawneh, M.A., Ricart, K.C., Roberts, B.R., Bomben, V.C., Basso, M., Ye, Y., Sahawneh, J., Franco, M.C., Beckman, J.S., and Estévez, A.G. (2010). Cu,Zn-superoxide dismutase increases toxicity of mutant and zinc-deficient superoxide dismutase by enhancing protein stability. *J. Biol. Chem.* 285, 33885–33897.
- Saito, Y., Yokota, T., Mitani, T., Ito, K., Anzai, M., Miyagishi, M., Taira, K., and Mizusawa, H. (2005). Transgenic small interfering RNA halts amyotrophic lateral sclerosis in a mouse model. *J. Biol. Chem.* 280, 42826–42830.
- Sakellariou, G.K., Davis, C.S., Shi, Y., Ivannikov, M. V, Zhang, Y., Vasilaki, A., Macleod, G.T., Richardson, A., Van Remmen, H., Jackson, M.J., et al. (2014). Neuron-specific expression of CuZnSOD prevents the loss of muscle mass and function that occurs in homozygous CuZnSOD-knockout mice. *FASEB J.* 28, 1666–1681.

- Sapp, P.C., Hosler, B.A., McKenna-Yasek, D., Chin, W., Gann, A., Genise, H., Gorenstein, J., Huang, M., Sailer, W., Scheffler, M., et al. (2003). Identification of two novel loci for dominantly inherited familial amyotrophic lateral sclerosis. *Am. J. Hum. Genet.* *73*, 397–403.
- Sasaki, S., and Iwata, M. (1996). Impairment of fast axonal transport in the proximal axons of anterior horn neurons in amyotrophic lateral sclerosis. *Neurology* *47*, 535–540.
- Sasaki, S., Shibata, N., Komori, T., and Iwata, M. (2000). iNOS and nitrotyrosine immunoreactivity in amyotrophic lateral sclerosis. *Neurosci. Lett.* *291*, 44–48.
- Sasaki, S., Aoki, M., Nagai, M., Kobayashi, M., and Itoyama, Y. (2009). Mitochondrial alterations in transgenic mice with an H46R mutant Cu/Zn superoxide dismutase gene. *J. Neuropathol. Exp. Neurol.* *68*, 365–373.
- Sato, T., Nakanishi, T., Yamamoto, Y., Andersen, P.M., Ogawa, Y., Fukada, K., Zhou, Z., Aoike, F., Sugai, F., Nagano, S., et al. (2005). Rapid disease progression correlates with instability of mutant SOD1 in familial ALS. *Neurology* *65*, 1954–1957.
- Sau, D., Rusmini, P., Crippa, V., Onesto, E., Bolzoni, E., Ratti, A., and Poletti, A. (2011). Dysregulation of axonal transport and motorneuron diseases. *Biol. Cell* *103*, 87–107.
- Saxena, S., Cabuy, E., and Caroni, P. (2009). A role for motoneuron subtype-selective ER stress in disease manifestations of FALS mice. *Nat. Neurosci.* *12*, 627–636.
- Schiffer, D., Cordera, S., Cavalla, P., and Migheli, A. (1996). Reactive astrogliosis of the spinal cord in amyotrophic lateral sclerosis. *J. Neurol. Sci.* *139 Suppl*, 27–33.
- Schuster, C., Kasper, E., Machts, J., Bittner, D., Kaufmann, J., Benecke, R., Teipel, S., Vielhaber, S., and Prudlo, J. (2013). Focal thinning of the motor cortex mirrors clinical features of amyotrophic lateral sclerosis and their phenotypes: a neuroimaging study. *J. Neurol.* *260*, 2856–2864.
- Schwartz, P.J., Reaume, A., Scott, R., and Coyle, J.T. (1998). Effects of over- and under-expression of Cu,Zn-superoxide dismutase on the toxicity of glutamate analogs in transgenic mouse striatum. *Brain Res.* *789*, 32–39.
- Seetharaman, S. V, Prudencio, M., Karch, C., Holloway, S.P., Borchelt, D.R., and Hart, P.J. (2009). Immature copper-zinc superoxide dismutase and familial amyotrophic lateral sclerosis. *Exp. Biol. Med.* (Maywood). *234*, 1140–1154.
- Seetharaman, S. V, Taylor, A.B., Holloway, S., and Hart, P.J. (2010). Structures of mouse SOD1 and human/mouse SOD1 chimeras. *Arch. Biochem. Biophys.* *503*, 183–190.
- Segovia-Silvestre, T., Andreu, A.L., Vives-Bauza, C., Garcia-Arumi, E., Cervera, C., and Gamez, J. (2002). A novel exon 3 mutation (D76V) in the SOD1 gene associated with slowly progressive ALS. *Amyotroph. Lateral Scler. Other Motor Neuron Disord.* *3*, 69–74.

- Shan, X., Vocadlo, D., and Krieger, C. (2009). Mislocalization of TDP-43 in the G93A mutant SOD1 transgenic mouse model of ALS. *Neurosci. Lett.* *458*, 70–74.
- Shaw, C.A., and Wilson, J.M.B. (2003). Analysis of neurological disease in four dimensions: insight from ALS-PDC epidemiology and animal models. *Neurosci. Biobehav. Rev.* *27*, 493–505.
- Shaw, P.J., and Ince, P.G. (1997). Glutamate, excitotoxicity and amyotrophic lateral sclerosis. *J. Neurol.* *244 Suppl*, S3–S14.
- Shaw, P.J., Ince, P.G., Falkous, G., and Mantle, D. (1995). Oxidative damage to protein in sporadic motor neuron disease spinal cord. *Ann. Neurol.* *38*, 691–695.
- Shefner, J.M., Reaume, A.G., Flood, D.G., Scott, R.W., Kowall, N.W., Ferrante, R.J., Siwek, D.F., Upton-Rice, M., and Brown, R.H. (1999). Mice lacking cytosolic copper/zinc superoxide dismutase display a distinctive motor axonopathy. *Neurology* *53*, 1239–1246.
- Sher, R.B., Heiman-Patterson, T.D., Blankenhorn, E.A., Jiang, J., Alexander, G., Deitch, J.S., and Cox, G.A. (2014). A major QTL on mouse chromosome 17 resulting in lifespan variability in SOD1-G93A transgenic mouse models of amyotrophic lateral sclerosis. *Amyotroph. Lateral Scler. Frontotemporal Degener.* *15*, 588–600.
- Sherman, L., Dafni, N., Lieman-Hurwitz, J., and Groner, Y. (1983). Nucleotide sequence and expression of human chromosome 21-encoded superoxide dismutase mRNA. *Proc. Natl. Acad. Sci. U. S. A.* *80*, 5465–5469.
- Shibata, N., Hirano, A., Kobayashi, M., Sasaki, S., Kato, T., Matsumoto, S., Shiozawa, Z., Komori, T., Ikemoto, A., and Umahara, T. (1994). Cu/Zn superoxide dismutase-like immunoreactivity in Lewy body-like inclusions of sporadic amyotrophic lateral sclerosis. *Neurosci. Lett.* *179*, 149–152.
- Shibata, N., Hirano, A., Kobayashi, M., Siddique, T., Deng, H.X., Hung, W.Y., Kato, T., and Asayama, K. (1996a). Intense superoxide dismutase-1 immunoreactivity in intracytoplasmic hyaline inclusions of familial amyotrophic lateral sclerosis with posterior column involvement. *J. Neuropathol. Exp. Neurol.* *55*, 481–490.
- Shibata, N., Asayama, K., Hirano, A., and Kobayashi, M. (1996b). Immunohistochemical study on superoxide dismutases in spinal cords from autopsied patients with amyotrophic lateral sclerosis. *Dev. Neurosci.* *18*, 492–498.
- Shibata, N., Nagai, R., Uchida, K., Horiuchi, S., Yamada, S., Hirano, A., Kawaguchi, M., Yamamoto, T., Sasaki, S., and Kobayashi, M. (2001). Morphological evidence for lipid peroxidation and protein glycoxidation in spinal cords from sporadic amyotrophic lateral sclerosis patients. *Brain Res.* *917*, 97–104.
- Shibata, N., Yamada, S., Uchida, K., Hirano, A., Sakoda, S., Fujimura, H., Sasaki, S., Iwata, M., Toi, S., Kawaguchi, M., et al. (2004). Accumulation of protein-bound 4-hydroxy-2-hexenal in spinal cords from patients with sporadic amyotrophic lateral sclerosis. *Brain Res.* *1019*, 170–177.

- Shimizu, H., Toyoshima, Y., Shiga, A., Yokoseki, A., Arakawa, K., Sekine, Y., Shimohata, T., Ikeuchi, T., Nishizawa, M., Kakita, A., et al. (2013). Sporadic ALS with compound heterozygous mutations in the SQSTM1 gene. *Acta Neuropathol.* *126*, 453–459.
- Siddique, T., and Ajroud-Driss, S. (2011). Familial amyotrophic lateral sclerosis, a historical perspective. *Acta Myol.* *30*, 117–120.
- Siklós, L., Engelhardt, J., Harati, Y., Smith, R.G., Joó, F., and Appel, S.H. (1996). Ultrastructural evidence for altered calcium in motor nerve terminals in amyotrophic lateral sclerosis. *Ann. Neurol.* *39*, 203–216.
- Simpson, E.P., Henry, Y.K., Henkel, J.S., Smith, R.G., and Appel, S.H. (2004). Increased lipid peroxidation in sera of ALS patients: a potential biomarker of disease burden. *Neurology* *62*, 1758–1765.
- Smith, C.D., Carney, J.M., Starke-Reed, P.E., Oliver, C.N., Stadtman, E.R., Floyd, R.A., and Markesbery, W.R. (1991). Excess brain protein oxidation and enzyme dysfunction in normal aging and in Alzheimer disease. *Proc. Natl. Acad. Sci. U. S. A.* *88*, 10540–10543.
- Smith, R.A., Miller, T.M., Yamanaka, K., Monia, B.P., Condon, T.P., Hung, G., Lobsiger, C.S., Ward, C.M., McAlonis-Downes, M., Wei, H., et al. (2006). Antisense oligonucleotide therapy for neurodegenerative disease. *J. Clin. Invest.* *116*, 2290–2296.
- Smith, R.G., Henry, Y.K., Mattson, M.P., and Appel, S.H. (1998). Presence of 4-hydroxynonenal in cerebrospinal fluid of patients with sporadic amyotrophic lateral sclerosis. *Ann. Neurol.* *44*, 696–699.
- Sreedharan, J., Blair, I.P., Tripathi, V.B., Hu, X., Vance, C., Rogelj, B., Ackerley, S., Durnall, J.C., Williams, K.L., Buratti, E., et al. (2008). TDP-43 mutations in familial and sporadic amyotrophic lateral sclerosis. *Science* *319*, 1668–1672.
- St Johnston, D. (2002). The art and design of genetic screens: *Drosophila melanogaster*. *Nat. Rev. Genet.* *3*, 176–188.
- Stadtman, E.R. (1992). Protein oxidation and aging. *Science* *257*, 1220–1224.
- Stadtman, E.R., and Berlett, B.S. (1997). Reactive oxygen-mediated protein oxidation in aging and disease. *Chem. Res. Toxicol.* *10*, 485–494.
- Stewart, H.G., Mackenzie, I.R., Eisen, A., Brännström, T., Marklund, S.L., and Andersen, P.M. (2006). Clinicopathological phenotype of ALS with a novel G72C SOD1 gene mutation mimicking a myopathy. *Muscle Nerve* *33*, 701–706.
- Strey, C.W., Spellman, D., Stieber, A., Gonatas, J.O., Wang, X., Lambris, J.D., and Gonatas, N.K. (2004). Dysregulation of stathmin, a microtubule-destabilizing protein, and up-regulation of Hsp25, Hsp27, and the antioxidant peroxiredoxin 6 in a mouse model of familial amyotrophic lateral sclerosis. *Am. J. Pathol.* *165*, 1701–1718.

- Ström, A.-L., Shi, P., Zhang, F., Gal, J., Kilty, R., Hayward, L.J., and Zhu, H. (2008). Interaction of amyotrophic lateral sclerosis (ALS)-related mutant copper-zinc superoxide dismutase with the dynein-dynactin complex contributes to inclusion formation. *J. Biol. Chem.* *283*, 22795–22805.
- Strong, M., and Rosenfeld, J. (2003). Amyotrophic lateral sclerosis: a review of current concepts. *Amyotroph. Lateral Scler. Other Motor Neuron Disord.* *4*, 136–143.
- Strong, M.J., Grace, G.M., Orange, J.B., and Leeper, H.A. (1996). Cognition, language, and speech in amyotrophic lateral sclerosis: a review. *J. Clin. Exp. Neuropsychol.* *18*, 291–303.
- Sturtz, L.A., Diekert, K., Jensen, L.T., Lill, R., and Culotta, V.C. (2001). A fraction of yeast Cu,Zn-superoxide dismutase and its metallochaperone, CCS, localize to the intermembrane space of mitochondria. A physiological role for SOD1 in guarding against mitochondrial oxidative damage. *J. Biol. Chem.* *276*, 38084–38089.
- Su, X.W., Broach, J.R., Connor, J.R., Gerhard, G.S., and Simmons, Z. (2014). Genetic heterogeneity of amyotrophic lateral sclerosis: implications for clinical practice and research. *Muscle Nerve* *49*, 786–803.
- Subramaniam, J.R., Lyons, W.E., Liu, J., Bartnikas, T.B., Rothstein, J., Price, D.L., Cleveland, D.W., Gitlin, J.D., and Wong, P.C. (2002). Mutant SOD1 causes motor neuron disease independent of copper chaperone-mediated copper loading. *Nat. Neurosci.* *5*, 301–307.
- Sugiyama, M., Takao, M., Hatsuta, H., Funabe, S., Ito, S., Obi, T., Tanaka, F., Kuroiwa, Y., and Murayama, S. (2013). Increased number of astrocytes and macrophages/microglial cells in the corpus callosum in amyotrophic lateral sclerosis. *Neuropathology* *33*, 591–599.
- Sumi, H., Kato, S., Mochimaru, Y., Fujimura, H., Etoh, M., and Sakoda, S. (2009). Nuclear TAR DNA binding protein 43 expression in spinal cord neurons correlates with the clinical course in amyotrophic lateral sclerosis. *J. Neuropathol. Exp. Neurol.* *68*, 37–47.
- Sun, M., Mondal, K., Patel, V., Horner, V.L., Long, A.B., Cutler, D.J., Caspary, T., and Zwick, M.E. (2012). Multiplex Chromosomal Exome Sequencing Accelerates Identification of ENU-Induced Mutations in the Mouse. *G3 (Bethesda)*. *2*, 143–150.
- Sundaramoorthy, V., Walker, A.K., Yerbury, J., Soo, K.Y., Farg, M.A., Hoang, V., Zeineddine, R., Spencer, D., and Atkin, J.D. (2013). Extracellular wildtype and mutant SOD1 induces ER-Golgi pathology characteristic of amyotrophic lateral sclerosis in neuronal cells. *Cell. Mol. Life Sci.* *70*, 4181–4195.
- Swerdlow, R.H., Parks, J.K., Cassarino, D.S., Trimmer, P.A., Miller, S.W., Maguire, D.J., Sheehan, J.P., Maguire, R.S., Pattee, G., Juel, V.C., et al. (1998). Mitochondria in sporadic amyotrophic lateral sclerosis. *Exp. Neurol.* *153*, 135–142.

- Synofzik, M., Fernández-Santiago, R., Maetzler, W., Schöls, L., and Andersen, P.M. (2010). The human G93A SOD1 phenotype closely resembles sporadic amyotrophic lateral sclerosis. *J. Neurol. Neurosurg. Psychiatry* *81*, 764–767.
- Synofzik, M., Ronchi, D., Keskin, I., Basak, A.N., Wilhelm, C., Gobbi, C., Birve, A., Biskup, S., Zecca, C., Fernández-Santiago, R., et al. (2012). Mutant superoxide dismutase-1 indistinguishable from wild-type causes ALS. *Hum. Mol. Genet.* *21*, 3568–3574.
- Tainer, J.A., Getzoff, E.D., Beem, K.M., Richardson, J.S., and Richardson, D.C. (1982). Determination and analysis of the 2 A-structure of copper, zinc superoxide dismutase. *J. Mol. Biol.* *160*, 181–217.
- Takahashi, M., Dinse, G.E., Foley, J.F., Hardisty, J.F., and Maronpot, R.R. (2002). Comparative prevalence, multiplicity, and progression of spontaneous and vinyl carbamate-induced liver lesions in five strains of male mice. *Toxicol. Pathol.* *30*, 599–605.
- Takahashi, T., Yagishita, S., Amano, N., Yamaoka, K., and Kamei, T. (1997). Amyotrophic lateral sclerosis with numerous axonal spheroids in the corticospinal tract and massive degeneration of the cortex. *Acta Neuropathol.* *94*, 294–299.
- Takehisa, Y., Ujike, H., Ishizu, H., Terada, S., Haraguchi, T., Tanaka, Y., Nishinaka, T., Nobukuni, K., Ihara, Y., Namba, R., et al. (2001). Familial amyotrophic lateral sclerosis with a novel Leu126Ser mutation in the copper/zinc superoxide dismutase gene showing mild clinical features and lewy body-like hyaline inclusions. *Arch. Neurol.* *58*, 736–740.
- Talbot, K. (2009). Another gene for ALS: mutations in sporadic cases and the rare variant hypothesis. *Neurology* *73*, 1172–1173.
- Tan, C.-F., Eguchi, H., Tagawa, A., Onodera, O., Iwasaki, T., Tsujino, A., Nishizawa, M., Kakita, A., and Takahashi, H. (2007). TDP-43 immunoreactivity in neuronal inclusions in familial amyotrophic lateral sclerosis with or without SOD1 gene mutation. *Acta Neuropathol.* *113*, 535–542.
- Telling, G.C., Scott, M., Mastrianni, J., Gabizon, R., Torchia, M., Cohen, F.E., DeArmond, S.J., and Prusiner, S.B. (1995). Prion propagation in mice expressing human and chimeric PrP transgenes implicates the interaction of cellular PrP with another protein. *Cell* *83*, 79–90.
- Teuling, E., van Dis, V., Wulf, P.S., Haasdijk, E.D., Akhmanova, A., Hoogenraad, C.C., and Jaarsma, D. (2008). A novel mouse model with impaired dynein/dynactin function develops amyotrophic lateral sclerosis (ALS)-like features in motor neurons and improves lifespan in SOD1-ALS mice. *Hum. Mol. Genet.* *17*, 2849–2862.
- Thonhoff, J.R., Gao, J., Dunn, T.J., Ojeda, L., and Wu, P. (2012). Mutant SOD1 microglia-generated nitroxidative stress promotes toxicity to human fetal neural stem cell-derived motor neurons through direct damage and noxious interactions with astrocytes. *Am. J. Stem Cells* *1*, 2–21.

Thorns, J., Jansma, H., Peschel, T., Grosskreutz, J., Mohammadi, B., Dengler, R., and Münte, T.F. (2013). Extent of cortical involvement in amyotrophic lateral sclerosis--an analysis based on cortical thickness. *BMC Neurol.* *13*, 148.

Thornton, C.E., Brown, S.D., and Glenister, P.H. (1999). Large numbers of mice established by in vitro fertilization with cryopreserved spermatozoa: implications and applications for genetic resource banks, mutagenesis screens, and mouse backcrosses. *Mamm. Genome* *10*, 987–992.

Tobisawa, S., Hozumi, Y., Arawaka, S., Koyama, S., Wada, M., Nagai, M., Aoki, M., Itoyama, Y., Goto, K., and Kato, T. (2003). Mutant SOD1 linked to familial amyotrophic lateral sclerosis, but not wild-type SOD1, induces ER stress in COS7 cells and transgenic mice. *Biochem. Biophys. Res. Commun.* *303*, 496–503.

Tohgi, H., Abe, T., Yamazaki, K., Murata, T., Ishizaki, E., and Isobe, C. (1999). Remarkable increase in cerebrospinal fluid 3-nitrotyrosine in patients with sporadic amyotrophic lateral sclerosis. *Ann. Neurol.* *46*, 129–131.

Tortarolo, M., Grignaschi, G., Calvaresi, N., Zennaro, E., Spaltro, G., Colovic, M., Fracasso, C., Guiso, G., Elger, B., Schneider, H., et al. (2006). Glutamate AMPA receptors change in motor neurons of SOD1G93A transgenic mice and their inhibition by a noncompetitive antagonist ameliorates the progression of amyotrophic lateral sclerosis-like disease. *J. Neurosci. Res.* *83*, 134–146.

Towne, C., Setola, V., Schneider, B.L., and Aebischer, P. (2011). Neuroprotection by gene therapy targeting mutant SOD1 in individual pools of motor neurons does not translate into therapeutic benefit in fALS mice. *Mol. Ther.* *19*, 274–283.

Traxinger, K., Kelly, C., Johnson, B.A., Lyles, R.H., and Glass, J.D. (2013). Prognosis and epidemiology of amyotrophic lateral sclerosis: Analysis of a clinic population, 1997-2011. *Neurol. Clin. Pract.* *3*, 313–320.

Traynor, B.J., Codd, M.B., Corr, B., Forde, C., Frost, E., and Hardiman, O.M. (2000). Clinical features of amyotrophic lateral sclerosis according to the El Escorial and Airlie House diagnostic criteria: A population-based study. *Arch. Neurol.* *57*, 1171–1176.

Troost, D., Sillevs Smitt, P.A., de Jong, J.M., and Swaab, D.F. (1992). Neurofilament and glial alterations in the cerebral cortex in amyotrophic lateral sclerosis. *Acta Neuropathol.* *84*, 664–673.

Tsang, C.K., Liu, Y., Thomas, J., Zhang, Y., and Zheng, X.F.S. (2014). Superoxide dismutase 1 acts as a nuclear transcription factor to regulate oxidative stress resistance. *Nat. Commun.* *5*, 3446.

Tsuda, T., Munthasser, S., Fraser, P.E., Percy, M.E., Rainero, I., Vaula, G., Pinessi, L., Bergamini, L., Vignocchi, G., and McLachlan, D.R. (1994). Analysis of the functional effects of a mutation in SOD1 associated with familial amyotrophic lateral sclerosis. *Neuron* *13*, 727–736.

- Tsunoda, S., Kawano, N., Miyado, K., Kimura, N., and Fujii, J. (2012). Impaired fertilizing ability of superoxide dismutase 1-deficient mouse sperm during in vitro fertilization. *Biol. Reprod.* *87*, 121.
- Tu, P.H., Raju, P., Robinson, K.A., Gurney, M.E., Trojanowski, J.Q., and Lee, V.M. (1996). Transgenic mice carrying a human mutant superoxide dismutase transgene develop neuronal cytoskeletal pathology resembling human amyotrophic lateral sclerosis lesions. *Proc. Natl. Acad. Sci. U. S. A.* *93*, 3155–3160.
- Turner, M. (2001). The treatment of motor neurone disease. *Practitioner* *245*, 530–532, 536–538.
- Turner, B.J., and Talbot, K. (2008). Transgenics, toxicity and therapeutics in rodent models of mutant SOD1-mediated familial ALS. *Prog. Neurobiol.* *85*, 94–134.
- Turner, B.J., Lopes, E.C., and Cheema, S.S. (2003). Neuromuscular accumulation of mutant superoxide dismutase 1 aggregates in a transgenic mouse model of familial amyotrophic lateral sclerosis. *Neurosci. Lett.* *350*, 132–136.
- Uchiyama, S., Shimizu, T., and Shirasawa, T. (2006). CuZn-SOD deficiency causes ApoB degradation and induces hepatic lipid accumulation by impaired lipoprotein secretion in mice. *J. Biol. Chem.* *281*, 31713–31719.
- Urushitani, M., Kurisu, J., Tsukita, K., and Takahashi, R. (2002). Proteasomal inhibition by misfolded mutant superoxide dismutase 1 induces selective motor neuron death in familial amyotrophic lateral sclerosis. *J. Neurochem.* *83*, 1030–1042.
- Urushitani, M., Sik, A., Sakurai, T., Nukina, N., Takahashi, R., and Julien, J.-P. (2006). Chromogranin-mediated secretion of mutant superoxide dismutase proteins linked to amyotrophic lateral sclerosis. *Nat. Neurosci.* *9*, 108–118.
- Valdmanis, P.N., and Rouleau, G.A. (2008). Genetics of familial amyotrophic lateral sclerosis. *Neurology* *70*, 144–152.
- Valdmanis, P.N., Belzil, V. V., Lee, J., Dion, P.A., St-Onge, J., Hince, P., Funalot, B., Couratier, P., Clavelou, P., Camu, W., et al. (2009). A mutation that creates a pseudoexon in SOD1 causes familial ALS. *Ann. Hum. Genet.* *73*, 652–657.
- Valentine, J.S., Doucette, P. a, and Zittin Potter, S. (2005). Copper-zinc superoxide dismutase and amyotrophic lateral sclerosis. *Annu. Rev. Biochem.* *74*, 563–593.
- Vance, C., Rogelj, B., Hortobágyi, T., De Vos, K.J., Nishimura, A.L., Sreedharan, J., Hu, X., Smith, B., Ruddy, D., Wright, P., et al. (2009). Mutations in FUS, an RNA processing protein, cause familial amyotrophic lateral sclerosis type 6. *Science* *323*, 1208–1211.
- Vassall, K.A., Stubbs, H.R., Primmer, H.A., Tong, M.S., Sullivan, S.M., Sobering, R., Srinivasan, S., Briere, L.-A.K., Dunn, S.D., Colón, W., et al. (2011). Decreased stability and increased formation of soluble aggregates by immature superoxide dismutase do not account for disease severity in ALS. *Proc. Natl. Acad. Sci. U. S. A.* *108*, 2210–2215.

Verma, A. (2013). Protein aggregates and regional disease spread in ALS is reminiscent of prion-like pathogenesis. *Neurol. India* *61*, 107–110.

Volkening, K., Leystra-Lantz, C., Yang, W., Jaffee, H., and Strong, M.J. (2009). Tar DNA binding protein of 43 kDa (TDP-43), 14-3-3 proteins and copper/zinc superoxide dismutase (SOD1) interact to modulate NFL mRNA stability. Implications for altered RNA processing in amyotrophic lateral sclerosis (ALS). *Brain Res.* *1305*, 168–182.

De Vos, K.J., Chapman, A.L., Tennant, M.E., Manser, C., Tudor, E.L., Lau, K.-F., Brownlees, J., Ackerley, S., Shaw, P.J., McLoughlin, D.M., et al. (2007). Familial amyotrophic lateral sclerosis-linked SOD1 mutants perturb fast axonal transport to reduce axonal mitochondria content. *Hum. Mol. Genet.* *16*, 2720–2728.

Walker, A.K., and Atkin, J.D. (2011). Stress signaling from the endoplasmic reticulum: A central player in the pathogenesis of amyotrophic lateral sclerosis. *IUBMB Life* *63*, 754–763.

Wang, J. (2003). Copper-binding-site-null SOD1 causes ALS in transgenic mice: aggregates of non-native SOD1 delineate a common feature. *Hum. Mol. Genet.* *12*, 2753–2764.

Wang, J., Xu, G., Gonzales, V., Coonfield, M., Fromholt, D., Copeland, N.G., Jenkins, N.A., and Borchelt, D.R. (2002a). Fibrillar inclusions and motor neuron degeneration in transgenic mice expressing superoxide dismutase 1 with a disrupted copper-binding site. *Neurobiol. Dis.* *10*, 128–138.

Wang, J., Xu, G., and Borchelt, D.R. (2002b). High molecular weight complexes of mutant superoxide dismutase 1: age-dependent and tissue-specific accumulation. *Neurobiol. Dis.* *9*, 139–148.

Wang, J., Xu, G., Slunt, H.H., Gonzales, V., Coonfield, M., Fromholt, D., Copeland, N.G., Jenkins, N.A., and Borchelt, D.R. (2005a). Coincident thresholds of mutant protein for paralytic disease and protein aggregation caused by restrictively expressed superoxide dismutase cDNA. *Neurobiol. Dis.* *20*, 943–952.

Wang, J., Xu, G., Li, H., Gonzales, V., Fromholt, D., Karch, C., Copeland, N.G., Jenkins, N.A., and Borchelt, D.R. (2005b). Somatodendritic accumulation of misfolded SOD1-L126Z in motor neurons mediates degeneration: alphaB-crystallin modulates aggregation. *Hum. Mol. Genet.* *14*, 2335–2347.

Wang, J., Xu, G., and Borchelt, D.R. (2006). Mapping superoxide dismutase 1 domains of non-native interaction: roles of intra- and intermolecular disulfide bonding in aggregation. *J. Neurochem.* *96*, 1277–1288.

Wang, J., Farr, G.W., Zeiss, C.J., Rodriguez-Gil, D.J., Wilson, J.H., Furtak, K., Rutkowski, D.T., Kaufman, R.J., Ruse, C.I., Yates, J.R., et al. (2009a). Progressive aggregation despite chaperone associations of a mutant SOD1-YFP in transgenic mice that develop ALS. *Proc. Natl. Acad. Sci. U. S. A.* *106*, 1392–1397.

- Wang, L., Sharma, K., Deng, H.-X., Siddique, T., Grisotti, G., Liu, E., and Roos, R.P. (2008). Restricted expression of mutant SOD1 in spinal motor neurons and interneurons induces motor neuron pathology. *Neurobiol. Dis.* *29*, 400–408.
- Wang, L., Sharma, K., Grisotti, G., and Roos, R.P. (2009b). The effect of mutant SOD1 dismutase activity on non-cell autonomous degeneration in familial amyotrophic lateral sclerosis. *Neurobiol. Dis.* *35*, 234–240.
- Wang, L., Deng, H.-X., Grisotti, G., Zhai, H., Siddique, T., and Roos, R.P. (2009c). Wild-type SOD1 overexpression accelerates disease onset of a G85R SOD1 mouse. *Hum. Mol. Genet.* *18*, 1642–1651.
- Wang, L., Grisotti, G., and Roos, R.P. (2010). Mutant SOD1 knockdown in all cell types ameliorates disease in G85R SOD1 mice with a limited additional effect over knockdown restricted to motor neurons. *J. Neurochem.* *113*, 166–174.
- Wang, L., Popko, B., and Roos, R.P. (2011a). The unfolded protein response in familial amyotrophic lateral sclerosis. *Hum. Mol. Genet.* *20*, 1008–1015.
- Wang, L., Gutmann, D.H., and Roos, R.P. (2011b). Astrocyte loss of mutant SOD1 delays ALS disease onset and progression in G85R transgenic mice. *Hum. Mol. Genet.* *20*, 286–293.
- Wang, L., Pytel, P., Feltri, M.L., Wrabetz, L., and Roos, R.P. (2012). Selective knockdown of mutant SOD1 in Schwann cells ameliorates disease in G85R mutant SOD1 transgenic mice. *Neurobiol. Dis.* *48*, 52–57.
- Warita, H., Itoyama, Y., and Abe, K. (1999). Selective impairment of fast anterograde axonal transport in the peripheral nerves of asymptomatic transgenic mice with a G93A mutant SOD1 gene. *Brain Res.* *819*, 120–131.
- Watanabe, M., Aoki, M., Abe, K., Shoji, M., Iizuka, T., Ikeda, Y., Hirai, S., Kurokawa, K., Kato, T., Sasaki, H., et al. (1997a). A novel missense point mutation (S134N) of the Cu/Zn superoxide dismutase gene in a patient with familial motor neuron disease. *Hum. Mutat.* *9*, 69–71.
- Watanabe, M., Dykes-Hoberg, M., Culotta, V.C., Price, D.L., Wong, P.C., and Rothstein, J.D. (2001). Histological evidence of protein aggregation in mutant SOD1 transgenic mice and in amyotrophic lateral sclerosis neural tissues. *Neurobiol. Dis.* *8*, 933–941.
- Watanabe, Y., Kuno, N., Kono, Y., Nanba, E., Ohama, E., Nakashima, K., and Takahashi, K. (1997b). Absence of the mutant SOD1 in familial amyotrophic lateral sclerosis (FALS) with two base pair deletion in the SOD1 gene. *Acta Neurol. Scand.* *95*, 167–172.
- Watanabe, Y., Yasui, K., Nakano, T., Doi, K., Fukada, Y., Kitayama, M., Ishimoto, M., Kurihara, S., Kawashima, M., Fukuda, H., et al. (2005). Mouse motor neuron disease caused by truncated SOD1 with or without C-terminal modification. *Brain Res. Mol. Brain Res.* *135*, 12–20.

- Watanabe, Y., Morita, E., Fukada, Y., Doi, K., Yasui, K., Kitayama, M., Nakano, T., and Nakashima, K. (2008). Adherent monomer-misfolded SOD1. *PLoS One* *3*, e3497.
- Waterston, R.H., Lindblad-Toh, K., Birney, E., Rogers, J., Abril, J.F., Agarwal, P., Agarwala, R., Ainscough, R., Alexandersson, M., An, P., et al. (2002). Initial sequencing and comparative analysis of the mouse genome. *Nature* *420*, 520–562.
- Weisberg, S.J., Lyakhovetsky, R., Werdiger, A., Gitler, A.D., Soen, Y., and Kaganovich, D. (2012). Compartmentalization of superoxide dismutase 1 (SOD1G93A) aggregates determines their toxicity. *Proc. Natl. Acad. Sci. U. S. A.* *109*, 15811–15816.
- Wen, H.-L., Lin, Y.-T., Ting, C.-H., Lin-Chao, S., Li, H., and Hsieh-Li, H.M. (2010). Stathmin, a microtubule-destabilizing protein, is dysregulated in spinal muscular atrophy. *Hum. Mol. Genet.* *19*, 1766–1778.
- Weydert, C.J., and Cullen, J.J. (2010). Measurement of superoxide dismutase, catalase and glutathione peroxidase in cultured cells and tissue. *Nat. Protoc.* *5*, 51–66.
- Wicks, P., Abrahams, S., Papps, B., Al-Chalabi, A., Shaw, C.E., Leigh, P.N., and Goldstein, L.H. (2009). SOD1 and cognitive dysfunction in familial amyotrophic lateral sclerosis. *J. Neurol.* *256*, 234–241.
- Wiedemann, F.R., Winkler, K., Kuznetsov, A. V, Bartels, C., Vielhaber, S., Feistner, H., and Kunz, W.S. (1998). Impairment of mitochondrial function in skeletal muscle of patients with amyotrophic lateral sclerosis. *J. Neurol. Sci.* *156*, 65–72.
- Wijesekera, L.C., and Leigh, P.N. (2009). Amyotrophic lateral sclerosis. *Orphanet J. Rare Dis.* *4*, 3.
- Wilcox, K.C., Zhou, L., Jordon, J.K., Huang, Y., Yu, Y., Redler, R.L., Chen, X., Caplow, M., and Dokholyan, N. V (2009). Modifications of superoxide dismutase (SOD1) in human erythrocytes: a possible role in amyotrophic lateral sclerosis. *J. Biol. Chem.* *284*, 13940–13947.
- Williamson, T.L., and Cleveland, D.W. (1999). Slowing of axonal transport is a very early event in the toxicity of ALS-linked SOD1 mutants to motor neurons. *Nat. Neurosci.* *2*, 50–56.
- Williamson, T.L., Bruijn, L.I., Zhu, Q., Anderson, K.L., Anderson, S.D., Julien, J.P., and Cleveland, D.W. (1998). Absence of neurofilaments reduces the selective vulnerability of motor neurons and slows disease caused by a familial amyotrophic lateral sclerosis-linked superoxide dismutase 1 mutant. *Proc. Natl. Acad. Sci. U. S. A.* *95*, 9631–9636.
- Winklhofer, K.F., Tatzelt, J., and Haass, C. (2008). The two faces of protein misfolding: gain- and loss-of-function in neurodegenerative diseases. *EMBO J.* *27*, 336–349.
- Witan, H., Kern, A., Koziollik-Drechsler, I., Wade, R., Behl, C., and Clement, A.M. (2008). Heterodimer formation of wild-type and amyotrophic lateral sclerosis-causing

mutant Cu/Zn-superoxide dismutase induces toxicity independent of protein aggregation. *Hum. Mol. Genet.* *17*, 1373–1385.

Witan, H., Gorlovoy, P., Kaya, A.M., Koziollek-Drechsler, I., Neumann, H., Behl, C., and Clement, A.M. (2009). Wild-type Cu/Zn superoxide dismutase (SOD1) does not facilitate, but impedes the formation of protein aggregates of amyotrophic lateral sclerosis causing mutant SOD1. *Neurobiol. Dis.* *36*, 331–342.

Wong, M., and Martin, L.J. (2010). Skeletal muscle-restricted expression of human SOD1 causes motor neuron degeneration in transgenic mice. *Hum. Mol. Genet.* *19*, 2284–2302.

Wong, P.C., Pardo, C.A., Borchelt, D.R., Lee, M.K., Copeland, N.G., Jenkins, N.A., Sisodia, S.S., Cleveland, D.W., and Price, D.L. (1995). An adverse property of a familial ALS-linked SOD1 mutation causes motor neuron disease characterized by vacuolar degeneration of mitochondria. *Neuron* *14*, 1105–1116.

Wooley, C.M., Sher, R.B., Kale, A., Frankel, W.N., Cox, G.A., and Seburn, K.L. (2005). Gait analysis detects early changes in transgenic SOD1(G93A) mice. *Muscle Nerve* *32*, 43–50.

Wright, P.D., Wightman, N., Huang, M., Weiss, A., Sapp, P.C., Cuny, G.D., Iverson, A.J., Glicksman, M.A., Ferrante, R.J., Matson, W., et al. (2012). A high-throughput screen to identify inhibitors of SOD1 transcription. *Front. Biosci. (Elite Ed.)* *4*, 2801–2808.

Wu, C.-H., Fallini, C., Ticozzi, N., Keagle, P.J., Sapp, P.C., Piotrowska, K., Lowe, P., Koppers, M., McKenna-Yasek, D., Baron, D.M., et al. (2012). Mutations in the profilin 1 gene cause familial amyotrophic lateral sclerosis. *Nature* *488*, 499–503.

Wulfsberg, E.A., Carrel, R.E., Klisak, I.J., O'Brien, T.J., Sykes, J.A., and Sparkes, R.S. (1983). Normal superoxide dismutase-1 (SOD-1) activity with deletion of chromosome band 21q21 supports localization of SOD-1 locus to 21q22. *Hum. Genet.* *64*, 271–272.

Yamanaka, K., Chun, S.J., Boillee, S., Fujimori-Tonou, N., Yamashita, H., Gutmann, D.H., Takahashi, R., Misawa, H., and Cleveland, D.W. (2008a). Astrocytes as determinants of disease progression in inherited amyotrophic lateral sclerosis. *Nat. Neurosci.* *11*, 251–253.

Yamanaka, K., Boillee, S., Roberts, E.A., Garcia, M.L., McAlonis-Downes, M., Mikse, O.R., Cleveland, D.W., and Goldstein, L.S.B. (2008b). Mutant SOD1 in cell types other than motor neurons and oligodendrocytes accelerates onset of disease in ALS mice. *Proc. Natl. Acad. Sci. U. S. A.* *105*, 7594–7599.

Yang, Y., Gozen, O., Watkins, A., Lorenzini, I., Lepore, A., Gao, Y., Vidensky, S., Brennan, J., Poulsen, D., Won Park, J., et al. (2009). Presynaptic regulation of astroglial excitatory neurotransmitter transporter GLT1. *Neuron* *61*, 880–894.

Yang, Y., Gozen, O., Vidensky, S., Robinson, M.B., and Rothstein, J.D. (2010). Epigenetic regulation of neuron-dependent induction of astroglial synaptic protein GLT1. *Glia* *58*, 277–286.

Yip, P.K., and Malaspina, A. (2012). Spinal cord trauma and the molecular point of no return. *Mol. Neurodegener.* 7, 6.

Yoo, H.Y., Chang, M.S., and Rho, H.M. (1999a). The activation of the rat copper/zinc superoxide dismutase gene by hydrogen peroxide through the hydrogen peroxide-responsive element and by paraquat and heat shock through the same heat shock element. *J. Biol. Chem.* 274, 23887–23892.

Yoo, H.Y., Chang, M.S., and Rho, H.M. (1999b). Heavy metal-mediated activation of the rat Cu/Zn superoxide dismutase gene via a metal-responsive element. *Mol. Gen. Genet.* 262, 310–313.

Yoon, E.J., Park, H.J., Kim, G.Y., Cho, H.M., Choi, J.H., Park, H.Y., Jang, J.Y., Rhim, H.S., and Kang, S.M. (2009). Intracellular amyloid beta interacts with SOD1 and impairs the enzymatic activity of SOD1: implications for the pathogenesis of amyotrophic lateral sclerosis. *Exp. Mol. Med.* 41, 611–617.

Yoshida, T., Maulik, N., Engelman, R.M., Ho, Y.S., and Das, D.K. (2000). Targeted disruption of the mouse Sod I gene makes the hearts vulnerable to ischemic reperfusion injury. *Circ. Res.* 86, 264–269.

Zelko, I.N., Mariani, T.J., and Folz, R.J. (2002). Superoxide dismutase multigene family: a comparison of the CuZn-SOD (SOD1), Mn-SOD (SOD2), and EC-SOD (SOD3) gene structures, evolution, and expression. *Free Radic. Biol. Med.* 33, 337–349.

Zeng, R., Coates, J.R., Johnson, G.C., Hansen, L., Awano, T., Kolichski, a., Ivansson, E., Perloski, M., Lindblad-Toh, K., O'Brien, D.P., et al. (2014). Breed distribution of SOD1 alleles previously associated with canine degenerative myelopathy. *J. Vet. Intern. Med.* 28, 515–521.

Zetterström, P., Stewart, H.G., Bergemalm, D., Jonsson, P.A., Graffmo, K.S., Andersen, P.M., Brännström, T., Oliveberg, M., and Marklund, S.L. (2007). Soluble misfolded subfractions of mutant superoxide dismutase-1s are enriched in spinal cords throughout life in murine ALS models. *Proc. Natl. Acad. Sci. U. S. A.* 104, 14157–14162.

Zetterström, P., Graffmo, K.S., Andersen, P.M., Brännström, T., and Marklund, S.L. (2011). Proteins that bind to misfolded mutant superoxide dismutase-1 in spinal cords from transgenic amyotrophic lateral sclerosis (ALS) model mice. *J. Biol. Chem.* 286, 20130–20136.

Zetterström, P., Graffmo, K.S., Andersen, P.M., Brännström, T., and Marklund, S.L. (2013). Composition of soluble misfolded superoxide dismutase-1 in murine models of amyotrophic lateral sclerosis. *Neuromolecular Med.* 15, 147–158.

Zhang, B., Tu, P., Abtahian, F., Trojanowski, J.Q., and Lee, V.M. (1997). Neurofilaments and orthograde transport are reduced in ventral root axons of transgenic mice that express human SOD1 with a G93A mutation. *J. Cell Biol.* 139, 1307–1315.

Zhang, F., Ström, A.-L., Fukada, K., Lee, S., Hayward, L.J., and Zhu, H. (2007). Interaction between familial amyotrophic lateral sclerosis (ALS)-linked SOD1 mutants and the dynein complex. *J. Biol. Chem.* *282*, 16691–16699.

Zhao, W., Beers, D.R., Henkel, J.S., Zhang, W., Urushitani, M., Julien, J.-P., and Appel, S.H. (2010). Extracellular mutant SOD1 induces microglial-mediated motoneuron injury. *Glia* *58*, 231–243.

Zimmerman, M.C., Oberley, L.W., and Flanagan, S.W. (2007). Mutant SOD1-induced neuronal toxicity is mediated by increased mitochondrial superoxide levels. *J. Neurochem.* *102*, 609–618.

Zinman, L., Liu, H.N., Sato, C., Wakutani, Y., Marvelle, A.F., Moreno, D., Morrison, K.E., Mohlke, K.L., Bilbao, J., Robertson, J., et al. (2009). A mechanism for low penetrance in an ALS family with a novel SOD1 deletion. *Neurology* *72*, 1153–1159.

Zu, J.S., Deng, H.X., Lo, T.P., Mitsumoto, H., Ahmed, M.S., Hung, W.Y., Cai, Z.J., Tainer, J.A., and Siddique, T. (1997). Exon 5 encoded domain is not required for the toxic function of mutant SOD1 but essential for the dismutase activity: identification and characterization of two new SOD1 mutations associated with familial amyotrophic lateral sclerosis. *Neurogenetics* *1*, 65–71.

Zuccato, C., Valenza, M., and Cattaneo, E. (2010). Molecular mechanisms and potential therapeutical targets in Huntington's disease. *Physiol. Rev.* *90*, 905–981.

REVIEW ARTICLE

Is SOD1 loss of function involved in amyotrophic lateral sclerosis?

Rachele A. Saccon, Rosie K. A. Bunton-Stasyshyn, Elizabeth M. C. Fisher and Pietro Fratta

Department of Neurodegenerative Disease, Institute of Neurology, University College, London WC1N 3BG, UK

Correspondence to: Elizabeth Fisher
Department of Neurodegenerative Disease,
Institute of Neurology, University College,
London WC1N 3BG, UK
E-mail: elizabeth.fisher@ucl.ac.uk

Correspondence may also be addressed to Pietro Fratta. E-mail: p.fratta@prion.ucl.ac.uk

Mutations in the gene superoxide dismutase 1 (*SOD1*) are causative for familial forms of the neurodegenerative disease amyotrophic lateral sclerosis. When the first *SOD1* mutations were identified they were postulated to give rise to amyotrophic lateral sclerosis through a loss of function mechanism, but experimental data soon showed that the disease arises from a—still unknown—toxic gain of function, and the possibility that loss of function plays a role in amyotrophic lateral sclerosis pathogenesis was abandoned. Although loss of function is not causative for amyotrophic lateral sclerosis, here we re-examine two decades of evidence regarding whether loss of function may play a modifying role in *SOD1*–amyotrophic lateral sclerosis. From analysing published data from patients with *SOD1*–amyotrophic lateral sclerosis, we find a marked loss of *SOD1* enzyme activity arising from almost all mutations. We continue to examine functional data from all *Sod1* knockout mice and we find obvious detrimental effects within the nervous system with, interestingly, some specificity for the motor system. Here, we bring together historical and recent experimental findings to conclude that there is a possibility that *SOD1* loss of function may play a modifying role in amyotrophic lateral sclerosis. This likelihood has implications for some current therapies aimed at knocking down the level of mutant protein in patients with *SOD1*–amyotrophic lateral sclerosis. Finally, the wide-ranging phenotypes that result from loss of function indicate that *SOD1* gene sequences should be screened in diseases other than amyotrophic lateral sclerosis.

Keywords: amyotrophic lateral sclerosis; motor neuron disease; superoxide dismutase 1; loss of function**Abbreviations:** ALS = amyotrophic lateral sclerosis; tg*SOD1* = *SOD1* transgenic mice

Introduction

Amyotrophic lateral sclerosis (ALS) is a neurodegenerative disorder characterized by the progressive loss of upper and lower motor neurons. Its clinical course is relentlessly progressive and typically causes death within 3 to 5 years of onset, mostly due to respiratory failure (Haverkamp *et al.*, 1995). Similar to other major neurodegenerative disorders, such as Alzheimer's disease and

Parkinson's disease, ALS is typically sporadic, but 5–10% of cases have an autosomal dominant pattern of transmission and are termed 'familial' (Rothstein, 2009). In 1993 the first causative mutations were found within the gene encoding the enzyme, superoxide dismutase 1 (*SOD1*) (Deng *et al.*, 1993; Rosen *et al.*, 1993). Since then, over 155 *SOD1* mutations have been described (although pathogenicity has not been shown for all of these changes) and these mutations account for up to 20% of

superoxide levels (through casein kinase signalling); this role is independent of its function in oxidative stress (Reddi and Culotta, 2013). Other described functions are nitration of proteins (Beckman *et al.*, 1993), copper buffering (Culotta *et al.*, 1997), phosphate activation (Wang *et al.*, 1996), zinc homeostasis (Wei *et al.*, 2001), thiol oxidation, and immunomodulation—modulation of SOD1 activity may differentially affect the NO-dependent microbicidal activity and release of cytokines by activated macrophages (Marikovsky *et al.*, 2003). Further, SOD1 is produced at high levels that have not yet been explained by known functions, therefore, it may well play other roles both neuron-specific and generally (Reddi and Culotta, 2013).

The finding of loss of dismutase activity in patients with ALS and the distribution of ALS-causative mutations spread throughout the *SOD1* gene initially suggested loss of function as a mechanism (Deng *et al.*, 1993; Rosen *et al.*, 1993). However, evidence for a gain of function mechanism was quick to follow from analysis of mutant *SOD1* transgenic (tg*SOD1*) mouse models. The first of these, tg*SOD1*^{G93A}, carries an ALS-causative point mutation resulting in a glycine to alanine substitution at residue 93 (Gurney *et al.*, 1994). Currently there are more than 12 different published human mutant SOD1 transgenic strains (Joyce *et al.*, 2011) and most of them (including tg*SOD1*^{G93A}) have increased dismutase activity because they greatly overexpress transgenic mutant human SOD1 in addition to endogenous mouse SOD1 and they develop a progressive adult-onset motor phenotype, accompanied by a striking loss of lower motor neurons.

Thus a loss of function mechanism became less favoured compared with gain of function because: (i) in humans, a lack of correlation was found between SOD1 dismutase activity and aggressiveness of clinical phenotypes (Ratovitski *et al.*, 1999); (ii) in mice, a lack of overt ALS-like phenotype was found in *Sod1* null (*Sod1*^{-/-}) animals, the first of which was published by Reaume *et al.* (1996); whereas (iii) transgenic mouse models over-expressing mutant human SOD1 have increased SOD1 activity and a loss of motor neurons that models human ALS.

The death knell for loss of function came in a seminal study published by the Cleveland laboratory (Bruijn *et al.*, 1998) who analysed survival time in mice carrying a mutant *SOD1* transgene (tg*SOD1*^{G85R}) on a normal mouse background (i.e. with two copies of the endogenous mouse *Sod1* gene) compared with the same transgene on a *Sod1*^{-/-} background. They found no change in survival of the mice, thus concluding that survival was entirely due to a gain of function mechanism, and independent of mouse SOD1 loss of function. These findings essentially ended the debate for a role of loss of function as a contributor to SOD1-familial ALS (Bruijn *et al.*, 1998).

SOD1 mutations remained the only known cause of 'classical' ALS until causative mutations in the gene *TARDBP* were found (Sreedharan *et al.*, 2008), and therefore have been studied extensively in a variety of animal and cellular models (Ilieva *et al.*, 2009). The causative gain of function is indisputable and several mechanisms by which this occurs have been proposed and comprehensively reviewed (Turner and Talbot, 2008; Ilieva *et al.*, 2009; Rothstein, 2009). However, in recent years a number of laboratories have further investigated *Sod1* knockout mice, examining their neuromuscular involvement and non-neurological

features. Data from these investigations and recent experiments using transgenic *SOD1* overexpressing mice have pointed to the possibility of a modifying role played by loss of dismutase activity on familial ALS disease course.

Here we review what is known about SOD1 loss of function and the evidence to suggest it may play a role in ALS pathogenesis after all, possibly through increased susceptibility to neurodegeneration. It is important and timely to consider these data because they are relevant to current therapeutic strategies to reduce the level of mutant familial ALS-SOD1 in heterozygous individuals. Such strategies could provide badly needed approaches to ameliorating the ALS phenotype, but clearly SOD1 loss has effects on both neuronal and non-nervous system tissues. SOD1 loss of function data also strongly suggest that SOD1 should be screened in disorders other than ALS.

SOD1 dismutase activity is greatly reduced in patients with SOD1-familial amyotrophic lateral sclerosis

Dismutase activity is the best characterized function of SOD1. Two other dismutases, encoded by separate genes, have been identified in mammals: SOD2 (Mn-SOD), which has manganese (Mn) as a cofactor and localizes to the mitochondrial matrix (Fridovich, 1986; Zelko *et al.*, 2002) and SOD3 (Fe-SOD), which exists as a homotetramer and is mainly extracellular (Marklund *et al.*, 1982). The existence of three enzymes with dismutase activity may complicate measures of SOD1 activity alone.

Box 1 Methods of measuring SOD1 dismutase activity

Activity assay: A sample is collected from the tissue of interest, such as red blood cells. Xanthine–xanthine oxidase is added to the sample to generate superoxide anions (O_2^-), and then a chromagen is used as an indicator of O_2^- production. In the presence of SOD, O_2^- concentrations are reduced, resulting in decreased colorimetric signal. However, all three SOD isoforms contribute to the activity measured, and so SOD1 activity is obtained indirectly by subtracting SOD2 and SOD3 activity from total SOD activity. This is achieved by running a parallel assay with the addition of potassium cyanide which preferentially inhibits SOD1 (Roe *et al.*, 1988).

Gel assay: Proteins from the tissue of interest are separated by electrophoresis in a native gel which is subsequently stained using a solution of nitro blue tetrazolium and riboflavin. Riboflavin is a source of O_2^- when exposed to light. The superoxide anions interact with nitro blue tetrazolium, reducing the yellow tetrazolium within the gel to a blue precipitate. This reduction reaction stains the gel blue; however, SOD inhibits this reaction, resulting in colourless bands where SOD is present. As the intensity of these bands is relative to the amount of SOD present, quantification can be inferred by measuring the intensity of the bands at the correct molecular weight using digital software (Weydert and Cullen, 2010).

In patients with ALS, SOD1 activity has most commonly been measured using two methods, generally either (i) the 'activity assay' which measures total dismutase activity of all three enzymes and then subtracts SOD2 and SOD3 activity, to leave only SOD1 activity; or (ii) the 'gel assay' in which the three enzymes are separated by electrophoresis and then dismutase activity is measured within the band of the correct size for the SOD1 dimer (Box 1).

Intrinsic and overall SOD1 activity

The dismutase activity of SOD1 can be measured in two ways depending on whether the focus is on (i) the 'intrinsic' SOD1 activity, which reflects the enzymatic efficiency of the protein and is obtained by measuring the activity of recombinant SOD1 protein normalized to its quantity; or (ii) the 'overall' activity within a tissue sample, which may be affected by various factors in the cellular environment (as described below), and is obtained by normalizing dismutase activity to the quantity of tissue. This last measure has generally been used with patients with familial ALS, and is a reflection of the amount of activity present in a biological context.

Intrinsic activity influences the overall activity, but is only one of the determinants; the others being any factor that affects the quantity, biological availability and functionality of SOD1. Amongst these are SOD1 messenger RNA half-life, SOD1 protein half-life, correct folding of SOD1, Cu²⁺-loading of SOD1 and other post-translational modifications (Wilcox *et al.*, 2009). In general, the 'overall' activity is an unbiased measure that takes into account known and unknown influences on SOD1 enzyme activity. Measurements are generally expressed relative to normal control samples.

Overall SOD1 activity is reduced in human amyotrophic lateral sclerosis samples

Intrinsic SOD1 activity has been measured in at least eight mutant proteins, giving diverse results ranging from 0–150% of human wild-type SOD1 activity. Correlation between these values and clinical aspects of the disease was assessed and did not show significant links (Borchelt *et al.*, 1994; Ratovitski *et al.*, 1999).

However, overall SOD1 activity has most commonly been measured in red blood cells, fibroblasts and lymphoblastoid cell lines derived from patients carrying at least 48 different mutations, and has proved to be more homogeneous than measures of intrinsic activity. We have searched reports of SOD1 activity from 1993 to 2012 in patients with SOD1-familial ALS and found that the majority of 48 tested mutations all have a reduction of overall activity. The average loss of activity is notable and averages 58% (± 17 , SD) of normal values (Fig. 1). These results are of striking consistency given the variability arising from different

laboratories performing the measurements and the naturally occurring variation in activity documented in blood samples (de Lustig *et al.*, 1993; Borchelt *et al.*, 1994; Robberecht *et al.*, 1994).

Overall SOD1 activity is normal or only slightly reduced in two mutations: the D90A in both homozygous and heterozygous patients, and the L117V in heterozygotes; although measurement from a homozygous patient showed a reduction of 67% SOD1 activity compared with control subjects (Andersen *et al.*, 1995; Synofzik *et al.*, 2012). Both these mutations are atypical, for example (i) SOD1 misfolding is not detected in cells derived from patients carrying these mutations (see below for association between SOD1 misfolding and SOD1 activity); (ii) the disease allele is homozygous in the majority of patients with D90A ALS and in one of four reported patients with L117V ALS; (iii) penetrance in heterozygotes is low; and (iv) disease progression is unusually slow (Synofzik *et al.*, 2012). Possibly these mutants have a slightly increased propensity to aggregate that is sufficient to start the disease process, although with reduced frequency, in the CNS, but is not enough to determine misfolding and loss of dismutase activity in the periphery.

Of note is the non-correspondence between the overall patient activity and the intrinsic activity; for example, the SOD1^{G37R} mutant has 150% intrinsic activity but only 40% overall activity compared with normal control subjects. Given that the intrinsic activity is only one of the determinants of the overall activity, other factors, such as the stability of mutant SOD1 protein, have been investigated to try to account for this loss of activity.

Different mutant SOD1 proteins have been shown to have a variable half-life, but this is consistently reduced compared to the wild-type form (Sato *et al.*, 2005). Calculations combining the measurement of intrinsic activity and half-life of six SOD1-familial ALS mutant proteins predicted that the overall activity would have been only 50% of normal levels (Borchelt *et al.*, 1994). Other studies and Fig. 1 are in accord with this finding (Deng *et al.*, 1993; Birve *et al.*, 2010). Further, most measures of SOD1 activity from patients with ALS have been taken in red blood cells, and we note that these cells have no active protein synthesis and are on average 60 days old, making the system particularly responsive to detecting protein half-life changes (Broom *et al.*, 2008). Nevertheless, when tested in post-mortem brain and spinal cord, SOD1 activity was found to be reduced to levels similar to those measured in red blood cells (Bowling *et al.*, 1993; Rosen *et al.*, 1994; Watanabe *et al.*, 1997; Browne *et al.*, 1998; Jonsson *et al.*, 2004), and when activity in red blood cells and CNS was compared in the same subset of patients, results were strikingly concordant (Rosen *et al.*, 1994).

Is SOD1 dismutase activity reduction exacerbated in motor neurons?

SOD1 activity has not been specifically measured in motor neurons and other affected cell types from SOD1-familial ALS post-mortem material, owing to technical difficulties in conducting these assays on limited micro-dissected material. The level of

activity reduction in these cell types is therefore unknown; however, there is evidence that the dismutase activity reduction may be enhanced in motor neurons.

RNA

SOD1 messenger RNA was shown to form tissue-specific complexes with ribonucleoproteins from brain and spinal cord and these interactions prolong its half-life in these tissues. However, complex formation appears to be impaired when *SOD1* messenger RNA carries ALS-causing mutations, therefore potentially reducing the half-life of mutant *SOD1* messenger RNA preferentially in CNS of patients with *SOD1*-familial ALS (Ge *et al.*, 2006).

Aggregation

Indirect evidence indicates that *SOD1* aggregation reduces dismutase activity. For example, data from cell experiments in which *SOD1*^{G93A} and amyloid- β were co-expressed, suggesting that aggregation results in reduction of *SOD1* activity (Yoon *et al.*, 2009). Further, two transgenic mouse lines over-expressing human wild-type-*SOD1* at a high level and at 2-fold this level, were analysed for aggregation and *SOD1* activity. In liver and muscle samples, aggregation was not found to be present, *SOD1* protein levels were increased, as expected, 2-fold and *SOD1* activity increased accordingly. However, in spinal cord and brain, where *SOD1* aggregation was clearly found, protein levels had a similar increase as in muscle and liver, but importantly *SOD1* activity did not show an increase, strongly suggesting a link between protein aggregation and activity (Graffmo *et al.*, 2013). Furthermore, even if *SOD1* retains enzymatic activity in aggregates, it may not accomplish the same functions as when correctly targeted to the appropriate cell compartments. *SOD1* misfolding and aggregation are a hallmark of *SOD1*-familial ALS and have been extensively documented in *SOD1*-familial ALS (Jonsson *et al.*, 2008) and wild-type *SOD1* has also been shown to be present in spinal cord aggregates of both patients with familial ALS (Jonsson *et al.*, 2004) and *SOD1* mouse models (Deng *et al.*, 2006; Wang *et al.*, 2009a; Prudencio *et al.*, 2010), thus making a dominant negative loss of function plausible. The recent finding of *SOD1* aggregation in cases with sporadic ALS (Bosco *et al.*, 2010; Forsberg *et al.*, 2010) makes this mechanism potentially relevant also to sporadic disease.

Oxidative stress

Lastly, oxidative stress induces *SOD1* to monomerize as an intermediate step to aggregate formation and it is known that *SOD1* does not have dismutase activity in this form (Khare *et al.*, 2004; Rakhit *et al.*, 2004; Ezzi *et al.*, 2007; Wilcox *et al.*, 2009). Motor neurons are known to be particularly susceptible to oxidative stress (Barber and Shaw, 2010) making this process potentially more pronounced in these cell types.

The tissue-specific changes in *SOD1* messenger RNA half-life and the effect of *SOD1* aggregation and monomerization on dismutase activity, raise the possibility that *SOD1* activity in the affected neurons may be lower than that measured from blood.

How *SOD1* activity in blood relates to that in spinal cord motor neurons is a critical issue that remains to be addressed.

In summary, *SOD1* overall activity is consistently reduced in blood samples of patients with *SOD1*-familial ALS, likely owing to changes in protein activity and alterations in mutant protein half-life. Further, there is an additional possible tissue-specific dismutase activity reduction in neurons.

Sod1^{-/-} mice have neuromuscular, neuronal and extra-neuronal phenotypes

An approach to elucidating the effect of *SOD1* loss of function is to assess the phenotype of *Sod1* null (*Sod1*^{-/-}) mice. Homozygous *Sod1* null mice have been used to analyse the role of *SOD1* in ALS, and for other purposes such as studying oxidative radical-mediated toxicity in reproduction and development (Huang *et al.*, 1997; Matzuk *et al.*, 1998). To date five *Sod1* knockout mouse lines have been published: *Sod1*^{tm1Cpe} (Reaume *et al.*, 1996); *Sod1*^{tm1Cje} (Huang *et al.*, 1997); *Sod1*^{tm1Leb} (Matzuk *et al.*, 1998); *Sod1*^{tm1Ysh} (Ho *et al.*, 1998); and *Sod1*^{tm1Dkd} (Yoshida *et al.*, 2000). All were obtained by targeted deletion of different regions of the *Sod1* gene, ranging from a single exon to the entire genomic sequence. For all five lines, no *SOD1* protein is detectable in homozygous null mice and *SOD1* activity is absent or very low [which may represent the background of the enzyme assay or might be caused by an endogenous superoxide dismutase activity supplied by an alternative scavenging enzyme (Reaume *et al.*, 1996)].

Deletion of different portions of the same gene may result in different phenotypes, but the five *Sod1* knockout strains have been compared in a number of studies and are strikingly similar (Huang *et al.*, 1997; Kondo *et al.*, 1997; Kostrominova, 2010). For example, skeletal muscles of three different *Sod1* null strains were compared and all developed accelerated age-related muscle denervation (Kostrominova, 2010). Genetic background may also influence phenotypes, however the majority of the studies discussed here, have been carried out on *Sod1*^{-/-} mice on a congenic C57BL/6 background, making results from different laboratories comparable.

When *Sod1*^{-/-} mice were first generated, a key issue was whether they developed motor neuron degeneration. The first analysis, from Reaume *et al.* (1996), found no reduction in motor neuron number at 4 months of age, but an increase in small neurons and astrocytes in spinal cord ventral horns. Subsequent studies confirmed the lack of motor neuron loss at 6, 9 and 17 months (Flood *et al.*, 1999) and lack of vacuolation or chromatolysis, key features of ALS, at 4 and 18 months (Fischer *et al.*, 2012). Microgliosis and ubiquitinated protein accumulation in motor neurons were ruled out, but mild astrocytosis was found at 4 and 18 months (Fischer *et al.*, 2012). Evaluation of lumbar ventral roots confirmed no loss in motor neuron number, but interestingly axonal diameter was reduced at 6 and 19 months and evidence of degenerating and regenerating axons was seen in the ventral L3 root at the latter time point (Flood *et al.*, 1999),

although another study did not see these results when analysing the L4 root (Fischer *et al.*, 2012).

Although *Sod1* null mice do not develop overt motor neuron degeneration, there is now a considerable literature, summarized below and described in more detail in the Supplementary material, showing that compared with wild-type controls, these mice have a wide range of phenotypes, including several relevant to ALS, such as a slowly progressive motor deficit that manifests from early adulthood and likely involves defects in large motor axons.

Sod1 null mice develop an adult-onset progressive motor axonopathy

Behavioural data

Sod1 null animals appear indistinguishable from littermates at birth through to weaning (Reaume *et al.*, 1996). Weight reduces with age compared with wild-type littermates (Jang *et al.*, 2010; Larkin *et al.*, 2011) and voluntary wheel running diminishes, which is a sensitive test for early locomotor defects (Muller *et al.*, 2006). At 9 months of age Rotarod performance and stride-length worsen (Flood *et al.*, 1999; Muller *et al.*, 2006), although spontaneous locomotion is normal, thus changes in motivation are not likely to contribute to these results (Flood *et al.*, 1999; Muller *et al.*, 2006). At 1 year of age, *Sod1*^{-/-} mice also have a deficit in grip-strength, and tremors (Fischer and Glass, 2010)—hallmarks of neuromuscular disorders in mice (Muller *et al.*, 2006).

Neurophysiological data

Direct neurophysiological measurement of the response to stimulation of nerve and muscle eliminates behavioural/motivational variability from the outcome. Such studies showed *Sod1* null mice have a reduction in muscle strength suggesting a progressive deficit in innervation (Larkin *et al.*, 2011). Motor unit number is reduced at 3 months, with progressive loss with age (Shefner *et al.*, 1999). Complex repetitive discharges found on needle examination indicate a deficit in the terminal part of the motor axon (Shefner *et al.*, 1999). Measures of nerve conduction velocity and latency analysis on sensory and mixed nerves, show a reduction only where a motor component is present, compatible with a deficit in the largest motor axons (Flood *et al.*, 1999). Thus neurophysiological investigations show clear muscle denervation and deficits in motor axons and functional motor units in *Sod1* null mice.

Axonal damage and early involvement of neuromuscular junctions

Denervation in *Sod1*^{-/-} mice has been documented by neuromuscular junction analysis of both fast and slow twitch muscles (Flood *et al.*, 1999; Fischer *et al.*, 2011, 2012; Larkin *et al.*, 2011). Denervation progresses with age, maintaining a more aggressive pattern in fast-twitch rather than slow-twitch muscles (Jang *et al.*, 2010; Fischer *et al.*, 2012). Thus SOD1 is required for maintenance of motor axons and their terminals (Fischer *et al.* (2011) and without this protein, fast-twitch motor units are lost preferentially, as is also observed in patients with ALS and mouse models of familial ALS (Dengler *et al.*, 1990; Pun *et al.*, 2006). The

involvement of neuromuscular junctions as an early pathological target has been extensively documented in mouse models of SOD1–familial ALS (Murray *et al.*, 2010) and was shown to precede motor neuron cell body loss in early disease in a patient with ALS (Fischer *et al.*, 2004).

Muscle pathology is secondary to denervation

Muscle mass is progressively lost (Muller *et al.*, 2006; Jang *et al.*, 2010; Larkin *et al.*, 2011) but has not been reported for organs such as liver, heart or kidney (Muller *et al.*, 2006). Angular muscle fibres, indicating denervation, are present by 2 months of age (Flood *et al.*, 1999) and by later time points a massive reduction in fibre number occurs, preferentially affecting type 2b fibres (fast glycolytic type innervated by large motor neurons), along with an increase in angular fibres (Reaume *et al.*, 1996; Larkin *et al.*, 2011). This muscle profile also occurs in mouse models of familial ALS–SOD1 (Kennel *et al.*, 1996; Frey *et al.*, 2000) and is typical of the neurogenic changes that initially affect larger motor neurons, suggesting that muscle pathology is secondary to axonal events.

Confirmation of muscle pathology being secondary to axonal damage and denervation was obtained by crossing *Sod1*^{-/-} mice with transgenic mice expressing *Sod1* in the CNS but not in muscle. In double mutant progeny, muscle pathology was fully rescued despite the absence of SOD1 in muscle (Flood *et al.*, 1999). Further, in *Sod1*^{-/-} mice, measurements of steady state redox potential of glutathione (which is routinely used as indicator of the intracellular redox state) in tibial nerve and gastrocnemius muscle showed a selective involvement of the nerve at 4 months, again indicating the primary involvement of the axon (Fischer *et al.*, 2012). Thus muscle changes in *Sod1*^{-/-} mice are secondary to denervation; they are non-specific and also present in muscle biopsies from patients with ALS (Baloh *et al.*, 2007a).

Sod1^{-/-} motor neurons show increased vulnerability to stress

SOD1 activity is important for motor neuron survival after injury as shown by facial axotomy of *Sod1* null mice which resulted in a significant increase in motor neuron loss compared with wild-type controls. This is interesting when considering the potential role for injury and trauma in ALS (Pupillo *et al.*, 2012; Yip and Malaspina, 2012).

Selective susceptibility to damage of the motor system

An important feature of ALS is the selective involvement of motor neurons and their related circuits, and indeed the phenotypes induced by lack of SOD1 in mice preferentially affect motor neurons. *Sod1*^{-/-} mice have no significant deficits in somatosensory behaviour (Flood *et al.*, 1999). Further, neurophysiology testing showed preferential motor involvement in *Sod1*^{-/-} mice and, on histopathological examination, L3 dorsal roots at 19 months are normal in contrast to the ventral roots, which have signs of degeneration/regeneration (Flood *et al.*, 1999). Finally, analysis of *Sod1* null epidermal nerves, which are the most distal tracts of the sensory axons, showed no abnormality, in contrast to their severely affected motor counterparts, the neuromuscular junctions (Fischer *et al.*, 2012).

Loss of SOD1 affects mitochondrial function

Sod1^{-/-} mice lack superoxide scavenging function in the cytosol and mitochondrial intermembrane space, which contain O₂⁻ generated by complex III (Muller *et al.*, 2004). *Sod1* null mitochondria release significantly increased amounts of O₂⁻ and therefore increased oxidative stress in these compartments was hypothesized to account for the neuromuscular phenotype of the mice (Jang *et al.*, 2010). Fischer *et al.* (2011) demonstrated that mitochondrial density is reduced in *Sod1*^{-/-} axons and, remarkably, they reversed this loss and the neuromuscular phenotype, by replacing SOD1 selectively in the mitochondrial intermembrane space of these mice.

Mitochondrial dysfunction is associated with ALS (Faes and Callewaert, 2011) and mitochondria are important for distal axonal maintenance (Baloh *et al.*, 2007b; Cassereau *et al.*, 2011). Furthermore, mitochondrial transport abnormalities are described in tgSOD1-ALS mouse models (De Vos *et al.*, 2007). Also, abnormal mitochondrial accumulations have been described in lower motor neurons and proximal axons from patients with ALS, post-mortem (Sasaki *et al.*, 2009). Thus it seems likely that damage to mitochondria through raised levels of free radicals may have a significant effect on distal axons of motor neurons.

In summary *Sod1*^{-/-} mice appear normal up to the age of weaning, after which they develop a slowly progressive motor-neuronopathy that involves primarily the motor neuron axons and neuromuscular junctions and is accompanied by significant secondary denervation pathology in muscles (Supplementary Fig. 1). Sensory involvement is negligible. Although no motor neuron loss has been documented, these are more vulnerable to damage in *Sod1*^{-/-} mice.

Other neuronal and extra-neuronal *Sod1* null phenotypes

In addition to deficits in the motor system, *Sod1* null mice develop a range of other disorders including: progressive neuronal hearing loss; progressive retinal degeneration; greatly increased susceptibility to cerebral ischaemia and brain trauma. Most importantly for studies of ALS, these mice have an increased susceptibility to neurodegeneration, for example, when crossed to a mouse model of Alzheimer's disease (Supplementary Box 1).

Extra neuronal phenotypes are also striking, in particular the well-known susceptibility to hepatocellular carcinoma, a feature that also manifests in the human population; there is a positive correlation between SOD1 activity and postoperative hepatocellular carcinoma survival time, as well as low levels of SOD1 and severity of hepatocellular carcinoma (Elchuri *et al.*, 2005; Takahashi *et al.*, 2002; Casaril *et al.*, 1994; Liaw *et al.*, 1997; Lin *et al.*, 2001). Other non-neuronal features include impaired endothelial-dependent relaxation, thinning of the skin, osteoporosis and female infertility (Supplementary Box 1).

These remarkably wide-ranging phenotypes are perhaps not surprising in an animal that is missing such an important enzyme, but the tissue specificity partly points to effects in tissues with a high production of free radicals, such as the nervous system and liver. Further, the progressive nature of most of these phenotypes is striking and may be relevant to the mechanism of SOD1-familial ALS,

both in terms of deficits increasing with age and in terms of targeting of many of the deficits to neuronal tissues.

A SOD1 activity of 50% is not sufficient for normal neuronal function

Sod1^{+/-} mice have abnormal phenotypes including within the motor system

Sod1 null mice are invaluable for investigating *in vivo* consequences of SOD1 loss of function, and may provide clues for the effects of reduced enzyme activity in ALS. However, the 100% loss of enzyme activity is a different setting from the average 57% reduction in patients with ALS. Thus, although *Sod1* null mice clearly indicate a susceptibility of specific tissues to the effects of a loss of SOD1 function, any discussion in the context of ALS must look at phenotypes that arise in *Sod1*^{+/-} animals (Supplementary Fig. 1) that retain 50% SOD1 activity (Reaume *et al.*, 1996) and so mimic the physiological levels described in patients with SOD1-familial ALS. Although *Sod1*^{+/-} mice clearly do not develop an ALS-like syndrome, a wide range of studies show that *Sod1*^{+/-} mice have abnormal phenotypes involving progressive cellular damage and deficits in reaction to injury and toxic stimuli. Here we consider how these may have implications for human ALS.

Sod1^{+/-} motor neurons are more susceptible to cell death after axon injury

Sod1^{+/-} mice suffer significantly more motor neuron loss in response to facial nerve axotomy than wild-type mice. This result is intermediate between *Sod1*^{-/-} and control mice, suggesting a dose dependence of this effect and demonstrating that 50% SOD1 activity is not sufficient for a normal function of motor neurons in response to injury (Reaume *et al.*, 1996).

Facial nerve axotomy was also performed on copper chaperone for SOD1 null mice (*Ccs*^{-/-}), that retain only 20% of SOD1 activity, owing to the lack of this crucial protein for delivery of copper to SOD1 (Box 2). Motor neuron survival was significantly reduced in *Ccs*^{-/-} mice (Subramaniam *et al.*, 2002). This result,

BOX 2 *Ccs*^{-/-} null mice model SOD1 partial loss of activity

Another mouse model that is relevant to studying the effects of reduced SOD1 activity is the 'copper chaperone for SOD1' (*Ccs*) null mouse. Copper chaperones shuttle copper, which is toxic for cells in its free form, to intracellular target proteins. CCS delivers copper to SOD1 by direct protein-protein interaction and is required for full activation of SOD1 (Culotta *et al.*, 1997, 1999). Mice lacking CCS (*Ccs*^{-/-}) were generated by gene targeting and retain only 20% of normal SOD1 activity; CCS-independent copper loading into SOD1 probably accounts for the remaining activity. Although the dismutase activity is impaired, there is no difference in the levels of SOD1 protein among wild-type, *Ccs*^{+/-} and *Ccs*^{-/-} littermates (Wong *et al.*, 2000).

and the similar result from *Sod1*^{+/-} mice, is important in light of the potential role for injury and trauma as a trigger in ALS pathogenesis (Pupillo *et al.*, 2012; Yip and Malaspina, 2012).

Spontaneous denervation, motor neuron sensitivity and reduction in mitochondrial numbers are not significant in *Sod1*^{+/-} mice but all show trends

Although *Sod1*^{+/-} mice have been less studied than null animals, there have been comprehensive investigations of denervation in these mice (Fischer *et al.*, 2011, 2012). At 18 months, 80% of tibialis anterior muscle (neuromuscular junctions) were innervated in *Sod1*^{+/-} compared with 92% in controls (Fischer *et al.*, 2011). This result did not reach statistical significance, but this trend was repeated in a following study (Fischer *et al.*, 2012). Currently, there is no evidence for spontaneous denervation in *Sod1*^{+/-} mice. Experiments were conducted up to the time-point of 18 months, the maximum limit when investigating *Sod1*^{-/-} mice—which develop and die of liver cancer at this stage—but could be extremely informative at later time-points for the *Sod1*^{+/-} mice. Whether increased sample size or a later time-point would show a significant result, remains to be determined.

Glutamate toxicity is enhanced in *Sod1*^{+/-} mice

Glutamate toxicity is implicated in disease in patients with ALS and in animal models (Ilieva *et al.*, 2009). The role of SOD1 in neuronal sensitivity to glutamate toxicity was assessed *in vivo* by intrastriatal injection of *N*-methyl-D-aspartic acid and kainite glutamate receptor agonists. *Sod1*^{+/-} mice were more susceptible to the neurotoxic effects of both stimuli and had reduced glutamic acid decarboxylase and choline acetyltransferase activities compared with controls (Schwartz *et al.*, 1998). Thus SOD1 partial loss of function could play a role in facilitating damage from glutamate toxicity, which may have relevance to ALS.

Increased susceptibility to cerebral ischaemia in *Sod1*^{+/-} mice

Sod1^{+/-} mice have decreased survival after induced focal cerebral ischaemia, along with increased early blood–brain barrier disruption and increased infarct volume causing brain swelling. Apoptotic neuronal death is also increased demonstrating enhanced ischaemia–reperfusion injury (Kondo *et al.*, 1997). Intriguingly, an important mechanism involved in ischaemia–reperfusion injury is glutamate excitotoxicity, which as discussed above, is postulated to play a role in ALS pathogenesis (Beal, 1992).

We note that blood–brain barrier alterations are found in tgSOD1-ALS mouse models and that indirect evidence of disruption, such as increased cerebrospinal fluid (CSF) albumin/plasma albumin ratios, has been documented in patients with ALS (Leonardi *et al.*, 1984; Apostolski *et al.*, 1991).

Increased memory deficits and plaque formation in an Alzheimer's disease model on a *Sod1*^{+/-} background

Overexpression in mice of the *APP* gene carrying the Swedish mutation causes behavioural deficits and plaque formation and thus models Alzheimer's disease (Bodendorf *et al.*, 2002). When this mutation is expressed on a *Sod1*^{+/-} background, it results in increased deficits in behavioural tests used to assess memory and

in increased senile plaque formation, thus showing that lack of 50% of SOD1 activity does indeed increase the development of a neurodegenerative phenotype *in vivo*.

Ganglion neuron loss is increased with ageing in *Sod1*^{+/-} mice

A 50% reduction in SOD1 activity results in reduced neuronal survival *in vivo* with respect to ganglion cell density, although this does not cause an apparent hearing deficit (Keithley *et al.*, 2005).

DNA methylation is reduced in *Sod1*^{+/-} mice

The effects of reduced mouse SOD1 activity could be relevant to ALS because DNA methyltransferases, the enzymes involved in DNA methylation, and 5-methylcytosine, the end-product of DNA methylation, were found to be upregulated in human ALS, suggesting that aberrant regulation of DNA methylation is part of the pathobiology of ALS (Chestnut *et al.*, 2011). DNA methylation was significantly reduced at 2 months of age in *Sod1*^{+/-} mice, although this study focused on prostate tissue (Bhusari *et al.*, 2010).

Sod1^{+/-} mice exhibit a contractile vascular phenotype with ageing

High levels of superoxide play a major role in contractile vascular dysfunction and loss of a single copy of *Sod1* is enough to increase vascular superoxide levels and produce vascular contractile dysfunction with ageing (Didion *et al.*, 2006).

Loss of mouse SOD1 activity to 50% of normal levels does not cause death of motor neurons but may be relevant to human SOD1–familial amyotrophic lateral sclerosis

Sod1^{+/-} mice show an increased loss of specific neuronal subtypes with ageing and an increased susceptibility to injury and toxic stimuli. These results are relevant to SOD1-familial ALS given the similarity of enzyme activity levels between patients with SOD1-familial ALS and *Sod1*^{+/-} models. The vulnerability shown in motor neurons after injury, the susceptibility of neurons to glutamate toxicity, and the blood–brain barrier alterations seen in these mice are significant elements since they are mechanisms and alterations postulated to be involved in ALS pathogenesis.

Overall *Sod1*^{-/-} and *Sod1*^{+/-} animals do not recapitulate mouse ALS, but they have a wide range of phenotypes that are both related to ALS directly (for example, denervation, increased susceptibility to glutamate toxicity, increased susceptibility to axonal damage) and more generally to neuronal degeneration (for example, loss of ganglion and retinal cells) and therefore this raises the question of a contribution of SOD1 loss of function to disease. A further point to consider is that although several transgenic mice carrying SOD1 mutations have motor neuron degeneration and characteristics of human ALS, other mouse strains with well-characterized pathogenic mutations in different 'ALS genes' (for example, *TARDBP*) have phenotypes less clearly reminiscent of the human disease (Joyce *et al.*, 2011). Thus it remains debatable as to how a mouse–ALS syndrome might manifest, and so considering all phenotypes that develop in the CNS of these

models is essential for understanding how ALS mutations cause disease.

SOD1 activity and its influence on SOD1–familial amyotrophic lateral sclerosis mouse models

SOD1 loss of function does not influence survival of transgenic SOD1 disease models

The possibility that SOD1 loss of function contributes to ALS pathogenesis has been investigated by analysing the double mutant progeny of *Sod1*^{-/-} or of *Ccs*^{-/-} mice crossed to three tgSOD1-ALS lines overexpressing the human mutations, G93A, G37R and G85R. These crosses produce double mutant mice in which either the transgenic human mutant protein is the only SOD1 present (in the case of *Sod1*^{-/-} crosses) or both the endogenous and transgenically expressed SOD1 are mostly inactive due to the *Ccs*^{-/-} background.

As both G93A and G37R mutant SOD1 retain dismutase activity (Fig. 1) they are not informative for the effect of SOD1 dismutase loss of function when on a *Sod1* null background. Further, transgenes often form multiple copy concatamers and indeed both the tgSOD1^{G93A} and the tgSOD1^{G37R} lines have an increase of >6-fold of mouse SOD1 activity, compared with non-transgenic control mice (Bruijn *et al.*, 1997; Subramaniam *et al.*, 2002; Deng *et al.*, 2006). As a result, even on a *Ccs*^{-/-} background, these two transgenic lines still have SOD1 activity levels comparable with those of non-transgenic wild-type mice and so are not useful for examining the effects of SOD1 loss of function on disease course (Subramaniam *et al.*, 2002).

However, two experiments do examine the effect of mouse SOD1 loss of function on the disease developed by tgSOD1-ALS mouse models. These assess progeny from crosses of *Sod1*^{-/-} and *Ccs*^{-/-} with tgSOD1^{G85R}, a human ALS mutation that has no detectable intrinsic activity (Borchelt *et al.*, 1994; Bruijn *et al.*, 1997). Activity is predicted to fall to 0% when crossed with *Sod1*^{-/-} (Bruijn *et al.*, 1998) and shown to be 20% when crossed with *Ccs*^{-/-}, as expected, given the residual SOD1 activity of the *Ccs*^{-/-} line (Subramaniam *et al.*, 2002).

The tgSOD1^{G85R} line shows clinical signs of disease between 8–10 months of age, which aggressively progress to paralysis within a few weeks (Bruijn *et al.*, 1997). The disease onset is much later than many other tgSOD1-ALS mouse models, this is appropriate for evaluating any potential modifying effect of SOD1 loss of function. Crosses to both *Sod1*^{-/-} ($n = 5$ double mutant progeny) and *Ccs*^{-/-} ($n = 10$ double mutant progeny) did not show significant effects on lifespan (Bruijn *et al.*, 1997; Subramaniam *et al.*, 2002).

Both of these studies resulted in seminal papers that have been extremely important to the field and have answered critical questions about SOD1 gain of function in ALS. However, neither paper answered the separate question about whether loss of function

modifies ALS, presumably and quite reasonably because that was not the focus of the papers. Both studies were performed using a cohort size too small to detect potential subtle changes [$n = 5$ in Bruijn *et al.* (1997) and $n = 10$ in Subramaniam *et al.* (2002)] and the sex of the mice analysed was not reported, although it is clear that in both humans and mouse, gender plays a role in ALS natural history (Acevedo-Aroza *et al.*, 2011; Joyce *et al.*, 2011). Furthermore, neither study evaluated the age of disease onset or performed behavioural analysis therefore not addressing the possibility that SOD1 loss of function may have an impact on onset and disease course. Lastly, both studies lack a quantitative pathology analysis: Bruijn *et al.* (1997) noted $n = 2$ for axonal count in the L5 ventral roots, and Subramaniam *et al.* (2002) perform a qualitative analysis only, at end-stage, therefore missing any potential modifier effect occurring during the disease process.

Thus while it remains unclear if SOD1 loss of function modifies important disease characteristics such as age of onset or progression, it appears not to affect lifespan. The lack of effect on survival in the absence of mouse SOD1 activity is an important result because it shows that life expectancy in this line is determined uniquely by mutant SOD1. It has been also speculated that the lack of an effect on lifespan is due to the insufficient levels of endogenous SOD1 to counteract the oxidative stress present in the tgSOD1^{G85R} mice, and because the tgSOD1^{G85R} mice die before developing a significant oxidative stress-mediated motor axonopathy (Wang *et al.*, 2012). With respect to onset and disease course, a larger cohort would be required to note differences, particularly if they are subtle.

SOD1 activity may influence disease course of transgenic SOD1 disease models

While the effect of mouse SOD1 activity on disease onset and progression of tgSOD1-ALS models is unclear from the crosses to *Sod1* null mice, there are other experimental data indicating that SOD1 activity may play a role in modifying SOD1-familial ALS.

SOD1 overexpression and influence on disease

The effect of overexpression of wild-type human SOD1 on disease course has been tested by crossing mutant tgSOD1-ALS animals with transgenic mice overexpressing wild-type human SOD1 (tgSOD1-WT). Double mutant progeny carry both the wild-type and mutant human SOD1 transgenes, with two copies of the endogenous mouse *Sod1* in the genetic background (Bruijn *et al.*, 1998; Jaarsma *et al.*, 2000; Fukada *et al.*, 2001; Deng *et al.*, 2006; Wang *et al.*, 2009a, b; Prudencio *et al.*, 2010). Generally, a worsening of both age of onset and survival have been reported, compared with single mutant tgSOD1-ALS littermates. However, we note that tgSOD1-WT mice spontaneously develop motor neuron and axon loss and have misfolded SOD1 accumulations (Jaarsma *et al.*, 2000) and develop an ALS-like disease when

expression is further increased (Graffmo *et al.*, 2013), making the results of these crosses hard to interpret.

Of note, transgenic mice over-expressing CCS have also been generated and crossed to different tgSOD1 lines, and results have ranged from no effect to a significant worsening of the phenotype. However, CCS over-expression was shown to have biological effects in the absence of SOD1 enzymatic activation and also to have an influence on the reduced state of SOD1, making these results not helpful for dissecting the role of dismutase activity on disease (Proescher *et al.*, 2008; Son *et al.*, 2009; Graffmo *et al.*, 2013).

Tissue specific expression and inactivation of mutant SOD1 points to a modifying role for dismutase activity

To address questions regarding the cell-autonomy of SOD1-familial ALS, investigators have used Cre-*loxP* technology to conditionally eliminate mutant SOD1 expression in different cell lineages or used specific promoters to overexpress mutant SOD1 in selected cell types. Analysis of their results is beyond our scope here, but generally demonstrates a central role for neurons in the determination of age of onset and disease progression in SOD1-familial ALS, and has also pointed to a role for other cell types, such as astrocytes and microglia in influencing the course of the disease (Ilieva *et al.*, 2009).

Cre-*loxP* experiments were conducted using two mutant tgSOD1 lines: conditional tgSOD1^{G37R}, which retains intrinsic dismutase activity, and conditional tgSOD1^{G85R}, which lacks activity. Neuronal excision experiments in both lines showed a beneficial effect on disease onset and survival. Interestingly, for consideration of the effects of dismutase activity, significant differences were found between the conditional tgSOD1^{G37R} and conditional tgSOD1^{G85R} lines after mutant SOD1 excision from microglia and from astrocytes.

A more profound amelioration was observed with the tgSOD1^{G85R} line in both experiments, with an effect on early disease with microglia excision and also on disease onset with excision in astrocytes; neither result occurred in the tgSOD1^{G37R} experiments (Ilieva *et al.*, 2009; Wang *et al.*, 2009b, 2011). A possible explanation for these divergent results has been proposed to lie in differences in dismutase activity (Wang *et al.*, 2012). If in addition to the toxic gain of function effects, tgSOD1^{G37R} has neuroprotective effects in microglia and astrocytes due to its enzymatic activity, then a knockdown of tgSOD1^{G37R} expression would have less ameliorative effects on the disease course than knockdown of the inactive SOD1^{G85R} (Wang *et al.*, 2009b, 2011).

In support of a modifying effect of SOD1 dismutase activity are findings obtained with the excision of tgSOD1^{G37R} from Schwann cells. Excision from the tgSOD1^{G37R} made the disease progression in the mice more severe. Lobsiger *et al.* (2009) proposed that SOD1^{G37R} activity in Schwann cell had a neuroprotective effect. Conversely, excision of the inactive SOD1^{G85R} caused a delay in disease onset, an increased survival and an amelioration of pathology (Wang *et al.*, 2012). Furthermore, increasing SOD1^{G93A} expression specifically in Schwann cells of the tgSOD1^{G93A} mouse had a beneficial effect on disease (Turner *et al.*, 2010).

In conclusion, the experimental data overall point to a protective role of SOD1 dismutase activity, at least in some cell types, on non-cell autonomous degeneration and disease in SOD1-ALS.

Conclusions

SOD1 loss of function models share many commonalities with amyotrophic lateral sclerosis indicating specific cell-type sensitivities

SOD1 loss of function was initially thought to play a role in ALS due to the discovery of disease-causing mutations in the SOD1 gene and due to the well-established link between oxidative stress and neurodegeneration (Smith *et al.*, 1991; Stadtman 1992; Stadtman and Berlett, 1997). Indeed free radical damage has been shown in CSF, serum and urine from patients with ALS (Smith *et al.*, 1998; Simpson *et al.*, 2004; Mitsumoto *et al.*, 2008) and proteins, lipids and DNA were shown to have elevated oxidative damage in ALS post-mortem material (Shaw *et al.*, 1995; Fitzmaurice *et al.*, 1996; Shibata *et al.*, 2001). As SOD1-familial ALS undoubtedly arises primarily from SOD1 toxic gain of function, the loss of dismutase activity may play a modifying role. The most useful tools to study this possibility *in vivo* have been the *Sod1*^{-/-} mice. These mice are a model of chronic oxidative stress, but do not develop a disease that models human ALS.

Long term studies of *Sod1*^{-/-} mice show striking features related to ALS. Notably, these mice develop a progressive distal motor axonopathy and ALS has indeed been postulated to start by affecting the distal portions of the neurons including neuromuscular junctions and axons (Murray *et al.*, 2010). The most affected motor units in *Sod1*^{-/-} mice are fast-twitch, which is in accordance with observations in ALS models (Frey *et al.*, 2000). Motor neurons in *Sod1* null mice have an increased susceptibility to injury and importantly, stimuli such as trauma, could play a role in initiating ALS (Pupillo *et al.*, 2012) where humans, even if carrying disease-causing mutations, are healthy for decades. Further, in *Sod1*^{-/-} mice, motor neurons are preferentially affected compared to sensory neurons, recapitulating the selectivity observed clinically and pathologically in ALS.

The neuromuscular phenotype in *Sod1* null mice has been demonstrated to be caused by the lack of SOD1 in the mitochondrial intermembrane space and a related decrease in axonal mitochondrial density (Fischer *et al.*, 2011). The involvement of mitochondria in ALS and other forms of motor neuron disease such as spinal muscular atrophy, has been shown in animal and cellular models and indirectly in post-mortem material (Baloh *et al.*, 2007b; De Vos *et al.*, 2007; Acsadi *et al.*, 2009; Sasaki *et al.*, 2009; Wen *et al.*, 2010; Faes and Callewaert, 2011). As described, *Sod1*^{-/-} mice have other phenotypes that underline the importance of this gene in neuronal ageing and in neurodegeneration. Among these are the spontaneous progressive loss of retinal cells and auditory ganglion neurons, the increased susceptibility to APP induced neurodegeneration and the increased

susceptibility to apoptotic cell death following brain trauma and ischaemic injury.

SOD1 activity is greatly reduced in human SOD1-familial amyotrophic lateral sclerosis

SOD1 activity is generally reduced to approximately half of normal in patients with SOD1-familial ALS, as measured in red blood cells, lymphoblastoid cells and fibroblasts (Fig. 1). Indirect evidence raises the possibility that a more severe reduction could occur in susceptible tissues and cell types, owing to reduced mutant *SOD1* messenger RNA half-life in the CNS and due to possible effects of SOD1 protein misfolding and aggregation on activity.

Data from other human diseases involving loss of enzyme activity shows many of these are recessive and heterozygotes are generally unaffected (Mitchell *et al.*, 2011). However, this is clearly not the case in the *Sod1*^{+/-} mouse; these animals have increased neuronal loss and increased susceptibility to injury. Further, the stimuli to which these mice are more susceptible are motor neuron axonal damage and glutamate toxicity, both closely related to ALS pathogenesis. In addition, the blood–brain barrier is more permeable following injury in these mice; indirect evidence of a similar state has also been described in patients with ALS and in mouse models of ALS. Exacerbation of neurodegenerative phenotypes in an Alzheimer's disease mouse model when on a *Sod1*^{+/-} background also indicates a potential predisposition to neurodegeneration of mice with a 50% reduction in SOD1 activity. Lastly, as *Sod1*^{+/-} mice show a spontaneous loss of spiral ganglion cells this confirms that decreased dismutase activity has direct consequences on neuronal survival.

A human SOD1 loss of function phenotype?

Although both *Sod1*^{-/-} and *Sod1*^{+/-} mice develop characteristics that have obvious relevance to ALS, we have found no data from human genetic analyses to suggest that SOD1 loss of function alone causes the human disease. >155 mutations in SOD1 have been described (Fig. 1), but there have been no truncation mutations occurring in the N-terminal part of SOD1 that would generate an effectively null allele (i.e. due to reduced expression from nonsense mediated decay of the messenger RNA or from inactivity of just a short stretch of N-terminal amino acids). We note a frameshift in exon 2 generating a predicted 35 amino acid protein that might be a null, has been reported in a family with ALS, but data regarding segregation are unclear making conclusions uncertain (Hu *et al.*, 2012).

Further, we could find no description of patients with full loss of SOD1 activity, even when SOD1 mutations are found in homozygosity. Of the six homozygous SOD1 mutations (L84F, N86S, D90A, L117V, L126S and G27delGGACCA) described, activities for four (D90A, L117V, L126S and G27delGGACCA) have been measured and vary between 25% and 93% of normal levels (Andersen *et al.*, 1995; Boukaftane *et al.*, 1998; Hayward *et al.*, 1998; Kato *et al.*, 2001; Zinman *et al.*, 2009; Synofzik *et al.*,

2012). Of note, a patient with a CCS homozygous mutation has been described with SOD1 activity of ~25% of normal. This patient showed a complex neurodevelopmental phenotype; however, this is attributed to a mutation in *SLC33A1* and not a loss of SOD1 function (Huppke *et al.*, 2012).

SOD1 gain and loss of function could complement each other in amyotrophic lateral sclerosis pathogenesis

A reduction in SOD1 activity is not causative for ALS (which is certainly what the mouse data show), however, it may modify disease, as suggested by results from the mouse cross experiments described above. It seems likely such modifying effects would come through an increased susceptibility to neurodegeneration either directly through, for example, the increased susceptibility to axonal damage seen in *Sod1*^{+/-} mice, or indirectly through, for example, effects on respiration in high energy consumers such as motor neurons—note the recent finding that SOD1 is a critical focus for integrating O₂, glucose and superoxide levels, through casein kinase signalling, to repress respiration and directing energy metabolism, and that this role is independent of its function in oxidative stress (Reddi and Culotta, 2013). Thus SOD1 loss of function will likely have effects on cellular metabolism and, further, as it is still unclear why this enzyme is produced at such high levels, SOD1 may well have other as yet unknown roles in neuronal function.

Loss and gain of function mechanisms coexist in other neurodegenerative diseases as shown in models of Huntington's disease (Zuccato *et al.*, 2010), Parkinson's disease (Winklhofer *et al.*, 2008) and spinocerebellar ataxia 1 (Lim *et al.*, 2008; Crespo-Barreto *et al.*, 2010). Indeed both loss and gain of function have been hypothesized to contribute to pathogenesis in ALS caused by *TARDBP* and *FUS* mutations (Lagier-Tourenne and Cleveland, 2009; Guo *et al.*, 2011).

SOD1 has a crucial role in superoxide clearance and its loss of function generates an increased state of oxidative stress. In a tgSOD1-ALS mouse model, SOD1 is itself a major target of oxidation (Andrus *et al.*, 1998) and SOD1 oxidation and glutathionylation, which occurs in response to oxidative stress, both increase the propensity of the dimer to dissociate and become misfolded (Khare *et al.*, 2004; Rakhit *et al.*, 2004; Ezzi *et al.*, 2007; Wilcox *et al.*, 2009).

These findings set the scene for a potential co-operation of SOD1 loss and gain of function in ALS pathogenesis. Indeed, a vicious circle can be hypothesized in which oxidized SOD1 has an increased propensity to misfold, causing seeding and aggregation of SOD1 and resulting in a reduction of dismutase activity, which therefore feeds more potential oxidative stress to the start of the loop (Fig. 2). We note that the strong link between SOD1 misfolding and its loss of function (see above) make the two effects very difficult to assess independently.

A number of recent findings have underlined how such a mechanism could be relevant not only to SOD1-familial ALS, but also to sporadic cases. Hyperoxidized and misfolded SOD1 have been demonstrated in sporadic ALS cases (Bosco *et al.*, 2010; Forsberg

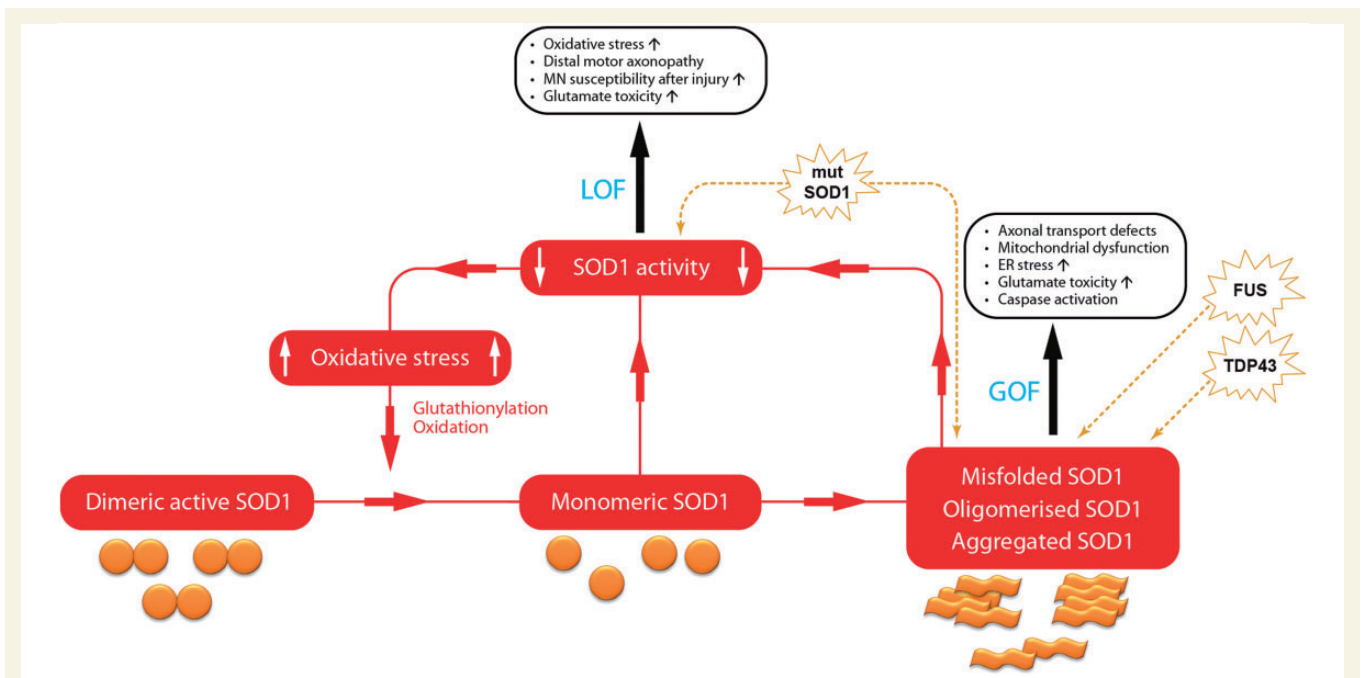


Figure 2 The cycle of SOD1 loss of function, schematic representation of a potential co-operation between SOD1 loss and gain of function in SOD1-familial ALS pathogenesis. SOD1 loss of function (LOF) increases levels of oxidative stress, which through glutathionylation and oxidation, can facilitate the monomerisation of dimeric SOD1. Once monomerized, SOD1 is more prone to become misfolded, oligomerized and aggregated. The monomerization of previously active dimeric SOD1 and the recruitment of SOD1 into aggregates further enhance the loss of function, feeding back to the beginning of the loop. In this way the gain of function (GOF) effects of misfolded, oligomerized and aggregated SOD1, which are known to cause motor neuron degeneration, are amplified by the loss of function circle. Mutant SOD1 (mutSOD1) has both a direct effect on reduction of SOD1 activity and induces SOD1 misfolding and aggregation. Mislocalisation of both TDP43 and FUS result in misfolding of SOD1. ER = endoplasmic reticulum; MN = motor neuron.

et al., 2010; Guareschi *et al.*, 2012) and misfolding of SOD1 was shown to be induced by both TDP43 and FUS mislocalization (Pokrishevsky *et al.*, 2012), events that occur in the majority of sporadic patients with ALS (Maekawa *et al.*, 2009; Deng *et al.*, 2010; Matsuoka *et al.*, 2011). Recent studies demonstrating that SOD1 aggregation can be seeded *in vitro* from mouse tgSOD1^{G93A} spinal cord material (Chia *et al.*, 2010), and 'transmitted' between cells (Munch *et al.*, 2011) extend the potential role for these pathogenic mechanisms to the clinical and pathological 'spread' of ALS (Ravits *et al.*, 2007; Pokrishevsky *et al.*, 2012). Of note, SOD1 was also found to be oxidized in Alzheimer's disease and Parkinson's disease (Choi *et al.*, 2005).

In fact, it is possible to speculate that the absence of SOD1 in the loss of function mouse model omits one of the most important targets of oxidative stress in ALS—that is, SOD1 itself—leaving the pathogenic cascade incomplete.

Finally, we note the lack of studies addressing the expression of the SOD1 *trans* allele in SOD1-familial ALS and the possibility that this plays a role in modifying the disease. Indeed, a 50 base pair deletion in the promoter region of SOD1 has been described to influence SOD1 expression and there have been attempts to correlate this with clinical characteristics in sporadic ALS, although so far results have not been replicated (Broom *et al.*, 2008). To our knowledge no studies analyse the SOD1 *trans*-allele in SOD1-familial ALS cases for the presence of this variant or other factors influencing the expression of the *trans*-allele.

Implications of SOD1 loss of function for current therapeutic approaches for amyotrophic lateral sclerosis and other diseases

Therapies are being developed for ALS and other neurodegenerative disease caused by dominant mutations, which entail knock-down of the mutant allele RNA (Smith *et al.*, 2006; Kordasiewicz *et al.*, 2012; Lu and Yang 2012). This approach is showing promise for Huntington's disease; a recent report has shown suppression of huntingtin in Huntington's disease mouse models and in the non-human primate brain, and a 75% suppression of huntingtin throughout the CNS appears to be well tolerated (Kordasiewicz *et al.*, 2012).

A number of analogous strategies have been tested for SOD1 (Ralph *et al.*, 2005; Raoul *et al.*, 2005; Saito *et al.*, 2005; Smith *et al.*, 2006; Wang *et al.*, 2010; Towne *et al.*, 2011; Wright *et al.*, 2012) and have shown very encouraging results. Excitingly, a phase 1 clinical trial has been conducted in SOD1-ALS (Fratta, 2013; Miller *et al.*, 2013) using antisense oligonucleotides that silence both mutant and wild-type SOD1, that were previously shown to be effective in a transgenic SOD1-ALS rat model (Smith *et al.*, 2006). The main aim of this study, the first of its kind, was to assess safety and so the treatment was undertaken for periods too brief to obtain a biological effect on SOD1 levels, so although the regime is reported

to be well-tolerated, it remains to be determined whether SOD1 downregulation causes unwanted effects.

The *Sod1* knockout mouse data presented here are important for these types of studies in illustrating the need to understand the full implications of such strategies. These are not only neuronal; for example, the reason most *Sod1* null (and a small percentage of *Sod1*^{+/-}) mice die is liver cancer. Thus particular attention must be paid to delivery routes, protein levels and distribution.

We note that the null mice lack *Sod1* completely, from the earliest time in development, and no appropriate model appears to be available currently for evaluating the effects of long-term endogenous *Sod1* knockdown from adulthood. The preclinical trials with RNA interference technologies used tgSOD1-ALS adult models to investigate SOD1 reduction on a very early onset and fast progressing disease, but did not study potential long term effects (Raoul *et al.*, 2005; Smith *et al.*, 2006). Experiments using conditional *Sod1* alleles would help clarify the situation. A hopeful note for ALS from the Huntington's disease study is that transient knockdown ameliorates disease for an extended period (Kordasiewicz *et al.*, 2012).

The data from *Sod1*^{+/-} animals indicate that in patients with SOD1-ALS there may be a case for epidemiological studies of the known phenotypes that arise with a 50% enzyme loss; for example, is there a greater incidence of cardiovascular disease and stroke in families with SOD1-familial ALS? Do these families have an increased incidence of liver cancer or, protection from tumours such as lung cancer, given that the majority of human lung adenocarcinomas express SOD1 at higher than normal levels (Somwar *et al.*, 2011).

Finally, knowledge of the effects of SOD1 loss of activity clearly indicates that this gene should be screened in cohorts with diseases such as hereditary distal motor neuropathies, age-related macular degeneration and progressive hearing loss, because both homozygous and heterozygous loss of function are compatible with life, at least in mice, but have abnormal phenotypes.

Acknowledgements

We thank Dr Peter Joyce and Dr Abraham Acevedo-Arozena for comments and Mr Ray Young for graphics.

Funding

P.F. is funded by Medical Research Council / Motor Neuron Disease Association Lady Edith Wolfson Fellowship. R.S. and E.M.C.F. are funded by the UK Motor Neuron Disease Association. R.K.A.B.-S., E.M.C.F. are funded by the UK Medical Research Council and the Thierry Latran Foundation.

Supplementary material

Supplementary material is available at *Brain* online.

References

- Acevedo-Arozena A, Kalmar B, Essa S, Ricketts T, Joyce P, Kent R, *et al.* A comprehensive assessment of the SOD1G93A low-copy transgenic mouse, which models human amyotrophic lateral sclerosis. *Dis Model Mech* 2011; 4: 686–700.
- Acsadi G, Lee I, Li X, Khaidakov M, Pecinova A, Parker GC, *et al.* Mitochondrial dysfunction in a neural cell model of spinal muscular atrophy. *J Neurosci Res* 2009; 87: 2748–56.
- Andersen PM, Al Chalabi A. Clinical genetics of amyotrophic lateral sclerosis: what do we really know? *Nat Rev Neurol* 2011; 7: 603–15.
- Andersen PM, Nilsson P, Ala-Hurula V, Keranen ML, Tarvainen I, Haltia T, *et al.* Amyotrophic lateral sclerosis associated with homozygosity for an Asp90Ala mutation in CuZn-superoxide dismutase. *Nat Genet* 1995; 10: 61–6.
- Andrus PK, Fleck TJ, Gurney ME, Hall ED. Protein oxidative damage in a transgenic mouse model of familial amyotrophic lateral sclerosis. *J Neurochem* 1998; 71: 2041–8.
- Apostolski S, Nikolic J, Bugarski-Prokopljivic C, Miletic V, Pavlovic S, Filipovic S. Serum and CSF immunological findings in ALS. *Acta Neurol Scand* 1991; 83: 96–8.
- Baloh RH, Rakowicz W, Gardner R, Pestronk A. Frequent atrophic groups with mixed-type myofibers is distinctive to motor neuron syndromes. *Muscle Nerve* 2007a; 36: 107–10.
- Baloh RH, Schmidt RE, Pestronk A, Milbrandt J. Altered axonal mitochondrial transport in the pathogenesis of Charcot-Marie-Tooth disease from mitofusin 2 mutations. *J Neurosci* 2007b; 27: 422–30.
- Barber SC, Shaw PJ. Oxidative stress in ALS: key role in motor neuron injury and therapeutic target. *Free Radic Biol Med* 2010; 48: 629–41.
- Beal MF. Role of excitotoxicity in human neurological disease. *Curr Opin Neurobiol* 1992; 2: 657–62.
- Beckman JS, Carson M, Smith CD, Koppenol WH. ALS, SOD and peroxynitrite. *Nature* 1993; 364: 584.
- Bhusari SS, Dobosy JR, Fu V, Almassi N, Oberley T, Jarrard DF. Superoxide dismutase 1 knockdown induces oxidative stress and DNA methylation loss in the prostate. *Epigenetics* 2010; 5: 402–9.
- Birve A, Neuwirth C, Weber M, Marklund SL, Nilsson AC, Jonsson PA, *et al.* A novel SOD1 splice site mutation associated with familial ALS revealed by SOD activity analysis. *Hum Mol Genet* 2010; 19: 4201–6.
- Bodendorf U, Danner S, Fischer F, Stefani M, Sturchler-Pierrat C, Wiederhold KH, *et al.* Expression of human beta-secretase in the mouse brain increases the steady-state level of beta-amyloid. *J Neurochem* 2002; 80: 799–806.
- Borchelt DR, Lee MK, Slunt HS, Guarnieri M, Xu ZS, Wong PC, *et al.* Superoxide dismutase 1 with mutations linked to familial amyotrophic lateral sclerosis possesses significant activity. *Proc Natl Acad Sci USA* 1994; 91: 8292–6.
- Bosco DA, Morfini G, Karabacak NM, Song Y, Gros-Louis F, Pasinelli P, *et al.* Wild-type and mutant SOD1 share an aberrant conformation and a common pathogenic pathway in ALS. *Nat Neurosci* 2010; 13: 1396–403.
- Boukaftane Y, Khoris J, Moulard B, Salachas F, Meininger V, Malafosse A, *et al.* Identification of six novel SOD1 gene mutations in familial amyotrophic lateral sclerosis. *Can J Neurol Sci* 1998; 25: 192–6.
- Bowling AC, Schulz JB, Brown RH Jr., Beal MF. Superoxide dismutase activity, oxidative damage, and mitochondrial energy metabolism in familial and sporadic amyotrophic lateral sclerosis. *J Neurochem* 1993; 61: 2322–5.
- Broom WJ, Greenway M, Sadri-Vakili G, Russ C, Auwarter KE, Glajch KE, *et al.* 50bp deletion in the promoter for superoxide dismutase 1 (SOD1) reduces SOD1 expression *in vitro* and may correlate with increased age of onset of sporadic amyotrophic lateral sclerosis. *Amyotroph Lateral Scler* 2008; 9: 229–37.
- Browne SE, Bowling AC, Baik MJ, Gurney M, Brown RH Jr., Beal MF. Metabolic dysfunction in familial, but not sporadic, amyotrophic lateral sclerosis. *J Neurochem* 1998; 71: 281–7.

- Brujin LI, Becher MW, Lee MK, Anderson KL, Jenkins NA, Copeland NG, et al. ALS-linked SOD1 mutant G85R mediates damage to astrocytes and promotes rapidly progressive disease with SOD1-containing inclusions. *Neuron* 1997; 18: 327–38.
- Brujin LI, Houseweart MK, Kato S, Anderson KL, Anderson SD, Ohama E, et al. Aggregation and motor neuron toxicity of an ALS-linked SOD1 mutant independent from wild-type SOD1. *Science* 1998; 281: 1851–4.
- Casari M, Corso F, Bassi A, Capra F, Gabrielli GB, Stanzial AM, et al. Decreased activity of scavenger enzymes in human hepatocellular carcinoma, but not in liver metastases. *International Journal of Clinical and Laboratory research* 1994; 24: 94–97.
- Cassereau J, Chevrollier A, Gueguen N, Desquiret V, Verny C, Nicolas G, et al. Mitochondrial dysfunction and pathophysiology of Charcot-Marie-Tooth disease involving GADP1 mutations. *Exp Neurol* 2011; 227: 31–41.
- Chang LY, Slot JW, Geuze HJ, Crapo JD. Molecular immunocytochemistry of the CuZn superoxide dismutase in rat hepatocytes. *J Cell Biol* 1988; 107: 2169–79.
- Chestnut BA, Chang Q, Price A, Lesuisse C, Wong M, Martin LJ. Epigenetic regulation of motor neuron cell death through DNA methylation. *J Neurosci* 2011; 31: 16619–36.
- Chia R, Tattum MH, Jones S, Collinge J, Fisher EM, Jackson GS. Superoxide dismutase 1 and tgSOD1 mouse spinal cord seed fibrils, suggesting a propagative cell death mechanism in amyotrophic lateral sclerosis. *PLoS One* 2010; 5: e10627.
- Choi J, Rees HD, Weintraub ST, Levey AI, Chin LS, Li L. Oxidative modifications and aggregation of Cu,Zn-superoxide dismutase associated with Alzheimer and Parkinson diseases. *J Biol Chem* 2005; 280: 11648–55.
- Crapo JD, Oury T, Rabouille C, Slot JW, Chang LY. Copper,zinc superoxide dismutase is primarily a cytosolic protein in human cells. *Proc Natl Acad Sci USA* 1992; 89: 10405–9.
- Crespo-Barreto J, Fryer JD, Shaw CA, Orr HT, Zoghbi HY. Partial loss of ataxin-1 function contributes to transcriptional dysregulation in spinocerebellar ataxia type 1 pathogenesis. *PLoS Genet* 2010; 6: e1001021.
- Culotta VC, Klomp LW, Strain J, Casareno RL, Krems B, Gitlin JD. The copper chaperone for superoxide dismutase. *J Biol Chem* 1997; 272: 23469–72.
- Culotta VC, Lin SJ, Schmidt P, Klomp LW, Casareno RL, Gitlin J. Intracellular pathways of copper trafficking in yeast and humans. *Adv Exp Med Biol* 1999; 448: 247–54.
- de Lustig ES, Serra JA, Kohan S, Canziani GA, Famulari AL, Dominguez RO. Copper-zinc superoxide dismutase activity in red blood cells and serum in demented patients and in aging. *J Neurol Sci* 1993; 115: 18–25.
- De Vos KJ, Chapman AL, Tennant ME, Manser C, Tudor EL, Lau KF, et al. Familial amyotrophic lateral sclerosis-linked SOD1 mutants perturb fast axonal transport to reduce axonal mitochondria content. *Hum Mol Genet* 2007; 16: 2720–8.
- Deng HX, Hentati A, Tainer JA, Iqbal Z, Cayabyab A, Hung WY, et al. Amyotrophic lateral sclerosis and structural defects in Cu,Zn superoxide dismutase. *Science* 1993; 261: 1047–51.
- Deng HX, Shi Y, Furukawa Y, Zhai H, Fu R, Liu E, et al. Conversion to the amyotrophic lateral sclerosis phenotype is associated with intermolecular linked insoluble aggregates of SOD1 in mitochondria. *Proc Natl Acad Sci USA* 2006; 103: 7142–7.
- Deng HX, Zhai H, Bigio EH, Yan J, Fecto F, Ajroud K, et al. FUS-immunoreactive inclusions are a common feature in sporadic and non-SOD1 familial amyotrophic lateral sclerosis. *Ann Neurol* 2010; 67: 739–48.
- Dengler R, Konstanzer A, Kuther G, Hesse S, Wolf W, Struppler A. Amyotrophic lateral sclerosis: macro-EMG and twitch forces of single motor units. *Muscle Nerve* 1990; 13: 545–50.
- Didion SP, Kinzenbaw DA, Schrader LI, Faraci FM. Heterozygous CuZn superoxide dismutase deficiency produces a vascular phenotype with aging. *Hypertension* 2006; 48: 1072–9.
- Elchuri S, Oberley TD, Qi W, Eisenstein RS, Jackson RL, Van Remmen H, et al. CuZnSOD deficiency leads to persistent and widespread oxidative damage and hepatocarcinogenesis later in life. *Oncogene* 2005; 24: 367–380.
- Etzi SA, Urushitani M, Julien JP. Wild-type superoxide dismutase acquires binding and toxic properties of ALS-linked mutant forms through oxidation. *J Neurochem* 2007; 102: 170–8.
- Faes L, Callewaert G. Mitochondrial dysfunction in familial amyotrophic lateral sclerosis. *J Bioenerg Biomembr* 2011; 43: 587–92.
- Fischer LR, Culver DG, Tennant P, Davis AA, Wang M, Castellano-Sanchez A, et al. Amyotrophic lateral sclerosis is a distal axonopathy: evidence in mice and man. *Exp Neurol* 2004; 185: 232–40.
- Fischer LR, Glass JD. Oxidative stress induced by loss of Cu,Zn-superoxide dismutase (SOD1) or superoxide-generating herbicides causes axonal degeneration in mouse DRG cultures. *Acta Neuropathol* 2010; 119: 249–59.
- Fischer LR, Igoudjil A, Magrané J, Li Y, Hansen JM, Manfredi G, et al. SOD1 targeted to the mitochondrial intermembrane space prevents motor neuropathy in the Sod1 knockout mouse. *Brain* 2011; 134: 196–209.
- Fischer LR, Li Y, Asres SA, Jones DP, Glass JD. Absence of SOD1 leads to oxidative stress in peripheral nerve and causes a progressive distal motor axonopathy. *Exp Neurol* 2012; 233: 163–71.
- Fitzmaurice PS, Shaw IC, Kleiner HE, Miller RT, Monks TJ, Lau SS, et al. Evidence for DNA damage in amyotrophic lateral sclerosis. *Muscle Nerve* 1996; 19: 797–8.
- Flood DG, Reaume AG, Gruner JA, Hoffman EK, Hirsch JD, Lin YG, et al. Hindlimb motor neurons require Cu/Zn superoxide dismutase for maintenance of neuromuscular junctions. *Am J Pathol* 1999; 155: 663–72.
- Forsberg K, Jonsson PA, Andersen PM, Bergemalm D, Graffmo KS, Hultdin M, et al. Novel antibodies reveal inclusions containing non-native SOD1 in sporadic ALS patients. *PLoS One* 2010; 5: e11552.
- Fratta P. Antisense makes sense for ALS. *Lancet Neurol* 2013; 12: 416–417.
- Frey D, Schneider C, Xu L, Borg J, Spooren W, Caroni P. Early and selective loss of neuromuscular synapse subtypes with low sprouting competence in motoneuron diseases. *J Neurosci* 2000; 20: 2534–42.
- Fridovich I. Biological effects of the superoxide radical. *Arch Biochem Biophys* 1986; 247: 1–11.
- Fridovich I. Superoxide radical and superoxide dismutases. *Annu Rev Biochem* 1995; 64: 97–112.
- Fukada K, Nagano S, Satoh M, Tohyama C, Nakanishi T, Shimizu A, et al. Stabilization of mutant Cu/Zn superoxide dismutase (SOD1) protein by coexpressed wild SOD1 protein accelerates the disease progression in familial amyotrophic lateral sclerosis mice. *Eur J Neurosci* 2001; 14: 2032–6.
- Ge WW, Leystra-Lantz C, Sanelli TR, McLean J, Wen W, Strong W, et al. Neuronal tissue-specific ribonucleoprotein complex formation on SOD1 mRNA: alterations by ALS SOD1 mutations. *Neurobiol Dis* 2006; 23: 342–50.
- Graffmo KS, Forsberg K, Bergh J, Birve A, Zetterstrom P, Andersen P, et al. Expression of wild-type human superoxide dismutase-1 in mice causes amyotrophic lateral sclerosis. *Human Mol Genet* 2013; 22: 51–60.
- Guareschi S, Cova E, Cereda C, Ceroni M, Donetti E, Bosco DA, et al. An over-oxidized form of superoxide dismutase found in sporadic amyotrophic lateral sclerosis with bulbar onset shares a toxic mechanism with mutant SOD1. *Proc Natl Acad Sci USA* 2012; 109: 5074–9.
- Guo W, Chen Y, Zhou X, Kar A, Ray P, Chen X, et al. An ALS-associated mutation affecting TDP-43 enhances protein aggregation, fibril formation and neurotoxicity. *Nat Struct Mol Biol* 2011; 18: 822–30.
- Gurney ME, Pu H, Chiu AY, Dal Canto MC, Polchow CY, Alexander DD, et al. Motor neuron degeneration in mice that express a human Cu,Zn superoxide dismutase mutation. *Science* 1994; 264: 1772–5.

- Haverkamp LJ, Appel V, Appel SH. Natural history of amyotrophic lateral sclerosis in a database population. Validation of a scoring system and a model for survival prediction. *Brain* 1995; 118: 707–19.
- Hayward C, Brock DJH, Minns RA, Swingler RJ. Homozygosity for Asn86Ser mutation in the CuZn superoxide dismutase gene produces a severe clinical phenotype in a juvenile onset case of familial amyotrophic lateral sclerosis. *J Med Genet* 1998; 35: 174.
- Ho YS, Gargano M, Cao J, Bronson RT, Heimler I, Hutz RJ. Reduced fertility in female mice lacking copper-zinc superoxide dismutase. *J Biol Chem* 1998; 273: 7765–9.
- Hu J, Chen K, Ni B, Li L, Chen G, Shi S. A novel SOD1 mutation in amyotrophic lateral sclerosis with a distinct clinical phenotype. *Amyotroph Lateral Scler* 2012; 13: 149–54.
- Huang TT, Yasunami M, Carlson EJ, Gillespie AM, Reaume AG, Hoffman EK, et al. Superoxide-mediated cytotoxicity in superoxide dismutase-deficient fetal fibroblasts. *Arch Biochem Biophys* 1997; 344: 424–32.
- Huppke P, Brendel C, Korenke GC, Marquardt I, Donsante A, Yi L, et al. Molecular and biochemical characterization of a unique mutation in CCS, the human copper chaperone to superoxide dismutase. *Hum Mutat* 2012; 33: 1207–15.
- Ilieva H, Polymenidou M, Cleveland DW. Non-cell autonomous toxicity in neurodegenerative disorders: ALS and beyond. *J Cell Biol* 2009; 187: 761–72.
- Jaarsma D, Haasdijk ED, Grashorn JA, Hawkins R, van Duijn W, Verspaget HW, et al. Human Cu/Zn superoxide dismutase (SOD1) overexpression in mice causes mitochondrial vacuolization, axonal degeneration, and premature motoneuron death and accelerates motoneuron disease in mice expressing a familial amyotrophic lateral sclerosis mutant SOD1. *Neurobiol Dis* 2000; 7: 623–43.
- Jang YC, Lustgarten MS, Liu Y, Muller FL, Bhattacharya A, Liang H, et al. Increased superoxide *in vivo* accelerates age-associated muscle atrophy through mitochondrial dysfunction and neuromuscular junction degeneration. *FASEB J* 2010; 24: 1376–90.
- Jonsson PA, Bergemalm D, Andersen PM, Gredal O, Brannstrom T, Marklund SL. Inclusions of amyotrophic lateral sclerosis-linked superoxide dismutase in ventral horns, liver, and kidney. *Ann Neurol* 2008; 63: 671–5.
- Jonsson PA, Ernhill K, Andersen PM, Bergemalm D, Brannstrom T, Gredal O, et al. Minute quantities of misfolded mutant superoxide dismutase-1 cause amyotrophic lateral sclerosis. *Brain* 2004; 127: 73–88.
- Joyce PI, Fratta P, Fisher EM, Acevedo-Arozena A. SOD1 and TDP-43 animal models of amyotrophic lateral sclerosis: recent advances in understanding disease toward the development of clinical treatments. *Mamm Genome* 2011; 22: 420–48.
- Kato M, Aoki M, Ohta M, Nagai M, Ishizaki F, Nakamura S, et al. Marked reduction of the Cu/Zn superoxide dismutase polypeptide in a case of familial amyotrophic lateral sclerosis with the homozygous mutation. *Neurosci Lett* 2001; 312: 165–8.
- Keithley EM, Canto C, Zheng QY, Wang X, Fischel-Ghodsian N, Johnson KR. Cu/Zn superoxide dismutase and age-related hearing loss. *Hear Res* 2005; 209: 76–85.
- Keller GA, Warner TG, Steimer KS, Hallelwell RA. Cu,Zn superoxide dismutase is a peroxisomal enzyme in human fibroblasts and hepatoma cells. *Proc Natl Acad Sci USA* 1991; 88: 7381–5.
- Kennel PF, Finiels F, Revah F, Mallet J. Neuromuscular function impairment is not caused by motor neurone loss in FALS mice: an electromyographic study. *Neuroreport* 1996; 7: 1427–31.
- Khare SD, Caplow M, Dokholyan NV. The rate and equilibrium constants for a multistep reaction sequence for the aggregation of superoxide dismutase in amyotrophic lateral sclerosis. *Proc Natl Acad Sci USA* 2004; 101: 15094–9.
- Kobayashi J, Kuroda M, Kawata A, Mochizuki Y, Mizutani T, Komori T, et al. Novel G37V mutation of SOD1 gene in autopsied patient with familial amyotrophic lateral sclerosis. *Amyotroph Lateral Scler* 2012; 13: 570–72.
- Kondo T, Reaume AG, Huang TT, Carlson E, Murakami K, Chen SF, et al. Reduction of CuZn-superoxide dismutase activity exacerbates neuronal cell injury and edema formation after transient focal cerebral ischemia. *J Neurosci* 1997; 17: 4180–9.
- Kordasiewicz HB, Stanek LM, Wancewicz EV, Mazur C, McAlonis MM, Pytel KA, et al. Sustained therapeutic reversal of Huntington's disease by transient repression of huntingtin synthesis. *Neuron* 2012; 74: 1031–44.
- Kostrominova TY. Advanced age-related denervation and fiber-type grouping in skeletal muscle of SOD1 knockout mice. *Free Radic Biol Med* 2010; 49: 1582–93.
- Lagier-Tourenne C, Cleveland DW. Rethinking ALS: the FUS about TDP-43. *Cell* 2009; 136: 1001–4.
- Larkin LM, Davis CS, Sims-Robinson C, Kostrominova TY, Remmen HV, Richardson A, et al. Skeletal muscle weakness due to deficiency of CuZn-superoxide dismutase is associated with loss of functional innervation. *Am J Physiol Regul Integr Comp Physiol* 2011; 301: R1400–7.
- Leonardi A, Abbruzzese G, Arata L, Cocito L, Vische M. Cerebrospinal fluid (CSF) findings in amyotrophic lateral sclerosis. *J Neurol* 1984; 231: 75–8.
- Liaw KY, Lee PH, Wu FC, Tsai JS, Lin-Shiau SY. Zinc, copper, and superoxide dismutase in hepatocellular carcinoma. *Am J Gastroenterol* 1997; 92: 2260–2263.
- Lim J, Crespo-Barreto J, Jafar-Nejad P, Bowman AB, Richman R, Hill DE, et al. Opposing effects of polyglutamine expansion on native protein complexes contribute to SCA1. *Nature* 2008; 452: 713–8.
- Lin MT, Wang MY, Liaw KY, Lee PH, Chien SF, Tsai JS, et al. Superoxide dismutase in hepatocellular carcinoma affects patient prognosis. *Hepatology* 2001; 48: 1102–1105.
- Lobsiger CS, Boillee S, McAlonis-Downes M, Khan AM, Feltri ML, Yamanaka K, et al. Schwann cells expressing dismutase active mutant SOD1 unexpectedly slow disease progression in ALS mice. *Proc Natl Acad Sci USA* 2009; 106: 4465–70.
- Lu XH, Yang XW. "Huntingtin Holiday": Progress toward an antisense therapy for Huntington's disease. *Neuron* 2012; 74: 964–6.
- Maekawa S, Leigh PN, King A, Jones E, Steele JC, Bodi I, et al. TDP-43 is consistently co-localized with ubiquitinated inclusions in sporadic and Guam amyotrophic lateral sclerosis but not in familial amyotrophic lateral sclerosis with and without SOD1 mutations. *Neuropathology* 2009; 29: 672–83.
- Marikovsky M, Ziv V, Nevo N, Harris-Cerruti C, Mahler O. Cu/Zn superoxide dismutase plays important role in immune response. *J Immunol* 2003; 170: 2993–3001.
- Marklund SL, Holme E, Hellner L. Superoxide dismutase in extracellular fluids. *Clin Chim Acta* 1982; 126: 41–51.
- Matsuoka T, Fujii N, Kondo A, Iwaki A, Hokonohara T, Honda H, et al. An autopsied case of sporadic adult-onset amyotrophic lateral sclerosis with FUS-positive basophilic inclusions. *Neuropathology* 2011; 31: 71–6.
- Matzuk MM, Dionne L, Guo Q, Kumar TR, Lebovitz RM. Ovarian function in superoxide dismutase 1 and 2 knockout mice. *Endocrinology* 1998; 139: 4008–11.
- Miller T, Pestronk A, David W, Rothstein J, Simpson E, Appel SH, et al. A Phase I, randomised, first-in-human study of an antisense oligonucleotide directed against SOD1 delivered intrathecally in SOD1-familial ALS patients. *Lancet Neurol* 2013; 12: 435–442.
- Mitchell JJ, Trakadis YJ, Scriver CR. Phenylalanine hydroxylase deficiency. *Genet Med* 2011; 13: 697–707.
- Mitsumoto H, Santella RM, Liu X, Bogdanov M, Zipprich J, Wu HC, et al. Oxidative stress biomarkers in sporadic ALS. *Amyotroph Lateral Scler* 2008; 9: 177–83.
- Muller FL, Liu Y, Van Remmen H. Complex III releases superoxide to both sides of the inner mitochondrial membrane. *J Biol Chem* 2004; 279: 49064–73.
- Muller FL, Song W, Liu Y, Chaudhuri A, Pieke-Dahl S, Strong R, et al. Absence of CuZn superoxide dismutase leads to elevated oxidative stress and acceleration of age-dependent skeletal muscle atrophy. *Free Radic Biol Med* 2006; 40: 1993–2004.
- Munch C, O'Brien J, Bertolotti A. Prion-like propagation of mutant superoxide dismutase-1 misfolding in neuronal cells. *Proc Natl Acad Sci USA* 2011; 108: 3548–53.

- Murray LM, Talbot K, Gillingwater TH. Review: neuromuscular synaptic vulnerability in motor neurone disease: amyotrophic lateral sclerosis and spinal muscular atrophy. *Neuropathol Appl Neurobiol* 2010; 36: 133–56.
- Pasinelli P, Brown RH. Molecular biology of amyotrophic lateral sclerosis: insights from genetics. *Nat Rev Neurosci* 2006; 7: 710–23.
- Pokrishevsky E, Grad LI, Yousefi M, Wang J, Mackenzie IR, Cashman NR. Aberrant localization of FUS and TDP43 is associated with misfolding of SOD1 in amyotrophic lateral sclerosis. *PLoS One* 2012; 7: e35050.
- Pramatarova A, Figlewicz DA, Krizus A, Han FY, Ceballos-Picot I, Nicole A, et al. Identification of new mutations in the Cu/Zn superoxide dismutase gene of patients with familial amyotrophic lateral sclerosis. *Am J Genet* 1995; 56: 592–6.
- Proescher JB, Son M, Elliott JL, Culotta VC. Biological effects of CCS in the absence of SOD1 enzyme activation: implications for disease in a mouse model for ALS. *Hum Mol Genet* 2008; 17: 1728–37.
- Prudencio M, Durazo A, Whitelegge JP, Borchelt DR. An examination of wild-type SOD1 in modulating the toxicity and aggregation of ALS-associated mutant SOD1. *Hum Mol Genet* 2010; 19: 4774–89.
- Pun S, Santos AF, Saxena S, Xu L, Caroni P. Selective vulnerability and pruning of phasic motoneuron axons in motoneuron disease alleviated by CNTF. *Nat Neurosci* 2006; 9: 408–19.
- Pupillo E, Messina P, Logroschino G, Zoccolella S, Chio A, Calvo A, et al. Trauma and amyotrophic lateral sclerosis: a case-control study from a population-based registry. *Eur J Neurol* 2012; 19: 1509–17.
- Rakhit R, Crow JP, Lepock JR, Kondejewski LH, Cashman NR, Chakrabarty A. Monomeric Cu,Zn-superoxide dismutase is a common misfolding intermediate in the oxidation models of sporadic and familial amyotrophic lateral sclerosis. *J Biol Chem* 2004; 279: 15499–504.
- Ralph GS, Radcliffe PA, Day DM, Carthy JM, Leroux MA, Lee DC, et al. Silencing mutant SOD1 using RNAi protects against neurodegeneration and extends survival in an ALS model. *Nat Med* 2005; 11: 429–33.
- Raoul C, Abbas-Terki T, Bensadoun JC, Guillot S, Haase G, Szulc J, et al. Lentiviral-mediated silencing of SOD1 through RNA interference retards disease onset and progression in a mouse model of ALS. *Nat Med* 2005; 11: 423–8.
- Ratovitski T, Corson LB, Strain J, Wong P, Cleveland DW, Culotta VC, et al. Variation in the biochemical/biophysical properties of mutant superoxide dismutase 1 enzymes and the rate of disease progression in familial amyotrophic lateral sclerosis kindreds. *Hum Mol Genet* 1999; 8: 1451–60.
- Ravits J, Laurie P, Fan Y, Moore DH. Implications of ALS focality: rostral-caudal distribution of lower motor neuron loss postmortem. *Neurology* 2007; 68: 1576–82.
- Reaume AG, Elliott JL, Hoffman EK, Kowall NW, Ferrante RJ, Siwek DF, et al. Motor neurons in Cu/Zn superoxide dismutase-deficient mice develop normally but exhibit enhanced cell death after axonal injury. *Nat Genet* 1996; 13: 43–7.
- Reddi AR, Culotta VC. SOD1 integrates signals from oxygen and glucose to repress respiration. *Cell* 2013; 152: 224–35.
- Robberecht W, Sapp P, Viaene MK, Rosen D, McKenna-Yasek D, Haines J, et al. Cu/Zn superoxide dismutase activity in familial and sporadic amyotrophic lateral sclerosis. *J Neurochem* 1994; 62: 384–7.
- Roe JA, Butler A, Scholler DM, Valentine JS, Marky L, Breslauer KJ. Differential scanning calorimetry of Cu,Zn-superoxide dismutase, the apoprotein, and its zinc-substituted derivatives. *Biochemistry* 1988; 27: 950–8.
- Rosen DR, Bowling AC, Patterson D, Usdin TB, Sapp P, Mezey E, et al. A frequent ala 4 to val superoxide dismutase-1 mutation is associated with a rapidly progressive familial amyotrophic lateral sclerosis. *Hum Mol Genet* 1994; 3: 981–7.
- Rosen DR, Siddique T, Patterson D, Figlewicz DA, Sapp P, Hentati A, et al. Mutations in Cu/Zn superoxide dismutase gene are associated with familial amyotrophic lateral sclerosis. *Nature* 1993; 362: 59–62.
- Rothstein JD. Current hypotheses for the underlying biology of amyotrophic lateral sclerosis. *Ann Neurol* 2009; 65 (Suppl 1): S3–9.
- Saito Y, Yokota T, Mitani T, Ito K, Anzai M, Miyagishi M, et al. Transgenic small interfering RNA halts amyotrophic lateral sclerosis in a mouse model. *J Biol Chem* 2005; 280: 42826–30.
- Sasaki S, Aoki M, Nagai M, Kobayashi M, Itoyama Y. Mitochondrial alterations in transgenic mice with an H46R mutant Cu/Zn superoxide dismutase gene. *J Neuropathol Exp Neurol* 2009; 68: 365–73.
- Sato T, Nakanishi T, Yamamoto Y, Andersen PM, Ogawa Y, Fukada K, et al. Rapid disease progression correlates with instability of mutant SOD1 in familial ALS. *Neurology* 2005; 65: 1954–7.
- Schwartz PJ, Reaume A, Scott R, Coyle JT. Effects of over- and under-expression of Cu,Zn-superoxide dismutase on the toxicity of glutamate analogs in transgenic mouse striatum. *Brain Res* 1998; 789: 32–39.
- Shaw PJ, Ince PG, Falkous G, Mantle D. Oxidative damage to protein in sporadic motor neuron disease spinal cord. *Ann Neurol* 1995; 38: 691–5.
- Shefner JM, Reaume AG, Flood DG, Scott RW, Kowall NW, Ferrante RJ, et al. Mice lacking cytosolic copper/zinc superoxide dismutase display a distinctive motor axonopathy. *Neurology* 1999; 53: 1239–46.
- Shibata N, Nagai R, Uchida K, Horiuchi S, Yamada S, Hirano A, et al. Morphological evidence for lipid peroxidation and protein glycoxidation in spinal cords from sporadic amyotrophic lateral sclerosis patients. *Brain Res* 2001; 917: 97–104.
- Simpson EP, Henry YK, Henkel JS, Smith RG, Appel SH. Increased lipid peroxidation in sera of ALS patients: a potential biomarker of disease burden. *Neurology* 2004; 62: 1758–65.
- Smith CD, Carney JM, Starke-Reed PE, Oliver CN, Stadtman ER, Floyd RA, et al. Excess brain protein oxidation and enzyme dysfunction in normal aging and in Alzheimer disease. *Proc Natl Acad Sci USA* 1991; 88: 10540–3.
- Smith RA, Miller TM, Yamanaka K, Monia BP, Condon TP, Hung G, et al. Antisense oligonucleotide therapy for neurodegenerative disease. *J Clin Invest* 2006; 116: 2290–6.
- Smith RG, Henry YK, Mattson MP, Appel SH. Presence of 4-hydroxynonenal in cerebrospinal fluid of patients with sporadic amyotrophic lateral sclerosis. *Ann Neurol* 1998; 44: 696–9.
- Somwar R, Erdjument-Bromage H, Larsson E, Shum D, Lockwood WW, Yang G, et al. Superoxide dismutase 1 (SOD1) is a target for a small molecule identified in a screen for inhibitors of the growth of lung adenocarcinoma cell lines. *Proc Natl Acad Sci USA* 2011; 108: 16375–80.
- Son M, Fu Q, Puttappathi K, Matthews CM, Elliott JL. Redox susceptibility of SOD1 mutants is associated with the differential response to CCS over-expression *in vivo*. *Neurobiol Dis* 2009; 34: 155–62.
- Sreedharan J, Blair IP, Tripathi VB, Hu X, Vance C, Rogelj B, et al. TDP-43 mutations in familial and sporadic amyotrophic lateral sclerosis. *Science* 2008; 319: 1668–72.
- Stadtman ER. Protein oxidation and aging. *Science* 1992; 257: 1220–4.
- Stadtman ER, Berlett BS. Reactive oxygen-mediated protein oxidation in aging and disease. *Chem Res Toxicol* 1997; 10: 485–94.
- Sturtz LA, Diekert K, Jensen LT, Lill R, Culotta VC. A fraction of yeast Cu,Zn-superoxide dismutase and its metallochaperone, CCS, localize to the intermembrane space of mitochondria. A physiological role for SOD1 in guarding against mitochondrial oxidative damage. *J Biol Chem* 2001; 276: 38084–9.
- Subramaniam JR, Lyons WE, Liu J, Bartnikas TB, Rothstein J, Price DL, et al. Mutant SOD1 causes motor neuron disease independent of copper chaperone-mediated copper loading. *Nat Neurosci* 2002; 5: 301–7.
- Synofzik M, Ronchi D, Keskin I, Basak AN, Wilhelm C, Gobbi C, et al. Mutant superoxide dismutase-1 indistinguishable from wild-type causes ALS. *Hum Mol Genet* 2012; 21: 3568–74.
- Takahashi M, Dinse GE, Foley JF, Hardisty JF, Maronpot RR. Comparative prevalence, multiplicity, and progression of spontaneous and vinyl carbamate-induced liver lesions in five strains of male mice. *Toxicol Pathology* 2002; 30: 599–605.

- Towne C, Setola V, Schneider BL, Aebischer P. Neuroprotection by gene therapy targeting mutant SOD1 in individual pools of motor neurons does not translate into therapeutic benefit in fALS mice. *Mol Ther* 2011; 19: 274–83.
- Turner BJ, Ackerley S, Davies KE, Talbot K. Dismutase-competent SOD1 mutant accumulation in myelinating Schwann cells is not detrimental to normal or transgenic ALS model mice. *Hum Mol Genet* 2010; 19: 815–24.
- Turner BJ, Talbot K. Transgenics, toxicity and therapeutics in rodent models of mutant SOD1-mediated familial ALS. *Prog Neurobiol* 2008; 85: 94–134.
- Wang J, Xu G, Borchelt DR. Mapping superoxide dismutase 1 domains of non-native interaction: roles of intra- and intermolecular disulfide bonding in aggregation. *J Neurochem* 2006; 96: 1277–88.
- Wang L, Deng HX, Grisotti G, Zhai H, Siddique T, Roos RP. Wild-type SOD1 overexpression accelerates disease onset of a G85R SOD1 mouse. *Hum Mol Genet* 2009a; 18: 1642–51.
- Wang L, Grisotti G, Roos RP. Mutant SOD1 knockdown in all cell types ameliorates disease in G85R SOD1 mice with a limited additional effect over knockdown restricted to motor neurons. *J Neurochem* 2010; 113: 166–74.
- Wang L, Gutmann DH, Roos RP. Astrocyte loss of mutant SOD1 delays ALS disease onset and progression in G85R transgenic mice. *Hum Mol Genet* 2011; 20: 286–93.
- Wang L, Pytel P, Feltri ML, Wrabetz L, Roos RP. Selective knockdown of mutant SOD1 in Schwann cells ameliorates disease in G85R mutant SOD1 transgenic mice. *Neurobiol Dis* 2012; 48: 52–7.
- Wang L, Sharma K, Grisotti G, Roos RP. The effect of mutant SOD1 dismutase activity on non-cell autonomous degeneration in familial amyotrophic lateral sclerosis. *Neurobiol Dis* 2009b; 35: 234–0.
- Wang X, Culotta VC, Klee CB. Superoxide dismutase protects calcineurin from inactivation. *Nature* 1996; 383: 434–7.
- Watanabe Y, Kuno N, Kono Y, Nanba E, Ohama E, Nakashima K, et al. Absence of the mutant SOD1 in familial amyotrophic lateral sclerosis (FALS) with two base pair deletion in the SOD1 gene. *Acta Neurol Scand* 1997; 95: 167–72.
- Wei JP, Srinivasan C, Han H, Valentine JS, Gralla EB. Evidence for a novel role of copper-zinc superoxide dismutase in zinc metabolism. *J Biol Chem* 2001; 276: 44798–803.
- Wen HL, Lin YT, Ting CH, Lin-Chao S, Li H, Hsieh-Li HM. Stathmin, a microtubule-destabilizing protein, is dysregulated in spinal muscular atrophy. *Hum Mol Genet* 2010; 19: 1766–78.
- Weydert CJ, Cullen JJ. Measurement of superoxide dismutase, catalase and glutathione peroxidase in cultured cells and tissue. *Nat Protoc* 2010; 5: 51–66.
- Wilcox KC, Zhou L, Jordon JK, Huang Y, Yu Y, Redler RL, et al. Modifications of superoxide dismutase (SOD1) in human erythrocytes: a possible role in amyotrophic lateral sclerosis. *J Biol Chem* 2009; 284: 13940–7.
- Winklhofer KF, Tatzelt J, Haass C. The two faces of protein misfolding: gain- and loss-of-function in neurodegenerative diseases. *EMBO J* 2008; 27: 336–49.
- Wong PC, Waggoner D, Subramaniam JR, Tessarollo L, Bartnikas TB, Culotta VC, et al. Copper chaperone for superoxide dismutase is essential to activate mammalian Cu/Zn superoxide dismutase. *Proc Natl Acad Sci USA* 2000; 97: 2886–91.
- Wright PD, Wightman N, Huang M, Weiss A, Sapp PC, Cuny GD, et al. A high-throughput screen to identify inhibitors of SOD1 transcription. *Front Biosci (Elite Ed)* 2012; 4: 2801–8.
- Yip PK, Malaspina A. Spinal cord trauma and the molecular point of no return. *Mol Neurodegener* 2012; 7: 6.
- Yoon EJ, Park HJ, Kim GY, Cho HM, Choi JH, Park HY, et al. Intracellular amyloid beta interacts with SOD1 and impairs the enzymatic activity of SOD1: implications for the pathogenesis of amyotrophic lateral sclerosis. *Exp Mol Med* 2009; 41: 611–7.
- Yoshida T, Maulik N, Engelman RM, Ho YS, Das DK. Targeted disruption of the mouse Sod1 gene makes the hearts vulnerable to ischemic reperfusion injury. *Circ Res* 2000; 86: 264–9.
- Zelko IN, Mariani TJ, Folz RJ. Superoxide dismutase multigene family: a comparison of the CuZn-SOD (SOD1), Mn-SOD (SOD2), and EC-SOD (SOD3) gene structures, evolution, and expression. *Free Radic Biol Med* 2002; 33: 337–49.
- Zinman L, Liu HN, Sato C, Wakutani Y, Marvelle AF, Moreno D, et al. A mechanism for low penetrance in an ALS family with a novel SOD1 deletion. *Neurology* 2009; 72: 1153–9.
- Zuccato C, Valenza M, Cattaneo E. Molecular mechanisms and potential therapeutic targets in Huntington's disease. *Physiol Rev* 2010; 90: 905–81.

ORIGINAL ARTICLE

A novel SOD1-ALS mutation separates central and peripheral effects of mutant SOD1 toxicity

Peter I. Joyce¹, Philip Mcgoldrick^{2,†}, Rachele A. Saccon^{2,†}, William Weber^{3,†}, Pietro Fratta², Steven J. West⁴, Ning Zhu⁴, Sarah Carter¹, Vinaya Phatak¹, Michelle Stewart¹, Michelle Simon¹, Saumya Kumar¹, Ines Heise¹, Virginie Bros-Facer², James Dick², Silvia Corrochano¹, Macdonnell J. Stanford³, Tu Vinh Luong⁵, Patrick M. Nolan¹, Timothy Meyer⁶, Sebastian Brandner², David L.H. Bennett⁴, P. Hande Ozdinler³, Linda Greensmith^{2,*}, Elizabeth M.C. Fisher^{2,*}, and Abraham Acevedo-Arozena^{1,*}

¹MRC Mammalian Genetics Unit, Harwell, Oxfordshire OX11 0RD, UK, ²MRC Centre for Neuromuscular Disease, UCL Institute of Neurology, Queen Square, London WC1N 3BG, UK, ³Department of Neurology, Northwestern University, Feinberg School of Medicine, Chicago, IL 60611, USA, ⁴Nuffield Department of Clinical Neurosciences, University of Oxford, Oxford OX3 9DU, UK, ⁵Department of Cellular Pathology, Royal Free London NHS Foundation Trust, Pond Street, London NW3 2QG, UK, and ⁶UCL Cancer Institute, Paul O’Gorman Building, 72 Huntley Street, London WC1E 6BT, UK

*To whom correspondence should be addressed at: Medical Research Council Mammalian Genetics Unit, Harwell, Oxfordshire OX11 0RD, UK. Email: a.acevedo@har.mrc.ac.uk (A.A.-A.); Institute of Neurology and MRC Centre for Neuromuscular Disease, UCL, Queen Square, London WC1N 3BG, UK. Email: e.fisher@prion.ucl.ac.uk (E.M.C.F.); Institute of Neurology and MRC Centre for Neuromuscular Disease, UCL, Queen Square, London WC1N 3BG, UK. Email: l.greensmith@ucl.ac.uk (L.G.)

Abstract

Transgenic mouse models expressing mutant *superoxide dismutase 1* (SOD1) have been critical in furthering our understanding of amyotrophic lateral sclerosis (ALS). However, such models generally overexpress the mutant protein, which may give rise to phenotypes not directly relevant to the disorder. Here, we have analysed a novel mouse model that has a point mutation in the endogenous mouse *Sod1* gene; this mutation is identical to a pathological change in human familial ALS (fALS) which results in a D83G change in SOD1 protein. Homozygous *Sod1*^{D83G/D83G} mice develop progressive degeneration of lower (LMN) and upper motor neurons, likely due to the same unknown toxic gain of function as occurs in human fALS cases, but intriguingly LMN cell death appears to stop in early adulthood and the mice do not become paralyzed. The D83 residue coordinates zinc binding, and the D83G mutation results in loss of dismutase activity and SOD1 protein instability. As a result, *Sod1*^{D83G/D83G} mice also phenocopy the distal axonopathy and hepatocellular carcinoma found in *Sod1* null mice (*Sod1*^{-/-}). These unique mice allow us

[†] These authors contributed equally to this work.

Received: July 29, 2014. Revised: October 30, 2014. Accepted: November 27, 2014

© The Author 2014. Published by Oxford University Press.

This is an Open Access article distributed under the terms of the Creative Commons Attribution License (<http://creativecommons.org/licenses/by/4.0/>), which permits unrestricted reuse, distribution, and reproduction in any medium, provided the original work is properly cited.

to further our understanding of ALS by separating the central motor neuron body degeneration and the peripheral effects from a fALS mutation expressed at endogenous levels.

Introduction

Amyotrophic lateral sclerosis (ALS) is a devastating neurodegenerative disease characterized by a loss of upper and lower motor neurons (LMNs), which causes muscle weakness, paralysis and ultimately death, typically within 3–5 years of disease onset. Approximately 10% of ALS cases have a clear family history (fALS), caused by mutations in specific genes, usually with a dominant pattern of inheritance (1–3). Mutations in *superoxide dismutase 1* (SOD1) account for 10–20% of fALS cases (although pathogenicity has not been demonstrated for all these changes), and to date >155 mutations have been identified throughout all five exons of the SOD1 gene, >95% of which are dominant (4).

SOD1 is a 153 amino acid metalloenzyme (also called Cu/Zn SOD1) that forms a homodimer whose main known function is to remove superoxide radicals through creating molecular oxygen and hydrogen peroxide, although other functions are known (5). Mutant SOD1 takes on a toxic gain-of-unknown function in SOD1-fALS, causing many cellular abnormalities that ultimately result in death of motor neurons (6). Recent research has identified misfolded wild-type (WT) SOD1 in non-SOD1-fALS and in ‘sporadic’ ALS suggesting that it may also play a role in the pathogenesis of these ALS cases (7–10).

SOD1 is highly conserved across species (11) and >12 different transgenic mouse models have been created that overexpress mutant forms of human SOD1 (6,12,13) and in one case mouse *Sod1* (14). The majority of these mice recapitulate many characteristics of ALS, including progressive motor deficits, hindlimb paralysis, motor neuron degeneration and early death (6,12,13). A mouse strain carrying a spontaneous point mutation in mouse *Sod1* has been previously described (15), although the equivalent mutation in humans has not been identified as pathogenic.

However, concerns remain regarding the translation of these models to human SOD1-fALS—particularly because SOD1 is generally overexpressed in transgenics and such raised expression levels affect the pathology of these animals (6,12). For example, the most widely used model of SOD1-fALS, the high-copy SOD1^{G93A} transgenic, carries ~24 copies of the mutant human SOD1 gene, expresses SOD1 protein at ~17-fold over the endogenous level, and has greatly accelerated disease compared with SOD1^{G93A^{dl}} mice, a strain derived from the SOD1^{G93A} founder line but with lower levels of SOD1 protein because of a deletion in the transgene array (~8–10 copies of SOD1^{G93A} gene, 8-fold SOD1 protein expression over WT) (16–18). As well as raised levels of mutant SOD1 affecting phenotype, increased levels of WT SOD1 also give rise to neurodegeneration—overexpression of WT human SOD1 at levels comparable with that found in SOD1^{G93A} transgenics results in an ALS-like syndrome with progressive loss of spinal motor neurons and premature death (19). Thus SOD1 ‘dose’ is clearly important for determining phenotype—and as well as overexpression, reduced expression also gives rise to neuronal and non-neuronal phenotypes in heterozygous and homozygous SOD1 knockout mice (reviewed in 4).

Mutations in SOD1-ALS cause a toxic gain of function, which leads to motor neuron degeneration. However, curiously, the majority of studies that have analysed dismutase activity of SOD1-fALS patient samples show that SOD1 dismutase activity

is reduced to an average of ~58% of normal levels (reviewed in 4). SOD1 transgenic models overexpress mutant SOD1 and also express two copies of endogenous mouse *Sod1*, so dismutase activity is not reduced in these animals. Therefore, although SOD1 transgenics clearly model the SOD1 toxic gain-of-function leading to motor neuron degeneration, they do not generally model the possible effects on ALS pathogenesis of a reduction in dismutase activity, as observed in the majority of SOD1-fALS patient samples.

The effects of SOD1 loss of function on motor neurons have been recently readdressed through the study of *Sod1*^{-/-} mice (20,21), which suffer from a severe progressive denervation of hindlimb muscles, leading to striking motor phenotypes (20). Importantly however, several reports show that aged *Sod1*^{-/-} mice do not develop motor neuron degeneration at any age (20,22,23). Thus, SOD1 activity is critical in maintaining innervation of neuromuscular junctions, but its removal does not result in motor neuron cell body loss.

In order to create the genetically closest model of SOD1 ALS to date, and to investigate the effects of a SOD1 mutation at endogenous expression levels, we identified a mutant line that carries an N-ethyl-N-nitrosourea (ENU)-induced point mutation in the mouse *Sod1* gene. Fortuitously, this mutation is identical to the nucleotide change found in human SOD1 D83G dominant fALS cases (24). In a D83G SOD1-fALS family, four of the five affected individuals had a rapid disease duration (range: 6–12 months), whilst one family member had a long disease duration (151 months). Two of the affected SOD1 D83G family members who were clinically examined in detail first presented with symptoms of LMN deficits, which were followed with upper motor neuron (UMN) symptoms (24).

Results

Identification of an ENU-induced point mutation in the mouse *Sod1* gene

To identify mouse lines carrying the equivalent of human ALS causative pathogenic mutations, we screened for mutations in *Sod1* using genomic DNA from an ENU-induced mutagenesis archive containing over 10 000 mice (25,26). We identified a mouse mutant carrying an adenosine-to-guanine missense mutation resulting in a D83G substitution (Supplementary Material, Fig. S1). Importantly, the same point mutation (A–G) gives rise to dominant D83G SOD1-fALS (24).

For all subsequent studies, female and male mice carrying the *Sod1*^{D83G} mutation were assessed on a C57BL/6J genetic background, backcrossed at least four generations and then intercrossed. Homozygous *Sod1*^{D83G/D83G} mice were not produced in Mendelian ratios from *Sod1*^{+ /D83G} intercrosses (in total: 167 WT, 362 *Sod1*^{+ /D83G}, 101 *Sod1*^{D83G /D83G}) (Supplementary Material, Table S1).

Upper and LMNs die in *Sod1*^{D83G/D83G} mice

Since degeneration of both LMN and UMN is the defining hallmark of ALS and occurs in fALS patients carrying the D83G mutation (24), we first examined the survival of LMN and UMN. The number of LMN in the sciatic motor pool in lumbar spinal cord

was assessed at 6, 15 and 52 weeks of age. At 6 weeks, we found no loss of motor neurons in heterozygous $Sod1^{+/D83G}$ or homozygous $Sod1^{D83G/D83G}$ mice (WT 483 ± 12 LMN; $Sod1^{+/D83G}$ 481 ± 10 LMN; $Sod1^{D83G/D83G}$ 495 ± 8 LMN; $n \geq 5$ per genotype). However, by 15 weeks there was a 23% reduction in the number of LMNs

in $Sod1^{D83G/D83G}$ mice only (359 ± 9 LMN) compared with WT littermates (442 ± 11 LMN; $P < 0.001$) (Fig. 1A and B), and this remained stable at 52 weeks (Fig. 1B). Thus, homozygous $Sod1^{D83G/D83G}$ mice develop significant LMN degeneration between 6 and 15 weeks of age, which does not progress.

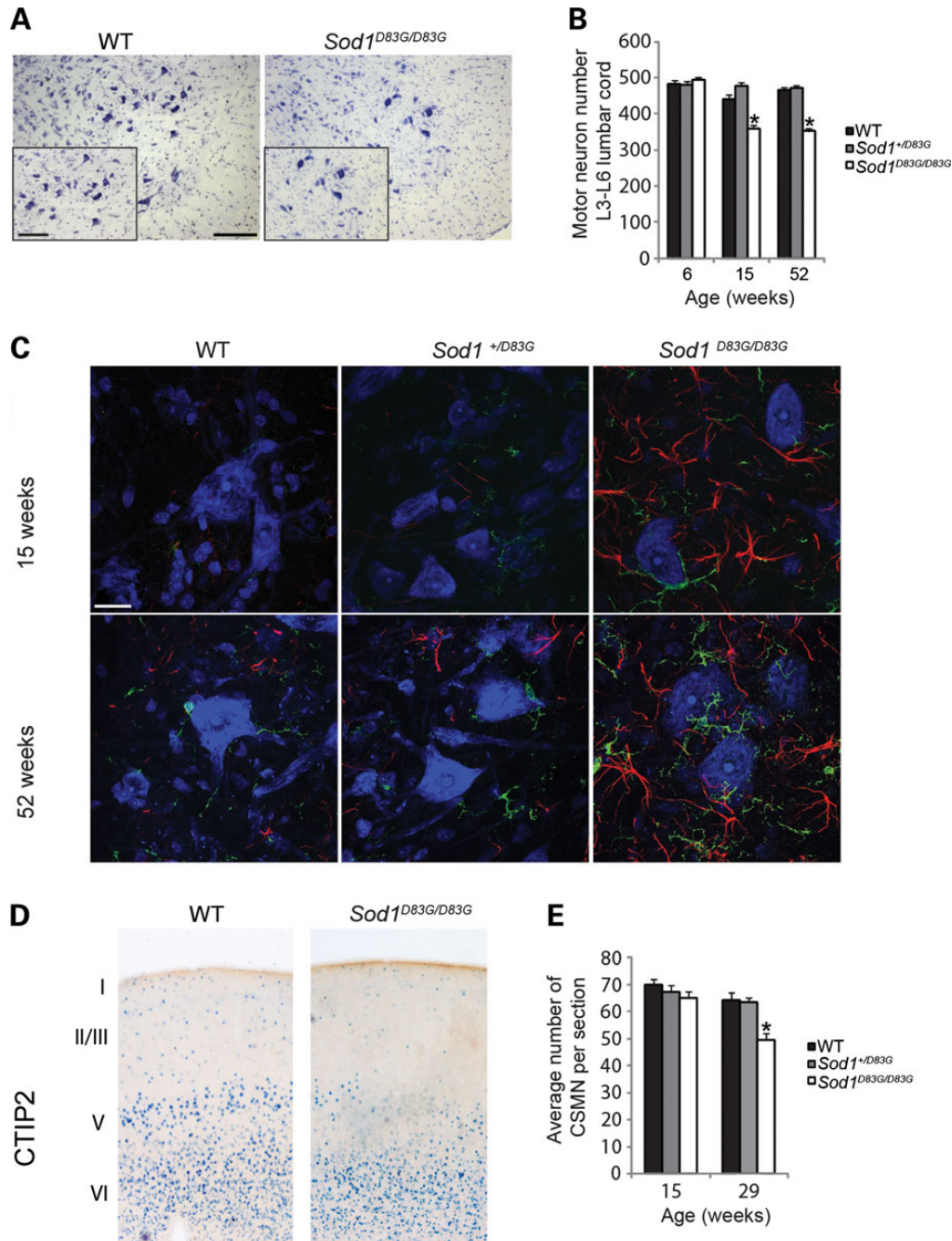


Figure 1. The $Sod1^{D83G}$ mutation causes LMN and UMN degeneration. (A) Representative images of lumbar spinal cord ventral horn sections stained for Nissl from WT and 15-week-old $Sod1^{D83G/D83G}$ mice; sciatic pool of motor neurons depicted in inset image. Scale bars: main 200 μ m, inset 100 μ m. (B) LMN numbers at 6, 15 and 52 weeks of age in female littermates. At 6 weeks of age counts are comparable, but by 15 weeks of age in $Sod1^{D83G/D83G}$ mice have a 23% loss of LMNs (359 ± 9) compared with WT littermates (469 ± 11) and $Sod1^{+/D83G}$ (477 ± 11). Motor neuron survival of $Sod1^{D83G/D83G}$ mice (353 ± 9) at 52 weeks is not significantly reduced compared with that at 15 weeks (359 ± 9 ; $P = 0.47$). $n \geq 5$ animals per group ($*P < 0.001$). (C) Representative images of ventral horn of lumbar spinal cord from 15- to 52-week-old mice stained for IBA-1 (green), GFAP (red) and Nissl (blue). Immunoreactivity for micro- and astrogliosis is increased in 15-week-old $Sod1^{+/D83G}$ mice, and yet further in 52-week-old $Sod1^{D83G/D83G}$ mice compared with WT littermates. Scale bar is 20 μ m. (D) CTIP2 expression is detected in the striatum, in layer VI, and is restricted to CSMN within layer V of the motor cortex. (E) CSMN survival of female mice at 15 and 29 weeks of age. CSMNs are reduced in $Sod1^{D83G/D83G}$ mice at 29 weeks (49.7 ± 2.4) compared with WT littermates (64.1 ± 2.8). CSMNs within layer V were averaged across three slides per animal; $n = 5$ per group. Scale bar is 50 μ m. Numbers represent the mean \pm SEM ($*P < 0.01$).

Reactive gliosis of both astrocytes and microglia is observed in ALS patients and mouse models. In *Sod1^{D83G/D83G}* mice, lumbar spinal cord sections from 15-week-old mice showed striking astrogliosis (GFAP) and microgliosis (IBA1), which increased further at 52 weeks of age (Fig. 1C). *Sod1^{+D83G}* mice did not show elevation in reactive gliosis compared with WT littermates (Fig. 1C).

To investigate UMNs in *Sod1^{D83G/D83G}* mice, we examined the survival of corticospinal motor neurons (CSMNs) at 15 and 29 weeks of age (Fig. 1D and E). Although Nissl staining of the cerebral cortex did not reveal obvious abnormalities in *Sod1^{D83G/D83G}* mice at either age (Supplementary Material, Figure S2A), analysis of Cry-mu, a selective marker of CSMNs in layer V of the motor cortex (27), revealed signs of cellular degeneration in *Sod1^{D83G/D83G}* mice at 29 weeks (Supplementary Material, Figure S2B). This was supported by staining for the molecular marker chicken ovalbumin upstream promoter transcription factor-interacting protein 2 (CTIP2), a transcription factor expressed by CSMN in layer V of the motor cortex and a subset of layer VI neurons (27) (Fig. 1D). CTIP2 expression helps distinguish between a possible reduction in molecular marker expression and cellular degeneration, and is restricted to the nucleus, allowing for reliable quantitative analysis.

CSMN numbers were comparable between WT, *Sod1^{+D83G}* and *Sod1^{D83G/D83G}* littermates at 15 weeks of age (WT 70 ± 4; *Sod1^{+D83G}* 67 ± 5; *Sod1^{D83G/D83G}* 65 ± 5) (Fig. 1E), but reduced by 22% at 29 weeks in *Sod1^{D83G/D83G}* mice (WT 64 ± 6; *Sod1^{+D83G}* 64 ± 4; *Sod1^{D83G/D83G}* 50 ± 5; $P < 0.05$) (Fig. 1D and E). This degeneration was restricted to CSMNs since analysis of callosal projection neurons (CPNs), which are developmentally closely related to CSMN but less vulnerable in ALS, showed that staining with CPN-specific markers LIM domain only four (LMO4) and special AT-rich sequence-binding protein 2 (SATB2), did not differ between WT and *Sod1^{D83G/D83G}* littermates, at either age (Supplementary Material, Fig. S2C and D). These results therefore suggest a selective and progressive CSMN degeneration (UMN) within the cortical component of motor neuron circuitry, which is likely to affect the motor capability of *Sod1^{D83G/D83G}* mice.

Analysis of functional motor units reveals a distal motor neuropathy in *Sod1^{D83G/D83G}* mice

In view of the MN degeneration observed in *Sod1^{D83G/D83G}* mice, we next determined the number of functional motor neurons that innervated the extensor digitorum longus (EDL) hindlimb muscle by physiological analysis of motor unit survival (MUNE). We found no differences in EDL motor unit survival across genotypes at 15 weeks of age, suggesting that the loss of LMN cell bodies detected at this age is restricted to populations of motor neurons that innervate hindlimb muscles other than EDL. Indeed, EDL has been previously shown to be less vulnerable to disease in transgenic SOD1 models (28). However, by 52 weeks of age, we observed a significant reduction in the number of motor units in EDL muscles of *Sod1^{D83G/D83G}* mice compared with WT littermates ($P < 0.001$; Fig. 2A and B). Comparison between WT and *Sod1^{+D83G}* littermates did not reveal any significant differences in EDL motor units at 15, 52 or 96 weeks of age (Fig. 2A).

Morphological analysis of the innervation pattern of endplate neuromuscular junctions (NMJ) of the EDL muscle confirmed the distal progressive denervation occurring between 15 and 52 weeks of age in *Sod1^{D83G/D83G}* mice (Fig. 2C–E). In agreement with the MUNE analysis, no significant differences in denervated EDL endplate NMJ were observed between any of the genotypes at 15 weeks of age (Fig. 2E). However, by 52 weeks of age, a significantly

different proportion of endplate NMJ in *Sod1^{D83G/D83G}* EDL is denervated (WT 2.6 ± 0.9; *Sod1^{+D83G}* 2.6 ± 1.1; *Sod1^{D83G/D83G}* 14.8 ± 2.8; $P < 0.001$) (Fig. 2E). Since no additional LMN body degeneration occurs between 15 and 52 weeks of age in *Sod1^{D83G/D83G}* mice, the progressive denervation and loss of EDL motor units are likely a peripheral neuropathy that is not the result of motor neuron death.

Sod1^{D83G/D83G} mice display progressive motor and behavioural deficits

We next examined whether the loss of motor neurons and progressive denervation in *Sod1^{D83G/D83G}* mice was reflected in deficits in motor function. Longitudinal phenotypic characterization of WT, *Sod1^{+D83G}* and *Sod1^{D83G/D83G}* littermates showed motor function of *Sod1^{D83G/D83G}* mice deteriorates progressively with age, and these mice develop tremors, gait abnormalities and become severely kyphotic (Supplementary Material, Video S1).

We found a reduction in body weight of *Sod1^{D83G/D83G}* from 4 weeks of age compared with WT littermates (females, $P = 0.001$; males, $P = 0.034$) (Fig. 3A; Supplementary Material, Fig. S3A). To evaluate the weight differences between littermates, the relative levels of lean and fat mass were determined using Echo MRI (29). Fifty-two-week-old male and female *Sod1^{D83G/D83G}* mice showed significantly less fat mass compared with sex-matched WT littermates, while there were no differences observed between WT and *Sod1^{+D83G}* littermates at 6, 35, 52 or 88 weeks of age (Fig. 3B; Supplementary Material, Fig. S3B).

To assess motor function, we examined grip strength and performance on an accelerating rotarod, starting at 6 and 7 weeks of age, respectively. We observed reduced grip strength in female and male *Sod1^{D83G/D83G}* mice from 6 weeks of age (females, $P \leq 0.002$; males, $P < 0.05$), but not in *Sod1^{+D83G}* mice (Fig. 3C; Supplementary Material, Fig. S3C). Female *Sod1^{D83G/D83G}* mice displayed earlier deficits in accelerating rotarod compared with males (23 weeks versus 67 weeks) (Fig. 3D; Supplementary Material, Fig. S3D).

We also examined the performance of WT, *Sod1^{+D83G}* and *Sod1^{D83G/D83G}* littermates using a modified SHIRPA analysis, which comprises of a battery of simple phenotypic tests with an emphasis on neurological function (30,31). Three traits differed between genotypes: the presence and progression of tremors, pelvic elevation and the ability to walk down a vertical wire grate (negative geotaxis) (Table 1).

We found subtle behavioural deficits in heterozygous *Sod1^{+D83G}* animals when examining the performance of mice on an in-cage wheel running system (32). A similar system has previously been used to identify presymptomatic motor abnormalities in *SOD1^{G93A}* transgenic mice (33). WT and *Sod1^{+D83G}* littermates were assessed at 44 and 88 weeks of age by recording activity over 7 days. *Sod1^{+D83G}* animals exhibited a significant deficit in nightly total distance travelled compared with WT littermates ($P < 0.05$), which declined further with age (Fig. 3E). In addition, while WT mice at 88 weeks of age showed an increase in the duration for each running bout (duration per run) when compared with 44 weeks of age, 88-week-old *Sod1^{+D83G}* mice showed a reduction in duration. *Sod1^{+D83G}* mice also displayed a reduction in the duration per running bout at 44 and 88 weeks of age compared with WT littermates (Fig. 3F). Thus, *Sod1^{+D83G}* mice present with subtle yet progressive deficits in motor function in the home cage, showing that the deleterious effects of the SOD1 D83G mutation are not restricted to homozygous mice.

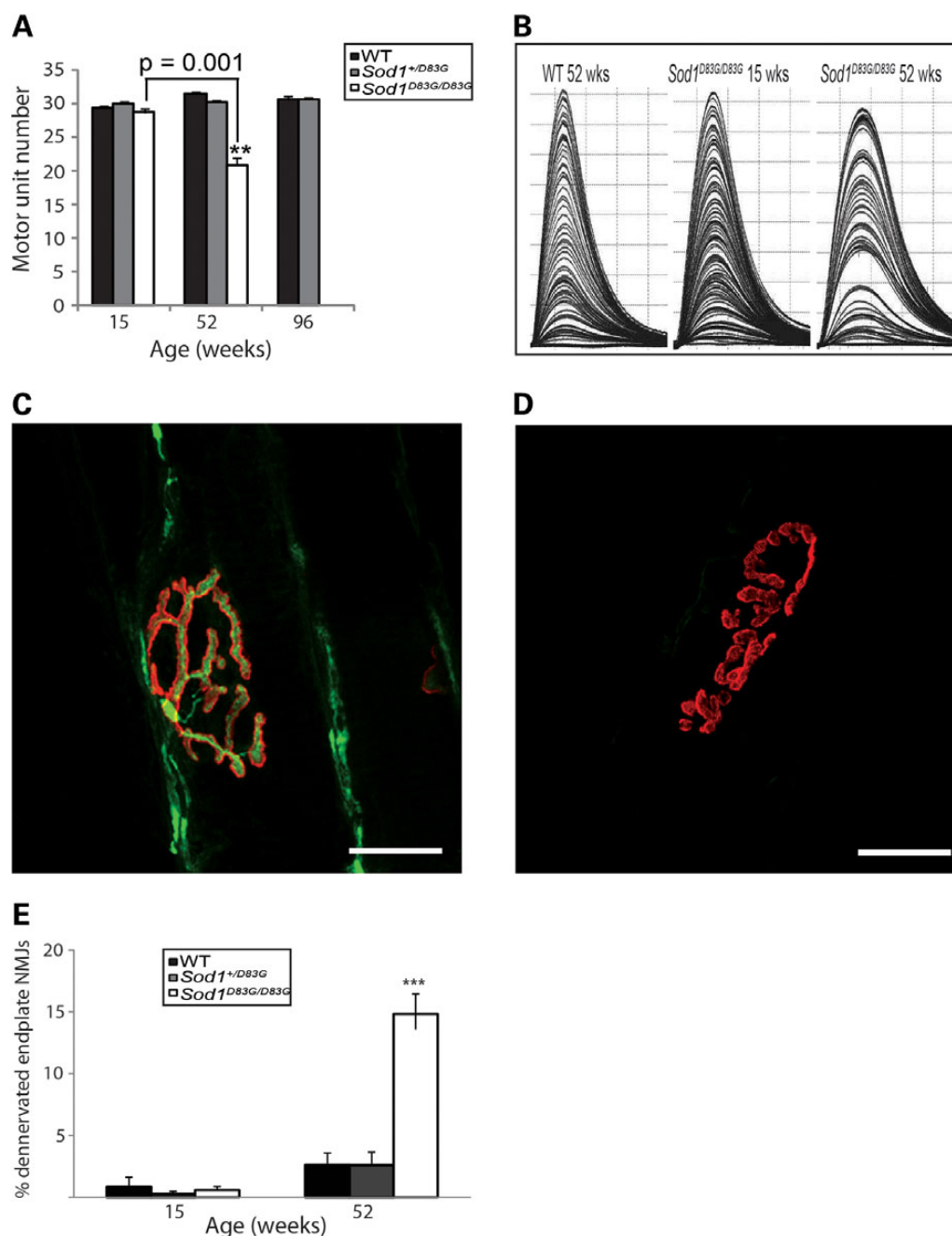


Figure 2. MUNE and endplate NMJ analysis from EDL muscle. (A and B) Surviving motor units for the EDL, which are reduced in 52-week-old *Sod1*^{D83G/D83G} mice (21 ± 1) compared with WT littermates (39 ± 0.4). (B) Representative traces from (A); each twitch trace recording is a single motor unit. Numbers represent the mean \pm SEM, at least nine legs were assessed per group. (C–E) Percentage of denervated endplate NMJ from EDL muscle at 15 and 52 weeks of age. Motor endplates are identified via α -bungarotoxin staining (red). Axons are revealed via neurofilament and SV2 (green). Representative images of (C) innervated and (D) denervated NMJ endplates. (E) Quantitative analysis of the percentage of denervated EDL endplate NMJ (denervated NMJ/total NMJ counted \times 100) from all three genotypes at 15 weeks of age reveal no significant differences between any of the genotypes. By 52 weeks of age, a significant difference in the percentage of denervated endplate NMJ appear between *Sod1*^{D83G/D83G} and the other two genotypes (WT and *Sod1*^{+/D83G}). At 15 weeks of age, at least 700 NMJ endplates were counted per genotype. At 52 weeks of age, at least 465 NMJ endplates were counted per genotype. Percentage of denervated endplate NMJ at 52 weeks: WT: 2.6 ± 0.9 ; *Sod1*^{+/D83G}: 2.6 ± 1.1 ; *Sod1*^{D83G/D83G}: 14.8 ± 2.8 . *** $P < 0.001$. Scale bar is 20 μ m.

Sod1^{D83G/D83G} mice lose muscle force with age

To gain a detailed understanding of the effect of the *Sod1*^{D83G} mutation on motor neuron and muscle function, we undertook a physiological analysis of the tibialis anterior (TA) and EDL hind-limb muscles of female WT, *Sod1*^{+/D83G} and *Sod1*^{D83G/D83G}

littermates at 15 and 52 weeks age. We also assessed *Sod1*^{+/D83G} mice at 96 weeks of age.

TA muscle of 15-week-old *Sod1*^{D83G/D83G} mice was significantly weaker than in WT littermates ($P = 0.02$), and muscle force declined further at 52 weeks of age (Fig. 4A and B). This may reflect

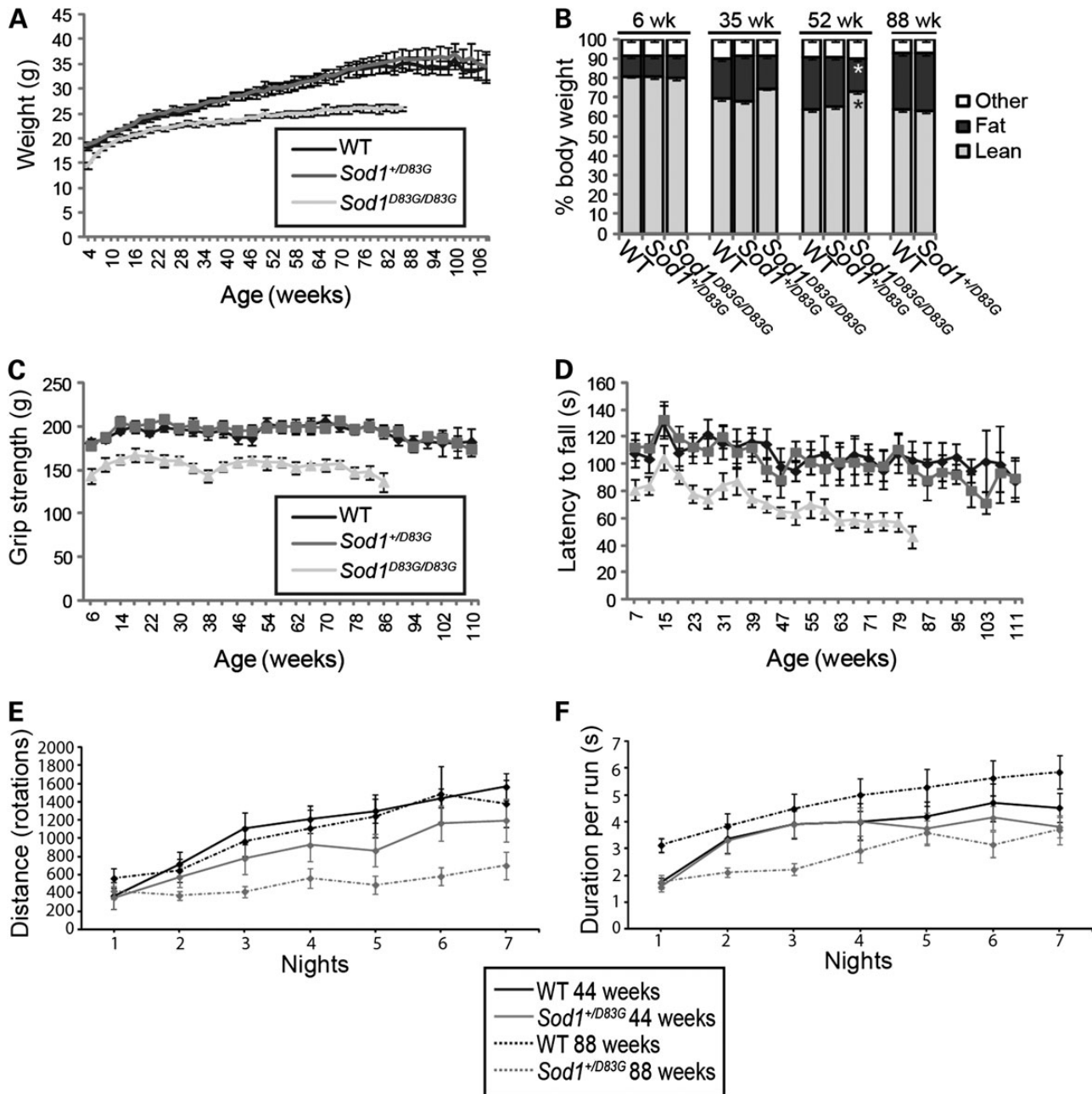


Figure 3. Body mass, behavioural and motor deficits in female *Sod1*^{D83G/D83G} mice. (A) Weights recorded weekly from 4 weeks of age to the humane endpoint; cohort sizes for (A, C and D) started as 11 WT, 13 *Sod1*^{+/D83G}, 11 *Sod1*^{D83G/D83G}, due to the death of mice with age, at least five mice were assessed per genotype at later time points. Weight is reduced in *Sod1*^{D83G/D83G} mice from 4 weeks of age (P = 0.001). (B) Echo MRI assessment of lean and fat mass for mice at 6, 35, 52 and 88 weeks of age. Fat mass is reduced and lean mass increased in 52-week-old *Sod1*^{D83G/D83G} mice by comparison with WT littermates (*P < 0.001). (C) Grip strength recorded monthly from 6 weeks of age to humane endpoint. Grip strength is reduced in *Sod1*^{D83G/D83G} mice (P < 0.002 from 6 weeks). (D) Rotarod recorded monthly from 7 weeks of age to humane endpoint. Rotarod performance is reduced in *Sod1*^{D83G/D83G} mice (P < 0.05 from 23 weeks). (E and F) Wheel running activity over 7 days from 44- and 88-week-old singly housed female WT and *Sod1*^{+/D83G} littermates. The distance run (E) is shorter in 44-week-old *Sod1*^{+/D83G} mice compared with WT (P < 0.01), while the distance run (E) and duration per run (F) both deteriorate with age in *Sod1*^{+/D83G} mice (44 versus 88 weeks) compared with WT littermates (P < 0.05). n = 7 per genotype per time point. Numbers shown represent the mean ± SEM.

the LMN degeneration detected in the spinal cord at this stage (Fig. 1B). However, as observed with motor unit survival and NMJ innervation, no deficit in EDL muscle force was detected in *Sod1*^{D83G/D83G} mice at 15 weeks, confirming that this muscle is less vulnerable to the effects of mutant SOD1 than other hind-limb fast twitch muscles. However, by 52 weeks, EDL muscle force in *Sod1*^{D83G/D83G} mice was significantly reduced by ~35% compared with WT (P < 0.001; Fig. 4C and D). Therefore, TA and

EDL muscles undergo a progressive loss in muscle strength in *Sod1*^{D83G/D83G} animals between 15 and 52 weeks of age, at a time when there is no progression in the death of LMN. In addition, as with SOD1 transgenic mouse models, the TA is affected earlier than EDL (28).

TA and EDL are fast twitch muscles that normally fatigue rapidly when repeatedly stimulated. Changes in the fatigue characteristics of fast twitch muscles are a typical feature of disease in

Table 1. Semi-quantitative-modified SHIRPA phenotypic analysis of WT (*Sod1*^{+/+}), *Sod1*^{+/D83G} and *Sod1*^{D83G/D83G} littermates

Genotype	Sample size	Mild tremors		Severe tremors		Reduced pelvic elevation		Negative geotaxis	
		Onset (weeks)	%	Onset (weeks)	%	Onset (weeks)	%	Onset (weeks)	%
<i>Sod1</i> ^{+/+} ♂	12	96	17	–	–	88	33	60	42
<i>Sod1</i> ^{+/D83G} ♂	15	94	13	–	–	86	20	69	60
<i>Sod1</i> ^{D83G/D83G} ♂	11	20	100	62	82	39	100	29	100
<i>Sod1</i> ^{+/+} ♀	13	98	15	–	–	86	46	90	8
<i>Sod1</i> ^{+/D83G} ♀	14	96	36	–	–	78	71	–	–
<i>Sod1</i> ^{D83G/D83G} ♀	12	22	100	67	58	32	100	49	75

Onset values are the mean age at onset, in weeks, for mice presenting each phenotype. Percentage represents the proportion of mice per line presenting each phenotype at least twice during their lifetime.

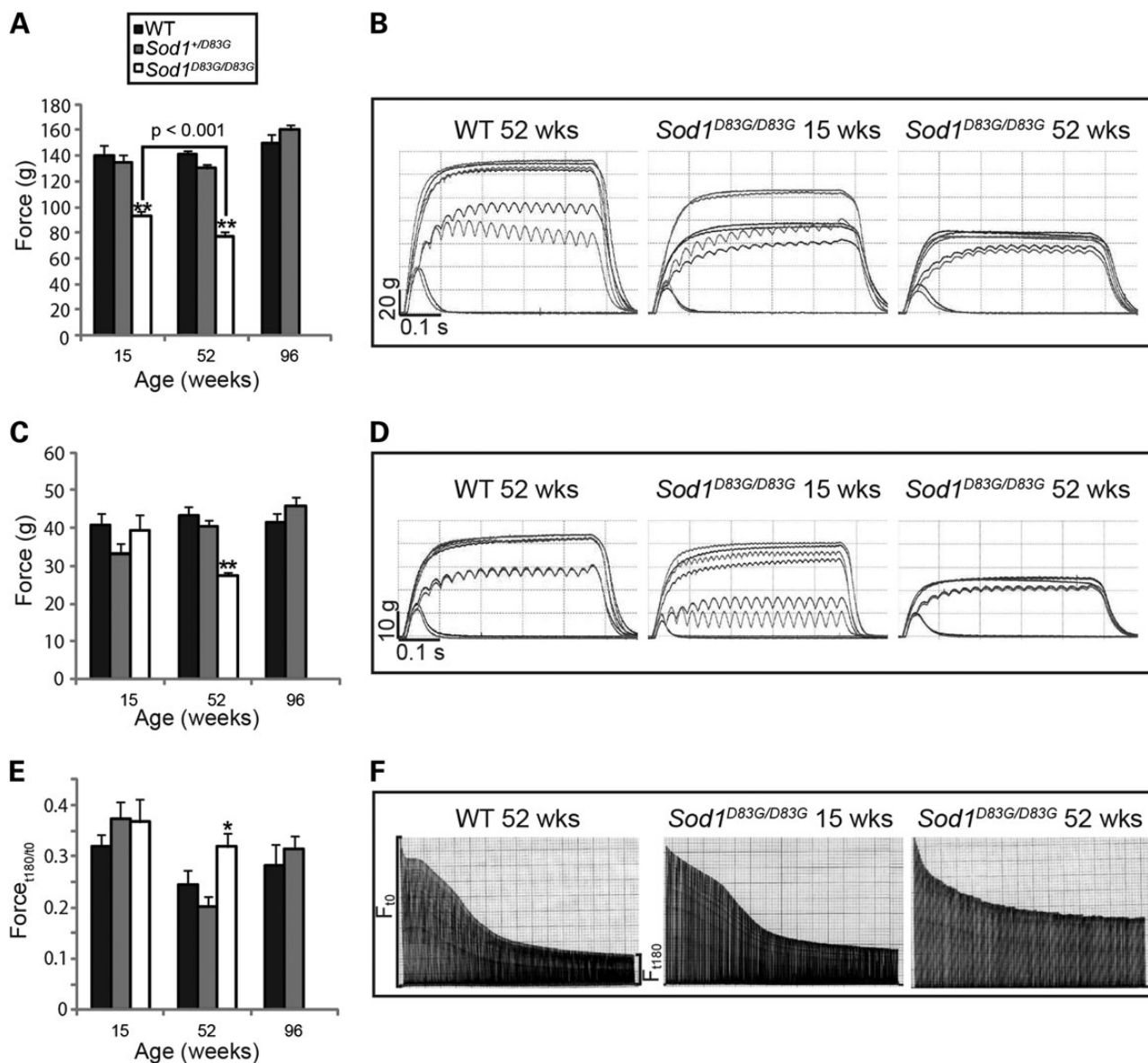


Figure 4. Functional deficits in muscle function in female *Sod1*^{D83G/D83G} mice. (A) TA tetanic muscle force for mice at 15, 52 and 88 weeks of age; 15-week-old *Sod1*^{D83G/D83G} TA tetanic muscle force (93 g ± 4 g) is reduced compared with WT littermates (140 ± 8 g) and deteriorates further at 52 weeks of age (77 ± 4 g). (B) Representative traces of TA tetanic tension from WT and *Sod1*^{D83G/D83G} mice. (C) EDL tetanic muscle force: 52-week-old *Sod1*^{D83G/D83G} EDL tetanic muscle force (29 ± 1 g) is reduced compared with WT littermates (43 ± 2 g). (D) Representative traces of EDL tetanic tension from WT and *Sod1*^{D83G/D83G} mice. (E) FI of EDL muscle for mice at 15, 52 and 88 weeks of age. FI of 52-week-old *Sod1*^{D83G/D83G} mice (0.32 ± 0.03) is increased compared with WT littermates (0.24 ± 0.03). (F) Representative fatigue traces from WT, and *Sod1*^{D83G/D83G} mice, produced by repeated stimulation of the EDL muscle for 180 s. Each line in the trace represents a single tetanic tension; line length is proportional to force produced (see Materials and Methods). **P* < 0.05, ***P* < 0.001.

SOD1 transgenic mouse models (34) and so we undertook a fatigue test of EDL muscles in *Sod1*^{D83G/D83G} mice (Fig. 4E and F). The force measured at the beginning of a 3 min period of stimulation was compared with that at the end of the test to produce a Fatigue Index (FI), a measure of the fatigability of the muscle. The results highlight the progressive deterioration of EDL in these mice, so that at 15 weeks, the FI of EDL in *Sod1*^{D83G/D83G} mice is no different from WT, but by 52 weeks of age, EDL FI is increased by 30% in *Sod1*^{D83G/D83G} mice compared with WT ($P = 0.04$) (Fig. 4E and F). Comparison between WT and *Sod1*^{+D83G} littermate mice did not reveal any significant differences in TA or EDL muscle function at 15, 52 or 96 weeks of age (Fig. 4).

Sod1^{D83G/D83G} mice have ALS-like changes in the histochemical phenotype of fast twitch muscles

To further characterize the effect of the *Sod1*^{D83G} mutation on muscle physiology, we examined the oxidative capacity of the muscle fibres in the TA and EDL muscles, by staining for the oxidative enzyme succinate dehydrogenase (SDH) at 15 and 52 weeks of age. Even at 15 weeks of age, *Sod1*^{D83G/D83G} TA muscle show a clear change in the histochemical properties of their muscle fibres (Supplementary Material, Fig. S4A and B). Fast twitch muscles, such as the TA and EDL, normally contain a large proportion of glycolytic fibres that stain only lightly for SDH activity, a marker of oxidative fibres. However, in the TA of *Sod1*^{D83G/D83G} mice at 15 weeks of age, grouping of intensely stained type I slow oxidative muscle fibres was observed and by 52 weeks almost all of the muscle fibres in the TA of *Sod1*^{D83G/D83G} mice stain intensely for SDH, indicating an oxidative phenotype that is more characteristic of slow twitch, type I muscle fibres (Supplementary Material, Fig. S4A). EDL muscles of 15-week-old *Sod1*^{D83G/D83G} mice, had a similar SDH staining pattern to WT littermates, but by 52 weeks, there was a marked increase in the proportion of intensely stained, likely type I muscle fibres (Supplementary Material, Fig. S4B). These results once again indicate that in mice expressing mutant SOD1, EDL muscles are affected later in the disease than other hindlimb muscles such as the TA.

Sod1^{D83G/D83G} mice have selective sensory deficits

Although ALS is predominantly a motor neuron disorder, a subset of ALS patients and *SOD1*^{G93A} transgenic mice develop deficits in the sensory system (35,36). Thus, we performed behavioural sensory phenotypic analyses with four sensory tests on female mice at 22 weeks of age ($n \geq 10$ per group): (i) cold plate (noxious cold stimulus), (ii) Randall Sellito test of mechanosensation (withdrawal to a high-threshold ramp mechanical stimulus), (iii) Von Frey (low threshold mechanical stimulus), (iv) Hargreaves method (noxious heat stimulus) (Fig. 5A–D). Interestingly, *Sod1*^{D83G/D83G} mice have significant sensory deficits in response to both a low threshold mechanical stimulus (von Frey; $P < 0.05$) (Fig. 5C) and a noxious heat stimulus (Hargreaves method; $P < 0.01$) (Fig. 5D) but no deficit toward a noxious cold stimulus (cold plate) (Fig. 5A) or a high-threshold mechanical stimulus (Randall Sellito) (Fig. 5B). These results suggest that different primary afferent populations have selective vulnerabilities to the *Sod1*^{D83G} mutation, or they may be a consequence of central sensorimotor integration.

SOD1 D83G protein is dismutase inactive and at reduced levels in *Sod1*^{D83G/D83G} mice

The D83 residue coordinates zinc binding to SOD1, and is required for the correct folding of human SOD1 (37). Thus, mutating

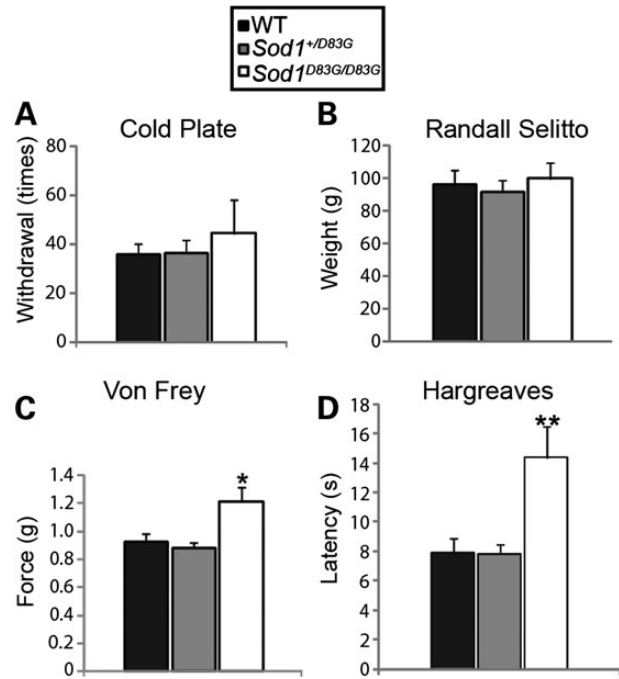


Figure 5. Behavioural sensory deficits in female *Sod1*^{D83G/D83G} mice. No significant differences in cold nociceptive sensitivity (A, cold plate) or mechanical pressure threshold (B, Randall Sellito) between genotypes. (C) von Frey: *Sod1*^{D83G/D83G} (1.22 g ± 0.10 g) display increased basal paw withdrawal threshold to von Frey filaments compared with WT littermates (0.92 g ± 0.06 g). (D) Hargreaves: *Sod1*^{D83G/D83G} (14.3 s ± 2.1 s) display increased baseline heat withdrawal latency compared with WT littermates (7.9 ± 1.0 s). Numbers shown represent the mean ± SEM. At least 10 animals were assessed per genotype and time point (* $P < 0.05$, ** $P < 0.01$).

the D83 residue is likely to interfere with the correct folding of SOD1 and potentially affect SOD1 activity. We measured SOD1 dismutase activity from the brains of WT, *Sod1*^{+D83G}, and *Sod1*^{D83G/D83G} littermates, and found *Sod1*^{D83G/D83G} mice showed almost no SOD1 dismutase activity (1 ± 2%), whereas *Sod1*^{+D83G} brain homogenates have 56 ± 7% ($n = 3$ per genotype) of WT littermate SOD1 activity (Fig. 6A and B).

To assess if the D83G mutation affects SOD1 protein stability, we also measured protein levels of SOD1 in spinal cord from WT, *Sod1*^{+D83G} and *Sod1*^{D83G/D83G} littermates. Intriguingly, SOD1 D83G protein levels are 12% ± 0.4% in *Sod1*^{D83G/D83G} mice compared with 100% ± 9% in WT littermates, while in *Sod1*^{+D83G} mice SOD1 protein levels are intermediate at 70% ± 5% ($n = 3$ per genotype) (Fig. 6C and D).

The reduction of mutant SOD1 D83G in the soluble fraction might be due to an unfolding and sequestration to the insoluble fraction. Therefore, we measured the level of SOD1 in the RIPA-insoluble fractions from spinal cords of WT, *Sod1*^{+D83G} and *Sod1*^{D83G/D83G} littermates and found low levels of insoluble SOD1 in all genotypes, with a similar reduction in SOD1 D83G protein levels in *Sod1*^{+D83G} and *Sod1*^{D83G/D83G} mice as that observed in the soluble fraction (Supplementary Material, Fig. S5A). Thus, SOD1 D83G protein does not accumulate in the insoluble fraction.

We were unable to identify misfolded SOD1 by immunoprecipitation using either the SEDI or USOD misfolded SOD1 antibodies from *Sod1*^{+D83G} and *Sod1*^{D83G/D83G} tissue extracts or immunohistochemistry (Supplementary Material, Figs. S5B and S6A), or detect overt inclusion pathology using p62 or ubiquitin staining in *Sod1*^{+D83G} and *Sod1*^{D83G/D83G} mice from spinal cord and brain (Supplementary Material, Figs. S5C and S6B).

To examine whether *Sod1*^{D83G} mRNA is differentially regulated from WT *Sod1*, we performed quantitative PCR of *Sod1* mRNA isolated from brains of 9-week-old WT, *Sod1*^{+D83G}, *Sod1*^{D83G/D83G} littermates and did not observe a difference between genotypes (Supplementary Material, Fig. S7A). In addition, we directly compared the relative levels of *Sod1* WT and D83G mRNA levels from the brains of 9-week-old *Sod1*^{+D83G} mice using quantitative pyrosequencer analysis (see Materials and Methods) and did not see a difference between the relative

expression levels of WT and mutant alleles (Supplementary Material, Fig. S7B).

Sod1^{D83G/D83G} have some phenotypes of *Sod1* null mice

Since *Sod1*^{D83G/D83G} mice are dismutase inactive (Fig. 6A and B), they are likely to phenocopy at least some aspects of *Sod1* null mice (*Sod1*^{-/-}). *Sod1*^{-/-} mice develop a progressive peripheral motor neuropathy, in which motor axons retract from neuromuscular junctions resulting in muscle denervation (20,22). However, unlike *Sod1*^{D83G/D83G} mice, there is no reported motor neuron loss in *Sod1*^{-/-} mice at any age (20,22,23). To verify that LMN loss in *Sod1*^{D83G/D83G} mice is not due to a loss of SOD1 activity and to confirm that motor neuron survival is unaffected in *Sod1*^{-/-} mice, we compared LMN survival in female *Sod1*^{D83G/D83G} and *Sod1*^{-/-} mice at 15 weeks of age; both genotypes were backcrossed to a C57BL/6J background. In contrast to *Sod1*^{D83G/D83G} mice and in agreement with all previous reports, *Sod1*^{-/-} mice do not develop motor neuron cell body loss and the survival of motor neurons in the sciatic pool is similar in WT (484 ± 9 MN, n = 6) and *Sod1*^{-/-} (489 ± 6 MN, n = 5; P = 0.47) mice. Therefore, unlike *Sod1*^{-/-} mice, *Sod1*^{D83G/D83G} mice have an additional toxic gain of function that causes the degeneration of motor neuron cell bodies.

Lifespan is reduced in transgenic SOD1 mice that overexpress mutant SOD1 and in *Sod1*^{-/-} mice. We set the humane endpoint of life in *Sod1*^{D83G/D83G} mice as either the time at which a loss of 20% of maximum bodyweight occurs or the onset of piloerection (an involuntary erection of fur that is indicative of loss of health). The majority of WT, *Sod1*^{+D83G} and *Sod1*^{D83G/D83G} littermates were culled due to a loss of 20% bodyweight (~70% of *Sod1*^{D83G/D83G} mice), while the rest (~30%) were culled for the presence of piloerection. The survival of *Sod1*^{D83G/D83G} mice is shortened compared with *Sod1*^{+D83G} and WT mice (Table 2 and Fig. 7A). We also found that male *Sod1*^{D83G/D83G} mice had a significantly reduced lifespan compared with female *Sod1*^{D83G/D83G} mice (495 ± 22 days versus 588 ± 24 days; P = 0.024).

At autopsy, *Sod1*^{D83G/D83G} mice had significantly more liver tumours than WT and *Sod1*^{+D83G} littermates (Table 2; P < 0.001). Interestingly, it has previously been shown that *Sod1*^{-/-} mice also develop liver tumours, most likely as a result of an increase in oxidative damage (38). Given that *Sod1*^{D83G/D83G} mice are dismutase inactive for SOD1 (Fig. 6A and B), it is likely that the loss of SOD1 activity in these mice is the cause of liver tumours.

The identification of liver tumours in *Sod1*^{D83G/D83G} mice led us to examine end-stage male *Sod1*^{D83G/D83G} mouse livers. Livers from WT littermates had no pathology other than variable perivenular lymphocytic infiltration (Fig. 7B). In *Sod1*^{D83G/D83G} mice, tumours occurred in the presence of otherwise pathologically normal and abnormal livers. In Figure 7C, there is a single, well-circumscribed and well-differentiated hepatocellular carcinoma occurring in a liver that is otherwise morphologically

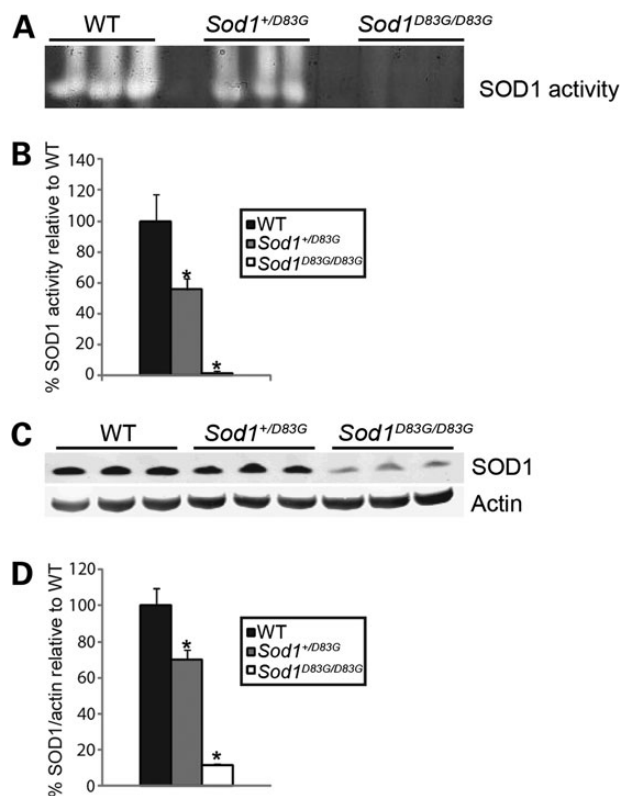


Figure 6. SOD1 D83G is dismutase inactive and unstably expressed. (A and B) SOD1 dismutase activity of brain homogenates from 65-week-old WT, *Sod1*^{+D83G} and *Sod1*^{D83G/D83G} littermates, assessed using a nitroblue treazolium (NBT) in-gel assay. (A) Cleared areas indicate SOD activity. (B) Quantification of SOD1 dismutase activity across the three genotypes shows *Sod1*^{+D83G} (56% ± 7%) and *Sod1*^{D83G/D83G} (1% ± 2%) homogenates have significantly less activity than WT (100% ± 17%) (*P = 0.002). (C and D) Immunoblot analysis of spinal cord soluble fractions for SOD1 protein levels from 65-week-old mice showing reduced SOD1 protein levels in *Sod1*^{+D83G} (70% ± 5%) and *Sod1*^{D83G/D83G} (12 ± 0.4%) extracts compared with WT littermate extracts. Actin provides a protein loading reference; SOD1 levels are normalized to actin (*P < 0.001). Numbers represent the mean ± SEM. Values represent the average from three independent experiments.

Table 2. Incidence of hepatocarcinogenesis and average survival of *Sod1*^{D83G/D83G} mice

Genotype	No. of animals examined		Average survival (days)		No. of animals with abnormal liver ^a	
	Males	Females	Males	Females	Males	Females
<i>Sod1</i> ^{+/-}	9	11	710 ± 21	754 ± 22	1 (11%)	0 (0%)
<i>Sod1</i> ^{+D83G}	15	13	696 ± 14	779 ± 15	2 (13%)	0 (0%)
<i>Sod1</i> ^{D83G/D83G}	11	9	495 ± 22	588 ± 24	10 (91%)	7 (78%)

^aGross analysis of liver and presence of abnormal nodules.

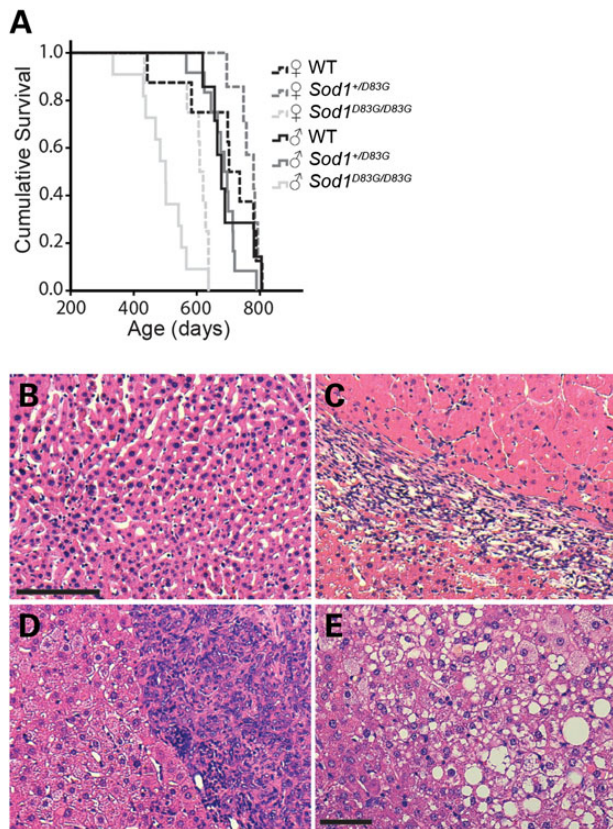


Figure 7. Lifespan of *Sod1^{D83G/D83G}* mice and the presence of hepatocellular carcinoma. (A) Survival of male and female WT, *Sod1^{+/-D83G}* and *Sod1^{D83G/D83G}* littermates to humane endpoint (see Materials and Methods). *Sod1^{D83G/D83G}* mice reach end-stage sooner than WT and *Sod1^{+/-D83G}* littermates (Table 2) and male *Sod1^{D83G/D83G}* mice (495 ± 22 days) reach end-stage earlier than females (588 ± 24 days) ($P = 0.024$). (B–E) Hematoxylin and eosin (H&E) stained liver sections from age-matched (B) WT and (C–E) end-stage *Sod1^{D83G/D83G}* mice. Livers from *Sod1^{D83G/D83G}* mice contain well-defined hepatocellular carcinoma (C) within an otherwise morphologically normal liver. (D) A poorly differentiated hepatocellular carcinoma or cholangiocarcinoma (E) within an otherwise inflamed liver background. Scale bar for (B)–(D) is 100 μm , and for (E) is 50 μm .

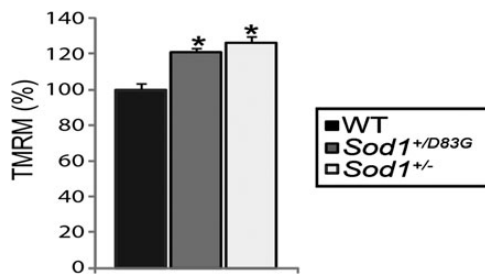


Figure 8. Mitochondrial potential in *Sod1^{+/-D83G}* and *Sod1^{+/-}* motor neurons. Resting $\Delta\psi_m$, estimated using TMRM, from embryonic WT littermates, *Sod1^{+/-D83G}* and *Sod1^{+/-}* motor neurons (WT, 100% \pm 3.4%; *Sod1^{+/-D83G}*, 121% \pm 1.9%; *Sod1^{+/-}*, 126% \pm 3.8%). Data are normalized to resting $\Delta\psi_m$ for WT littermates (100%) and represent the mean \pm SEM. Recordings taken from at least 75 cells from 2 or more independent embryonic motor neuron cultures ($P < 0.001$).

normal. In contrast, another *Sod1^{D83G/D83G}* liver demonstrated multiple ill-defined hepatocellular carcinomas and a well-circumscribed nodular lesion, composed of sheets of pleomorphic

tumour cells with vesicular nuclei and basophilic cytoplasm compatible with a poorly differentiated hepatocellular carcinoma or cholangiocarcinoma (Fig. 7D). This liver also showed diffuse nuclear anisocytosis, moderate parenchymal inflammation and patchy fatty change (Fig. 7E). Hence, pathological analysis reveals that the hepatocellular carcinomas in *Sod1^{D83G/D83G}* mice occurred in the presence of both morphologically normal and abnormal livers.

Mitochondrial membrane potential defects in *Sod1^{+/-D83G}* embryonic motor neurons

Mitochondrial dysfunction has been identified as one of the earliest defects in motor neurons of transgenic SOD1 mice and it has been suggested that mitochondrial dysfunction may play a pivotal role in motor neuron degeneration in ALS (39). We therefore analysed the mitochondrial membrane potential ($\Delta\psi_m$) of embryonic motor neurons. $\Delta\psi_m$ is an indicator of mitochondrial energetic state and can be measured using tetramethylrhodamine methylester (TMRM) (40). Those from *Sod1^{D83G/D83G}* (as previously reported for *Sod1^{-/-}*) did not survive for >72 h in culture and therefore $\Delta\psi_m$ could only be examined in motor neurons from WT and *Sod1^{+/-D83G}* littermates. We have previously shown that $\Delta\psi_m$ in embryonic motor neurons from *SOD1^{G93A}* transgenic mice is disrupted (41). In embryonic motor neurons of *Sod1^{+/-D83G}* mice, $\Delta\psi_m$ was significantly elevated compared with WT littermates (Fig. 8; $P < 0.001$).

Since the *Sod1^{+/-D83G}* mice have an ~45% reduction in SOD1 dismutase activity, it was unclear whether the elevation in $\Delta\psi_m$ in *Sod1^{+/-D83G}* motor neurons was due to a loss of SOD1 dismutase activity, or a gain of function of SOD1 D83G protein. We therefore analysed the $\Delta\psi_m$ of embryonic motor neurons derived from WT and *Sod1^{+/-}* littermates and found that *Sod1^{+/-}* motor neurons also have elevated $\Delta\psi_m$ (Fig. 8). This indicates that the mitochondrial defects present in *Sod1^{+/-D83G}* motor neurons are likely caused by a partial loss of SOD1 function.

Discussion

We have identified and characterized the first mouse model carrying the equivalent of a human ALS pathogenic mutation in the endogenous mouse *Sod1* gene, and this mutation is identical to a human fALS mutation (24). Since the mutation is within the endogenous *Sod1* gene, mutant SOD1 is not overexpressed. Here we show that homozygous *Sod1^{D83G/D83G}* mice develop upper and LMN degeneration, unlike *Sod1* null animals. This is therefore likely due to a toxic gain of function of mutant SOD1—presumably modelling that which causes motor neuron death in human ALS cases.

We found ~20% loss of UMN by 29 weeks of age in homozygotes, but did not look at later time points and so do not know if this phenotype progresses. Given the importance of mutant SOD1 protein dose in accelerating the ALS-like phenotype (16), it is possible heterozygotes may develop UMN loss later in life. Alternatively, a copy of WT SOD1 might be protective; this remains to be determined.

We showed 23% loss of LMN in the lumbar spinal cord of homozygous *Sod1^{D83G/D83G}* mutants by 15 weeks of age that remained stable at 52 weeks of age. We speculate whether further ageing, or a ‘second hit’ might be required to cause a more dramatic loss of LMN in this mouse mutant; however, this remains to be determined. We note that a similar loss of MN in humans is unlikely to cause sufficient loss of motor function to prompt a visit to a physician. *Sod1^{+/-D83G}* heterozygous mutants displayed

no LMN loss up to 52 weeks of age, either because the dose of mutant SOD1 was insufficient or because WT SOD1 might have a protective effect.

Our analyses of the *Sod1*^{D83G} mouse mutant show that mutation in the endogenous mouse *Sod1* gene models critical features of human ALS (U and LMN cell death), albeit with a different profile than found in mice expressing human mutant SOD1 transgene arrays. This corroborates earlier findings in which a mutant genomic mouse *Sod1* transgenic was used to model human SOD1 G85R-fALS—'Sod1 G86R' mice with 'high transgene expression' had both U and LMN degeneration by 3–4 months of age (14). Therefore, the endogenous mouse SOD1 D83G mutation is informative for determining why some U and LMN die in ALS but removes any possible confounding effects of overexpression observed in SOD1 transgenic mice. We note that we and others have not observed MN cell body degeneration in *Sod1*^{-/-} mice at any stage, and therefore MN loss in *Sod1*^{D83G/D83G} mice likely arises from a toxic gain of function of the mutant SOD1 protein, as in ALS (20–22).

The significant reduction in SOD1 D83G protein is not due to allele-specific differences at the transcriptional level, but the dose-dependent decreases in SOD1 protein in heterozygous and homozygous D83G mutant mice may result from instability of mutant SOD1 and its subsequent degradation (42). It has been previously reported that mutant SOD1 has decreased half-life compared with WT SOD1 (42), and potentially the inability of D83G SOD1 to coordinate zinc may contribute to its instability (37,43,44).

Given that SOD1 expression levels in different transgenic mouse models show dose-dependent toxicity (16,18), the low levels of SOD1 D83G protein may only be sufficient to cause moderate motor neuron degeneration. The low SOD1 mutant protein level (~10% of WT in homozygotes) may be sufficient to elicit a degree of motor neuron degeneration but not the levels of loss seen in ALS, and may at least partially explain why loss of motor neurons within the sciatic motor pool appears not to progress between 15 and 52 weeks of age.

With respect to loss-of-function effects, which are of interest because of the loss of dismutase activity in the majority of human pathogenic SOD1-fALS mutations (average dismutase activity in SOD1-fALS is ~58% of normal (4)), we found mitochondrial membrane potentials ($\Delta\psi_m$) of both *Sod1*^{+D83G} and *Sod1*^{+/-} embryonic MNs are hyperpolarized. Thus, SOD1 loss of dismutase function to just 56% of WT (*Sod1*^{+D83G} level) contributes to mitochondrial abnormalities. Distal axonopathy in *Sod1*^{-/-} mice can be rescued by expressing mitochondrial-targeted WT SOD1 (20); the relevance of this to ALS remains to be determined.

Sod1^{D83G/D83G} mice develop a severe peripheral neuropathy similar to that arising from the loss of function in *Sod1*^{-/-} mice. This peripheral neuropathy is likely driving the phenotypic deterioration from 15 weeks of age in *Sod1*^{D83G/D83G} mice (Supplementary Material, video S1), as no further LMN loss occurs after that. As dismutase activity is only 1% of WT animals in the SOD1 D83G homozygotes, this peripheral neuropathy may be due to a loss of dismutase activity, potentially leading to increased vulnerability of peripheral motor axons to oxidative stress (45). It is also possible that the neuropathy develops because of a loss-of-unknown SOD1 function.

In at least one patient with diagnosed ALS who unexpectedly died from other causes, NMJ degeneration was found to precede motor neuron cell body death (45). Similarly, in transgenic human mutant SOD1 mouse models (with normal dismutase levels), NMJ degeneration leading to synaptic dysfunction precedes motor neuron cell body death and behavioural motor deficits

(45,46). These findings led to the concept of ALS as a "dying back" disorder in which muscle denervation precedes the death of the motor neuron cell body, and suggests that SOD1 gain of function can also lead to NMJ degeneration—and potentially also contributing to the distal neuropathy seen in *Sod1*^{D83G/D83G} mice.

Here our data, and that from other SOD1 mouse models, suggests that the axonal and neuronal cell body degeneration may be separate events that could be modulated by different sets of genes and/or environmental factors. In further support of this hypothesis, ablation of *Bax* in the human G93A SOD1 transgenic mouse model leads to complete dissociation between motor neuron soma death and motor dysfunction via distal denervation (47). While cell bodies are protected in *Bax* deficient G93A SOD1 transgenic mice, the degree of NMJ denervation and overall survival is not altered compared with G93A transgenic mice alone. Thus, *Sod1*^{D83G/D83G} mice provide a novel model to test therapeutics aimed at preserving NMJ as well as ameliorating the early stages of motor neuron cell body degeneration.

Overall, these results suggest that *Sod1*^{D83G/D83G} mice not only model the early stages of human ALS but are also able to separate the effects of central neuronal death from the peripheral distal neuropathy in a system in which the mutant gene is expressed at endogenous levels.

The *Sod1*^{D83G} model is the first of its kind carrying a known pathogenic point mutation in the mouse endogenous *Sod1* gene, which is identical to a human fALS mutation. Homozygous *Sod1*^{D83G/D83G} mice develop a degree of UMN and LMN degeneration, as well as progressive motor dysfunction due to a distal neuropathy, and hence model key aspects of the early stages of ALS. The *Sod1*^{D83G} model therefore provides a unique mammalian system in which to assess the contribution of both central neuronal loss and peripheral axonal dysfunction, which will further our understanding of ALS.

Materials and Methods

Mice

Ethics statement: all experiments were performed under licence from the UK Home Office. WT, *Sod1*^{+D83G} and *Sod1*^{D83G/D83G} mice were initially on a C57BL/6J-C3H background and backcrossed at least four generations to C57BL/6J. For all experiments, littermates for all genotypes were used, produced by intercrossing *Sod1*^{+D83G} mice. Experiments were performed blind to genotype and lifespan was defined as a loss of 20% of maximum body weight or the presence of piloerection. Animals were assessed daily and weighed at least biweekly.

Identification of *Sod1*^{D83G} mutation

The Harwell ENU-DNA archive (http://www.har.mrc.ac.uk/services/dna_archive/) was screened with high-resolution melting analysis using the LightScanner platform (Idaho Technology Inc., Salt Lake City, Utah, USA) (48). Coding sequence from exon 4 of *Sod1* including flanking (~70 bp) splice sites was tested in DNA derived from ~10 000 F1 ENU mutagenized animals. *Sod1* exon 4 was amplified with the following primers: SOD1_4F CATCCACT CATACGTATTTGAC, SOD1_4R ACCATAAAGTCATGGGAAGG using the lightscanner mastermix plus LC green (Idaho Technology Inc.) and possible mutations analysed with Sanger sequencing (GATC, Germany). We identified the chromosome 16 A90,224, 530G mutation, corresponding to the D83G amino acid change in SOD1. The mouse line was rederived using sperm from the

(C57BL/6J × C3H) F1 founder by *in vitro* fertilization. Genomic DNA from the F1 founder carrying the *Sod1* D83G mutation was deep sequenced (see Supplementary Material, Materials and Methods for details) to identify any other possible ENU-induced mutations linked to *Sod1* on mouse chromosome 16. The closest ENU-induced coding mutation was ~46 Mb proximal to the *Sod1* gene and did not segregate with lifespan or weight abnormalities in *Sod1*^{D83G/D83G} mice.

Behavioural analysis

See Supplementary Material, Materials and Methods for a description of behavioural and Echo MRI analysis.

Physiological assessment of hindlimb muscle force, motor units and fatigue index

Muscle force, motor unit number and muscle fatigue characteristics for female WT, *Sod1*^{+ /D83G} and *Sod1*^{D83G/D83G} littermates were examined at 15 and 52 weeks of age, and female WT and *Sod1*^{+ /D83G} littermates also at 88 weeks of age, as described previously (49). Cohort sizes per time point were at 15 weeks: 5 WT, 5 *Sod1*^{+ /D83G} and 5 *Sod1*^{D83G/D83G} animals; 52-weeks: 5 WT, 7 *Sod1*^{+ /D83G} and 6 *Sod1*^{D83G/D83G} animals; 88 weeks: 5 WT, 7 *Sod1*^{+ /D83G}. Briefly, mice were anaesthetized (4.5% chlorohydrate), the distal tendons of the TA and EDL muscles in both hindlimbs cut and attached to isometric force transducers (Dynamometer UFI Devices, UK), and the sciatic nerves exposed and sectioned. Isometric contractions were elicited by stimulating the nerve to the TA or EDL muscles using squarewave pulses of 0.02 ms duration at supra-maximal intensity. The number of motor units innervating the EDL muscle was determined by stimulating the motor nerve with stimuli of increasing intensity, resulting in incremental increases in twitch tension due to successive recruitment of motor axons with increasing threshold. The number of increments in twitch force was counted giving an estimate of the number of functional motor units present in muscle. The fatigue characteristics of EDL were examined by undertaking a fatigue test in which the EDL muscle was repeatedly stimulated at 40 Hz for 250 ms every second for 180 s. The resulting contractions were recorded on a pen recorder (Lectromed Multitrace 2) producing a fatigue trace from which an FI, a measure of muscle fatigability, can be determined by expressing the force at the end of the test as a ratio of the force at the start: $FI = F_{t180}/F_{t0}$. A muscle that is completely fatigue resistant has an FI approaching 1.0.

Morphological assessment of muscle and neuronal tissue

For assessment of survival of motor neurons in the sciatic pool of the lumbar spinal cord (16,18), animals were perfused with saline followed with 4% paraformaldehyde (PFA) fixation. Spinal cords were removed, postfixed in 4% PFA and cryopreserved in 30% sucrose. Transverse sections (20 μm) of the lower L2–lower L6 lumbar region of fixed spinal cords cut on a cryostat serially onto glass slides and stained for Nissl (galloyanin) (50). Nissl-stained motor neurons in the sciatic pool in every third section of the L3–L6 lumbar region, over 40 sections in total, were counted. Only large, polygonal neurons with a distinguishable nucleus and nucleolus and clearly identifiable Nissl structure were included in the counts. This method avoids the possibility of counting the same motor neuron in consecutive sections. At least five mice were analysed from each experimental group per time point.

For assessment of CSMNs, brains were removed intact from animals perfused as above, postfixed (4% PFA, overnight), and

stored in PBS with sodium azide (0.01%) at 4°C. Brains were sectioned in 50 μm coronal planes and serially collected in 12-well plates. Sections mounted on Superfrost Plus glass slides (VWR) were stained for Nissl (cresyl violet). Antibodies used for assessment of CSMNs: anti-CTIP2 (1 : 1000; Abcam), anti-Cry-mu (1 : 500, Sigma), anti-Satb2 (1 : 1000; Abcam) and anti-LMO4 (1 : 500, Millipore). Sections for LMO4 were pretreated with 0.05% trypsin EDTA at 37°C for 10 min, followed by washes in blocking solution (0.5% BSA, 2% FBS, 0.1% Triton X-100 and 0.01% saponin, 0.02% sodium azide) and treatment with 50 mM ammonium chloride for 30 min. All sections were incubated with primary antibodies in blocking solution overnight at 4°C. Appropriate secondary antibodies (1 : 500 alkaline phosphatase conjugated, Santa Cruz Biotechnology; 1 : 500 Cy3-conjugated, Millipore) were applied. Sections with Cy3-conjugated antibodies were stained with DAPI (1 : 5000 in PBS) for 5 min. Sections for CTIP2 were processed with Vector blue AP substrate kit (Vector Laboratories) according to manufacturer's instructions. Sections were analysed using a Nikon Eclipse TE2000-E fluorescence microscope equipped with Intensilight C-HGFI (Nikon). Epifluorescent images were acquired using Digital Sight DS-Qi1MC CCD camera (Nikon). Three well-defined sections spanning the motor cortex (Bregma 0.86 mm, interaural 4.66 mm; Bregma 0.02 mm, interaural 3.82 mm; Bregma -1.22 mm, interaural 2.58 mm) (51) were used for quantitative analysis, as previously described (27,52).

Muscle histochemistry was performed on TA and EDL muscle sections by staining for the oxidative enzyme, as previously described (53). Briefly, serial cross-sections of fresh frozen TA and EDL were cut on a cryostat at 12 μm, collected on glass slides and stained for SDH activity to determine the oxidative capacity of the muscle fibres.

Neuromuscular junction quantification

EDL muscles were dissected from mice of all three genotypes at 15 and 52 weeks of age. The numbers of whole EDL muscles analysed at 15 weeks of age: 7 WT, 4 *Sod1*^{+ /D83G} and 8 *Sod1*^{D83G/D83G}. At 52 weeks: 11 WT, 8 *Sod1*^{+ /D83G} and 8 *Sod1*^{D83G/D83G}. Mice were perfused trans-cardial with saline solution and 4% PFA. Muscles were postfixed in 4% PFA and cryopreserved in sucrose. Whole EDL muscles were then embedded in OCT media (Tissue-Tek), frozen on dry-ice and stored at -80°C. A Bright™ cryostat was used to cut 20 μm longitudinal section of frozen EDL muscles which were subsequently collected onto poly-lysine-coated slides. Primary antibodies used: mouse monoclonal anti-synaptic vesicle (Developmental Studies Hybridoma Bank) Mouse monoclonal anti-neurofilament (165 kDa) (Developmental Studies Hybridoma Bank). M.O.M. biotinylated secondary antibody (Vector Labs) was used following manufacturer instructions. α-Bungarotxin-rhodamine was used to label postsynapsis and sections mounted. Images were acquired on a confocal microscope (Leica DFC 420C) and NMJ were manually counted.

Immunocytochemistry

See Supplementary Material, Materials and Methods for immunocytochemistry experiments.

qPCR, western blotting, dismutase activity and immunoprecipitations

qPCR, western blotting, dismutase activity and immunoprecipitation protocols are available in Supplementary Material, Materials and Methods.

Embryonic motor neuron culture and mitochondrial membrane potential

Motor neuron culture and measurement of mitochondrial membrane potential are described in Supplementary Material, Materials and Methods.

Statistical analysis

An ANOVA test was used to compare between WT, *Sod1*^{+/^{D83G}} and *Sod1*^{D83G/D83G} genotypes per time point followed by Bonferroni's multiple comparisons testing correction for weight, dismutase activity, protein quantification, Echo MRI analysis, grip strength, rotarod, startle response and sensory analysis. Wheel running behaviour was analysed using a repeated measures ANOVA. Cox survival analysis was used to analyse SHIRPA and survival data. The Mann–Whitney test was used to compare between genotypes per time point or *Sod1*^{D83G/D83G} cohorts across time points for TA and EDL maximum muscle force, surviving motor units, FI and motor neuron survival. Two-tailed tests were used in all instances and significance level was set at $P < 0.05$.

Supplementary Material

Supplementary Material is available at HMG online.

Acknowledgements

We are indebted to Jim Humphries, Jenny Corrigan, Liz Darley, Elizabeth Joynson, Natalie Walters, Sara Wells, Barney Bryson and the whole necropsy, histology, genotyping and MLC ward 6 teams at MRC Harwell for excellent technical assistance. We thank Jean-Pierre Julien, Avi Chakrabarty and Janice Robertson for the generous gift of antibodies.

Conflict of Interest statement. None declared.

Funding

This work was supported by the Motor Neurone Disease Association (A.A., E.F.), Packard Center for ALS at Johns Hopkins (A.A., E.F., L.G.), Wellcome Trust (DLHB, 095698/Z/11/Z), Medical Research Council (E.F., A.A.) and Les Turner ALS Foundation (P.H.O.). L.G. and E.F. are funded by the European Community's Seventh Framework Programme (FP7/2007–2013). L.G. is the Graham Watts Senior Research Fellow, funded by The Brain Research Trust. Funding to pay the Open Access publication charges for this article was provided by the Medical Research Council.

References

- Leblond, C.S., Kaneb, H.M., Dion, P.A. and Rouleau, G.A. (2014) Dissection of genetic factors associated with amyotrophic lateral sclerosis. *Exp. Neurol.*, doi: 10.1016/j.expneurol.2014.04.013.
- Renton, A.E., Chio, A. and Traynor, B.J. (2014) State of play in amyotrophic lateral sclerosis genetics. *Nat. Neurosci.*, **17**, 17–23.
- Turner, M.R., Hardiman, O., Benatar, M., Brooks, B.R., Chio, A., de Carvalho, M., Ince, P.G., Lin, C., Miller, R.G., Mitsumoto, H. et al. (2013) Controversies and priorities in amyotrophic lateral sclerosis. *Lancet Neurol.*, **12**, 310–322.
- Saccon, R.A., Bunton-Stasyshyn, R.K.A., Fisher, E.M.C. and Fratta, P. (2013) Is SOD1 loss of function involved in amyotrophic lateral sclerosis? *Brain*, **136**, 2342–2358.
- Reddi, A.R. and Culotta, V.C. (2013) SOD1 integrates signals from oxygen and glucose to repress respiration. *Cell*, **152**, 224–235.
- Joyce, P.I., Fratta, P., Fisher, E.M.C. and Acevedo-Aroza, A. (2011) SOD1 and TDP-43 animal models of amyotrophic lateral sclerosis: recent advances in understanding disease toward the development of clinical treatments. *Mamm. Genome*, **22**, 420–448.
- Bosco, D.A., Morfini, G., Karabacak, N.M., Song, Y., Gros-Louis, F., Pasinelli, P., Goolsby, H., Fontaine, B.A., Lemay, N., McKenna-Yasek, D. et al. (2010) Wild-type and mutant SOD1 share an aberrant conformation and a common pathogenic pathway in ALS. *Nat. Neurosci.*, **13**, 1396–1403.
- Guareschi, S., Cova, E., Cereda, C., Ceroni, M., Donetti, E., Bosco, D.A., Trotti, D. and Pasinelli, P. (2012) An over-oxidized form of superoxide dismutase found in sporadic amyotrophic lateral sclerosis with bulbar onset shares a toxic mechanism with mutant SOD1. *Proc. Natl. Acad. Sci. USA*, **109**, 5074–5079.
- Pokrishevsky, E., Grad, L.I., Yousefi, M., Wang, J., Mackenzie, I.R. and Cashman, N.R. (2012) Aberrant localization of FUS and TDP43 is associated with misfolding of SOD1 in amyotrophic lateral sclerosis. *PLoS ONE*, **7**, e35050.
- Rotunno, M.S. and Bosco, D.A. (2013) An emerging role for misfolded wild-type SOD1 in sporadic ALS pathogenesis. *Front. Cell. Neurosci.*, **7**, 253.
- Fridovich, I. (1995) Superoxide radical and superoxide dismutases. *Annu. Rev. Biochem.*, **64**, 97–112.
- McGoldrick, P., Joyce, P.I., Fisher, E.M.C. and Greensmith, L. (2013) Rodent models of amyotrophic lateral sclerosis. *Biochim. Biophys. Acta – Mol. Basis Dis.*, **1832**, 1421–1436.
- Turner, B.J. and Talbot, K. (2008) Transgenics, toxicity and therapeutics in rodent models of mutant SOD1-mediated familial ALS. *Prog. Neurobiol.*, **85**, 94–134.
- Ripps, M.E., Huntley, G.W., Hof, P.R., Morrison, J.H. and Gordon, J.W. (1995) Transgenic mice expressing an altered murine superoxide-dismutase gene provide an animal-model of amyotrophic-lateral-sclerosis. *Proc. Natl. Acad. Sci. USA*, **92**, 689–693.
- Luche, R.M., Maiwald, R., Carlson, E.J. and Epstein, C.J. (1997) Novel mutations in an otherwise strictly conserved domain of CuZn superoxide dismutase. *Mol. Cell. Biochem.*, **168**, 191–194.
- Acevedo-Aroza, A., Kalmar, B., Essa, S., Ricketts, T., Joyce, P., Kent, R., Rowe, C., Parker, A., Gray, A., Hafezparast, M. et al. (2011) A comprehensive assessment of the SOD1 (G93A) low-copy transgenic mouse, which models human amyotrophic lateral sclerosis. *Dis. Models Mech.*, **4**, 686–700.
- Gurney, M.E., Pu, H., Chiu, A.Y., Dal Canto, M.C., Polchow, C.Y., Alexander, D.D., Caliendo, J., Hentati, A., Kwon, Y.W. and Deng, H.X. (1994) Motor neuron degeneration in mice that express a human Cu,Zn superoxide dismutase mutation. *Science*, **264**, 1772–1775.
- Jonsson, P.A., Graffmo, K.S., Andersen, P.M., Brannstrom, T., Lindberg, M., Oliveberg, M. and Marklund, S.L. (2006) Disulphide-reduced superoxide dismutase-1 in CNS of transgenic amyotrophic lateral sclerosis models. *Brain*, **129**, 451–464.
- Graffmo, K.S., Forsberg, K., Bergh, J., Birve, A., Zetterstrom, P., Andersen, P.M., Marklund, S.L. and Brannstrom, T. (2013) Expression of wild-type human superoxide dismutase-1 in mice causes amyotrophic lateral sclerosis. *Hum. Mol. Genet.*, **22**, 51–60.
- Fischer, L.R., Igoudjil, A., Magrane, J., Li, Y.J., Hansen, J.M., Manfredi, G. and Glass, J.D. (2011) SOD1 targeted to the

- mitochondrial intermembrane space prevents motor neuropathy in the Sod1 knockout mouse. *Brain*, **134**, 196–209.
21. Fischer, L.R., Li, Y.J., Asress, S.A., Jones, D.P. and Glass, J.D. (2012) Absence of SOD1 leads to oxidative stress in peripheral nerve and causes a progressive distal motor axonopathy. *Exp. Neurol.*, **233**, 163–171.
 22. Flood, D.G., Reaume, A.G., Gruner, J.A., Hoffman, E.K., Hirsch, J.D., Lin, Y.G., Dorfman, K.S. and Scott, R.W. (1999) Hindlimb motor neurons require Cu/Zn superoxide dismutase for maintenance of neuromuscular junctions. *Am. J. Pathol.*, **155**, 663–672.
 23. Reaume, A.G., Elliott, J.L., Hoffman, E.K., Kowall, N.W., Ferrante, R.J., Siwek, D.F., Wilcox, H.M., Flood, D.G., Beal, M.F., Brown, R.H. et al. (1996) Motor neurons in Cu/Zn superoxide dismutase-deficient mice develop normally but exhibit enhanced cell death after axonal injury. *Nat. Genet.*, **13**, 43–47.
 24. Millicamps, S., Salachas, F., Cazeneuve, C., Gordon, P., Bricka, B., Camuzat, A., Guillot-Noel, L., Russaouen, O., Bruneteau, G., Pradat, P.F. et al. (2010) SOD1, ANG, VAPB, TARDBP, and FUS mutations in familial amyotrophic lateral sclerosis: genotype-phenotype correlations. *J. Med. Genet.*, **47**, 554–560.
 25. Acevedo-Arozena, A., Wells, S., Potter, P., Kelly, M., Cox, R.D. and Brown, S.D. (2008) ENU mutagenesis, a way forward to understand gene function. *Annu. Rev. Genomics Hum. Genet.*, **9**, 49–69.
 26. Quwailid, M.M., Hugill, A., Dear, N., Vizor, L., Wells, S., Horner, E., Fuller, S., Weedon, J., McMath, H., Woodman, P. et al. (2004) A gene-driven ENU-based approach to generating an allelic series in any gene. *Mamm. Genome*, **15**, 585–591.
 27. Ozdinler, P.H., Benn, S., Yamamoto, T.H., Guzel, M., Brown, R. H. and Macklis, J.D. (2011) Corticospinal motor neurons and related subcerebral projection neurons undergo early and specific neurodegeneration in hSOD1(G93A) transgenic ALS mice. *J. Neurosci.*, **31**, 4166–4177.
 28. Kalmar, B., Novoselov, S., Gray, A., Cheetham, M.E., Margulis, B. and Greensmith, L. (2008) Late stage treatment with arimoclomol delays disease progression and prevents protein aggregation in the SOD1 mouse model of ALS. *J. Neurochem.*, **107**, 339–350.
 29. Taicher, G.Z., Tinsley, F.C., Reiderman, A. and Heiman, M.L. (2003) Quantitative magnetic resonance (QMR) method for bone and whole-body-composition analysis. *Anal. Bioanal. Chem.*, **377**, 990–1002.
 30. Rogers, D.C., Fisher, E.M., Brown, S.D., Peters, J., Hunter, A.J. and Martin, J.E. (1997) Behavioral and functional analysis of mouse phenotype: SHIRPA, a proposed protocol for comprehensive phenotype assessment. *Mamm. Genome*, **8**, 711–713.
 31. Rogers, D.C., Peters, J., Martin, J.E., Ball, S., Nicholson, S.J., Witherden, A.S., Hafezparast, M., Latcham, J., Robinson, T. L., Quilter, C.A. and Fisher, E.M. (2001) SHIRPA, a protocol for behavioral assessment: validation for longitudinal study of neurological dysfunction in mice. *Neurosci. Lett.*, **306**, 89–92.
 32. Mandillo, S., Heise, I., Garbugino, L., Tocchini-Valentini, G.P., Giuliani, A., Wells, S. and Nolan, P. (2014) Early motor deficits in mouse disease models are reliably uncovered using an automated home-cage wheel-running system: a cross-laboratory validation. *Dis. Models Mech.*, **7**, 397–407.
 33. Bruestle, D.A., Cutler, R.G., Telljohann, R.S. and Mattson, M.P. (2009) Decline in daily running distance presages disease onset in a mouse model of ALS. *Neuromol. Med.*, **11**, 58–62.
 34. Kieran, D. and Greensmith, L. (2004) Inhibition of calpains, by treatment with leupeptin, improves motoneuron survival and muscle function in models of motoneuron degeneration. *Neuroscience*, **125**, 427–439.
 35. Guo, Y.S., Wu, D.X., Wu, H.R., Wu, S.Y., Yang, C., Li, B., Bu, H., Zhang, Y.S. and Li, C.Y. (2009) Sensory involvement in the SOD1-G93A mouse model of amyotrophic lateral sclerosis. *Exp. Mol. Med.*, **41**, 140–150.
 36. Pugdahl, K., Fuglsang-Frederiksen, A., de Carvalho, M., Johnsen, B., Fawcett, P.R.W., Labarre-Vila, A., Liguori, R., Nix, W.A. and Schofield, I.S. (2007) Generalised sensory system abnormalities in amyotrophic lateral sclerosis: a European multicentre study. *J. Neurol. Neurosurg. Psychiatry*, **78**, 746–749.
 37. Krishnan, U., Son, M., Rajendran, B. and Elliott, J.L. (2006) Novel mutations that enhance or repress the aggregation potential of SOD1. *Mol. Cell Biochem.*, **287**, 201–211.
 38. Elchuri, S., Oberley, T.D., Qi, W.B., Eisenstein, R.S., Roberts, L. J., Van Remmen, H., Jepstein, C.J. and Huang, T.T. (2005) CuZnSOD deficiency leads to persistent and widespread oxidative damage and hepatocarcinogenesis later in life. *Oncogene*, **24**, 367–380.
 39. Faes, L. and Callewaert, G. (2011) Mitochondrial dysfunction in familial amyotrophic lateral sclerosis. *J. Bioenerg. Biomembr.*, **43**, 587–592.
 40. Duchen, M.R., Surin, A. and Jacobson, J. (2003) Imaging mitochondrial function in intact cells. *Biophotonics, Part B*, **361**, 353–389.
 41. Bilsland, L.G., Nirmalanathan, N., Yip, J., Greensmith, L. and Duchen, M.R. (2008) Expression of mutant SOD1(G93A) in astrocytes induces functional deficits in motoneuron mitochondria. *J. Neurochem.*, **107**, 1271–1283.
 42. Kabuta, T., Suzuki, Y. and Wada, K. (2006) Degradation of amyotrophic lateral sclerosis-linked mutant Cu,Zn-superoxide dismutase proteins by macroautophagy and the proteasome. *J. Biol. Chem.*, **281**, 30524–30533.
 43. Choi, I., Yang, Y.I., Song, H.D., Lee, J.S., Kang, T., Sung, J.J. and Yi, J. (2011) Lipid molecules induce the cytotoxic aggregation of Cu/Zn superoxide dismutase with structurally disordered regions. *Biochim. Biophys. Acta – Mol. Basis Dis.*, **1812**, 41–48.
 44. Nordlund, A., Leinartaite, L., Saraboji, K., Aisenbrey, C., Grobner, G., Zetterstrom, P., Danielsson, J., Logan, D.T. and Oliveberg, M. (2009) Functional features cause misfolding of the ALS-provoking enzyme SOD1. *Proc. Natl. Acad. Sci. USA*, **106**, 9667–9672.
 45. Fischer, L.R., Culver, D.G., Tennant, P., Davis, A.A., Wang, M.S., Castellano-Sanchez, A., Khan, J., Polak, M.A. and Glass, J.D. (2004) Amyotrophic lateral sclerosis is a distal axonopathy: evidence in mice and man. *Exp. Neurol.*, **185**, 232–240.
 46. Murray, L.M., Talbot, K. and Gillingwater, T.H. (2010) Review: Neuromuscular synaptic vulnerability in motor neurone disease: amyotrophic lateral sclerosis and spinal muscular atrophy. *Neuropathol. Appl. Neurobiol.*, **36**, 133–156.
 47. Gould, T.W., Buss, R.R., Vinsant, S., Pevette, D., Sun, W., Knudson, C.M., Milligan, C.E. and Oppenheim, R.W. (2006) Complete dissociation of motor neuron death from motor dysfunction by Bax deletion in a mouse model of ALS. *J. Neurosci.*, **26**, 8774–8786.
 48. Voegelé, C., Tavtigian, S.V., de Silva, D., Cuber, S., Thomas, A. and Calvez-Kelm, F. (2007) A laboratory information management system (LIMS) for a high throughput genetic platform aimed at candidate gene mutation screening. *Bioinformatics*, **23**, 2504–2506.
 49. Sharp, P.S., Dick, J.R. and Greensmith, L. (2005) The effect of peripheral nerve injury on disease progression in the SOD1 (G93A) mouse model of amyotrophic lateral sclerosis. *Neuroscience*, **130**, 897–910.

50. Kellett, B.S. (1963) Galloxyanin-chrome alum: a routine stain for Nissl substance in paraffin sections. *J. Med. Lab. Technol.*, **20**, 196–198.
51. Paxinos, G.F. (2001) *The Mouse Brain in Stereotaxic Coordinates*. Academic Press, San Diego.
52. Jara, J.H., Villa, S.R., Khan, N.A., Bohn, M.C. and Ozdinler, P.H. (2012) AAV2 mediated retrograde transduction of corticospinal motor neurons reveals initial and selective apical dendrite degeneration in ALS. *Neurobiol. Dis.*, **47**, 174–183.
53. Boerio, D., Kalmar, B., Greensmith, L. and Bostock, H. (2010) Excitability properties of mouse motor axons in the mutant SOD1(G93A) model of amyotrophic lateral sclerosis. *Muscle Nerve*, **41**, 774–784.

SOD1 Function and Its Implications for Amyotrophic Lateral Sclerosis Pathology: New and Renascent Themes

Rosie K. A. Bunton-Stasyshyn, Rachele A. Saccon, Pietro Fratta and Elizabeth M. C. Fisher

Neuroscientist published online 9 December 2014

DOI: 10.1177/1073858414561795

The online version of this article can be found at:

<http://nro.sagepub.com/content/early/2014/12/09/1073858414561795>

Published by:



<http://www.sagepublications.com>

Additional services and information for *The Neuroscientist* can be found at:

Open Access: Immediate free access via SAGE Choice

Email Alerts: <http://nro.sagepub.com/cgi/alerts>

Subscriptions: <http://nro.sagepub.com/subscriptions>


Reprints: <http://www.sagepub.com/journalsReprints.nav>

Permissions: <http://www.sagepub.com/journalsPermissions.nav>

>> [OnlineFirst Version of Record](#) - Dec 9, 2014

[What is This?](#)

SOD1 Function and Its Implications for Amyotrophic Lateral Sclerosis Pathology: New and Renascent Themes

The Neuroscientist
1–11
© The Author(s) 2014
Reprints and permissions:
sagepub.com/journalsPermissions.nav
DOI: 10.1177/1073858414561795
nro.sagepub.com


Rosie K. A. Bunton-Stasyshyn¹, Rachele A. Saccon¹, Pietro Fratta¹, and Elizabeth M. C. Fisher¹

Abstract

The canonical role of superoxide dismutase 1 (SOD1) is as an antioxidant enzyme protecting the cell from reactive oxygen species toxicity. *SOD1* was also the first gene in which mutations were found to be causative for the neurodegenerative disease amyotrophic lateral sclerosis (ALS), more than 20 years ago. ALS is a relentless and incurable mid-life onset disease, which starts with a progressive paralysis and usually leads to death within 3 to 5 years of diagnosis; in the majority of cases, the intellect appears to remain intact while the motor system degenerates. It rapidly became clear that when mutated SOD1 takes on a toxic gain of function in ALS. However, this novel function remains unknown and many cellular systems have been implicated in disease. Now it seems that SOD1 may play a rather larger role in the cell than originally realized, including as a key modulator of glucose signaling (at least so far in yeast) and in RNA binding. Here, we consider some of the new findings for SOD1 in health and disease, which may shed light on how single amino acid changes at sites throughout this protein can cause devastating neurodegeneration in the mammalian motor system.

Keywords

amyotrophic lateral sclerosis, ALS, motor neuron, superoxide dismutase 1, SOD1

Introduction

Amyotrophic lateral sclerosis (ALS) is a fatal adult-onset neurodegenerative disease characterized by degeneration and death of upper and lower motor neurons (MNs). Patients typically suffer from progressive motor weakness, which starts focally and spreads through the body leading to paralysis and ultimately death within a few years of diagnosis. Although usually sporadic (without a family history), approximately 10% of ALS cases are familial (fALS) and of those, ~20% are caused by mutations in the gene *superoxide dismutase 1 (SOD1)* (Kiernan and others 2012). More than 160 mutations in *SOD1* have been identified in ALS sufferers, the majority of which are missense point mutations resulting in a dominant mode of inheritance. At least 75 of SOD1's 154 amino acids have been reported as mutated in ALS and their positions are scattered throughout the five exons of the gene (Saccon and others 2013).

SOD1 is highly conserved throughout evolution (Wang and others 2006), ubiquitously expressed and makes up 1-2% of the total soluble protein in the central nervous system (Pardo and others 1995). Its primary function is thought to be as a cytosolic and mitochondrial

antioxidant enzyme, converting superoxide to molecular oxygen and hydrogen peroxide; however, in yeast at least, less than 1% of total SOD1 is required to carry out this canonical function (Corson and others 1998; Reddi and Culotta 2013) leaving the question open as to whether SOD1 plays other equally important role(s), which might account for its abundance.

Many lines of evidence have led to the conclusion that mutations in SOD1 cause ALS via an as yet unidentified gain of function, although it has been proposed that a loss of function may also play a secondary role in disease, at least in some cases (Saccon and others 2013). A great number of cellular mechanisms has been implicated as potentially involved in SOD1-fALS pathogenesis, however, distinguishing cause from effect and identifying the critical processes remains challenging (Redler and

¹Department of Neurodegenerative Disease, Institute of Neurology, University College London, London, UK

Corresponding Author:

Elizabeth M. C. Fisher, Department of Neurodegenerative Disease, Institute of Neurology, University College London, London, WC1N 3BG, UK.

Email: e.fisher@prion.ucl.ac.uk

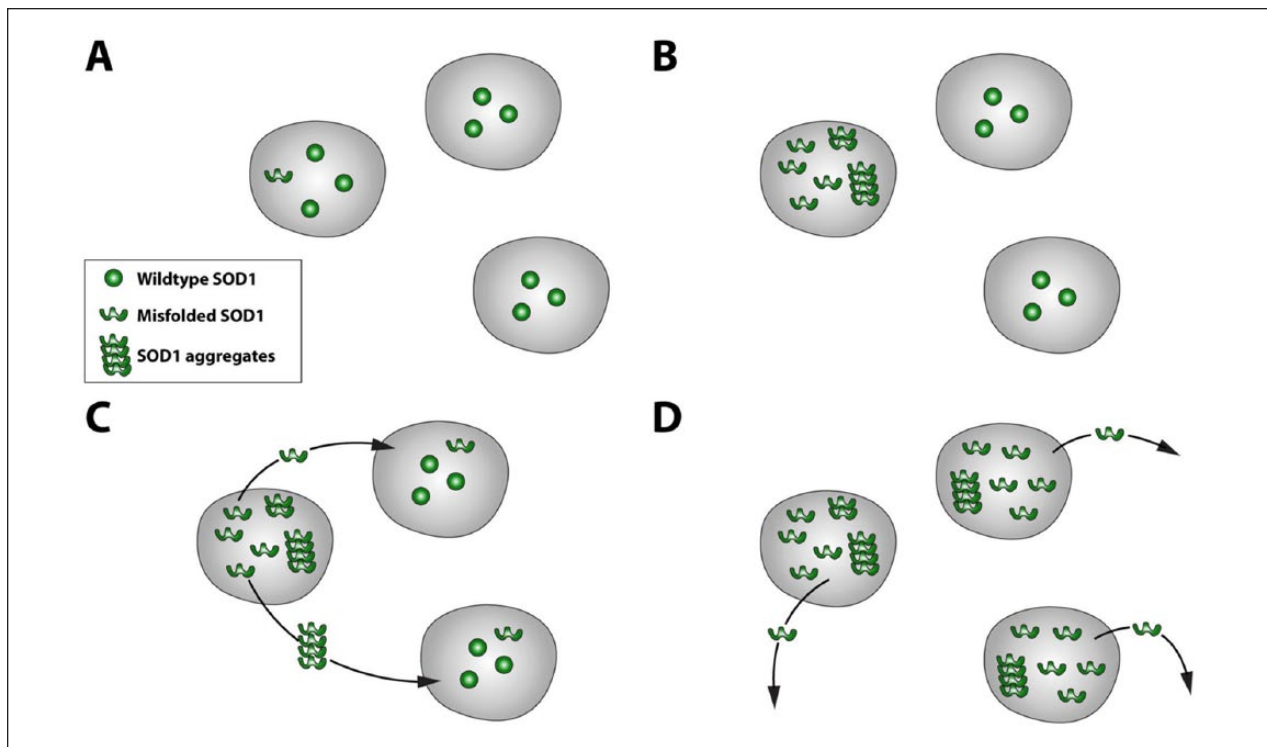


Figure 1. Superoxide dismutase I (SOD1) may have prion-like properties. (A) Misfolded SOD1 within a cell could (B) sequester and misfold wildtype SOD1, ultimately producing aggregates, and (C) if secreted and taken up by neighboring cells could (D) cause a “chain reaction” of misfolding, aggregate formation, and transmission in a prion-like manner. The exact nature of this process—for example, the roles of monomers and aggregates—remains unknown.

Dokholyan 2012). Here, we describe emerging themes in SOD1 biology that suggest this enzyme is involved in a widening array of cellular processes in both health and disease; this may shed new light on the pathogenesis of SOD1-ALS.

Transmission of SOD1

Some causative proteins for neurodegenerative diseases may have “prion-like” properties: the ability to sequester wildtype proteins and seed their aggregation or misfolding, and to act as transmissible agents between cells (Polymenidou and Cleveland 2012) (Fig. 1). SOD1 displays prion-like properties *in vitro* and in cellular and now in animal models, which is particularly of interest for SOD1-fALS, given the focal start of ALS, the finding that motor neuron death is not cell-autonomous (e.g., see Ilieva and others 2009), and the implications for therapy to halt the spread of pathology. These findings are also important for a potential mechanism for spread, and possibly even pathogenesis in *sporadic* ALS (sALS), given the presence of aggregated SOD1 in sALS cases (Bosco and others 2010; Forsberg and others 2010; Grad and Cashman 2014).

SOD1 Seeded Aggregation *In Vitro*

In vitro assays measuring aggregation propensity show recombinant wildtype and ALS-mutant SOD1 can seed aggregation of themselves (self-seeding) and of each other (cross-seeding). Seeded amyloid fibrilization of SOD1 occurred at acidic pH and in the presence of a chaotrope (Chia and others 2010), and non-amyloid seeded fibrilization was seen at physiological pH (Hwang and others 2010). Spinal cord tissue homogenate from a *SOD1^{G93A}* transgenic mouse (which models human ALS) was then shown to efficiently self- and cross-seed the amyloid fibrilization of recombinant wildtype and mutant SOD1 *in vitro* (Chia and others 2010). However, self- and cross-seeding does not, alone, indicate prion-like properties; the prion-like nature of a protein also comes from its ability to transmit between cells and indeed between organisms.

Transmission in Cell Models

Mutant SOD1 is found in medium from primary cultures of whole spinal cord and of astrocytes from SOD1-ALS transgenic mice (Basso and others 2013; Urushitani and

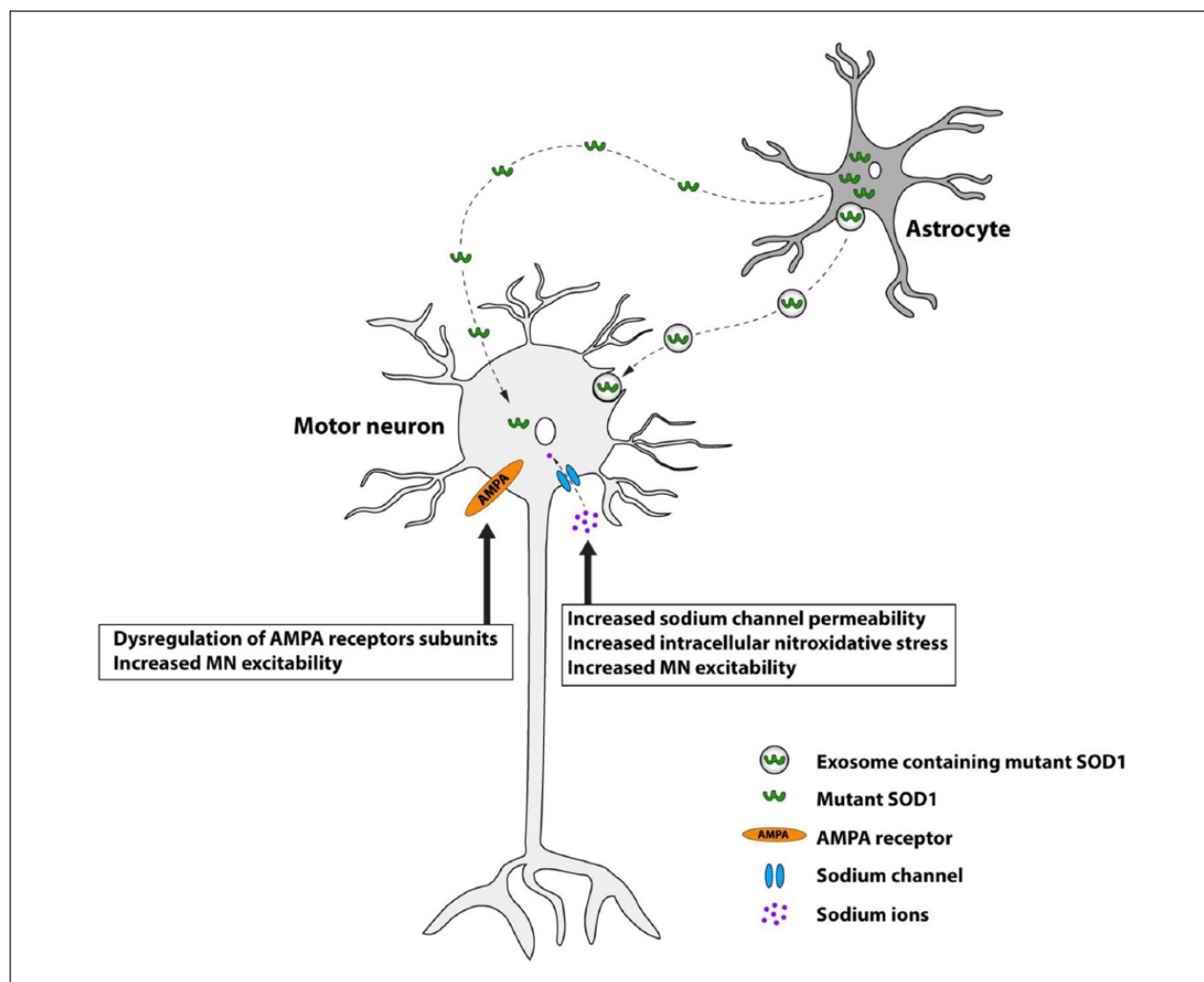


Figure 2. Mutant superoxide dismutase I (SOD1) may be transmitted from astrocytes to motor neurons, causing cell death. Mutant SOD1 is secreted in exosomes by astrocytes and may be taken in by motor neurons; propagation of misfolding may then proceed within the cell (see Fig. 1). Exposure of motor neurons to mutant SOD1 results in increased sodium channel permeability, induction of nitroxidative stress, hyperexcitability likely through dysregulation of AMPA receptors as well as sodium channel dysfunction and reduced viability.

others 2006). Furthermore, mutant SOD1 is secreted in exosomes from primary astrocytes and neuronal-like stable cell lines, (Basso and others 2013; Grad and Cashman 2014) (Fig. 2). Thus there is a mechanism for mutant SOD1 to get out of cells.

In terms of getting into cells, a range of recombinant forms of SOD1 (including wildtype and mutant, aggregated and non-aggregated) are efficiently internalized by neuronal-like stable cell lines, via the non-selective mechanism, macropinocytosis (Grad and Cashman 2014; Münch and others 2011; Sundaramoorthy and others 2013). Primary mouse spinal cord cultures and neuronal-like cell lines also take in wildtype and mutant SOD1 via internalization of exosomes (Basso and others 2013; Grad and others 2014).

Once internalized, recombinant aggregated mutant SOD1 can self-seed aggregation of stably expressed mutant SOD1; this is sustained for up to 1 month and through multiple passages of a mouse neuroblastoma-derived cell line, long after the exogenous seeds had apparently been cleared from the cells (Münch and others 2011). Furthermore, recombinant mutant SOD1 (both aggregated and non-aggregated forms) can also cross-seed endogenous wildtype SOD1—which can also be self-seeded by recombinant aggregated wildtype SOD1 (Sundaramoorthy and others 2013).

Self-seeded aggregation of endogenous SOD1 by conditioned medium has been shown in stable cell lines through multiple passages; this was blocked by both *SOD1* knock-down and immuno-depletion of misfolded

SOD1 in the medium (Grad and others 2011; Grad and Cashman 2014).

Transmission between Mouse Models

Recently, transmissibility of mutant SOD1 and motor neuron disease pathology between different transgenic mouse models appears to have been demonstrated. Spinal cord homogenates from *SOD1^{G93A}* mice were injected into the spinal cords of different *SOD1* transgenic models and motor neuron disease was induced in an otherwise unaffected transgenic animal expressing low levels of a different (SOD1 G85R) mutant SOD1 protein (Ayers and others 2014). Remarkably, when tissues from the induced mice were used to inoculate new *SOD1^{G85R}* mice (“second passage homogenates”) disease onset was earlier in recipient animals, exactly as seen in prion disease models. Other data shows potential SOD1 “strains” akin to prion strains (Ayers and others 2014). This article offers compelling data to indicate the physiological prion-like transmission of mutant SOD1 and motor neuron disease pathology in vivo. Of note, one-third of the *SOD1^{G85R}* mice inoculated with homogenates from wildtype *SOD1* transgenic mice also developed the motor neuron degeneration phenotype, while self-seeding experiments in two other mutant *SOD1* transgenic lines failed to accelerate disease in these mice. Future work to identify whether a misfolded SOD1 species is both necessary and sufficient to induce disease, and to determine whether the phenomenon is applicable to other SOD1 variants will be needed.

Mutant SOD1 Expressing Glia Are Toxic to Motor Neurons

Data from transgenic mice with tissue specific/restricted expression of mutant SOD1 demonstrate that non-neuronal cells are involved in the progression of disease-related phenotypes (reviewed in Ilieva and others 2009). In vitro experiments also clearly demonstrate the toxicity of mutant SOD1-expressing glia to motor neurons.

Astrocytes

Toxicity of astrocytes, to motor neurons has been demonstrated by co-culture, and by the application of astrocyte conditioned medium (ACM) (Basso and others 2013; Haidet-Phillips and others 2011; Meyer and others 2014; Nagai and others 2007). Intriguingly, this interaction appears to be cell-type specific: mutant SOD1 expressing primary astrocytes reduced viability of both primary and embryonic stem cell-derived MNs in co-culture, but interneurons, GABAergic neurons, or dorsal root ganglion neurons were not affected. Mutant

SOD1 fibroblasts, microglia, cortical neurons, or myocytes were not toxic to co-cultured MNs (Nagai and others 2007).

Induction of nitroxidative stress and hyperexcitability has been proposed as a possible mode of astrocyte toxicity to motor neurons: within 30 minutes of applying mutant SOD1 ACM, primary spinal MNs had increased excitability and increased sodium channel permeability; this exposure, followed by 4 days of culture with normal medium, was sufficient to cause ~50% MN death (Fritz and others 2013). ACM also produced an increase in intracellular nitroxidative stress in cultured MNs (Rojas and others 2014) (Fig. 2). Similarly, co-treatment with ACM and sodium channel blockers protected MNs from hyperexcitability, nitroxidative stress, and cell death, while antioxidants protected against nitroxidative stress and significantly improved MN survival, although their effect on sodium channel activity was not assessed (Fritz and others 2013; Rojas and others 2014). MNs co-cultured with mutant SOD1 expressing astrocytes have been shown to have dysregulated AMPA receptor subunits and increased excitability (Van Damme and others 2007).

However, conversely, a separate study of mutant *SOD1* transgenic mouse models found MNs with lowest basal excitability were the most vulnerable, and pharmacologically increasing MN activity reduced misfolded SOD1 pathology and markers of cellular stress while decreasing activity had the opposite, detrimental, effects (Saxena and others 2013).

The toxic factor released by astrocytes has not yet been identified and may well be/include mutant SOD1 because exosome depletion prevents ACM toxicity (Basso and others 2013). Interestingly, astrocytes from mutant TDP43 transgenic mice, sALS and *C9orf72* expansion patients have also been shown to cause MN toxicity by co-culture and by ACM (Haidet-Phillips and others 2011; Meyer and others 2014; Rojas and others 2014) suggesting some common toxic pathway in sALS and fALS.

Microglia

Activated microglia are thought to play an initially protective role in ALS, but then possibly become toxic due to increasing neuroinflammatory processes as disease advances (Lewis and others 2012). Microglia purified from mutant *SOD1* mice are toxic to stem cell-derived human MNs and this toxicity appears to be dependent on prostaglandin signalling: activation of prostaglandin D2 (PGD2) receptor 1 (DP1) in wildtype mouse and human microglia prior to co-culture with MNs, induced significant MN toxicity. Conversely, pretreatment of mutant *SOD1* mouse microglia with a pharmacological inactivator of DP1, or genetic ablation of DP1 expression, significantly attenuates toxicity to MNs (de Boer and others 2014).

Expression of mutant SOD1 up-regulates *PGD2 receptor 1 (PTGDR)* transcript levels in mouse and human microglia, and increases the release of PGD2 in rat microglia and astrocytes suggesting a possible interaction between these glial cell types (Thonhoff and others 2011). Nitroxidative stress may mediate microglial toxicity to MNs; however, this appears to be specific to microglia prepared from symptomatic mutant SOD1 expressing mice, so this effect is unlikely to be a primary cause of MN degeneration (Thonhoff and others 2011).

Protein Homeostasis

Unfolded Protein Response/Endoplasmic Reticulum Stress

The endoplasmic reticulum (ER) is a cellular compartment in which post-translation protein processing, including chaperone-assisted protein folding, is carried out. When the function of the ER is perturbed, ER stress activates two adaptive pathways: (1) the unfolded protein response (UPR) to refold misfolded proteins, and (2) ER-associated degradation (ERAD) to export misfolded proteins from the ER to the ubiquitin proteasome system (UPS) for degradation. Although ER stress pathways are initially protective responses, prolonged activation can lead to pro-apoptotic consequences.

The UPR has three main pathways (the activating transcription factor 6 [ATF6], endoplasmic reticulum to nucleus signaling 1 (also known as inositol-requiring kinase 1) [IRE1], and eukaryotic translation initiation factor 2- α kinase 3 (also known as protein kinase RNA-activated (PKR)-like ER kinase) [PERK] pathways) that are all activated in spinal MNs in SOD1-ALS mouse models (Walker and Atkin 2011). This activation appears to be an early, presymptomatic, event in *SOD1^{G93A}* mice, with toxic consequences for the affected cells (Saxena and others 2009). Similarly, RNA profiles of MNs derived from a *SOD1^{+A4V}* fALS patient, show activation of ER stress and the UPR, compared with non-mutant isogenic controls (Kiskinis and others 2014).

Endoplasmic reticulum stress initially increases phosphorylation of eIF2 α via PERK activation, which stalls protein synthesis (anti-apoptotic ER stress pathways). However, chronic ER stress activates GADD34 which dephosphorylates eIF2 α , reinitiating protein translation in a pro-apoptotic pathway (Fig. 3). Blocking the dephosphorylation of p-eIF2 α , increased survival of *SOD1^{+A4V}* MNs (Kiskinis and others 2014), and this could be due to stopping the pro-apoptotic action of GADD34. However, as the basal state of *SOD1^{+A4V}* MNs was of increased p-eIF2 α these results are difficult to interpret.

Mutant *SOD1^{G85R}* transgenic mice in which *Perk* is reduced (heterozygous knockout), have shortened disease

duration and lifespan, perhaps because the UPR is overwhelmed by misfolded mutant SOD1, whereas *SOD1^{G85R}* transgenic mice in which the effect of PERK is increased by reduction of *Gadd34* (heterozygous knockout), have an ameliorated disease and prolonged lifespan (Wang and others 2011; Wang and others 2014).

Mutant SOD1 has been implicated in the direct activation of ER stress through interaction with subunits of coatomer coat protein II complex (COPII) in a transfected cell model and in mutant *SOD1* transgenic mice as early as 10 days of age (Atkin and others 2014). COPII is essential for ER-Golgi transport, and expression of mutant SOD1 caused ER-Golgi transport disturbance before either the earliest markers for ER stress or aggregate formation, implicating the interaction and its effect as an early upstream event in mutant SOD1 toxicity. Disrupting ER-Golgi transport in this way results in activation of ER stress responses (Fig. 4). In cellular models, co-expression of COPII subunits with mutant SOD1 significantly reduced SOD1-induced apoptosis (Atkin and others, 2014).

SOD1 as an ER Stress Activating Zinc Sensor

Another recently proposed role for SOD1 is as a zinc sensor, activating ER stress and up-regulating zinc transporters by binding to Derlin1 in zinc-deficient conditions (Homma and others 2013). Derlin1 is an ERAD protein involved in export of misfolded proteins from the ER to the UPS. Under conditions of zinc depletion SOD1, which is a copper/zinc dependent enzyme, binds Derlin1 at a normally hidden Derlin1 binding region, and the resulting dysfunction of both Derlin1 and the ERAD process causes a build-up of misfolded protein in the ER and elicits ER stress (Fig. 5). ATF6, a transcription factor activated by ER stress, as well as up-regulating ER chaperones, also promotes transcription of the zinc transporter *ZIP14*, which may act to restore intracellular zinc levels (Homma and others 2013).

SOD1 mutation in ALS may result in constitutive exposure of the Derlin1 binding region and chronic ER stress and ERAD dysfunction. Mutant SOD1 activates ER stress and the IRE1-ASK1 pro-apoptotic pathway in a Derlin1 binding-dependent manner (Nishitoh and others 2008); further, of 132 ALS associated SOD1 mutations, 124 co-immunoprecipitated with Derlin1 in transfected HEK cells (Fujisawa and others 2012). The mutants which did not co-precipitate with Derlin1 also failed to activate ER stress and were less toxic in cellular assays (Fujisawa and others 2012). In a *SOD1^{G93A}* transgenic mouse model of ALS, knocking-out *Ask1* improved survival and reduced MN death, showing that this pathway is also important in vivo, however, age at disease onset was unchanged (Nishitoh and others 2008).

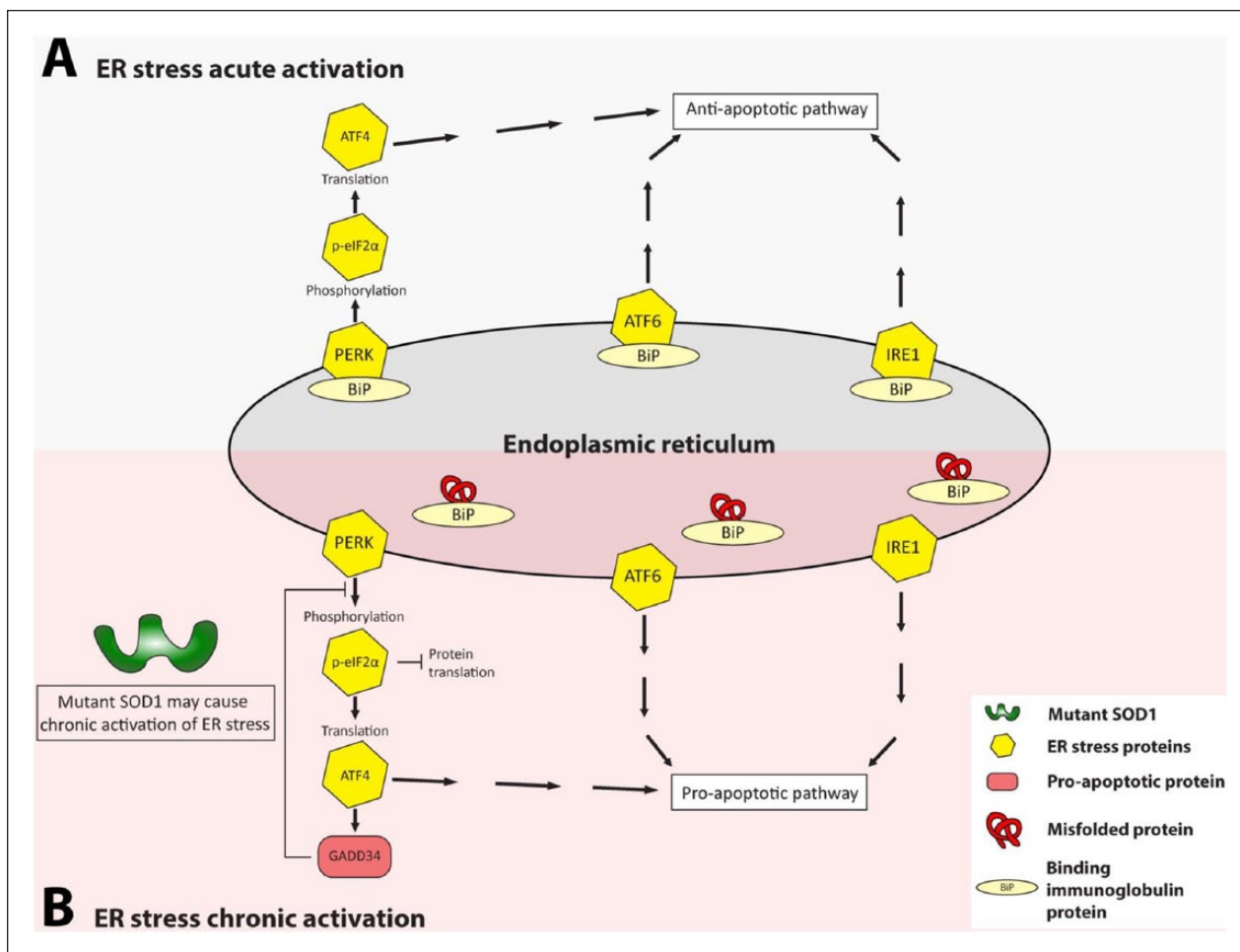


Figure 3. Mutant superoxide dismutase I (SOD1) may cause chronic activation of endoplasmic reticulum (ER) stress. Acute anti-apoptotic and chronic pro-apoptotic ER stress pathways: (A) during acute activation of ER stress the three signal transduction pathways (the PERK, ATF6, and IRE1 pathways) mediate the unfolded protein response. PERK, ATF6, and IRE1 proteins are associated with BiP (binding immunoglobulin protein). (B) However, if there is chronic activation of the ER stress PERK, ATF6, and IRE1 dissociate from BiP causing the activation of pro-apoptotic pathways. GADD34 is activated in the PERK pathway, promoting the dephosphorylation of p-eIF2 α and the reinitiation of protein synthesis. Chronic activation of ER stress, may mediate the unfolded protein response (UPR) and the ER-associated degradation (ERAD) mechanism.

Motor neurons may have an increased basal level of ER stress as compared with other neuronal and non-neuronal cell types; this difference might be a source of the selective vulnerability of MNs in ALS (Kiskinis and others 2014) and might also make them more susceptible to perturbation of Derlin1 function by mutant SOD1.

Autophagy

The autophagy pathway for protein clearance has been implicated as dysfunctional in sALS and fALS patients (unidentified genotypes) and transgenic mouse models of SOD1-fALS (Hetz and others 2009, and reviewed in Song and others 2012). Pharmacological and genetic manipulation of autophagy pathways in SOD1-fALS

mice and *Caenorhabditis elegans* models has resulted in conflicting findings suggesting both protective and toxic roles for autophagy (Hetz and others 2009; Li and others 2013; Song and others 2012; Zhang and others 2011; Nassif and others 2014).

A direct role for mutant SOD1 in abnormal autophagy is suggested as, when overexpressed in a neuronal-like cell line, mutant SOD1 was found to co-precipitate with beclin 1 (BECN1), an autophagy activator, and with BCL2L1, a suppressor of BECN1 activity, whereas wildtype SOD1 only precipitated with BCL2L1 (Nassif and others 2014). The BECN1–BCL2L1 complex was weakened by co-expression with mutant SOD1, suggesting mutant SOD1 may activate autophagy by releasing BECN1 from the suppression of BCL2L1. However,

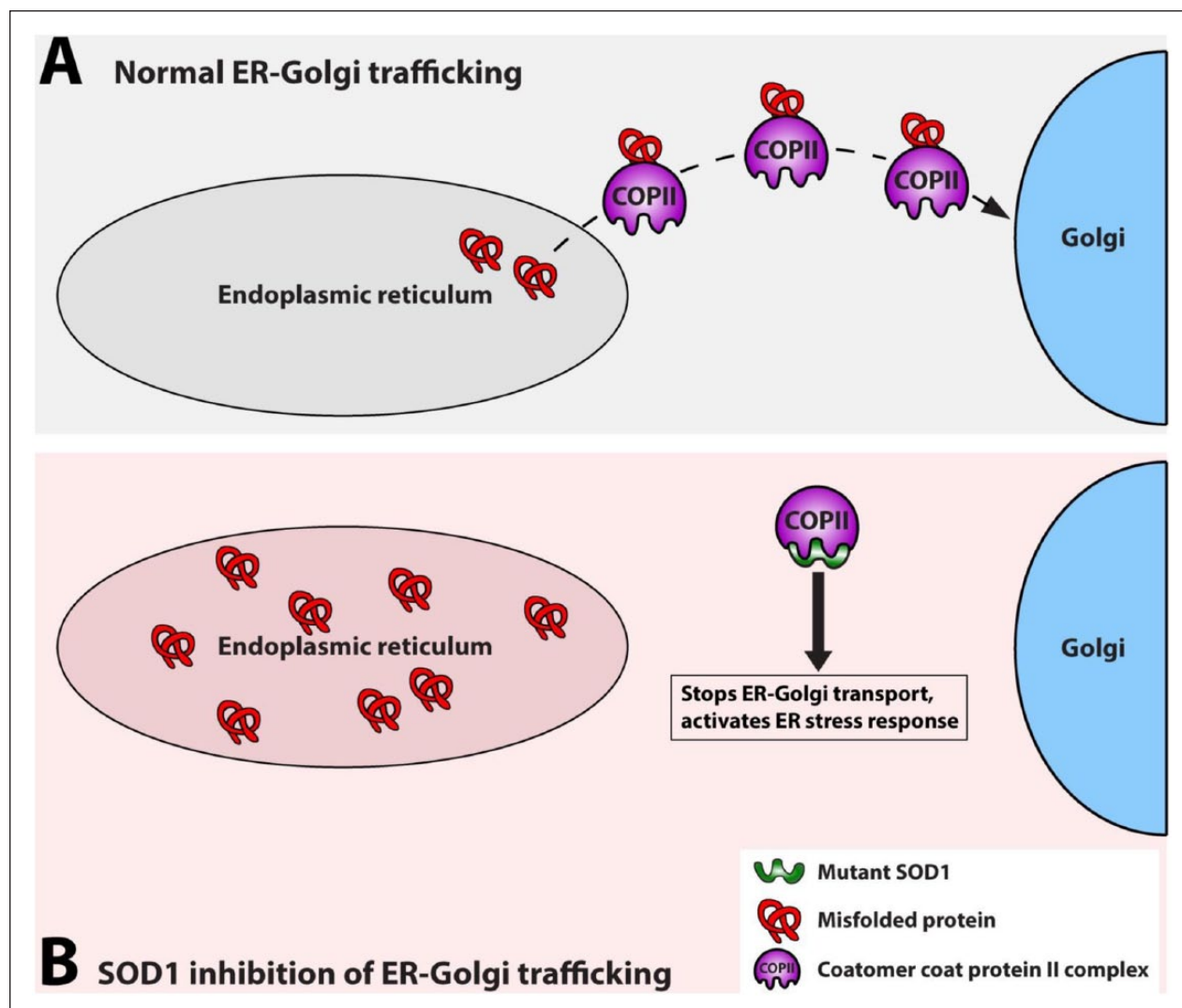


Figure 4. Mutant superoxide dismutase I (SOD1) activates endoplasmic reticulum (ER) stress by disrupting ER-Golgi trafficking through binding to coatmer coat protein II complex (COPII). (A) In normal conditions, COPII transports normal and misfolded proteins from the ER to the Golgi (only misfolded proteins are show in the figure) but (B) when mutant SOD1 is present, it interacts with a COPII subunit disrupting ER-Golgi trafficking resulting in a buildup of misfolded proteins in the ER, leading to ER stress.

the effect of wildtype SOD1, or any other co-expressed protein, on the BECN1-BCL2L1 complex was not assessed, therefore it is not possible to attribute the effect specifically to mutant SOD1 rather than increased protein expression per se. The activation of autophagy by mutant SOD1 could also be a downstream consequence of early effects on axonal transport and ER stress and ERAD (Hetz and others 2009; Zhang and others 2007).

Other Emerging Roles for SOD1

Several causative “ALS genes” encode RNA binding proteins, and this has highlighted how disruption of

processes involving RNA may play a primary role in the pathogenesis of the disease. Among these proteins, TDP43 and FUS are to date the most studied (Ling and others 2014; Nassif and others 2014). However, recent findings also point to a potential role of SOD1 in nucleic acid metabolism, as below.

SOD1 as a Transcription Factor

Although this is not their best characterized role, both TDP43 and FUS have been shown to act as transcription factors and, similarly, recent evidence has shown that SOD1 can regulate transcription in response to oxidative stress stimuli by moving into the nucleus and binding to

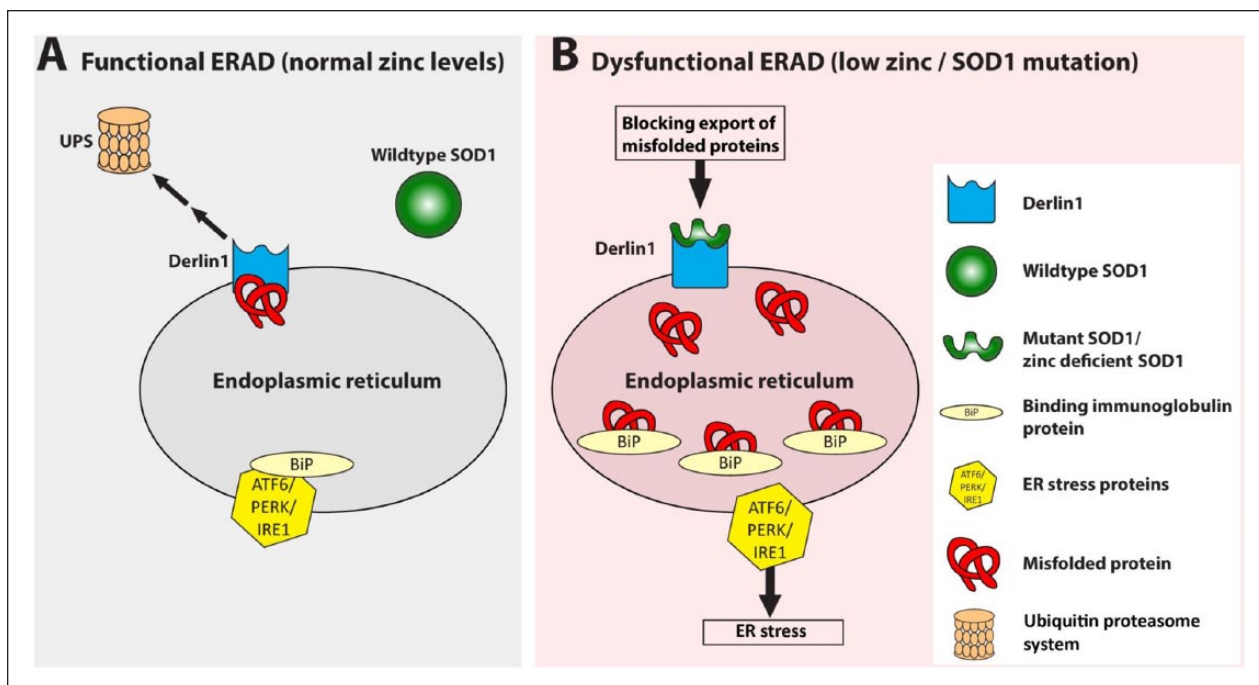


Figure 5. Superoxide dismutase I (SOD1) as an endoplasmic reticulum (ER) stress activating zinc sensor. (A) Under normal conditions wildtype SOD1 does not bind Derlin1, allowing export of misfolded proteins to the ubiquitin proteasome system (UPS). The three ER stress signal transducers PERK, ATF6, and IRE1 remain inactive and associated with binding immunoglobulin protein (BiP). (B) When mutant and/or in conditions of zinc depletion SOD1 assumes a mutant-like conformation exposing a binding site for Derlin1. The SOD1-Derlin1 interaction causes an accumulation of misfolded proteins which sequester BiP away from PERK, ATF6, and IRE1, activating the homeostatic ER stress response. Therefore, mutation of SOD1 in amyotrophic lateral sclerosis (ALS) may lead to constitutive Derlin1–SOD1 binding and ER stress activation.

promoters to regulate the expression of oxidative resistance genes (Hu and others 2009; Tsang and others 2014).

SOD1 as an RNA Binding Protein

TDP43 (Transactive response DNA Binding protein 43kDa) and FUS (Fused in Sarcoma) are involved in mRNA splicing, miRNA biogenesis, and mRNA stabilization and transport (Ling and others 2014). Whilst evidence of a role for SOD1 in the former two is still lacking, mutant SOD1 can bind mRNAs and play a role in their stabilization (Lu and others 2007; Lu and others 2009; Chen and others 2014). Wildtype SOD1 has further been shown to interact with TDP43, suggesting a potential common action in the regulation of specific RNA stability (Volkening and others 2009).

Mutant SOD1 binds sequence elements within the 3' UTR of *VEGF* (Vascular Endothelial Growth Factor) mRNA and forms complexes with other ribonucleoproteins such as TIAR and HuR. These interactions, which are specific to mutant SOD1, negatively affect levels of *VEGF* mRNA, which is a neuroprotective factor for motor neurons (Lu and others 2007; Lu and others 2009). Similarly, mutant SOD1 has been shown to bind the 3'

UTR of the neurofilament light chain (*NFL*) mRNA and negatively affect its stability. In an induce Pluripotential Stem Cell-derived cell model of ALS this reduction of *NFL* mRNA level mediates axonal degeneration, which could be a critical first step in ALS (Chen and others 2014).

SOD1 as a Signaling Molecule

SOD1 and Cell Metabolic State Signaling. Using yeast and human cell lines Reddi and Culotta (2013) identified a new role in cellular metabolism for SOD1: to integrate signals from oxygen and glucose in order to repress respiration within cells. In the mechanism proposed SOD1 binds the casein kinase gamma homologues Yck1p and Yck2p preventing their degradation via its enzymatic activity (Fig. 6). This results in repression of aerobic respiration and promotion of aerobic fermentation. Without SOD1, Yck1p and Yck2p are degraded, resulting in aerobic respiration. This finding gives insight into how rapidly proliferating cells may favor anaerobic glycolysis. Although effects in neurons remain to be determined the authors note the link between this signaling pathway and responses to hypoxia, a toxic state for motor neurons

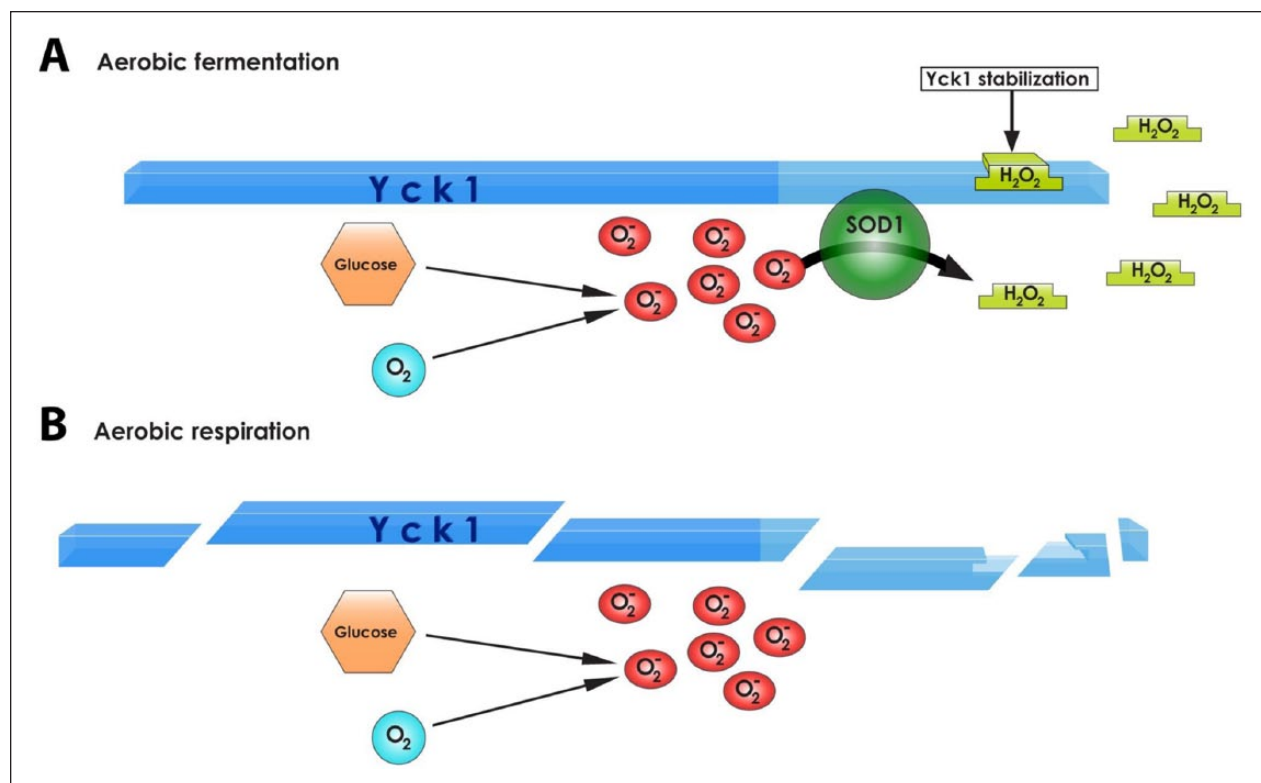


Figure 6. The role of superoxide dismutase (SOD1) in cellular metabolism, in yeast. (A) In an environment rich in glucose and oxygen SOD1 binds to the C-terminal degron of Yck1p and prevents its degradation, producing hydrogen peroxide that stabilizes the complex, so enabling the cells to utilise aerobic fermentation. (B) When SOD1 is not present Yck1p is degraded causing the cells to undergo aerobic respiration.

(Reddi and Culotta 2013). It is also interesting to note that a *de novo* mutation in casein kinase 1 gamma 3 (*CSNK1G3*) was recently identified as a potential ALS risk factor (Chesi and others 2014) and, in a yeast screen *YCK2*, a homologue of the human casein kinase 1 gamma 2, was identified as an enhancer of TDP43 toxicity (Kim and others 2014), offering hints that the putative interaction between SOD1 and casein kinase 1 gamma could be relevant to ALS.

Conclusions and Outstanding Questions

In ALS, SOD1 takes on a toxic unknown gain of function. However, as with many proteins involved in neurodegenerative disease, it is still not clear what the *normal* functions are for SOD1, and which cellular pathways rely on this protein. We know that it is abundant and ubiquitous, but protein levels appear to be far above what would be required solely for its role as an antioxidant in the cytosol.

New functions are now coming to light, and intriguingly—given the roles of other causative ALS genes—SOD1 is involved in RNA metabolism, including acting

as a nuclear transcription factor, and in metabolic signaling. Almost certainly there is much more to be discovered about SOD1 function in the normal situation, as well as in ALS, where there are interesting links and converging themes involving excitotoxicity (AMPA receptors, sodium channel activation) and ER stress, as well as cell specific effects from astrocytes and microglia.

Study of these functions present new opportunities for badly needed therapeutics to modulate disease progression in *SOD1-fALS*, and possibly even sALS, perhaps in combination with anti-sense oligonucleotide therapies (Musarò 2013; Yang and others 2013). However, until we have a considerably better understanding of SOD1 functions, much about this small protein remains enigmatic.

Declaration of Conflicting Interests

The author(s) declared no potential conflicts of interest with respect to the research, authorship, and/or publication of this article.

Funding

The author(s) disclosed receipt of the following financial support for the research, authorship, and/or publication of this

article: The authors have been supported by the Motor Neuron Disease Association (RAS, PF, EMCF), the Thierry Latran Foundation (PF, EMCF), the UK Medical Research Council (RKAB-S, PF, EMCF) and the NIHR-UCLH Biomedical Research Centre (PF).

References

- Atkin JD, Farg MA, Soo KY, Walker AK, Halloran M, Turner BJ, and others. 2014. Mutant SOD1 inhibits ER-Golgi transport in amyotrophic lateral sclerosis. *J Neurochem* 129:190–204.
- Ayers JJ, Fromholt S, Koch M, DeBosier A, McMahon B, Xu G, and others. 2014. Experimental transmissibility of mutant SOD1 motor neuron disease. *Acta Neuropathol* 128:791–803.
- Basso M, Pozzi S, Tortarolo M, Fiordaliso F, Bisighini C, Pasetto L, and others. 2013. Mutant copper-zinc superoxide dismutase (SOD1) induces protein secretion pathway alterations and exosome release in astrocytes: implications for disease spreading and motor neuron pathology in amyotrophic lateral sclerosis. *J Biol Chem* 288:15699–711.
- Bosco DA, Morfini G, Karabacak NM, Song Y, Gros-Louis F, Pasinelli P, and others. 2010. Wild-type and mutant SOD1 share an aberrant conformation and a common pathogenic pathway in ALS. *Nat Neurosci* 13:1396–403.
- Chen H, Qian K, Du Z, Cao J, Petersen A, Liu H, and others. 2014. Modeling ALS with iPSCs reveals that mutant SOD1 misregulates neurofilament balance in motor neurons. *Cell Stem Cell* 14:796–809.
- Chesi A, Staahl BT, Jovicic A, Courhous J, Fasolino M, Raphael AR, and others. 2014. Exome sequencing to identify de novo mutations in sporadic ALS trios. *Nat Neurosci* 16:851–6.
- Chia R, Tattum MH, Jones S, Collinge J, Fisher EMC, Jackson GS. 2010. Superoxide dismutase 1 and tgSOD1G93A mouse spinal cord seed fibrils, suggesting a propagative cell death mechanism in amyotrophic lateral sclerosis. *PLoS One* 5:e10627.
- Corson LB, Strain JJ, Culotta VC, Cleveland DW. 1998. Chaperone-facilitated copper binding is a property common to several classes of familial amyotrophic lateral sclerosis-linked superoxide dismutase mutants. *Proc Natl Acad Sci U S A* 95:6361–6.
- de Boer AS, Koszka K, Kiskinis E, Suzuki N, Davis-Dusenbery BN, Eggan K. 2014. Genetic validation of a therapeutic target in a mouse model of ALS. *Sci Transl Med* 6:248ra104.
- Forsberg K, Jonsson PA, Andersen PM, Bergemalm D, Graffmo KS, Hultdin M, and others. 2010. Novel antibodies reveal inclusions containing non-native SOD1 in sporadic ALS patients. *PLoS One* 5:e11552.
- Fritz E, Izaurieta P, Weiss A, Mir FR, Rojas P, Gonzalez D, and others. 2013. Mutant SOD1-expressing astrocytes release toxic factors that trigger motoneuron death by inducing hyperexcitability. *J Neurophysiol* 109:2803–14.
- Fujisawa T, Homma K, Yamaguchi N, Kadowaki H, Tsuburaya N, Naguro I, and others. 2012. A novel monoclonal antibody reveals a conformational alteration shared by amyotrophic lateral sclerosis-linked SOD1 mutants. *Ann Neurol* 72:739–49.
- Grad LI, Cashman NR. 2014. Prion-like activity of Cu/Zn superoxide dismutase. Implications for amyotrophic lateral sclerosis. *Prion* 8:33–41.
- Grad LI, Guest WC, Yanai A, Pokrishevsky E, O'Neill MA, Gibbs E, et al. 2011. Intermolecular transmission of superoxide dismutase 1 misfolding in living cells. *Proc Natl Acad Sci U S A* 108:16398–403.
- Grad LI, Yerbury JJ, Turner BJ, Guest WC, Pokrishevsky E, O'Neill MA, and others. 2014. Intercellular propagated misfolding of wild-type Cu/Zn superoxide dismutase occurs via exosome-dependent and -independent mechanisms. *Proc Natl Acad Sci U S A* 111:3620–5.
- Haidet-Phillips AM, Hester ME, Miranda CJ, Meyer K, Braun L, Frakes A, and others. 2011. Astrocytes from familial and sporadic ALS patients are toxic to motor neurons. *Nat Biotechnol* 29:824–8.
- Hetz C, Thielen P, Matus S, Nassif M, Court F, Kiffin R, and others. 2009. XBP-1 deficiency in the nervous system protects against amyotrophic lateral sclerosis by increasing autophagy. *Genes Dev* 23:2294–306.
- Homma K, Fujisawa T, Tsuburaya N, Yamaguchi N, Kadowaki H, Takeda K, and others. 2013. SOD1 as a molecular switch for initiating the homeostatic ER stress response under zinc deficiency. *Mol Cell* 52:75–86.
- Hu S, Xie Z, Onishi A, Yu X, Jiang L, Lin J, and others. 2009. Profiling the human protein-DNA interactome reveals ERK2 as a transcriptional repressor of interferon signaling. *Cell* 139:610–22.
- Hwang YM, Stathopoulos PB, Dimmick K, Yang H, Badiei HR, Tong MS, and others. 2010. Nonamyloid aggregates arising from mature copper/zinc superoxide dismutases resemble those observed in amyotrophic lateral sclerosis. *J Biol Chem* 285:41701–11.
- Ilieva H, Polymenidou M, Cleveland DW. 2009. Non-cell autonomous toxicity in neurodegenerative disorders: ALS and beyond. *J Cell Biol* 187:761–72.
- Kiernan MC, Vucic S, Cheah BC, Turner MR, Eisen A, Hardiman O, and others. 2012. Amyotrophic lateral sclerosis. *Lancet* 377:942–55.
- Kim HJ, Raphael AR, Ladow ES, McGurk L, Weber RA, Trojanowski JQ, and others. 2014. Therapeutic modulation of eIF2 α phosphorylation rescues TDP-43 toxicity in amyotrophic lateral sclerosis disease models. *Nat Genet* 46:152–160.
- Kiskinis E, Sandoe J, Williams L, Boulting G, Moccia R, Wainger B, and others. 2014. Pathways disrupted in human ALS motor neurons identified through genetic correction of mutant SOD1. *Cell Stem Cell* 14:781–95.
- Lewis C-A, Manning J, Rossi F, Krieger C. 2012. The neuroinflammatory response in ALS: the roles of microglia and T cells. *Neurol Res Int* 2012:803701.
- Li J, Huang KX, Le WD. 2013. Establishing a novel *C. elegans* model to investigate the role of autophagy in amyotrophic lateral sclerosis. *Acta Pharmacol Sin* 34:644–50.
- Ling SC, Polymenidou M, Cleveland DW. 2014. Converging mechanisms in ALS and FTD: disrupted RNA and protein homeostasis. *Neuron* 79:416–38.
- Lu L, Wang S, Zheng L, Li X, Suswam EA, Zhang X, and others. 2009. Amyotrophic lateral sclerosis-linked mutant

- SOD1 sequesters Hu antigen R (HuR) and TIA-1-related protein (TIAR). Implications for impaired post-transcriptional regulation of vascular endothelial growth factor. *J Biol Chem* 284:33989–98.
- Lu L, Zheng L, Viera L, Suswam E, Li Y, Li X, and others. 2007. Mutant Cu/Zn-superoxide dismutase associated with amyotrophic lateral sclerosis destabilizes vascular endothelial growth factor mRNA and downregulates its expression. *J Neurosci* 27:7929–38.
- Meyer K, Ferraiuolo L, Miranda CJ, Likhite S, McElroy S, Renusch S, and others. 2014. Direct conversion of patient fibroblasts demonstrates non-cell autonomous toxicity of astrocytes to motor neurons in familial and sporadic ALS. *Proc Natl Acad Sci U S A* 111:829–32.
- Münch C, O'Brien J, Bertolotti A. 2011. Prion-like propagation of mutant superoxide dismutase-1 misfolding in neuronal cells. *Proc Natl Acad Sci U S A* 108:3548–53.
- Musarò A. 2013. Understanding ALS: new therapeutic approaches. *FEBS J* 280:4315–22.
- Nagai M, Re DB, Nagata T, Chalazonitis A, Jessell TM, Wichterle H, and others. 2007. Astrocytes expressing ALS-linked mutated SOD1 release factors selectively toxic to motor neurons. *Nat Neurosci* 10:615–22.
- Nassif M, Valenzuela V, Rojas-Rivera D, Vidal R, Matus S, Castillo K, and others. 2014. Pathogenic role of BECN1/Beclin 1 in the development of amyotrophic lateral sclerosis. *Autophagy* 10:1256–71.
- Nishitoh H, Kadowaki H, Nagai A, Maruyama T, Yokota T, Fukutomi H, and others. 2008. ALS-linked mutant SOD1 induces ER stress- and ASK1-dependent motor neuron death by targeting Derlin-1. *Genes Dev* 22:1451–64.
- Pardo CA, Xu Z, Borchelt DR, Price DL, Sisodia SS, Cleveland DW. 1995. Superoxide dismutase is an abundant component in cell bodies, dendrites, and axons of motor neurons and in a subset of other neurons. *Proc Natl Acad Sci U S A* 92:954–8.
- Polymenidou M, Cleveland DW. 2012. Prion-like spread of protein aggregates in neurodegeneration. *J Exp Med* 209:889–93.
- Reddi AR, Culotta VC. 2013. SOD1 integrates signals from oxygen and glucose to repress respiration. *Cell* 152:224–35.
- Redler RL, Dokholyan NV. 2012. The complex molecular biology of amyotrophic lateral sclerosis (ALS). *Prog Mol Biol Transl Sci* 107:215–62.
- Rojas F, Cortes N, Abarzua S, Dyrda A, van Zundert B. 2014. Astrocytes expressing mutant SOD1 and TDP43 trigger motoneuron death that is mediated via sodium channels and nitroxidative stress. *Front Cell Neurosci* 8:24.
- Saccon RA, Bunton-Stasyshyn RKA, Fisher EMC, Fratta P. 2013. Is SOD1 loss of function involved in amyotrophic lateral sclerosis? *Brain* 136:2342–58.
- Saxena S, Cabuy E, Caroni P. 2009. A role for motoneuron subtype-selective ER stress in disease manifestations of FALS mice. *Nat Neurosci* 12:627–36.
- Saxena S, Roselli F, Singh K, Leptien K, Julien JP, Gros-Louis F, and others. 2013. Neuroprotection through excitability and mTOR required in ALS motoneurons to delay disease and extend survival. *Neuron* 80:80–96.
- Song CY, Guo JF, Liu Y, Tang BS. 2012. Autophagy and its comprehensive impact on ALS. *Int J Neurosci* 122:695–703.
- Sundaramoorthy V, Walker AK, Yerbury J, Soo KY, Farg MA, Hoang V, and others. 2013. Extracellular wildtype and mutant SOD1 induces ER-Golgi pathology characteristic of amyotrophic lateral sclerosis in neuronal cells. *Cell Mol Life Sci* 70:4181–95.
- Thonhoff JR, Gao J, Dunn TJ, Ojeda L, Wu P. 2011. Mutant SOD1 microglia-generated nitroxidative stress promotes toxicity to human fetal neural stem cell-derived motor neurons through direct damage and noxious interactions with astrocytes. *Am J Stem Cells* 1:2–21.
- Tsang CK, Liu Y, Thomas J, Zhang Y, Zheng XF. 2014. Superoxide dismutase 1 acts as a nuclear transcription factor to regulate oxidative stress resistance. *Nat Commun* 5:3446.
- Urushitani M, Sik A, Sakurai T, Nukina N, Takahashi R, Julien JP. 2006. Chromogranin-mediated secretion of mutant superoxide dismutase proteins linked to amyotrophic lateral sclerosis. *Nat Neurosci* 9:108–18.
- Van Damme P, Bogaert E, Dewil M, Hersmus N, Kiraly D, Scheveneels W, and others. 2007. Astrocytes regulate GluR2 expression in motor neurons and their vulnerability to excitotoxicity. *Proc Natl Acad Sci U S A* 104:14825–30.
- Volkening K, Leystra-Lantz C, Yang W, Jaffee H, Strong MJ. 2009. Tar DNA binding protein of 43 kDa (TDP-43), 14-3-3 proteins and copper/zinc superoxide dismutase (SOD1) interact to modulate NFL mRNA stability. Implications for altered RNA processing in amyotrophic lateral sclerosis (ALS). *Brain Res* 1305:168–82.
- Walker AK, Atkin JD. 2011. Stress signaling from the endoplasmic reticulum: a central player in the pathogenesis of amyotrophic lateral sclerosis. *IUBMB Life* 63:754–63.
- Wang J, Xu GL, Borchelt DR. 2006. Mapping superoxide dismutase 1 domains of non-native interaction: roles of intra- and intermolecular disulfide bonding in aggregation. *J Neurochem* 96:1277–88.
- Wang L, Popko B, Roos RP. 2011. The unfolded protein response in familial amyotrophic lateral sclerosis. *Hum Mol Genet* 20:1008–15.
- Wang L, Popko B, Roos RP. 2014. An enhanced integrated stress response ameliorates mutant SOD1-induced ALS. *Hum Mol Genet* 23:2629–38.
- Yang YM, Gupta S, Kim KJ, Powers BE, Cerqueira A, Wainger BJ, and others. 2013. A small molecule screen in stem-cell-derived motor neurons identifies a kinase inhibitor as a candidate therapeutic for ALS. *Cell Stem Cell* 12:713–26.
- Zhang F, Ström AL, Fukada K, Lee S, Hayward LJ, Zhu H. 2007. Interaction between familial amyotrophic lateral sclerosis (ALS)-linked SOD1 mutants and the dynein complex. *J Biol Chem* 282:16691–9.
- Zhang X, Li L, Chen S, Yang D, Wang Y, Zhang X, and others. 2011. Rapamycin treatment augments motor neuron degeneration in SOD1^{G93A} mouse model of amyotrophic lateral sclerosis. *Autophagy* 7:412–25.